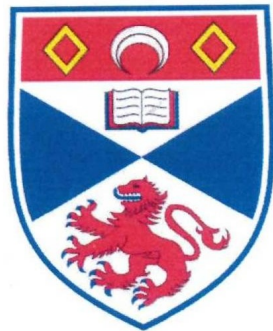


An Investigation into the *Trypanosoma brucei*
CDP-DAG Synthase and Downstream Pathways

Alison Catherine Lilley



This thesis is submitted in partial fulfilment for the degree of PhD
at the
University of St Andrews

19 September 2012

Table of Contents

Abstract.....	7
List of Figures.....	8
List of Tables	14
Candidate’s declarations:.....	15
Supervisor’s declaration:.....	16
Permission for electronic publication:	17
Acknowledgements.....	18
List of Abbreviations.....	19
Chapter 1: Introduction	22
1.1 African Trypanosomiasis.....	22
1.1.1 The Human Disease.....	22
1.1.2 Current HAT Treatments.....	24
1.2 <i>Trypanosoma brucei</i>	25
1.2.1 Taxonomy.....	25
1.2.2 Cell Structure.....	27
1.2.3 Life cycle	28
1.2.4 <i>T. brucei</i> as a model organism.....	30
1.2.5 Variant Surface Glycoprotein and the Glycosylphosphatidyl Inositol Anchor	30
1.3 Lipid Metabolism in <i>T. brucei</i>	32
1.3.1 Uptake of Components from Host for Lipid Biosynthesis in <i>T. brucei</i>	32
1.3.2 Fatty Acid Synthesis.....	32
1.3.3 Glycerophospholipids.....	34
1.3.4 Glycerophospholipid Biosynthesis Overview	36
1.3.4.a Synthesis of PA, CDP-DAG and Kennedy Pathways.....	36
1.3.4.b Synthesis of PG and CL	38
1.3.4.c Synthesis of Phosphatidylserine.....	38
1.3.4.d Synthesis of Phosphatidylethanolamine.....	39
1.3.4.e Synthesis of Phosphatidylcholine.....	40
1.3.4.f GPI anchor Biosynthesis.....	41
1.3.5 Products of the CDP-DAG Pathway	42
1.3.5.a CDP-DAG.....	43

1.3.5.b Phosphatidylserine.....	45
1.3.5.c Phosphatidylglycerol and CL.....	45
1.3.5.d Phosphatidylinositol and PIPs	46
1.4 CDP-DAG Synthase	49
1.4.1 Gene.....	50
1.4.2 Sequence Analyses/Structure	51
1.4.3 Sub-cellular localisation	52
1.4.4 Enzyme Specificity/Kinetics	54
1.4.5 Reverse Reaction	56
1.4.6 Expression/Regulation.....	56
1.4.7 Inhibitors.....	60
1.4.8 CDP-DAG synthase as a Drug Target in <i>T. brucei</i>	60
1.5 PI Synthase	60
1.5.1 Gene.....	61
1.5.2 Sequence/Structure	61
1.5.3 Subcellular Localisation	62
1.5.4 Specificity/Kinetics	63
1.5.5 Inhibitors.....	65
1.5.6 Exchange reaction.....	66
1.5.7 Expression/Regulation.....	66
1.5.8 PI Synthase as a Drug Target in <i>T. brucei</i>	67
1.6 Objectives	67
Chapter 2: Materials and Methods	69
2.1 General.....	69
2.1.1 Reagents	69
2.1.2 Bioinformatics	69
2.1.3 PCR.....	70
2.1.4 RT-PCR	74
2.1.5 Restriction Enzyme Digestion	74
2.1.6 Ligation Reactions.....	75
2.1.7 Northern Blotting.....	75
2.1.7.a Synthesis of DIG-labelled probes	75
2.1.7.b In vitro transcription	76
2.1.7.c Quantification.....	76
2.1.7.d Gel Loading and Transfer	76

2.1.7.e Hybridisation	77
2.1.7.f Probe Detection	77
2.1.8 Southern Blotting.....	78
2.1.8.a Digests for TbCDS Southern	78
2.1.8.b DNA gel electrophoresis for Southern Analysis	78
2.1.8.c Transfer.....	78
2.1.8.d DIG Probe Labelling.....	78
2.1.8.e Probe Quantification	79
2.1.8.f Probe detection	79
2.1.9 Western Blotting.....	80
2.1.10 Transformation of <i>E. coli</i>	80
2.1.11 Plasmid Purification	81
2.1.12 Sequencing	81
2.1.13 ES-MS	81
2.1.14 Recombinant Protein Expression	82
2.1.14.a Construction of pET-32b HIS ₆ -TbCDS-HIS ₆	82
2.1.14.b Overproduction	82
2.1.14.c Crude Membrane Preparation	82
2.1.14.d Overexpression for Lipid Extraction.....	83
2.1.14.e Detergent Extraction	83
2.2 <i>Trypanosoma brucei</i> methods	83
2.2.1 <i>T. brucei</i> cell culture.....	83
2.2.2 <i>T. brucei</i> genomic DNA extraction and ethanol precipitation.....	84
2.2.3 <i>T. brucei</i> Transformation.....	84
2.2.4 <i>T. brucei</i> RNAi	84
2.2.5 Creation of TbCDS conditional knockout.....	85
2.2.5.a Creation of Tetracycline Inducible Ectopic TbCDS copy.....	85
2.2.5.b Construction of Endogenous Gene Knockout Cassettes.....	85
2.2.5.c Conditional Gene Knockouts	87
2.2.6 Cell Counting.....	88
2.2.7 <i>In vivo T. brucei</i> metabolic labelling.....	88
2.2.8 Cell Free System Assay of GPI Biosynthesis.....	89
2.2.9 TbCDS cell free activity assay	90
2.2.10 Extraction and Analysis of NTPs	90

2.2.11 Cell Fixing and Staining	91
2.2.12 Mitotracker staining.....	92
2.2.12 Microscopy	92
2.2.13 Lipid Extraction from <i>T. brucei</i>	92
2.3 Yeast Methods	93
2.3.1 <i>Saccharomyces cerevisiae</i> culture	93
2.3.2 Yeast Colony PCR.....	93
2.3.3 Yeast Transformation	93
2.3.5 Construction of TbCDS and CDS1 pRS-426 Met25.....	94
2.3.6 Complementation of <i>cds1::KanMX</i> with TbCDS and Yeast CDS by Tetrad Analysis	94
2.3.7 Construction of TbCDS and CDS1 p405-TEF1	94
2.3.8 Plasmid Shuffle	95
Chapter 3: Characterisation of <i>Trypanosoma brucei</i> Cytidine Diphosphate Diacylglycerol Synthase	96
3.1 Introduction	96
3.2 Identification and Sequencing of TbCDS 427.....	96
3.3 Predicted TbCDS Proteomics	99
3.4 Phylogenetics.....	105
3.5 Expression of TbCDS in <i>E. coli</i>	108
3.6 Yeast rescue.....	114
3.7 Summary and Conclusions	125
Chapter 4 - Cytidine Diphosphate Diacylglycerol Synthase in Bloodstream Form <i>Trypanosoma brucei</i>	127
4.1 Introduction	127
4.2 Transcription of TbCDS in <i>T. brucei</i>	128
4.3 TbCDS activity in Bloodstream Form <i>T. brucei</i>	129
4.4 RNAi of TbCDS in Bloodstream Form <i>T. brucei</i>	129
4.4.1 Confirmation of Construct Integration	133
4.4.2 Morphological Phenotyping of Bloodstream Form TbCDS RNAi Cell line	134
4.4.3 Biochemical Phenotyping of Bloodstream Form TbCDS RNAi Cell Line. 136	
4.4.3.a In vivo Radiolabelling of Bloodstream Form TbCDS RNAi	136
4.4.3.b. Lipid Profile of Bloodstream Form TbCDS RNAi Cell Line by ES-MS/MS.....	142
4.4.3.c NTP levels	161
4.5 Knockout of TbCDS in bloodstream form <i>T. brucei</i>	162
4.5.1 Creation of a TbCDS Conditional Knockout Cell Line	163

4.5.2 Confirmation of the TbCDS CKO Genotype	165
4.5.3 Growth Phenotype of TbCDS CKO	166
4.5.4 Morphological Phenotype of TbCDS CKO.....	168
4.5.5 Biochemical Phenotyping of Bloodstream Form TbCDS CKO.....	170
4.5.5.a. In vivo radiolabelling	170
4.5.5.b. Cell Free System for GPI Anchor Synthesis	172
4.5.5.c ES-MS/MS of Lipids.....	175
4.6 Summary and Conclusions	190
Chapter 5 - Cytidine Diphosphate Diacylglycerol Synthase in Procyclic Form	
<i>Trypanosoma brucei</i>	193
5.1 Introduction	193
5.2 RNAi of TbCDS in Procyclic Form <i>T. brucei</i>	194
5.2.1 Confirmation of Construct Integration	198
5.2.2 Morphological Phenotyping of Procyclic Form TbCDS RNAi Cell line....	199
5.2.3 Mitochondrial Functioning in Procyclic Form TbCDS RNAi Cell line.....	203
5.2.4 Biochemical Phenotyping of Procyclic Form RNAi Cell Line	206
5.2.4.a In Vivo Radiolabelling	206
5.2.4.b Lipid Profile of Procyclic Form TbCDS RNAi Cell Line by ES-MS	213
5.5 Summary and Conclusion.....	231
Chapter 6: Overexpression and Subcellular Localisation of TbCDS in <i>T. brucei</i>	234
6.1 Introduction	234
6.2 TbCDS Overexpression in Bloodstream Form <i>T. brucei</i>	235
6.2.1 Growth Phenotype of Bloodstream Form <i>T. brucei</i> over expressing TbCDS	235
6.2.2 Lipidomics of Bloodstream Form <i>T. brucei</i> over expressing TbCDS.....	236
6.2.2.a Positive Survey Scan	236
6.2.2.b Negative Survey Scan	238
6.2.2.c Choline-Phosphate Containing Lipids.....	242
6.2.2.d Inositol-Phosphate Containing Lipids	244
6.2.2.e Glycerol-Phosphate Containing Lipids	246
6.2.3 Subcellular Localisation of TbCDS in Bloodstream Form <i>T. brucei</i>	248
6.3 Overexpression of TbCDS in Procyclic Form <i>T. brucei</i>	251
6.3.1 Lipidomics of Procyclic Form <i>T. brucei</i> overexpressing TbCDS	252
6.3.1.a Positive Survey Scan	252
6.3.1.b Negative Survey Scan	254

6.2.3.c Choline-Phosphate Containing Lipids	256
6.2.3.d Inositol-Phosphate Containing Lipids.....	258
6.2.3.e Glycerol-Phosphate Containing Lipids	260
6.2.3.f CL.....	262
6.4 Subcellular Localisation of TbCDS in Procyclic Form <i>T. brucei</i>	264
6.5 Conclusions	267
Chapter 7: Overexpression and Subcellular Localisation of TbPIS in	270
<i>T. brucei</i>	270
7.1 Introduction	270
7.2 TbPIS Overexpression in Bloodstream Form <i>T. brucei</i>	271
7.2.2 Lipidomics of Bloodstream Form <i>T. brucei</i> over expressing TbPIS.....	273
7.2.2.a Positive Survey Scan	273
7.2.2.b Negative Survey Scan	276
7.2.2.c Inositol-Phosphate Containing Lipids	278
7.2.3 Subcellular Localisation of TbPIS in Bloodstream Form <i>T. brucei</i>	280
7.3 TbPIS Overexpression in Procyclic Form <i>T. brucei</i>	282
7.3.1 Lipidomics of Procyclic Form <i>T. brucei</i> Overexpressing TbPIS	284
7.3.1.a Positive Survey Scan	284
7.3.1.b Negative Survey Scan	286
7.3.1.c Choline-Phosphate Containing Lipids.....	289
7.3.1.d Inositol-Phosphate Containing Lipids.....	291
7.3.2 Subcellular Localisation of TbPIS in Procyclic Form <i>T. brucei</i>	294
7.4 Conclusions	296
Chapter 8: Conclusions and Future Work	300
Bloodstream Form <i>Trypanosoma brucei</i>	300
Procyclic Form <i>Trypanosoma brucei</i>	303
References	306
Appendix A	323

Abstract

Lipid metabolism in *Trypanosoma brucei*, the causative agent of African sleeping sickness, differs from its human host, allowing a plethora of novel drug targets to be discovered and validated. Cytidine diphosphate diacylglycerol (CDP-DAG) is a central lipid intermediate produced by the enzyme CDP-DAG synthase (CDS), but nothing was known about CDS in *T. brucei*. Only one gene encodes CDS in *Trypanosoma brucei* (Tb927.7.220) and this was shown to encode a functional CDS by overexpression in *E. coli* and complementation of a yeast CDS null, which was created during this study. Expression and activity of TbCDS was confirmed in *T. brucei*, and was shown to be essential in both life cycle stages. Disruption of TbCDS altered the lipid profile of *T. brucei*, confirming a central role for CDP-DAG in phospholipid synthesis. Biochemical and morphological characterisation of mutants in TbCDS expression elucidated at least two separately localised and regulated pools of CDP-DAG and phosphatidylinositol in *T. brucei*. In bloodstream form these pools are localised to the Golgi and the ER, however in procyclics it is possible that both of these pools are localised to the Golgi, since no phosphatidylinositol synthase protein was detected in the ER of procyclics. Reduction in TbCDS was shown to affect cell cycle regulation and Golgi segregation possibly due to a depletion of phosphorylated phosphatidylinositols (PIPs). These studies also indicate that phosphatidylglycerol may be synthesised by the phosphatidylglycerol-phosphate synthase which may be capable of using phosphatidylserine as a substrate in a headgroup swapping reaction. TbCDS has now been genetically validated as a drug target, and has highlighted novel aspects of lipid biosynthesis in *T. brucei*. Collectively, these findings highlight the central role played by TbCDS and the new knowledge gained here may lead to the discovery and validation of other novel drug targets against African sleeping sickness.

List of Figures

1.1	Distribution of Human African Trypanosomiasis species	23
1.2	Taxonomic relationships in the Euglenozoa	26
1.3	Cartoon of <i>Trypanosoma brucei</i> showing major structural features	28
1.4	Life cycle of <i>Trypanosoma brucei</i>	29
1.5	VSG and its GPI anchor in <i>T. brucei</i>	31
1.6	<i>De novo</i> fatty acid synthesis by four microsomal elongases	33
1.7	Structure of a glycerophospholipid	35
1.8	Phospholipid composition in <i>T. brucei</i>	36
1.9	Predicted pathways for glycerophospholipid synthesis in <i>T. brucei</i>	37
1.10	Pathways for GPI biosynthesis in <i>T. brucei</i>	42
1.11	Products of the CDP-DAG pathway	44
1.12	Intracellular cycle of phosphoinositide-mediated signal transduction in mammals	48
1.13	Reaction catalysed by cytidine diphosphate diacylglycerol synthase	49
1.14	Reaction catalysed by phosphatidylinositol synthase	60
1.15	Minimum Structural recognition for <i>T. brucei</i> phosphatidylinositol synthase	65
2.1	Orientation of TbCDS probe in pHRL-CMV vector	74
2.2	Schematic showing the transfer stack used for Southern and Northern blots	76
2.3	Schematic of TbCDS knockout construct creation	85
3.1	TbCDS in the genome	95
3.2	Cloning of putative TbCDS ORF and UTRs from PCR into Topo for sequencing	95
3.3	DNA sequence of putative TbCDS strain 427 open reading frame (Tb427.07.220) plus 5' and 3' UTRs	96
3.4	Predicted hydrophobicity and trans-membrane regions of TbCDS protein	98
3.5	PROSITE sequence logo for phosphatidyl cytidyltransferase pattern	99

3.6	Protein sequences of known CDS proteins with TbCDS and other predicted kinetoplastid proteins, aligned using ClustalW	100
3.7	Protein sequences of predicted prokaryotic CDS proteins with kinetoplastid prokaryotic-like proteins, aligned using ClustalW	101
3.8	Unrooted phylogeny of known and putative CDS protein sequences	104
3.9	Unrooted phylogeny of known and putative CDS prokaryotic protein sequences with kinetoplastid CDS sequences	105
3.10	Recombinant expression of TbCDS in <i>E. coli</i>	107
3.11	Overexpression of TbCDS in <i>E. coli</i> causes a change in phospholipid composition -PG species	109
3.12	Overexpression of TbCDS in <i>E. coli</i> causes a change in phospholipid composition - CL species	111
3.13	Yeast rescue constructs	112
3.14	Schematic showing complementation of a yeast CDS1 null with the putative TbCDS	114
3.15	Haploid <i>S. cerevisiae</i> from tetrad analysis	118
3.16	Construction of p405-TEF1 rescue plasmids	119
3.17	Plasmid shuffle shows TbCDS can complement the yeast <i>cds1::KanMX</i> knockout	121
3.18	Negative survey scan of lipids from yeast - CDS rescue	122
4.1	TbCDS is transcribed in <i>T. brucei</i> , and cells have CDP-DAG synthase activity	126
4.2	Construction of TbCDS RNAi knockdown plasmid	127
4.3	TbCDS is essential in bloodstream form <i>T. brucei</i> - clone 1	129
4.4	TbCDS is essential in bloodstream form <i>T. brucei</i> - clone 6	130
4.5	Presence of hygromycin phosphotransferase (HYG) gene from TbCDS p2T7 RNAi construct in bloodstream form <i>T. brucei</i> genomic DNA	132
4.6	Morphology of Single Marker and TbCDS RNAi 48 hours + tetracycline	133
4.7	Biochemical analysis of bloodstream form TbCDS RNAi in the absence and presence of tetracycline at 42 hours by <i>in vivo</i> radiolabelling	135
4.8	Positive ion survey scan of lipids from Single Marker and bloodstream form TbCDS RNAi + tetracycline	142

4.9	Negative survey scan of lipids from Single Marker and bloodstream form TbCDS RNAi + tetracycline	144
4.10	Daughter ion spectrum of m/z 686 [M-H] ⁻ ion	146
4.11	Mass spectrometric analyses of choline-phosphate containing phospholipids from SM and bloodstream form TbCDS RNAi + Tet	148
4.12	Mass spectrometric analyses of ethanolamine-phosphate containing phospholipids from SM and bloodstream form bloodstream form TbCDS RNAi + tetracycline	150
4.13	Mass spectrometric analyses of inositol-phosphate containing phospholipids from SM and bloodstream form TbCDS RNAi + tetracline	152
4.14	Mass spectrometric analyses of glycerol-phosphate containing lipids in Single Marker and bloodstream form TbCDS RNAi + Tet	154
4.15	Daughter ion spectra of PG species	155
4.16	Mass spectrometric analyses of serine-phosphate containing phospholipids in SM and bloodstream form TbCDS RNAi	158
4.17	NTP quantification in SM and bloodstream form TbCDS RNAi by multireactant monitoring mass spectrometry (MRM-MS)	159
4.18	Construction of TbCDS knockout and endogenous expression pLEW100 constructs	161
4.19	PCR Confirmation of bloodstream form TbCDS CKO	163
4.20	TbCDS is essential for the survival of bloodstream form <i>T. brucei</i> in culture	164
4.21	Morphology of SM and TbCDS CKO 48 hours - tetracycline	166
4.22	Biochemical analysis of bloodstream form TbCDS CKO by <i>in vivo</i> radiolabelling + and - tetracycline for 42 hours	169
4.23	TbCDS is essential for formation of GPI intermediates	170
4.24	Positive ion survey scan of lipids from SM and TbCDS CKO - tetracycline	173
4.25	Negative survey scan of lipids from SM and TbCDS CKO - Tet	175
4.26	Daughter ion spectrum of m/z 700 [M-H] ⁻ ion	176
4.27	Mass spectrometric analyses of choline-phosphate containing phospholipids in SM and bloodstream form TbCDS CKO - tetracycline	178

4.28	Mass spectrometric analyses of ethanolamine-phosphate containing phospholipids in SM and TbCDS CKO - tetracycline	180
4.29	Mass spectrometric analyses of inositol-phosphate containing phospholipids from SM and bloodstream form TbCDS CKO - tetracycline	182
4.30	Mass spectrometric analyses of serine-containing phospholipids from SM and bloodstream form TbCDS CKO tetracycline	184
4.31	Mass spectrometric analyses of glycerophospholipids from SM and bloodstream form TbCDS CKO - tetracycline	186
5.1	Construction of TbCDS p2T7-177 vector	192
5.2	Essentiality of TbCDS in procyclic form <i>T. brucei</i>	194
5.3	Presence of phleomycin resistance gene (BLE) from TbCDS p2T7-177 RNAi construct in procyclic form <i>T. brucei</i> genomic DNA	195
5.4	Knockdown of TbCDS in procyclic form cells showing detached flagella and cell-cycle stalled mutants	198
5.5	Effect of TbCDS knockdown in procyclic form cells on mitochondrial membrane potential 7 days plus tetracycline	201
5.6	Knockdown of TbCDS in procyclic form cells results loss of mitochondrial membrane potential after 14 days plus tetracycline	202
5.7	Biochemical analysis of clone 1 procyclic form TbCDS RNAi by <i>in vivo</i> radiolabelling 48 hours - and + tetracycline	205
5.8	Positive ion survey scan of lipids from DM and procyclic form TbCDS RNAi + tetracycline	211
5.9	Negative survey scan of lipids from DM and procyclic form TbCDS RNAi + tetracycline	213
5.10	Mass spectrometric analyses of choline-phosphate containing phospholipids from DM and procyclic TbCDS RNAi + tetracycline	215
5.11	Mass spectrometric analyses of ethanolamine-containing phospholipids from DM and procyclic TbCDS RNAi + tetracycline	217
5.12	Mass spectrometric analyses of inositol-phosphate containing phospholipids from DM and procyclic TbCDS RNAi + tetracycline	220
5.13	Mass spectrometric analyses of serine containing phospholipids from DM and procyclic TbCDS RNAi + tetracycline	222
5.14	Mass spectrometric analyses of glycerol-phosphate containing phospholipids from DM and procyclic TbCDS RNAi + tetracycline	225

5.15	Negative survey scan of lipids from DM and procyclic TbCDS RNAi + tetracycline - high m/z.	227
6.1	Overexpression of TbCDS in BSF <i>T. brucei</i> results in an initial increase in growth rate	233
6.2	Positive ion survey scan of lipids from SM and bloodstream form and TbCDS pLEW100 + tetracycline	235
6.3	Negative survey scan of lipids from SM and bloodstream form TbCDS pLEW100 + tetracycline	238
6.4	Mass spectrometric analyses of choline-phosphate containing phospholipids from SM and bloodstream form TbCDS pLEW100 + tetracycline	240
6.5	Mass spectrometric analyses of inositol-phosphate containing phospholipids from SM and bloodstream form TbCDS pLEW100 + tetracycline	242
6.6	Mass spectrometric analyses of glycerol-phosphate containing phospholipids from SM and bloodstream form TbCDS pLEW100 + tetracycline	244
6.7	Subcellular localisation of TbCDS-HA in TbCDS conditional knockout bloodstream form <i>T. brucei</i>	247
6.8	Positive ion survey scan of lipids from DM and procyclic form TbCDS pLEW100 + tetracycline	250
6.9	Negative survey scan of lipids from DM and procyclic form TbCDS pLEW100 + tetracycline	252
6.10	Mass spectrometric analyses of choline-phosphate containing phospholipids from DM and procyclic form TbCDS pLEW100 + tetracycline	254
6.11	Mass spectrometric analyses of inositol-phosphate containing phospholipids from DM and procyclic form TbCDS pLEW100 + tetracycline	256
6.12	Mass spectrometric analyses of glycerol-phosphate containing phospholipids from DM and procyclic form TbCDS pLEW100 + tetracycline	258

6.13	High m/z negative survey scan of lipids from DM and procyclic form TbCDS pLEW100 + tetracycline	260
6.14	Subcellular localisation of TbCDS-HA in TbCDS single knockout, procyclic form <i>T. brucei</i>	263
7.1	Overexpression of TbPIS in BSF <i>T. brucei</i> causes a decrease in growth rate.	269
7.2	Positive ion survey scan of lipids in SM and bloodstream form TbPIS pLEW100 + tetracycline	272
7.3	Negative survey scan of lipids in SM and bloodstream form TbPIS pLEW100 + tetracycline	274
7.4	Mass spectrometric analyses of inositol-phosphate containing phospholipids in SM and bloodstream form TbPIS pLEW100 + tetracycline	276
7.5	Subcellular localisation of TbPIS-HA in bloodstream form <i>T. brucei</i>	278
7.6	TbPIS-HA protein expressed from TbPIS pLEW100 construct in procyclic form <i>T. brucei</i>	280
7.7	Positive ion survey scan of lipids from DM and procyclic form TbPIS pLEW100 + tetracycline	282
7.8	Negative survey scan of lipids from DM and procyclic form TbPIS pLEW100 + tetracycline	284
7.9	Daughter ion spectrum from A. 774 m/z [M-H] ⁻ ion, B. 751 m/z [M-H] ⁻ ion C. 963 m/z [M-H] ⁻ ion	285
7.10	Mass spectrometric analyses of choline-phosphate containing phospholipids from DM and procyclic form TbPIS pLEW100 + tetracycline	287
7.11	Mass spectrometric analyses of inositol-phosphate containing phospholipids from DM and procyclic form TbPIS pLEW100 + tetracycline	281
7.12	Daughter ion spectrum from A. 863 m/z [M-H] ⁻ ion. B. 910 m/z [M-H] ⁻ ion.	290
7.13	Subcellular localisation of TbPIS-HA in procyclic form <i>T. brucei</i>	292
8.1	Revised pathways for glycerophospholipid synthesis in bloodstream form <i>T. brucei</i>	299
8.2	Revised pathways for glycerophospholipid synthesis in BSF <i>T. brucei</i>	300

List of Tables

1.1	<i>T. brucei</i> genes predicted to encode PI kinases.	49
2.1	Primer sequences and PCR conditions for TbCDS and TbPIS	71-73
3.1.	Tetrad Dissection of MET15 his3leu2ura3 cds1::KanMX [pRS425-MET25 yeast CDS1].	117
3.2	Tetrad Dissection Strain of MET15 his3leu2ura3 cds1::KanMX [pRS425-MET25 TbCDS]	118

Candidate's declarations:

I, Alison Lilley, hereby certify that this thesis, which is approximately 77,700 words in length, has been written by me, that it is the record of work carried out by me and that it has not been submitted in any previous application for a higher degree.

I was admitted as a research student in September, 2008 and as a candidate for the degree of Doctor of Philosophy in September, 2009; the higher study for which this is a record was carried out in the University of St Andrews between 2008 and 2012.

Date signature of candidate

Supervisor's declaration:

I hereby certify that the candidate has fulfilled the conditions of the Resolution and Regulations appropriate for the degree of Doctor of Philosophy in the University of St Andrews and that the candidate is qualified to submit this thesis in application for that degree.

Datesignature of supervisor

Permission for electronic publication:

In submitting this thesis to the University of St Andrews I understand that I am giving permission for it to be made available for use in accordance with the regulations of the University Library for the time being in force, subject to any copyright vested in the work not being affected thereby. I also understand that the title and the abstract will be published, and that a copy of the work may be made and supplied to any bona fide library or research worker, that my thesis will be electronically accessible for personal or research use unless exempt by award of an embargo as requested below, and that the library has the right to migrate my thesis into new electronic forms as required to ensure continued access to the thesis. I have obtained any third-party copyright permissions that may be required in order to allow such access and migration, or have requested the appropriate embargo below.

The following is an agreed request by candidate and supervisor regarding the electronic publication of this thesis:

Embargo on both printed copy and electronic copy for the same fixed period of 2 years, on the ground that publication would preclude future publication.

Date signature of candidatesignature of supervisor

Acknowledgements

I am extremely grateful to my supervisor, Terry Smith, for his constant support and patience throughout my PhD, and particularly his help with ES-MS.

Thanks are also due to Prof. Mike Stark for provision of yeast strains and his invaluable help with yeast work.

I especially wish to thank the entire TKS group for helping a hopeless zoologist in, and out of the lab, as well as proofreading, banter and cake.

List of Abbreviations

5-FOA	5-fluoroorotic acid
AAG	Alkyl- acyl glycerol
ACS	Fatty acyl-CoA synthetase
BSA	Bovine serum albumin
CCT	CTP: phosphocholine cytidyltransferase
cDNA	Complimentary DNA
CDP-DAG	Cytidine diphosphate diacylglycerol
CDS	Cytidine diphosphate diacylglycerol synthase
CK	Choline kinase
cKO	Conditional knockout
CL	Cardiolipin
CoA	Coenzyme A
CPT	CDP- choline-phosphotransferase
CTP	Cytidine triphosphate
DAG	Diacylglycerol
DAGK	DAG kinase
dCTP	Deoxycytidine-5'-triphosphate
DeAc	GPI inositol deacylase
DHAP	dihydroxyacetonephosphate
DNA	Deoxyribonucleic acid
DTT	Dithiothreitol
ECL	Enhanced chemiluminescence
ECT	CTP: phosphoethanolamine cytidyltransferase
EDTA	Ethylenediaminetetraacetic acid
EK	Ethanolamine kinase
EPC	Ethanolaminephosphorylceramide
EPC	ethanolamine phosphorylceramide
EPT	ethanolamine phosphotransferase
ER	Endoplasmic Reticulum
ES-MS	Electrospray ionisation mass spectrometry
ES-MS/MS	Electrospray ionisation tandem mass

	spectrometry
G-3-P	Glycerol-3-phosphate
GAT1	Glycerol-3-phosphate acyltransferase
GAT2	1-acyl- <i>sn</i> -glycerol-3-phosphate acyltransferase
GlcNAc	Acetylglucosamine
GPI	Glycosylphosphatidylinositol
GT	GPI-GlcNAc transferase
HA	Haemagglutinin
HAT	Human African Trypanosomiasis
HP-TLC	High performance thin layer chromatography
HRP	Horseradish peroxidase
HYG	Hygromycin phosphotransferase
IAT	Inositol acyltransferase
IP ₃	Inositol-1,4,5-triphosphate
IPC	Inositol phosphorylceramide
IPC	Inositol phosphorylceramide
IPTG	Isopropyl-β-D-thiogalactopyranoside
kDA	Kilodalton
LB	Luria-Bertani medium
MAM	Mitochondria-associated membranes
mRNA	Messenger RNA
MT	Mannosyltransferase
ORF	Open reading frame
PAC	Puromycin acetyltransferase
PAP	Phosphatidic acid phosphatase
PBS	Phosphate buffered saline
PC	Phosphatidylcholine
PCR	Polymerase chain reaction
PE	Phosphatidylethanolamine
PEMT	Phosphatidylethanolamine methyltransferases
PG	Phosphatidylglycerol
PGP	Phosphatidylglycerophosphate
PGPS	Phosphatidylglycerolphosphate synthase

PI	Phosphatidylinositol
PIG-L	GlcNAc-PI de- <i>N</i> -acetylase
PIPs	Phosphorylated PI species
PIS	PI synthase
PLA ₁	Phospholipase A ₁
PS	Phosphatidylserine
PSD	Phosphatidylserine decarboxylase
PSS1	PS synthase-1
PSS2	PS synthase-2
RNA	Ribonucleic acid
RNAi	RNA interference
RT-PCR	Reverse transcription PCR
SC	Synthetic complete
SDS-PAGE	Sodium dodecyl sulfate polyacrylamide gel electrophoresis
SLS	Sphingolipid synthase
SMase	Sphingomyelinase
SpM	Sphingomyelin
SQDQ	Sulfoquinosyl diacylglycerol
TbCDS	<i>Trypanosoma brucei</i> cytidine diphosphate diacylglycerol synthase
TbELO	<i>Trypanosoma brucei</i> elongase
TbINO1	<i>Trypanosoma brucei</i> myo-inositol-3-phosphate synthase
Tris	Tris(hydroxymethyl)aminomethane
UAS _{INO}	Upstream activation sequence sensitive to inositol
UTR	Untranslated region
VSG	Variant surface glycoprotein
WHO	World Health Organisation

Chapter 1: Introduction

1.1 African Trypanosomiasis

African Trypanosomiasis is a fatal disease caused by the eukaryotic parasite *Trypanosoma brucei*. The disease occurs in 36 sub-Saharan African countries where it is transmitted by the bite of blood feeding tsetse flies. People exposed to the disease tend to be of poor, rural populations and therefore there is little financial incentive to produce drugs or treatments.

In 2009, following extensive control and monitoring efforts the World Health Organisation reported the number of cases had dropped below 10,000 for the first time in 50 years. In 2010 only 7,139 new cases were reported. However, data is difficult to collect and often underestimated due to the limited access of those at risk to health centres and diagnostics, and the estimated number of actual cases is currently 30,000 (Simarro et al., 2011).

Nevertheless, throughout the last century there have been a number of epidemics. War, poverty and population displacement are all key factors which lead to increased transmission and reappearance of the disease in areas where it had previously almost disappeared.

In addition to their importance to human health, *Trypanosoma* species are the causative agents of a wasting disease of cattle known as Nagana (a Zulu word meaning “to be depressed”), which reduces cattle production and is a major obstacle to economic development in affected areas (Van den Bossche and Delespaux, 2011).

1.1.1 The Human Disease

Human African Trypanosomiasis (HAT) or African sleeping sickness is caused by two subspecies: *Trypanosoma brucei gambiense* and *Trypanosoma brucei rhodesiense* (Figure 1.1) *T.b. gambiense* accounts for 95% of reported cases and is found in West and Central Africa. *T. b. rhodesiense* occurs in Eastern and Southern Africa and currently accounts for less than 5% of reported cases (Simarro et al., 2011).

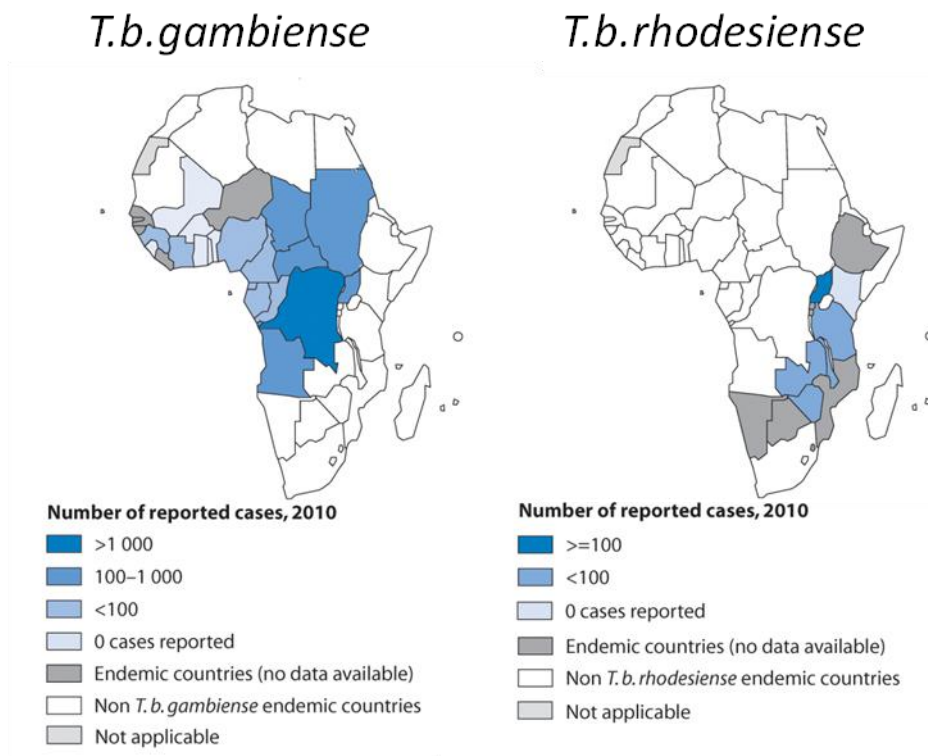


Figure 1.1. Distribution of Human African Trypanosomiasis species. *Trypanosoma brucei gambiense* (West African Sleeping Sickness) and *Trypanosoma brucei rhodesiense* (East African Sleeping Sickness) in 2010. Source: Simarro et al (2011)

HAT is a disease of two stages. The initial or acute stage occurs upon infection of the human host by *Trypanosoma brucei*. As the trypanosomes multiply in the bloodstream the infected person may experience fever, itching, joint pains and general malaise - symptoms which can be confused with many other diseases including influenza and malaria. In infections of *T. b. gambiense* the first stage of the disease may be virtually asymptomatic and can last for months or even years. In *T. b. rhodesiense* the symptoms are normally more violent and the acute disease is quicker to progress to the second stage (Barrett et al., 2003).

This second, neurological or chronic stage of the disease occurs when the trypanosomes cross the blood brain barrier and enter the cerebrospinal fluid. Symptoms of the second stage include disruption of sleeping patterns which give the disease its common name - sleeping sickness. Other symptoms include headaches, confusion, sensory disturbance and lack of coordination. If untreated, HAT will invariably lead to coma and death (Barrett et al., 2003).

1.1.2 Current HAT Treatments

There are currently no vaccines available against HAT, and production of a vaccine would be highly problematic due to antigenic variation of the major cell surface antigen of bloodstream form *T. brucei* Variant Surface Glycoprotein (VSG), discussed later. Due to the lack of financial incentive to create new drugs against the disease, available treatments are limited. Most of the drugs available have been in use for more than 60 years and have several drawbacks.

One of the key difficulties in treatment is that in order to treat the late stage of the disease, the drug must cross the blood brain barrier. Not only does this limit the range of usable molecules, but drugs that are able to cross the barrier often have severe unwanted side effects.

Pentamidine and suramin are currently used in the early stage of the disease against *T. b. gambiense* and *T. b. rhodesiense* respectively. Both these drugs have significant unwanted side effects, with hypotension and hypoglycaemia being the most commonly reported in pentamidine and a variety of severe effects such as anaphylactic shock, severe skin reactions, neurotoxicity and renal failure being associated with suramin.

The key treatment option against the second stage of the disease was previously melarsoprol, which has been in use since 1949. This drug is an arsenical and as a result has many side effects, the worst being encephalopathy which is responsible for fatalities in 3-10% of those treated (Kennedy, 2004). A more recent option, registered in 1990 is eflornithine. This molecule is considerably less toxic than melarsoprol but can still cause diarrhoea, convulsions and hallucinations (Kennedy, 2004). Moreover, it is expensive, only effective against *T.b. gambiense* and must be administered intravenously four times a day for two weeks, a regime which is difficult to apply in field hospitals and mobile units. Investigations are currently underway into an orally administered eflornithine, which would have clear advantages (Simarro et al., 2011).

The appearance of cases where treatment is ineffective suggests resistance is becoming a problem (recently reviewed in Barrett et al. (2011)). Given how long current drugs have been in use, coupled with factors leading to non-compliance with treatment regimes, such as civil unrest and inadequate resources, this is hardly

surprising. Some mechanisms of drug resistance have been elucidated, for example both pentamidine and melarsoprol are taken up the purine transporter P2, so loss or mutation of this transporter can mean that drug import into the cell is far lower. Drug resistance has also been linked to enhanced drug export, mediated by a multidrug resistance-associated protein called TbMRPA (reviewed by (Gehrig and Efferth, 2008)).

One way to decrease the emergence of drug resistance is by using existing drugs together in combination therapies. If these drugs are synergistic they may also allow reduction of dosage which could mitigate toxic effects. In April 2009, combination therapy using nifurtimox and eflornithine was added to the WHO Essential Medicines list for the treatment of late stage *T. b. gambiense* HAT (Simarro et al., 2011). Nifurtimox is a cheap, orally administered drug that is used to treat American trypanosomiasis (Chagas disease) but had previously been shown to have varying efficacy against HAT (Janssens and Demuyne, 1977, Moens et al., 1984, Pepin et al., 1992). This combination therapy treatment is significantly simpler than eflornithine alone (only 14 infusions over 7 days compared to 56 infusions over 14 days) and works out much cheaper, with less side effects for a similar efficacy (Yun et al., 2010). Unfortunately, this regime is still not effective against *T. b. rhodesiense*.

It is clear that the impact of African Trypanosomiasis to both human health and agriculture in regions where the disease is prevalent can be devastating. It is therefore imperative that drugs are developed which are safer, more effective, easier to administer, stable in the African environment and inexpensive.

1.2 *Trypanosoma brucei*

1.2.1 Taxonomy

The parasite which causes this devastating disease is the species *Trypanosoma brucei*. *T. brucei* are single celled eukaryotes which belong to the phylum Euglenozoa. Figure 1.2 shows taxonomy of the Euglenozoa based on molecular phylogenetic analyses. This group of flagellated, single celled organisms contains both free living and parasitic species. They branch early from the base of the eukaryotic phylogenetic tree suggesting they are an ancient group (Maslov et al.,

1999, Simpson et al., 2002, Simpson and Roger, 2004, Simpson et al., 2006, Moreira et al., 2004, Breglia et al., 2007).

The subgroup kinetoplastida are characterised by extensive mitochondrial DNA contained within a unique organelle, the kinetoplast. The kinetoplastida are further subdivided into three groups. The earliest branching of these groups is the prokinetoplastina which have only recently been defined on the basis of molecular phylogeny, in particular the spliced leader and single subunit RNA genes (Moreira et al., 2004, Breglia et al., 2007, Simpson and Roger, 2004, Simpson et al., 2006). The two known representatives are morphologically very different from each other and so it is difficult to define any phenotypic characteristics of this group.

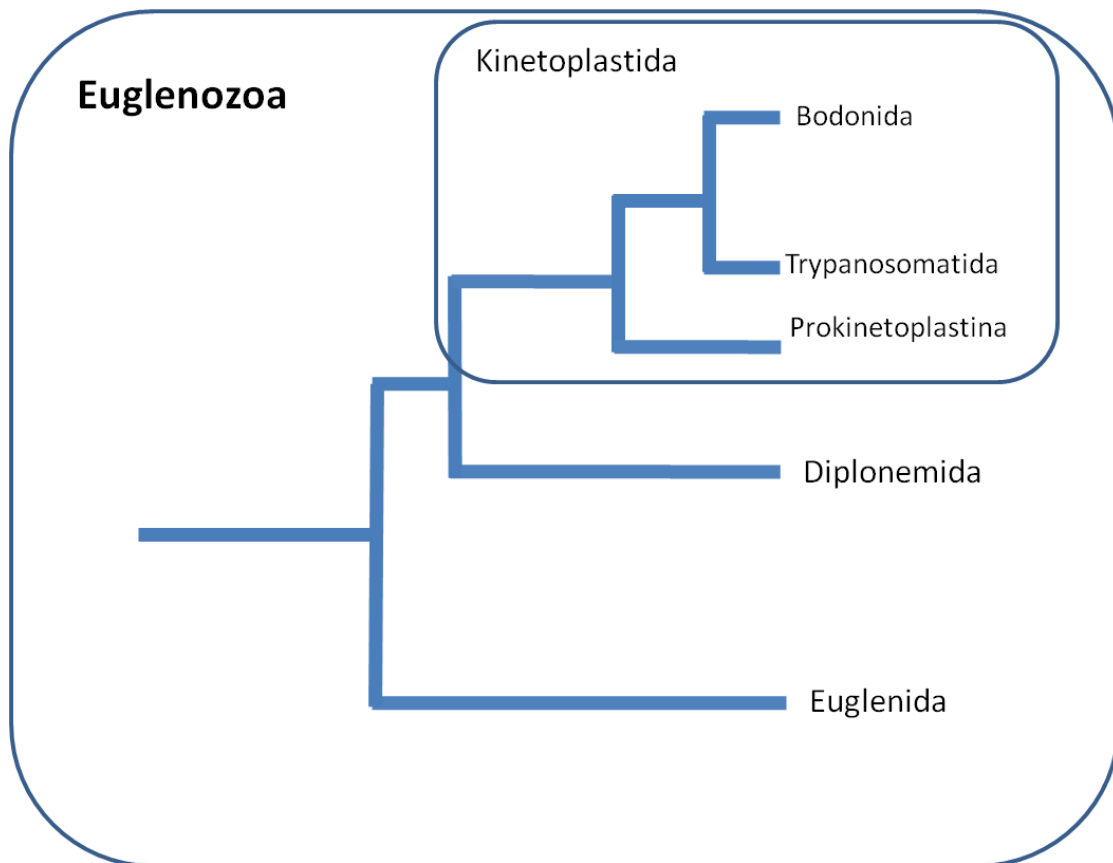


Figure 1.2 Taxonomic relationships in the Euglenozoa. Relationships within the *Euglenozoa* based on molecular phylogenetic analyses primarily of ribosomal RNA genes and nucleus-encoded protein genes (Maslov et al. 1999; Simpson et al., 2002, 2006; Simpson and Roger 2004; Moreira et al. 2004; Breglia et al. 2007). *Relationships within the kinetoplastida* - bodonids are biflagellate and a more diverse group than the uniflagellate trypanosomatids. Relationships from molecular data (Simpson et al, 2006.) The Prokinetoplastina are the earliest branch of the kinetoplastida, and have been defined only recently on the basis of molecular phylogeny, in particular the spliced leader and SSU RNA genes (Moreira et al., 2004; Simpson et al., 2006). The two known representatives are morphologically very different from each other. Reproduced from the Tree of Life Web Project, Pages Euglenozoa (Leander et al, 2008) and Kinetoplastida (Lukes, 2009)

The other two groups in the kinetoplastida can be defined by the number of flagella - the *Bodonida* contain two flagella, whereas the *Trypanosomatida* contain only one (Vickerman, 1974) and these groupings are also well supported by molecular evidence (Simpson et al., 2006). The *Trypanosomatida* contains many parasitic species in addition to *T. brucei*, such as *Trypanosoma cruzi* - the causative agent of Chagas disease, and various *Leishmania* species which cause a variety of diseases ranging from cutaneous ulcers to deadly visceral infections. Trypanosomatid parasites can have complex life cycles and a characteristic feature of trypanosomatids is their ability to change their morphology during their life cycle. However there are certain characteristic features of the cells such as a single flagellum supported by a prominent paraflagellar rod, a single, usually reticulated mitochondrion, glycosomes, and a corset of subpellicular microtubules. These characteristic features are all discussed below (Vickerman and Preston, 1976).

1.2.2 Cell Structure

In *Trypanosoma brucei*, the cell is long and slender, tapering at either end (Figure 1.3). The single flagellum is a long structure with two major components: a typical eukaryotic axoneme - a compact structure with an arrangement of nine pairs of microtubules around a central pair, which is the motor of the cell (Luck, 1984) - and the paraflagellar rod. The paraflagellar rod is unique to trypanosomatids, euglenids and dinoflagellates. It is composed of filamentous proteins and extends along the length of the flagellum, giving it support (Deflorin et al., 1994). The flagellum emerges from the basal body out of an invagination in the cell membrane called the flagellar pocket, which is the only place in the trypanosome where endocytosis and exocytosis take place (reviewed by Field and Carrington (2009)). This flagellum is attached along the length of the cell by a cytoskeletal membrane domain known as the flagellum attachment zone (Sherwin and Gull, 1989). Subpellicular microtubules run along the length of the cells forming a sturdy skeleton which is the major determinant of cell shape

T. brucei contain all the normal organelles of eukaryotic cells - nucleus, endoplasmic reticulum and Golgi apparatus. A single mitochondrion is present containing the kinetoplast, but the mitochondrial structure varies greatly between life cycle stages. The cell also contains membrane bound organelles containing glycolytic enzymes.

These organelles are known as glycosomes and are thought to be derived from peroxisomes (Parsons, 2004).

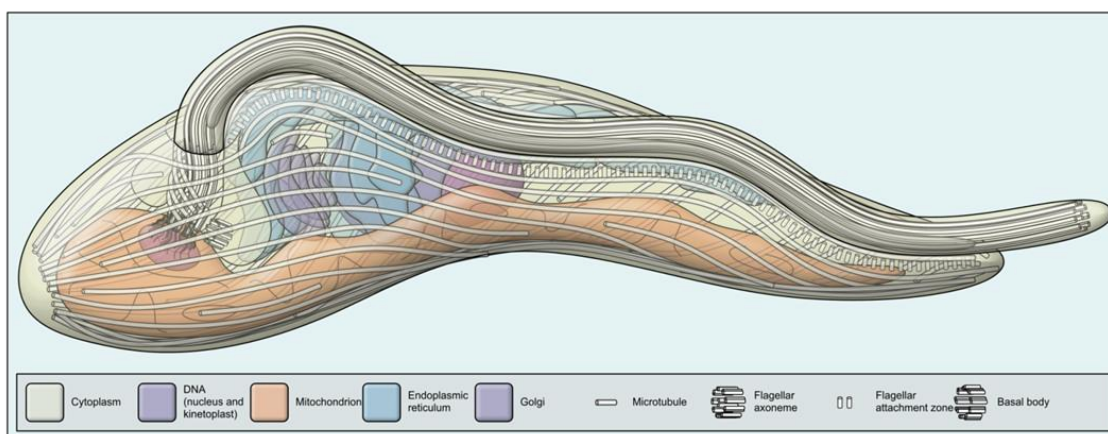


Figure 1.3 Cartoon of *Trypanosoma brucei* showing major structural features (not to scale). Image by Richard Wheeler (www.richardwheeler.net)

1.2.3 Life cycle

The life cycle of *T. brucei* is complex, and involves two hosts (Figure 1.4). Following the bite of an infected tsetse fly, pre-adapted, non-dividing metacyclic trypanosomes enter the lymphatic system via the skin (Figure 1.4, step 1). They pass into the bloodstream, where they transform into slender bloodstream trypomastigotes, with narrow tubular mitochondria (Figure 1.4 step 2). In the bloodstream, they make their energy through glycolysis of blood glucose. The trypomastigotes rapidly proliferate by binary fission, spreading throughout the blood and tissue fluids causing the first stage of the disease as described above (Figure 1.4, steps 3-4). Eventually, the cells penetrate the endothelium and choroid plexus and spread to the central nervous system, causing the second stage of the disease.

As parasitaemia increases, some slender bloodstream form trypomastigotes arrest cell division and differentiate into “stumpy” form trypomastigotes (Matthews, 2005). These stumpy forms have an enlarged mitochondrion with more cristae in comparison to the bloodstream forms, and if taken up by a tsetse fly are capable of establishing an infection in the fly’s midgut.

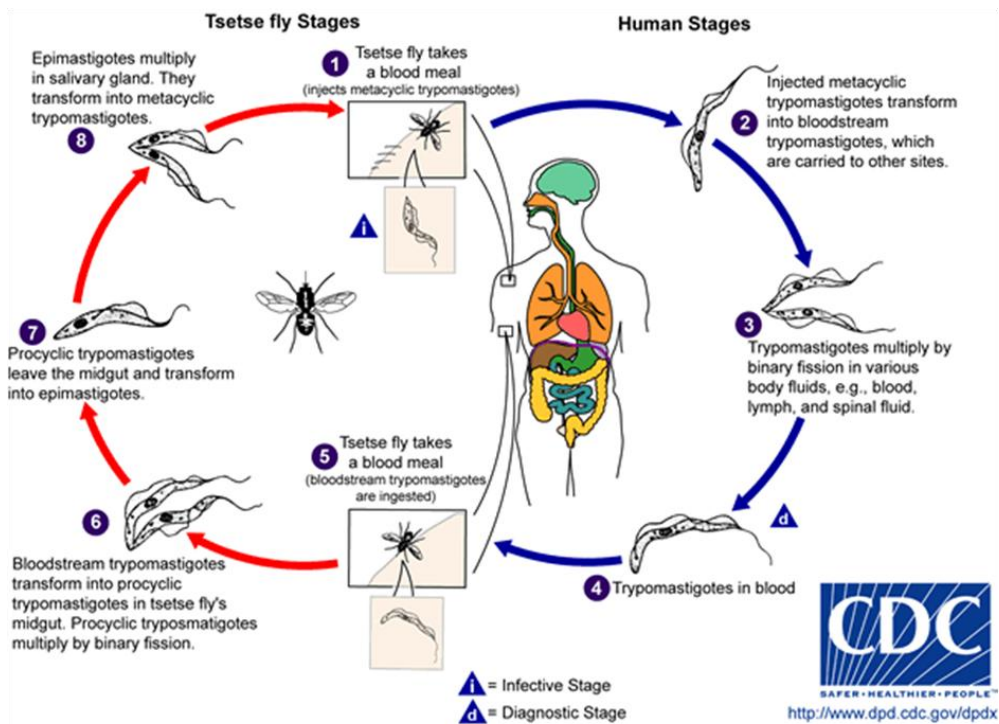


Figure 1.4 Life cycle of *Trypanosoma brucei* – schematic showing the life cycle stages. Source – Centre for Disease Control.

Stumpy trypomastigotes in the bloodstream are ingested by tsetse flies when they take a blood meal (Figure 1.4, step 5). Once in the fly's mid-gut, the bloodstream form trypomastigotes transform into procytic trypomastigotes containing an extensive, branched mitochondrion with discoid cristae (Figure 1.4, step 6) (Vickerman, 1985, Matthews, 2005). In the fly, the trypanosomes generate energy by amino acid oxidation. Procytics multiply in the tsetse fly mid-gut and then migrate to the salivary glands where they undergo asymmetric cell division to form long and short epimastigotes (Figure 1.4, step 7) (Van den Abbeele et al., 1999). The short epimastigotes attach to the salivary gland wall where they proliferate and are thought to undergo sexual exchange (Figure 1.4, step 8) (Gibson et al., 2006). Finally, the trypanosomes mature to metacyclic forms and detach from the salivary gland (Tetley et al., 1987). They are now infectious to mammals and are injected into the mammalian host when the tsetse takes a blood meal.

The complex life cycle of *T. brucei* means that it is able to adapt to a number of very different, often hostile, physiological environments. Whilst the ability of the parasite to adapt and survive is key to the problems it causes to human health and agriculture, it also makes it a very interesting organism from a scientific viewpoint.

1.2.4 *T. brucei* as a model organism

As an organism of scientific interest, *T. brucei* are fascinating not only because of their complex life cycle, but their phylogenetic history. Since they belong to an early diverging eukaryotic lineage they may provide insights into the ancestral eukaryotes and possibly into the evolution of parasitism. Indeed, *Trypanosoma* have many metabolic peculiarities including, but by no means limited to polycistronic transcription (reviewed by (Campbell et al., 2003) and lack of polymerase II transcriptional regulation (Gunzl et al., 2003). Moreover, several biological processes such as glycosylphosphatidyl inositol (GPI) anchoring, trans-splicing and antigenic variation were first elucidated in *T. brucei* meaning that the study of *T. brucei* has been far reaching in its contribution to the scientific field.

1.2.5 Variant Surface Glycoprotein and the Glycosylphosphatidyl Inositol Anchor

Of particular interest is the variable surface glycoprotein (VSG) coat which covers the bloodstream parasite (Figure 1.5, A). As previously mentioned, *T. brucei* experiences many different hostile environments throughout its life cycle, and all of these are extracellular. The bloodstream form parasites have the advantage of being bathed in a nutrient rich medium, but are highly visible to the host's immune system. The VSG coat protects the bloodstream form parasite not only physically from the alternative complement pathway but from specific immune responses which it is able to do by antigenic variation (Cross, 1996). The *T. brucei* genome, in addition to containing up to 200 genes for different VSG variants, contains a further 1600 silent genes meaning the potential for mosaic variation is staggering (Berriman et al., 2005, Marcello and Barry, 2007). However, under normal circumstances the parasite will only express one at a time (Vanderploeg et al., 1982). Whilst the majority of the population will express the same VSG, some will switch to a different variant. This means that when the host immune system produces an antibody against the first VSG species it will clear the majority of the population but those parasites expressing a different surface antigen will survive to perpetuate the infection. This pattern of parasite antigenic switching, immune system clearance and growth of a different population makes for the characteristic "waves of parasitaemia" (Figure 1.5, E.) that were first observed in the blood stream of infected cattle by Ross and Thompson in 1910.

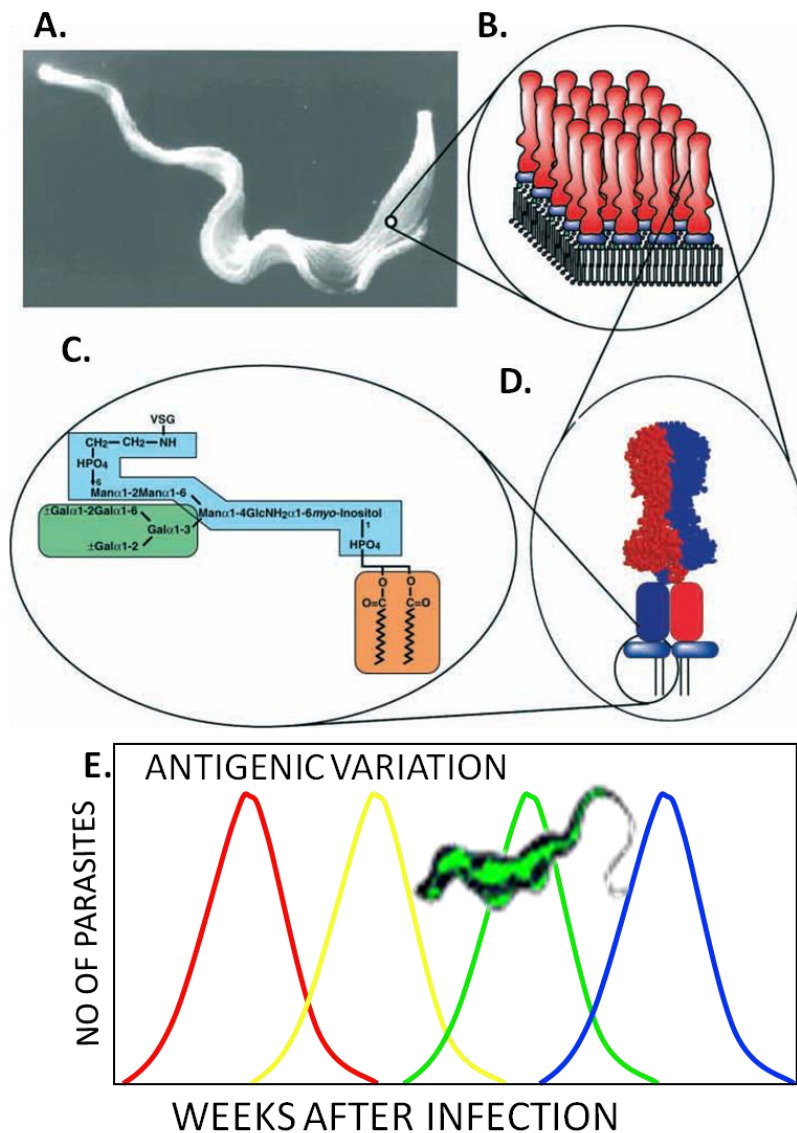


Figure 1.5. VSG and its GPI anchor in *T. brucei*. A. Scanning electron micrograph (courtesy of Michael Duszenko) of a bloodstream form of *T. brucei*. B. A cartoon model of a 20 nm x 20 nm section of the plasma membrane (Ferguson, 1997). C. Structure of a VSG dimer, based on the N-terminal crystal structure (Blum et al., 1993) D. the primary structure of the GPI anchor (Ferguson et al., 1988). The section of the GPI anchor structure shown in blue is conserved throughout the eukaryotes. The galactose side-chain (shown in green) and the fatty acids of the PI moiety, which are both myristate (shown in pink), are unique to VSGs. Image from Ferguson, 1999. E . Graph indicating the waves of parasitaemia that occur after weeks of infection due to the changing VSG coats. Each colour represents a different coat. (A-D from Ferguson, 1999, E. – courtesy of Terry Smith.)

The 5×10^6 VSG dimers are held in the outer leaflet plasma membrane of the parasite by glycosylphosphatidyl inositol (GPI) anchors. Trypanosome research has been at the forefront of research into GPI anchors, where their structure,

biosynthesis and function has been extensively studied (reviewed by Ferguson (1999) and their biosynthesis will be outlined later. Whilst GPI research in trypanosomes has contributed much to the general field, GPI biosynthesis in *T. brucei* has been shown to differ in several respects to that of mammals and has been validated both genetically (Nagamune et al., 2000) and chemically (Smith et al., 2004) as a drug target. It has also opened the door for further research into *T. brucei* lipid metabolism, and, most importantly, the possibilities it may present for drug development.

1.3 Lipid Metabolism in *T. brucei*

1.3.1 Uptake of Components from Host for Lipid Biosynthesis in *T. brucei*

Trypanosomes can acquire some lipids from their host by uptake of protein bound fatty acids and *lyso*-phospholipids or by receptor mediated endocytosis of lipoprotein particles that also contain cholesterol (Dixon et al., 1971, Samad et al., 1988, Coppens et al., 1988, Bowes et al., 1993, Coppens and Courtoy, 1995). Choline, ethanolamine and *myo*-inositol are important precursors to glycerophospholipids and spingolipids. Surprisingly, *T. brucei* bloodstream form are unable to uptake choline (experimentally verified with radio and stable isotope labelled choline, T.K. Smith, unpublished observations), and instead must take up choline containing lipids phosphatidylcholine (PC), *lyso*-PC and sphingomyelin (SpM), many of which will be endocytosed as components of low density lipoprotein particles in order to obtain this headgroup (Bowes et al., 1993, Rifkin et al., 1995, Overath and Engstler, 2004). Ethanolamine, serine and *myo*-inositol are efficiently taken up by both bloodstream form and procyclic form. However, transporters for ethanolamine and serine have not been identified in *T. brucei*, whereas a *myo*-inositol transporter has been identified in the procyclic form (Gonzalez-Salgado et al., 2012).

1.3.2 Fatty Acid Synthesis

For a long time it was thought that *T. brucei* could not synthesise fatty acids *de novo*. This was mostly based on an early experiment where fatty acids in the parasite could not be labelled by [¹⁴C]acetate (Dixon et al., 1971). However, it became clear that there must be some form of *de novo* fatty acid synthesis due to the requirement

of myristate for GPI remodelling. In bloodstream form *T. brucei*, GPI anchors exclusively contain two molecules of myristate fatty acids, but myristate is present at very low levels in the mammalian bloodstream (Ferguson and Cross, 1984). It seemed, therefore, that in addition to scavenging fatty acids from the host, *T. brucei* must possess a unique system for *de novo* fatty acid synthesis (reviewed in Lee et al. (2007)).

It was initially thought that *de novo* synthesis of myristate occurred via a mitochondrial type II prokaryotic-like synthase which makes predominantly C8, but also longer fatty acids up to C16 (Morita et al., 2000, Paul et al., 2001), but it was discovered that this synthesis is not sufficient for the GPI requirement (Lee et al., 2006).

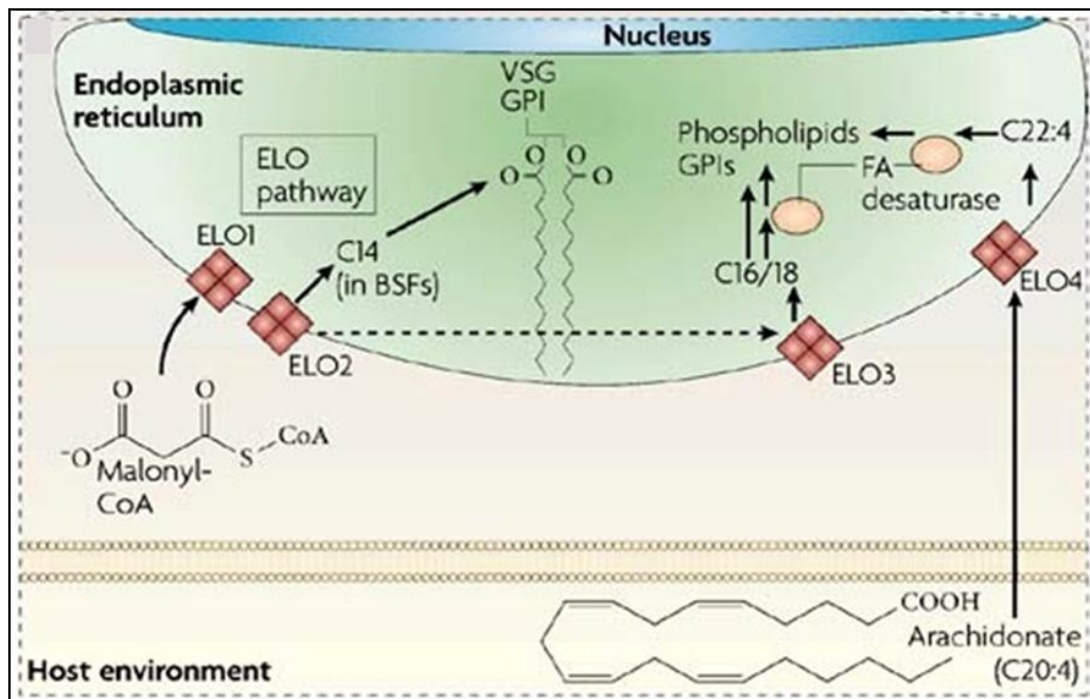


Figure 1.6. *De novo* fatty acid synthesis in *T. brucei* by four microsomal elongases. Elongase – 1 (ELO 1) and elongase 2 (ELO 2) use malonyl-CoA to elongate a butyryl-CoA primer to myristate (C14). Myristate can be incorporated into the variant surface glycoprotein (VSG) GPI anchor (in the bloodstream form) or it can be elongated by elongase 3 (ELO 3) to make C16 and C18. Longer fatty are used directly in GPIs and phospholipids, or modified by fatty acid desaturases before their incorporation into phospholipids. ELO4 elongates arachidonate (C20:4 from extracellular sources) to C22:4, which can be elongated and desaturated further. Arachidonate and other polyunsaturated fatty acids are incorporated into phospholipids. Image from Lee et al, 2007.

In fact, *T. brucei* uses a family of 4 microsomal elongases (TbELO1-4) for the majority of its *de novo* fatty acid synthesis (Figure 1.6)(Lee et al., 2006). In other organisms, elongase pathways are used primarily for the elongation of long chain fatty acids, but what is unique about the *T. brucei* system is that it is primed by short chain acetyl-coA meaning it is an effective method of *de novo* fatty acid synthesis. TbELO1 elongates C4 to C10, TbELO2 elongates C10 to C14 and TbELO3 elongates C14 to C18, although there is some overlap in specificity in these elongases. In bloodstream forms, down-regulation of TbELO3 (which converts C14 to C18) explains the high production of myristate required for GPI anchors (Lee et al., 2006). TbELO4 is specific for polyunsaturated fatty acids and is known to extend arachidonate (C20:4), acquired from the host, by two carbons (Lee et al., 2007). Polyunsaturated fatty acids can be desaturated further by a plant-like fatty acid desaturase to make long, unsaturated fatty acids such as C22:5 and C22:6 (Tripodi et al., 2006). Both the mitochondrial type II fatty acid synthase (Stephens et al., 2007) and the microsomal elongases (Lee et al., 2006) are essential to *T. brucei*. The failure of the labelling experiment by Dixon and colleagues (1971) was because, surprisingly, *T. brucei* do not take up acetate (Morita et al., 2000).

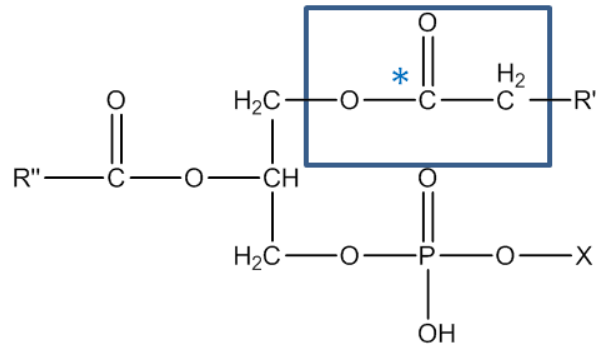
Before incorporation into glycerophospholipids, fatty acids must undergo activation to CoA derivatives. This is usually accomplished by a family of enzymes called fatty acyl-CoA synthetases. Currently, five of eight of these potential acyl-CoA synthetases have been characterised in *T. brucei* (Smith and Buetikofer, 2010).

1.3.3 Glycerophospholipids

Glycerophospholipids are the major components of cell membranes and are a fascinating class of molecules, not only because of their role in the stability of membranes and membrane proteins but in their role as second messengers in cell signalling. These molecules contain a glycerol backbone which is linked to a polar headgroup by a phosphodiester bond, and two hydrophobic carbon chains linked to position *sn*-1 and *sn*-2 and can either be acyl chains, linked via ester bonds or alkyl and alkenyl chains linked by ether bonds (Figure 1.7). Certain individual classes of phospholipids and their properties will be discussed later.

Trypanosomes contain all the major phospholipid classes present in mammalian cells (Figure 1.8). They do not use intact phospholipids gained from their host organism, but *de novo* synthesise their own specific species as will be discussed below (Patnaik

et al., 1993, Dixon and Williams, 1970). Only a few phospholipid biosynthetic genes of *T. brucei* have been studied (reviewed in Smith and Buetikofer (2010)) but the completion of its genome has allowed identification of putative homologues of many genes necessary for *de novo* phospholipid biosynthesis. As phospholipid synthesis is elucidated in *T. brucei*, differences are emerging between them and their mammalian host which could lead to novel targets for therapeutics.



Glycerophospholipid (diacyl)

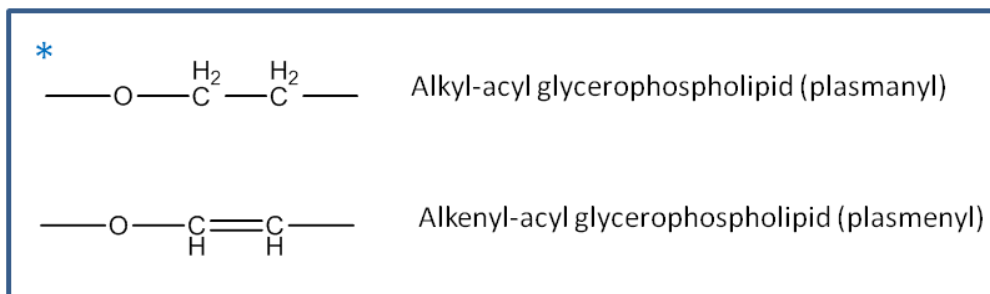


Figure 1.7. Structure of a glycerophospholipid. X = headgroup, r' and r'' = lipid chains which can be attached to the glycerol by acyl, alkyl or alkenyl links.

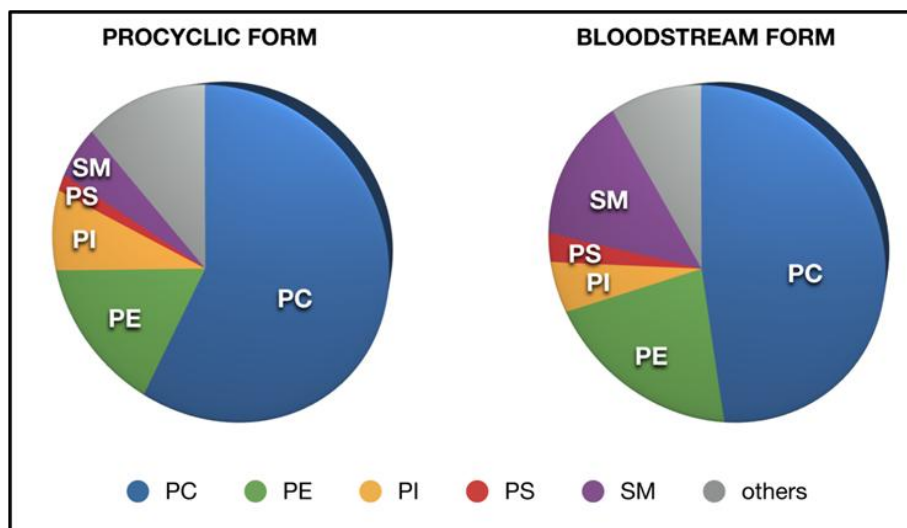


Figure 1.8. Phospholipid composition in *T. brucei*. Relative distribution of the phospholipid classes phosphatidylcholine (PC), phosphatidylethanolamine (PE), phosphatidylinositol (PI), phosphatidylserine (PS) and sphingomyelin (SM) in *T. brucei* procyclic and bloodstream forms. Others include inositolphosphorylceramide (IPC), ethanolamine phosphorylceramide (EPC), cardiolipin (CL), phosphatidylglycerol (PG), phosphatidylinositol phosphates (PIPs), phosphatidic acid (PA), lyso – phospholipids, phosphorylated prenyls, dolichol phosphates (Dol-Ps). Image from Smith & Butikofer, 2010.

1.3.4 Glycerophospholipid Biosynthesis Overview

1.3.4.a Synthesis of PA, CDP-DAG and Kennedy Pathways

Figure 1.9, box A shows the first steps of phospholipid biosynthesis in all organisms - two successive acylations of glycerol-3-phosphate by glycerol-3-phosphate acyltransferase and 1-acyl-*sn*-glycerol-3-phosphate acyltransferase to produce phosphatidic acid (PA) (Moore, 1982, Carman and Henry, 1989, Kent, 1995). Additionally, in the case of ether lipids (Figure 1.9, box B) dihydroxyacetonephosphate (DHAP) is converted to 1-alkyl-2-acyl-G-3-P in 4 steps by the enzymes acyl-coA:dihydroxyacetonephosphate acyltransferase, 1-alkyl-dihydroxyacetonephosphate synthase and alkyldihydroxyacetonephosphate oxidoreductase. The following steps of phospholipid synthesis differ depending on the organism.

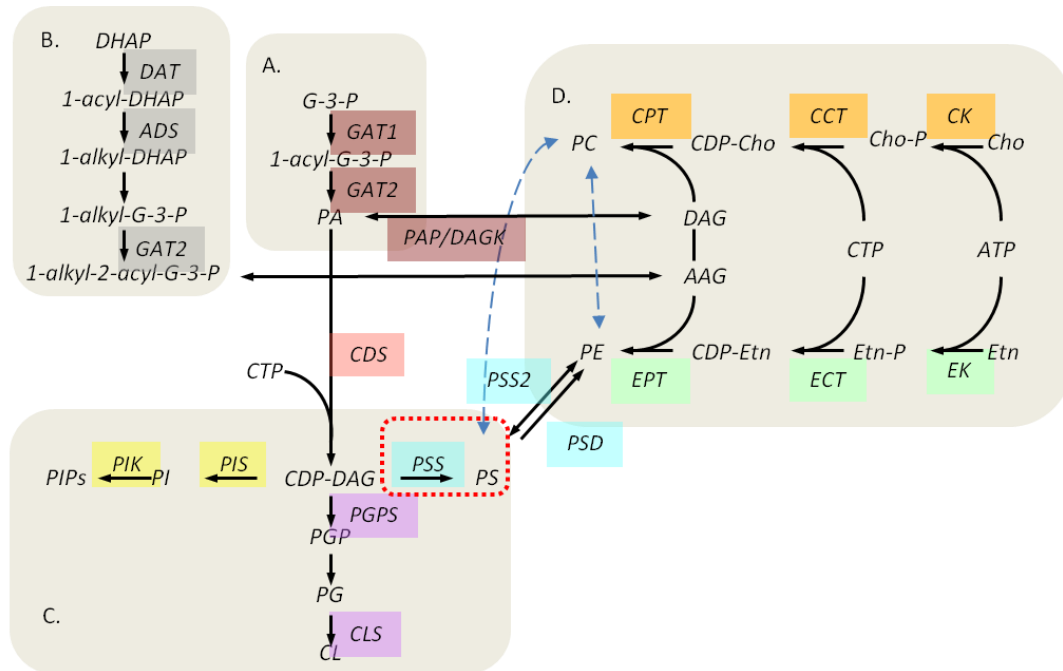


Figure 1.9. Predicted pathways for glycerophospholipid synthesis in *T. brucei*. Enzymes for which candidate genes have been identified are indicated. Red dashed box – PS synthesis from CDP-DAG not present in higher eukaryotes. Dashed blue arrows indicate head group exchange pathways present in other organisms, but not in *T. brucei*. **Metabolite abbreviations:** DHAP – dihydroxyacetonephosphate, G-3-P – glycerol-3-phosphate, PA – phosphatidic acid; CDP-DAG – cytidine diphosphate diacylglycerol; PGP – phosphatidylglycerophosphate; PG – phosphatidylglycerol, CL – cardiolipin, PS- phosphatidylserine, PE – phosphatidylethanolamine; PI – phosphatidylinositol; PIPs – phosphorylated derivatives of phosphatidyl inositol; DAG – diacylglycerol; AAG – alkylacylglycerol, TAG – triacylglycerol, Etn – ethanolamine; P-Etn – ethanolamine phosphate; CDP-Etn – cytidine diphosphate-ethanolamine; PE – phosphatidylethanolamine; Cho – choline; P-Cho – choline phosphate; CDP-cho – cytidine diphosphate choline. **Enzyme abbreviations:** DAT – dihydroxyacetonephosphate acyltransferase, ADS – 1- alkyl-dihydroxyacetonephosphate synthase, GAT1 – glycerol-3-phosphate acyltransferase GAT2 – 1-acyl-*sn*-glycerol-3-phosphate acyltransferase, CDS – cytidine diphosphate diacylglycerol synthase, PGPS – phosphatidylglycerolphosphate synthase, CLS – cardiolipin synthase, PIS phosphatidylinositol synthase, PIK - phosphatidylinositol kinase, PSS – phosphatidylserine synthase, PSS2 – phosphatidylserine synthase, PSD – phosphatidylserine decarboxylase, EK – ethanolamine kinase, ECT – ethanolamine-phosphate cytidyltransferase, EPT – ethanolamine phosphotransferase, CK – choline kinase, CCT – choline-phosphate cytidyltransferase, CPT – choline phosphotransferase, PAP – phosphatidic acid phosphatase, DAGK – DAG kinase. Adapted from Smith & Butikofer, 2010.

In bacteria, phosphatidic acid (PA) is converted to cytidine diphosphate diacylglycerol (CDP-DAG) via the enzyme CDP-DAG synthase (CDS). CDP-DAG is the precursor to phosphatidylglycerol (PG) and phosphatidylserine (PS) which in turn are precursors to cardiolipin (CL) and phosphatidylethanolamine (PE), respectively (Dowhan, 1997). In eukaryotes, including *T. brucei*, PA is partitioned between CDP-DAG and diacylglycerol (DAG)(Figure 1.9). CDP-DAG gives rise to phosphatidylinositol (PI - absent in most prokaryotes) and its phosphorylated derivatives (PIPs); phosphatidylglycerol (PG) and CL; and in some organisms phosphatidylserine (PS) (Figure 1.9, box C). DAG gives rise to PC (also absent in most prokaryotes) and phosphatidylethanolamine (PE) via CDP-choline or CDP ethanolamine respectively (Figure 1.9, box D) - the pathway from DAG to PE and PC is known as the Kennedy pathway.

1.3.4.b Synthesis of PG and CL

PG is synthesised from CDP-DAG in two steps (shown in Figure 1.9, box C). In the first step phosphatidylglycerophosphate (PGP) is produced via a phospholipid phosphodiester synthase (PGPS) (Lykidis, 2007) of which there is a eukaryotic-like homologue in *T. brucei*. PGP is then hydrolysed to produce PG.

CL can be formed from PG in two different ways: in prokaryotes it is formed using two molecules of PG and a phospholipase D-like CL synthase (CLS). In most eukaryotes, however, CL is formed from a CDP-DAG and a PG molecule using a CDP-alcohol dependent CL synthase (Figure 1.9, box C). In *T. brucei* there does not appear to be any homologue of the eukaryotic type CL synthase, but a homologue of the prokaryotic CL synthase has been characterised and localised to the mitochondrion in the procyclic form, which uses two molecules of PG for CL synthesis (Serricchio and Buetikofer, 2012).

1.3.4.c Synthesis of Phosphatidylserine

In higher eukaryotes, for example mammals, phosphatidylserine is not produced directly from CDP-DAG, but is instead synthesised by base head-group exchange from other phospholipids (Kent, 1995). These exchange reactions are mediated by two serine-exchange enzymes, PS synthase-1 (PSS1) and PS synthase-2 (PSS2) which have specificities for phosphatidylcholine and phosphatidylethanolamine, respectively. Plants contain both pathways for PS synthesis - by headgroup exchange or from CDP-DAG (reviewed in Vance and Steenbergen (2005). Not much is known about the

method for biosynthesis of PS in *T. brucei*, but it has been suggested that *T. brucei* can synthesise PS from base head-group exchange (Rifkin et al., 1995, Signorell et al., 2008) and a putative PSS-2 has been identified in the *T. brucei* genome (Figure 1.9). In procyclic form *T. brucei*, [³H]serine labelling of PS was massively reduced when expression of a terminal enzyme of ethanolamine branch of the Kennedy pathway - diacylglycerol: ethanolamine phosphotransferase (EPT) - was knocked down, suggesting that PS can only be synthesised from headgroup exchange with PE (Signorell et al., 2008) and that unlike *Plasmodium* and yeast it has not retained the prokaryotic system for PS synthesis via CDP-DAG. However in the bloodstream form, conditional knockout of a preceding enzyme in the ethanolamine branch of the Kennedy pathway - ethanolamine-phosphate cytidyltransferase (ECT) - did not sufficiently alter the incorporation of [³H]serine into PS (Gibellini et al., 2009). These differing results suggest that synthesis of PS in the two cell types may be different, but further work and direct comparison between the two cell types is required to fully understand what is going on.

1.3.4.d Synthesis of Phosphatidylethanolamine

Figure 1.9, box D shows both the ethanolamine and the choline branch of the Kennedy pathway. The ethanolamine branch of the Kennedy pathway starts with the phosphorylation of ethanolamine by ethanolamine kinase (EK) followed by activation of this ethanolamine-phosphate with CTP by the enzyme ethanolamine-phosphate cytidyltransferase (ECT) to make CDP-ethanolamine. Both EK and ECT enzymes are found in the cytosol. Finally, ethanolamine phosphotransferase (EPT), a membrane bound protein of the ER, transfers the activated headgroup to diacylglycerol.

In most eukaryotes, in addition to its synthesis via the Kennedy pathway, PE can be made from CDP-DAG via PS through successive decarboxylation by prokaryotic/mitochondrial PS decarboxylase I or endoplasmic reticulum (ER) localised PS decarboxylase 2 (reviewed in Schuiki and Daum (2009)). In mammalian cells, the relative contributions of the Kennedy pathway or PS decarboxylation to PE formation is cell-type dependent (Vance, 2008).

In *T. brucei* a PS decarboxylase I has been identified and is expressed. The recombinant protein expressed in *E. coli* is active, and preliminary results indicate it is essential in the bloodstream form parasite (T.K Smith, unpublished observations). Radiolabelling experiments in both bloodstream form and procyclic form *T. brucei*

appear to show [³H]serine can be incorporated into PE (Menon et al., 1993, Rifkin et al., 1995, Signorell et al., 2008); but it is thought that, at least in the procyclic form, this is due to base headgroup exchange of the [³H]serine with existing PS followed by decarboxylation of [³H]PS to [³H]PE and therefore net synthesis of PE via PS is not occurring (Signorell et al., 2008). This is supported by the fact that PS decarboxylation is unable to compensate for the loss of *de novo* synthesised PE in bloodstream form (Gibellini et al., 2009) or procyclic form (Signorell et al., 2008) cells.

However, PS decarboxylation to PE was not observed at all during stable isotope labelling of bloodstream form with d₃-serine (Gibellini et al., 2009), whilst the d₃-serine was readily incorporated into d₃-PS. Whether these results show true differences in cell type or are due to differences in experimental method is unclear. However, combined with the differences seen in PS synthesis between bloodstream form and procyclic form *T. brucei* (Gibellini et al., 2009, Signorell et al., 2008) it would seem to indicate that PS metabolism is different in the two cell types.

1.3.4.e Synthesis of Phosphatidylcholine

The CDP choline branch of the Kennedy pathway is very similar to that of the ethanolamine branch (Figure 1.9, box D). Choline is phosphorylated and activated in the cytoplasm via choline kinase (CK) and choline-phosphate cytidyltransferase (CCT) respectively. In the ER, CDP-choline is converted to phosphatidylcholine by cholinephosphotransferase (CPT).

In some organisms PC can be made by three consecutive methylations of PE by S-adenosyl-L-methionine methyltransferases (PEMT) (Pessi et al., 2004, Palavalli et al., 2006, Nuccio et al., 2000). In yeast this is the most important route for PC and PE synthesis when ethanolamine and choline are not present in the medium, with the Kennedy pathway being more important when there is a problem in the CDP-DAG pathway (Carman and Henry, 1989, Carman and Henry, 1999, Carman and Han, 2011). *T. brucei*, however, is unable convert PE to PC, and it does not contain homologues for any methyltransferase (Rifkin et al., 1995). This has been confirmed by stable isotope labelling with d₄-ethanolamine followed by analysis of PE and PC by ES-MS/MS (Richmond et al., 2010). The genome of *T. cruzi* also appears to be lacking any PE N-methyltransferase whilst *Leishmania* species genomes do contain methyltransferases and their function has been experimentally confirmed (T.K.

Smith, unpublished observation). *Plasmodium falciparum* appear to have an alternative, plant like N-methyl transferase genes (Pessi et al., 2004).

1.3.4.f GPI anchor Biosynthesis

As previously discussed, a key area of *T. brucei* lipid research - and one which has contributed much to the general scientific field - has been the structure, function and biosynthesis of GPI anchors. In bloodstream form *T. brucei*, these molecules are essential due to their function in anchoring the protective VSG coat (Figure 1.5) and the biosynthesis of GPI anchors in this cell type has been studied extensively. The core of the GPI anchor is the glycerophospholipid PI, which is synthesised from *myo*-inositol and CDP-DAG by the enzyme PI synthase (as above, and shown in Figure 1.9). PI made from *de novo* synthesised *myo*-inositol is almost exclusively used for GPI anchor synthesis (Martin and Smith, 2006a). The biosynthesis of GPI anchors has been mostly elucidated using a cell free assay for their synthesis with synthetic or radiolabelled substrates (Masterson et al., 1989, Masterson, 1990, Menon et al., 1990a, Menon et al., 1990b, Guther and Ferguson, 1995). A review of GPI anchor biosynthesis is given by Ferguson (1999). The pathways for GPI anchor biosynthesis in *T. brucei* are shown in Figure 1.10. The first step of GPI synthesis in all organisms is the transfer of GlcNAc (acetylglucosamine) from UDP-GlcNAc to PI by a GPI-GlcNAc transferase (GT). The GlcNAc-PI is then de-*N*-acetylated by GlcNAc-PI de-*N*-acetylase (PIG-L) to form GlcN-PI (Doering et al., 1989, Milne et al., 1994, Watanabe et al., 2000). GlcN-PI then is then mannosylated three times by mannosyltransferases. The first mannosylation, catalysed by α -1-4-mannosyltransferase (MT-I) is unusual in trypanosomes because, unlike in most other eukaryotes, it occurs before the acylation of PI which is catalysed by an inositol acyltransferase (IAT). The other two mannosylations are carried out by α -1-6-Mannosyltransferase (MT-II) and α -1-2-mannosyltransferase (MT-III). After the action of all three mannosyltransferases and inositol acyltransferase, ethanolamine phosphate produced by the Kennedy pathway (above and Figure 1.9) is transferred to Man₃-GlcN-(acyl)PI to form Etn-P-Man₃-GlcN-(acyl)PI. In bloodstream form, this GPI precursor is then deacylated by GPI inositol deacylase (DeAc) and its fatty acid chains are remodelled by replacing both with myristate giving mature GPI - Etn-P-Man₃-GlcN-(dimyristoyl-) PI (Masterson et al., 1990). In procyclic form, the acyl-PI component of Etn-P-Man₃GlcN-acyl-PI is acted upon by a phospholipase to form Etn-P-Man₃GlcN-(2-*O*-acyl-lyso-) PI. In the bloodstream form, the mature GPI is then attached to VSG protein by a GPI

transamidase complex (Nagamune et al., 2003) before further processing and exocytosis to the cell surface via endosomes.

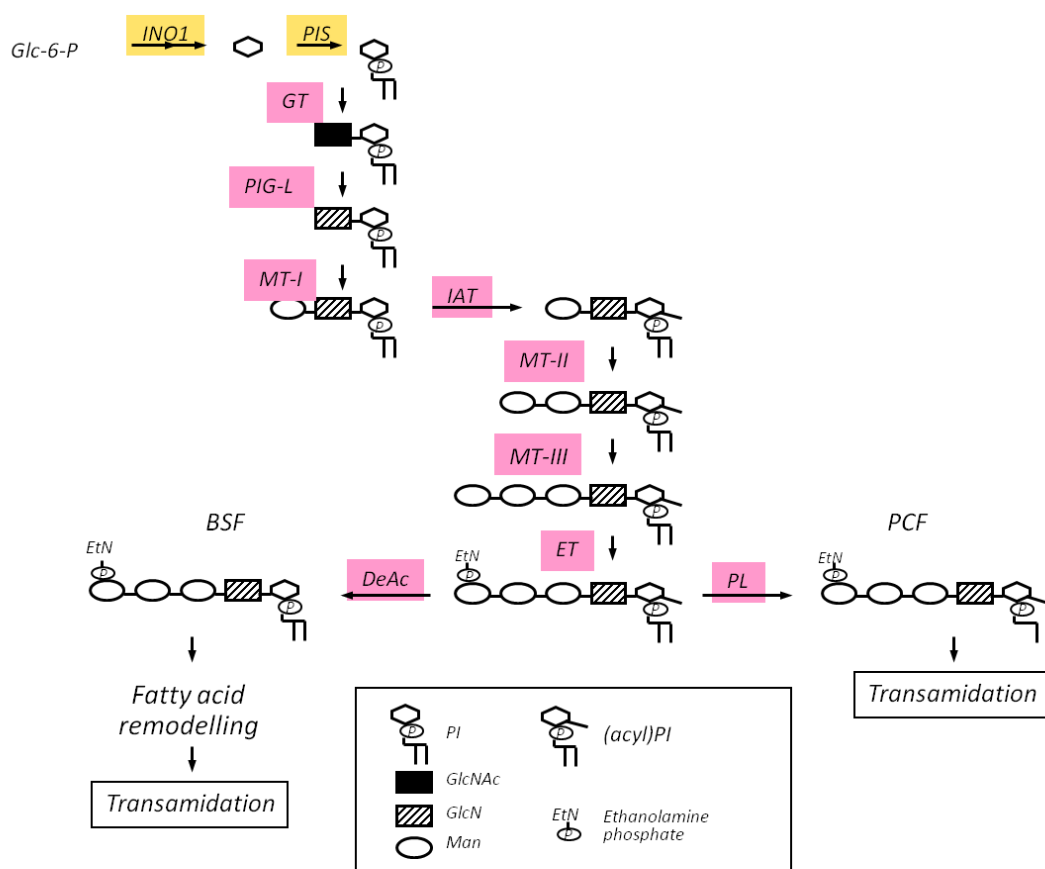


Figure 1.10. Pathways for GPI biosynthesis in *T. brucei*. **Glc-6-P** = glucose-6-phosphate, **PI** = phosphatidylinositol, **GlcNAc** = N-acetylglucosamine, **GlcN** = glucosamine, **Man** = Mannose, **BSF** – bloodstream form, **PCF** – procyclic form. Enzyme abbreviations and GeneDB accession numbers, where known, are as follows: **INO1** – Inositol-3-phosphate synthase (Tb927.10.7110); **PIS** - phosphatidylinositol synthase (Tb09.160.0530); **GT** – GPI-GlcNAc transferase (Tb927.2.1780, Tb927.3.4570, Tb927.10.16140); **PIG-L** – GlcNAc-PI-de-N-acetylase (Tb11.01.3900); **MT-1** – α -1-4-Mannosyltransferase (Tb927.6.3300); **IAT** – Inositol acyltransferase; **MT-II** – α -1-6-Mannosyltransferase (Tb927.10.13160); **MT-III** – α -1-2-Mannosyltransferase (Tb927.10.5560); **ET** – Ethanolamine-phosphate transferase (Tb.11.02.2720, Tb927.10.13290); **DeAc** – GPI inositol deacylase (Tb927.3.2610); **PL** – phospholipases. Image from Smith and Butikofer (2010).

1.3.5 Products of the CDP-DAG Pathway

This study will focus on the formation of CDP-DAG, and the CDP-DAG pathway in glycerophospholipid synthesis. In order to assess its importance to *T. brucei*, and whether it will present suitable drug targets it is pertinent to consider the properties of the phospholipid products of the CDP-DAG pathway, and their possible functions in the parasite.

1.3.5.a CDP-DAG

Cytidine diphosphate diacylglycerol (CDP-DAG) (Figure 1.11, box A) is a liponucleotide containing a cytidine headgroup. The actual pool of CDP-DAG at any time in a cell is vanishingly small, as the turnover rate is so rapid. Whilst it is not thought to have many specific functions, it is an activated lipid intermediate and a key precursor to several important phospholipids (Figure 1.9, box C, and discussed below). It is also an important molecule in the phosphoinositide cycle where alterations in its synthesis have been shown to affect the signal transduction pathway in *Drosophila* vision (Wu et al., 1995) and the cytokine signalling response in endothelial cells (Weeks et al., 1997). Additionally it is a direct inhibitor of neuroblastoma cell phosphatidylinositol-3-kinase (Lavie and Agranoff, 1996). Surprisingly, it has recently been shown that a wide range of antidepressants of diverse chemical and pharmacological classes strongly increase the production of CDP-DAG in the mammalian brain, which may help to replenish or supplement the pool of available phosphatidylinositols for phosphoinositide-related signalling (Tyeryar et al., 2008).

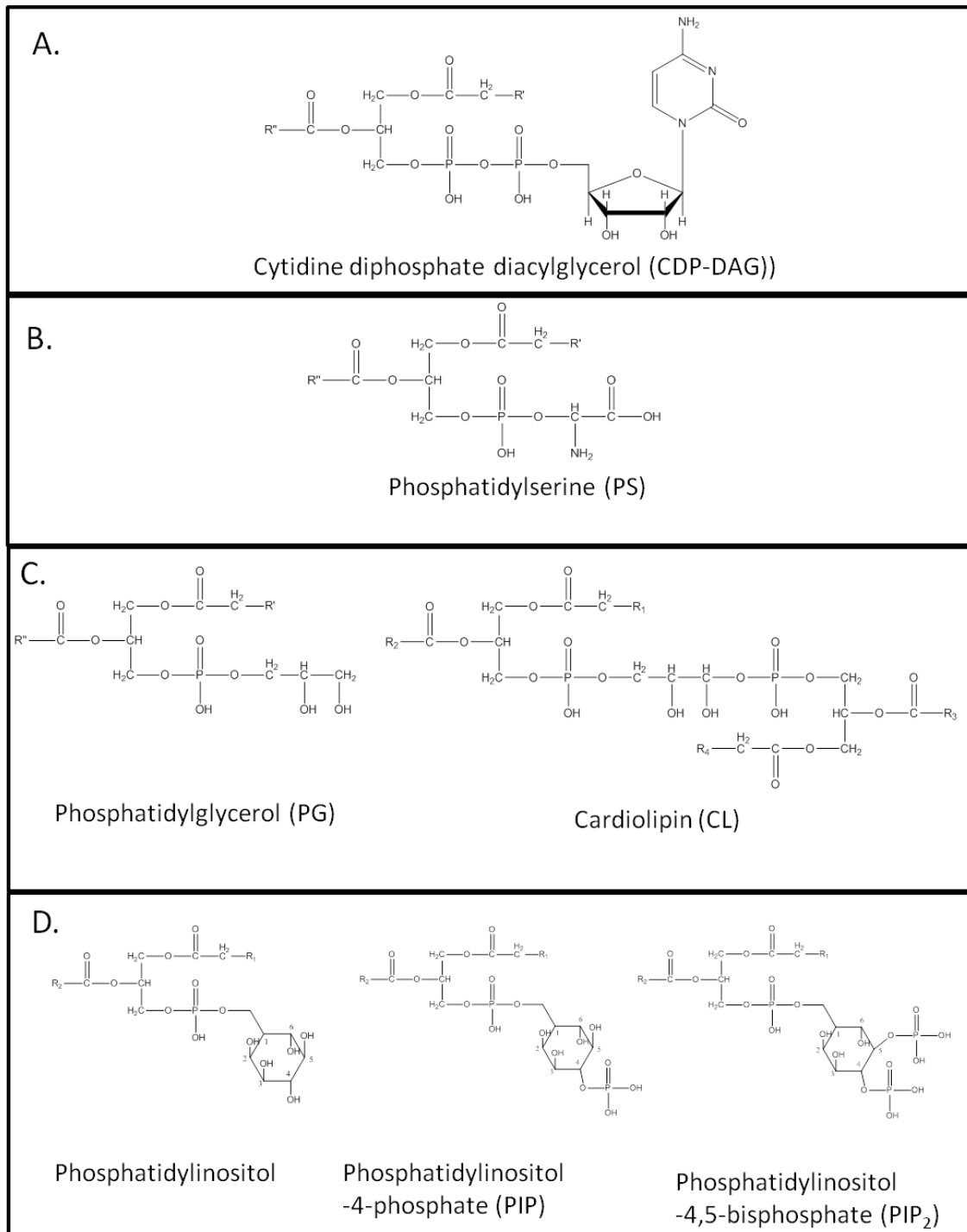


Figure 1.11. Products of the CDP-DAG pathway. R' and R'' – lipid chains which can be attached to the glycerol by acyl, alkyl or alkenyl links.

1.3.5.b Phosphatidylserine

PS contains the amino acid serine as a headgroup (Figure 1.11, box B). It is a relatively minor membrane phospholipid, comprising 3-10% of membrane phospholipid in mammalian cells and about 3% in *T. brucei* (Richmond et al., 2010) (Figure 1.8).

Despite its low abundance in membranes, in many cells PS is an essential biosynthetic intermediate as a precursor to PE via PS decarboxylation (see earlier, and Figure 1.9) but this is not the case in *T. brucei* where it seems that PS is not a significant source of PE (Menon et al., 1993, Rifkin et al., 1995, Signorell et al., 2008, Gibellini et al., 2009). In cells where PS is essential for PE formation, loss of PS synthase activity can be overcome by the addition of ethanolamine (Voelker and Frazier, 1986), PE (Kuge and Nishijima, 1997) or, in yeast, choline (Atkinson et al., 1980, Nikawa and Yamashita, 1981) to the medium. In *E. coli* the addition of divalent cations to the medium appear to be able to change the physical properties of CL so that it can substitute for PE, and so overcome PS auxotrophy for PE (Dechavigny et al., 1991, Raetz, 1976). These results seem to suggest that PS itself is not a key membrane phospholipid in these organisms.

PS is, however, enriched in certain tissues and subcellular locations such as brain in mammals and in the plasma membrane (Vance and Steenbergen, 2005). In mammalian plasma membranes, PS has an asymmetric distribution, with the majority being found on the inner leaflet (Vance and Steenbergen, 2005). Exposure of PS on the cell surface occurs late in apoptosis, after which it is recognised by a PS receptor and the apoptotic cell is phagocytosed (Wong et al., 2010).

Additionally, in many higher eukaryotes PS has a role as a co-factor for several proteins such as protein kinase C (Takai et al., 1979, Bittova et al., 2001) and Raf1 Kinase (Ghosh et al., 1994, Ghosh et al., 1996, Nagai et al., 1999). These results indicate that the essentiality of PS may be very variable dependent on the organism and cell type.

1.3.5.c Phosphatidylglycerol and CL

CDP-DAG is the only known precursor to the mitochondrial phospholipids PG and CL (Figures 1.9 and 1.11, box C). Whilst PG is not a major phospholipid, it is required for the synthesis of CL. However, in yeast in the absence of the CL synthase, PG

accumulates and can partially compensate for several cellular functions of CL (Jiang et al., 2000).

CL is a major membrane component of bacteria and due to its unusual structure - four hydrophobic chains and a small negatively charged head group - it has unique properties and tends to form non-bilayer structures. CL is a key mitochondrial phospholipid, the vast majority of CL found on the inner mitochondrial membrane, with only about 25% of total CL being found on the outer mitochondrial membrane (Gebert et al., 2009). In the mitochondrion, it is important not only for structure but may play a key role in the function and stabilisation of many mitochondrial proteins and complexes, transport of proteins to the mitochondria and apoptosis (reviewed in Osman et al. (2011)). In mammalian cells, mutations in PGP synthase eliminate PG and CL pools, resulting in altered mitochondrial structure and function (Ohtsuka et al., 1993a, Ohtsuka et al., 1993b).

In *T. brucei*, mass spectrometry shows only small amounts of CL in the mitochondrial fraction of procyclics (Guler et al., 2008). The synthesis of CL via the prokaryotic-like CL synthase has been shown to be essential in procyclic where ablation of its activity by conditional knockout caused reduction in mitochondrial membrane potential, mitochondrial fragmentation and cell death (Serricchio and Buetikofer, 2012). Additionally, CL synthase was found to be part of a large protein complex, and its depletion resulted in the decrease of mitochondrial respiratory complexes III and IV (Serricchio and Buetikofer, 2012).

1.3.5.d Phosphatidylinositol and PIPs

Phosphatidylinositols (Figure 1.11, box D), which contain a *myo*-inositol headgroup, are important structural phospholipids as components of membranes, and as part of GPI anchors. Most prokaryotes are deficient in PI, but it is found in some actinomycetes, myxobacteria and *Treponema* species, where it is used for lipid anchoring of important molecules and is therefore essential for membrane and cell wall stability (Jackson et al., 2000).

In *T. brucei*, PI synthase (Tb09.160.0530) is essential for the production of GPI anchors in bloodstream form (Martin and Smith, 2006b). Interestingly, whilst a bloodstream form null mutant of GPI GlcNAc de-N-acetylase, the enzyme that catalyses the second step in the formation of GPIs, is not viable (Chang et al., 2002),

Figure 1.10), the procyclic null is viable (Guther et al., 2006). This may suggest that PI is not essential for GPI anchor formation in procyclics, and the essentiality of PIS in procyclics has not been confirmed. However, recently a *T. brucei* myo-inositol transporter has been shown to be essential in procyclic cells for the formation of cellular PI and inositol phosphorylceramide (IPC), which may indicate that PIS is also essential (Gonzalez-Salgado et al., 2012). Interestingly, whilst RNAi knockdowns of the transporter showed a massive reduction in the synthesis of PI and IPC, GPI anchor synthesis appeared unaffected (Gonzalez-Salgado et al., 2012). This is consistent with the knowledge that *de novo* synthesised inositol is used for the formation of GPI anchors (Martin and Smith, 2006a), but also adds that *de novo* synthesised inositol cannot be used for the formation of cellular PI and IPC and will be discussed later.

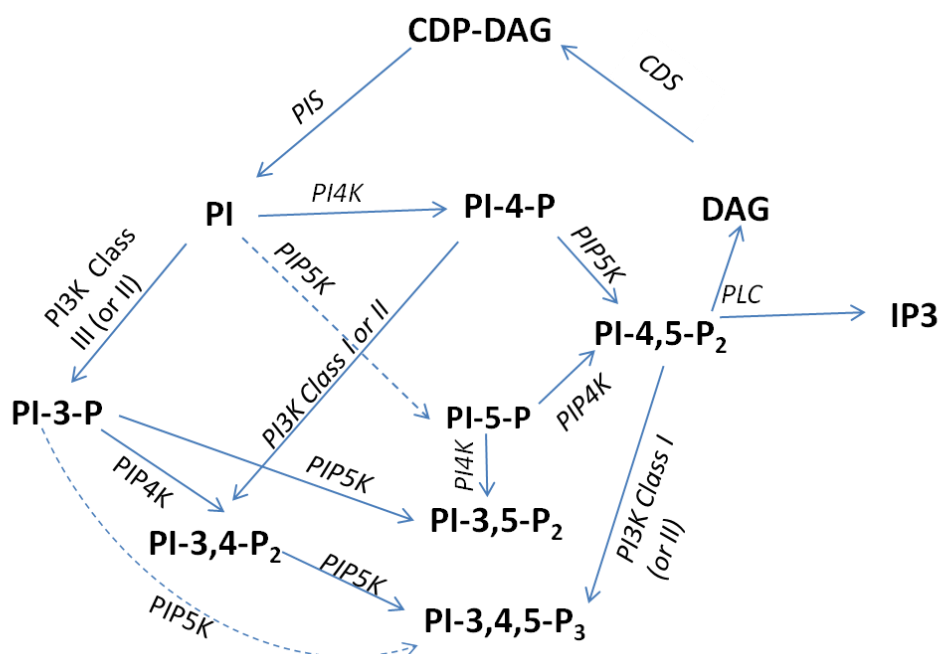


Figure 1.12. Intracellular cycle of phosphoinositide-mediated signal transduction in mammals. Solid arrows indicate established steps, whilst broken arrows indicated postulated steps. **CDP-DAG** = cytidine diphosphate diacylglycerol, **PI** = phosphatidylinositol, **PI-4-P** = phosphatidylinositol-4-phosphate, **DAG** = diacylglycerol, **PI-3-P** = phosphatidylinositol-3-phosphate, **PI-5-P** = phosphatidylinositol-5-phosphate, **PI-4,5-P₂** = phosphatidylinositol-4,5-bisphosphate, **PI-3,4-P₂** = phosphatidylinositol-3,4-bisphosphate, **PI-3,5-P₂** = phosphatidylinositol -3,5 -bisphosphate, **PI-3,4,5-P₃** = phosphatidylinositol-3,4,5-trisphosphate. **PIS** = phosphatidylinositol synthase, **CDS** = cytidine diphosphate diacylglycerol synthase, **PI4K** = phosphatidylinositol-4-kinase, **PIP5K** = phosphatidylinositol-phosphate 5-kinase, **PI3K** = phosphatidylinositol-3-kinase, **PIP4K** = phosphatidylinositol-phosphate 4-kinase, **PIP5K** = phosphatidylinositol-phosphate 5-kinase, **PLC** = phospholipase C, **PIP4K** = phosphatidylinositol-phosphate 4-kinase. Image adapted from Fruman et al, 1998.

However, in the general research field it is the phosphorylated derivatives of PI (PIPs) that have sparked the most interest (Figure 1.11, box D). PI-4-phosphate (PIP)

and PI-4,5-bisphosphate (PIP₂) contain additional phosphate groups esterified at carbon 4 or carbons 4 and 5 of the inositol headgroup. Figure 1.12 shows an overview of phosphoinositide signalling cycles in mammals. Hydrolysis of PIP₂ by phospholipase C produces the second messengers DAG and inositol-1,4,5-triphosphate (IP₃). IP₃ acts to mobilise intracellular Ca²⁺ leading to activation of calcium inducible signal transduction pathways and DAG activates protein kinase C signalling pathways. In eukaryotic cells PIPs are vital as second messengers in cell signalling, involved in a variety of cellular process including vesicular transport (DeCamilli et al., 1996), cytoskeletal organisation (Janmey, 1994, Hartwig et al., 1995, Gilmore and Burridge, 1996), Golgi maintenance (Liu et al., 2008, Rodgers et al., 2007) and regulation of protein kinase activities (Franke et al., 1997).

Little is known about the importance of phosphatidylinositols as second messengers in eukaryotic parasites. In *Plasmodium* there is evidence of a phosphoinositide cycle (Elabbadi et al., 1994) and in *T. cruzi* PI signalling pathways affect growth control (Malaquias and Oliveira, 1999). Though nothing has been shown in *T. brucei*, several putative PI kinases have been identified in the genome (van Hellemond and Tielens, 2006, Smith and Buetikofer, 2010)(Table 1.1) but there is a lack of genes encoding class I or II PI 3-kinases. A class III PI 3-kinase has been implicated in Golgi segregation and endocytic trafficking (Hall et al., 2006) and a PI-4-kinase is required for maintenance of Golgi structure, protein trafficking, normal cellular shape and cytokinesis in procyclic form trypanosomes (Rodgers et al., 2007). Moreover, all of the mono- and bisphosphorylated PI species have been confirmed in *T. brucei* (Richmond et al., 2010).

Table 1.1. <i>T. brucei</i> genes predicted to encode PI kinases.		
Enzyme name	<i>T. brucei</i> gene	Yeast gene
PI3 kinase Class (III)	Tb927.8.6210	Pik1
PI4 kinase	Tb927.4.1140	Stt4
PI4 kinase	Tb927.3.4020	
PIK-related	Tb927.4.800	TOR-like
PI3 kinase	Tb927.4.420	TOR2
PI3 kinase	Tb927.1.1930	
PIK-related	Tb927.2.2260	
PI3 kinase related	Tb11.01.6300	

1.4 CDP-DAG Synthase

The production of CDP-DAG is accomplished by the enzyme CDP-DAG synthase (CDS) (EC 2.7.7.41/Tb927.7.220) from cytidine triphosphate (CTP) and phosphatidic acid (PA) (Figure 1.13). This enzyme has not previously been studied in *T. brucei*, but is likely to be essential since it is the precursor to so many other important phospholipids, some of which have already been genetically validated as essential.

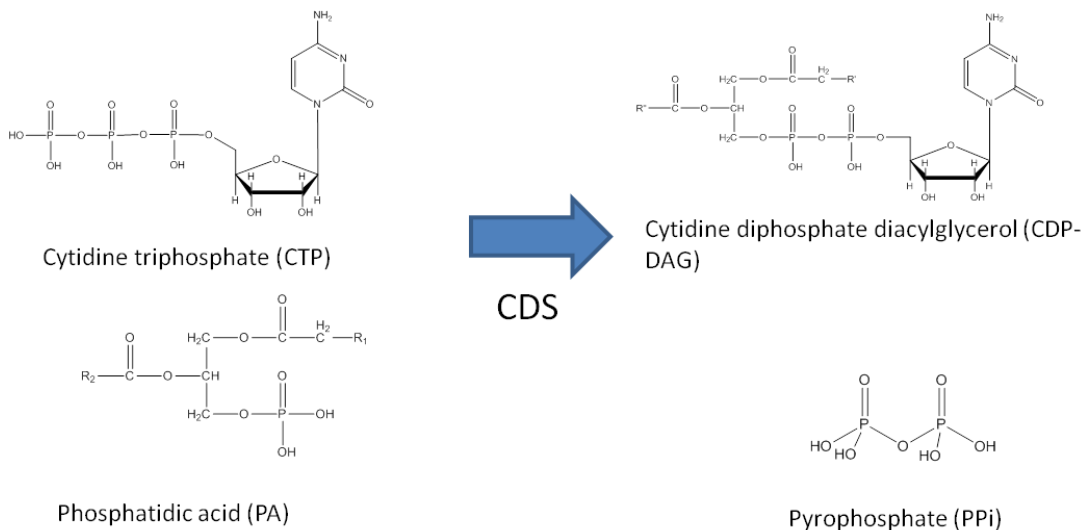


Figure 1.13. Reaction catalysed by cytidine diphosphate diacylglycerol synthase (CDS). R' and R'' – lipid chains which can be attached to the glycerol by acyl, alkyl or alkenyl links.

1.4.1 Gene

A gene encoding CDP-DAG synthase activity was first discovered when *E. coli* mutants were isolated exhibiting defects in the activity. Above pH 8, these mutants exhibited massive accumulation of PA, a phenotype which was similar to cytidine starvation of a CTP auxotroph. *De novo* synthesis of PE and PG were greatly inhibited and at pH 8.5 for 60 minutes the mutant lost viability, at which point the liponucleotide pool was about one seventh of that of an isogenic wildtype (Ganong et al., 1980, Ganong and Raetz, 1982). These mutants made it possible to clone the CDS encoding gene, and a plasmid over-expressing CDS was created (Icho et al., 1985). This paved the way for subsequent purification and characterisation studies.

Interest in the CDS gene was greatly increased when a CDS homologous to the bacterial one was isolated from photoreceptor cells in *Drosophila melanogaster* (Wu et al., 1995). Overexpression of this gene resulted in amplification of light response in photoreceptor cells, whilst a mutant deficient in this gene product underwent light dependent retinal degradation (Wu et al., 1995). The role of CDS as a possible regulatory step in phosphoinositide signalling and vision lead to more research, particularly into the mammalian enzyme, and CDS genes were subsequently cloned from yeast (Shen et al., 1996), human (Heacock et al., 1996, Halford et al., 1998), rat brain (Saito et al., 1997) and mouse (Volta et al., 1999, Inglis-Broadgate et al., 2005). The genes from *Drosophila*, yeast, mammals and plants all show high sequence similarity, suggesting a high degree of conservation during evolution.

CDS homologues have now been identified in all eukaryotic organisms sequenced to date and some appear to have multiple copies (Lykidis, 2007). *Arabidopsis thaliana* has five different predicted CDS genes, which may encode up to ten different proteins (Haselier et al., 2010). Three of these CDS genes are derived from the same ancestral eukaryotic gene, whilst two are thought to have derived from the photosynthetic endosymbiont via horizontal gene transfer, and their proteins are targeted to the plastids (Haselier et al., 2010). *Danio rerio* (zebrafish) has 3 eukaryotic copies, whilst mammals have 2 copies, designated CDS1 and CDS2 which appear to be differently expressed and regulated (Lykidis et al., 1997, Inglis-Broadgate et al., 2005, Volta et al., 1999, Kopka et al., 1997). Conversely, only one gene has been found in *S. cerevisiae* and *Drosophila*. In yeast, the single gene identified is essential for cell growth (Shen et al., 1996), so it seems likely it encodes

the only CDS activity. The gene, however, has no targeting sequence and is not thought to be alternatively spliced (Shen et al., 1996), but activity has been found in several sub-cellular locations (Kuchler et al., 1986, Kinney and Carman, 1990, Kelley and Carman, 1987). It is therefore not known how the enzyme is targeted to the different cellular locations, although there is the possibility of an alternative transcription start site (Shen et al., 1996). In contrast, the only isolated *Drosophila* transcript appears to solely be expressed in retinal cells and mutants deficient in the transcript, apart from showing retinal degeneration, develop normally and are viable (Wu et al., 1995). This is not consistent with eye-CDS being the only CDS gene in the organism. Indeed, transposase induced excisions of the P-element insert into the CDS allele yielded three mutations that are homozygous lethal. Progeny of these mutants lacked the eye-CDS protein, indicating that the eye-specific and general CDS enzymes are encoded by the same gene. Analysis of the genomic structure of CDS has confirmed the presence of alternatively spliced CDS isoforms. Such post-transcriptional regulation of the transcript would allow for specialisation of the different CDS isoforms (Wu et al., 1995)

1.4.2 Sequence Analyses/Structure

All eukaryotic CDS proteins sequenced so far are quite similar in size, ranging from 399 amino acids in *Arabidopsis thaliana* CDS5 (Haselier et al., 2010) to 461 amino acids in human CDS1 (Heacock et al., 1996). The exception to this is the *Plasmodium falciparum* gene which encodes a protein 667 amino acids long. However, this enzyme is proteolytically processed to yield two smaller proteins, the larger one responsible for the CDS activity (Martin et al., 2000).

The most homologous regions in all CDS protein sequences studied so far are found towards the C-terminus, where there are domains sharing more than 80% identity (Saito et al., 1997). These regions mostly correspond to intra-cytoplasmic loops and may be domains of the active site essential for enzyme function (Volta et al., 1999). All eukaryotic CDS proteins possess an N-terminal hydrophilic region, and no typical signal peptide. In *S. cerevisiae*, *Drosophila* and rat the region prior to the first hydrophilic domain is about 80 amino acids long but in *P. falciparum* it is 269 amino acids long, and is the part which is cleaved off during proteolytic processing (Martin et al., 2000). The hydrophilic N-terminal region of eukaryotic CDS is not found in the *E. coli* or *Mycobacterium smegmatis* homologues. Both of these bacterial enzymes

are much shorter, suggesting that N-terminal and C-terminal extensions are not required for catalytic activity (Heacock and Agranoff, 1997).

In a yeast CDS mutant, a base change resulting in a cysteine to tyrosine substitution was sufficient to reduce the level of CDS protein by at least 70%, causing the mutant to be deficient in phospholipid synthesis and to excrete inositol (Shen et al., 1996, Shen and Dowhan, 1996). This amino acid substitution occurs at the interphase between a hydrophobic and a hydrophilic region but does not appear to be conserved in CDS sequences from other organisms.

There are some cysteine residues that are conserved in both the eukaryotic and prokaryotic enzymes (Heacock and Agranoff, 1997), and the yeast (Kelley and Carman, 1987) and human (Heacock and Agranoff, 1997) enzymes are sensitive to sulfhydryl inhibitors, suggesting that sulfhydryl groups are important at the active site. Conversely, Belendiuk et al found the partially purified yeast enzyme had full activity in the presence of iodoacetamide (Belendiuk et al., 1978) and Langley and Kennedy found that N-ethylmaleimide did not inhibit the partially purified *E. coli* enzyme (Langley and Kennedy, 1978). Belendiuk and colleagues also found their partially purified enzyme to be active in the presence of phenylmethylsulfonyl fluoride, indicating serine hydroxyl groups were also not required for catalytic activity (Belendiuk et al., 1978).

All proteins are highly hydrophobic and are predicted to have several membrane spanning domains, indicating they are integral membrane proteins (Volta et al., 1999, Heacock et al., 1996, Martin et al., 2000, Nigou and Besra, 2002).

The structure of the CDS enzyme has currently not been solved for any of the isolated copies. The enzyme from *S. cerevisiae* appears to exist as a dimer composed of two identical 56 kDa subunits (Kelley and Carman, 1987) whilst the enzyme from *E. coli* is composed of a single subunit weighing 27 kDa (Sparrow and Raetz, 1985).

1.4.3 Sub-cellular localisation

All CDS enzymes identified so far are integral membrane proteins. In prokaryotes, the majority of CDS activity is found on the inner membrane of the cell envelope (Bell et al., 1971, White et al., 1971). In yeast, CDS activity is distributed between the mitochondria and the ER (Kuchler et al., 1986, Kelley and Carman, 1987) and some activity has also been reported in the Golgi, nucleus, secretory vesicles destined for

the plasma membrane and the plasma membrane (Kinney and Carman, 1990, Jelsema and Morre, 1978). In mammals the bulk of CDS activity is found in the endoplasmic reticulum and in human COS-7 cells is particularly localised to the perinuclear and tubular regions. In the rat liver mitochondria, the majority of the enzyme activity copurifies with the inner mitochondrial membrane enriched fraction (Mok et al., 1992). In plants, all CDS isozymes had highest activity in the mitochondrial fractions. The CDS in plant chloroplasts is encoded by a plastidial gene and is mainly involved in PG synthesis (Andrews and Mudd, 1985, Haselier et al., 2010). Recently, CDS has been shown to be present in a unique, non-raft sub domain of the ER which is rich in the chaperone protein calnexin (Waugh et al., 2011).

In spite of the presence of CDS in multiple locations, no signal sequence has been identified in any of the eukaryotic CDS genes identified so far (Saito et al., 1997, Wu et al., 1995, Kelley and Carman, 1987, Martin et al., 2000).

In rat liver cells, where the bulk of CDS activity is found in the ER, mitochondrial CDS activity accounts for only 5-10% of total CDS activity (Bishop and Strickland, 1976, Mok et al., 1992) but the reaction appears to be distinct in the two different locations. The availability of PA, for example, appears to be a limiting factor for the formation of the microsomal, but not the mitochondrial enzyme, whilst GTP significantly stimulated the enzyme from the microsomal fraction but not the mitochondrial enzyme, where it actually seemed to slightly inhibitory (Mok et al., 1992). This would appear to suggest the existence of two separate isozymes, or, as suggested by Heacock and Agranoff, could reflect differences due to the environment or due to post-translational modification (Heacock and Agranoff, 1997). Given current knowledge that mammals encode two separate CDS genes, CDS1 and CDS2, it seems prudent to consider that the two genes encode separately compartmentalised enzymes. The two proteins show different expression patterns in tissues - the CDS2 being highly and ubiquitously expressed, while CDS1 expression is much more restricted but is found in the inner segment of the photoreceptor layer in the retina (Saito et al., 1997, Volta et al., 1998, Volta et al., 1999, Inglis-Broadgate et al., 2005) whereas CDS2 is not expressed in the adult retina (Volta et al., 1999). However, PSORTII and DAS trans-membrane computer prediction programmes indicate that both CDS1 and CDS2 enzymes appear to be localised to the ER, (Inglis-Broadgate et al., 2005, Volta et al., 1999) but further studies are required to address substrate specificity and exact localisation.

There is some evidence that separately compartmentalised CDS enzymes could be used to produce CDP-DAG for particular metabolic fates, in particular for PI destined for the phosphoinositide pathway in some higher eukaryotes (Heacock and Agranoff, 1997).

1.4.4 Enzyme Specificity/Kinetics

It might be expected that the fatty acid composition of CDP-DAG would closely match that of its precursor PA, but in mammals this is not the case. There is much less palmitate (C16:0) and much more stearate (C18:0) composing the major fatty acids of CDP-DAG than PA, as well as considerably more of the unsaturated fatty acid arachidonate (C20:4). The composition of the fatty acids of PI, however, is very similar to those of CDP-DAG, whilst those of PG and CL more closely resemble those of PA (Thompson and Macdonald, 1975).

This could suggest that CDS is actively selecting for particular species of PA. Indeed, substrate specificity for C18:0/20:4 over di-C18:1 and little or no activity with di-C12:0 or di-C18:0 was found in a CDS enzyme isolated from rat brain (Saito et al., 1997). This may suggest that this isozyme selectively participates in the phosphoinositide cycle. The *Mycobacterium smegmatis* enzyme showed a preference for C16 PA species, which are the predominant species found in this organism (Nigou and Besra, 2002) and the two *Arabidopsis* CDS isozymes showed highest activity with di-C18:1 PA. However, other researchers found mammalian CDS enzymes to exhibit little or no selectivity (Bishop and Strickland, 1976, Thompson and Macdonald, 1975) but more than one CDS isozyme could have been present in these assay preparations. In plants (potato tuber, pea leaf and soya-bean microsome) PA and CDP-DAG contain similar amounts of the same species of PA but PI contains only two distinct species (16:0/18:2 and 16:0/18:3) (Justin and Mazliak, 1992) suggesting that acyl substrate specificity is at the PI synthase level.

There is evidence that the PA species containing unsaturated fatty acids are better substrates for CDP-DAG, however it seems likely that this is due to their solubility, even in detergent, rather than enzyme specificity (Bishop and Strickland, 1976, Holub and Piekarski, 1976). The *E. coli* enzyme did not utilise lyso-PA (Sparrow and Raetz, 1985).

The *E. coli* CDS can accept both dCTP and CTP as substrates (Raetz and Kennedy, 1973), and both dCDP-DAG and CDP-DAG can be utilised by the downstream enzymes PS and PG synthase. Similar results have been obtained in some *in vitro* studies for eukaryotic enzymes (Thompson, 1977, Baelee and Carman, 1984, Kelley and Carman, 1987, Saito et al., 1997) but are not thought to occur *in vivo* as no dCDP-DAG has ever been detected in a eukaryotic organism. The ratio of dCDP-DAG to CDP-DAG in *E. coli* was found to be 0.8-1 whilst the ratio of dCTP to CTP in *E. coli* is thought to be between 0.1 and 0.2 suggesting dCTP is utilised more efficiently, although the reported K_m and V_{max} values with CTP and dCTP are virtually identical (Raetz and Kennedy, 1973, Sparrow and Raetz, 1985). The downstream enzymes showed differential preferences for the two forms of CDP-DAG: the rate of PS synthesis was five times faster with CDP-DAG than with dCDP-DAG, whilst in the synthesis of PGP dCDP-DAG was more active (Raetz and Kennedy, 1973). This suggests that presence of the two different forms may be relevant in the partitioning of CDP-DAG with dCDP-DAG as a precursor to the mitochondrial phospholipids PG and CL, and CDP-DAG being the precursor of PE via PS. However, in the CDS conditional null mutant described by Ganong and Raetz, increase of pH to 8.5 (and hence inhibition of CDS activity) resulted in a shift in the ratio of dCDP-DAG to CDP-DAG to about 3:1, whilst the ratio of PE to PG did not change. This argues against the role for the relative amount of the two forms being involved in regulating the ratio of these phospholipids *in vivo* (Ganong and Raetz, 1982). All nucleotides other than CTP (or dCTP) are poor substrates for CDS (Carter and Kennedy, 1966, Raetz and Kennedy, 1973, Thompson, 1977, Sievers et al., 2011, Kelley and Carman, 1987).

Analysis of the *E. coli* and *S. cerevisiae* enzymes suggest that they follow typical saturation kinetics toward CTP and PA which are consistent with a sequential reaction mechanism (Sparrow and Raetz, 1985, Kelley and Carman, 1987). In yeast, the enzyme binds to CTP before PA, and PPi is released prior to CDP-DAG in the reaction sequence (Kelley and Carman, 1987, Belendiuk et al., 1978).

CDS from all sources has an absolute requirement for divalent cations for activity, with Mg^{2+} being the most effective. Where tested, other divalent cations Mn^{2+} , Ca^{2+} and Fe^{2+} gave, at most, half the rate observed with Mg^{2+} (Carter and Kennedy, 1966, Nigou and Besra, 2002). Additionally, in all studies CDS shows preference for K^+ and non ionic detergent. The *Mycobacterium smegmatis* CDS was also stimulated by Na^+ , but to a lesser extent than by K^+ (Nigou and Besra, 2002).

1.4.5 Reverse Reaction

No CDS isolated to date catalyses the hydrolysis of CDP-DAG. In prokaryotes, a separate, membrane bound pyrophosphatase specific for CDP-DAG catalyses this reaction (Raetz et al., 1972) but no eukaryotic homologue has been found. However, all labs have reported that CDS is capable of carrying out the reverse reaction where the presence of PPi is an absolute requirement. In yeast (Kelley and Carman, 1987) and *E. coli* (Sparrow and Raetz, 1985), the reverse reaction appeared to be favoured *in vitro*, however it is likely that *in vivo* the forward reaction is favoured due to low levels of CDP-DAG and/or the presence of inorganic pyrophosphatase.

1.4.6 Expression/Regulation

The pool of CDP-DAG is much smaller than that of PA in *E. coli* (Raetz and Kennedy, 1973), beef liver (Thompson and Macdonald, 1975) and *S. cerevisiae* (Nickels et al., 1994). This, along with the position of CDP-DAG at a branch point suggests that the synthesis of CDP-DAG may be a rate-limiting step in phospholipid synthesis.

Much research in the regulation of phospholipid biosynthesis has been done in *S. cerevisiae*. The inositol-responsive *cis*-acting element (UAS_{INO}) and the corresponding *trans*-acting factors (the gene products of INO2 (Ino_{2p}) INO4 (Ino_{4p}) and OPI1 (Opi_{1p})) have been well characterized for transcriptional regulation of phospholipid synthesis genes. A detailed review of the regulation is given in Carman and Han (2011).

Briefly, an upstream activation sequence sensitive to inositol (UAS_{INO}) has been found 5' to the *S. cerevisiae* CDS sequence (Shen et al., 1996). The Ino_{2p}-Ino_{4p} gene product complex binds to the UAS_{INO} sequence and stimulates transcription (Carman and Han, 2007, Chen et al., 2007). Opi_{1p} binds PA and Acs_{2p} at the nuclear/ER membrane, but on lowering concentration of PA is released and enters the nucleus where it represses transcription of UAS_{INO}-controlled genes by binding to INO2 (Loewen et al., 2004, Carman and Han, 2007). PA concentration is therefore central in the regulation of phospholipid synthesis and enzymes involved in PA metabolism, such as PA phosphatase and DAG kinase, have a role in the regulation of UAS_{INO} containing genes (Han et al., 2008, Han et al., 2007). PA phosphatase and DAG kinase are both in turn regulated by the concentration of CDP-DAG (Wu and Carman, 1996, Shen et al., 1996), showing that CDS is central to regulation of phospholipid

metabolism. Interestingly, CDP-DAG levels also directly affect transcription of the inositol-3-phosphate synthase (INO1) and phosphatidylserine synthase (PSS) genes independent of INO2-INO4 genes or inositol, choline or ethanolamine concentration in the growth medium (Shen and Dowhan, 1997).

Other factors triggering regulation of UAS_{INO} genes include nutrient availability and growth stage. For example, expression of these genes is activated when zinc is available in the medium (Iwanyshyn et al., 2004, Carman and Han, 2007) whilst ethanolamine and choline result in a reduction of CDS activity, but only when inositol is present (Carman and Henry, 2007, Ashburner and Lopes, 1995, Carman and Han, 2009, Chen et al., 2007). UAS_{INO}-containing genes have their highest level of expression during the exponential phase of *S. cerevisiae* cell growth, whilst they are repressed in stationary phase (Chen et al., 2007, Carman and Henry, 1999, Carman and Henry, 2007). Whilst most phospholipid enzymes containing UAS_{INO} have several copies of the sequence, CDS only has one (Shen et al., 1996) which could explain why its expression is not so dramatically up regulated in response to inositol, choline or ethanolamine (Homann et al., 1985) compared to other phospholipid synthesis enzymes (Shen and Dowhan, 1996).

In addition to the role of CDS in transcriptional regulation, it has been shown that a marked fall in PI synthase (PIS1) activity follows a decrease in CDS activity without a parallel change in the level of PIS1 mRNA, suggesting this effect is not at the transcriptional level, and may related to enzyme stability (Shen and Dowhan, 1997, Dowhan, 1997).

In the rat heart and in embryonic rat heart-derived H9c2 myoblast cells, CDS may be a rate-limiting enzyme for CL biosynthesis (Hatch, 1994, Hatch and McClarty, 1996).

E. coli mutants deficient in CDS activity exhibited a massive accumulation in PA, followed by inhibition of both PE and PG synthesis resulting in a severe reduction of overall cell phospholipid and death (Ganong and Raetz, 1982). A yeast null in CDS failed to germinate whilst a clone with 10% of wild type CDS activity excreted inositol into the medium, and exhibited a decrease in the initial rate of PI synthesis but an increase in the rate of PS synthesis, which was mirrored in the overall cell phospholipid content (Shen and Dowhan, 1996). The increased sensitivity of PI to the lack of CDP-DAG seems surprising given that the yeast PI and PS synthases both have equivalent affinity for CDP-DAG (Carman and Baelee, 1992, Baelee and Carman,

1984, Kelley and Carman, 1987). However, these K_m values were measured *in vitro* at saturation concentration of their other substrate (inositol or serine), and in enzymes with two substrates the K_m of one is inversely related to the concentration of the other. *In vivo*, whilst the PS synthase is saturated at the concentration of serine present, the available concentration of inositol for PI synthase is 9 fold below its K_m , and therefore PI has a higher K_m for CDP-DAG under physiological conditions (Kelley et al., 1988). An interesting point from the study by Shen and Dowhan is that 10% of yeast CDS activity was enough to support normal growth in these yeast cells (Shen and Dowhan, 1996).

In *Arabidopsis*, inactivation of both the plastid CDS genes inhibited the formation of plastidial (but not mitochondrial or microsomal) PG. This led to incorrect development of thylakoid membranes, a drastic reduction in chlorophyll and the inability of the mutants to grow photoautotrophically (Haselier et al., 2010). Similarly, in the cyanobacterium *Synochocystis* a null mutant of CDS was lethal to the cells when cultured photoautotrophically, but growth could be rescued by supplementation with PG (Sato et al., 2000). In this, and other photosynthetic organisms, the summed level of anionic phospholipids sulfoquinovosyl diacylglycerol (SQDG) and PG is kept fairly constant, with an increase in one species if synthesis of the other is impaired, however in the *Syechocystis* CDS null the SQDG level remained constant at various levels of PG supplementation. This may indicate that, whilst sufficient for growth, the incorporated PG was not able to regulate levels of the anionic lipids (Sato et al., 2000).

Interestingly, overexpression of the *E. coli* CDS gene, and of human CDS1 in COS-7 cells did not result in significant proportional increases in the cellular CDP-DAG levels, suggesting that this is not a rate-limiting step (Lykidis et al., 1997, Icho et al., 1985). However, the group did find an affect of CDS overexpression in *E. coli* cytidine auxotrophs. When starved of cytidine this auxotrophic cell line accumulated PA, likely because this blocked the pathway due to a lack of the CDS substrate CTP. However an accumulation of PA did not occur when CDS was over-expressed, perhaps suggesting that increased CDS can improve competition for limiting CTP (Icho et al., 1985). The cytidine-starved *E. coli* cells also accumulated total lipid, but again this was stopped by the overproduction of CDS. It is a possibility, therefore, that CDP-DAG is somehow required for regulation, possibly signalling total lipid content (Icho et al., 1985). In yeast, overexpression of CDS caused a marked increase in PI

synthesis, but a decrease in PS synthesis which was also reflected in the overall phospholipid composition of the cells - the inverse of the mutant with low CDS activity. There was also a small but significant increase in PA (Shen and Dowhan, 1996).

In rat liver, GTP has been reported to stimulate the microsomal, but not the mitochondrial CDS enzyme (Liteplo and Sribney, 1980, Mok et al., 1992, Monaco and Feldman, 1997). It does this by decreasing the enzyme's affinity for PA, with no change in the V_{max} of (rat liver) microsomal synthesis, suggesting the activation could involve the covalent modification of the enzyme or of a protein associated with it (Mok et al., 1992). Other investigators, however, found that in human CDS1, this stimulatory effect was not limited to GTP, but was also caused by GDP and ATP (Lykidis et al., 1997). ATP stimulated the guinea pig liver enzyme, but only in experiments that were allowed to proceed for 1-2 hours, and it was presumed that this was due to it preventing the breakdown of CTP by microsomal phosphatases (Carter and Kennedy, 1966). AMP was found to stimulate the partially purified *E. coli* CDS when CTP was used as a substrate, however this stimulation was less pronounced with dCTP, possibly because AMP inhibits the CDP-DAG hydrolase, and CDP-DAG hydrolase does not hydrolyse dCDP-DAG (Langley and Kennedy, 1978). Neither mono, di- or tri phosphorylated adenosine, cytidine, guanosine or uridine have any effect on *S. cerevisiae* CDS activity (Kelley and Carman, 1987), whilst ATP, GTP and UTP were found to be strongly inhibitory in *M. smegmatis* (Nigou and Besra, 2002) and ATP strongly inhibited the rat microsomal enzyme (Sribney et al., 1977) possibly by competing for the active site.

There is some evidence of alternatively spliced forms of CDS in *Drosophila*, *P. falciparum* and mammals, which may have some role in regulation, whereas in *E. coli* the presence of CDP- and dCDP-DAG may be significant in the regulation. Additionally, several of the sequences identified contain recognition sites for kinases and phosphorylases, and in the rat brain enzyme the immuno-reactive band of protein is larger than the deduced mass of the CDS protein (Saito et al., 1997) suggesting that, as in the *P. falciparum* enzyme, post translational protein modifications are occurring which may also be involved in regulation of CDS.

1.4.7 Inhibitors

The reaction products PPI and CDP-DAG are both inhibitors of CDS activity in *M. smegmatis* (Nigou and Besra, 2002) and rat liver (Monaco and Feldman, 1997) suggesting a negative feedback mechanism. dCTP (Kelley and Carman, 1987, Belendiuk et al., 1978) and thiophosphatidate (Bonnell et al., 1989) are competitive inhibitors of the yeast enzyme, whilst CMP has a strong, non competitive inhibitory effect on the enzyme from *Bacillus subtilis* (Gaillard et al., 1983). In whole cell lysates of COS cells transfected with the rat CDS cDNA, PIP₂ has also been found to have an inhibitory effect (Saito et al., 1997). This is contradicted by Monaco and Feldman who worked with the microsomal pellet, and suggest that the difference could be due to their lack of detergent use which may have meant inadequate lipid solubilisation (Monaco and Feldman, 1997). The inhibition of CDS by PIP₂ could suggest that the phosphoinositide cycle is regulated by negative feedback control (see Figure 1.12).

1.4.8 CDP-DAG synthase as a Drug Target in *T. brucei*

In order for CDP-DAG synthase to be a drug target in *T. brucei*, it must be shown to be essential. Null mutants in yeast (Shen et al., 1996), *E. coli* (Ganong and Raetz, 1982) and *Synechocystis* (Sato et al., 2000) are inviable. These organisms, like *T. brucei*, appear to only have one gene encoding CDS activity. Considering the parasite's essential requirements for the phospholipids whose synthesis is CDP-DAG dependent can assess its essentiality in *T. brucei*.

1.5 PI Synthase

Phosphatidylinositol is synthesised from *myo*-inositol and CDP-DAG in a condensing reaction by the enzyme PIS (PI synthase; EC 2.7.8.11/Tb09.160.0530) releasing CMP (Figure 1.14). Additionally, in the absence of CDP-DAG, PI can be made from an existing PI and a free *myo*-inositol by a headgroup exchange reaction. Whilst PI synthase has been studied in bloodstream form *T. brucei*, nothing is yet known about the enzyme in the procyclic form.

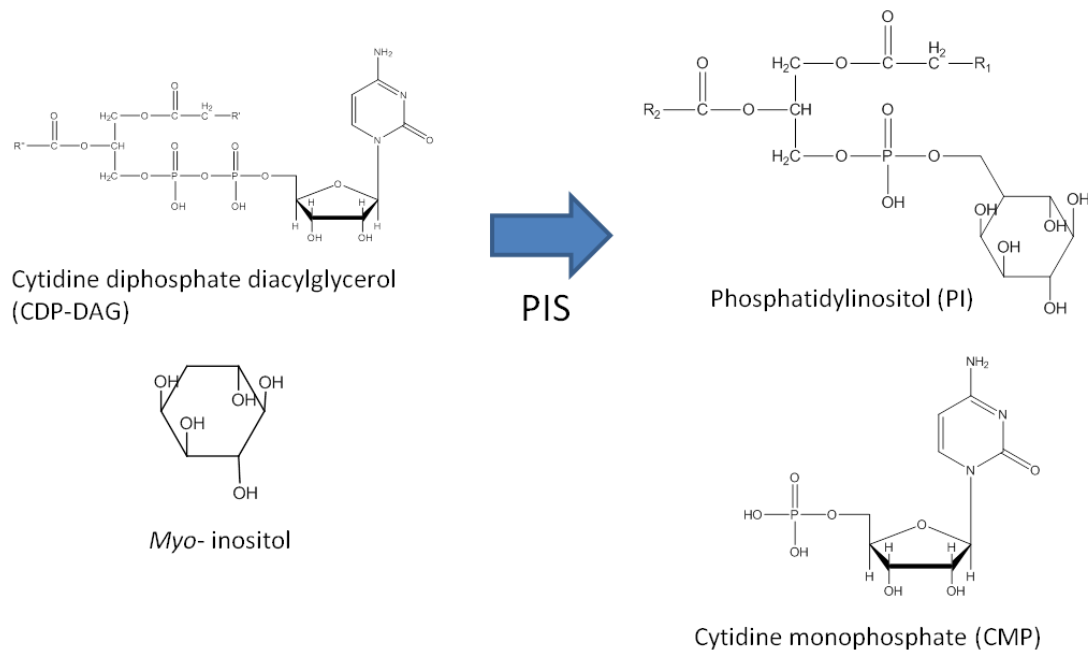


Figure 1.14. Reaction catalysed by Phosphatidylinositol synthase (PIS). R' and R'' – lipid chains which can be attached to the glycerol by acyl, alkyl or alkenyl links.

1.5.1 Gene

A PI synthase gene was first discovered in yeast by complementing a mutant that was null in PI synthesis (Nikawa et al., 1987a), followed by inducible expression of this yeast PIS1 gene in *E. coli*, which itself lacks the enzyme (Nikawa et al., 1988). The gene has now been cloned from a variety of sources including rat liver (Tanaka et al., 1996), human placenta (Lykidis et al., 1997) *Arabidopsis thaliana* (Collin et al., 1999, Haselier et al., 2010), *Toxoplasma gondii* (Seron et al., 2000) and *T. brucei* (Martin and Smith, 2006b).

Phylogenetic analysis by Lykidis (2007) showed the eukaryotic PIS genes formed a monophyletic group. This means that the PIS gene probably evolved just once in an ancestral eukaryote. In the few prokaryotic groups which do encode PIS activity the gene involved (PGSA) appears to be unrelated to the eukaryotic gene, suggesting the gene involved independently in these lineages (Lykidis, 2007).

1.5.2 Sequence/Structure

In *A. thaliana* the cDNA AtPIS1 is predicted to encode a protein 227 amino acids long with a molecular weight of 25.9 kDa (Collin et al., 1999). The yeast PIS is 25 kDa

(Nikawa et al., 1987a) and mammalian enzymes have an apparent molecular mass of between 20 and 25 kDa (Antonsson, 1997).

All PI synthases are hydrophobic, with the protein from rat containing 60% hydrophobic amino acids in three main clusters (Tanaka et al., 1996) with at least five trans-membrane regions in an *A. thaliana* protein (Collin et al., 1999).

There is a conservative domain common to several alcohol phosphotransferases: D(X)₂DG(X)₂AR(X)₂N(X)₅G(X)₃D(X)₃D. This is in the hydrophilic region of the yeast and *Arabidopsis* PIS protein and is thought to be a domain of the active site (Collin et al., 1999). Several organisms encode enzymes with putative phosphorylation sites.

1.5.3 Subcellular Localisation

In all organisms studied so far, PI synthase has been shown to be a multiple membrane bound protein and PI synthase activity is predominantly associated with the ER. The enzyme has also been localised to the mitochondria in yeast (Cobon et al., 1974, Kuchler et al., 1986) and the plants - cauliflower and potato (Sumida and Mudd, 1970, de Virville et al., 2010) but not in *A. thaliana* or *Nicotiana benthamiana* (de Virville et al., 2010). There has also been activity reported from the nuclear membrane of rabbit cerebral cortex (Baker and Chang, 1990) and Golgi in rat liver (Williamson and Morre, 1976). Finally, in several organism PI synthesis activity has been associated with the plasma membrane (Kinney and Carman, 1990, Imai and Gershengorn, 1987, Chicha et al., 1993, Galvao and Shayman, 1990, McPhee et al., 1991).

There is much debate about the presence of the PI synthase activity in plasma membranes. In rat pituitary, the PI synthase activity from plasma membrane was found to be more extractable than its ER counterpart by high salt concentrations (3M NaCl₂ or KCl₂). This salt extractable activity differed in its pH optima, dependence on Mg²⁺ and the K_m for *myo*-inositol (Imai and Gershengorn, 1987). This could be due to two different enzymes, or it could just be due to differences in the local environment. However, PI synthase activity from rabbit proximal tubule plasma membranes was not shown to have significant kinetic differences to that from the ER (Galvao and Shayman, 1990).

One thought on the dual localisation of PI synthase in mammals is attributed to its requirement for phosphoinositide signalling. It has been suggested that there are two

pools of PI in mammalian cells - one which is sensitive to hormone induced hydrolysis, and one which is not (Koreh and Monaco, 1986, Cubitt and Gershengorn, 1989). In a cell free system using turkey erythrocytes the hormone sensitive pool of PI was re-synthesised in the plasma membrane fraction alone (Vaziri et al., 1993). It is tempting to think that the membrane localised PI synthesis activity has a role in producing PI for cell signalling fates, however this is far from proven. Certainly, requirement for different PI pools would not give evidence for separately compartmentalised PI synthase enzymes since the transport of PI between cellular compartments by PI transport proteins is well characterised - reviewed in (Wirtz, 2006).

The conundrum of the presence of plasma membrane localised PIS may be explained by a recent investigation by Kim and co-workers who have produced results indicating that PI synthesis occurs in a unique, highly mobile membrane compartment designated the PIPEROsome (PI Producing ER-derived Organelle) that makes contact with multiple cellular compartments, including the plasma membrane (Kim et al., 2011).

Interestingly, in bloodstream form *T. brucei* a single tagged PI synthase enzyme was found to be present in both the ER and the Golgi (Martin and Smith, 2006b). Since it has been shown that *de novo* synthesised inositol is used exclusively for the synthesis of PI for GPI anchors (Martin and Smith, 2006a) it seems that the two enzyme locations correspond to separate pools of inositol - one pool of PI in the Golgi made from exogenously acquired inositol and used for bulk phospholipid; and one pool of PI in the ER made from *de novo* synthesised inositol and used for GPI anchors. This has been confirmed in procyclic *T. brucei* where knockdown of an inositol transporter localising to both the plasma and Golgi membrane depleted cellular PI and IPC but had no effect on the formation of GPI anchors (Gonzalez-Salgado et al., 2012).

1.5.4 Specificity/Kinetics

All PIS proteins expressed so far, including the *T. brucei* enzyme expressed in *E. coli* (Martin and Smith, 2006b) require divalent cations Mg^{2+} and/or Mn^{2+} for activity, and have an alkaline pH optimum.

For the mammalian enzyme (Antonsson, 1994), and that from *Candida albicans* (Antonsson and Klig, 1996) Mn^{2+} was efficient at activating the enzyme at lower

concentrations (0.1 - 1 mM) whilst higher concentrations were inhibitory, and at around 50 mM the enzyme showed complete inhibition. The optimal concentration of Mg^{2+} was between 10 and 100 mM but the optimal activity obtained from the enzyme was 2 - 4 fold higher than that obtained with manganese. In the yeast enzyme, the converse was true with manganese being more efficient an activator than magnesium (Fischl and Carman, 1983). The *C. albicans* enzyme on the other hand, was not affected by manganese (Antonsson and Klig, 1996).

Manganese also had a stabilising effect on the extracted enzyme which was not present with magnesium (Antonsson, 1994, Parries and Hokinneaverson, 1984, Monaco et al., 1994). Divalent cations of zinc and calcium inhibited the human placental (Antonsson, 1994) and the *Candida albicans* enzyme (Antonsson and Klig, 1996).

The affinity of PIS for its substrates varies between different enzyme sources. The reported K_m of the *T. brucei* PIS for *myo*-inositol is 2 μM - considerably less than those previously reported from other sources including yeast enzyme at 0.1-0.21 mM (Fischl and Carman, 1983, Kelley et al., 1988) and human placenta at 0.28 mM (Antonsson, 1994). There are nine possible stereoisomers of inositol (*myo*-, *muco*-, *neo*-, *epi*-, *D*(+)-*chiro*-, *L*(-)-*chiro*-, *cis*-, *allo*- and *scyllo*-) but only *myo*-inositol has been found incorporated into phospholipids (Agranoff and Fisher, 1991). With the exception of some earlier reports (Paulus and Kennedy, 1960, Benjamins and Agranoff, 1969), all investigators have found other inositol isomers to be poor substrates for PIS enzymes (Antonsson, 1997). The enzyme from *T. brucei* is no exception, where at 25 μM only *myo*-inositol was able to affect the incorporation [3H] *myo*- inositol into [3H] PI (Martin and Smith, 2006b).

For CDP-DAG, the reported K_m value for the rat liver enzyme is 9.5 μM , whilst the human and *Candida albicans* enzymes have 36 μM affinities. In all these organisms, CDP-DAG concentrations above 0.4 - 0.5 mM are inhibitory. PIS from human placenta can also equally well use dCDP-DAG (45 μM) as CDP-DAG (36 μM) a substrate (Antonsson, 1994). dCDP-DAG also did not show inhibition at high concentrations, so the maximum activity was 25% higher with dCDP-DAG compared to CDP-DAG. The same pattern is not seen for the enzyme from *C. albicans* where the K_m for dCDP-DAG was only 29 μM (compared to CDP-DAG at 36 μM) and although dCDP-DAG showed no

inhibition, maximal activity was only 36% of that seen with CDP-DAG (Antonsson and Klig, 1996).

Whilst it has been investigated, and some differences have been found, there is no conclusive evidence about preference of PIS for lipid chain length or degree of saturation on CDP-DAG (Benjamins and Agranoff, 1969, Bishop and Strickland, 1976, Li et al., 1988).

The yeast enzyme catalyses a Bi-Bi sequential reaction mechanism, whereby PI synthase binds to CDP-DAG before inositol and PI is released before CMP (Fischl and Carman, 1983).

1.5.5 Inhibitors

For both human placenta and *C. albicans* PIS enzymes, nucleoside tri-phosphates had a greater more inhibitory effect than nucleoside di-phosphates. Nucleoside mono-phosphates had no effect on the human enzyme but CMP and AMP inhibited the *C. albicans* enzyme to a low extent. For both enzyme sources the strongest inhibition came from pyro- and ortho-phosphates (K_i 0.2 and 0.8 mM) (Antonsson, 1994, Antonsson and Klig, 1996).

Chlorinated analogues of PI hexachlorocyclohexanes have been shown to inhibit incorporation of inositol into PI. The strongest inhibitors were isomers with the same stereochemistry as *myo*-inositol (Parries and Hokinneaverson, 1985, Pulido et al., 1992). However, this inhibition was not competitive or specific to the inositol processing enzymes. Other *myo*-inositol derivatives substituted at the 3-position on the inositol ring were used as substrates by the human enzyme, suggesting that this position is not important in the reaction with the enzyme (Johnson et al., 1993). However, in the *T. brucei* enzyme, high concentrations of *neo*-, *epi*-, L(-)-*chiro*-, *allo*-, *scyllo*-, 1-deoxy-1-fluoro-*scyllo*-, 2-OMe-*myo*-, 1-deoxy-1-fluoro-*myo*-, 3-deoxy-3-fluoro-*myo*- and D₆-*myo*- inositol caused a reduction in the incorporation of [³H]*myo*-inositol into [³H]PI. These results show that at this very high concentration they were able to interact with the TbPIS, and that the orientation of the 1-, 3- and 4- hydroxyls were important and represent the minimum recognition motif for TbPIS (Figure 1.15) (Martin and Smith, 2006b).

Some analogues of CDP-DAG have also been tested as inhibitors. When the phosphate was replaced by a methyl group it was found to competitively inhibit the human enzyme with a K_i of 32 nm (Vargas et al., 1984).



Figure 1.15. Minimum Structural recognition for *T. brucei* phosphatidylinositol synthase. Martin and Smith found the orientation of the 1-, 3- and 4- hydroxyls on the inositol ring were important for enzyme recognition (Martin and Smith, 2006)

1.5.6 Exchange reaction

The reaction for synthesis of PI by exchange of a new *myo*-inositol headgroup with that on an existing PI has been found in the ER of animals, plants, a slime mould, *Crithidia fasciculata* and *Chlamydomonas reinhardtii* (Blouin et al., 2003). This reaction also needs Mn^{2+} but has a lower pH optimum lower than that of the transferase activity. However, evidence suggests that both these activities are carried out by the same enzyme and the ability of known PI synthases to carry out this reaction have been demonstrated in recombinant PIS enzymes from *S. cerevisiae* (Klezovitch et al., 1993), *A. thaliana* (Justin et al., 2002) and *T. brucei* (Martin and Smith, 2006b). In *T. brucei* this activity is greatly stimulated by 4 μ M CMP.

1.5.7 Expression/Regulation

As is the case with CDP-DAG synthase, the mechanism of regulation of PI synthase in yeast (encoded by PIS1) has been well studied, and is reviewed by Carman and Han (2011). Expression of the PIS1 gene, unlike the CDS gene, does not respond directly to inositol, although a UAS_{INO} sequence is found upstream of the coding sequence (Fischl et al., 1986). Instead, PIS1 expression is transcriptionally regulated by carbon source (Anderson and Lopes, 1996). PIS gene expression is reduced by the presence of glycerol in the growth medium as opposed to glucose, and increased when cells

are grown on galactose. This regulation involves binding of the Mcm1 protein to the *cis*-MCEs sequence and the involvement of two-component regulatory gene *SLN1* (Anderson and Lopes, 1996). Inositol supplementation causes a rapid and dramatic increase in the synthesis of PI by increased substrate availability for PI synthase, but also by directly inhibiting the activity of PS synthase, which increases availability of CDP-DAG for PIS (Kelley et al., 1988). Increase in the CDP-DAG substrate by overexpression of CDS increases PIS activity, while decrease in CDS activity also decreases that of PIS. This occurs without a change in transcription levels of PIS1 (Shen and Dowhan, 1997). Independent of inositol concentration, zinc depletion causes increased expression of PIS1 by the interaction of transcriptional activator protein Zap1p with a zinc responsive *cis*-acting element (UAS_{ZRE}) in the promoter (Han et al., 2005). Other than in yeast, little about regulation is known. In mammals PI synthesis activity is up-regulated in response to hormone induced phospholipase C mediated hydrolysis of IP₃, but the mechanism is unknown (Monaco and Adelson, 1991). Additionally, PI synthesis maybe regulated by feedback inhibition from PI (Imai and Gershengorn, 1987).

1.5.8 PI Synthase as a Drug Target in *T. brucei*

Phosphatidylinositol synthase has already been shown to be essential in bloodstream form *T. brucei* (Martin and Smith, 2006b) but nothing has been shown in the procyclic form. However, it was thought that bloodstream form cells were dying due to their inability to make GPI anchors, and as previously mentioned the procyclic null of an enzyme involved in GPI anchor formation is viable (Guther et al., 2006), so PI may not be essential for GPI anchor formation in the procyclic form. Nevertheless, PI is responsible for the formation of IPC and PIPs, which could give insight into an essential role phosphoinositide signaling has in these parasites.

1.6 Objectives

Phospholipid synthesis in *T. brucei* is being elucidated, and differences are being found between the parasite and its human host which can hopefully be exploited in drug development. For example, the lack of cross-talk between branches of the Kennedy pathway and the essential requirement for GPI anchor synthesis may make the parasite vulnerable to inhibition of these pathways. Little is currently known about the CDP-DAG pathway and its downstream uses and products but the

essentiality of downstream enzymes, such as PI synthase and CL synthase certainly indicate that the pathway is important.

The objective of this work was to investigate the synthesis of the key, high energy donor lipid intermediate CDP-DAG in *T. brucei* by the enzyme CDP-DAG synthase, with particular emphasis on its affect on the GPI anchor biosynthetic pathway. In order to investigate the impact of its altered expression upon other phospholipid pathways, CDS expression mutants were created in both bloodstream form and procyclic form parasites.

Additionally, further investigation of PI synthesis was undertaken. In addition to further investigation into its localisation, the procyclic PI pathways were studied in order to determine its affect on the GPI biosynthetic pathway, as well as its contribution to IPC and PIPs.

Chapter 2: Materials and Methods

2.1 General

2.1.1 Reagents

Unless otherwise stated, chemicals were purchased from either Sigma-Aldrich or BDH (VWR international). Restriction endonucleases and DNA modifying enzymes were obtained from either New England BioLabs or Promega. [2-³H]Ethanolamine (50 Ci/mmol) and D-[2-³H]mannose (15 Ci/mmol) were purchased from Amersham. [9,10-³H(N)]-Tetradecanoic acid (myristic acid) (47 Ci/mmol) was obtained from Perkin Elmer and L-[³⁵S]methionine (1175 Ci/mmol) from MP Biochemicals. The remainder of radiolabelled substrates were from American Radiolabelled Chemicals: [2-³H]-Glucose (30 Ci/mmol); GDP-[2-³H]-Man (20 Ci/mmol); [1-³H]-UDP-GlcNAc (20 Ci/mmol); [2-³H]-inositol (20 Ci/mmol); L-[3-³H]-serine (20 Ci/mmol); [5-³H]CTP (25 Ci/mmol); [1,2,3-³H]-glycerol (20 Ci/mmol).

Kodak Biomax MS film came from Kodak SA and Amersham Hyperfilm MP came from GE Healthcare Life Sciences.

Competent *E. coli* strains DH5 α and Top10 (Invitrogen) were used for routine manipulation, and Rosetta 2 (DE3) competent cells (Merck Millipore) were used for protein overexpression. Culturing media for *E. coli* were provided by the media kitchen at the University of St. Andrews.

Primers were synthesised by either Thermo Scientific or Eurogentec.

2.1.2 Bioinformatics

The following databases were used in order to obtain DNA and protein sequence information: for general information, NCBI GenBank (<http://www.ncbi.nlm.nih.gov>) and associated BLAST tools were used, for specific information on Trypanosomatid and *S. cerevisiae* sequences, TriTrypDB (<http://tritrypdb.org/tritrypdb>) and *Saccharomyces* database (SDB) (<http://www.yeastgenome.org>) were used, respectively.

Phylogenetic analysis was performed using MobyLe@Pasteur platform from the Institut Pasteur "Projets et Développements en Bioinformatique" Team and the Ressource Parisienne en Bioinformatique Structurale (<http://mobyLe.pasteur.fr>). Sequences were aligned using Mafft (Kato et al., 2002, Kato et al., 2005, Kato and Toh, 2008), Clustal O 1.0.2 or Clustal W: Multiple Alignment (Sievers et al., 2011) algorithms. Alignments were manually checked and gap regions and ambiguously aligned regions were excluded from further analysis. Distance matrices were created using ProtDist, (Felsenstein, 1980b), and distance based phylogeny reconstructions were computed using BioNJ (Gascuel, 1997), QuickTree (Howe et al., 2002) Fitch, Kitsch or Neighbor (Felsenstein, 1980a, Felsenstein, 1980b). Maximum likelihood and Maximum Parsimony (ProtPars) were both performed using PHYML (Felsenstein, 1980b).

Sequence hydrophobicity analysis and topology prediction of protein sequence was performed using TopPred 0.01 (Claros and Vonheijne, 1994, Vonheijne, 1992) using the Kyte-Doolittle (KD) scale (Kyte and Doolittle, 1982).

2.1.3 PCR

Polymerase chain reaction (PCR) was carried out in either MJ Mini™ Personal Thermal Cycler (BioRad) or the GeneAmp® PCR System 2700 (Applied Biosystems).

For applications where high fidelity of the DNA polymerase was essential, KOD Hot Start DNA Polymerase from Novagen® was used. A standard reaction contained 4 µl of 25 mM MgSO₄, 5 µl of dNTP mix (2 mM each), 5 µl of 10X buffer for KOD Hot Start DNA polymerase and 1 µl of KOD DNA polymerase (1 U/µl) all supplied by Novagen. 1 µl of each 20 µM primer was used, and usually 1 µl of template DNA (usually diluted to 10-100 ng/µl). The reaction was brought to a total volume of 50 µl using sterile, deionised water. A standard temperature cycle consisted of 1 cycle of 95°C for 3 minutes, 35 cycles of 95°C for 20 seconds, annealing temperature for 15 seconds and 70°C for 10-15 s/kb product size. This was followed by a final extension step at 70°C for 4 minutes. Primers sequences and annealing temperatures are given in Table 2.1.

Table 2.1 Primer sequences and PCR conditions for TbCDS and TbPIS

Template	Region Amplified [PCR product length [bp]]	Primers (5' to 3')	PCR parameters
<i>T. brucei brucei</i> Lister 427 genomic DNA	TbCDS 5'UTR + ORF [1737]	TbCDS F1 - ATAAGTAAgcgggcgcTGATTAACGCACCC TbCDS pLEW R- TGCTtaattaaCTATCCTGTGAGAACCTATTAAG	95°C – 3 min 35 cycles: [95°C – 20s 52°C – 20s 70°C – 30s] 70°C – 5 min (KOD polymerase)
<i>T. brucei brucei</i> Lister 427 genomic DNA	TbCDS ORF + 179bp 3'UTR [1400]	TbCDS pLEW F TbCDS R2' AGTAAgcgggcgcCCTTGAAAACAATGGTGTATAC	95°C – 3 min 35 cycles: [95°C – 20s 54°C – 15s 70°C – 40s] 70°C – 4 min (KOD polymerase)
<i>T. brucei brucei</i> Lister 427 genomic DNA	TbCDS ORF [1221]	TbCDS pET F – GAGgagatccGATGAAAAACAAGTCCAGCAAG TbCDS pET R - GAGGctcgaagTTCTGTGAGAGACCTATTAAG	95°C – 3 min 35 cycles: [95°C – 20 s 58°C – 20 s 70°C – 30 s] 70°C – 5 min (KOD polymerase)
<i>T. brucei brucei</i> Lister 427 genomic DNA	TbCDS ORF [1221]	TbCDS pET F – as above TbCDS-YeastRescue-R CGGctcgaagCCTATTCTGTGAGAGACCTATTAAGAGTCGAG	95°C – 3 min 35 cycles: [95°C – 20 s 62°C – 20 s 70°C – 30 s] 70°C – 5 min (KOD polymerase)
<i>S. cerevisiae</i> genomic DNA	Yeast CDS1 ORF [1374]	yeastCDS1 F CCCaagcttATGTCTTGACAACCTGGAGATGAA YeastCDS1 R CGGctcgaagTTCAAGAGTGATTGGTCAATGATTTCTGGTCAC	95°C – 3 min 35 cycles: [95°C – 20 s 65°C – 20 s 70°C – 40 s] 70°C – 5 min (KOD polymerase)

Template	Region Amplified [PCR product length (bp)]	Primers (5' to 3')	PCR parameters
<i>T. brucei brucei</i> Lister 427 total RNA	TbCDS mRNA [≥1221]	Mini Exon – AACGCTATTATTAGAACAGTTTCTGTACTATA TT new CDS 82R (as above)	55°C – 30 min 94°C – 2 min 35 cycles: [94°C – 15 s 58°C – 30 s 72°C – 1.5min] 7°C – 5 min (Superscript III rt/Platinum Taq and GoTaq)
<i>T. brucei brucei</i> Lister 427 genomic DNA	TbCDS ORF [1221]	New CDS pLEW F GAGaagcttATGAAAAACAAGTCCAGCAAG New CDS pLEW R TGCTtaattaaCTTTTCTGTGAGAGACCTATTAA G	95°C – 3 min 35 cycles: [95°C – 20 s 58°C – 20 s 70°C – 30 s] 70°C – 5 min (KOD polymerase)
<i>T. brucei brucei</i> Lister 427 genomic DNA	TbCDS 5'UTR [516]	TbCDS F1 Tb CDS R1 - CGTTTAAACTTACGGACCGT CaagcttCTAGAC GCTTTCCTGAAAAATGC	95°C – 2 min 35 cycles: [95°C – 20 s 60°C – 15 s 70°C – 40 s] 70°C – 4 min (KOD polymerase)
<i>T. brucei brucei</i> Lister 427 genomic DNA	TbCDS 3'UTR [179]	CDS F2 CDS R2'	95°C – 2 min 35 cycles: [95°C – 20 s 60°C – 15 s 70°C – 10 s] 70°C – 4 min (KOD polymerase)
<i>S. cerevisiae</i> genomic DNA	Yeast CDS1 ORF [1374]	YeastCDS1 F CCCaagcttATGTCTTGACAACCTGGAGATGA A YeastCDS1 R CGGgtcgaagTTCAAGAGTGATTGGTCAATGAT TTCTTGGTCAC	95°C – 3 min 35 cycles: [95°C – 20 s 65°C – 20 s 70°C – 40 s] 70°C – 5 min (KOD polymerase)

Template	Region Amplified [PCR product length (bp)]	Primers (5' to 3')	PCR parameters
TbCDS 3' UTR and TbCDS 5' UTR	TbCDS Knitted UTRs [695]	TbCDS F1 TbCDS R2'	1. Knitting PCR 95°C – 5 min 5 cycles: [95°C - 1 min 54°C – 1 min 74°C – 2 min] 3. Add primers and amplify 35 cycles: [95°C – 20 58°C – 15 74°C – 30s] 74°C – 4 min
<i>T. brucei brucei</i> Lister 427 CDS- HA ^{T1} ΔCDS::PAC/ΔCDS::HYG genomic DNA	PURO ORF + CDS 3' UTR [779]	Puro F AAGCTTATGACCGAGTACAAGCCCACGGTGCGCC TbCDS R2'	95°C – 2 min 35 cycles: [95°C – 20 s 58°C – 10 s 70°C – 30s] 70°C – 5 min (KOD polymerase)
<i>T. brucei brucei</i> Lister 427 CDS- HA ^{T1} ΔCDS::PAC/ΔCDS::HYG genomic DNA	HYG ORF + CDS 3' UTR [1205]	HYG F AAGCTTATGAAAAGCCTGAACTCACCGCGAC TbCDS R2'	95°C – 2 min 35 cycles: [95°C – 20 s 58°C – 10 s 70°C – 30s] 70°C – 5 min (KOD polymerase)
<i>T. brucei brucei</i> Lister 427 genomic DNA TbCDS p2T7	HYG ORF [1026]	HYG F HYG R GGATCCCTATTCCCTTGCCCTCGGACGAGTGCTGGGGCG	95°C – 5 min 35 cycles: [95°C – 20 s 60°C – 15 s 70°C – 30s] 70°C – 4 min (KOD polymerase)
<i>T. brucei brucei</i> Lister 427 genomic DNA TbCDS p2T7 - 177	PHLEO ORF [374]	PHLEO F CCCAAGCTTGGGATGGCCAAGTTGACCAAGTCCCGTTCC PHLEO R CGCGGATCCGCGTCAGTCTGCTCCTCGGCCACGAAGTGC	95°C – 5 min 35 cycles: [95°C – 20 s 65°C – 15 s 70°C – 30s] 70°C – 4 min (KOD polymerase)
<i>T. brucei brucei</i> Lister 427 genomic DNA	TbCDS ORF internal region [283]	TbCDSProbeF - ATAAGTAAgcgccgcGCCAGGGTGCAGCAACATGC TbCDSProbeR - AGTAAgctagcAACGCCGTTGCTCCTCGGGT	95°C – 2 min 35 cycles: [95°C – 30 s 65°C – 10 s 70°C – 55 s] 70°C – 5 min (KOD polymerase)

Primers F – forward primer; R – reverse primer; Not1 restriction sites are in lower case; NheI restriction sites are in lowercase, italic; HindIII restriction sites are in lowercase, underline; BamHI are in lowercase, underline, italic; PacI restriction sites are in lowercase, bold; XhoI restriction sites are in lowercase, bold, italic, underline. Linking regions are in blue, underlined. Red base indicates a mutation.

For diagnostic PCR reactions where fidelity was less important, the GoTaq[®] kit from Promega was used. A standard reaction contained 10 µl of 5X green GoTaq[®] reaction buffer, 1 µl of PCR Nucleotide Mix at 10 mM each, 1 µl of each primer at 20 µM each, 0.25 µl of GoTaq[®] DNA polymerase at 5 U/µl and 1 µl of template DNA (usually diluted to between 10-100 ng/µl). The final reaction volume was brought to 50 µl with sterile, deionised water. A standard temperature cycle consisted of one cycle of 2 minutes denaturation at 95°C, and 35 cycles of denaturation at 95°C for 1 minute, annealing temperature for 1 minute and 72°C extension for minute/kb. A final extension cycle of 72°C for 5 minutes was used.

For *E. coli* colony PCR, 1 colony was transferred into 6 µl of LB and mixed by vortexing. 1 µl of this was then used as a template in a PCR reaction as shown above but with a 10 minute initial denaturation time and with a final PCR volume of 10 µl.

2.1.4 RT-PCR

The absence of DNA from RNA was confirmed by performing standard PCR reactions with primers of known conditions to check no product was formed. Reverse transcription PCR was performed using the SuperScript[™] One-Step RT-PCR kit with Platinum[®] Taq (Invitrogen) following the manufacturers recommendation. Reaction components 2X Reaction Mix; 10 pg - 1 µg template RNA, 10 µM sense primer, 10 µM anti-sense primer, 1 µl 0.2 µM RT/ Platinum[®] Taq Mix, DEPC treated water to 50 µl. cDNA synthesis and pre-denaturation were performed with 1 cycle of 55°C for 30 minutes and 2 minutes at 94°C. PCR amplification was performed by 35 cycles of: 94°C for 15 s, 68-72°C for 1 min/kb, final extension was performed by 1 cycle of 72°C for 5 minutes. Primer sequences and conditions used are given in Table 2.1.

2.1.5 Restriction Enzyme Digestion

Standard restriction enzyme digests were performed using one unit of each restriction enzyme per µg of DNA, 2 µl of 10X buffer supplied by the restriction enzyme manufacturer and 0.2 µl of BSA (if required) in a total reaction volume of 20 µl. Where more DNA was to be digested, the reaction was scaled up accordingly. The reaction was allowed to proceed for 1-24 hours.

2.1.6 Ligation Reactions

Ligation of DNA was carried out using T4 DNA ligase (Promega). A typical ligation reaction consisted of DNA insert and DNA plasmid vector in a molar ratio of 3:1, one unit of T4 DNA ligase and T4 DNA ligase buffer made up to 10 µl total reaction. Ligations were incubated at room temperature for at least 30 minutes prior to transformation into DH5α *E. coli*.

2.1.7 Northern Blotting

2.1.7.a Synthesis of DIG-labelled probes

The plasmid phRL-CMV (with renilla ORF removed) containing the T7 promoter was obtained from Dr Ben Brennan, University of St. Andrews. Primers were designed to amplify a fragment of the CDS open reading frame (ORF) adding a *NotI* site to the forward primer, and *NheI* to the reverse primer (Figure 2.1, Table 2.1). The PCR product obtained with these primers was purified and digested with the restriction enzymes. This digested purified product was then cloned into *NheI* and *NotI* digested phRL-CMV vector in the reverse orientation, i.e. with the 3' end of the PCR product (the reverse primer) next to the T7 promoter in order that negative sense RNA was produced to detect positive sense RNA (Figure 2.1).

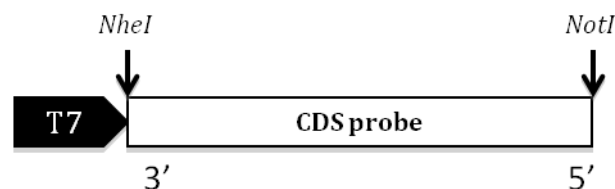


Figure 2.1. Orientation of CDS probe in phRL-CMV vector. In order that riboprobe transcripts could detect +ve sense RNA, the CDS probe PCR product was inserted into the cloning site in the 3'->5' direction.

NotI produces a 5' overhang at the end of the gene of interest, as templates with a 5' overhang allow more efficient *in vitro* transcription than those with a 3' overhang or blunt end (Roche). The DNA was then run on an agarose gel and purified using the QiaQuick gel extraction kit (Quiagen). 5 µg of plasmid DNA were digested and the linearised product was eluted in 30 µl.

2.1.7.b *In vitro* transcription

1 µg of template DNA in 20 µl diethylpyrocarbonate (DEPC) treated deionised water was combined with 8 µl 5X transcription buffer (Promega), 4 µl 100 mM DTT (Promega), 4 µl DIG labelling mix (Roche) and 80 U T7 RNA polymerase (Promega). The reaction mixture was incubated at 37°C for 2 hours. Two units of RQ1 RNase-free DNase (Promega) was then added and the mixture incubated at 37°C for a further 15 min. The reaction mixture was diluted 10-fold in DEPC-treated deionised water (up to 400 µl).

2.1.7.c *Quantification*

Quantification of DIG-labelled probes was carried out by serial dilution and direct detection, as described in the manufacturer's protocol.

2.1.7.d *Gel Loading and Transfer*

5 µg RNA was made up to a final volume of 60% formamide, 10X RNA loading dye (50 mM Tris-HCl pH 7.6; 0.25% bromophenol blue; 60% glycerol) and 1 µl ethidium bromide per sample. Samples were denatured at 70°C for 5 minutes and chilled immediately on ice for 5 minutes. Samples were run on a 1.2% agarose gel made up with 1X TAE buffer (40 mM Tris, 20 mM acetic acid, 1 mM EDTA), which was also used as the running buffer. After running, gel was washed twice in 10 x SSC (1.5 M NaCl, 0.15 M Tri-sodium citrate, pH 7). A piece of Amersham Hybond™ N⁺ membrane was prepared by soaking in 10X SSC. The blotting stack was prepared by soaking two pieces of Whatman paper in 10X SSC, and leaving another two pieces of paper dry, along with a wick the same width as the DNA gel and paper pieces. The stack was prepared as shown in Figure 2.2. From the bottom: a stack of paper towels, followed by two pieces of dry Whatman, one piece of wet Whatman, the membrane, the agarose gel (at which point the agarose gel wells were marked onto the membrane) and the second piece of wet Whatman. This stack was insulated using Clingfilm, and the Whatman wick was drawn through the trough of transfer buffer and placed across the top of the insulated stack with each end in a trough of buffer. The wick was only allowed to make contact with the wet Whatman at the top of the stack. The gel was allowed to transfer overnight. After blotting, the membrane was washed in 2X SSC for 5 minutes and allowed to dry. RNA was cross linked to the membrane using Stratalinker® UV Crosslinker (Stratagene) on the auto cross link setting.

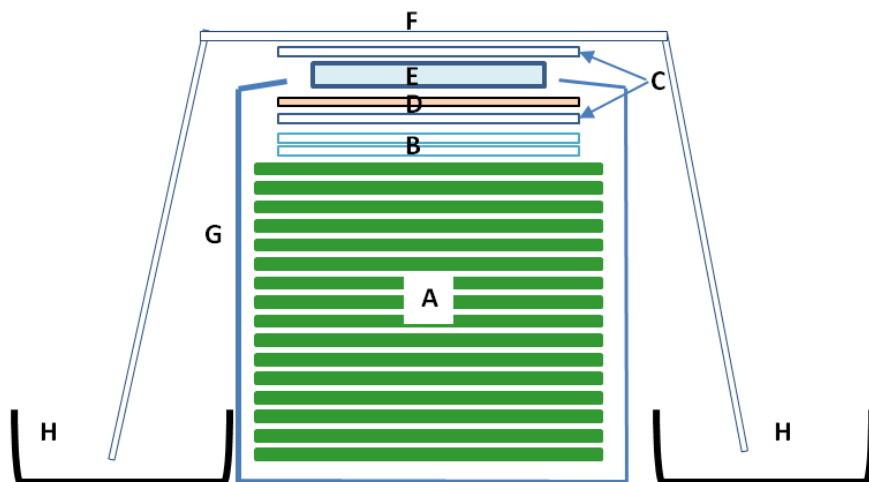


Figure 2.2. Schematic showing the transfer stack used for Southern and Northern blots. **A.** Paper towel stack. **B.** Two pieces of dry Whatman 3mm paper. **C.** Two pieces of Whatman 3mm paper soaked in transfer buffer. **D.** Charged transfer membrane. **E.** Agarose gel. **F.** Wick of Whatman 3mm paper. **G.** Clingfilm around whole stack to ensure wick only makes contact with top of stack. **H.** Troughs containing transfer buffer.

2.1.7.e Hybridisation

The membrane was placed in a hybridisation tube with 10 ml of 50% formamide hybridisation buffer (50% deionised formamide, 5X SSC, 0.1% (w/v) lauroyl sarcosine, 0.02% (w/v) SDS, 2% blocking reagent (Roche) preheated to 68°C and allowed to pre-hybridise at 68°C for 30 minutes with rotation. 150 ng of DIG-labelled probes were denatured by boiling for 5 minutes and then cooled rapidly in ice water. 150 ng of probe was added to 10 mls of 50% formamide hybridisation buffer, and the pre-hybridisation buffer was poured off the membrane and replaced with the formamide hybridisation buffer plus probe. The membrane was allowed to hybridise overnight with the probe at 68°C. After the hybridisation step, the membrane was washed twice in 2X SSC /0.1% SDS at room temperature for 15 minutes (low stringency wash) followed by two washes with 0.1X SSC/ 0.1% SDS at 68°C for 30 minutes (high stringency wash).

2.1.7.f Probe Detection

The membrane was rinsed briefly in washing buffer (0.15 M NaCl, 0.1 M maleic acid pH 7.5, 0.3% Tween-20) and blocked in 10 ml blocking buffer (1X blocking reagent in 0.1 M maleic acid, 0.4 M NaCl pH 7.5) for 30 minutes with constant agitation. The DIG labelled probes were detected by first incubating with 75 mU/ml anti-Digeoxigenin-AP (Roche) in 10 ml blocking buffer for 1 hour, followed by two 30

minute wash steps with 10 ml washing buffer. The membrane was equilibrated for 5 minutes in 10 ml detection buffer (0.15 M NaCl, 0.1 M maleic acid, pH 9.5) before detection. The membrane was placed in a plastic envelope and detection was performed using 3-4 drops of CDP-Star[®] chemiluminescent substrate (Roche) diluted in ~1 ml of detection reagent and applied to the membrane. The plastic was folded over the membrane and the reagent rolled out to cover the membrane, which was then incubated for about 5 minutes. The excess liquid was then rolled out and the membrane exposed to film.

2.1.8 Southern Blotting

2.1.8.a Digests for TbCDS Southern

Approximately 5 µg of DNA was digested with 2-10 U restriction enzyme, the appropriate buffer and BSA where required in a total volume of 40 µl. The mixture was incubated at the optimum enzyme temperature for at least four hours, usually overnight.

2.1.8.b DNA gel electrophoresis for Southern Analysis

A 1% agar in TAE buffer gel was prepared using only 2.5 µl of ethidium bromide/100 ml gel volume (40 mM Tris, 20 mM acetic acid, 1 mM EDTA). The 40 µl DNA digest plus 5X loading dye was run in one lane, beside 3 µl of Hyperladder (Bioline). The DNA gel was run at 50 V for 3-4 hours after which it was removed to a rocker and DNA was denatured with 0.4 M NaOH for 10-20 mins. The gel was rinsed briefly in deionised water, then neutralised by soaking in at least 50 ml 2X SSC (300 mM NaCl; 15 mM Na₃C₆H₅O₇) for 30 minutes. The solution was refreshed and soaking was continued for a further 15 minutes.

2.1.8.c Transfer

Transfer of DNA onto Amersham Hybond[™]-N⁺ membrane was performed as described for Northern blotting above, Figure 2.2, except that the transfer buffer was 2X SSC.

The stack was left to transfer for 20 min per mm of agarose gel thickness.

2.1.8.d DIG Probe Labelling

Probes were produced from PCR products using the DIG High Prime Labelling Kit (Roche). 3 µg of PCR product was labelled in a total reaction volume of 16 µl. This

was heated to 95°C for 10 minutes in order to denature the DNA, followed by the addition of 4 µl DIG High Prime (Roche). The mixture was then incubated at 37°C for 20 hours after which the labelling was terminated by incubating at 65°C for 10 minutes, and the probe mixture was stored in the freezer until required.

2.1.8.e Probe Quantification

Quantification of DIG-labelled probes was carried out by serial dilution and direct detection as described in the manufacturer's protocol.

2.1.8.f Probe detection

After transfer, the membrane was moved onto clean, dry Whatman paper and cross linked using the UV crosslinker. The membrane was added to a hybridisation tube in a rotary incubator containing 10 ml of DIG Easy Hyb (Roche) pre-warmed to 42-65°C, and incubated at this temperature for 30 minutes for pre-hybridisation

DIG labelled probes were de-natured at 95°C for 5 minutes, chilled briefly on ice water and added to a fresh 10 ml of pre-warmed DIG Easy Hyb at a concentration of 25 ng/ml. The membrane was then incubated with this probe mixture and allowed to hybridise overnight at 42-65°C. Stringency washes were performed at 42-65°C, for example twice for 5 minutes in 2X SSC, 0.1% SDS, twice for 15 minutes in 0.1-0.5X SSC, 0.1% SDS.

The membrane was then rinsed briefly in washing buffer (0.1 M maleic acid, 0.15 M NaCl pH 7.5, 0.3% (w/v) Tween 20) and blocked with copious blocking solution (1X blocking reagent (Roche) diluted in 0.1 M Maleic acid, 0.15 M NaCl pH 7.5) for at least 30 minutes.

The membrane was incubated in 20 ml antibody solution (75 mU/ml anti-Digeoxigenin-AP in blocking solution) for 30 minutes, followed by 3 washes with washing buffer (10 min, half hour, half hour). The membrane was then equilibrated in detection buffer (0.1 M Tris-HCl, 0.1 M NaCl, pH 9.5).

Antibody-AP conjugate bound to the membrane was then detected by the application of CDP-Star[®] chemiluminescent substrate (Roche) diluted in ~1 ml of detection reagent and applied to the membrane. The plastic was folded over the membrane and the reagent rolled out to cover the membrane, which was then incubated like

this for about 5 minutes. The excess liquid was then squeezed off the blot and the membrane was exposed to film.

Southern blots using [³²P] labelled primer as probe (Hartmann Analytic) were carried out according to the same protocol, except that detection was carried out using Kodak High Energy film with a high intensity specific screen and exposed at -80 °C

2.1.9 Western Blotting

Protein samples were run on SDS-PAGE gels before transferring to nitrocellulose membrane (Hybond ECL, Amersham Biosciences). Six pieces of Whatman 3 MM paper were cut to a similar size as the gel and two pieces were soaked in anode 1 solution (0.3 M TRIS; 20% methanol); two pieces in anode 2 solution (25 mM Tris; 20% methanol) and two pieces in cathode solution (25 mM Tris; 40mM glycine, 20% methanol). The transfer stack was arranged (from bottom to top: anode 1, anode 2, membrane, gel, cathode) in a TE 70 Semi-Dry Transfer Unit (Amersham) and run for 1 hour at 45 mA. The membrane was blocked overnight at 4 °C in a solution of 5% skimmed milk powder in PBS. After overnight blocking, the membrane was allowed to reach room temperature before the detection of protein with anti-HIS HRP conjugated antibodies (Clonotech) (1:10000) to detect HIS tags or anti-HA high affinity rat monoclonal (Roche) (1:5000) to detect HA tags, followed by anti-RAT HRP (1:5000). Fluorescence was detected using Amersham ECL detection reagent (GE Healthcare) according to the manufacturer's instructions.

2.1.10 Transformation of *E. coli*

Transformation of *E. coli* cells with plasmid DNA was typically performed using 1 µl of a plasmid Miniprep (see later) or 5 µl of a ligation reaction (Section 2.1.6). Chemically competent *E. coli* cells were incubated with the plasmid on ice for at least 30 minutes and then heat shocked at 42 °C for 45 seconds. The cells were then chilled on ice for one minute before adding 150 µl of SOC medium (0.5% yeast extract, 2% tryptone, 10 mM NaCl, 2.5 mM KCl, 10 mM MgCl₂, 10 mM MgSO₄, 20 mM glucose) or LB medium (1% tryptone, 0.5% yeast extract, 1.0% NaCl pH 7.0) and shaken for one hour at 37 °C. The mixture was then plated out on LB agar containing the appropriate selection antibiotics for the plasmid. The plates were incubated at 37 °C overnight to obtain individual colonies.

2.1.11 Plasmid Purification

A single bacterial colony was picked from the transformation plate and transferred to 10 ml of liquid media (LB or T. broth (1% bacto-tryptone, 0.5% NaCl)) along with the appropriate antibiotics for selection of the plasmid. The culture was grown in a shaking incubator at 37°C overnight. Cells were harvested by 15 minutes centrifugation at 13,000 rpm in a Beckmann benchtop centrifuge. The cell pellet was washed in PBS and plasmid DNA extracted using QIAprep Spin MiniPrep Kit (Quiagen).

2.1.12 Sequencing

All sequencing of DNA was carried out either by DNA Sequencing & Services™ at the University of Dundee or GATC Biotech.

2.1.13 ES-MS

Total lipid extracts were dissolved in 15 µl of chloroform : methanol (1:2) and 15 µl of acetonitrile:isopropanol:water (6:7:2) and analysed with a Absceix 4000 QTrap, a triple quadrupole mass spectrometer equipped with a nanoelectrospray source.

Samples were delivered using either thin-wall nanoflow capillary tips or a Nanomate interface in direct infusion mode (~125 nl/min). The lipid extracts were analysed in both positive and negative ion modes using a capillary voltage of 1.25 kV. MS/MS scanning (daughter, precursor and neutral loss scans) were performed using nitrogen as the collision gas with collision energies between 35-90 V. Each spectrum encompasses at least 50 repetitive scans.

Tandem mass spectra (MS/MS) were obtained with collision energies as follows: 35-45V, PC/SpM in positive ion mode, parent-ion scanning of m/z 184; 35-55 V, PI/IPC in negative ion mode, parent-ion scanning of m/z 241; 35-65 V, PE in negative ion mode, parent-ion scanning of m/z 196; 20-35 V, PS in negative ion mode, neutral loss scanning of m/z 87; and 40-90 V, for all glycerophospholipids (including PA, PG and CL) detected by precursor scanning for m/z 153 in negative ion mode. MS/MS daughter ion scanning was performed with collision energies between 35-90 V. Assignment of phospholipid species is based upon a combination of survey, daughter, precursor and neutral loss scans, as well previous assignments (Richmond et al., 2010). The identity of phospholipid peaks was verified using the LIPID MAPS: Nature

Lipidomics Gateway (www.lipidmaps.org). In order to compare the peak heights relative to each other, peaks were measured by ruler and ratios were calculated.

2.1.14 Recombinant Protein Expression

2.1.14.a Construction of pET-32b HIS₆-TbCDS-HIS₆

TbCDS was amplified from genomic DNA using TbCDS pET F and TbCDS pET R primers, containing BamHI and XhoI restriction sites, respectively (Table 2.1). The PCR product was cloned into TOPO using a Zero Blunt PCR Cloning Kit (Invitrogen), confirmed with EcoRI restriction digest and sequenced. The pET-32b vector adds an N-terminal thioredoxin fragment and N- and C- terminal His₆-tags to the TbCDS in order to express a recombinant fusion protein of ~65 kDa which can be purified by affinity chromatography.

2.1.14.b Overproduction

In order to test expression of the TbCDS recombinant protein, Rosetta 2 (DE3) *E. coli* cells were transformed with the pET-32b HIS₆-TrxA-TbCDS-HIS₆ and selected on LB-agar plates containing ampicillin (100 µg/ml) and chloramphenicol (25 µg/ml). A single colony was used to inoculate 10 ml of LB media containing ampicillin and chloramphenicol, as above. The cells were grown overnight at 37°C with shaking, and 100 µl of overnight culture was used to induce 10 ml LB medium. Growth was monitored and at an optical density (OD) of 0.6 (measured by spectrophotometry) cultures were induced with 0.1 mM IPTG, and incubated overnight at 16°C with shaking.

Cells were harvested by centrifugation (3,500 g, 20 min, 4°C) and cell pellets were frozen until use. Recombinant protein production was monitored by Western blotting using HRP-conjugated anti-His antibodies (Clontech)(1:10,000)

2.1.14.c Crude Membrane Preparation

pET-32b TbCDS Rosetta 2 (DE3) cell pellets were lysed by resuspension in lysis buffer (50 mM Tris pH 7.5, 250 mM NaCl, 5 mM MgCl₂, 0.4 mg/ml lysozyme, 0.25 mM DTT) and incubation at 37°C for 30 min. Samples were then sonicated in 3 x 15 s pulses, with one minute of on ice between each. To obtain the cell membrane fraction containing the membrane bound TbCDS, the samples were spun at 14,500 g for 15 min at 4°C. The pellet was washed in buffer (as above, minus lysozyme).

2.2.14.d Overexpression for Lipid Extraction

To obtain lipids from Rosetta 2 (DE3) cells over-expressing pET32b TbCDS 20 mls of Rosetta 2 (DE3) pET32b TbCDS was prepared as described above and induced. At an OD of 0.6 this culture was split into two 10 ml cultures, one of which was induced with 1 mM IPTG, whilst the other was left un-induced. Cultures were incubated at 16 °C overnight with shaking and cell pellets were obtained and washed as described in section 2.1.14.b. Total lipids were extracted using the Bligh Dyer method (Bligh and Dyer, 1959). Cells from 10 mls of culture were resuspended in a glass vial in 100 µl PBS. 375 µl of 1:2 (v/v) CHCl₃:MeOH was added to each 100 µl PBS cell suspension sample, followed by vortexing and agitation for at least 30 min. After this, 125 µl of CHCl₃ and then 125 µl of water were added to the sample, vortexing after each addition. Samples were centrifuged at 1000 rpm and the lower/organic phase recovered to a fresh glass vial. Samples were washed using the upper phase of a centrifuged sample containing 100 µl H₂O, 275 µl 1:2 CHCl₃:MeOH, 125 µl CHCl₃, 125 µl H₂O. The organic phase was recovered to a fresh glass tube, dried down using an N₂ evaporator and stored at 4 °C.

2.1.14.e Detergent Extraction

For detergent extraction of recombinant pET32b TbCDS, crude membrane fraction was prepared as described above and resuspended in 500 µl buffer (50 mM Tris pH 7.5, 250 mM NaCl, 5 mM MgCl₂ and 0.25 mM DTT) containing varying amounts of TX-100. Samples were sonicated in a sonication bath for 5 min and centrifuged at 14,500 g for 15 min at 4 °C. The supernatant was taken to a fresh glass vial and the pellet re-extracted. The supernatants were then pooled.

2.2 Trypanosoma brucei methods

2.2.1 T. brucei cell culture

Bloodstream form *Trypanosoma brucei* strain 427, which have been previously modified to express T7 polymerase and tetracycline repressor proteins (Wirtz et al., 1999) were used as the baseline for all experiments and are referred here as single marker (SM) or wild type cells. The trypanosomes were cultured in HMI-9 (Hirumi and Hirumi, 1989) supplemented with 2.5 µg/ml G418. They were grown in flasks and incubated at 37 °C in an incubator with 5% CO₂.

The procyclic form of *T. brucei* strain 927 were cultured in SDM-79 (Brun and Schonemberger, 1979) supplemented with 10% foetal calf serum, G418 (15 µg/ml), hygromycin (50 µg/ml) and NaHCO₃ at 3.98 g/L to allow CO₂ buffering. They were grown in non tissue culture-treated flasks and incubated at 30 °C in an incubator with 5% CO₂.

2.2.2 *T. brucei* genomic DNA extraction and ethanol precipitation

T. brucei cells were pelleted from culture by centrifugation at 800 g for 10 minutes. The cell pellet was resuspended in 1 ml of media, transferred to a microcentrifuge tube and centrifuged for 30 s at full speed. The cell pellet was washed in Trypanosome Dilution Buffer (TDB, 5 mM KCl, 80 mM NaCl, 1 mM MgSO₄, 20 mM NaH₂PO₄, 2 mM NaH₂PO₄, 20 mM glucose, pH 7.7) if bloodstream form, PBS for procyclic form and then resuspended in lysis buffer (10 mM Tris, 100 mM NaCl, 25 mM EDTA pH 8, 0.5% SDS, 0.1 mg/ml proteinase K (Promega)). The mixture was incubated at 56 °C for at least 2 hours. 2.5 volumes of ice cold absolute ethanol were gently added, along with a 1/10 volume of 0.3 M sodium acetate. The resultant mixture was gently inverted until the DNA was seen to precipitate. Precipitated DNA was spooled and removed with a bent plastic inoculation loop and cleaned twice by dipping in 70% ethanol. The DNA was briefly allowed to air dry before dissolving in water or Quiagen EB (10 mM Tris-Cl, pH 8.5).

2.2.3 *T. brucei* Transformation

Cells were harvested from culture as described 2.2.2. The supernatant was discarded and the cell pellet resuspended in 100 µl of Nucleofector[®] solution (Lonza) containing 10 µg of linearised vector for transfection. This mixture was then transferred to a cuvette and electroporation was performed using the Nucleofector[®] device (Lonza) - programme X-001 for bloodstream forms or programme X-014 for procyclic form. The transfected trypanosomes were transferred to a flask of HMI-9/SDM-79 and allowed to recover overnight. The morning after the transfection, the appropriate selection antibiotic for the new construct was added to the flask and the flask contents were distributed across the wells of a 24 well tissue culture plate.

2.2.4 *T. brucei* RNAi

To create a construct for the knockdown of TbCDS, the TbCDS ORF was isolated from genomic DNA using the TbCDS pET F and TbCDS pET R primers containing BamHI and

XhoI restriction site (Table 2.1). The resultant PCR product of 1221 bp was then digested with BamHI and XhoI restriction enzymes to obtain a BamHI-XhoI fragment from the internal BamHI site to the reverse primer of 400 bp long. This fragment was ligated into the hygromycin selectable p2T7 (Wang et al., 2000) and the phleomycin selectable p2T7-177 (Wickstead et al., 2002) vectors using the BamHI and XhoI restriction sites. These vectors contain two opposing T7 promoters on either side of their multiple cloning sites, which are under the control of the tetracycline repressor protein. Addition of tetracycline binds the protein allowing transcription to occur, and double stranded RNA is produced, inducing the cell's RNAi mechanism.

After linearisation and transfection (see above) these vectors integrate into the genome of *T. brucei* by homologous recombination due to regions in the plasmid corresponding to genomic DNA in the parasite. The vector p2T7 integrates into the rDNA spacer region of the *T. brucei* genome and was used to transfect bloodstream form *T. brucei*. The vector p2T7-177 integrates into the transcriptionally silent mini-chromosome region and was used for transfection of procyclic form *T. brucei*.

2.2.5 Creation of TbCDS conditional knockout

2.2.5.a Creation of Tetracycline Inducible Ectopic TbCDS copy

The first step in creating the *T. brucei* TbCDS knockout was to create an inducible copy of the target gene. TbCDS ORF was amplified by PCR from TbCDS Topo using KOD polymerase with New CDS 82F and New CDS 82R primers (Table 2.1). The PCR product was then cloned into the pLEW100 vector and the pLEW82 vectors. Both of these vectors add a C-terminal haemagglutinin (HA) tag and a tetracycline regulatable promoter, integrate into the spacer rRNA and are selectable with phleomycin, but in pLEW100 the promoter is procyclin, and in pLEW82 the promoter is T7 (Wirtz et al., 1999). Addition of tetracycline allows transcription of the cloned gene, while in the absence of tetracycline, transcription is repressed. pLEW82 has a very high level of expression but is not very regulatable i.e. leaky expression occurs. pLEW100 produces a relatively much lower level of expression, but in the absence of tetracycline is essentially silent.

2.2.5.b Construction of Endogenous Gene Knockout Cassettes

To construct the knockout constructs, the 5' and 3' UTRs flanking the TbCDS gene in its genomic location were amplified.

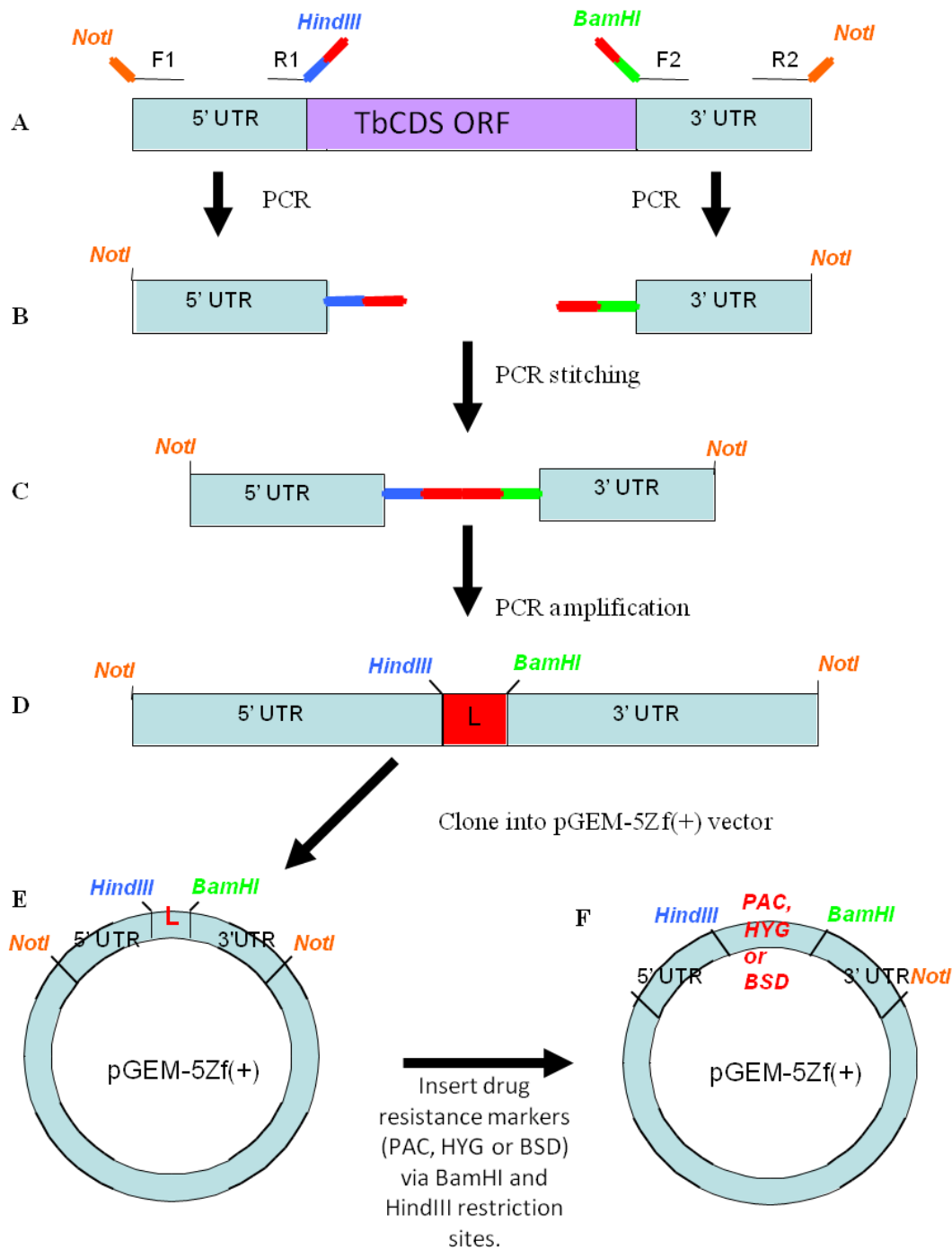


Figure 2.3 Schematic of CDS knockout construct creation. **A-B** Regions of 5' and 3' UTR of flanking the TbCDS ORF were isolated from *T. brucei* genomic DNA by PCR using primers which added restriction sites and complimentary linking regions to the UTRs. **C-D**. The complimentary regions of the two UTR's were stitched together using a knitting PCR reaction, and amplified. **E**. The knitted UTR construct was ligated into pGem-5Zf(+) vector. **F**. Drug resistance marker genes puromycin acetyltransferase (PAC) or hygromycin phosphotransferase (Hyg) or Blastidicin S deaminase (BSD) were then inserted between the UTRs using the BamHI and HindIII restriction sites.

The 5' UTR was amplified from Topo TbCDS 5' UTR + ORF using the TbCDS F1 and TbCDS R1' primers (Table 2.1, Figure 2.3, A-B). The 3' UTR was amplified from Topo-TbCDS 3'UTR + ORF using the TbCDS F2 and TbCDS R2 primers (Table. 2.1, Figure 2.3, A-B). The products were then stitched together in a knitting PCR reaction utilising a short linking region added by the TbCDS R1' and TbCDS F2 primers containing the restriction sites BamHI and HindIII, respectively (Table 2.1), in order to anneal the two UTRs (Figure 2.3, C-D).

The knitted UTRs were then ligated into pGEM-5Zf(+)(Promega) via the NotI sites added by the TbCDS F1 and TbCDS R2 primers (Table 2.1, Figure 2.3, E). The antibiotic resistant marker genes hygromycin phosphotransferase (HYG), puromycin acetyltransferase (PAC) or blasticidin S deaminase (BSD) were then ligated between the BamHI and HindIII restriction sites (Figure 2.3, F).

All constructs were purified using QIAprep MiniPrep Plasmid Kit (Qiagen) and linearised with NotI. 10 µg of linearised construct was precipitated with sodium acetate/ethanol as described, and the pellet washed twice with ethanol and resuspended directly into T-cell Nucleofector solution (Lonza) for transfection into *T. brucei* as described above.

2.2.5.c Conditional Gene Knockouts

The pLEW100 TbCDS construct was transfected into the SM cell line and, due to regions of rDNA homology flanking TbCDS in the pLEW100 (Wirtz et al., 1999), integrated into an rDNA locus by the process of homologous recombination. After recovery, cells were selected in the presence of phleomycin.

The first TbCDS allele was deleted from the TbCDS pLEW100 cell line using the TbCDS PAC knockout cassette in both bloodstream form and procyclic form cells. Successful transformants were selected in the presence of puromycin.

In order to allow for the deletion of the second TbCDS allele, TbCDS::PAC TbCDS pLEW100 cells were cultured in the presence of tetracycline for 24 hours in order to switch on expression of the exogenous, tetracycline inducible TbCDS copy. Cells were then transfected with the second knockout cassette (the HYG knockout cassette in bloodstream form or the BSD knockout in procyclic). After the cells had recovered from transfection, the correct transformants were selected for in the presence of the

appropriate selection antibiotic, plus tetracycline in order to maintain expression of the exogenous TbCDS.

Once conditional double knockouts were obtained they were grown in the absence of tetracycline in media containing tetracycline free foetal calf serum. This repressed the expression of the exogenous copy of the gene and therefore the cells were studied in the absence of any of the target protein.

2.2.6 Cell Counting

In order to assess growth of genetically modified clones, flasks were set up at a known cell density. To induce RNAi or the expression of exogenous gene copies, experimental flasks were induced by the addition or removal 1 µg/ml tetracycline to the media. To switch off exogenous gene copies in conditional knockouts, tetracycline was removed from the media, and cells were washed in tetracycline free media (containing tetracycline free foetal calf serum). Flasks were counted in duplicate at around the same time every day for bloodstream form and every second day for procyclics using a haemocytometer or a CASY cell counter and analyser (Roche). After counting they were diluted back down to a known density with fresh media containing appropriate selection drugs.

2.2.7 *In vivo T. brucei* metabolic labelling

$1-2 \times 10^7$ cells were harvested from mid log culture as described and washed in 1 ml of labelling media. Cells were then resuspended in 10 µl of fresh labelling media and added to a further 1 ml of labelling media pre-warmed to 37°C in a shaking water bath. Radiolabelled metabolites were added to cells in labelling media at 50 µCi per ml and gently agitated for 1 hour at 37°C for bloodstream form, or overnight at 30°C for procyclic.

Protein samples were harvested by centrifugation of the cells and resuspension of the pellet in 2X sample buffer preheated to 95°C. The cells and sample buffer were then incubated for 5 minutes at 95°C. Samples were stored at -20°C until analysis.

Lipid samples were also harvested by centrifugation. The pellet was resuspended in 100 µl of TDB before addition of 666 µl of 1:1 CHCl₃:MeOH to make the final sample composition 10:10:3 CHCl₃:MeOH:H₂O. Samples were shaken at 4°C for one hour before centrifuging at top speed for 1 min. The supernatant was reserved and the

pellet was re-extracted with 100 μ l of 10:10:3 CHCl₃:MeOH:H₂O. The resultant supernatant was added to the first supernatant. 200 μ l of butanol was added, followed by 200 μ l of water and the sample was vortexed and spun to separate the phases. The butanol phase was removed and reserved and two more butanol washes were performed, with the butanol phases being removed and pooled. The pooled BuOH phase was then back-washed twice with 200 μ l of fresh water.

10 μ l of the 600 μ l pooled, washed BuOH sample was added to 1ml of scintillation fluid for counting. The remaining samples were dried by Thermo Savant SpeedVac SPD121P Centrifugal Evaporator.

Samples were resuspended in 10 or 20 μ l of solvent and analysed by silica 60 HPTLC plates in solvent system 10:10:3 CHCl₃:MeOH:H₂O and/or 180:140:9:9:23 CHCl₃:MeOH:30% NH₃: 1 M NH₄Ac :H₂O . Dried HPTLC plates were sprayed with EnHance™ and radiolabelled lipids visualised by autoradiography.

2.2.8 Cell Free System Assay of GPI Biosynthesis

Membranes of *T. brucei* SM and bloodstream form TbCDS conditional null mutants grown in the absence of tetracycline for 42 hours were isolated. Washed *T. brucei* membranes were prepared fresh as follows: *T. brucei* cells were harvested from culture as described and washed twice in TDB followed by lysis with 800 μ l ice cold water. Membranes were then snap frozen in liquid nitrogen and stored at -80°C until they were required. 5 x 10⁶ cells were used per assay. Membranes were washed in 1 ml of ice cold wash buffer (50 mM HEPES pH 7.4, 25 mM KCl, 5 mM MgCl₂, 100 μ M tosyl-L-Lysine chromomethyl ketone (TLCK) and 1 μ g leupeptin). The membranes were then resuspended by sonication in 45 μ l of 2X incorporation buffer (100 mM HEPES pH 7.4, 50 mM KCl, 10 mM MgCl₂, 10 mM MnCl₂, 1 μ g/ml tunicamycin and 1 mM DTT). The resuspended membranes were then added to the assay tube containing an equal volume of GDP-[³H]mannose (0.5 μ Ci/labelling) plus or minus 1 mM UDP-N-acetylglucosamine (UDP-GlcNAc). The whole assay mixture was then sonicated for ~30 s followed by incubation at 30°C for one hour. The reaction was stopped by the addition of 267 μ l of 1:1 v/v CHCl₃:MeOH. Radiolabelled glycolipid products were recovered by shaking the 10:10:3 CHCl₃:MeOH:H₂O mixture at 4°C followed by evaporation to dryness. The reaction products were partitioned between butanol and water and analysed by silica 60 HPTLC plates in solvent system 10:10:3 (CHCl₃:MeOH:H₂O). Dried HPTLC plates were then sprayed with EnHance Spray

Surface Autoradiography Enhancer (PerkinElmer) and radiolabelled glycolipids visualised by fluorography.

2.2.9 TbCDS cell free activity assay

TbCDS activity assay was based on the methods described previously by Sparrow (Sparrow and Raetz, 1985, Wu et al., 1995, Nigou and Besra, 2002, Martin et al., 2000, Carman and Fischl, 1992).

Washed *T. brucei* membranes were prepared fresh as follows. *T. brucei* cells were harvested from culture as described in section 2.2.2 and washed twice in TDB followed by lysis with 800 µl ice cold water. For procyclic cells, glass beads were added and the mixture vortexed. 200 µl of 5X incorporation buffer (250 mM Tris-maleate pH 6.5; 15 mM MgCl₂; 5 mg/ml BSA, 1.25 mM DTT) was then added to the lysed cells, followed by centrifugation at 1000 rpm to remove beads (if used). Beads were then washed twice in incorporation buffer and the wash mix added to the cell membrane pellet. The cell membrane pellet was washed twice in incorporation buffer and the cell pellet was resuspended in 85 µl incorporation buffer followed by sonication. Resuspended membranes were added to reaction tubes to make a final assay volume of 100 µl containing 50 mM Tris-maleate pH 6.5; 3 mM MgCl₂; 1 mg/ml BSA; 0.25 mM DTT; 1 mM [³H]CTP at 9 µCi/mM; 1.5 mM PA and 15 mM TX-100. The assay mixture was sonicated briefly and incubated for 20 minutes at 30 °C. The reaction was stopped by the addition of 666 µl of 1:1 (v/v) CHCl₃:MeOH and radiolabelled glycolipids were extracted into the resulting 10:10:3 mixture by shaking at 4 °C for at least 1 hour. Assay mixtures were then spun at full speed and the supernatant evaporated to dryness. 200 µl CHCl₃ and 200 µl 0.1 M HCl were then added to the tubes which were vortexed and briefly vortexed. The chloroform layer was removed and washed twice with 0.1 M HCl, followed by evaporation to dryness. The resultant radiolabelled glycolipids were analysed by silica 60-HPTLC in solvent system 25:15:4:2 v/v CHCl₃:MeOH:CH₃COOH:H₂O. Dried HPTLC plates were sprayed with EnHance Spray and radiolabelled glycolipids visualised by fluorography.

2.2.10 Extraction and Analysis of NTPs

Nucleotide triphosphates (NTPs) were quantified using the method of Fyffe, Major and Smith (manuscript in preparation). A known number of cells were centrifuged at

800 g for ten minutes at room temperature and washed twice in cold trypanosome dilution buffer (TDB, 5 mM KCl, 80 mM NaCl, 1 mM MgSO₄, 20 mM NaH₂PO₄, 2 mM NaH₂PO₄, 20 mM glucose, pH 7.7). The cell pellet was lysed in 100 µl of ice cold 1M TCA. All following steps were carried out on ice or at 4°C. 150 pM of internal standard inosine-5-triphosphate (ITP) was added to the sample, which was then mixed and centrifuged at 15,000 g for 10 minutes at 4°C. The supernatant was transferred to a fresh tube and 25 µl of 10 mM EDTA pH 7.0 was added, followed by 50 µl of chloroform and 25 µl of trioctylamine. The sample was vortexed and centrifuged at 15,000 g for 10 minutes at 4°C. The upper phase was transferred to a fresh tube; snap frozen in liquid nitrogen and freeze dried. The sample was then resuspended in 60 µl of 50% methanol and introduced to the mass spectrometer (Quattro Ultima Triple Quadrupole, Waters or Absciex 4000 QTrap) by constant infusion at a rate of 30 µl or 125 nl per minute respectively. A multi reactant monitoring (MRM) program was created, which specifically focussed upon a set of mass transitions. The parent ion masses of GTP, ATP, UTP, CTP and the internal standard ITP were selected, and the number of ions of the principal daughter ion of each was recorded and normalised using the internal standard and standard curves. NTP levels were then calculated using the number of cells harvested, taking bloodstream form *T. brucei* cell volume of 5.89 µl per 1 x 10⁸ and procyclic *T. brucei* cell volume as 4.8 µl per 1 x 10⁸ (de Koning et al., 1998).

2.2.11 Cell Fixing and Staining

At least 1 x 10⁶ cells were harvested from culture by centrifugation at 800 g for ten minutes at room temperature and washed with TDB. Cells were fixed in PBS plus 4% paraformaldehyde and incubated at room temperature for 20 minutes. Cells were washed with and resuspended in PBS. Fixed cells in PBS were applied to polylysine coated slides and left overnight to adhere. Slides were washed briefly with PBS and incubated in 100 µl PBS/0.1 M glycine for five minutes at room temperature,

followed by three brief washes in PBS. Cells were permeabilised in PBS/0.1% TX-100 for 10 minutes and washed three times with PBS. The slides were then blocked in PBS/1% BSA for ten minutes at room temperature and washed before incubation with the primary antibody in blocking buffer for one hour.

Slides were washed three times with blocking buffer before incubation with the secondary antibody in blocking solution for one hour in a foil covered humid chamber.

After washing three times in PBS the slides were mounted in SlowFade® Gold Antifade Reagent with DAPI (Invitrogen) and a cover slip was placed over the slide. Slides were allowed to cure for 24 hours at room temperature before sealing the sides with nail varnish.

2.2.12 Mitotracker staining

4×10^5 cells were harvested from culture by centrifugation at 800 g for ten minutes at room temperature. The pellet was washed in 1 ml SDM-79 and spun for 3 min at 800 g. The cell pellet was then incubated at 37°C for 10 minutes in 1 ml SDM-79, 50 nm Mitotracker red (Invitrogen).

Cells were again spun at 800g, the supernatant removed and the cell pellet washed in SDM-79. The cells were then incubated in a fresh 1 ml of SDM-79 for 30 minutes at 37°C. Finally, cells were washed in PBS and fixed in PBS containing 4% paraformaldehyde. Mitotracker images were acquired with an exposure time of 500 ms.

2.2.12 Microscopy

All immunofluorescence microscopy was performed on a DeltaVision microscope (Applied Precision Inc) and processed using ImageJ software (Rasband, 1997-2012).

2.2.13 Lipid Extraction from *T. brucei*

Total lipids were extracted from *T. brucei* membranes using the Bligh Dyer method (Bligh and Dyer, 1959) as previously described in section 2.2.14.d.

2.3 Yeast Methods

2.3.1 *Saccharomyces cerevisiae* culture

The *Saccharomyces cerevisiae* strain YBR029c heterozygous for *cds1::KanMX* was created by the *Saccharomyces* Genome Deletion project (Winzeler et al., 1999) and obtained from Professor Mike Stark at the University of Dundee.

For general growth and maintenance of cultures *Saccharomyces cerevisiae* was either grown on liquid YPD containing 1% bacto-yeast extract, 2% bacto-peptone and 2% dextrose, or YPD plates containing 2% bacto-agar. Otherwise, auxotrophs were grown on complete minimal glucose medium (SC) containing 0.67% bacto-yeast nitrogen base without amino acids (Sigma) and 2% dextrose. This was supplemented with appropriate amino acid mix to select for plasmids with auxotrophic markers. Initially the amino acids were made up as sterile stocks and added as required, but later the appropriate amino acid mixes were bought in from Sigma-Aldrich.

Yeast cultures were grown at 30°C, with constant shaking when in liquid media.

2.3.2 Yeast Colony PCR

A yeast colony was picked and lysed in 15 µl of lysis buffer containing 0.1 M sodium phosphate buffer ($\text{Na}_2\text{HPO}_4:\text{NaH}_2\text{PO}_4$) pH 7.4 and 11 mg/ml Lyticase (from *Arthrobacter luteus* - Sigma). This was incubated at 37°C for one hour, followed by 10 minutes at 95-100°C. The solution was vortexed and the cell debris pelleted by centrifuging for one minute at 3,000 G. 2.5 µl of the resultant lysate was then used in a standard PCR reaction.

2.3.3 Yeast Transformation

Transformation was performed as described by Chen and colleagues (1992). A yeast colony was transferred to 150 µl of lysis buffer (0.4 M lithium acetate, 40% PEG 4000, 0.1 M DTT) containing 3 µl of a standard plasmid preparation. This was incubated at 45°C for 45 minutes. 1ml of YPD was then added and the culture allowed to recover at 30°C with shaking for 1 hour. 200 µl of this culture was plated onto appropriate media for the strain containing the new plasmid and incubated at 30°C.

2.3.5 Construction of TbCDS and CDS1 pRS-426 Met25

TbCDS was isolated from *T. brucei* strain 427 genomic DNA using the TbCDS pLEW F primer containing a HindIII site, and the TbCDS YeastRescue R primer containing a XhoI site (Table 2.a). Yeast CDS1 was isolated by colony PCR from *S. cerevisiae* using YeastCDS1 F primer containing a HindIII site, and Yeast CDS1 R containing a XhoI site (Table 2.a). Both CDS genes were cloned into the yeast expression vector pRS-426 MET25 using the HindIII and XhoI restriction sites. pRS-426 MET25 was obtained from Paul Denny at the University of Glasgow and contains the MET25 promoter, which is suppressed in the presence of methionine. It contains the URA3 selection marker for yeast and ampicillin resistance marker for *E. coli*. DH5 α were transformed with the ligation mixture, and selected on LB agar plus ampicillin. Successful transformants were screened by colony PCR using the above primers.

2.3.6 Complementation of *cds1::KanMX* with TbCDS and Yeast CDS by Tetrad Analysis

The *S. cerevisiae* *cds1::KanMX* heterozygous cell line was transfected with either the plasmid containing the yeast CDS1, the plasmid containing the *T. brucei* CDS or empty plasmid. The vector was selected for on media deficient in uracil and methionine. The three cell lines above, plus the original heterozygous CDS1 null were then taken for tetrad analysis. Sporulation was carried out by Professor Mike Stark in Dundee in the absence of methionine in order to allow expression of the CDS gene on the pRS-426 Met25 locus. After sporulation, viable spores were tested for lethality on SCD + Met in order to select against those spores containing the mutated CDS1 allele and therefore relying on the exogenously expressed CDS.

2.3.7 Construction of TbCDS and CDS1 p405-TEF1

TbCDS and yeast CDS1 were sub-cloned from pRS-426 MET25 to p405-TEF1 using the HindIII and XhoI restriction sites. p405-TEF1 was a gift from Nicholas Buchler (Addgene plasmid #15968). It is a high copy number plasmid containing the strong TEF1 promoter and is selectable with ampicillin resistance in *E. coli* and LEU2 in *S. cerevisiae*.

2.3.8 Plasmid Shuffle

Haploid CDS1 knockout containing yeast CDS1 on pRS-416 MET25 (MET15 his3leu2ura3 cds1::KanMX [pRS425-MET25 CDS1]) was used in a plasmid shuffle with TbCDS or Yeast CDS1 on p405-TEF1. The yeast knockout containing [pRS425-MET25 CDS1] was transfected with TbCDS on p405-TEF1, yeast CDS1 on p405-TEF1 or empty p405-TEF1. Successful transformants were selected SC-LEU-MET-URA to select for both plasmids. Cells were then cultured on SC-LEU-MET (+URA) followed by plating on SC-LEU+5-fluoro-orotic acid (5-FOA) to select against the URA3 containing pRS416-MET25 CDS1, whilst selecting for new p405-TEF1 TbCDS/CDS1/empty plasmid, to see if the genes on the new plasmid could complement the cds1::KanMX knockout.

Chapter 3: Characterisation of *Trypanosoma brucei* Cytidine Diphosphate Diacylglycerol Synthase

3.1 Introduction

No CDS gene or protein has previously been studied in *Trypanosoma brucei*, or any other kinetoplastid. Due to its central position in glycerophospholipid synthesis and the discovery that some downstream products are essential, it seems likely that this enzyme will also be essential. In particular *T. brucei*'s large and essential requirement for the downstream product; PI for GPI anchors (Martin and Smith, 2006a). Therefore a study of this enzyme is key to understanding the dynamics and regulation of the major glycerophospholipids synthesised in *T. brucei*. In the parasitic apicomplexan *Plasmodium falciparum* the CDS gene was essential and found to differ from the human gene in that it encoded a longer protein with a large N terminal extension which was proteolytically processed (Martin et al., 2000). Such differences between parasite biosynthetic pathways and those of their host can potentially be exploited by drug development. If the *T. brucei* TbCDS or CDP-DAG pathway is found to differ from that of its hosts it could provide a promising drug target. The first step of characterising this enzyme in *T. brucei*, and the first aim of this project was to identify a gene predicted to encode CDS from the *T. brucei* genome and to show the resulting protein is a functional and active CDS.

3.2 Identification and Sequencing of TbCDS 427

A BLAST-P search of the NCBI database and GeneDB using known CDS enzymes from other organisms revealed a single putative CDS homologue in the genome (trytrypdb.org) of *T. brucei* bloodstream form 927 (Tb927.7.220).

To sequence the entire open reading frame of the predicted TbCDS in *T. brucei* strain 427, the putative *T. brucei* TbCDS was used as a template for the design of a forward primer approximately 500 bp upstream from the predicted start codon (F1) and a

reverse primer approximately 500 bp downstream of the predicted stop codon (R2) (Table 2.a). Unfortunately, it was discovered that R2 annealed within the 311bp open reading frame of a putative 40s ribosomal protein S33 gene (Tb927.7.230) which began 245 bp downstream of the putative TBtCDS gene and contained a duplicate directly downstream (Tb927.7.240) (Figure 3.1), meaning the primer specifically bound at two different places approximately 500 bp apart. Therefore, a new R2 (R2') was designed to anneal within the untranslated region before the ribosomal gene giving a 3'UTR product of 179bp (Table 2.1).

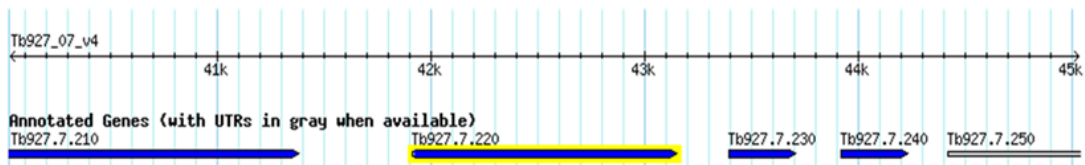


Figure. 3.1. TbCDS in the genome. A snapshot from the genome browser at TryTrypDB.org (TriTrypDB GBrowse v2.48) of a 5kbp stretch of chromosome 7 showing the TbCDS gene highlighted in yellow (Tb927.7.220) as well as the two identical putative 40s ribosomal protein S33 genes (Tb927.7.230 and Tb927.7.240).

PCR products were obtained from *T. brucei* strain 427 genomic DNA using the TbCDS F1 and TbCDS pLEW F primer combination (Figure 3.2, A.i) and TbCDS pLEW F and TbCDS R2 combinations (Figure 3.2, B.i) - primer sequences given in Table 2.1. Both of these products were cloned into Zero Blunt Topo for sequencing (Figure 3.2, A and B ii). The obtained DNA sequence, along with the predicted translation is shown in Figure 3.3.

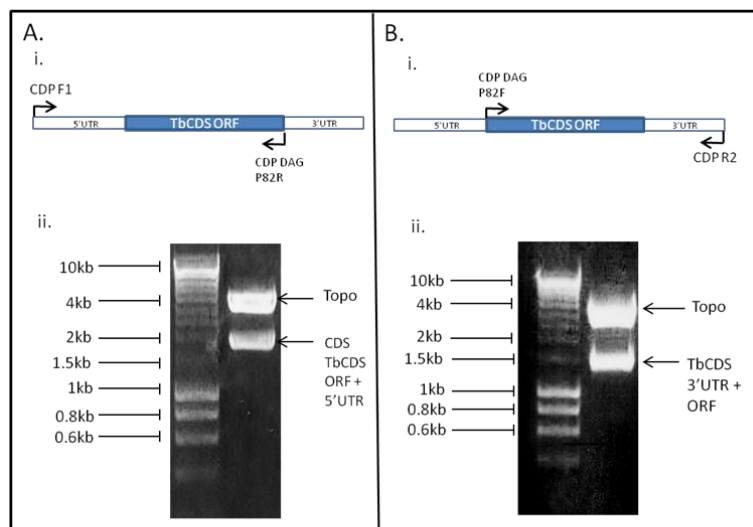


Figure 3.2. Cloning of putative TbCDS ORF and UTRs from PCR into Topo for sequencing. A.i) Schematic of the primers used and the region amplified. A.ii) EcoRI restriction enzyme digest of TbCDS ORF + 5' UTR (1740 bp) in Topo. (B.i) Schematic of the primers used and the region amplified B.ii) EcoRI restriction enzyme digest of TbCDS ORF + 3'UTR (1400) in Topo.

The sequenced 1916 bp of *T. brucei* strain 427 gDNA contains 11 single base differences from the database strain 927 sequence. Ten of these differences are point mutations which occur in the 5' UTR (highlighted red in Figure 3.3). Numbered as in Figure 3.3: position 116 adenine to guanine; position 182 thymine to cytosine; position 204 thymine to cytosine; a cluster from position 213 where ACTCCTTTATT becomes TTACTCCTTTA and an adenine to thymine at position 341. The final base change at position 524 is an adenine to guanine base change and results in an amino acid change from serine to asparagines (amino acid position 3). The predicted open reading frame for the TbCDS gene is 1221 bp long. The G+C content is 46% in the coding region, which is lower than the average for protein coding genes in *T. brucei*, which is 50% (Berriman et al 2005).

3.3 Predicted TbCDS Proteomics

The TbCDS ORF is predicted to encode a protein of 406 residues (translation show in Figure 3.3) with a theoretical molecular mass of ~46 kDa, which corresponds well to the sizes of other eukaryotic CDS proteins such as *Arabidopsis thaliana* CDS5 which is 399 amino acids long (Haselier et al., 2010) and the human CDS1 which is 461 amino acids long (Heacock et al., 1996). Like previously described CDS proteins, the predicted isoelectric point of TbCDS is 9.7, similar to that from *P. falciparum* CDS (9.74) (Martin et al., 2000), plant CDS proteins *Solanum tuberosum* (pl 10.4) and *Arabidopsis thaliana* (pl 9.9) (Kopka et al., 1997) for and *Mycobacterium tuberculosis*, (pl 8.8) but rather more basic than the mammalian homologues from mouse CDS1 at 7.62, mouse CDS2 at 6.6 (Inglis-Broadgate et al., 2005) and Human CDS1 7.57 (Weeks et al., 1997).

The protein is highly hydrophobic - with a grand average of hydrophathicity of 0.285 (Kyte and Doolittle, 1982) and is predicted to have seven membrane spanning domains (Figure 3.4). This is not unexpected as all CDS enzymes so far identified are integral membrane proteins with multiple membrane spanning domains (Saito et al., 1997, Volta et al., 1999, Heacock et al., 1996, Martin et al., 2000, Nigou and Besra, 2002). Topology predicts that both the N and C terminals are hydrophilic, which again corresponds with other known CDS proteins. The predicted TbCDS protein encodes a conserved domain characteristic of the cytidylyltransferase family (NCBI Superfamily cl00347). This family are integral membrane protein and includes phosphatidate cytidylyltransferase EC:2.7.7.41.

The predicted TbCDS also contains a typical phosphatidate cytidytransferase signature: S-x-[LIVMF]-K-R-x(4)-K-D-x-[GSA]-x(2)-[LIF]-[PGS]-x-H-G-G-[LIVMF]-x-D-R-[LIVMFT]-D- (graphical representation is show in Figure 3.5). This signature is shared by almost all predicted CDS proteins, both prokaryotic and eukaryotic, where it is found towards the C terminal end of the predicted protein. The predicted *T. brucei* protein is no exception, and the phosphatidate cytidyltransferase signature begins directly after the final predicted trans-membrane domain in a hydrophilic region (Figures 3.3 and 3.4).

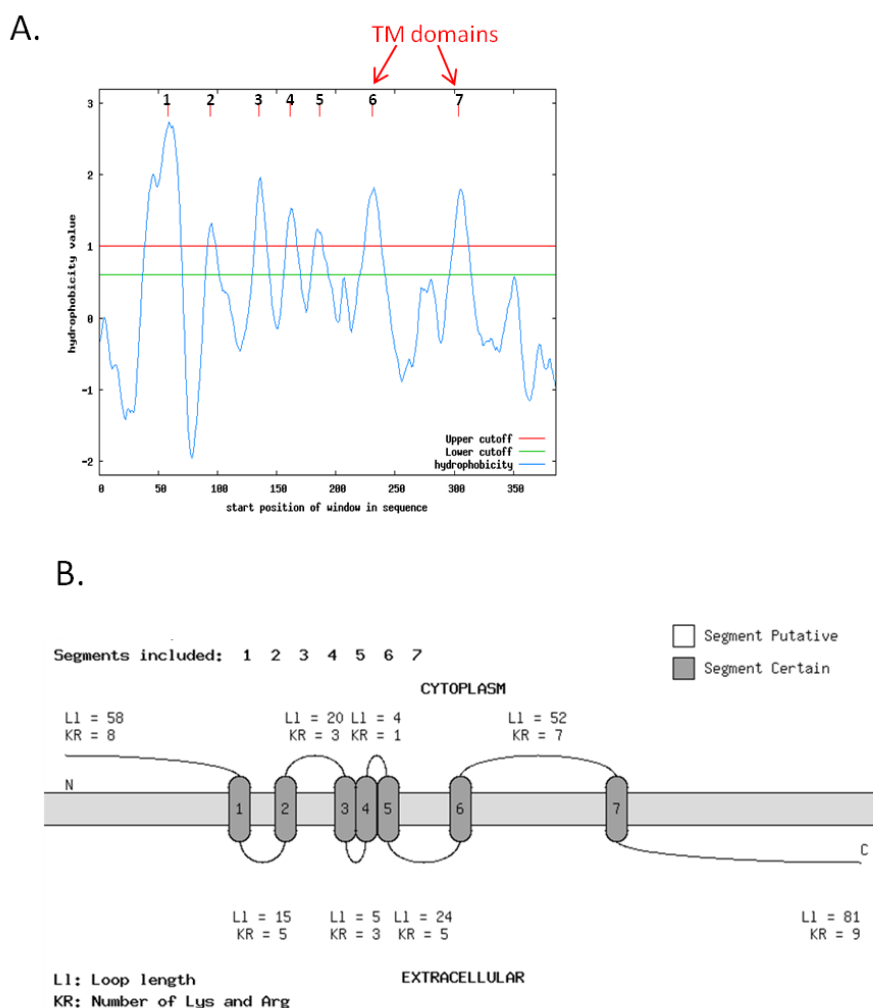


Figure 3.4. Predicted hydrophobicity and trans-membrane regions of TbCDS protein (A) Hydrophobicity analysis of predicted protein sequence encoded by TbCDS 427 according to the KD-scale (Kyte and Doolittle, 1982) (B) Schematic showing topology prediction and transmembrane domains of predicted protein sequence encoded by TbCDS 427 according to the KD-scale. Both images produced using TopPred 0.01 program for topology prediction of membrane proteins at mobyle.pasteur.fr (Von Hejne et al, 1992; Claros and Von Hejne, 1994; Deveaud and Schuerer)

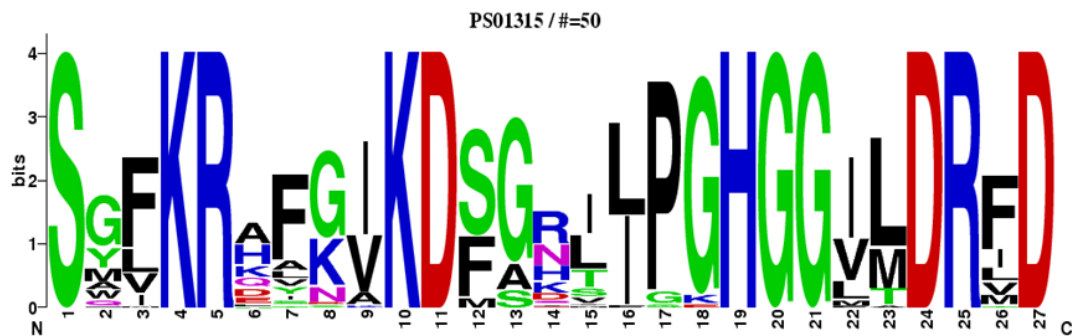


Figure 3.5 PROSITE sequence logo for phosphatidyl cytidyltransferase (CDS) pattern. Graphical display of a multiple sequence alignment consisting of colour-coded stacks of letters representing amino acids at successive positions. The total height of a logo position depends on the degree of conservation in the corresponding multiple sequence alignment column. The height of each letter in a logo position is proportional to the observed frequency of the corresponding amino acid in the alignment column. The letter of each stack is ordered from most to least frequent, so that it is possible to read the consensus sequence from the top of the stacks. '#' indicates the number of true positive hits detected in UniProtKB/Swiss-Prot. Accession number: PS01315.

Acquired from PROSITE (<http://prosite.expasy.org/cgi-bin/prosite>) built using WebLogo.

An alignment of the TbCDS 427 predicted protein with other predicted kinetoplastid CDS proteins and known eukaryotic CDS proteins is shown in Figure 3.6. The kinetoplastid CDS proteins are all closely related, with *T.b.brucei* strain 927 and *T.b. gambiense* predicted CDSs showing 99% identity with the *T. brucei* 427 TbCDS. The *T. brucei* 427 TbCDS shares 64% identity with *T. cruzi*, 60% with *T. vivax* and between 49-50% identity with *Leishmania* species. The putative TbCDS 427 also shows significant similarity to other eukaryotic CDS proteins, with 37% sequence identity to mouse and human CDS proteins and 37% identity with *S. cerevisiae* CDS1. Out with the Trypanosomatidae family the top BLAST hits are ascomycetes and cellular slime moulds also with around 37% identity. These results suggest that this CDS gene is an ancestral eukaryotic gene that is highly conserved. The highest degree of conservation is found towards the C-terminal end of the protein, particularly where the phosphatidate citidyltransferase pattern is found, giving further confirmation that this corresponds to a domain of the active site.

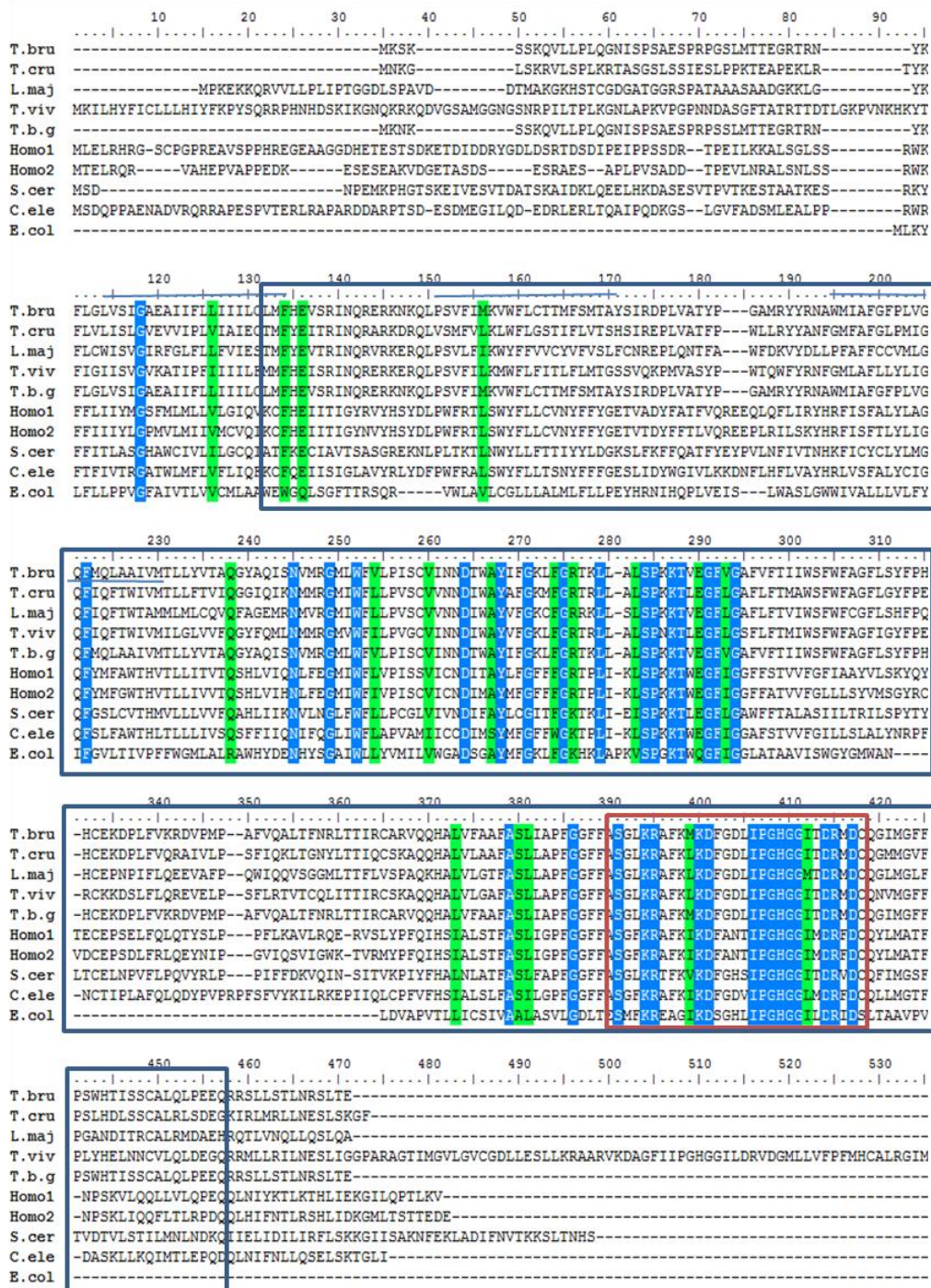


Figure 3.6. Protein sequences of known CDS proteins with TbCDS and other predicted kinetoplastid proteins, aligned using Clustal W. Blue shading indicates identical residues in all sequences, green shading indicates similar residues. Species and accession numbers: **T. brucei** = *T. brucei* - XP_845646.1; **T. cruzi** = *T. cruzi* - XP_810276.1; **L. major** = *L. major* - XP_001684166.1; **T. vivax** = *T. vivax* - CCC48662.1; **T. b. gambiense** = *T. b. gambiense* - CBH12030.; **Homo1** = *Homo sapiens 1* - NP_001254.2; **Homo2** = *Homo sapiens 2* - NP_003809.1; **S. cer** = *S. cerevisiae* - NP_009585.1; **C. ele** = *C. elegans* - NP_501297.1.s; **E. col** = *E. coli* - YP_003037629.1. Red box indicates the phosphatidyl cytidyltransferase signature (Figure 3.2)

Wider BLAST searches using prokaryotic CDS sequences (though also defined by EC:2.7.7.41) (Figure 3.7) recovered a second CDS gene in *Trypanosoma cruzi* (Tc00.1047053508707.140/TcCLB.508707.140) *Trypanosoma vivax* (TvY486_0025800) and *Leishmania* species (LinJ.32.3010, LmjF.32.2870; LmxM.31.2870, LtaP32.3050), but nothing in *T. b. brucei*. These genes have more identity with the prokaryotic CDS genes and are annotated with the alternate name “phosphatidate cytidyltransferase”, more commonly used when referring to the prokaryotic enzyme. A gene in *T.b.gambiense* (Tbg972.7.100) is also annotated as phosphatidate cytidyltransferase, but on closer inspection appears to be syntenic with the eukaryotic-like CDP-DAG synthase of *T. b. brucei* and other trypanosomatids. All these prokaryotic-like cytidyltransferases contain incomplete CTP-Transferase superfamily domains, with missing sections at the N-terminal ends. The phosphatidate cytidyltransferase gene in *T. cruzi* and *Leishmania* species is syntenic, but this is not the case with the *Trypanosoma vivax* gene. The *Leishmania* spp cytidyltransferase proteins show around 70% identity with each other and 34% with the *T. cruzi* protein, but only 26% identity with the *T. vivax* protein. Other than within the *Trypanosoma* family, the top hits for all proteins are firmicutes (~41% identity); fusobacteria (~40% identity) and proteobacteria, but there is only homology at the C-terminal end, less than a quarter of the gene. The rest of the proteins do not show significant homology to anything out with their family.

An alignment of these predicted proteins with some prokaryotic CDS sequences is shown in Figure 3.6. It is clear that the structure of these proteins is quite unique, and, interestingly, the phosphatidate cytidyltransferase signature that is present in almost all CDS proteins is incomplete in *L. tarentole*, and missing entirely in the *T. vivax* protein. This calls into question whether they can function as CDS enzymes at all, since this is predicted to be a domain of the active site and it may be that these sequences are incomplete, are pseudogenes, or that they have an alternative function.

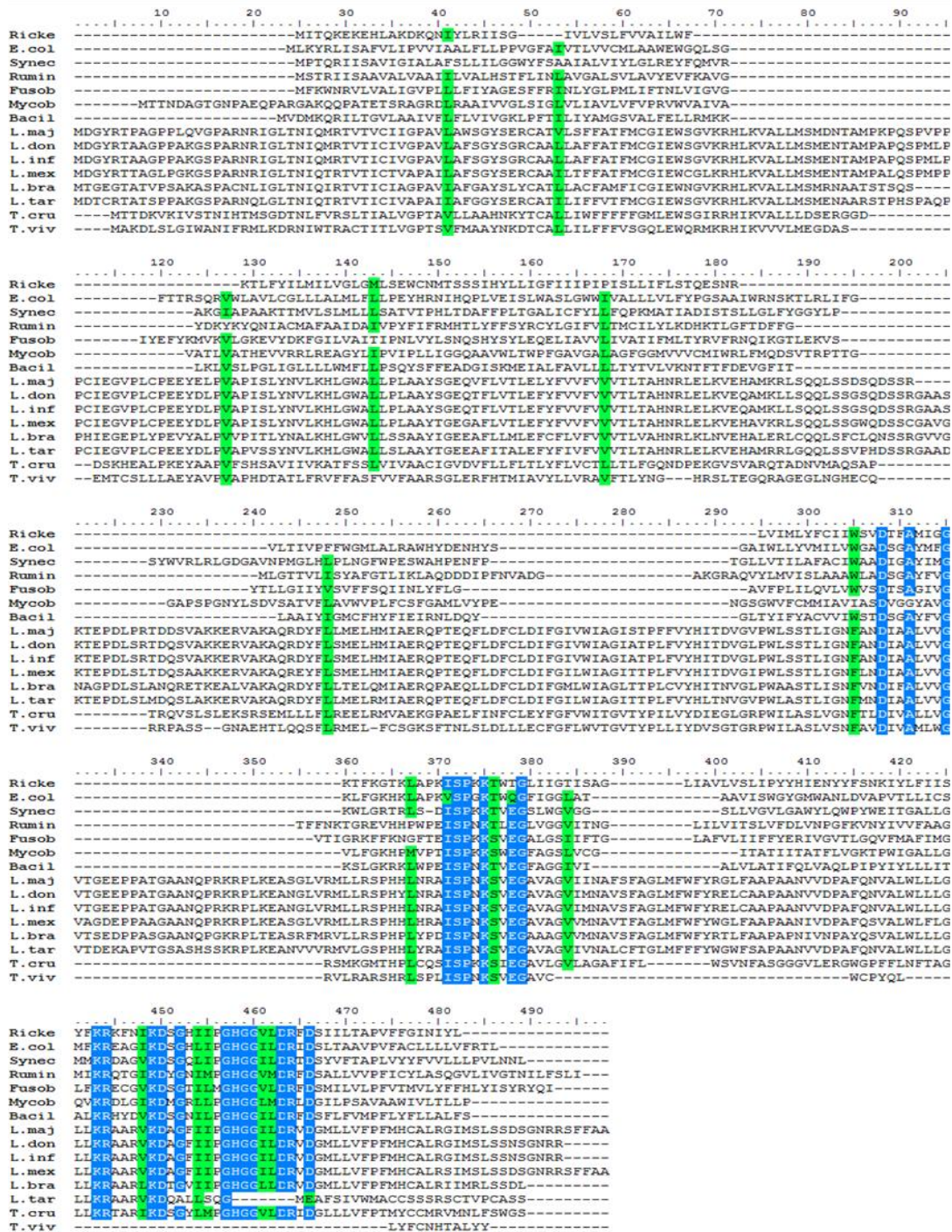


Figure 3.7. Protein sequences of predicted prokaryotic CDS proteins with kinetoplastid prokaryotic-like proteins, aligned using Clustal W. Blue shading indicates identical residues in 85% of sequences, green shading indicates similar residues. Species and accession numbers: **Ricke** = *Rickettsia*YP_067369.1 ; **E.col** = *E.coli* YP_003037629.1 - XP_810276.1; **Synec**= *L major* - XP_001684166.1; **T.viv** = *T. vivax* - CCC48662.1 ; **Homo1** = *Homo sapiens 1* - NP_001254.2; **Homo2** = *Homo sapiens 2*- NP_003809.1; **S.cer** = *S. cerevisiae* - NP_009585.1 - **C.ele** = *C. elegans* - NP_501297.1.s; **E. col** = *E.coli* - YP_003037629.1. Red box indicates the phosphatidyl cytidyltransferase signature (Figure 3.2)

3.4 Phylogenetics

Figure 3.8. shows an unrooted phylogram of the predicted eukaryotic like CDS proteins from kinetoplastids, along with some other eukaryotic CDSs some. The trypanosomatids form their own, well supported clade as a putative sister group to a large clade containing the mammalian species at the tip, with the ascomycetes *S. cerevisiae* and *T. melanosporum* branching earliest. This suggested the similarity shared with the ascomycetes may be as a result of a more conserved sequence from a common ancestor. The plasmodium sequence is the most divergent, branching near *Encephalitiozoon intestinalis* which is likely to indicate an artefact of long branch attraction due to saturation (a well known artefact of the parsimony method of phylogenetic reconstruction) in these two eukaryotes which are known to be highly divergent from other eukaryotes, rather than a close evolutionary relationship.

An unrooted phylogram of the extremely divergent or prokaryotic-like second kinetoplastid CDS genes and prokaryotic CDS proteins is shown in Figure 3.9. Unsurprisingly, these unusual proteins form their own, well supported clade. The *T. cruzi* and the *Leishmania* species form sister clades, suggesting the genes in these organisms share a common ancestor. If the prokaryotic-like CDS genes were originally the result of a horizontal gene transfer event from a prokaryotic endosymbiont, this transfer occurred before the *Trypanosoma* and *Leishmania* lineages split i.e. in their common ancestor. *T. vivax*, however, branches off before the common ancestor of *T. cruzi* and the *Leishmania* species. This split is well supported by bootstrap analysis and bears consideration. It may indicate that a lack of evolutionary pressure has allowed the gene to accumulate mutations and saturation has occurred. This lack of evolutionary pressure is well supported by the fact that *T. brucei* does not appear to contain a homologue of this gene, and the fact that the *T. vivax* gene appears to lack what is predicted to be a domain of the active site.

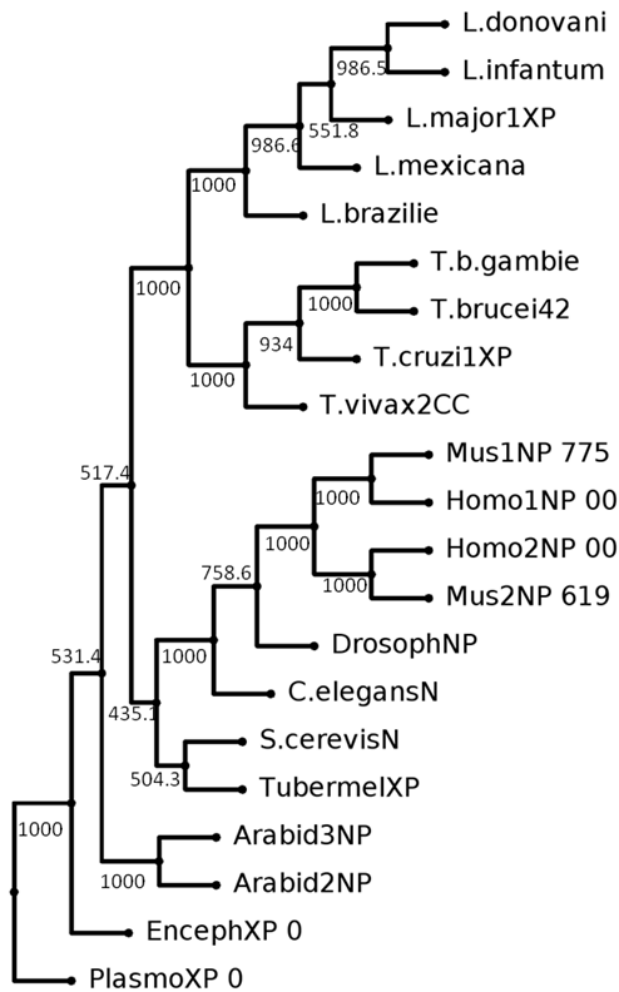


Figure 3.8. Unrooted phylogeny of known and putative CDS protein sequences . Sequences were aligned using Clustal Omega and manually edited to remove ambiguously aligned and gap regions, resulting in 448 unambiguously aligned positions. Phylogeny was inferred using the protein sequence parsimony method from the PHYLIP package (Phylipi 3.67 ProtPars) (Felsenstein 1989,) hosted by the moyble.pasteur.net. Numbers at nodes indicate the frequency of branch associations from 1000 bootstrap replicates. Full species names and accession numbers: **S.cerevisN** – *Saccharomyces cerevisiae*(NP_009585.1); **Homo1NP00** – *Homo sapiens* 1 (NP_001254.2); **Mus1NP775** – *Mus musculus* 1 (NP_775546.2); **Homo2NP00** – *Homo sapiens* 1 (NP_003809.1); **Mus2NP619** – *Mus musculus* 2 (NP_619592.1); **DrosophNP** – (*Drosophila melanogaster* (NP_524661.1); **C.elegansN** – *Canaerhabillis elegans* (NP_501297.1); **Arabid2NP** – *Arabidopsis thaliana* 2 (NP_176433.2); **Arabid3NP** – *Arabidopsis thaliana* 3 (NP_194407.5); **PlasmoXP0** – *Plasmodium falciparum* (XP_001348270.)1; **T.brucei427** – *Trypanosoma brucei* strain 427 (Figure 3.C); **EncephXP0** – *Encephalitozoon intestinalis* (YP_003072938.1); **L.major1XP** – *Leishmania major* (XP_001684166.1); **T.vivax2CC** – *Trypanosoma vivax* (CCC48662.1); **L.brazilie** – *Leishmania brazilliensis* (XP_001562395.1); **L.mexicana** – *Leishmania mexicana*(CBZ27982.1); **L.donovani** – *Leishmania donovani* (CBZ35048.1); **L.infantum** – *Leishmania infantum* (XP_001470506.1); **T.b.gambie** – *Trypanosoma brucei gambiense* (CBH12030.1); **TubermelXP**– *Tuber melanosporum*(XP_002839280.1).

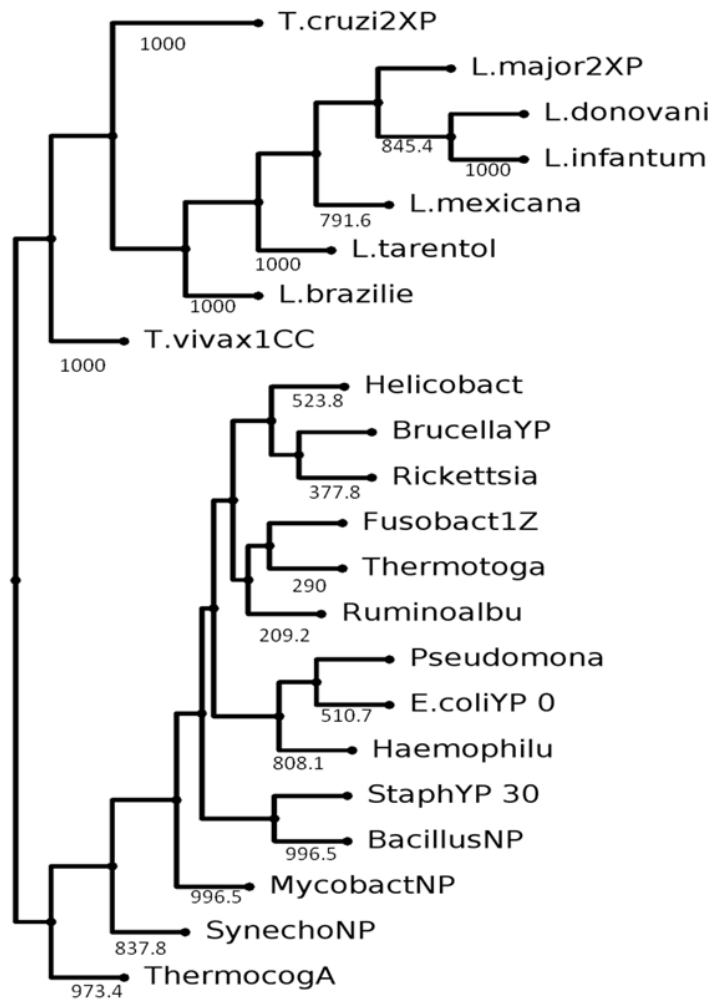


Figure 3.9. Unrooted phylogeny of known and putative CDS protein sequences with kinetoplastid CDS sequences. Sequences were aligned using Mafft and manually edited to remove ambiguously aligned and gap regions. Trees were built using alignments of 495 unambiguously aligned positions. Phylogeny was inferred using the protein sequence parsimony method from the PHYLIP package (Phylipi 3.67 ProtPars) (Felsenstein 1989, 1993) hosted by the moyble.pasteur.net. Numbers at nodes indicate the frequency of branch associations from 1000 bootstrap replicates. Full species names and accession numbers: **T.vivax2CC**:-*Trypanosoma vivax* (CCD19856.1) **Helicobact** - *Helicobacter pylori* (307636907); **E.coliYP 0** - *Escherichia coli* (YP_003037629.1); **Haemophiilu** - *Haemophilus influenzae* (NP_439079.1); **Pseudomona** - *Pseudomonas aeruginosa* (NP_252341.1); **Rickettsia** - *Rickettsia typhi* (YP_067369.1); **StaphYP30** - *Staphylococcus saprophyticus* (YP_301597.1); **BacillusNP** - *Bacillus subtilis* (NP_389536.1); **SynechoNP** -*Synechocystis* sp. (NP_440908.1); **BrucellaYP** - *Brucella ovis* (YP_001259075.1); **MycobactNP** - *Mycobacterium tuberculosis* (NP_217397.1); **Fusobact1Z** - *Fusobacterium nucleatum* (ZP_04970183.1); **Thermotoga** - *Thermotoga maritima* (NP_229198.1); **L.major2XP** - *Leishmania major* (XP_001685610.1); **T.cruzi2XP** - *Trypanosoma cruzi* (XP_812177.1); **L.infantum** - *Leishmania infantum* (XP_003392723.1); **Ruminoalbu** - *Ruminococcus albus* (YP_004105248); **Thermocog** - *Thermococcus gammatolerans* (ACS34635.1) **L.donovani** - *Leishmania donovani* (1CBZ37030.1); **L.mexicana** - *Leishmania mexicana* (1CBZ29682.1); **L.brazilie** - *Leishmania braziliensis1* (XP_001567663.1); **L.tarento** - *Leishmania tarentole* (P32.3050).

However, since the *T. vivax* gene is not syntenic with the others kinetoplast ones, this may indicate that it has an alternative origin i.e. the transfer of the *T. vivax* gene was a separate horizontal gene transfer event. On the other hand, if the common ancestor of *T. cruzi* and the *Leishmania* species genes suggest that this endosymbiotic transfer occurred in an ancestor of these two groups, this would mean that *T. vivax* contained the same gene. A separate transfer event that happened in *T. vivax* after it split from the other *Trypanosoma* species would have left this organism with two of these prokaryotic-like genes. Since this is not the case *T. vivax* must have lost the original gene, as appears to have happened with *T. brucei* after splitting with *T. vivax*. *T. vivax* presumably gained this alternative gene after splitting with *T. brucei*, or, if this gene transfer event occurred in the common ancestor of *T. brucei* and *T. vivax*, *T. brucei* must have lost this gene too. From this analysis, it is not possible to say whether the original prokaryotic-like *T. vivax* CDS gene was lost before or after the new gene was acquired.

Alternatively, the common ancestor of *Trypanosoma* and *Leishmania* may have had both genes, with *T. brucei* losing both, *T. cruzi* and the *Leishmanians* losing one and *T. vivax* losing the other. This hypothesis is less parsimonious as it would require far more horizontal gene transfer events and losses, but this does not necessarily discredit it. Further phylogenetic analyses would be required in order to determine which of these hypotheses is most likely to be true.

3.5 Expression of TbCDS in *E. coli*

Since no CDS gene has ever been studied in a trypanosomatid parasite, it was necessary to confirm whether the identified TbCDS open reading frame encoded CDP-DAG synthase activity. Overexpression of recombinant TbCDS cloned from *Trypanosoma brucei* was first attempted in *E. coli*. Since *E. coli* contains its own endogenous CDS activity, it was necessary to be able to detect any TbCDS activity over and above that of the endogenous *E. coli* CDS activity in order to confirm that the TbCDS was functional and active.

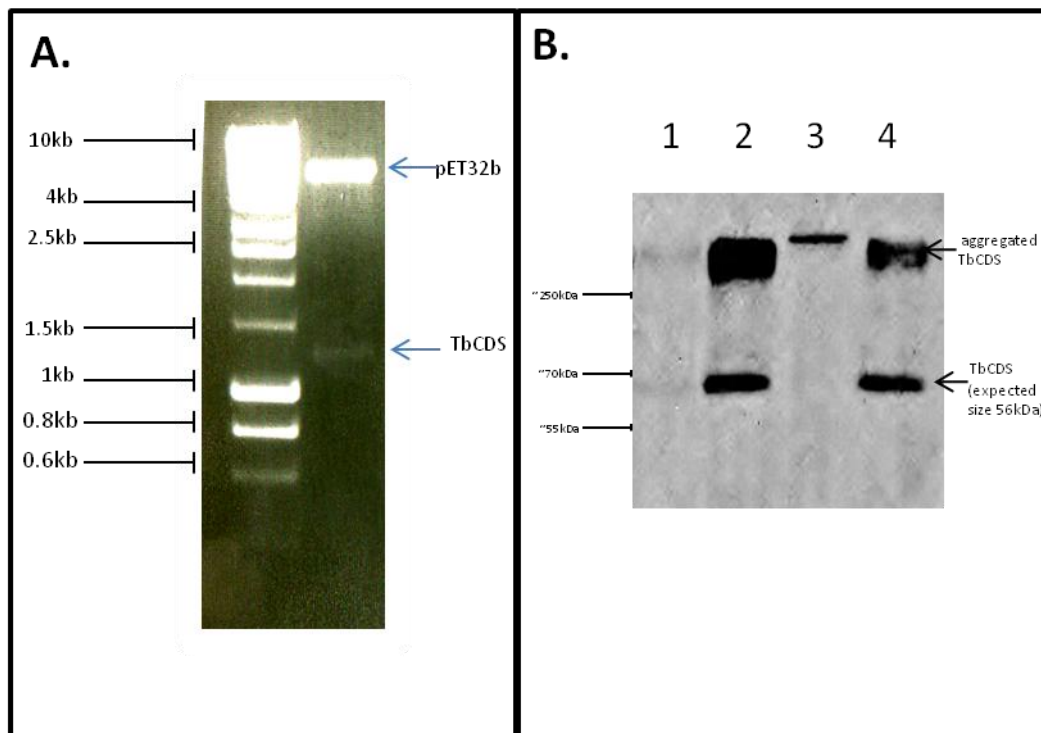


Figure 3.10 Recombinant expression of TbCDS in *E. coli*. (A) EcoRI, XhoI restriction enzyme digest of TbCDS in pET32b) Anti-HIS Western blot of TbCDS expressed on pET32b vector, containing an N terminal thioredoxin tag and N- terminal and C-terminal hexahistidine tags, in Rosetta 2 *E. coli* cells. Lane 1 – soluble fraction extracted with 0.1% TX-100. Lane 2 – insoluble pellet from 0.1% TX-100 extraction. Lane 3 – soluble fraction extracted with 0.5% TX-100. Lane 4 – insoluble pellet from 0.5% TX-100 extraction.

TbCDS was cloned into the *E. coli* overexpression plasmid pET-32b, using EcoRI and XhoI restriction enzyme sites (Figure 3.10, A). pET-32b adds N- and C- terminal His₆ tags and an N-terminal thioredoxin so that the protein can be enriched for by affinity chromatography. A variety of competent *E. coli* cells were transformed with the pET-32b TbCDS construct: C43, Rosetta 2, BL21 Gold PlysS and RIL cells. Each was induced with varying amounts of IPTG and allowed to grow at either 37°C for 3 hours or 16°C overnight in either LB, auto induction or TPB medium. The harvested cells were then lysed and separated into soluble and pellet fractions. Significant overexpression of any protein was not visible on coomassie stained SDS-PAGE gels, but some low expression of HIS-tagged protein was detected by Western blot (Figure 3.10, B).

Whilst still appreciably low, the best results were obtained in Rosetta 2 cells grown at 16°C overnight in LB, with the signal being found entirely in the pellet as expected from the hydrophobicity predictions of TbCDS. In order to obtain soluble protein, the

pellet was resuspended in various detergents and incubated in a sonication bath with frequent vortexing. The following detergents and concentrations were tried: TritonX-100 (0.1% - 1%) n-OG (0.3%), Sodium deoxycholate (0.5%) and SDS (0.1%). A soluble His-tagged protein at approximately 65 kDa - the correct size for the predicted recombinant protein - was detected by western blot from the TritonX-100 extraction (Figure 3.10, B, lane 3), however the signal was very low and there was a high degree of aggregation. With such poor expression, it was considered inappropriate to try and purify the protein by affinity chromatography.

Assay for TbCDS activity using an enriched membrane preparation from *E. coli* cells over expressing TbCDS was attempted, but no appreciable increase in CDS activity was observed over and above the *E. coli* endogenous activity. In order to perform a more sensitive test for the overexpression of TbCDS in *E. coli*, lipid extracts from induced and un-induced *E. coli* cells carrying the TbCDS overexpression plasmid were prepared for MS analysis.

Results are shown in Figures 3.11 and Figure 3.12. Figure 3.11 shows the negative ion scan for precursors of m/z 153 (glycerol-phosphate) in the mass range between 600 and 1000 m/z to show the PG and PE species.

There is proportionally less of what is the most abundant species in the uninduced *E. coli* - PG C36:2 species, composed of di-C18:2, and PG C34:1 (a mixture of C16:0/C18:1) becomes the most abundant species in the induced TbCDS expressing cell line. In the uninduced cell line, the peak corresponding to PG C34:1 is only 0.89 the intensity of the PG C36 peak, whilst in the induced cells the proportion of PG C34 becomes 1.16 that of the PG C36. PA species with corresponding lipid moieties are incorporated into CDP-DAG, which is used as a substrate for PG synthase and results in a change in the relative distribution of PG species. The *E. coli* CDS shows a preference for PA species containing at least one double bond in the diacyl group, but has a higher activity with C16:0/C18:1 than with C18:1/C18:1.

Since C36:2 is the most abundant PG species in the wild type *E. coli* scan, this indicates that the *E. coli* enzyme has a higher encounter rate with PA C36:2. It is possible that different localisation of the TbCDS in *E. coli* means that it has access to more C34:1 PA, or alternatively that the affinity of the TbCDS for this substrate is higher than that of the *E. coli* CDS. Similarly, there is a proportional increase in the peak at 720 m/z corresponding to PG C32:1 composed of C16:0/C16:1 and

C14:0/C18:1. These species were not tested in the *E. coli* enzyme, but it is again clear from these results that the TbCDS is either encountering more of these species in its subcellular localisation or that it has a higher affinity for these species.

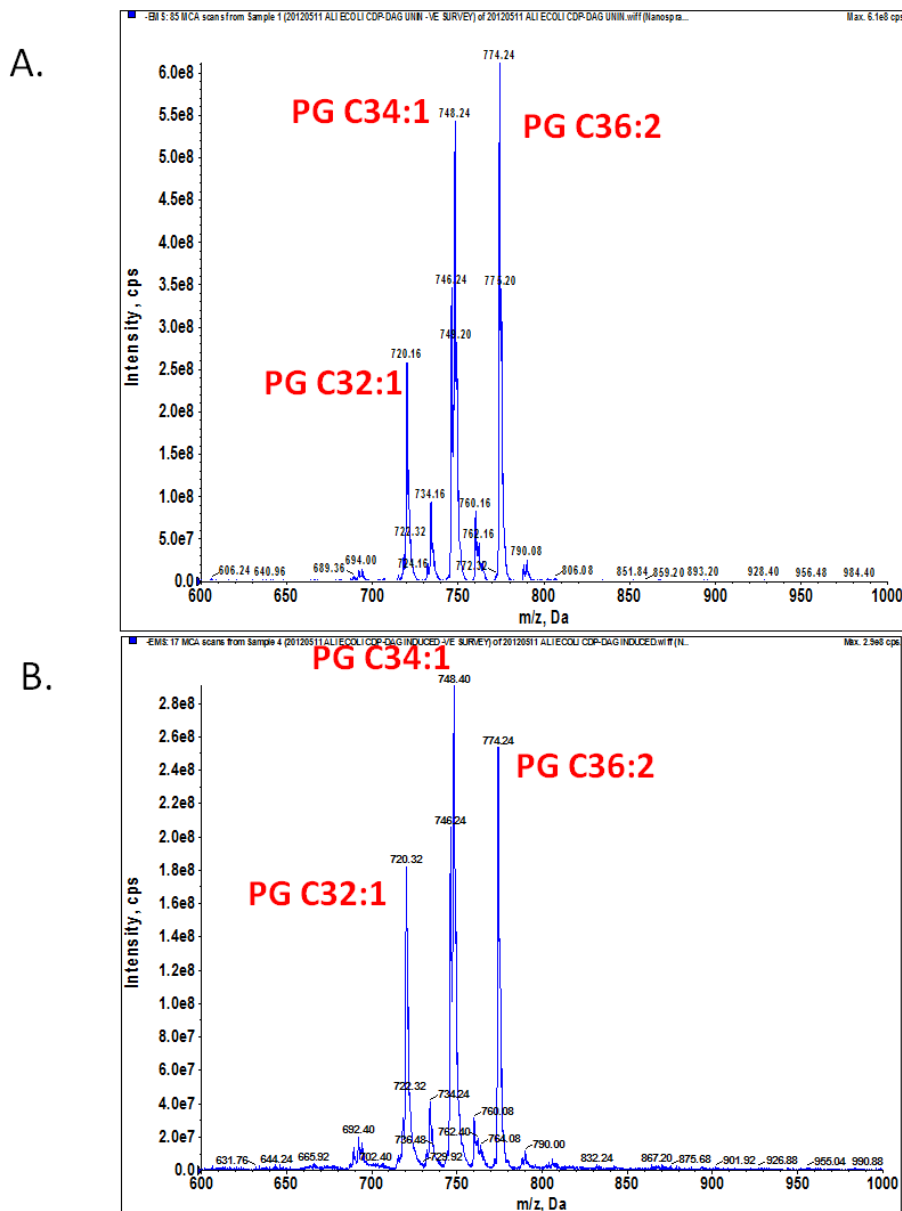


Figure 3.11. Overexpression of TbCDS in *E. coli* causes a change in phospholipid composition- PG species. A. ES-MS negative ion spectra of for m/z 153 in negative ion mode with a collision offset energy of 50 V specifically detected [M-H]⁻ ions from glycerophospholipids in a total lipid extract from Rosetta 2 *E. coli* cells carrying the TbCDS pET-32b plasmid under induced (A) and unduced (B) conditions. Mass range between 600 and 1000 m/z showing mainly PG species. Peaks are plotted as their intensity (cps) as a function of their mass/charge values (m/z). Since each class of phospholipid is detected with different optimal offset collision efficiencies, the phospholipid class peaks in these spectra do not represent their true abundance in the cell relative to other phospholipid classes.

The negative survey scan for high molecular weight species (Figure 3.12) shows the CL 1491 m/z corresponding to C74:0, whilst the peak at 1437 m/z, corresponding to CL C70 is increased from 0.63 to 0.81 of the peak corresponding to C72. in the overexpressing *E. coli* (Figure 3.12 compare A and B). Again, this could indicate that the TbCDS has an increased specificity for the shorter chained lipid species in comparison to the *E. coli* enzyme. Interestingly, there is also a significant decrease in peaks at 1450 m/z and m/z 1477 corresponding to the odd chain CL species C71:0 and C73:0 in the induced compared to the uninduced TbCDS expressing *E. coli* - from 0.45 to 0.27 and 0.52 to 0.37 of C72, respectively. Since fatty acid chains containing an odd number of carbons do not occur in trypanosomes it is highly possible that they are not good substrates for TbCDS and therefore not incorporated into CDP-DAG for PG synthesis and CL formation.

Combined, the alteration of PG and CL species in induced TbCDS expressing *E. coli* compared to the uninduced gives good evidence that TbCDS encodes a functional CDS, and that it has different specificities for PA species than the *E. coli* enzyme. However, further evidence was needed, and it seemed unlikely that such evidence could be obtained with such a relatively low level of expression in a high endogenous background.

The acquisition of a yeast CDS knockdown cell line allowed for the opportunity to test for TbCDS activity in a clean background.

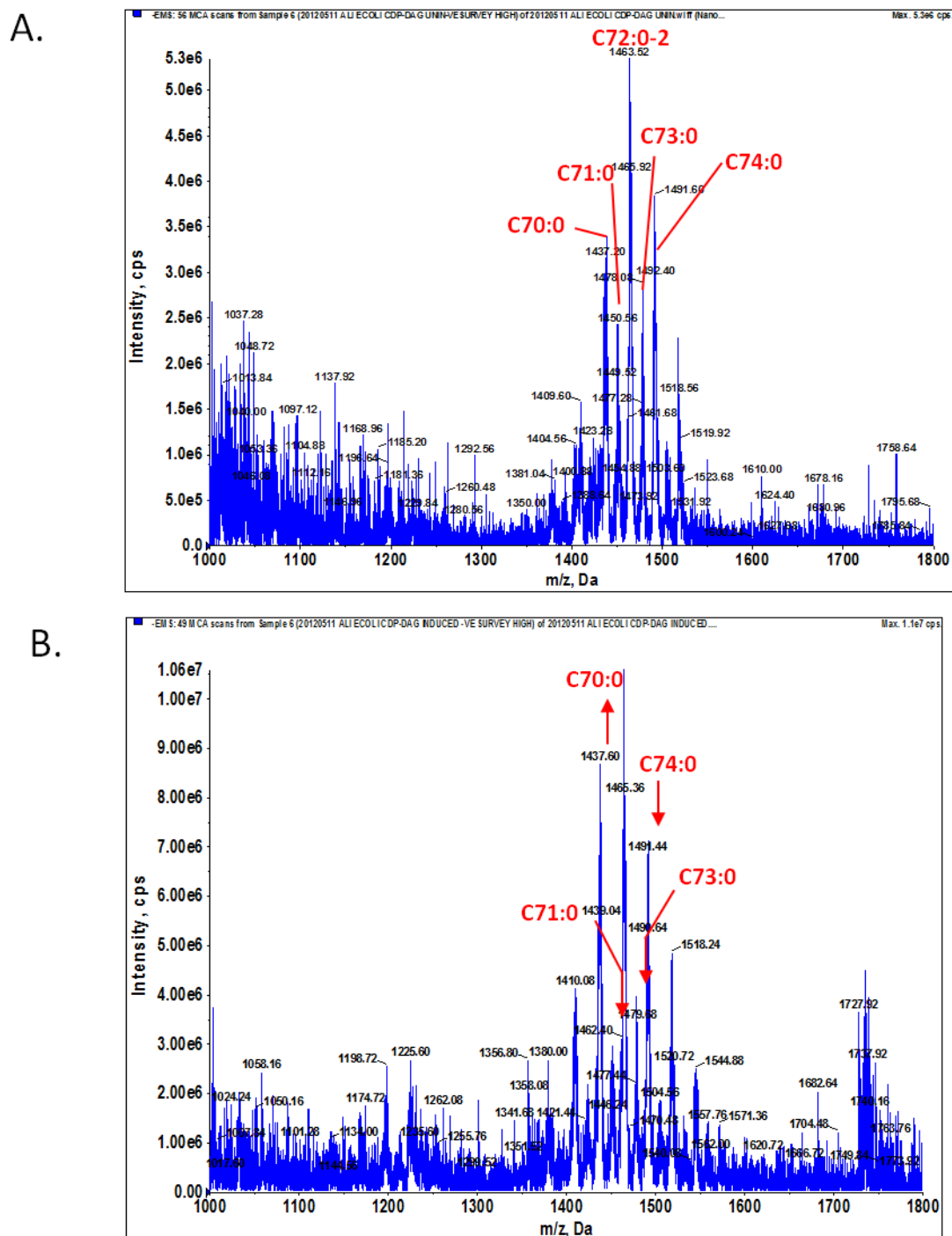


Figure 3.12. – Over expression of TbCDS in *E. coli* causes a change in phospholipid composition- CL species. ES-MS-MS negative ion spectra of for m/z 153 in negative ion mode with a collision offset energy of 50 V specifically detected [M-H]⁻ ions from glycerophospholipids in a total lipid extract from Rosetta 2 *E. coli* cells carrying the TbCDS pET-32b plasmid under uninduced (A) and induced (B) conditions. Mass range between 1000 and 1800 showing CL species. Peaks are plotted as their intensity (cps) as a function of their mass/charge values (m/z). Since each class of phospholipid is detected with different optimal offset collision efficiencies, the phospholipid class peaks in these spectra do not represent their true abundance in the cell relative to other phospholipid classes.

3.6 Yeast rescue

As CDS1 is an essential gene in *S. cerevisiae* (Shen et al., 1996) a double knockout cannot be obtained. A cell line heterozygous for the yeast *cds1::KanMX* was obtained from Professor Mike Stark at the University of Dundee. TbCDS and Yeast CDS1 were isolated by PCR and cloned into pRS426-MET25 uracil selectable yeast expression vector containing the MET promoter, which is suppressed in the presence of methionine (Figure 3.13; Figure 3.14, A). The full method used to rescue *S. cerevisiae cds1::KanMX/CDS1* is summarised by schematic in Figure 3.14. First, the *S. cerevisiae cds1::KanMX* heterozygous cell line was transfected with either the plasmid containing the yeast CDS1 (pRS426-MET25 yeast CDS1), the plasmid containing the *T. brucei* CDS (pRS426 MET24 TbCDS) or empty plasmid (Figure 3.14, A).

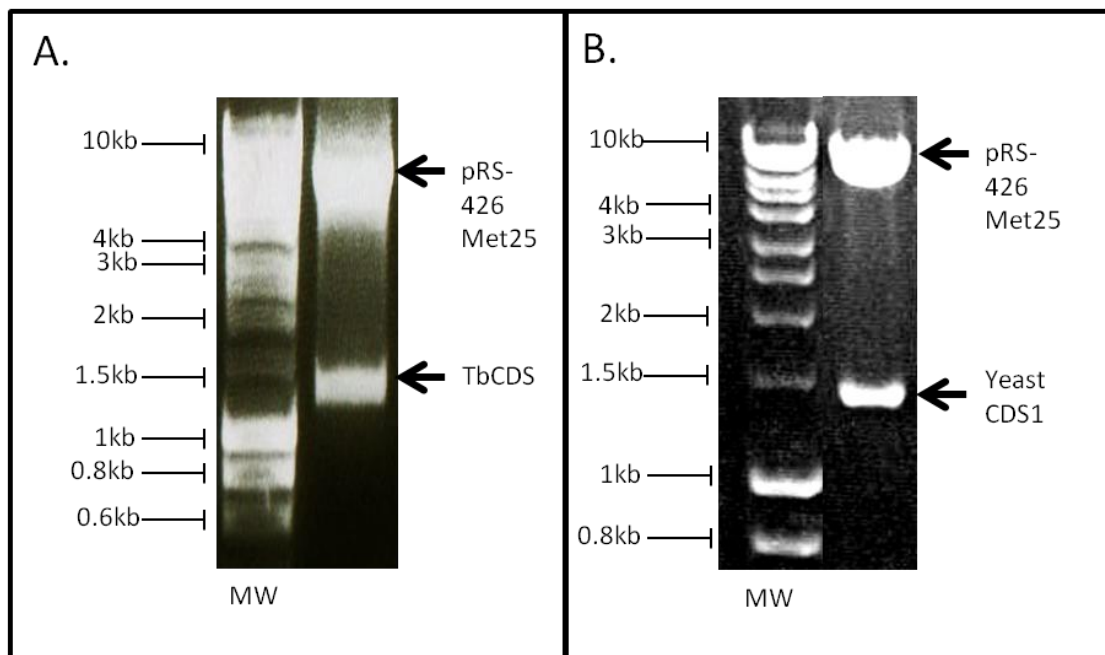


Figure 3.13. Yeast rescue constructs (A) HindIII-XhoI restriction enzyme digestion of TbCDS gene in pRS-426 Met25 (B) HindIII XhoI digest of Yeast CDS1 gene in pRS-426 Met25.

The vector was selected for in media deficient in uracil and methionine (Figure 3.14, B). The three cell lines above, plus the original heterozygous CDS1 null containing no plasmids were then taken for sporulation and tetrad analysis (performed by Mike Stark at the University of Dundee (Figure 3.14, C)). Sporulation and tetrad analysis was carried out in the absence of methionine in order to allow expression of the CDS

gene on the pRS426-MET25 locus. Unfortunately, at this stage it was noted that the background *S. cerevisiae* strain was heterozygous for the MET gene, meaning that half of the spores would be unviable in the methionine absent environment required for the expression of the exogenous CDS.

After sporulation, viable spores were tested for lethality on SCD + Met in order to select against those spores containing the mutated CDS1 allele and therefore relying on the exogenously expressed CDS (not shown in Figure 3.14). Unfortunately, all viable spores also grew in the presence of methionine. Since it has previously been shown that CDS is essential in *S. cerevisiae* this seems to suggest that all viable spores contained the wild type, single functional CDS1 allele. However, it was postulated that suppression of the exogenous gene in the presence of methionine may not be complete, and that the level of leaky expression may be enough for survival of the cells. In support of this, it has been shown that only 10% of wild type CDS activity is sufficient to support normal growth in *S. cerevisiae* (Shen et al., 1996). In order to test this hypothesis, the segregants were screened in the presence of G418 which selects for the knockout construct used to make the null, and in the absence of uracil to select for pRS426-MET25 (Figure 3.14, I). Finally, they were also screened with 5-fluoroorotic acid (5-FOA) which screens against the plasmid, since pRS426-MET25 confers prototrophy for uracil and is therefore able to convert 5-FOA into 5-fluoro uracil, which is lethal.

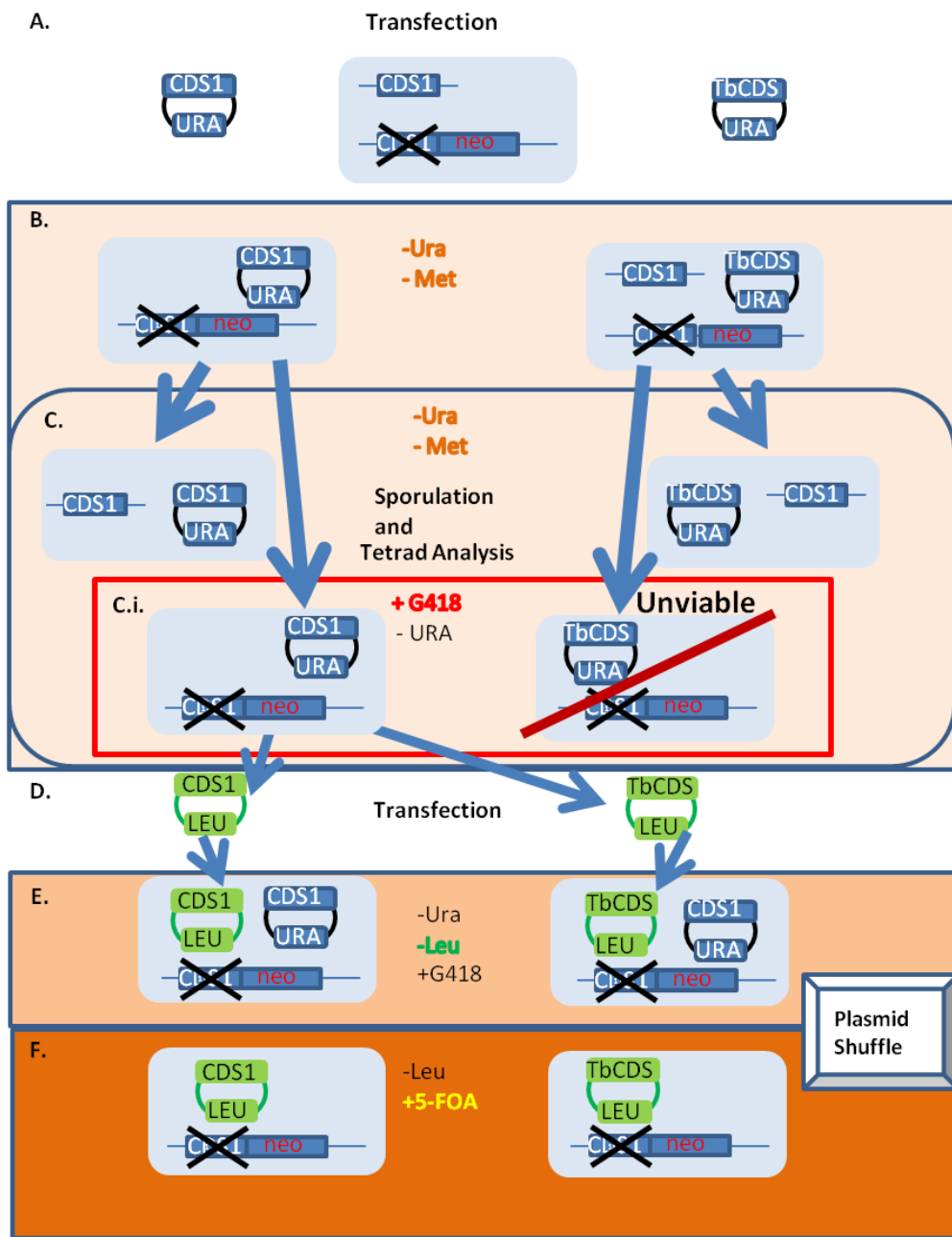


Figure 3.14. Schematic showing complementation of a yeast *CDS1* null with the putative *TbCDS*. (A) A *cds1::KanMX* single knockout containing the *neo* G418 resistance gene transfected with either yeast *CDS1* or *TbCDS* on the expression plasmid pRS-426 Met25 containing *URA3* auxotrophic marker for uracil. (B) Successful transformants were selected by uracil auxotrophy. (C) These diploid cells containing the exogenous gene copies were then sporulated and tetrads dissected on SCD-URA+G418 to select for the *cds1::KanMX* null allele and the pRS-426 MET25. Whilst yeast *CDS1* pRS-426 Met25 was able to rescue the spores containing the *cds1::KanMX* null allele, spores containing the *cds1::KanMX* null allele and the *TbCDS* pRS-426 Met25 were unviable. (D) In order to test if the *TbCDS* may be successful in a different expression vector, the haploid *cds1::KanMX* knockout containing yeast *CDS1* in a plasmid was transfected with a second plasmid, with a stronger promoter containing the leucine auxotrophy marker and either the yeast *CDS1* or the *TbCDS* gene. (E) Transformants with both plasmids were then selected for on plates lacking both uracil and leucine. (F) The initial plasmid was then selected against by the addition uracil and 5-FOA to the plates. The uracil synthesis plasmid converts 5-FOA to 5-Fluoro-orotic acid which is lethal, and the plasmid was shuffled out.

As expected, the heterozygous CDS1 null with no vector gave 0, 1 or 2 viable spores per tetrad dissection when dissected on SCD -Met. This confirms what was seen on the sporulation of a heterozygous yeast CDS1 null by Shen and colleagues (1996). The viable spores were all able to grow in the presence of methionine and sensitive to G418. This confirmed that the knockout was lethal and that the cell line is heterozygous for MET (not shown).

Tetrad dissection of the heterozygous CD1 null containing pRS426-MET25 yeast CDS1 (Table 3.a), showed clear complementation of the *cds1::KanMX* knockout- G418 resistant spores (containing *cds1::KanMX* knockout) grew on - Ura plates (contained the plasmid) but failed to grow in 5-FOA (are unviable without the plasmid) (Figure 3.14, C.i). There were also several strains that were sensitive to G418 (i.e. not knockouts) and growing on -URA (contain the plasmid) but that also grow on 5FOA (so can lose the plasmid and still be viable).

Tetrad dissection of the strain containing pRS426-MET25 TbCDS (Table 3.2) showed that the TbCDS was unable to complement the yeast *cds1* knockout. Several strains contained the plasmid (could grow on - URA) but were sensitive to G418 (not knockouts) and could grow on 5-FOA (without the plasmid) (Figure 3.14, C.ii). Interestingly, there were also two G418 resistant spores (knockouts) that germinated but did not have the plasmid (strains 4D and 16A in Table 3.2). This result cannot be easily explained but it is likely that something unusual has happened, and in any case was not useful for the present investigation.

Table 3.1. Tetrad Dissection of MET15 his3leu2ura3 cds1::KanMX [pRS425-MET25 yeast CDS1].

	Met	Ura	5-FOA	G418	YPAD			Met	Ura	5-FOA	G418	YPAD	
1A							11A						
1B							11B						
1C							11C						
1D							11D						
2A	(✓)	x	✓	x	✓		12A	✓	✓	x	✓	✓	
2B	(✓)	x	✓	x	✓		12B	(✓)	x	✓	x	✓	
2C	x						12C	(✓)	✓	x	✓	✓	
2D	x						12D	✓	✓	✓	x	✓	
3A	x						13A	(✓)	x	✓	x	✓	
3B	x						13B	✓	x	✓	x	✓	
3C	✓	✓	✓	x	✓		13C	x					
3D	✓	✓	x	✓	✓		13D	x					
4A	x						14A	✓	x	(x)	x	✓	
4B	x						14B	(✓)	x	✓	x	✓	
4C	(✓)	x	✓	x	✓		14C	(✓)	✓	x	✓	✓	
4D	(✓)	x	✓	x	✓		14D	✓	✓	x	✓	✓	
5A	✓	✓	x	✓	✓		15A	(✓)	x	(x)	x	✓	
5B	✓	✓	x	✓	✓		15B	(✓)	✓	x	✓	✓	
5C	(✓)	x	✓	x	✓		15C	✓	x	✓	x	✓	
5D	(✓)	x	✓	x	✓		15D	✓	✓	(x)	✓	✓	
6A	x						16A	✓	✓	✓	x	✓	
6B	(✓)	x	✓	x	✓		16B	(✓)	x	✓	x	✓	
6C	(✓)	✓	x	✓	✓		16C	(✓)	✓	x	✓	✓	
6D	x						16D	x					
7A	x						17A	(✓)	x	(✓)	x	✓	
7B	(✓)	x	✓	x	✓		17B	x					
7C	✓	x	✓	x	✓		17C	(✓)	x	✓	x	✓	
7D	x						17D	x					
8A	x						18A	✓	x	✓	x	✓	
8B	(✓)	✓	x	✓	✓		18B	x					
8C	✓	(x)	✓	x	✓		18C	x					
8D	(✓)	✓	x	✓	✓		18D	✓	x	✓	x	✓	
9A	x						19A	(✓)	x	✓	x	✓	
9B	✓	✓	x	✓	✓		19B	x					
9C	(✓)	x	✓	x	✓		19C	✓	x	✓	x	✓	
9D	✓	✓	✓	x	✓		19D	x					
10A	(✓)	x	✓	x	✓		20A	x					
10B	x						20B	x					
10C	✓	✓	✓	x	✓		20C	x					
10D	(✓)	✓	x	✓	✓		20D	x					

“X” only in the first Met column means the spore failed to germinate. Brackets around the tick or cross mean the growth was weak. Yellow highlights indicate that the spores grow on – Ura plates (have the plasmid) and fail to grow on 5-FOA (are unviable without the plasmid). Green highlights indicate strains that are G418 sensitive (not knockouts) and growing on – Ura (have the plasmid).

Table 3.2 Tetrad Dissection Strain of MET15 his3leu2ura3 cds1::KanMX [pRS425-MET25 TbCDS]

	Met	Ura	5-FOA	G418	YPAD			Met	Ura	5-FOA	G418	YPAD	
1A							11A						
1B							11B						
1C							11C						
1D							11D						
2A	X						12A	X					
2B	X						12B	X					
2C	(✓)	✓	✓	X	✓		12C	✓	X	✓	(X)	✓	
2D	(✓)	✓	✓	X	✓		12D	(✓)	X	✓	X	✓	
3A	X						13A	X					
3B	✓	✓	✓	X	✓		13B	(✓)	X	✓	X	✓	
3C	(✓)	✓	✓	X	✓		13C	X					
3D	X						13D	✓	X	✓	X	✓	
4A	✓	✓	✓	X	✓		14A	✓	✓	✓	X	✓	
4B	(✓)	✓	✓	X	✓		14B	X					
4C	X						14C	(✓)	✓	✓	X	✓	
4D	✓	X	✓	✓	✓		14D	X					
5A	✓	X	✓	X	✓		15A	X					
5B	X						15B	(✓)	✓	✓	X	✓	
5C	X						15C	X					
5D	X						15D	X					
6A	(✓)	X	✓	X	✓		16A	✓	X	✓	✓	✓	
6B	✓	X	✓	X	✓		16B	(✓)	✓	✓	X	✓	
6C	X						16C	X					
6D	X						16D	✓	✓	✓	X	✓	
7A	(✓)	X	✓	X	✓		17A	(✓)	✓	✓	X	✓	
7B	(✓)	X	✓	X	✓		17B	X					
7C	X						17C	✓	✓	✓	X	✓	
7D	X						17D	X					
8A	(✓)	X	✓	X	✓		18A	X					
8B	✓	X	✓	X	✓		18B	X					
8C	X						18C	(✓)	X	✓	X	✓	
8D	X						18D	✓	X	✓	X	✓	
9A	X						19A	✓	X	✓	X	✓	
9B	X						19B	X					
9C	✓	✓	✓	(X)	✓		19C	(✓)	X	✓	X	✓	
9D	X						19D	(✓)	X	✓	X	✓	
10A	✓	✓	✓	X	✓		20A	(✓)	X	✓	X	✓	
10B	X						20B	X					
10C	(✓)	✓	✓	X	✓		20C	✓	X	✓	(X)	✓	
10D	X						20D	X					

“X” only in the first Met column means the spore failed to germinate. Brackets around the tick or cross mean the growth was weak. Green highlights indicate strains that are G418 sensitive (not knockouts) and growing on – Ura (have the plasmid).

Since the yeast CDS1 on the pRS426-MET25 is able to complement the *cds1::KanMX* knockout, and the TbCDS on the same plasmid under the same conditions is possible that the *T. brucei* CDS is unable to functionally complement for the yeast one. However, this failure could plausibly be due to insufficient TbCDS expression as pRS426-MET25 is a low copy number, low expression level plasmid, and/or the cells not having sufficient exogenous CDS activity to undergo germination. Four haploid knockout strains containing the yeast CDS1 on pRS426-MET25 (MET15 his3leu2ura3 *cds1::KanMX* [pRS426-MET25 yeast CDS1]) were therefore used in a plasmid shuffle with TbCDS on p405-TEF1 to increase the chances of a complementation without the need for the cells to undergo sporulation and tetrad analysis. Figure 3.15 shows the growth patterns of the *cds1::KanMX* [pRS426-MET25 yeast CDS1] yeast strains under different growth conditions, as noted in Table 3.1. On synthetic complete (SC) medium both YBR029c (the heterozygous CDS1/*cds1::KanMX* knockout parent strain - auxotrophic for uracil) and the *cds1::KanMX*[pRS426-MET25 yeast CDS1] strains are able to grow (Figure 3.15, A). On SC - URA, only the *cds1::KanMX*[pRS426-MET25 yeast CDS1] strains can grow due to their prototrophic uracil marker (Figure 3.15, B). However, on SC+5-FOA only the parent strain can grow, due to their lack of the URA containing pRS426-MET25 plasmid (Figure 3.15, C). Under such conditions, the yeast *cds1* haploid can be thought of as a conditional knockout, since it cannot grow without the plasmid, and the affect of the CDS containing plasmid can be nullified by the addition of 5-FOA to the 5-media.

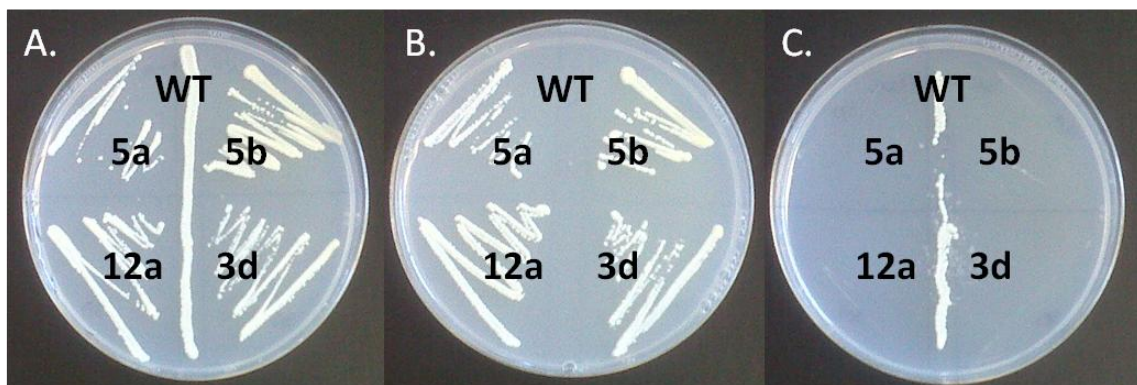


Figure 3.15. Haploid *S. cerevisiae* from tetrad analysis, genotype - MET15 his3leu2ura3 *cds1::KanMX* [pRS425-MET25 CDS1]. (A) Spores 5a, 5b, 12a, 3d (from tetrad analysis, table 3.a) and WT (wild type - wild type cells are in fact YBR029c strain cells – the parent cell of the original knockout, auxotrophic for uracil). on SC. (B) Spores 5a, 5b, 12a, 3d and WT (wild type) on SC-ura. (C) Spores 5a, 5b, 12a, 3d and WT (wild type) on SC+5-FOA.

In order to shuffle out pRS426-MET25, the plasmid p405-TEF1 was chosen due to its strong, constitutive expression and LEU2 selection marker meaning that it was compatible with the leucine auxotrophic phenotype of YBR029c and the URA selectable pRS426-MET25. TbCDS and Yeast CDS1 open reading frames were cloned into the plasmid using HindIII and XhoI restriction sites (Figure 3.16) and *cds1::KanMX*[pRS425-MET25 CDS1] were transformed with p405-TEF1 TbCDS and p405-TEF1 Yeast CDS1 plasmids, along with empty p405-Tef1 (Figure 3.14, D) and plated onto SC-URA-LEU in order to select for both plasmids, along with G418 to select for the original *cds1::KanMX* knockout construct (Figure 3.14, E).

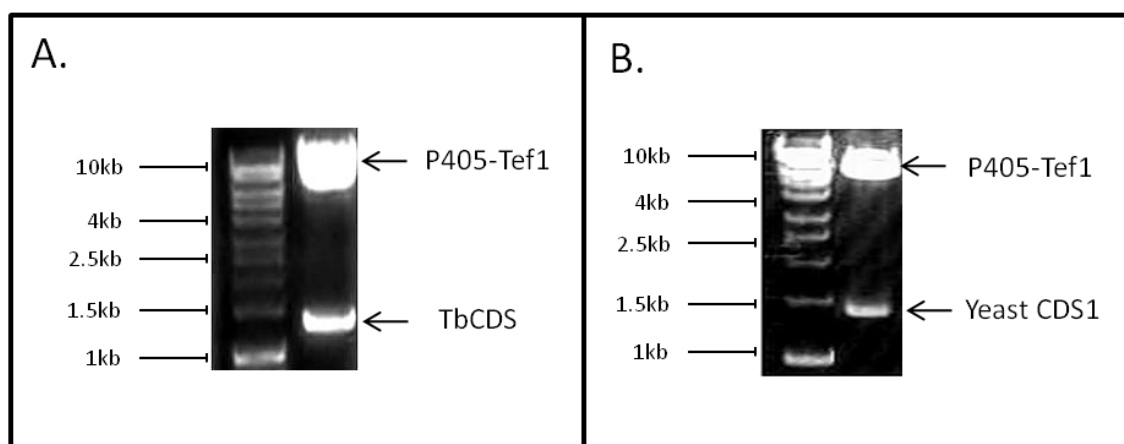


Figure 3.16. Construction of p405-TEF1 rescue plasmids (A) HindIII-XhoI restriction enzyme digest of TbCDS in p405-TEF1 yeast expression vector. (B) HindIII-XhoI restriction enzyme digest of Yeast CDS1 in p405-TEF1 Yeast expression vector.

The obtained colonies containing both plasmids (*cds1::KanMX*[pRS425-MET25 CDS1][empty p405-TEF1/p405-TEF1 CDS1/p40-TEF1 TbCDS]) plus the original haploid strain containing just the URA selectable pRS425-MET25 (*cds1::KanMX* [pRS425-MET25 CDS1]) were plated on YPD in order to obtain good growth and reduce dependence on the URA plasmid. All four strains were then plated onto YPD+5-FOA in order to select against the URA plasmid (Figure 3.14, F and Figure 3.17, A). Figure 3.17, A shows that there was good growth of the knockout strain containing yeast CDS1 on p405-TEF1, which shows the plasmid shuffle has worked and the yeast CDS1 can also complement the *cds1* null phenotype when on p405-TEF1. It also appears that TbCDS can complement the yeast *cds1* null phenotype, suggesting that the TbCDS open reading frame does indeed code for a functional CDS. However, in this experiment there should have been no growth of the original parent strain containing just the pRS426-MET25 yeast CDS1 plasmid, since the knockout requires the plasmid for

growth and the plasmid should be lost in the presence of 5-FOA. However there was some growth on the plate, although it was much less than that observed for the p405-TEF1 TbCDS and p405-TEF1 yeast CDS1 containing strains. Similarly, though to a far less extent, there is some growth of the cell line containing empty p405-TEF1. 5-FOA selection is sometimes known to be incomplete, particularly when it is used in YPD as opposed to minimal media. However, we found that in minimal media the strains were extremely slow growing and therefore plated yeast had to be left on the 5-FOA plates for long periods of time, which was not only inconvenient due to time constraints, but is not recommended due to the mutagenic effects of 5-FOA. It was also considered possible that the low growth on the 5-FOA plate was due to residual synthase activity from before the plasmid was lost, since it was found by Shen and co-workers that in haploid *S. cerevisiae* with a similar CDS1 null haploid background transformed with a yeast CDS1 expressing plasmid formed small colonies under non-inducing conditions for expression of yeast CDS1. When these colonies were streaked onto a fresh plate in non-inducing conditions they failed to grow (Shen et al., 1996). In order to test if residual yeast CDS1 activity had caused the growth in the negative control strains the strains from the YPD + 5-FOA 1 plate (Figure 3.17, B) were restreaked onto a fresh YPD + 5-FOA 2 plate (Figure 3.17, C). On this plate, both the strain containing the empty p405-TEF1, and the parent strain containing no viable plasmid failed to grow at all, as expected. Growth in strains containing the p405-TEF1 TbCDS plasmid and the control p405-TEF1 yeast CDS1 plasmid was definitely present, although rather low. This experiment provides definitive evidence that the TbCDS ORF encodes a functional CDS enzyme, and that it is able to rescue an otherwise non-viable yeast null background.

To see if expression of the TbCDS gene altered the lipid profile compared to wild type and/or the yeast CDS1 gene on p405-TEF1, lipids were extracted from these three different genotype yeast by the Bligh Dyer method, as previously described (Chapter 2). Lipids samples were then analysed by ES-MS. Figure 3.18 shows the negative survey scan of lipids from wild type *S. cerevisiae*, *cds1* null *S. cerevisiae* rescued by the yeast CDS1 on the p405-TEF1 (*cds1::KanMX* [yeast CDS1 p405-TEF1]) and the null *S. cerevisiae* rescued by the *T. brucei* TbCDS (*cds1::KanMX* [TbCDS1 p405-TEF1]).

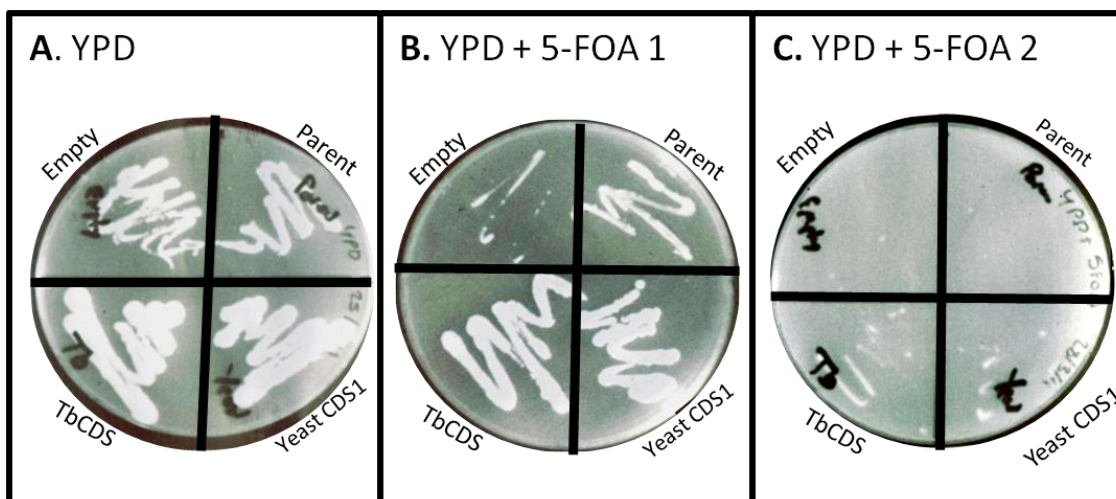


Figure 3.17. Plasmid shuffle shows TbCDS can complement the yeast *cds1::KanMX* knockout. A. After transformation of haploid *cds1::KanMX* [p425-MET25 yeast CDS1] with empty p405-TEF1, p405-TEF1 TbCDS or p405-TEF1 yeast CDS1 and selection for both plasmids, the three strains plus the original parent strain containing just p425-MET24 were plated on YPD, where all strains grew normally. B. Strains were then plated onto YPD+5-FOA in order to select against the p425-MET25 URA plasmid. Strains from this plate were then plated onto a fresh YPD+5-FOA plate. **Parent** = *cds1::KanMX* [p425-MET25 yeast CDS1]; **Empty** = *cds1::KanMX* [empty p405-TEF1]; **Yeast** = *cds1::KanMX* [p405-TEF1 yeast CDS1]; **TbCDS** = *cds1::KanMX* [p405-TEF1 TbCDS].

The presence of peaks corresponding to PI in Figure 3.18, B shows that the yeast CDS1 plasmid has rescued the CDS1 null. The peaks corresponding to all PI species are considerably reduced in comparison to other species, which may explain the slow growth of this cell line. For example, the PI species C32:1 decreased from 2.52 of PE C32 to 0.37, whilst PI C34:1 and PI C36:1 decrease from 1.58 to 0.375 and 0.52 to 0.08 of PE C32, respectively. In its genomic location, the yeast CDS1 is flanked by sequences which are important for expression, regulation and possibly localisation (see Chapter 2) and it is likely that a lack of such signals hinder wild type levels of expression. Surprisingly, whilst still below wild type levels, Figure 3.18, C shows the yeast CDS1 null rescued by TbCDS has considerably higher levels of PI than the yeast CDS1. The height of the PI C32:1 peak in the TbCDS rescue is 0.78 of PE C32 compared to 0.32 in yeast rescue; the PI C34:1 peak in TbCDS rescue is the same height as the PE C32, but only 0.375 of PE C32 in yeast and the PI C36 peak is 0.25 of PE C32 in TbCDS rescue but only 0.08 of PE C32 in the yeast rescue. This shows that the TbCDS is a better rescue than the yeast CDS1, possibly indicating that the enzyme has a higher affinity for its substrates. This is surprising, however, given that the TbCDS on the lower expression level pRS426-MET25 plasmid failed to rescue the yeast null, whilst the yeast CDS1 on the same plasmid was entirely successful.

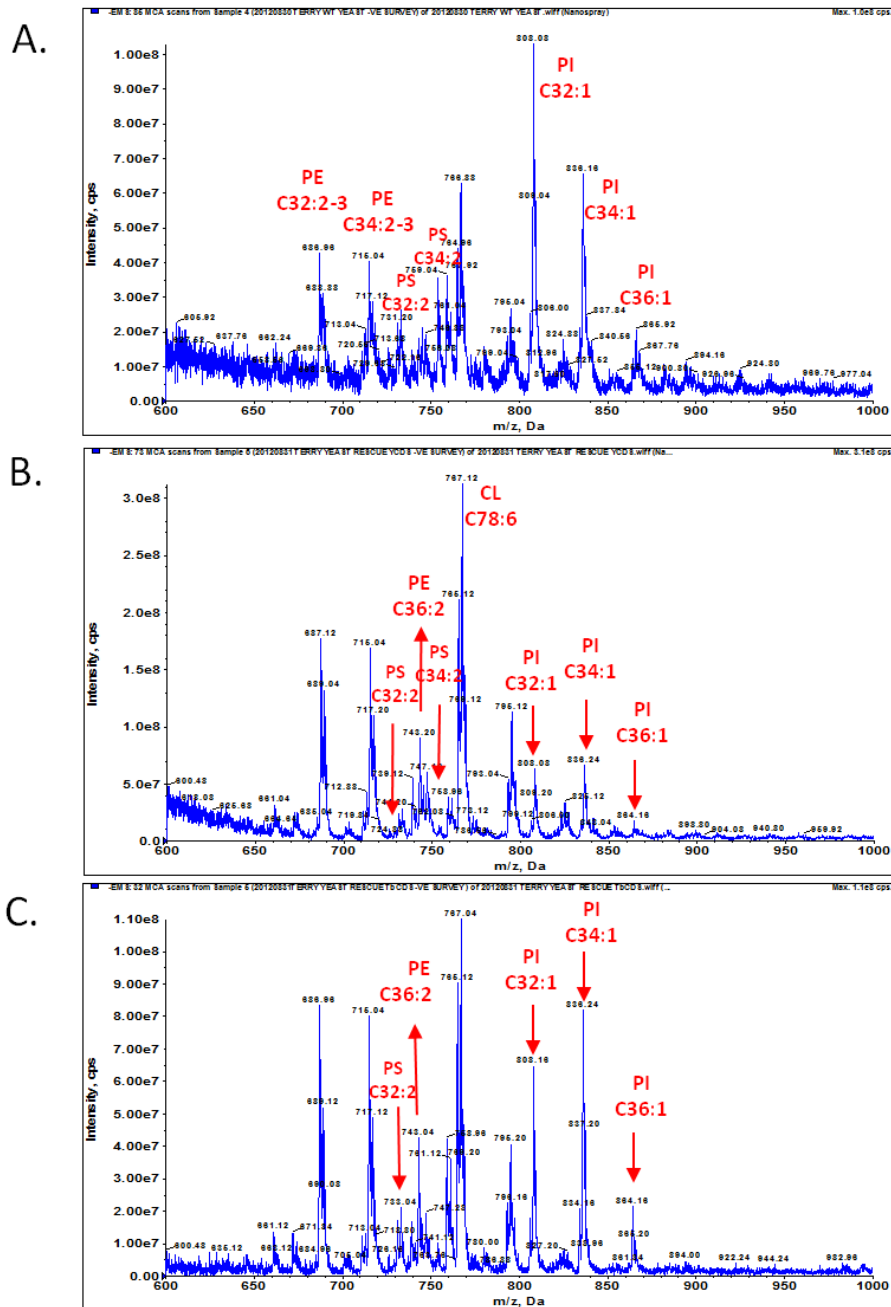


Figure 3.18. Negative survey scan of lipids from yeast CDS rescue. Mass spectrometric analyses of total phospholipids by negative survey scan ES-MS. A. wild type *S. cerevisiae*. B. *S. cerevisiae* *cds1::KANMX* [yeastCDS1 p405-TEF1] C. *S. cerevisiae* *cds1::KANMX* TbCDS1 p405-TEF1]. PE = phosphatidylethanolamine species, species, PI = phosphatidyl inositol. Red arrows indicate peaks which are different in the mutant, whilst the direction of the arrow indicates whether this peak is increased or decreased in the mutant. CX:Y = X – total number of carbons, Y – total number of double bonds in fatty acid chains of lipid species.

It is possible that lower than optimal levels of CDS expression may have not been sufficient for the cells to undergo sporulation, but are sufficient for growth. If the yeast gene is less efficient at rescue it would presumably not have been sufficient for sporulation either. It is possible that for some reason there was more residual CDS activity in the yeast single CDS1 knockout cells transfected with the yeast CDS1 ectopic gene than those transfected with the TbCDS ectopic gene. This would imply that the ability of the cells to sporulate was not in fact due to the exogenous gene, but due to varying background levels.

A reduction in PS species at 731 and 759 m/z in both the rescue phenotypes - from 0.64 in wild type to 0.17 and 0.25 in the yeast and the TbCDS rescues, respectively - is likely a response to the reduced availability of CDP-DAG. In yeast, a large quantity of PE is produced via headgroup exchange with PS, and PS is made via CDP-DAG (Atkinson et al., 1980). A block in the CDP-DAG pathway results in an increase of PE synthesis via the Kennedy Pathway (Shen and Dowhan, 1996). The decrease in PS but not in PE species shows that the Kennedy Pathway is picking up some of the slack from the less than optimal CDP-DAG pathway.

3.7 Summary and Conclusions

A gene predicted to encode CDS activity was found in the genome of *T. brucei* strain 927 and used to design primers in order to isolate the gene and surrounding UTRs from *T. brucei* strain 427. The 1916 bp sequenced contained a 1221 bp reading frame predicted to encode a multiple trans-membrane protein belonging to the cytidyltransferase super-family (cl00347) and containing a phosphatidate cytidyltransferase signature. This protein showed high sequence homology to predicted CDS proteins from other trypanosomatids, but also to other proven eukaryotic CDSs.

A second predicted CDS whose product encoded a protein with sequence homology to prokaryotic CDS proteins was found in the genome of other kinetoplastids *T. cruzi*, *T. vivax* and *Leishmania* species but noticeably absent from *T. brucei*. These proteins show sequence similarity to prokaryotic CDSs only at their C-terminal end, with no strong homology to other known proteins for the rest of the protein family.

Phylogenetic analysis of the eukaryotic like kinetoplast CDSs found them to form their own well supported clade branching early from the eukaryotes, suggesting it is

an ancient eukaryotic protein. The prokaryotic like kinetoplast CDSs also form their own well supported clade, suggesting that any horizontal gene transfer event must have occurred before the split between the *Trypanosoma* and the *Leishmania* species. Surprisingly, the prokaryotic-like *T. vivax* CDS branches off before the other *Trypanosoma* and *Leishmania* species common ancestor. This, combined with the evidence that this gene is not syntenic may suggest the *T. vivax* gene was acquired in a separate horizontal gene transfer event.

In order to verify that TbCDS encoded a functional CDS, a HIS-tagged recombinant protein was expressed in *E. coli* and detected by western blot. Mass spectrometric analysis of lipid extracts from *E. coli* expressing the TbCDS protein showed a slight change in the composition of downstream CDP-DAG pathway products i.e. PG and CL, with an increase in the proportion of species containing shorter acyl chains and a decrease in the phospholipids containing acyl chains with an odd number of carbons. This may suggest that the TbCDS enzyme has a stronger affinity for shorter substrates, and that PA species containing acyl groups with odd numbers of carbon (which are not present in *T. brucei*) are poor substrates for TbCDS. Alternatively, in *E. coli* the TbCDS may be differently localised than the native *E. coli* CDS meaning the enzyme has access to a different, shorter subset of PA species. This gives the first piece of evidence that the TbCDS encodes a functional CDS protein.

For further proof that TbCDS encodes CDS activity, a heterozygous yeast CDS1 knockout was obtained and transformed with the yeast CDS1 and TbCDS on expression plasmids. Tetrad analysis showed that the yeast CDS1 could complement the haploid yeast knockout spores under these conditions, but that the TbCDS could not. The haploid yeast knockout containing the yeast CDS1 on a plasmid was then used for a plasmid shuffle experiment using TbCDS on a higher expression level plasmid, without the need for sporulation. This experiment shows that TbCDS can complement the yeast null of CDS1 and must therefore encode a functional CDS.

Alteration of the lipid profile of *E. coli* over-expressing TbCDS, along with the rescue of a yeast CDS1 knockout by TbCDS give the first pieces of evidence for the predicted CDS in this organism encoding a functional CDS, which is the first step to finding if this gene is essential. Additionally, the discovery of a second, unique CDS in other kinetoplastids that shows very low homology to the human may also be useful in future drug development.

Chapter 4 – Cytidine Diphosphate Diacylglycerol Synthase in Bloodstream Form *Trypanosoma brucei*

4.1 Introduction

The discovery of an open reading frame in *T. brucei* that encodes CDS activity is an excellent start to this study, and provides the basis for an investigation into its suitability as a drug target. The next step was to ascertain whether TbCDS was expressed in both major life cycle stages of *T. brucei* and what effect a reduction of its activity might have on phospholipid synthesis and hence viability. In other organisms where TbCDS activity was reduced a variety of morphological and biochemical differences were seen, which were highly dependent on the organism and, in some cases, the gene encoding the activity. In yeast, where CDS is essential for viability, a mutant with low CDS activity excreted inositol, exhibited a cellular decrease in phosphatidylinositol and an increase in phosphatidylserine (Shen and Dowhan, 1996). Similarly, in *E. coli*, a lack of CDS resulted in death, preceded by a massive accumulation of PA and a decrease in PS and PE (of which CDP-DAG is the precursor in this organism, as there is no Kennedy Pathway) (Ganong and Raetz, 1982). In photosynthetic organisms *Arabidopsis* and *Synechocystis*, knockouts of plastidial CDS caused deformations of the chloroplast and an inability to photosynthesise (Haselier et al., 2010, Sato et al., 2000). However, the CDS isoform studied in *Drosophila* only affected the light response in the developing retina due to a decrease in the pool in phosphoinositides (Wu et al., 1995), and in humans a reduction in CDP-DAG is similarly linked to depletion of the phosphoinositide pool and is thought to be linked to depression (Tyeryar et al., 2008).

In order to be useful as a drug target against the human and animal disease, TbCDS must be expressed and active in the bloodstream form of the parasite, and essential

for parasite survival. The next aims of this project were as follows: first to confirm the expression and activity of TbCDS in bloodstream form *T. brucei*; secondly to investigate how a decrease in TbCDS expression affects the parasite morphologically and biochemically, with particular emphasis on glycerophospholipid metabolism and GPI anchor synthesis. This should identify whether bloodstream form *T. brucei* rely on TbCDS for cell viability.

4.2 Transcription of TbCDS in *T. brucei*

To confirm TbCDS transcription, RT-PCR was performed using the CDS 82 F and CDS 82 R primers (Table 2.1) to amplify the TbCDS ORF. A product at the correct size of 1.2 kb was seen when total RNA from bloodstream form or procyclic form were used as a template (Figure 4.1, A), clearly showing that TbCDS mRNA is present in both these life cycle stages.

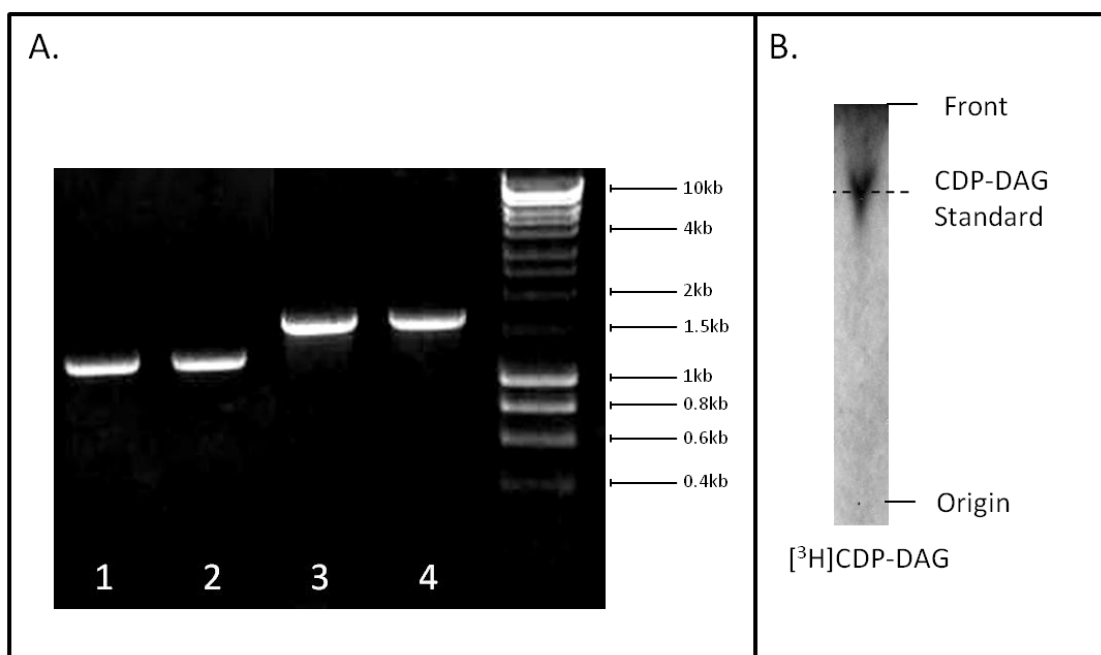


Figure 4.1. TbCDS is transcribed in *T. brucei*, and cells have CDP-DAG synthase activity (A) RT-PCR of TbCDS open reading frame from *T. brucei* RNA. Lane 1 – TbCDS RT-PCR from SM (bloodstream form) RNA. Lane 2 – TbCDS RT-PCR from DM (procyclic) RNA. Lanes 3 and 4 - loading control using INO1 primers on SM and DM RNA respectively. MW = molecular weight marker. (B) TbCDS assay of *T. brucei* lysate – TLC of lipid fraction shows $[^3\text{H}]$ CDP-DAG formation from $[^3\text{H}]$ CTP.

4.3 TbCDS activity in Bloodstream Form *T. brucei*

Whilst TbCDS was shown to encode CDS activity and to be transcribed in bloodstream form *T. brucei*, it was also important to show that CDS activity was present in *T. brucei*. This activity was tested in a cell free system using *T. brucei* membranes to catalyse the incorporation of [³H]CTP into lipid soluble [³H]CDP-DAG by the reaction $PA + [^3H]CTP \rightarrow [^3H]CDP-DAG + PPi$ (Figure 1.13). After incubation of washed membranes with [³H]CTP and PA the lipid phase was extracted and analysed by HP-TLC and autoradiography. A single band was seen on the HP-TLC and identified as [³H]CDP-DAG based upon its co-migration with a CDP-DAG (dipalmitoyl) standard (Figure 4.1, B). This showed for the first time the ability of bloodstream form *T. brucei* membranes to catalyse the formation of CDP-DAG from CTP and PA, previously shown to be the reaction catalysed by TbCDS. With the knowledge that bloodstream form express the TbCDS open reading frame and displays its activity, the next step was to see how bloodstream form *T. brucei* would cope with reduced levels of TbCDS expression, by the creation of a TbCDS RNAi knockdown cell line.

4.4 RNAi of TbCDS in Bloodstream Form *T. brucei*

To create a construct for the knockdown of TbCDS, a 400 bp DNA fragment corresponding to the 5' end of the TbCDS ORF was ligated into the p2T7 vector using BamHI and XhoI restriction sites (Figure 4.2). The vector p2T7 contains two opposing T7 promoters on either side of the multiple cloning site which produce double stranded RNA in the presence of tetracycline to induce the RNAi knockdown mechanism.

Bloodstream form *T. brucei* cells were transfected with TbCDS p2T7 and several positive transformants were selected using hygromycin. Two flasks of TbCDS p2T7 clone 1 were seeded at equal densities and RNAi was induced by the addition of tetracycline to one flask. Cells were counted at approximately the same time every day and split when they grew higher than $1 \times 10^6 \text{ ml}^{-1}$. The number of cells per ml was recorded over time and graphed (Figure 4.3, A and B). A growth defect was apparent after 48 hours in the plus tetracycline (TbCDS RNAi) flask, but with no obvious cell cycle stall. After 48 hours there was a slight recovery in growth, although nowhere near that of wild type, and after approximately 150 hours cells started to die off. No

viable cells were countable 216 hours after the addition of tetracycline, whilst the cells not induced with tetracycline continued growing like wild type.

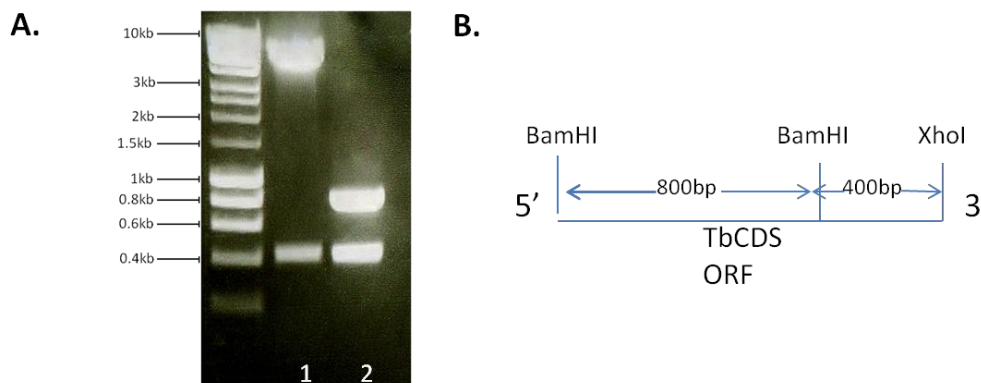


Figure 4.2. Construction of TbCDS RNAi knockdown plasmid. (A) 1% agarose gel Lane 1 – BamHI XhoI restriction digest of TbCDS fragment in p2T7. Lane 2 BamHI Digest of TbCDS ORF. (B) Schematic showing the position of BamHI and XhoI restriction enzyme sites in the TbCDS ORF amplified by TbCDS pET32b F and TbCDS pET32b R primers (Table 2.1).

Repetition of the experiment with clone 1 TbCDS p2T7 cells produced largely the same growth pattern, with an early major growth defect followed by death after 150 hours and no viable cells after 216 hours (Figure 4.3, C).

However, induction of clone 1 TbCDS RNAi cells at a later date failed to produce any growth defect and it seemed the cells had reverted during culture. This could have been due to the presence of small amounts of tetracycline in the foetal calf serum used as an ingredient of HMI-9. This tetracycline puts selective pressure on the TbCDS RNAi cells to break tetracycline control, and it has previously been noted that revertants can occur in the absence of added tetracycline with the p2T7 construct if gene knockdown is particularly toxic (LaCount et al., 2000, LaCount et al., 2002). Unfortunately, it was not noticed that the cells had reverted before the original set of long term storage stabilates had been used and the second set of stabilates contained revertant cells

For further experiments, clone 6 TbCDS p2T7 was revived and never allowed to remain in continuous culture for longer than necessary. Cell count experiments were repeated in duplicate with clone 6 CDS RNAi cells (Figure 4.4). The growth defect was found to be very similar to that noted for clone 1, with a growth defect always apparent after 48 hours.

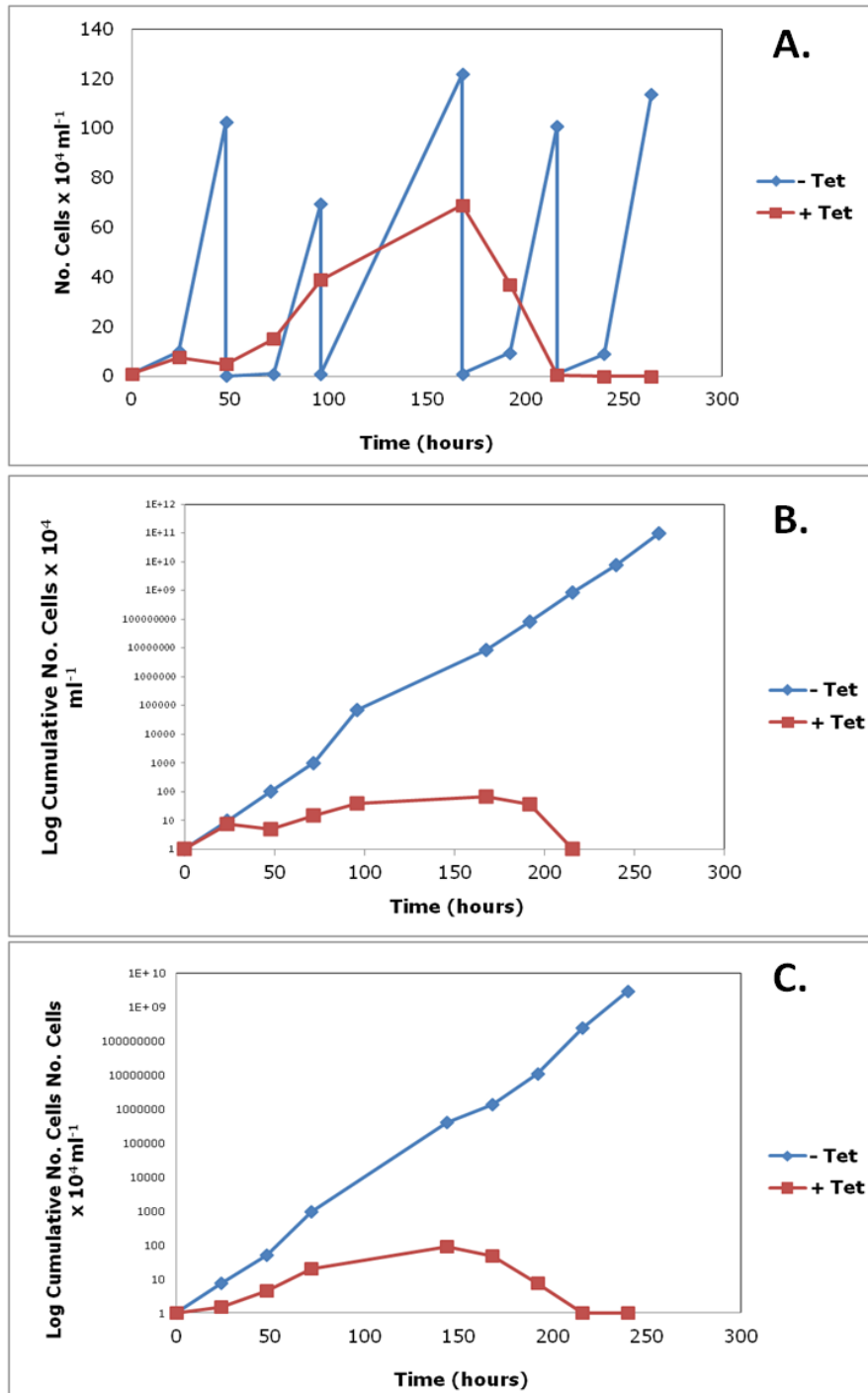


Figure 4.3. TbCDS is essential in BSF *T. brucei* – clone 1 (A, B) Clone 1 BSF TbCDS RNAi cell counts (A) Number of cells per ml of culture x 10⁴ over time in hours cultured in the presence (+ Tet = induction of TbCDS RNAi) or absence (- Tet) of tetracycline. (B) Graph showing log cumulative number of cells over time in the presence and absence of tetracycline. (C) Clone 1 BSF TbCDS RNAi cell counts 2 – graph of repeat experiment showing log cumulative number of cells over time in the presence and absence of tetracycline.

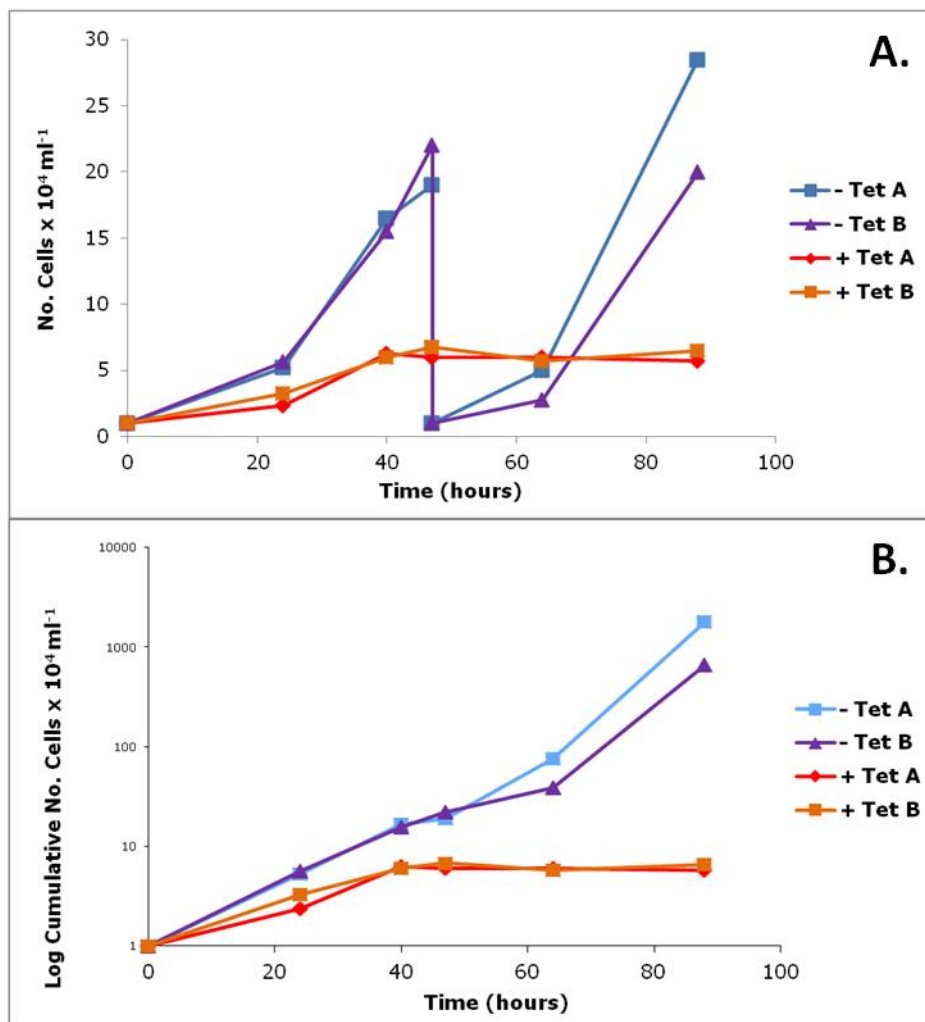


Figure 4.4. TbCDS is essential in bloodstream form *T. brucei* – clone 6. (A) Number of cells per ml of culture x 10⁴ over time in hours cultured in the presence (+ tet = induction of TbCDS RNAi) or absence (- Tet) of tetracycline. (B) Graph showing log cumulative number of cells over time in the presence and absence of tetracycline. A and B are two duplicate flasks of the same condition.

4.4.1 Confirmation of Construct Integration

Southern blot analysis was used to confirm that the p2T7 copy of TbCDS had integrated into the genomic locus. Genomic DNA from TbCDS p2T7 clone 1 and clone 6 *T. brucei* transformants was prepared and digested with several different enzymes (one enzyme per lane) in order to produce an easily detectable fragment size containing the ORF: XcmI produces a 2.5 kb and a 3.3 kb fragment; XhoI produces a 4kb labelled fragment; HindIII produces a 2.6 kb fragment and NcoI produces a fragment at 3.9 kb.

Attempts to probe southern blots using the DIG-labelled TbCDS ORF were unsuccessful under a variety of hybridisation temperatures, DNA and probe concentrations and different stringency washes. Probe labelling efficiency by serial dilution alongside labelled standards showed that at least 20 ng/ μ l of labelled probe was being synthesised. Direct detection confirmed that spots containing as little as 0.1 pg/ μ l of control DIG labelled DNA were detectable. A positive control carried out under the same conditions, probing NcoI digested SM gDNA with a DIG labelled TbINO1 (inositol phosphate synthase) open reading frame probe was successful, showing no kit component or protocol was inherently faulty.

Another positive control used the DIG-labelled TbCDS ORF probe on a blot containing 100 ng of pET32b plasmid containing the TbCDS ORF alongside 5 μ g of HindIII digested DM genomic DNA. The TbCDS probe produced a strong signal from the plasmid, but failed to produce any signal from the genomic DNA.

Since the TbCDS gene is thought to be present at low copy number, the TbCDS pET F32F primer (which was determined to be sufficiently specific for the CDS locus) was labelled with [32 P] by Hartmann Analytic's random primer labelling service to create a high energy probe that should be easily detectable. Genomic DNA was prepared, digested, blotted and probed as described in Chapter 2, section 1.8 with varying hybridisation temperatures. A variety of exposures (the longest at twelve days) failed to produce any signal.

In spite of failure to detect the p2T7 TbCDS copy by Southern blot, the hygromycin resistance of the cells, along with detection of the HYG ORF by PCR (Figure 4.5) were considered to be evidence of construct integration, and the morphological and biochemical phenotyping of the TbCDS RNAi cell line was continued.



Figure 4.5. Presence of hygromycin phosphotransferase (HYG) gene from TbCDS p2T7 RNAi construct in BSF *T. brucei* genomic DNA. 1% agarose gel stained with ethidium bromide showing PCR for HYG gene in 1. SM 2. TbCDS p2T7 clone 6 BSF gDNA 3. positive control – HYG in pGEM vector. Sequences for primers used are given in Table 2.1.

4.4.2 Morphological Phenotyping of Bloodstream Form TbCDS RNAi

Cell line

Growth of clone 6 bloodstream form TbCDS RNAi cells initially slows at 48 hours after the addition of tetracycline. These TbCDS RNAi cells were fixed and DAPI stained at this timepoint in order to examine their general morphology by light microscopy. Whilst there was no obvious morphological phenotype or cell cycle stall at this time point, Z-projections of DIC images showed more irregular, uneven cell surfaces than SM cells (Figure 4.6). This could be an artefact of fixing, however it was observed on several occasions with bloodstream form TbCDS RNAi cells prepared independently on several occasions. This may indicate the properties of the plasma the membrane were altered, possibly due to a change in phospholipid composition as a result of TbCDS knockdown.

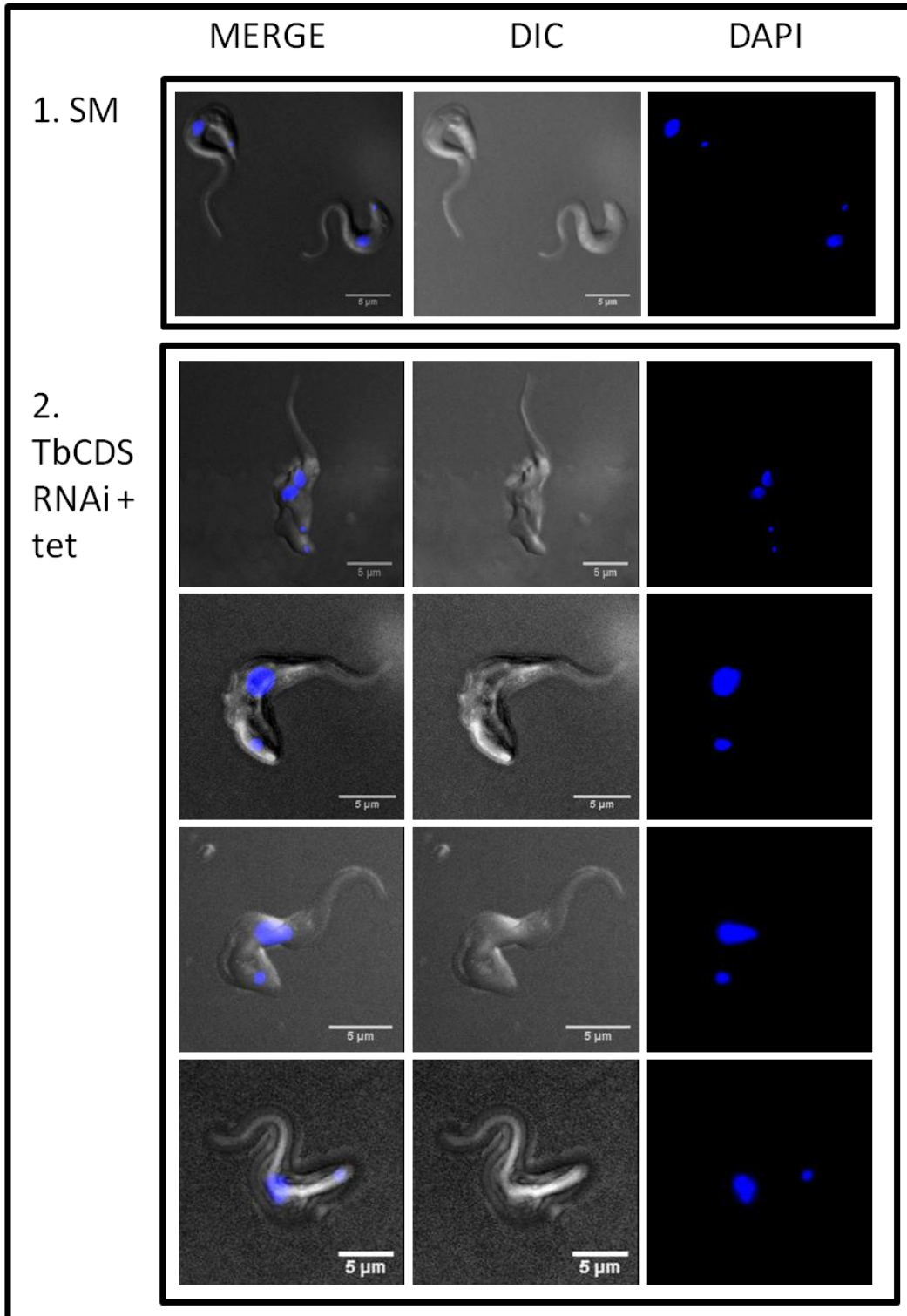


Figure 4.6. Morphology of SM and bloodstream form TbCDS RNAi *T. brucei* 48 hours + tetracycline. 3D projections of Z-series images taken by light microscopy. Middle panel shows DIC, right panel shows DAPI staining and left panel shows the merged image. Cells were fixed with 4% paraformaldehyde, allowed to adhere to polysine slides and mounted with anti-fade GOLD reagent containing DAPI. 1. SM cells harvested from mid-log culture and fixed in 4% paraformaldehyde. 2. TbCDS RNAi cells harvested from culture 48 hours after induction of RNAi and fixed in 4% paraformaldehyde.

4.4.3 Biochemical Phenotyping of Bloodstream Form TbCDS RNAi Cell

Line

To examine what was happening in the bloodstream form TbCDS RNAi cell line, biochemical phenotyping of the tetracycline induced cells was investigated. This was important to show what was happening at the metabolic level in the TbCDS RNAi cell line which was causing the growth defect, uneven cell surface and death. CDP-DAG itself is difficult to see by mass spectrometry because the actual pool of the nucleolipid is very small and dynamic. In addition to examining lipid metabolism by *in vivo* radiolabelling with lipid precursors, ESI MS/MS was used to examine the total lipid profile and to quantify the nucleotide substrate for CDS, CTP.

4.4.3.a *In vivo Radiolabelling of Bloodstream Form TbCDS RNAi*

To investigate how lipid metabolism in the bloodstream form TbCDS RNAi knockdown was affected, *in vivo* radiolabelling was carried out with various lipid precursor substrates 42 hours after the addition of tetracycline to the TbCDS RNAi cell line. At 42 hours a growth defect was initially apparent, but cells were presumed to still be biochemically active. TbCDS RNAi trypanosomes plus and minus tetracycline were incubated with the radiolabelled metabolite and then harvested.

To assess protein synthesis in the mutant trypanosomes compared to the wild type, cells were incubated with [³⁵S]methionine for 1 hour. Protein was harvested by direct lysis of washed cells in 95°C sample buffer, separated by SDS-PAGE, and coomassie stained to check for equal loading (Figure 4.7, A, lanes 1 and 2). The gel was then dried, soaked in liquid EnHance™ and exposed to autoradiography film. Figure 4.7, panel A shows the developed film alongside the coomassie stained gel. The incorporation of [³⁵S]methionine into cellular proteins is clear in both the - tetracycline and the + tetracycline 42 hr cells, proving that both cell lines are viable and protein synthesis is occurring. The coomassie stained gel shows the total amount of protein loaded to be approximately the same between the two cell lines. However, it is clear that the amount of newly synthesised protein in the TbCDS RNAi cells is slightly less, demonstrating the TbCDS RNAi cells are still viable, but protein synthesis is starting to slow down. This is in keeping with the growth plateau seen at this time point. It is worth mentioning that lipid metabolism is normally unaffected by total protein synthesis shutdown (Smith et al, 2009) so any decrease in lipid

metabolism would be directly linked to TbCDS knockdown and not a secondary effect due to a decrease in protein synthesis.

For *in vivo* radiolabelling of lipids, after incubation with labelled precursor, total cellular lipids were extracted, washed and counted. Samples were then analysed by HP-TLC, the plates sprayed with EnHance™ and put on film. The developed autoradiographs are shown in Figure 4.7, panel B

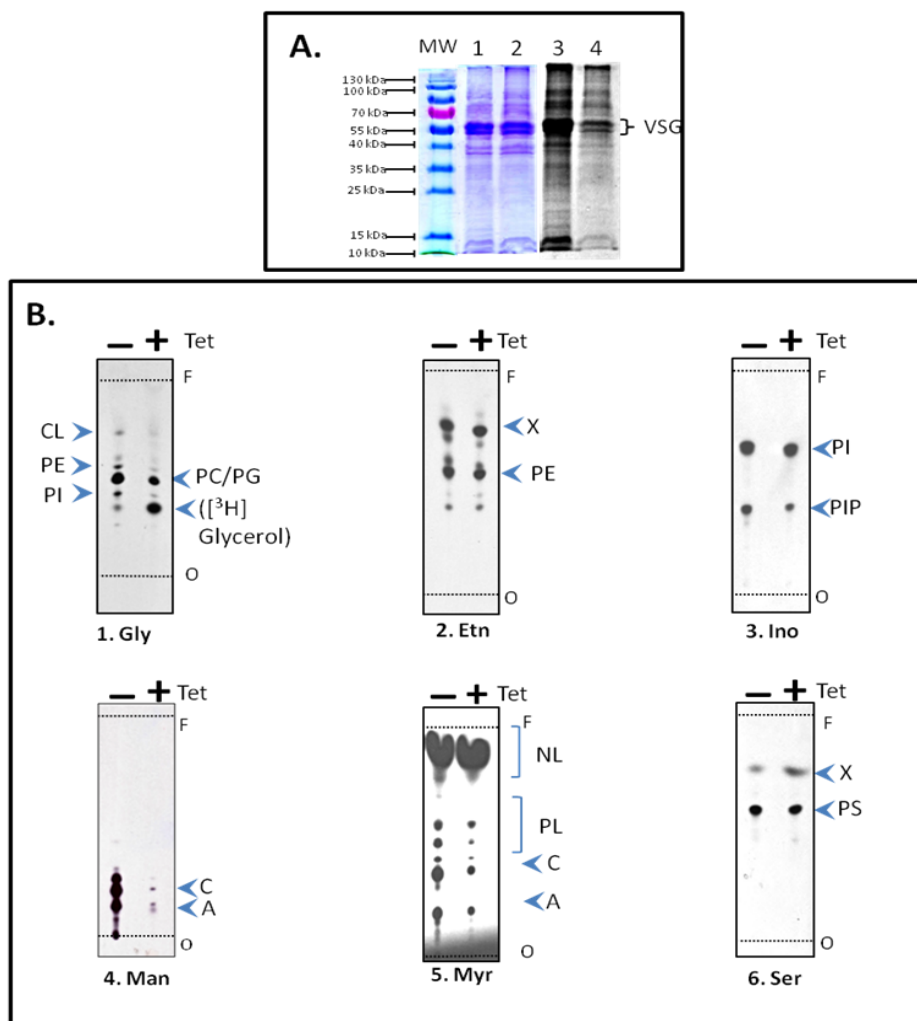


Figure 4.7. Biochemical analysis of BSF TbCDS RNAi in the absence and presence of tetracycline at 42 hours by *in vivo* radiolabelling. (A) Cells were labelled with [³⁵S] methionine and protein extracts separated on a 12% SDS-PAGE gel. Proteins were stained with Coomassie blue (lanes 1 and 2) or detected by autoradiography (lanes 3 and 4). Lanes 1 and 3 SM. Lanes 2 and 4 -TbCDS RNAi cells 48 hours + tetracycline. (B) Autoradiographs of HPTLC plates run with the lipid fraction of *in vivo* radiolabellings. -/+ (left and right of plate) = BSF TbCDS RNAi - and + tetracycline (left and right of plate) = BSF TbCDS RNAi - and + tetracycline. 1. Gly = [³H]Glycerol; 2.Etn= [³H]Ethanolamine (X = unidentified phospholipid that co-migrates with cardiolipin); 3.Ino= [³H]Inositol; 4. Man = [³H]Mannose (C = Glycolipid C, A = Glycolipid A); 5. Myr = [³H]Myristate (NL = neutral lipids, PL = phospholipids); 6. Ser = [³H]Serine. O = origin, F = front. Plates 1-4 were run in 180:140:9:9:23 CHCl₃:MeOH:30% NH₃: 1 M NH₂Ac :H₂O and plates 5 and 6 were run in 10:10:3 CHCl₃:MeOH:H₂O .

Glycerol is incorporated into glycerolipids as the backbone to which both the headgroup and fatty acid chains attach (Figure 1.7). Incubation of cells with [³H]glycerol should label the major diacyl glycerophospholipid species that are rapidly synthesised in the lipid fraction. In this experiment, [³H]glycerol labelled the expected species of phospholipids including PE, PI and PC, however the incorporation was less in the TbCDS RNAi + tetracycline 42 hours than in the TbCDS RNAi - tetracycline with biggest decreases in PE and a spot corresponding to PI. A spot thought to correspond to CL was also reduced (Figure 4.7, B.1). A reduction in labelling of all phospholipids would correlate with the global decrease in phospholipid seen in the *E. coli* CDS null strain (Ganong and Raetz, 1982) and with the global decrease in anionic phospholipids that was seen in a *Synechocystis* mutant defective in CDP-DAG synthesis (Sato et al., 2000). This fits with the proposed role of CDP-DAG as a precursor to PS, PI and PG. However, in *T. brucei* PE and PC are not thought to be made via CDP-DAG (Signorell et al., 2008, Gibellini et al., 2008, Gibellini et al., 2009). A reduction in PE and PC species could perhaps be explained by *T. brucei* needing to maintain the plasma membrane lipid composition required for proper function and the rapid endo- and exocytosis of GPI-anchored VSG (reviewed in Overath and Engstler (2004)).

Water soluble ethanolamine is the headgroup of PE and EPC, and can be incorporated into these lipids either by *de novo* synthesis via the Kennedy pathway, or by headgroup exchange with existing PE or other phospholipids PS and PC. Additionally in some organisms it can be made by decarboxylation of PS. However, headgroup exchange between PC and PE does not occur in *T. brucei*, and the extent to which PS to PE headgroup exchange or decarboxylation occurs is debatable since PS is unable to compensate for the loss of *de novo* synthesised PE in bloodstream form (Gibellini et al., 2009) or procyclic (Signorell et al., 2008) cells. Figure 4.7, B.2 shows the incorporation of [³H]ethanolamine into PE and another, higher band, labelled as X. Incorporation into PE appears to be relatively unaffected in the TbCDS RNAi cell line in comparison to the wild type, certainly less than the reduction of [³⁵S]methionine incorporation into protein and glycerol into phospholipids. This would confirm that CDP-DAG does not significantly contribute to the production of PE, through headgroup exchange with PS, as it does in some other organisms. This result appears contrary to Figure 4.7, B.1 where TbCDS RNAi showed a decrease in the labelling of [³H]PE with [³H]glycerol. However, the major species of PE in *T. brucei* are alkyl-

acyl, and would therefore not be labelled by exogenous [^3H]glycerol (see Figure 1.9, B and D). These results therefore show that the small pool of diacyl PE species may be reduced upon reduction of TbCDS activity, whilst the most common alkyl-acyl species are unaffected. The band which runs higher than PE migrates at the same height as CL, but [^3H]ethanolamine has not previously been shown to label this lipid. The same band appears in the [^3H]serine labelling, which may indicate that a metabolic product of serine/ethanolamine is somehow being incorporated into CL.

In bloodstream form trypanosomes, inositol is incorporated into lipid as the headgroup of PI and its phosphorylated derivatives. In the TbCDS RNAi cell line there is little or no change in the incorporation of [^3H]inositol into PI compared to wild type, but perhaps slightly less incorporated into PIPs (Figure 4.7, B.3). However, in neither case is this reduction in inositol lipids as much reduced as the incorporation of [^{35}S]methionine into proteins or [^3H]glycerol into phospholipids. Again, this shows that most lipid metabolism is normal despite a protein synthesis decrease, but this result is unexpected, since the only known route of PI synthesis is via CDP-DAG. However, PI synthase also catalyses headgroup exchange of inositol into existing PI, so it seems likely that this activity is increased, therefore masking any decrease in *de novo* synthesis. It is also possible that synthesis of alkyl-acyl PI species is increased; however these species are relatively rare in PI. It has been shown that bloodstream form *T. brucei* do not use exogenous inositol for the production of GPI anchors, suggesting that two separate pools of PI exist. In the ER, exclusively *de novo* synthesised inositol is incorporated into PI, which is then used for the synthesis of GPI anchors. In the Golgi, PI is synthesised from exogenous inositol and is used for bulk cellular PI (Martin and Smith, 2006a). In this scenario, it is possible that the flux through these pathways occurs at different rates, and a reduction in CDP-DAG does not affect bulk cellular PI to the same degree. The ER pool is very small and if only this pool were affected, a decrease in glycerol labelled PI would be difficult to see. Corroborating this, no change was seen in the pool of glycerol labelled PI in a knockout of inositol phosphate synthase despite the fact that the pool of ER PI for GPI anchors was severely depleted (Martin and Smith, 2006a).

Whilst [^3H]inositol does not normally label GPI anchors, they can be labelled using [^3H]mannose. [^3H]Mannose is converted into GDP-[^3H]mannose and dolichol-P-[^3H]mannose allowing easy incorporation into GPI precursors via a series of three mannosylations. Mature glycolipids A and C are then formed by ethanolamine-

phosphate capping and acyl remodelling with myristate. In the TbCDS RNAi + tetracycline 42 hr cells, the incorporation of [³H]mannose into glycolipid C and A is drastically reduced with respect to TbCDS RNAi - tetracycline (Figure 4.7, B.4) - far beyond that of any general metabolic slowing suggested by the reduction of protein synthesis. This loss of GPI anchor synthesis could well be the cause of cell death, since chemical and genetic validation of the *T. brucei* GPI pathway as a drug target showed that soon after GPI biosynthesis had decreased by more than 90% the cells lost viability (Chang et al., 2002, Nagamune et al., 2000, Smith et al., 2004). It seems likely that a reduction in CDP-DAG precursor means the parasite is unable to make PI for GPI anchors, since a similar reduction in GPI anchor synthesis was seen when PI synthase was knocked out in bloodstream form *T. brucei* (Martin and Smith, 2006b). This result indicates that PI synthesis in the ER utilising *de novo* synthesised inositol is reduced by the decrease in CDP-DAG synthesis. This also indicates the possibility of a separate CDP-DAG pool which is responsible for bulk cellular PI synthesis in the Golgi. In the case of PI, the two separate pools are synthesised by the same gene product but in different cellular locations - i.e. ER and Golgi (Martin and Smith, 2006b). This shows a similar need for CDP-DAG in both the ER and the Golgi and may indicate that like TbPIS, TbCDS is also dually localised.

In order to get a more general look at overall lipid synthesis, the incorporation of a labelled fatty acid can be monitored. In the case of bloodstream form *T. brucei*, [³H]myristate is an excellent choice because it is readily utilised. Figure 4.7, B.5 shows [³H]myristate labelling of the TbCDS RNAi cells. There is less incorporation of [³H]myristate into all lipid classes, including glycolipid C and A. This indicates that the reduction in TbCDS activity does not have a drastic effect on general lipid metabolism in the time frame studied here.

There is some ambiguity surrounding the synthesis and metabolism of PS in both bloodstream form and procyclic *T. brucei*. It is debated whether or not PS is synthesised from CDP-DAG as in prokaryotes, yeast and plasmodium, or exclusively from PE, as is the case in higher eukaryotes. In order to address this question it seemed particularly important to examine the incorporation of [³H]serine into lipid. [³H]serine labels PS, but can also label sphingolipids due to its incorporation into ceramide. Figure 4.7, B.6 shows the incorporation of [³H]serine into lipid in both SM and bloodstream form TbCDS RNAi cells. There is no obvious difference between the incorporation of [³H]serine into PS between these two cell lines, indicating PS

synthesis is unaffected by the depletion of CDP-DAG. It is difficult to say if this is also the case in the [³H]glycerol labelling as signal may be low and in the solvent system used, PS was predicted to migrate to a similar height as PI. This may give evidence that in *T. brucei*, PS is not synthesised via CDP-DAG, but through headgroup exchange with PE, as was suggested of the procyclic form (Signorell et al., 2008), but in contradiction to what was seen previously in the bloodstream form when conditional knockout of ECT did not affect the incorporation of [³H]serine into [³H]PS (Gibellini et al., 2009). There could also be an increase in headgroup swapping, as was seen in PE and PI, which could mask the difference in *de novo* synthesis. There is also a possible slight increase in the incorporation of [³H]serine into a higher band, labelled “X” in Figure 4.7, B.6. This band was also seen in the [³H]ethanolamine labelling (Figure 4.7, B.2) and co-migrates with CL in 180:140:9:9:23 (CHCl₃:MeOH:30% NH₃:1M NH₄Ac:H₂O) and in 10:10:3 (CHCl₃:MeOH:30% NH₃Ac:H₂O) - see Appendix A. CL is decreased in the [³H]glycerol labelling, whilst the band labelled X is unchanged in the ethanolamine labelling and slightly increased in the serine labelling. This may indicate these species do not correspond to the same lipid, or that incorporation of these precursors into the lipid is differently effected by TbCDS knockdown.

In summary, the results from the radiolabelling experiments have raised several questions. Incorporation of glycerol into PE and PI in the TbCDS RNAi 42 hrs + tetracycline was decreased, however incorporation of ethanolamine into PE and inositol into PI is unaffected. In both cases, these results may suggest an increase in headgroup exchange activity is masking a decrease in the phospholipid, or in the case of PE that only the less common diacyl species are reduced. An increase in headgroup exchange may be a quick and efficient way to respond to changing phospholipid composition in the CDP-DAG depleted cells.

The incorporation of [³H]mannose into GPI anchor intermediates glycolipids A and C was dramatically reduced in the TbCDS RNAi knockdown, which could certainly cause a growth stall due to the cells unwillingness to deplete their GPI anchored VSG coat by cell division. This suggests that the pool of PI for GPI anchors in the ER is dramatically reduced in the TbCDS RNAi cells. Since this pool does not incorporate exogenous inositol, it could partly explain the difference in the [³H]glycerol and [³H]inositol labelling, but an increase in headgroup exchange activity could also have this effect, and a decrease in just the ER localised GPI pool may not be sufficient to

cause the [³H]glycerol labelling decrease that was seen in the TbCDS knockdown. In order to examine the lipid profile of the bloodstream from TbCDS RNAi knockdown cells in more detail, and to find an answer to some of the questions raised by the radiolabelling, total cellular phospholipid from the knockdown cell lines was analysed by ESI MS/MS.

4.4.3.b. Lipid Profile of Bloodstream Form TbCDS RNAi Cell Line by ES-MS/MS

Total lipids were extracted from TbCDS RNAi cells at 42 hours after the addition of tetracycline, TbCDS RNAi cells minus tetracycline and SM cells as described previously. Lipid samples were first analysed by scanning ESI-MS for all species in order to get an idea of the general abundance of the different groups of lipids. Where individual fatty acid chain lengths are not known, diacyl species are represented as a sum of both the fatty acid chain carbons in the form CX:Y where X is the total number of fatty acid carbons and Y is the total number of double bonds in the lipid moiety. Most peaks have been fragmented previously and the main aryl composition identified. Each peak in these figures corresponds to a series of molecular species in a particular class with the same number of carbons but different masses due to differences in the degree of saturation of their lipid moiety. In the positive scans, it is not possible to distinguish between alkyl (ether) and alkenyl (vinyl ether) *sn*-1 linked fatty acids since an ether-linked (alkyl-linked) fatty acid containing X number of carbons and 1 double bond (a-CX:1) has identical mass to a vinyl ether (alkenyl-linked) fatty acid containing number of carbons and zero double bonds (e-CX:0).

In bloodstream form *T. brucei* the major species of PE, PC, PI and PS contain C18:0 in the *sn*-1 position. In ether-linked lipids, there is usually an unsaturated fatty acid in the *sn*-2 position - most often C18:2, whilst in diacyl lipids this position is usually occupied by either C18:2 and C22:4 and to a lesser extent C20:4 (Richmond et al., 2010).

4.4.3.b.i Positive Survey Scan

Figure 4.8 shows a scanning ES-MS in positive ion mode, which detects PC and SpM, and, to a lesser extent, PS and PE. In SM *T. brucei*, five of the largest peaks correspond to PC series. In order of *m/z*, starting with the smallest, the peak at 780.59 *m/z* corresponds to PC C36 and SpM C22; 794 *m/z* represents a PC a-C38 series; 808 *m/z* is composed of PC C38; 832 *m/z* is PC C40 and the peak at about 856

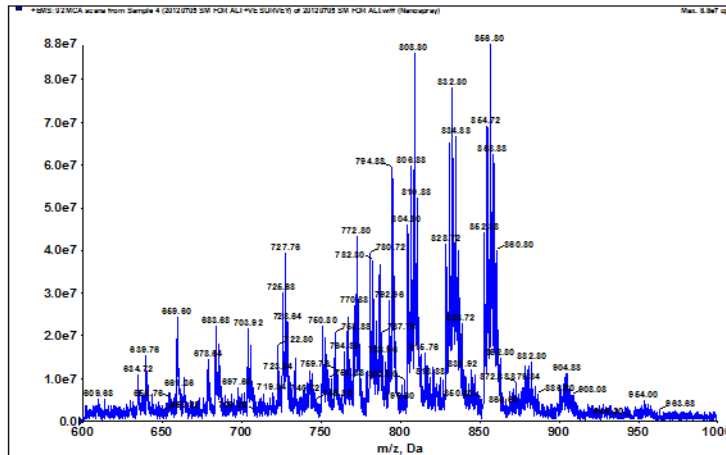
m/z represents the diacyl PC C42 species. Other intense peaks correspond to the most abundant PE species - PE a-C36 at around 727 m/z; and the most abundant PS species e/a-C36 at around 772 m/z.

On comparing lipid scans from SM, TbCDS RNAi - tetracycline and TbCDS RNAi + tetracycline 42 hours, it is apparent that the - tetracycline scan is not equivalent to the SM scan. In fact, in many cases the TbCDS RNAi - tetracycline cells were intermediate in their lipid profile between SM and TbCDS RNAi + tetracycline scans. This indicates that the expression of the p2T7 RNAi construct was leaky and that there has been some level of TbCDS knockdown even in un-induced cells. Since revertants were readily obtained upon continuous culture in HMI-9, this may indicate that the HMI-9 contained more than trace levels of tetracycline. There is much precedence for leaky expression of the p2T7 construct (Guler et al., 2008, LaCount et al., 2002, Fridberg et al., 2008). For this reason, TbCDS RNAi minus tetracycline scans are not shown later, and SM scans are used for comparison TbCDS RNAi + tetracycline lipid scans.

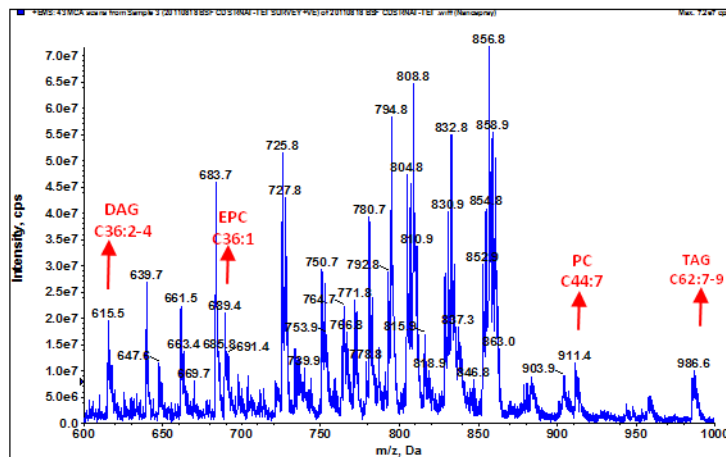
On further examination of the spectra in Figure 4.8., it is clear that in all cell types there is generally a similar distribution of all the expected lipid classes. Since an internal standard was not included it is not possible to quantify lipids in these scans, but the relatively similar distribution indicates that, at this time point, many lipid species show similar distributions.

Paying more attention to individual species, there are a few peaks that do show a significant change in the TbCDS RNAi + tetracycline cell type compared to the TbCDS RNAi - tetracycline and SM, and these are indicated by red arrows in Figure 4.8. The most increased peak is at m/z 615.5. Since this peak does not appear in any other scan, including that for p153 glycerol-phosphate, m/z 615.5 is not a glycerophospholipid, and therefore corresponds to DAG C36, the key component being C36:4. This peak is not above baseline in SM cells, but increases to 0.23 of PC C42 in TbCDS RNAi - tetracycline and 1.275 of PC C42 in TbCDS RNAi + tetracycline, making it the most abundant species in TbCDS RNAi + tetracycline (Figure 4.8, B,C). A considerable peak in TbCDS RNAi + tetracycline at m/z 689.4 likely corresponds to ethanolamine phosphorylceramide (EPC) dC20:1/C16:0. Again, this is not above baseline in SM but increases to 0.25 of PC C42 in TbCDS RNAi - tetracycline and 0.9 of PC C42 in TbCDS RNAi + tetracycline.

A. SM



B. TbCDS RNAi - tetracycline



C. TbCDS RNAi + tetracycline

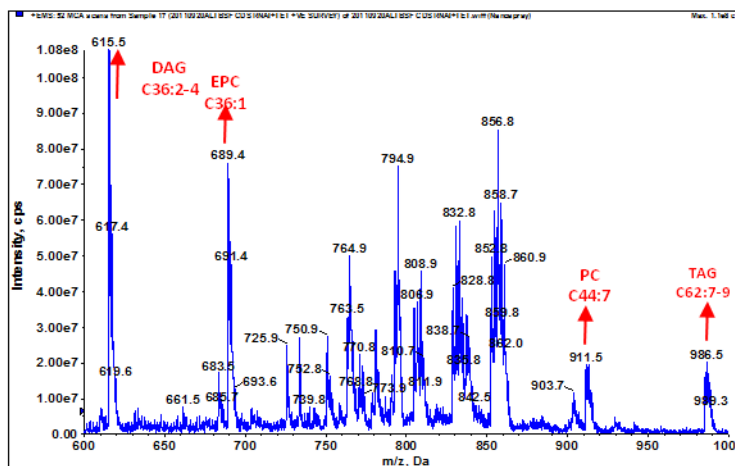


Figure 4.8. Positive ion survey scan of lipids from SM and BSF TbCDS RNAi + and minus tetracycline. Mass spectrometric analyses of total phospholipids by positive survey scan ESI-MS. A. wild type single marker cells (SM). B. BSF TbCDS RNAi cells grown in the absence of tetracycline. C. BSF TbCDS RNAi cells grown in the presence of tetracycline for 42 hours. DAG = diacylglycerol species, TAG = triacylglycerol species, PC = phosphatidylcholine species, EPC = ethanolamine phosphorylceramide species. Red arrows and text indicate peaks which are different in the mutant, whilst the direction of the arrow indicates whether this peak is increased or decreased in the mutant. CX:Y = X – total number of carbons, Y – total number of double bonds in fatty acid chains of lipid species. e = alkenyl-acyl- linked lipid, a = alkyl-acyl- linked lipid.

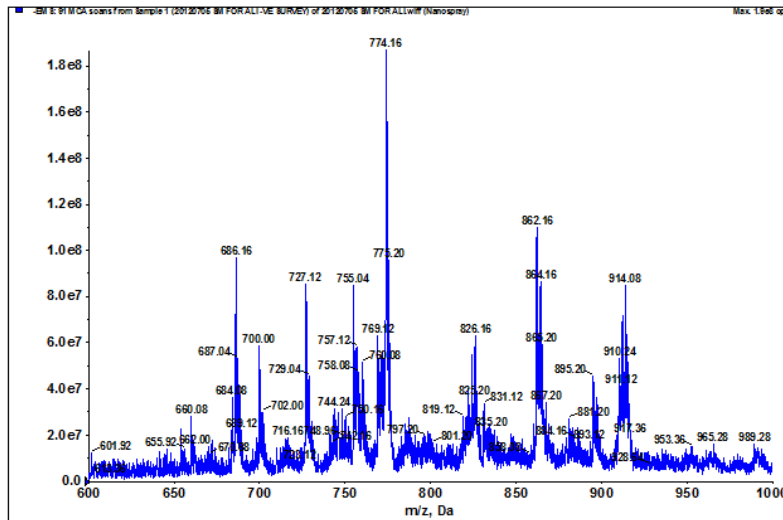
This is unexpected and may correspond to alteration of SpM levels or a cellular response to the disruption of another phospholipid. Another peak at m/z 986.5 probably corresponds to TAG C62, mostly TAG C62:8. It is 0.125 of PC C42 in TbCDS RNAi - tetracycline and increases to 0.25 of PC C42 in TbCDS RNAi + tetracycline. Finally, the appearance of a peak at 911.5 m/z must correspond to a sodium adduct of PC C44:7, since this species is also increased in the scan for choline-phosphate containing lipids (Figure 4.11).

The increase in DAG and TAG seen in the TbCDS RNAi + tetracycline scan may indicate that lack of TbCDS activity has meant that its substrate PA has accumulated and has been dephosphorylated to DAG. The accumulation of PA in a cell is harmful due to its role as a second messenger, linked with apoptosis (reviewed in Wang et al., 2006), whereas dephosphorylation of PA to DAG renders it less harmful to the cell. Indeed, in yeast both PA phosphatase and DAG kinase are regulated by CDP-DAG concentration (Wu and Carman, 1996, Shen et al., 1996). Why these DAG species are not further utilised for the production of PE and PC is unclear. It may be that the Kennedy Pathways are already operating at maximum capacity and therefore cannot use any extra DAG. It may also be interesting that these DAG species in particular accumulate. One explanation would be that unsaturated C36 species of PA are incorporated into CDP-DAG rather than DAG under normal conditions due to an enzyme preference or compartmentalisation, and these CDP-DAG species are incorporated into a particular downstream lipid species, PG, PI or PS. A comprehensive lipidomic analysis of bloodstream form *T. brucei* shows that C36:2-4 species are common in PI, PS and PG species, but also in PC species (Richmond et al., 2010).

4.4.3.b.ii Negative Survey Scan

Negative survey scans are shown in Figure 4.9. In bloodstream form *T. brucei* negative ion mode detects $[M-H]^-$ of PE, PS, PG and PA. Additionally, the ethanolamine containing phospholipid ethanolamine phosphorylceramide (EPC) - a sphingolipid made from ceramide and PE which may be used in signalling and is unique to the bloodstream form - can be detected. In the SM scan, a peak at 659 m/z corresponds to EPC C18:1/C16:0 (Sutterwala et al., 2008). Other peaks at lower molecular weights mainly represent PA species: 699 m/z and 685 m/z correspond to PA C36 series - mostly C18:0/C18:2 and the ether linked PA C36 series, e.g. e-C18:0/18:2, respectively.

A. SM



B. TbCDS RNAi + tetracycline

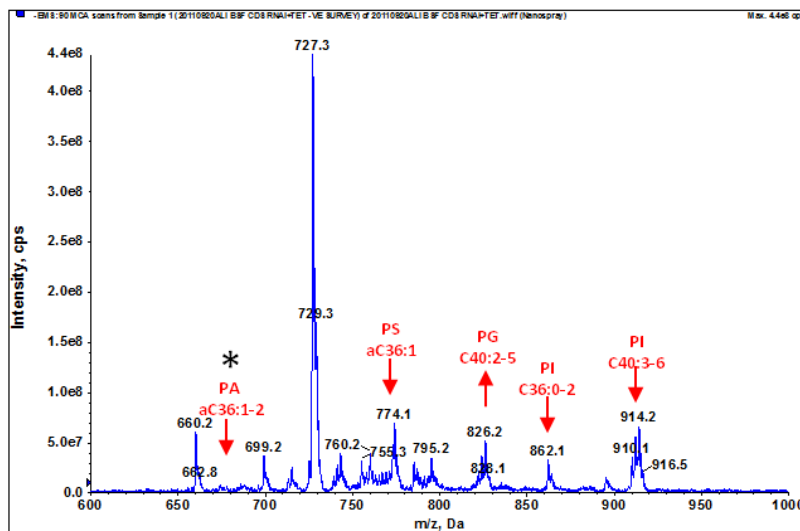


Figure 4.9. Negative survey scan of lipids from SM and TbCDS RNAi + tetracycline. Mass spectrometric analyses of total phospholipids by negative survey scan ESI-MS/MS. A. Wild type single marker cells (SM). B. BSF TbCDS RNAi cells grown in the presence of tetracycline for 42 hours. PA = phosphatidic acid species, PE = phosphatidylethanolamine species, PS = phosphatidylserine species, PG = phosphatidyl glycerol, PI = phosphatidyl inositol. Asterix indicates ion which has been further fragmented. For further information see Figure 4.8.

An intense peak at about 727 m/z corresponds to the most abundant PE series - a-C36 and another intense peak at 774 m/z is comprised of the key PS series - e-C36. Other peaks at around 743 m/z, 754 m/z and 794 m/z correspond to other abundant PE series - PE C36, PE a-C38 and PE C40, respectively. Finally, two higher molecular weight peaks represent the majority of PI species. PI C36 is at about 862 m/z and PI C40 at approximately 911 m/z.

Comparing the negative survey scan from TbCDS RNAi 42 hr + tetracycline (Figure 4.9, B) with that of SM (Figure 4.9, A), there is a dramatic difference. There is a decrease in the intensity of all the anionic lipids with respect to m/z 727, which corresponds to plasmenyl PE - mostly α -C36:4, confirming what was seen in the [3 H]ethanolamine labelling where PE species were unaffected. PI C36 goes from 1.28 of PE α -C36 in SM to 0.05 in TbCDS RNAi + tet, whilst the peak of PI C40 goes from being the same height as PE α -C36 in SM to just 0.14 of this peak in TbCDS RNAi + tet. This result confirms the decrease in the incorporation of [3 H]glycerol into the TbCDS RNAi + tetracycline cell line compared to the incorporation in uninduced cells, and confirms that the lack of a change in [3 H]inositol labelling must be due to an increase in headgroup exchange activity into existing phospholipid (Figure 4.7.B.3). The decrease seen in the major peak of plasmenyl-PS from 2.16 of PE α -C36 in SM to 0.16 of PE α -C36 in TbCDS RNAi + tetracycline is unexpected, however, given that incorporation of [3 H]serine into PS was shown to be unaffected. This could indicate that an increase in headgroup exchange activity into existing PS is masking the absolute decrease in the PS pool.

A peak at m/z 686 is entirely absent from the TbCDS RNAi + tetracycline scan. This ion was further fragmented from the SM sample to produce the daughter ion spectrum shown in Figure 4.10, and corresponds to PA α -C18:0/C18:2. PA is the lipid precursor to CDP-DAG and therefore would be expected to build up when TbCDS activity is decreased, rather than disappear, but too much PA is likely to be damaging to the cell due to its role as a signalling molecule in apoptosis and therefore PA phosphatases are likely upregulated in a response to a depletion of CDP-DAG to convert PA to DAG for incorporation into the Kennedy Pathway (Wu and Carman, 1996, Shen et al., 1996). This alkyl-acyl- linked C36:2 lipid moiety is a common component of Kennedy Pathway products PE and PC, but less common in downstream CDP-DAG products PI, PG and PS. Upregulation of the Kennedy Pathway could be occurring in order to try to compensate for a reduction in phospholipid resulting from CDP-DAG deficit and that this could cause depletion of the PA α -C18:0/C18:2 pool.

Interestingly, there is a relative increase of a peak at m/z 826.2 in the TbCDS RNAi + tetracycline scan which appears to correspond to the PG species C40 (mostly 40:4). This is unexpected since PG is not usually a very abundant lipid and can rarely be seen in a negative survey scan. Moreover, since CDP-DAG is the only known precursor

to PG, it seems strange that a knockdown of CDP-DAG synthesis would cause increase in a distinct class of PG, but could either be an adaptation to cope with depleted phospholipids PI and PS, or an indicator that there is an alternative pathway or enzyme involved in the formation of PG.

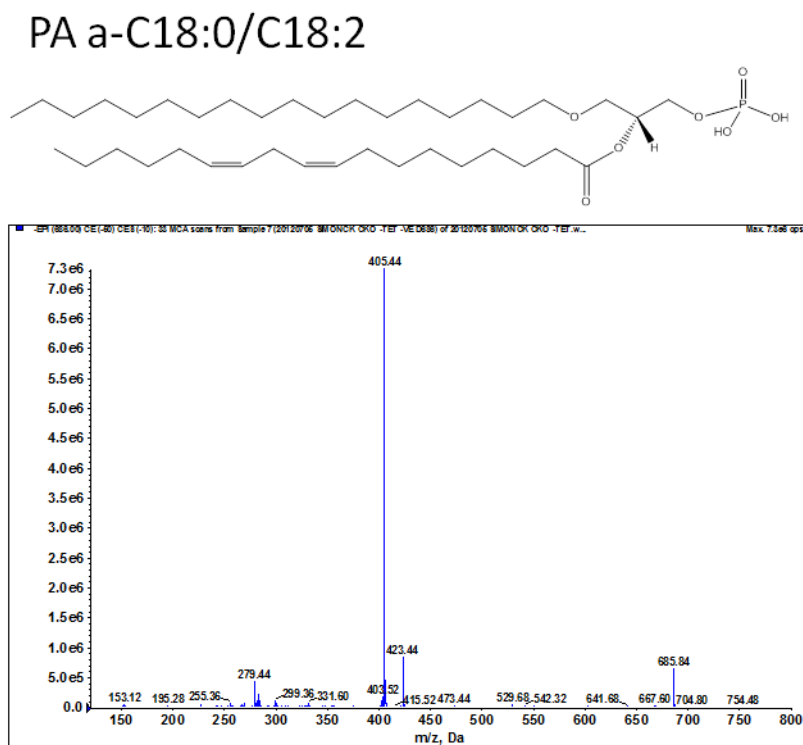


Figure 4.10. Daughter ion spectrum of m/z 686 $[M-H]^-$ ion. PA = phosphatidic acid. a = alkyl-acyl- linked. CX:Y = number of carbons:number of carbon-carbon double bonds.

The results from the ES-MS positive and negative survey spectra indicate diverse changes in phospholipid pools as a result of TbCDS knockdown. In order to look more closely at these pathways, ES-MS scans were performed for specific lipids.

4.4.3.b.iii Choline Containing Lipids

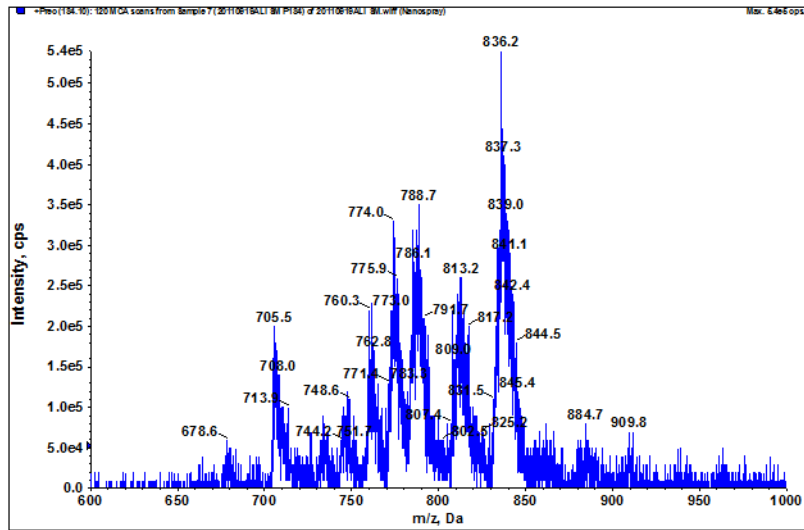
The spectra in Figure 4.11 were produced by a scan for precursors fragmenting to produce the unique ion fragment phosphorylcholine at $184 m/z$. The lipid species the seen all contain choline-phosphate. *T. brucei* contain a large number of different molecular species containing choline-phosphate, which is unsurprising given that PC and SpM make up more than two thirds of the total phospholipid pools in both

bloodstream form and procyclic life cycle stages (Richmond et al, 2010). This pool of lipids contains both diacyl and ether species in a ratio of about 3:1, and for nearly every diacyl species there is also an alkylacyl/alkenylacyl one (Richmond et al., 2010). PC species in bloodstream form fall into four main series: C40:y, C36:y, C38:y and e/a-C36:y and also contain the longer, often unsaturated species C42:y and C44:y.

From Figure 4.11 it is clear that the TbCDS RNAi + tetracycline mutant contains all four main series of choline-phosphate containing lipid at similar abundances to what is seen in the wild type. There is a slight increase in the e/a-C36:y series relative to the others, which may correspond to the depletion of the PA e/a-C36:2 pool that was seen on the negative survey scan (Figure 4.9). For example e/a-C36 is increased from 0.62 of PC C42 in SM to 0.96 of PC C42 in the TbCDS RNAi + tetracycline. This PA e/a-C36:2 would have been dephosphorylated to e/a-DAG C36:2 and utilised by Kennedy Pathway to form PC e/a-C36. There is also an increase in the peak corresponding to the long, unsaturated lipid moiety C44 (mostly C44:7) at m/z 888 which corresponds to the 911 m/z peak that was seen in the positive survey scan in a sodium adduct.

At the other end of the scale, a small peak at 678.6 m/z, corresponding to SpM C14:0 is completely absent from the TbCDS RNAi + tetracycline scan. Why this sphingolipid should be affected by depletion of CDP-DAG is unclear, but does show that TbCDS may have a central role in phospholipid content and regulation.

A. SM



B. TbCDS RNAi + tetracycline

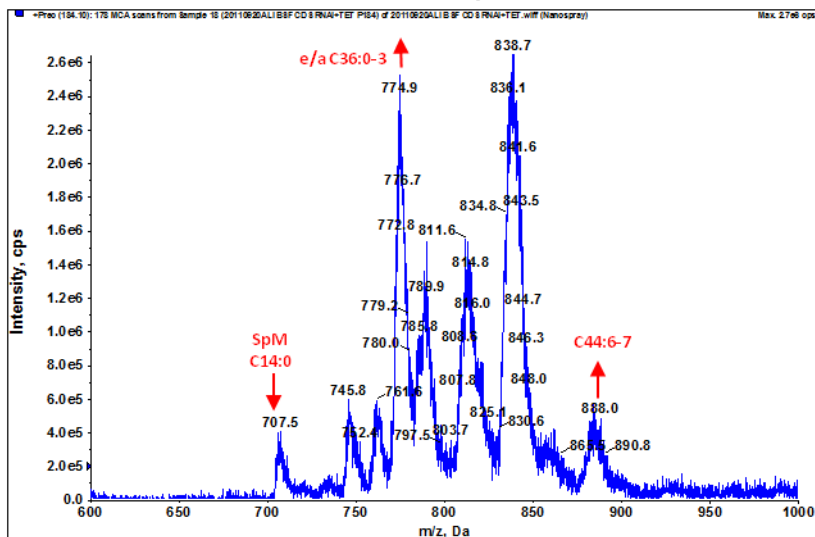


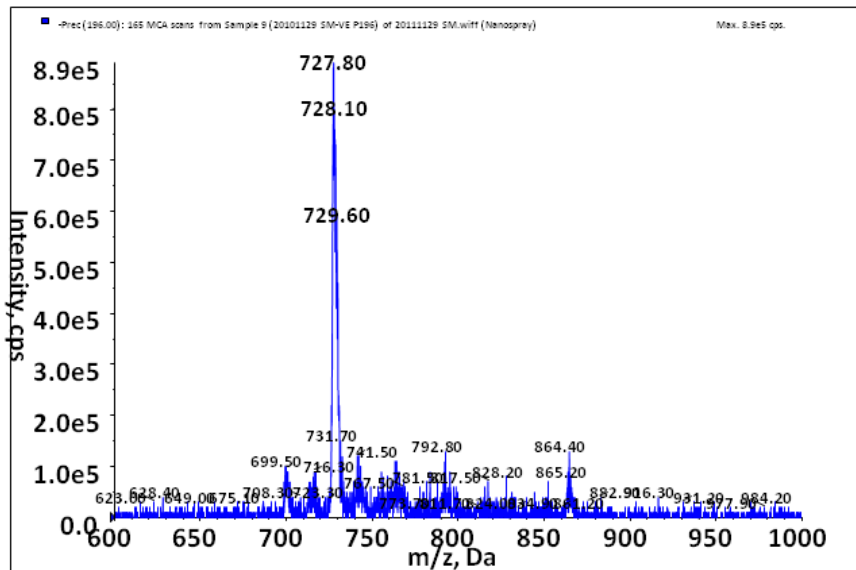
Figure 4.11. Mass spectrometric analyses of choline-phosphate containing phospholipids from SM and BSF TbCDS RNAi + tetracycline. Total lipids were analysed by ESI-MS/MS in positive ion mode using parent-ion scanning of the collision induced fragment for phosphorylcholine at 184 m/z. A. Wild type single marker cells (SM). B. BSF TbCDS RNAi cells grown in the presence of tetracycline for 42 hours. SM = sphingomyelin. For further information see Figure 4.8.

4.4.3.b.iv Ethanolamine Containing Lipids

Unlike with choline-phosphate containing lipids, the spectra of ethanolamine-phosphate containing lipids is dominated by one series: that of PE e/a-36:y, which is known to be composed mostly of plasmalyl e-C18:1/C18:2, and only about a third of PE species in bloodstream form *T. brucei* are diacyl (Richmond et al., 2010).

Figure 4.12. clearly shows that m/z 726-728, pertaining to the e/a-36:y series is the most abundant in the TbCDS RNAi + tetracycline spectrum, as in SM. Comparison of the relative abundance of ethanolamine containing species does not show up any obvious differences between the wild type and the TbCDS RNAi + tetracycline scans - this is similar to the choline-phosphate containing lipid scan (Figure 4.11). The absence of any really noticeable changes in the distribution of PE species suggests that, as with the PC species, the knockdown of TbCDS does not have a strong effect on the relative abundance of PE species. A decrease in diacyl species of PE was indicated from the [³H]glycerol labelling as compared to the [³H]ethanolamine labelling, but this is not clear here, although the relatively small size of the diacyl peaks of PE makes them difficult to compare. This may indicate that the decrease in synthesis of diacyl PE species has not yet had an effect on the total pool of PE species at this time point.

A. SM



B. TbCDS RNAi + tetracycline

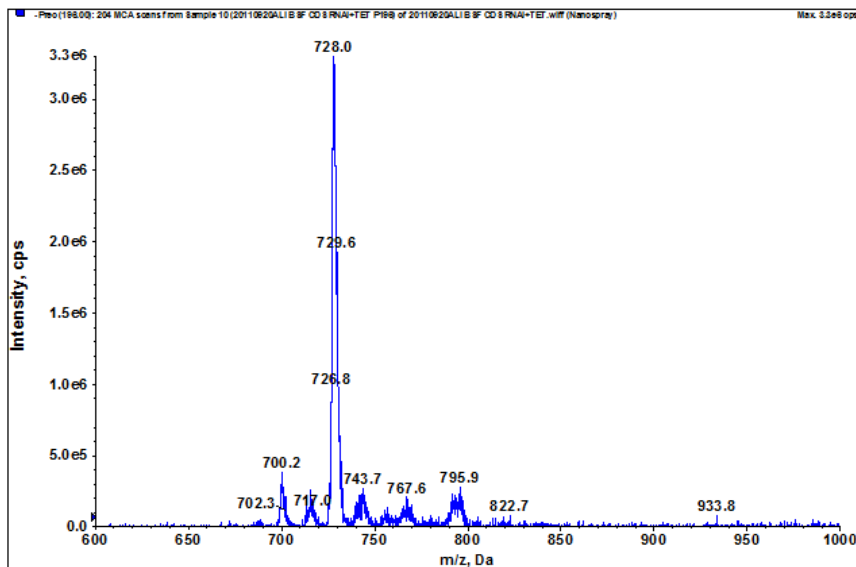


Figure 4.12. Mass spectrometric analyses of ethanolamine-phosphate containing phospholipids from SM and BSF TbCDS RNAi + tetracycline. Total lipids were analysed by ESI-MS in negative ion mode using parent-ion scanning of the collision induced fragment for phosphorylethanolamine at 196 m/z. A. Wild type single marker cells. B. BSF TbCDS RNAi cells grown in the presence of tetracycline for 42 hours. For further information see Figure 4.8.

4.4.3.b.v Inositol Containing Lipids

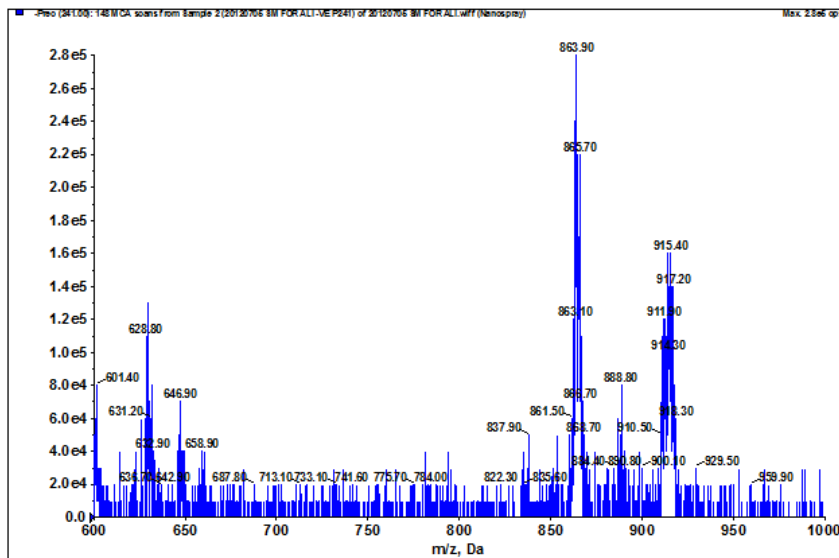
In bloodstream form *T. brucei*, the most abundant series of inositol-phosphate containing phospholipids is PI C40:y, mostly composed of C18:0/22:4-6, and C36:y - largely C18:0/18:1-2. The majority of inositol lipids contain acyl linked fatty acid chains, and both diacyl and ether species containing fatty acids shorter than C18 are not usually seen in bloodstream form (Richmond et al., 2010).

Inositol-phosphate containing lipids were specifically detected by scanning for precursors of 241 *m/z* in negative ion mode. Figure 4.13 shows that the two most abundant PI series are clearly present in the TbCDS bloodstream form, and C36 PI appears to be decreased more than C40 PI - the ratio of PI C36 to PI C40 changes from 1.79 in SM to 0.47 in TbCDS RNAi + tetracycline. A decrease in C36 PI also corresponds to the increase that was seen in C36 DAG (Figure 4.8). C36 PA that is not being utilised by TbCDS to make C36 CDP-DAG for C36 PI could be dephosphorylated into C36 DAG. In procyclic *T. brucei*, PI species C18:0/C18:2 and C18:0/C18:1 are preferentially incorporated into GPI precursor GlcNAc-PI (Guther et al., 2006) and in a knockout of the bloodstream form *T. brucei* inositol phosphate synthase the pool of C36 PI was decreased relative to the pool of C40 PI, and the cells were unable to make GPI anchors (Martin and Smith, 2006a). Together, these results clearly show that the pool of PI for GPI anchors synthesised from *de novo* synthesised inositol in the ER consists largely of C36 PI. The disproportionate decrease in C36 PI in this *T. brucei* TbCDS RNAi, combined with the result clearly showing GPI anchor synthesis was severely hindered show that the pool of PI for GPI anchors is differentially effected by a depletion in TbCDS activity. One reason for this could be that the flux through the GPI anchor synthesis pathway is very fast, so a decrease in PI would affect it more quickly than the slower moving pathway of synthesis for bulk PI.

The TbCDS RNAi + tetracycline sample scan reveals a peak at 781 *m/z* which may correspond to an IPC species. IPC is made of ceramide and phosphatidylinositol, and is not normally detectable in bloodstream form *T. brucei*, but has been shown in the procyclic where they are thought play an important role in the mitochondria (Guler et al., 2008). Since downstream CDP-DAG products PG and CL are also important mitochondrial phospholipids, it is possible that perturbation in levels of these phospholipids may cause an increase in IPC to compensate. Alternatively, IPC may be formed due to a lack of PC in the correct location to make SpM. IPC may also be formed as a result of a biochemical slowdown triggered by as yet unknown signals

similar to what is observed in slender bloodstream form differentiation to stumpy form (Sutterwala et al., 2008).

A. SM



B. TbCDS RNAi + tetracycline

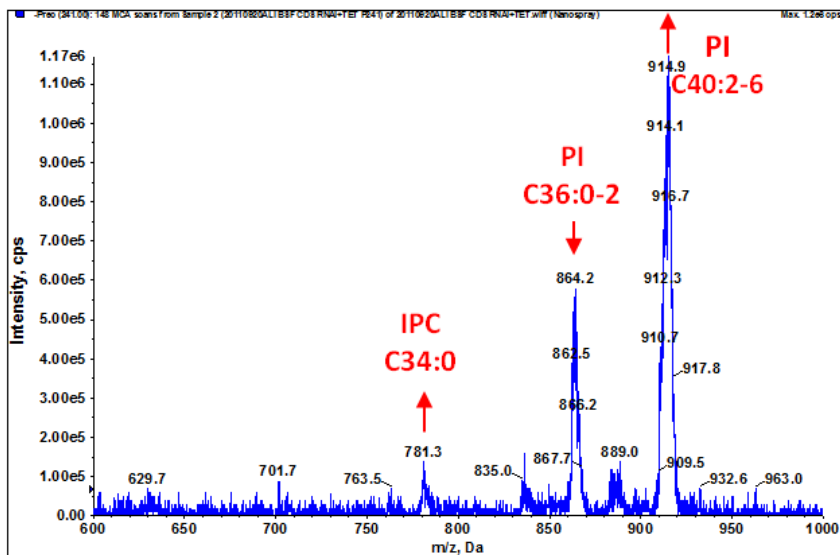


Figure 4.13. Mass spectrometric analyses of inositol-phosphate containing phospholipids from SM and BSF TbCDS RNAi + tetracycline. Total lipids were analysed by ESI-MS in negative ion mode using parent-ion scanning of the collision induced fragment at 241 m/z. A. Wild type single marker cells. B. BSF TbCDS RNAi cells grown in the presence of tetracycline for 42 hours. For further information see Figure 4.8.

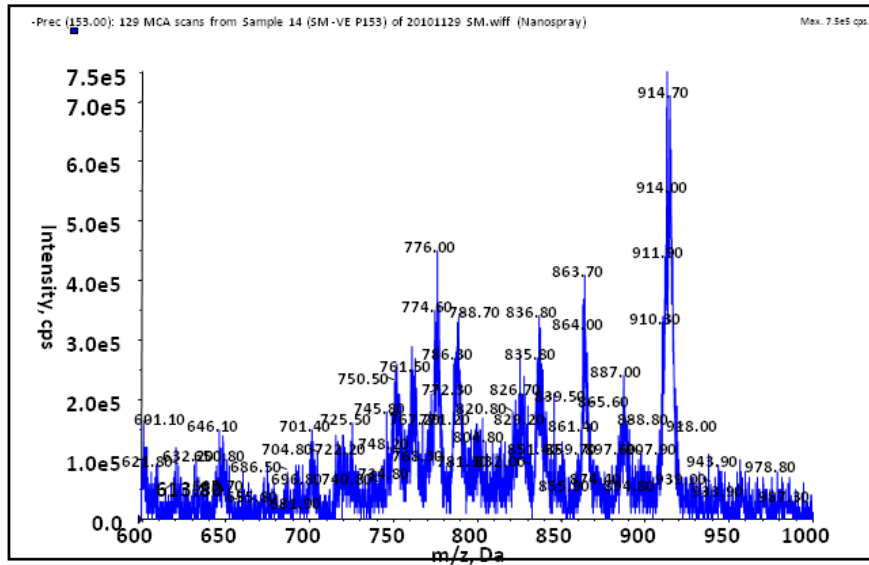
4.4.3.b.vi PA and PG

PA is not a particularly abundant phospholipid in *T. brucei* due to its high turnover rate. Its species distribution seems to be similar to that of the phospholipids to which it is a precursor. It contains both alkyl and acyl species as well as long chain highly unsaturated species.

PG is difficult to detect due to its neutral headgroup, but has been shown as a minor membrane component in bloodstream form *T. brucei*, and of mitochondria as a precursor to CL. As with the other phospholipid species discussed, ether PG is present in *T. brucei* (Richmond et al., 2010). In order to detect PA and PG species, which were clearly of interest due to their roles as substrate and downstream product of TbCDS, a scan was carried out for precursors of 153 m/z (glycerol-phosphate) which detects all anionic glycerophospholipids, but in particular PA and PG (Figure 4.14). It was also helpful to confirm the identities of some of the species from previous scans. For example the hugely abundant 615 m/z species seen in the TbCDS RNAi + tetracycline positive ion scan but not in the corresponding SM sample was not present in the p153 m/z scan of TbCDS RNAi + Tet, which confirmed that it was a DAG species and not a PA species (not a glycerophospholipid).

The general abundance of glycerophospholipids in TbCDS RNAi + tetracycline is not very different from that of SM. However, ratios between PG species do not remain the same. PG a-C36, C36 and C40 are increased relative to PI species. Relative to PI C40, PA C40 is increased from 0.34 to 0.66; PG a-36 is increased from 0.48 to 0.98, PG C36 is increased from 0.48 to 0.98 and PG C40 is increased from 0.27 to 0.72. There was not a general increase in PA species and a decrease in PG species as may have been expected given that they are precursor and downstream products of TbCDS, respectively. In fact, the peak which was most increased in the TbCDS RNAi + tetracycline was at 827.0 m/z in the TbCDS RNAi + tetracycline. This peak was also comparatively increased in the negative survey scan of the TbCDS RNAi + tetracycline in comparison to the SM. Its appearance in this scan and not the p241, p196 or p84 scans confirms that it was likely a glycerophospholipid composed mostly of C40:3 and C40:4. This may correspond to an increase in PA C40 at m/z 761.3.

A. SM



B. TbCDS RNAi + tetracycline

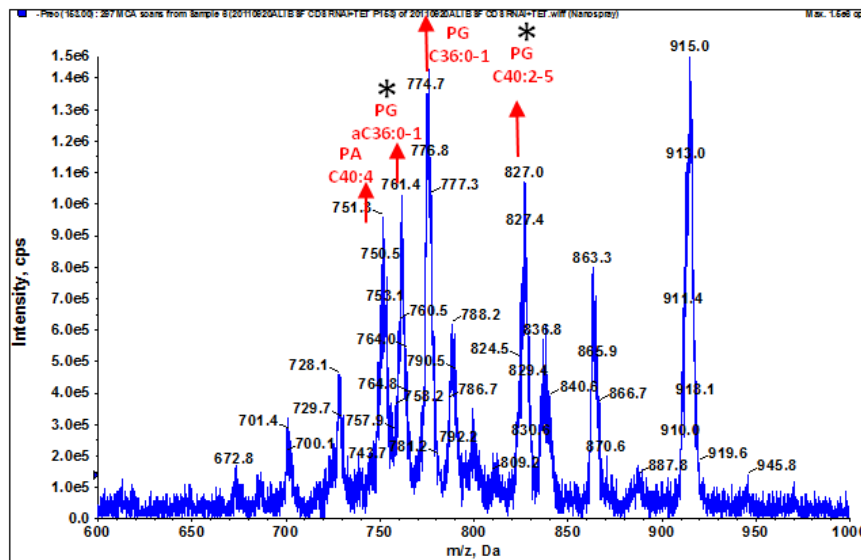
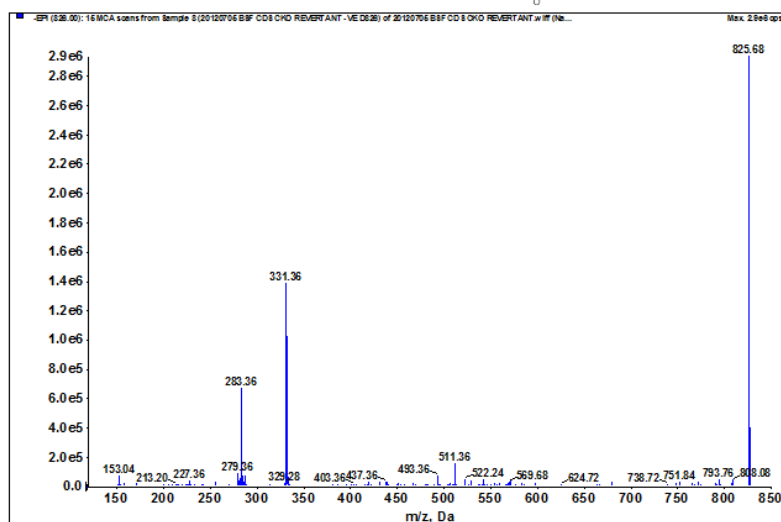
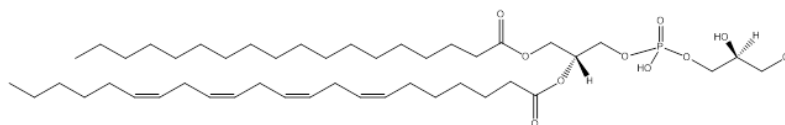


Figure 4.14. Mass spectrometric analyses of glycerol-phosphate containing lipids in SM and BSF TbCDS RNAi + tetracycline. Total lipids were analysed by ESI-MS in negative ion mode using precursor ion scanning for the collision induced fragment for glycerol-phosphate at 153 m/z. A. Wild type single marker cells. B. BSF TbCDS RNAi cells grown in the presence of tetracycline for 42 hours. Asterixes indicate peaks which have been further fragmented (Figure 4.15). For further information see Figure 4.8.

A. PG C18:0/C22:4



B. PG a-C18:0/C18:2

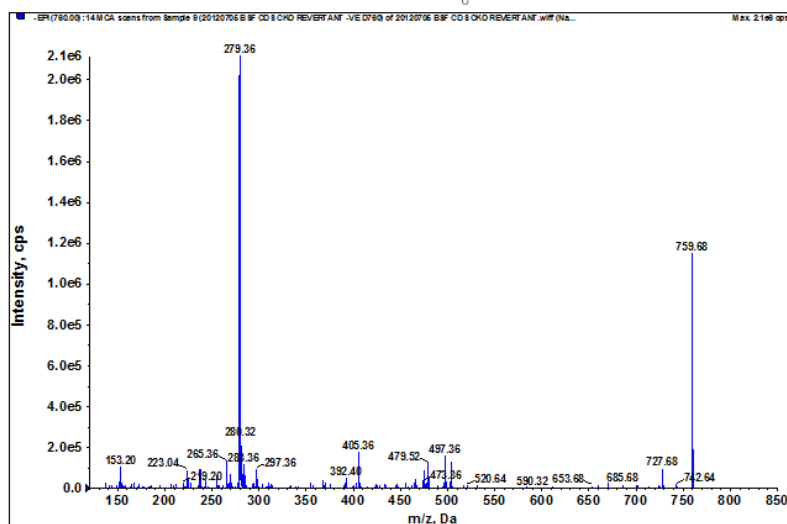
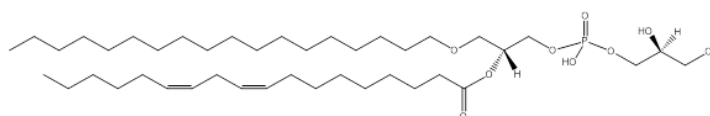


Figure 4.15. Daughter ion spectra of PG species. Daughter ion spectra of two species which were increased in the TbCDS RNAi + tetracycline p153 precursor ion scan. A. m/z 826 [M-H]⁻ ion. B. m/z 760 [M-H]⁻ ion. PG = phosphatidylglycerol. a = alkyl-acyl-linked. CX:Y = number of carbons:number of carbon-carbon double bonds.

Daughter ion fragmentation of this peak further identified it as PG C18:0/C22:4 (Figure 4.15, A). The corresponding C40 PA species at 751 m/z is also somewhat increased. Slight relative increases are also seen in C36 PG species at m/z 774.7, along with a-C36 PG at 761 m/z. An increase in PG species is unexpected since CDP-DAG was considered to be the only lipid precursor to PG in *T. brucei*.

In human and bacteria, a phospholipase D type enzyme is capable of carrying out a trans-phosphatidyl transfer reaction from PC using glycerol as the electron acceptor to produce PG (Dittrich and Ulbrich-Hofmann, 2001, Piazza and Marmer, 2007, Sakagami et al., 2005). Whilst there are no homologues to this PC specific phospholipase D in *T. brucei*, it belongs to a large family of enzymes which have a duplicated phospholipase D domain. Searching the *T. brucei* genome for any such enzymes revealed two: phosphatidylglycerol phosphate synthase (PGPS - Tb927.8.1720) and CL synthase (CLS - Tb927.4.2560). CLS is essential in *T. brucei*, and is unusual in that it is of prokaryotic origin and produces CL from two molecules of PG rather than from PG and CDP-DAG as the eukaryotic enzyme does (Serricchio and Buetikofer, 2012). CL is not a major phospholipid in bloodstream form *T. brucei* and is therefore difficult to see by MS. It is possible that CLS is capable of breaking down CL into PG, but this does not seem likely as PG is mainly thought to be important as a precursor to CL, which is known to be essential for mitochondrial function in the procyclic (Serricchio and Buetikofer, 2012). CL breakdown to PG may occur in the bloodstream form if a certain level of PG is essential. Alternatively, preliminary work also indicates that the *T. brucei* PGPS is essential (Smith and Buetikofer, 2010) and this enzyme shows strong similarity to the prokaryotic PS synthase. If PGPS can bind PS, it could possibly catalyse a phosphatidyl-transferase reaction similar to PC specific eukaryotic phospholipase D using glycerol-phosphate as an acceptor and therefore producing PGP. Further evidence for this hypothesis was found by comparing the profile of serine-phosphate containing lipid in TbCDS RNAi + tetracycline with that in SM.

4.4.3.b.vii Serine Containing Lipids

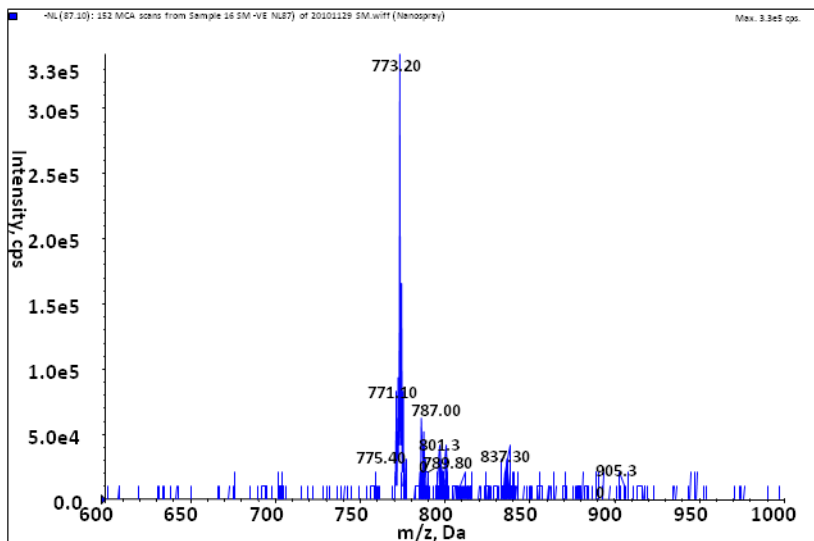
Serine containing lipids are also comprised of a variety of diacyl and ether molecular species, the majority of the ether species being alkyl-acyl- (Richmond et al., 2010). The most abundant series of serine containing lipids by far is a-C36:y, and in bloodstream form trypanosomes a further quarter of the species fall into the C36:y series (Richmond et al., 2010).

Figure 4.16 shows the spectra of the scan for serine-phosphate containing phospholipid species in SM and TbCDS RNAi + tetracycline cell lines. Unfortunately, the signal was not very high so it was difficult to draw any firm conclusions. However, unusually, given that serine labelling of PS was largely unaffected in the TbCDS RNAi + tetracycline cell line, there seems to be rather a large change in the relative abundance of different PS species. The a-C36:y series still has the greatest intensity, but the diacyl C36:y series has disappeared, and there is instead a huge increase in C38:y, specifically C38:2 and C38:1 which normally only accounts for about 5% of serine containing lipid in bloodstream form *T. brucei* (Richmond et al., 2010). In this scan, it has gone from not being above background to 0.55 the intensity of the a-C36 PS. Since the reduction in TbCDS expression does not reduce labelling of PS by [³H]serine, the increase in C38 PS must correspond to a decrease in a-C36 PS. This is perhaps unexpected if the dominant peak of PS is made from headgroup exchange with PE a-C36 species, which is itself not decreased, however, it may correspond with the increase in PG a-C36. Similarly, the increase in diacyl PG C36 may explain the decrease in diacyl C36 PS. Why C38 PS builds up is unclear - C38 is not a particularly common lipid moiety of PE, but is reasonably common in PA, PC and PG species.

Whilst giving some proof for the theory that PG can be made from PS, the disturbance in the pools of PS species makes it difficult to say whether PS is synthesised from CDP-DAG or not. The conflicting results seen by (Signorell et al., 2008) and (Gibellini et al., 2009) whereby disruption in the PE synthesis pathway depleted PS in procyclic but not bloodstream form *T. brucei* could possibly be explained if PC were able to act as a substrate for PSS. A build up of C38 PS may therefore indicate an increase in exchange activity with PC, since this phospholipid contains far more C38 species.

Alternatively, the decrease in C40 PS (of which the largest component is C40:5) could correlate with the decreased contribution of CDP-DAG, since C40:5 is a major species of its lipid precursor and its downstream product PI, but not of PC or PE (Richmond et al., 2010). The decrease in C36:y PS corresponds with the decrease in C36:y PI and a large increase in C36 DAG, though the C36 PS peak is mostly C36:2 whilst the C36:y DAG peak is C36:4.

A. SM



B. TbCDS RNAi + tetracycline

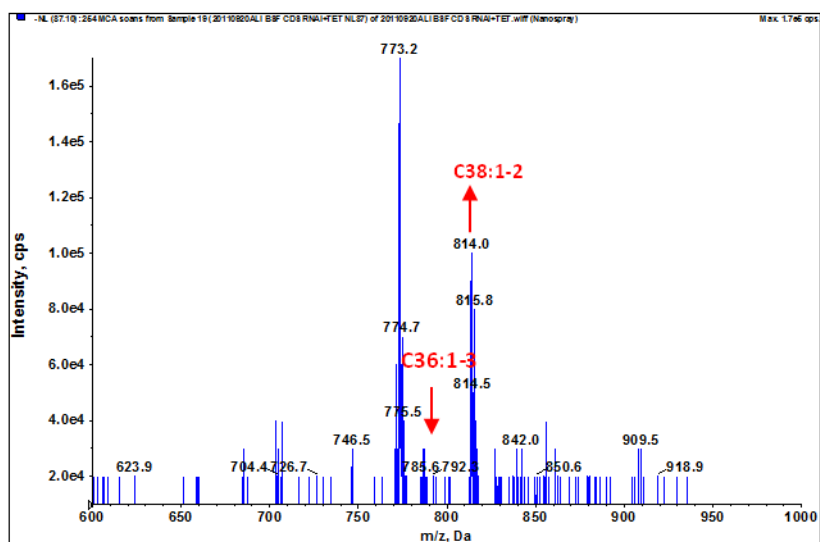


Figure 4.16. Mass spectrometric analyses of serine-phosphate containing phospholipids in SM and BSF TbCDS RNAi. Total lipids were analysed by ESI-MS in negative ion mode using neutral loss scanning for 87 m/z. A. Wild type single marker cells. B. BSF TbCDS RNAi cells grown in the presence of tetracycline for 42 hours. For further information see Figure 4.8.

4.4.3.c NTP levels

NTP samples were taken at 48 and 120 hours after the induction of TbCDS RNAi in clone 1, as well as from SM cells. These time points correspond to the time at which growth slows (48 hours), and just before cells start to die (150 hours). An internal standard was added to each sample, and the samples were analysed by multiple reactant monitoring (Fyffe, Major and Smith - manuscript in preparation) in order to compare average NTP levels per cell. The results are shown in Figure 4.17. After 48 hours, the levels of ATP, GTP and UTP are approximately that of wild type cells, however, CTP is higher. The graphed NTP values are a result of 3 scans on the same sample, and so it is not possible to draw statistical significance from the result. However, the increase in CTP is not unexpected as CTP is a substrate for CDP-DAG synthase and a decrease in the enzyme level may result in increased substrate. After 120 hours, all NTP levels are higher than in wild type. This has previously been shown to be characteristic of cells where a growth stall has occurred (Fyffe, Major and Smith) - the NTPs are still being synthesised but are no longer being incorporated into DNA and other metabolic processes. This is likely to be a symptom of the phenotype rather than a cause of the failing cells.

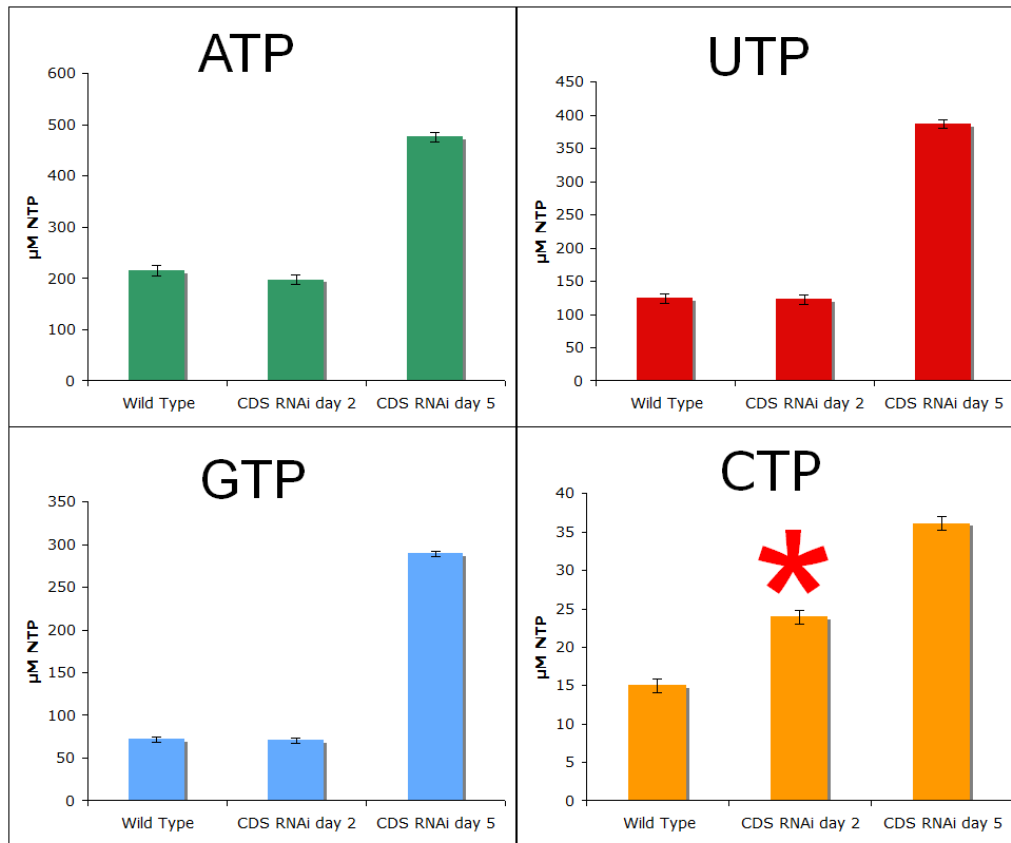


Figure 4.17. NTP quantification in SM and BSF TbCDS RNAi by multireactant monitoring mass spectrometry (MRM-MS). Quantification of each NTP in $\mu\text{M}/\text{cell}$ in wild type (SM), clone 1 TbCDS RNAi at day 2 and day 5 after the addition of tetracycline.

4.5 Knockout of TbCDS in bloodstream form *T. brucei*

RNAi knockdown of TbCDS showed some significant alterations in cell growth, metabolism and lipid content. Unfortunately, these cells were not particularly stable and there was some clone to clone variation along with a lack of reproducibility in the growth phenotype beyond five days of tetracycline induction. Because RNAi produces a knockdown rather than a null, cells were adapting to low levels of CDP-DAG, possibly masking normal biosynthetic pathways. This made it difficult to assess the usual functions of TbCDS. It is known that whilst CDS an essential gene in yeast, only 10% of wild type activity is needed to support wild type growth (Shen et al., 1996) suggesting that cells do not necessarily need a large amount of CDP-DAG. In order to look further into the essentiality of TbCDS, a conditional null mutant was created to see how the cells coped with this gene being knocked out altogether.

4.5.1 Creation of a TbCDS Conditional Knockout Cell Line

The first step in the creation of a conditional knockout was to transfect the cells with an inducible ectopic copy of TbCDS. *T. brucei* 427 cells constitutively express the T7 polymerase and tetracycline repressor protein, so the TbCDS ORF was cloned into the phleomycin selectable pLEW100 vector to produce an HA-tagged ectopic TbCDS with a procyclin promoter (GPEET) which is constitutively expressed in both bloodstream form and procyclic (Pays et al., 1990) and two tetracycline operators, flanked by two stretches of *T. brucei* rDNA (Wirtz et al., 1999) (Figure 4.18, G). This construct is designed to allow tightly regulated expression of a gene in *T. brucei* under the control of tetracycline. In the absence of tetracycline, there is no expression from this construct. The TbCDS-HA pLEW100 vector was linearised and transfected into *T. brucei* 427 SM cells where it integrated into the ribosomal DNA spacer region via homologous recombination. Selection with phleomycin allowed the creation of the TbCDS-HA (Figure 4.18, G). cell line (Table 2.1, Figure 4.18, A) and inner primers R1 and F2 designed according to the sequence obtained previously.

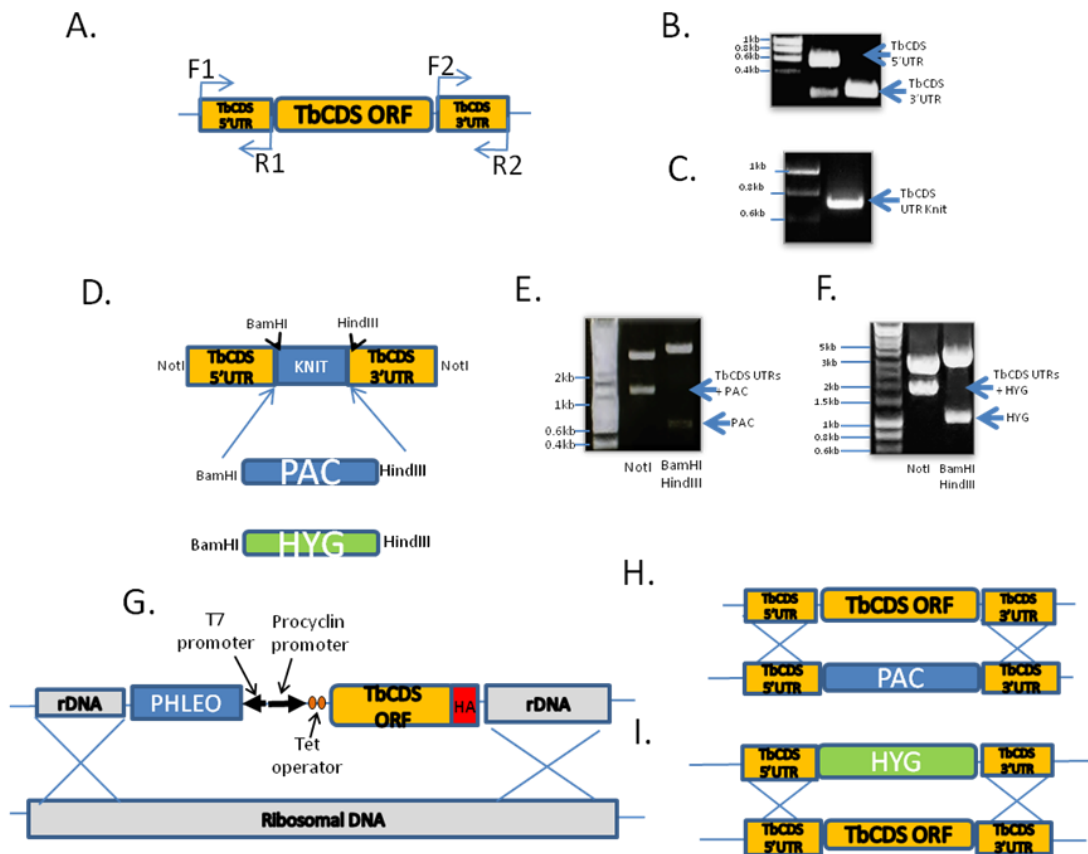


Figure 4.18. Construction of TbCDS knockout and endogenous expression pLEW100 constructs. (A) Schematic showing the position of TbCDS primers F1, R1, F2 and R2 (Table 2.1) designed to isolate the TbCDS UTRs. (B) The 5' and 3' TbCDS UTRs were PCR amplified using the primer combinations TbCDS F1, R1 and TbCDS F2,R2. (C) The two UTRs were linked together via complimentary regions in the R1 and F2 primers in a knitting PCR reaction. After subcloning, the puromycin resistance (PAC) or hygromycin resistance (HYG) cassette was ligated in between the TbCDS stitched UTR regions using BamHI and HindIII sites.(E-F) Knockout constructs were ligated into pGEM and checked by NotI restriction enzyme digest to dropped out the entire knockout construct, or BamHI and HindIII to drop out the PAC (E) or HYG (F) construct. (G) TbCDS was transfected into a SM background using the pLEW 100 plasmid which contains the gene under tetracycline inducible promoter, along with a phleomycin resistance gene (PHLEO) and homologous regions to rRNA. The plasmid was linearised and transfected in order to integrate it into the rDNA spacer regions by homologous recombination. (H) After selection for cells containing the tetracycline inducible, ectopic TbCDS, the cells were transfected with the PURO knockout cassette. The linearised construct integrated into the genome by homologous recombination with the TbCDS UTRs and knocked out the first genomic TbCDS copy, replacing it with PURO. Successful transformants were selected with puromycin. (I) In the presence of tetracycline, to switch on the ectopic TbCDS copy, the TbCDS single knockouts were transfected with the HYG knockout cassette, and successful transformants were selected with hygromycin.

An adenine was changed to a cytosine in the R1 primer 10 base pairs upstream of the TbCDS start codon in order to mutate out a HindIII restriction enzyme recognition site -from AAGCTT to ACGCTT (Figure 3.3, Table 2.1, Figure 4.18, A). F1 and R1, and F2 and R2 primer combinations were then used in two separate PCR reactions in order to isolate the 5' and 3' UTR regions (Table 2.1, Figure 4.19, A). These PCR products were annealed together in a knitting PCR, using the linking regions added by the R1 and F2 primers (Figure 4.18, C and 4.18, D) and the knitted construct was ligated into pGEM-5ZF using NotI restriction sites added by the F1 and R2 primers. The linking region was then cut out of the knitted construct and replaced by the drug resistance genes puromycin acetyltransferase (PAC) or hygromycin phosphotransferase (HYG) which were ligated between the 5' and 3' TbCDS UTRs using BamHI and HindIII restriction sites (Figure 4.18, D, E and F).

The first TbCDS allele was knocked out of the TbCDS-HA cell line by transfection with the PAC knockout construct (Figure 4.18, H), so that the PAC gene replaced the TbCDS gene by homologous recombination and cells which had undergone knockout were selectable with puromycin. This created a single knockout cell line with an inducible copy of TbCDS - Δ TbCDS::PAC TbCDS-HA.

It is often impossible to knock out the second allele of a gene if this gene is essential, therefore, in order to allow deletion of the second TbCDS allele, Δ TbCDS::PAC TbCDS-HA cells were cultured in the presence of tetracycline for 24 hours to allow the exogenous TbCDS-HA to be switched on and relieve cell dependence on the second allele. The single knockout cells containing the ectopic TbCDS were then transfected with the HYG knockout construct (Figure 4.18, I) and selected with hygromycin in the presence of tetracycline. This allowed the creation of the conditional double knockout cell line Δ TbCDS::PAC/ Δ TbCDS::HYG TbCDS-HA.

4.5.2 Confirmation of the TbCDS CKO Genotype

The genotype of the conditional mutant was verified by PCR analysis using the PuroF with TbCDS R2 primers; HygF with TbCDS R2; and CDPDAG p82F with TbCDS R2 (Figure 4.19, A). Whilst the first two primer combinations produced a product when used with TbCDS CKO gDNA as a template, they produced no product with SM gDNA. This proved the presence of the knockout constructs in the gDNA of TbCDS CKO. The final primer combination (CDPDAG p82F, TbCDS R2) produced no product when used

on the TbCDS CKO gDNA but did produce a product from SM, showing that in the TbCDS CKO the TbCDS gene was no longer present in its genomic locus.

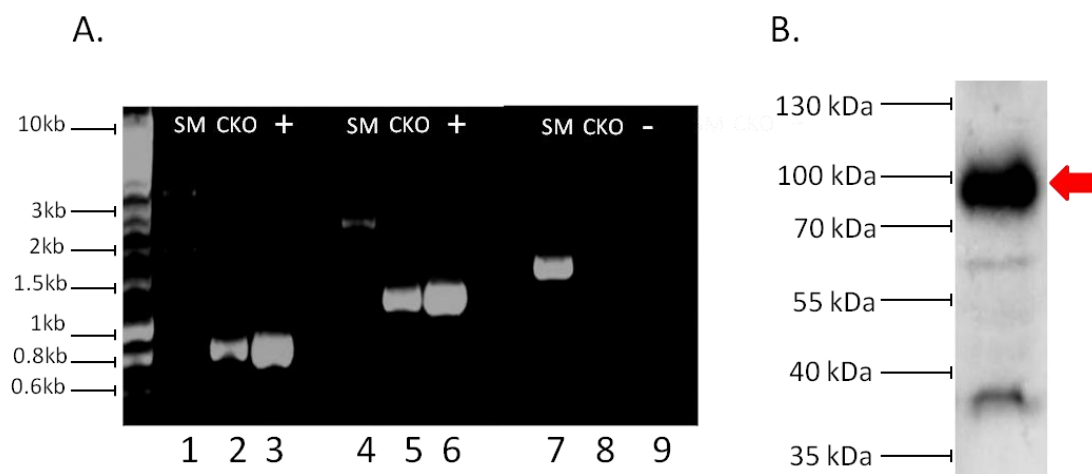


Figure 4.19. PCR Confirmation of BSF TbCDS CKO (A) 1% agarose DNA gel of diagnostic PCR using genomic DNA from single marker and TbCDS conditional knockout. 1-3 Puro F and TbCDS R2 primers to amplify part of the PURO knockout construct. Template: Lane 1 – SM gDNA, lane 2 TbCDS CKO gDNA, lane 3 TbCDS PURO KO construct in pGEM. Lanes 4-6 – Hyg F and TbCDS R2 primers to amplify part of the HYG TbCDS knockout construct. Template : Lane 4 – SM gDNA, lane 5 – TbCDS CKO gDNA, lane 6 – TbCDS HYG KO construct in pGEM . Lane 7 -9 TbCDS ORF F and TbCDS R2 primers to amplify TbCDS in its genomic location. Template: Lane 7 – SM gDNA, Lane 8 – CKO gDNA, Lane 9 – TbCDS HYG KO knockout in pGEM. (B) Confirmation that *T. brucei* TbCDS CKO are expressing HA tagged TbCDS protein from the exogenous, tetracycline controlled pLEW 100 TbCDS copy - Anti-HA Western blot of total *T. brucei* TbCDS CKO 24 hours after the addition tetracycline to the culture. Red arrow indicates TbCDS-HA. The predicted size of the HA tagged protein is 47 kDa, but it runs aggregated, presumably due to its multiple trans-membrane domains.

Western blot confirmed that the conditional knockouts were expressing HA-tagged TbCDS in the presence of tetracycline (Figure 4.19, B). Interestingly, expression of HA tagged TbCDS was not detectable in the pLEW100 TbCDS-HA cell line (containing both the wild type genomic TbCDS alleles) in the presence of tetracycline, perhaps suggesting that the cells exert some post-transcriptional control over the levels of TbCDS protein.

4.5.3 Growth Phenotype of TbCDS CKO

To examine the growth phenotype of Δ TbCDS::PAC/ Δ TbCDS::HYG TbCDS-HA cell counts were performed in the presence and absence of tetracycline in order to switch on or off the expression of the endogenous TbCDS copy and therefore the presence or absence of TbCDS (Figure 4.20). A growth defect was present after 24

hours, and after 48 hours cells started to die. There were no live cells countable by 100 hours. These results clearly show that TbCDS is essential to bloodstream form *T. brucei* in culture.

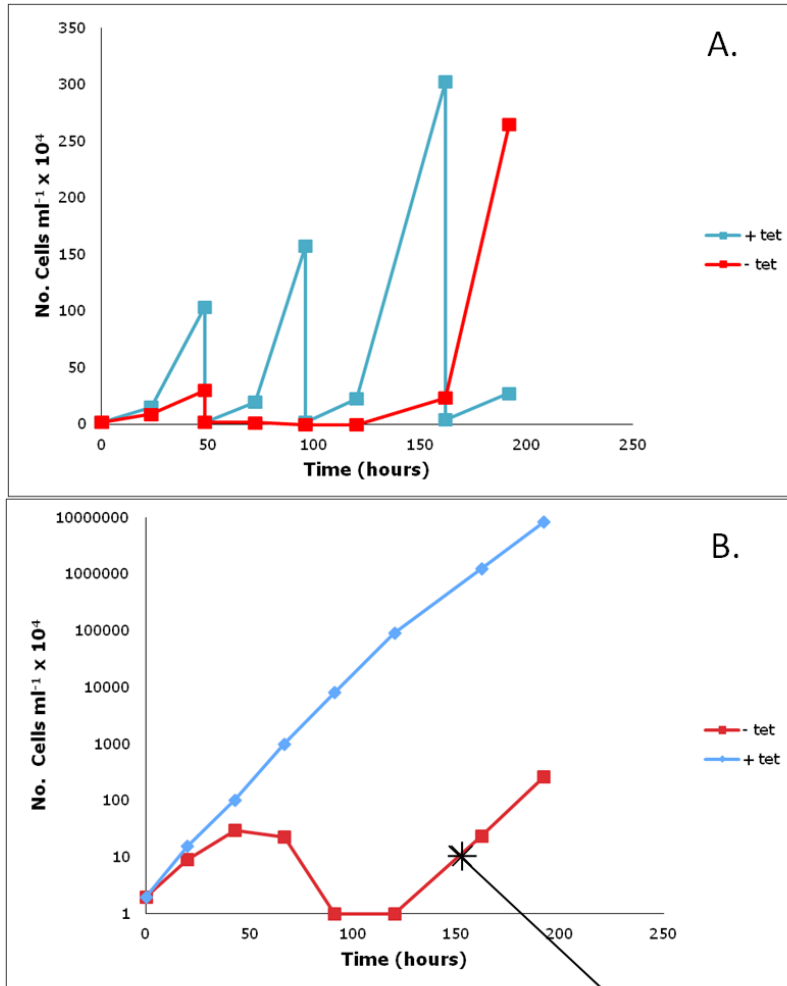
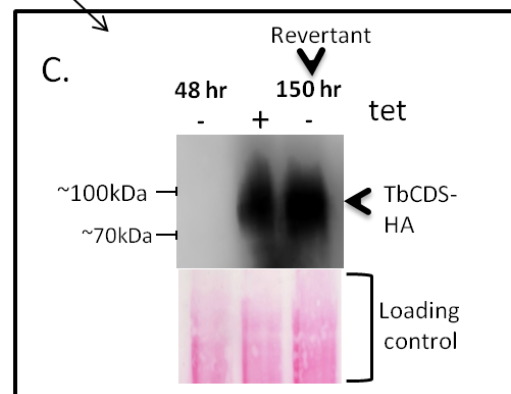


Figure 4.20. TbCDS is essential for the survival of BSF *T. brucei* in culture. (A,B) Growth curves of *T. brucei* CKO in the absence (red squares) or presence (red squares) of tetracycline (tet) (A) actual number of cells per ml of culture x 10⁴ after number of hours cultured in the presence or absence of tetracycline. (B) Growth curves of log cumulative number of cells over time in the presence and absence of tetracycline. (C) Reoccurrence of HA tagged TbCDS despite the absence of tetracycline suggests regrowth is due to cells reverting and breaking the tetracycline control of TbCDS expression. Loading control is ponceau stained western blotted membrane.



After about 120 hours, growth resumed as normal. It seemed likely that this was revertant growth due to the cells breaking the tetracycline control as loss of tetracycline control has previously been shown in knockouts of essential genes (Chang et al., 2002, Milne et al., 2001, Roper et al., 2002). Indeed, anti-HA western blot confirmed that the revertant cells had resumed the production of the HA tagged TbCDS in the absence of tetracycline (Figure 4.20, C).

4.5.4 Morphological Phenotype of TbCDS CKO

By observation of the Δ TbCDS::PAC/ Δ TbCDS::HYG TbCDS-HA^{Ti} cells in the absence of tetracycline, a more obvious phenotype was visible than had been seen in the TbCDS RNAi knockdown cell line. Figure 4.21 shows the morphology of SM cells compared to the TbCDS CKO cell line after 48 hours in the absence of tetracycline. Similarly to the TbCDS RNAi cell line, these cells seemed to have a rougher surface than the wild type. The most obvious phenotype was what appeared to be a cell cycle stall after the replication of the flagella. DAPI staining showed that, in most cases, these cells were 1K2N, often with unusual looking nuclei perhaps due to the nuclei trying and failing to undergo further replication. In *T. brucei* cells undergoing RNAi against VSG, there is a precytokinesis cell stall and the majority of these cells have two flagella. However in the VSG RNAi cell line both these flagella are internal (Shedden et al., 2005), and this is not the case here, since free flagella can be seen. It has been shown that *T. brucei* lack certain common eukaryotic cell checkpoints in cell division and can undergo cytokinesis without completing mitosis (Das et al., 1994, Robinson et al., 1995, Ploubidou et al., 1999). The kinetoplast is the first of the two DNA containing cell bodies to divide and therefore 2K1N cells are common in a normal population. Stalled mutants tend to have more kinetoplasts than nuclei and it is thought that the division of the kinetoplastid is intimately linked to cell cycle progression (Jetton et al., 2009, Hammarton et al., 2007a). The initiation of cell division begins with the maturation of an immature basal body, followed by kinetoplast duplication and the growth of a new flagellum alongside that of the old flagellum. The basal body is physically linked to the kinetoplast, so theoretically it should not be possible for the flagella to replicate without the kinetoplast (Hammarton et al., 2007b).

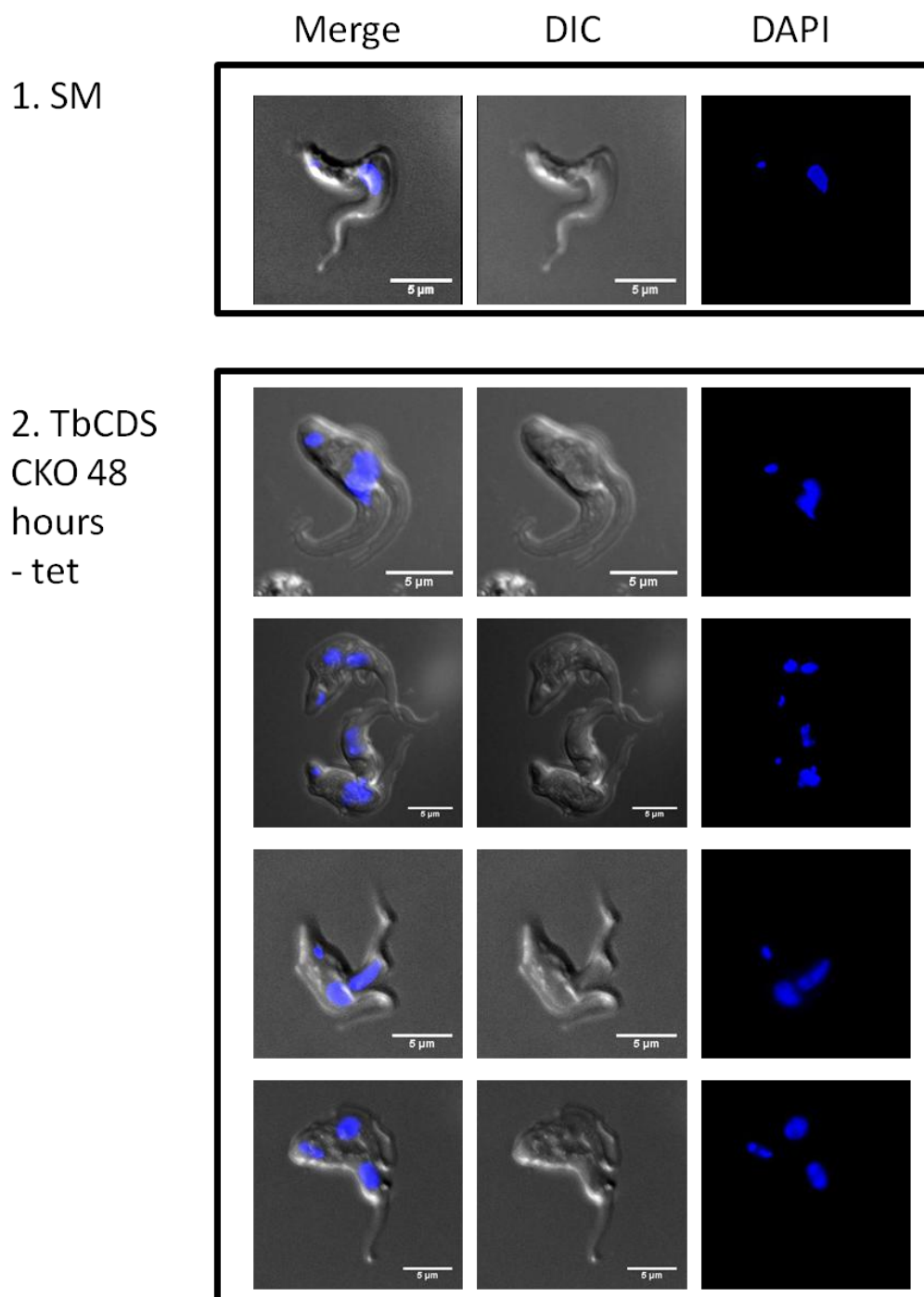


Figure 4.21. Morphology of SM and TbCDS CKO 48 hours - tetracycline. Maximum intensity of projections of Z-series images taken by light microscopy. Middle panel shows DIC, right panel shows DAPI staining and left panel shows the merged Image. Cells were fixed with 4% paraformaldehyde, allowed to adhere to poly-lysine slides and mounted with anti-fade GOLD reagent containing DAPI. 1. SM cells harvested from mid log culture and fixed in 4% paraformaldehyde. 2. TbCDS CKO cells harvested from culture 48 hours after the removal of tetracycline.

From these images, it cannot be ruled out that the kinetoplastid has replicated, but it failed to segregate. RNAi of the protein Mob1 in bloodstream form *T. brucei*, which binds to and activates protein kinase partners stimulating protein kinase activity, caused a phenotype where the cells had multiple nuclei and kinetoplasts, often with the number of nuclei larger than the number of kinetoplasts, indicating that kinetoplast division was affected (Hammarton et al., 2005). They postulate that this protein may be part of a kinetoplast replication/segregation checkpoint in trypanosomes. The fact that mutants of two very different proteins should produce similar phenotypic affects are extremely interesting, particularly since there has been a link established between PIPs and protein kinase regulation (Franke et al., 1997). These results could indicate for the first time a role for phosphoinositide signalling in regulation of kinetoplastid replication, cell-cycle progression and organised cell division in *T. brucei*.

4.5.5 Biochemical Phenotyping of Bloodstream Form TbCDS CKO

4.5.5.a. In vivo radiolabelling

Building on from the radiolabelling of the TbCDS RNAi cell line, in the bloodstream form TbCDS CKO cell line it was decided to look at labelling of total lipid ($[^3\text{H}]$ myristate), total glycerolipid ($[^3\text{H}]$ glycerol) and PI ($[^3\text{H}]$ inositol)(Figure 4.22). The time point for labelling was 42 hours after the removal of tetracycline from the media as at this point the cells are clearly growing more slowly, but are not yet dying and therefore biochemical phenotyping could give an indication of what is causing death.

As was the case in TbCDS RNAi, there was no change in the labelling of overall lipid by $[^3\text{H}]$ myristate, although there did seem to be a slight increase in neutral lipids in the TbCDS CKO and a slight reduction in glycolipids A and C (Figure 4.22, A). This shows that normal overall lipid synthesis is occurring in the TbCDS CKO, and also that the cells are still metabolically active at this time point. The increase in neutral lipid in the knockout may reflect the increase in species of DAG and TAG that was seen in the TbCDS RNAi knockdown although these would have to contain C14 or C18 lipid moieties in order to be labelled by myristate. This can be confirmed later when the results from ES-MS of lipids are discussed. Unlike in the TbCDS RNAi knockdown, where the incorporation of $[^3\text{H}]$ glycerol into most glycerolipid species appeared to be

equally reduced (Figure 4.22, B.1), a differential effect was seen in the incorporation of [³H]glycerol into different glycerophospholipids in TbCDS CKO (Figure 4.22, B). There is less labelling of PE and PI by [³H]glycerol in the mutant - as was seen in TbCDS RNAi + tetracycline, but PC and/or PS seem unaffected. The decrease in PI labelling by [³H]glycerol is expected, but the decrease in PE labelling is not. Again, glycerol does not label the majority of PE species as they are plasmenyl. This decrease in diacyl PE species may reflect a cellular response to a decline in other phospholipid species as the cells try to adapt to the change in membrane composition. The fact that PC labelling is not affected is not unexpected, given that this route of synthesis of choline containing lipids is separate from the CDP-DAG pathway - i.e. the Kennedy Pathway. The lack of a change in PS labelling may indicate that it is not made via CDP-DAG or that any deficit due to the lack of CDP-DAG can be made up by synthesis via PE and possibly PC by the headgroup swapping enzyme PSS. Most interestingly, there is an increase in the band corresponding to PG. Again, this is surprising since CDP-DAG is the only known route to PG synthesis, however the TbCDS RNAi + tetracycline ES-MS showed that not only did the PG species not decrease relative to other lipid species, but certain species were increased.

Surprisingly, but again reflecting what was seen in the TbCDS RNAi knockdown, the incorporation of [³H]inositol into PI is unaffected in the TbCDS CKO (Figure 4.22, C). Since TbPIS is known to catalyse a headgroup swapping reaction of inositol with pre-existing PI, it seems likely that this lack of a decrease in [³H]PI is due to the headgroup swapping of [³H]inositol into cold PI. Since [³H]glycerol labelling of PI was decreased in the TbCDS CKO, it is clear that *de novo* synthesis of PI via CDP-DAG and inositol (*de novo* synthesised and exogenous) is decreased overall, as would be expected.

It has previously been shown here that in TbCDS RNAi knockdown cells the incorporation of [³H]mannose into GPI anchors was severely compromised. To see if the cells decreased ability to form GPI anchors was due to depletion of PI rather than any other block in the pathway, washed trypanosomal lysate formed from SM and TbCDS CKO - tetracycline *T. brucei* were used in a cell free system to test their ability to catalyse different steps of the GPI anchor biosynthetic pathway.

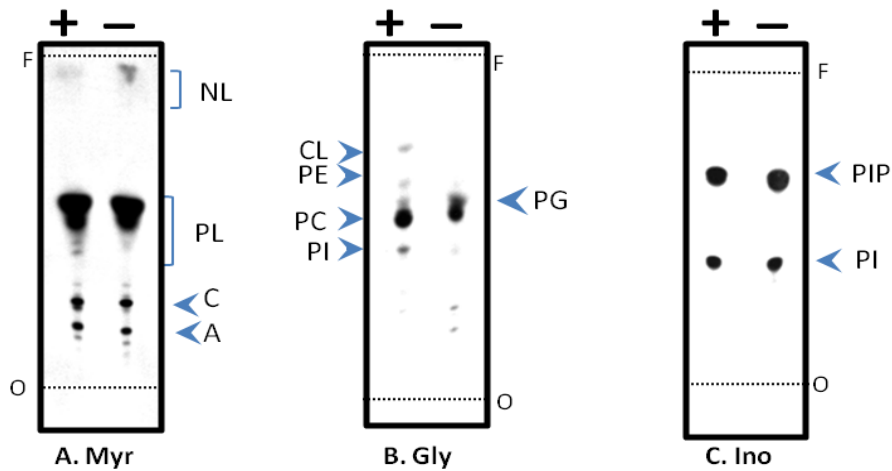


Figure 4.22. Biochemical analysis of BSF TbCDS CKO by *in vivo* radiolabelling after growth + and - tetracycline for 42 hours. Autoradiographs of HPTLC plates run with the lipid fraction of cells labelled with: A. Myr = [³H]Myristate; B. Gly = [³H]Glycerol; C. Ino = [³H]Inositol; (NL = neutral lipids, PL = phospholipids) -/+ (left and right of plate) = TbCDS CKO + tetracycline, TbCDS CKO - tetracycline. O = origin, F = front. A, B and C run in 180:140:9:9:23 CHCl₃:MeOH:30% NH₃:1M NH₄Ac:H₂O.

4.5.5.b. Cell Free System for GPI Anchor Synthesis

Washed membranes from SM and TbCDS CKO cells at 42 hours minus tetracycline were incubated with the radiolabelled GPI precursor GDP-[³H]Man in the presence or absence of UDP-GlcNAc. In the presence of *T. brucei* membranes, GDP-[³H]Man forms dolichol-phosphate-[³H]mannose (DPM). With the addition of UDP-GlcNAc, the [³H]mannosylated GPI intermediates Man₁GlcN-PI (M1), Man₂GlcN-PI (M2) Man₃GlcN-PI (M3), Man₃GlcN-(acyl)-PI(aM3), EtN-P-Man₃GlcN-PI (A') are formed (synthesis pathway shown in Figure 1.10). In the absence of UDP-GlcNAc as a negative control, only DPM is formed.

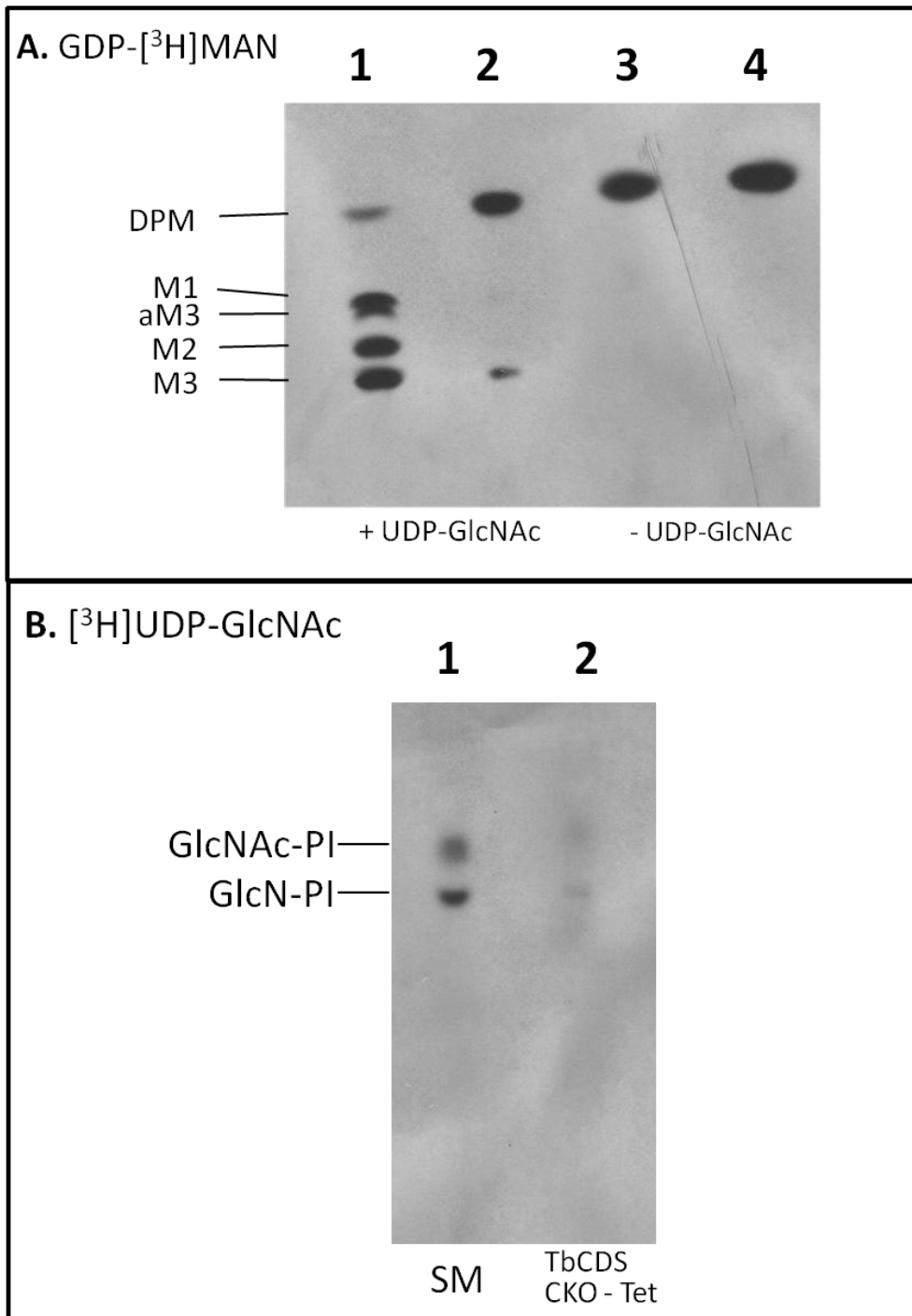


Figure 4.23. TbCDS is essential for formation of GPI intermediates. (A.) Cell free system of SM (lanes 1 and 3) and TbCDS CKO 42 hours – tetracycline (lanes 2 and 4) membranes incubated with GDP-[³H]Man in the presence (lanes 1 and 2) and absence (lanes 3 and 4) of UDP-GlcNAc. (B) Cell free system of SM (lane one) and TbCDS CKO 48 hour minus tetracycline (lane 2) membranes incubated with UDP-[³H]GlcNAc.

In the absence of UDP-GlcNAc, both SM and TbCDS CKO membranes formed only DPM as expected (Figure 4.23, A, lanes 3 and 4). When SM membranes were incubated in the presence of UDP-GlcNAc, GDP-[³H]mannose labelled DPM, M1, aM3, M2 and M3 were formed, as expected (Figure 4.23, A, lane 1). When TbCDS CKO membranes were incubated in the presence of UDP-GlcNAc and GDP-[³H]mannose, only DPM and a very faint M3 band were labelled (Figure 4.23, A, lane 2). Since there is a lack of mannosylated intermediates it is clear that the block occurs very early in the pathway and may be due to a lack of PI which is required to initiate the pathway. To further back this up, SM membranes incubated in a new cell free system assay with UDP-[³H]GlcNAc in the absence of GDP-Man, formed two strong bands corresponding to GlcNAc-PI and GlcN-PI (Figure 4.23, B, lane 1) whilst the same two bands were very faint when TbCDS CKO - tetracycline membranes were incubated in the same conditions (Figure 4.23, B, lane 2). These results together show that TbCDS CKO-tetracycline cells are severely compromised in their ability to make GPI anchors, and that this is due to a lack of endogenous PI in the correct membrane location (ER) that can act as an acceptor allowing the completion of the initial step of GPI biosynthesis - synthesis of GlcNAc-PI.

These results, together with those from the [³H]glycerol labelling of PI clearly show that the *de novo* synthesis of PI is decreased in the TbCDS CKO. However, [³H]inositol labelling of PI shows no change. [³H]inositol cannot be incorporated into the ER pool of PI since the PI synthase enzyme is only thought to have access to inositol-phosphate synthesised from glucose which is then dephosphorylated inside the ER. *T. brucei* lack exogenous inositol transport across the ER membrane (Gonzalez-Salgado et al., 2012). This could be taken as evidence that only the ER pool of PI is affected by the TbCDS knockout, however in an INO1 knockout which specifically decreased the pool of PI for GPI anchors there was no overall decrease of [³H]glycerol labelled PI, presumably due to the ER pool of PI being so small. Since a significant decrease in [³H]glycerol is seen here, both pools of PI must be affected. This indicates that the lack of change seen in the incorporation of [³H]inositol into PI is due to an increase in headgroup swapping of the [³H]inositol into existing PI. Such an increase of the headgroup swapping reaction is possibly stimulated by an increase of the inositol pool relative to the CDP-DAG pool - yeast mutants deficient in CDS activity excrete inositol into the medium (Shen and Dowhan, 1996) - and may help to maintain a dynamic turnover of good quality PI. However, [³H]glucose incorporation

into PI is greatly decreased indicating that either the ER pool of PI is more greatly affected in the TbCDS knockout (possibly due to a high rate of flux through the pathway) and/or headgroup exchange is not up-regulated in the ER. A differential effect of CDP-DAG depletion on the two different pools of PI could indicate two separate pools of CDP-DAG, possibly synthesised by dually localised TbCDS in the membranes of the two different organelles, as is the case with PIS (Martin and Smith, 2006b).

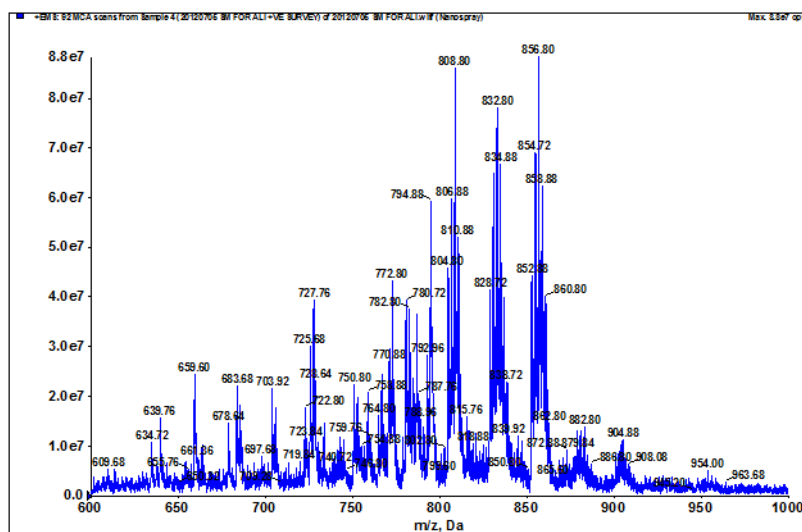
4.5.5.c ES-MS/MS of Lipids

4.5.5.c.i Positive Survey Scan

Comparison of the TbCDS CKO - tetracycline positive survey scan with that from the TbCDS knockdown (Figure 4.24) shows that they are remarkably similar, though DAG C36 at 615 m/z (mostly 36:5) and EPC C36 at 689 m/z (mostly C42:9) are greatly increased. In both cases they are not above background in SM but form significant peaks in TbCDS CKO - tetracycline. DAG C36 and EPC C36 peaks in TbCDS CKO - tetracycline are 0.97 and 0.64 of PC α -C38, respectively. At the other end of the spectra PC C44:7, along with TAG C62 (mostly C62:9) are also increased. The fact that these species are increased in both the knockdown and knockout shows that they are not an anomaly. As previously mentioned, since the accumulation of the TbCDS precursor PA is potentially harmful to the cells, PA species are probably dephosphorylated to neutral lipids DAG and TAG. This hypothesis is supported by the regulation of DAG kinase and PA phosphatase activities by CDP-DAG concentration in yeast (Shen et al., 1996). The DAG may not be utilised by the Kennedy Pathway if this pathway is already at saturation, and/or the DAG species produced from dephosphorylation of PA may not be readily incorporated into the Kennedy Pathway. The increase in neutral lipid is supported by the [³H]myristate labelling of the TbCDS CKO lipid fraction (Figure 4.22, A) which indicates an increase in neutral lipids containing C14 or C18 acyl chains.

The increase in EPC C36:1 is accompanied by a decrease in the shorter chained C34:1 EPC species. It seems likely that this is due to an increase in the availability of C36 lipid moieties due to their reduction in PI.

A. SM



B. TbCDS CKO - tetracycline

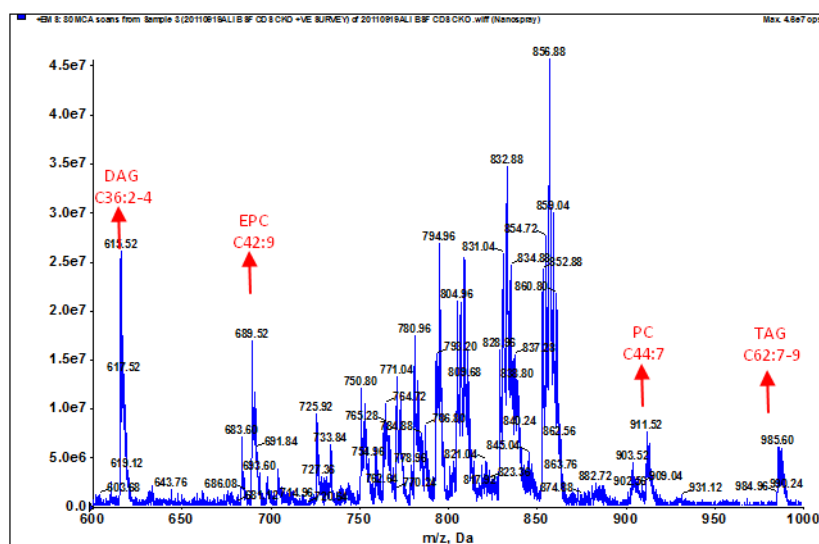


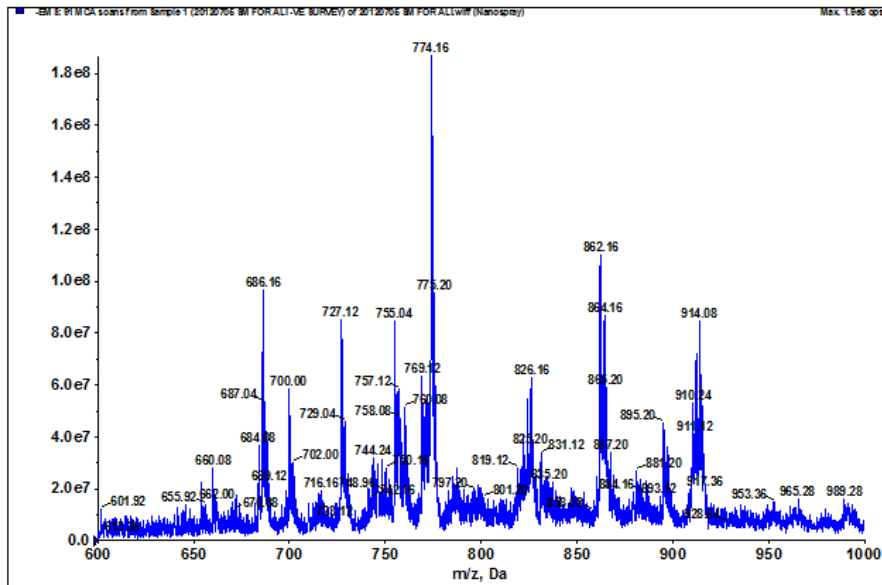
Figure 4.24. Positive ion survey scan of lipids from SM and TbCDS CKO – tetracycline. Mass spectrometric analyses of total phospholipids by positive survey scan ESI-MS. A. Wild type single marker cells. B. TbCDS CKO cells grown in the absence of tetracycline for 42 hours. For further information see Figure 4.8.

4.5.5.c.ii Negative Survey Scan

The negative survey scan of the TbCDS CKO also shows some similarities to that of the TbCDS knockdown (Figure 4.9). As with the TbCDS RNAi negative survey scan, because all peaks are so altered it is difficult to say which peaks are decreased relative to others. The PE m/z 727 peak which represents a-C36 PE is one of the most intense. The m/z 686 peak, previously identified by fragmentation as PA a-C18:0/18:2 (Figure 4.10) is also absent from this scan, as it was in the RNAi, but in addition the peak at m/z 700 is absent, which further fragmentation confirmed to be the diacyl counterpart of the other missing PA, PA C18:0/C18:2 (Figure 4.26). A peak at m/z 761 is present in the TbCDS CKO scan which is not a defined peak in the SM. This peak was previously identified as PG a-C18:0/C18:2 (Figure 4.15, B) and is increased in the TbCDS RNAi + tetracycline p153 scan (Figure 4.14), and in the negative survey scan of the TbCDS knockdown (Figure 4.9), but at a very low intensity. The m/z 825.9 peak, previously identified to compose mostly of PG C18:0/C22:4 (Figure 4.15, A) that was increased in the TbCDS RNAi + tetracycline is much larger in the TbCDS CKO. An increase in PG species in a total TbCDS CKO gives clear evidence that PG is formed from another lipid precursor than CDP-DAG, and this will be discussed later.

There is an decrease in the relative amount of PI C36 to PI C40 from 1.29 in SM to 0.38 echoing what was seen in the TbCDS RNAi + tet where the ratio of PI C36 to PI C40 was also 0.38.

A. SM



B. TbCDS CKO – tetracycline 42 hours

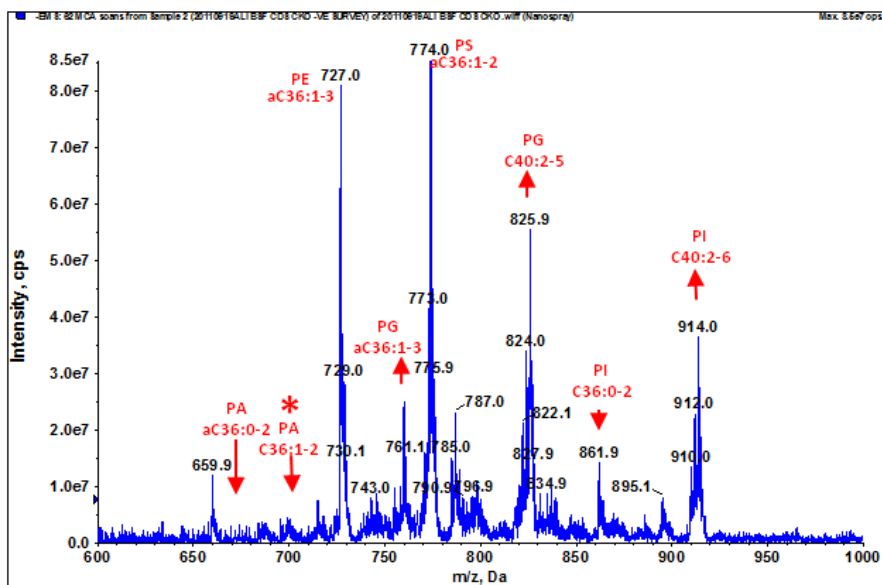


Figure 4.25. Negative survey scan of lipids from SM and TbCDS CKO – tetracycline. Mass spectrometric analyses of total phospholipids by negative survey scan ESI-MS. A. Wild type single marker cells. B. TbCDS CKO cells grown in the absence of tetracycline for 42 hours. PA = phosphatidic acid, PG = phosphatidylglycerol, PI = phosphatidylinositol, PE = phosphatidylethanolamine, PS = phosphatidyl serine. Asterisk indicates species which have been further fragmented (Figure 4.27). For further annotation refer to Figure 4.8.

PA C18:0/C18:2

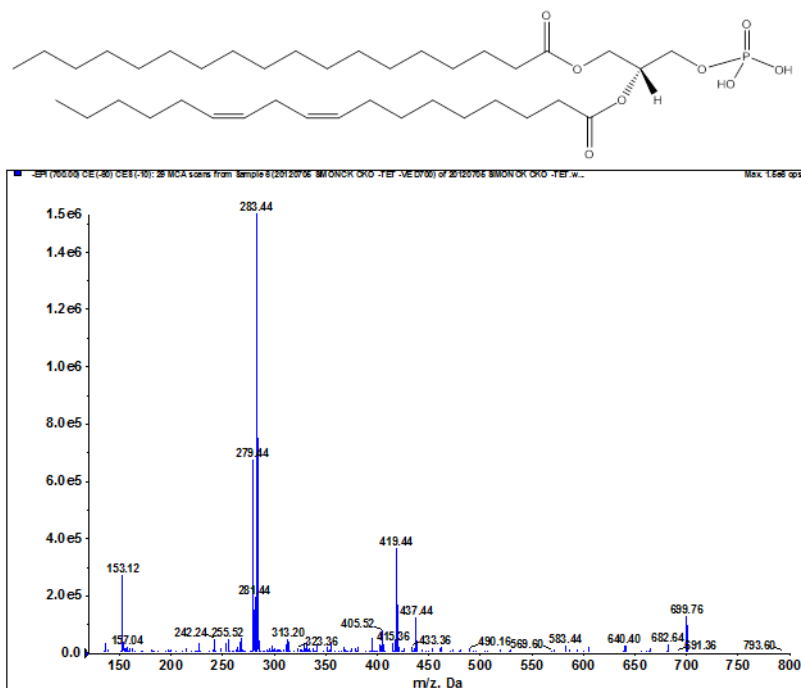


Figure 4.26. Daughter ion spectrum of m/z 700 [M-H]⁻ ion. PA = phosphatidic acid. CX:Y = number of carbons:number of carbon-carbon double bonds.

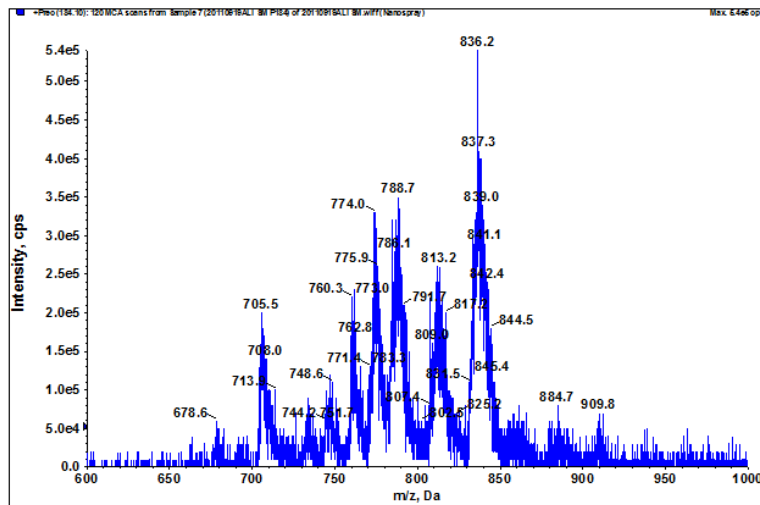
4.5.5.C.iii Choline Containing Lipids

As in the TbCDS RNAi knockdown, it was also considered important to examine the effect of TbCDS knockout on the Kennedy Pathways. Whilst the major phospholipids PC and PE do not require CDP-DAG for their synthesis, CDP-DAG knockdown had a dramatic effect on phospholipid composition in TbCDS RNAi + tetracycline, including increased DAG, feeding into the Kennedy Pathway. It was therefore important to see how TbCDS knockout effected these key pathways.

In fact, there was little alteration to the distribution of choline-phosphate containing lipid species in the TbCDS knockout (Figure 4.27) with the four key PC series largely unaltered, as was seen in the TbCDS knockdown. This confirms the [³H]glycerol labelling results, and indicates that PC synthesis is tightly regulated separately from the CDP-DAG pathway. If PC is being utilised to make up any deficit in PS it might be expected that there would be some reduction in certain PC species. However, the quantity of PS in the cell is very minor compared to the quantity of PC and in this respect may make little impact on overall PC levels, which may be tightly regulated

anyway. The only slight difference in distribution of PC species an increase in the 888 m/z peak (884 m/z in SM) the most abundant species of which being C44:7 in the mutant and C44:9 in SM. This peak was only 0.15 of PC C40 in SM, but increased to 0.33 in the TbCDS CKO - tetracycline. C44 species have been found in bloodstream form and procyclic form PC species, but only in bloodstream form PS species (Richmond et al., 2010). This may give clues with respect to the dependence of the procyclic form, but not the bloodstream form on the synthesis of PE for PS synthesis by headgroup swapping via PSS, but this remains to be seen. As in the TbCDS knockdown, there is an increase in the saturation of choline containing lipid species in the TbCDS knockout.

A. SM



B. TbCDS CKO - tetracycline

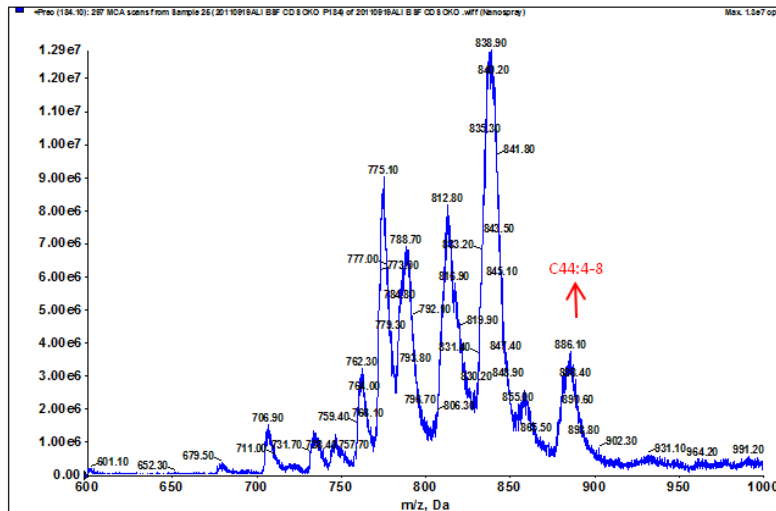


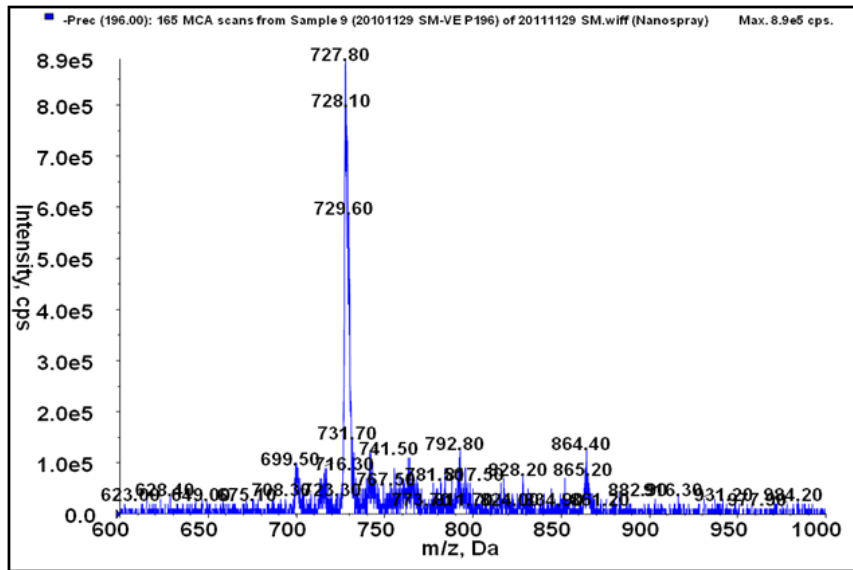
Figure 4.27. Mass spectrometric analyses of choline-phosphate containing phospholipids in SM and TbCDS CKO - tetracycline. Total lipids were analysed by ESI-MS in positive ion mode using parent-ion scanning of the collision induced fragment for phosphorylcholine at 184 m/z. A. Wild type single marker cells. B. BSF TbCDS CKO cells grown in the absence of tetracycline for 42 hours. For further annotation refer to Figure 4.8.

4.5.5.c.iv Ethanolamine Containing Lipids

Just as in the TbCDS knockdown, the TbCDS CKO scan of ethanolamine containing lipids shows very little change compared to that of the SM (Figure 4.28). [³H]glycerol showed a reduction in diacyl PE, whilst [³H]ethanolamine labelling showed no change, suggesting that diacyl PE was reduced but PE overall was not affected. Since the ES-MS scan shows that all species remain similarly distributed in the TbCDS CKO with respect to SM, an alternative explanation is required. The decrease in [³H]glycerol labelling could be indicative of a global decline in PE species that is being masked by headgroup exchange of [³H]ethanolamine into existing PE, as appears to be the case in PI. Upregulation of headgroup exchange could be an adaptation to disruption in cellular phospholipid balance in order to maintain the best possible pool of phospholipid in a limited supply of lipid. If PG is normally made via CDP-DAG, the large increase in its synthesis via PE and PS may be putting pressure on the PE pools, which may lead to such a global decline.

In terms of species specific alterations in PE, as in the knockdown the only obvious difference is the disappearance of a small peak of PE at 824.7 m/z, composed mostly of PE C42:3. The reasons for this are not clear, but since it is present in both the knockdown and the knockout, it must be significant. It may be that this DAG species is being utilised by PC as a response to changing lipid composition, and there is a very slight increase in the peak containing PC C42:3 from the choline-phosphate scan (Figure 4.27).

A. SM



B. TbCDS CKO -

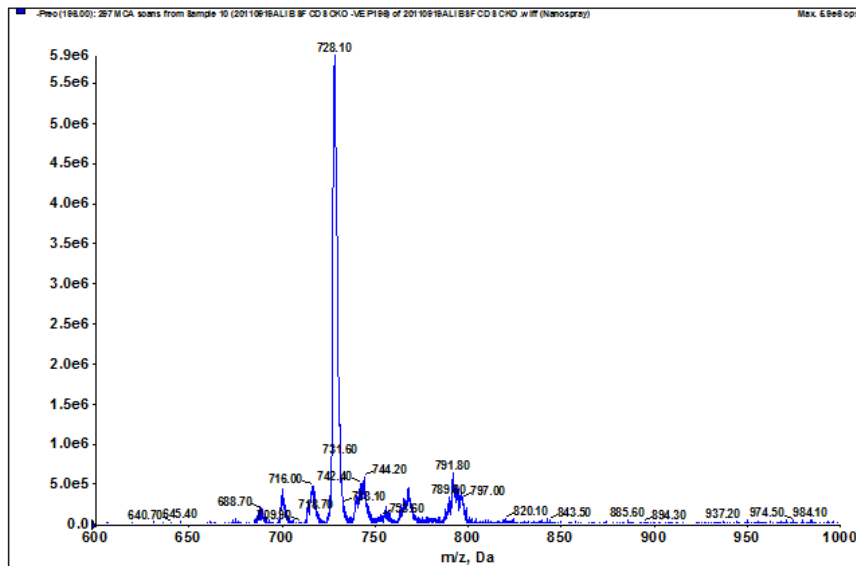


Figure 4.28. Mass spectrometric analyses of ethanolamine-phosphate containing phospholipids in SM and TbCDS CKO – tetracycline. Total lipids were analysed by ESI-MS/MS in negative ion mode using parent-ion scanning of the collision induced fragment for ethanolamine at 196 m/z . A. wild type single marker cells. B. BSF TbCDS CKO cells grown in the absence of tetracycline for 42 hours. For further annotation refer to Figure 4.8.

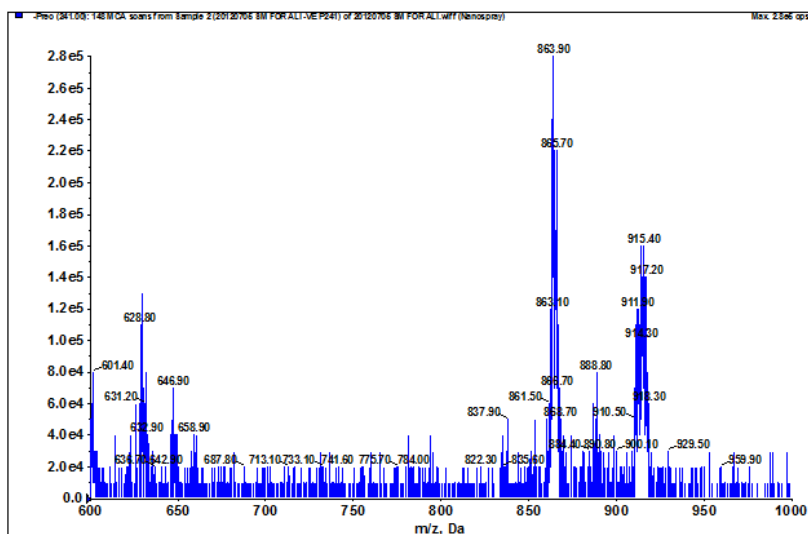
4.5.5.c.v Inositol Containing Lipids

The inositol-phosphate containing lipid spectra of TbCDS CKO - tetracycline shows almost identical changes to that of the TbCDS knockdown in comparison to SM (Figure 4.13). Whilst total PI cannot be quantified by this scan, it is known from [³H]glycerol labelling that the synthesis of these PI species are both decreased. There is also a relative decrease in the intensity of the peak pertaining to PI C36 compared to PI C40 from 1.78 in SM to 0.42 in TbCDS CKO - tetracycline (compared to 0.47 in TbCDS RNAi + tetracycline). Again, there is the appearance of a peak not normally present in bloodstream form *T. brucei*, possibly corresponding to IPC C34:0. As mentioned previously, the appearance of IPC may be a response to a metabolic slow down as seen in slender bloodstream form forms differentiating to stumpy forms (Sutterwala et al., 2008).

PI C36 species are thought to be preferentially incorporated into GlcNAc-PI for the initiation of the GPI synthesis pathway. These results suggest some segregation of PI species within subcellular compartments in *T. brucei*. In this bloodstream form TbCDS CKO, and in the bloodstream form TbCDS RNAi knockdown, there was a decrease in the C36 peak of PI relative to the PI C40 peak. This, combined with the decrease in the ability of the TbCDS CKO cells to synthesise GPI anchors, gives strong evidence that the pool of PI made from *de novo* synthesised inositol in the ER and destined for GPI anchors contains a higher proportion of C36:y PI. Similarly, the pool of PI synthesised from exogenous inositol in the Golgi, and utilised for bulk cellular PI may contain a higher proportion of C40:y PI. A differential effect of TbCDS activity reduction on the two pathways may be not be unexpected since flux through the ER pathways is likely much higher than that through the Golgi pathway, even if the actual pool of PI for GPI anchors is very small. Since CDP-DAG is clearly required in both the Golgi and the ER it is possible that like PIS, TbCDS is also dually localised.

Alternatively, though less likely, the pool of Golgi PI may acquire some lipid precursor from another pathway, for example by the presence of an alternate enzyme which shows little or no homology to other known CDS enzymes. Since it seems likely from phylogenetic analysis that *T. brucei* formerly had at least one CDS enzyme of prokaryotic origin (as discussed in Chapter 3) it is possible that another horizontally transferred enzyme exists which does not contain a classic phosphatidate cytidyltransferase pattern or cytidyltransferase domain.

A. SM



B. TbCDS CKO - tetracycline

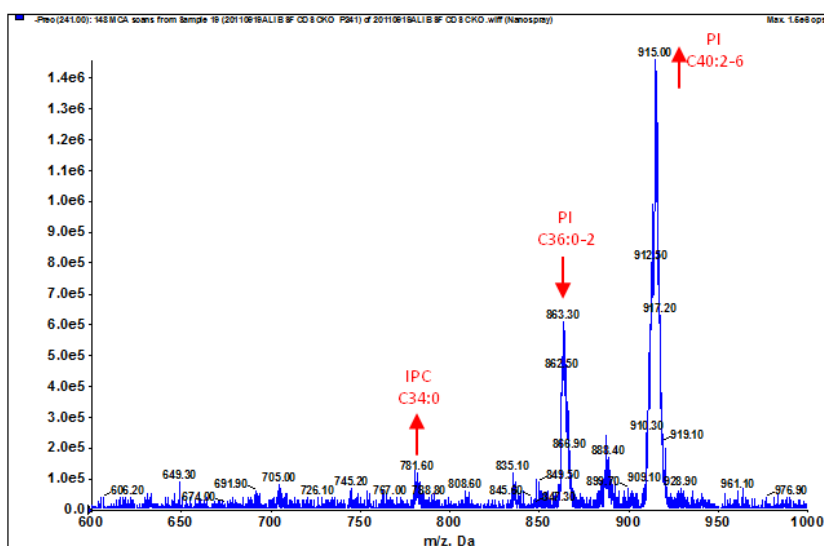


Figure 4.29. Mass spectrometric analyses of inositol-phosphate containing phospholipids from SM and TbCDS CKO - tetracycline. Total lipids were analysed by ESI-MS in negative ion mode using parent-ion scanning of the collision induced fragment at 241 m/z. A. Wild type single marker cells. B. BSF TbCDS CKO cells grown in the absence of tetracycline for 42 hours. For further annotation refer to Figure 4.8.

It is not known whether the *T. vivax* prokaryotic-like gene is expressed or functional, and if it is active, it may not contain a complete phosphatidate cytidyltransferase pattern and therefore may act in a different way to known CDSs. If further mutation

has occurred within a potential second, prokaryotic-like *T. brucei* CDS, it would not be easy to identify.

In some mammals it has been suggested that there is an alternative pool of PI for PIP signalling, that resides specifically in highly mobile membrane sub compartment termed the PIPERosome (Kim et al., 2011). Since results presented here indicate a role for TbCDS in the regulation of kinetoplast cell division via CDP-DAG derived PIPs, it would not be unreasonable to suggest there may be a third pool of PI present in such a compartment or organelle within *T. brucei*.

4.5.5.c.vi Serine Containing Lipids

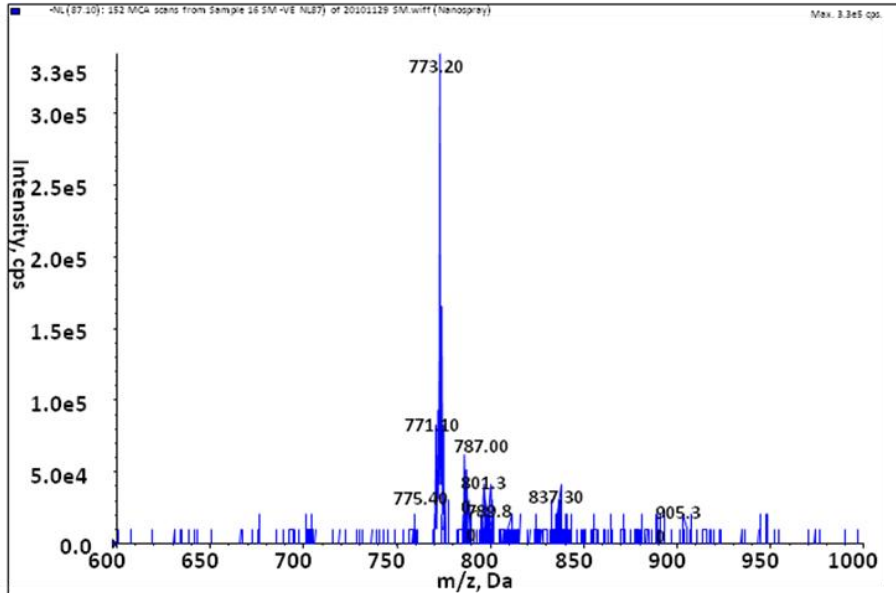
Figure 4.31 shows the spectrum of the scan for serine-phosphate containing phospholipid species in SM and TbCDS CKO. The scan is not of a very high intensity, but as in the TbCDS RNAi knockdown, there is a large change in the relative abundance of different PS species. From the [³H]glycerol labelling it was hard to tell if synthesis of PS was decreased, as in the solvent system used it co-migrates with PI and therefore a large increase in PI could mask any changes in PS, which is less abundant than PI and therefore has a lower signal.

Just as in the knockdown, the a-C36:y series still has the greatest intensity, but there is a significant increase in C38:3-4 from not above background in SM to 0.48 of the PS a-C36 in TbCDS CKO - tetracycline. These results show the reduction in TbCDS activity has a dramatic effect on the relative abundance of the PS species. Whilst an alteration of the PS profile as a result of TbCDS knockout may appear to indicate a role for CDP-DAG in the synthesis of PS, this alteration could also be due to an increase of PS requirement to synthesise PG in the absence of CDP-DAG. It has previously been suggested here that an increase in PG in the TbCDS knockdown and knockout may be due to a novel synthesis pathway, for example from PS via the enzyme PGPS.

If this is the case, it may be that CDP-DAG is not in fact an important route of synthesis for PS, as was suggested of the procyclic form by Signorell and colleagues (Signorell et al., 2008). The alteration that is seen in PS species could be a secondary affect of a decrease in PG synthesis via CDP-DAG resulting in the utilisation of the PS pool to compensate for reduced PG. This is supported by the fact that the PG species that are increased (PG a-C36:2 and C40:4) are also key PS species. To confirm that this hypothesis also fits the TbCDS knockout phenotype, it was necessary to look

more closely at the PA and PG species in the TbCDS knockout cells in the absence of tetracycline.

A. SM



B. TbCDS CKO - tetracycline

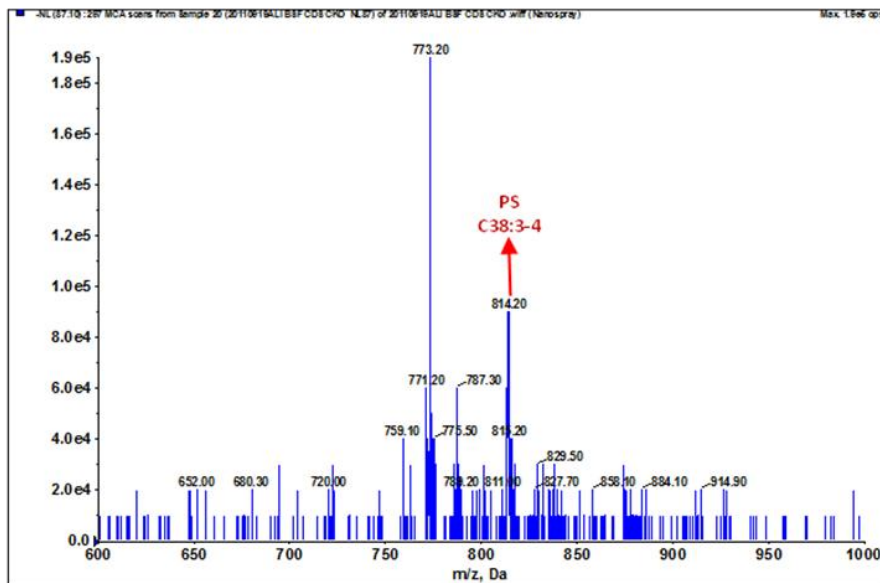


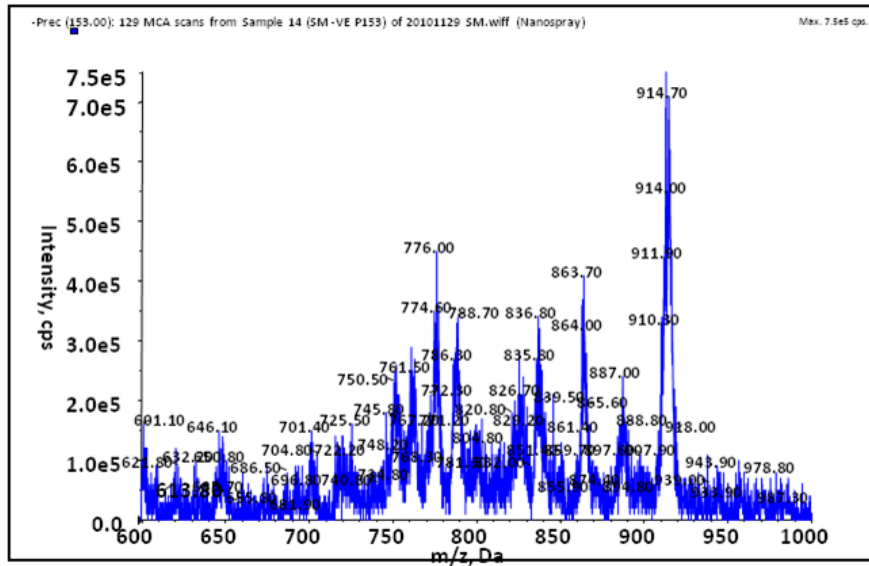
Figure 4.30. Mass spectrometric analyses of serine-containing phospholipids from SM and TbCDS CKO tetracycline. Total lipids were analysed by ESI-MS in negative ion mode using neutral loss scanning for 87 m/z. A. Wild type single marker cells. B. BSF TbCDS CKO cells grown in the absence of tetracycline for 42 hours. For further information see Figure 4.8.

4.5.5.c.vii PA and PG

ES-MS showed surprising results with respect to PA and PG species in the TbCDS RNAi knockdown. Rather than the predicted increase in PA and decrease in PG, quite the opposite was observed (Figure 4.14). Examination of the lipid by precursor ion scanning for p153 in TbCDS CKO showed similar results (Figure 4.14). The lack of alteration in PA levels is perhaps not unexpected since it is probably not allowed to accumulate and is dephosphorylated to DAG. However, the lack of a decrease in PG levels was extremely unexpected. In fact, the majority of PG species appear to have increased relative to the other peaks in the spectra, which was supported by [³H]glycerol labelling.

As in the TbCDS RNAi knockdown, the largest increases were seen in PG a-C36:2, PG C40:4 and PG C36:1 (Figure 4.31) from 0.33, 0.6, 0.43 and 0.28 of PI C40 in SM to 1, 2.73, 2.23 and 1.9 of PI C40 in TbCDS CKO - tetracycline, respectively. This gives further evidence for either an alternative CDS enzyme, or pathway for the synthesis of PG that does not rely on CDP-DAG. If PG is being made via PS, the same species may be expected to be altered/changed in both PS and PG. The PG species that are increased the most are PG a-36:2 and PG 40:4. PS a-C36:2 is a major species, and seems to be increased in TbCDS CKO, whilst PS C40 is difficult to see in the available scans but may also be increased. However, acyl remodelling of PG is known to occur (Yang et al., 2004), so the source of PG may not have the same aryl chains as the resultant PG species.

A. SM



B. TbCDS CKO - tetracycline

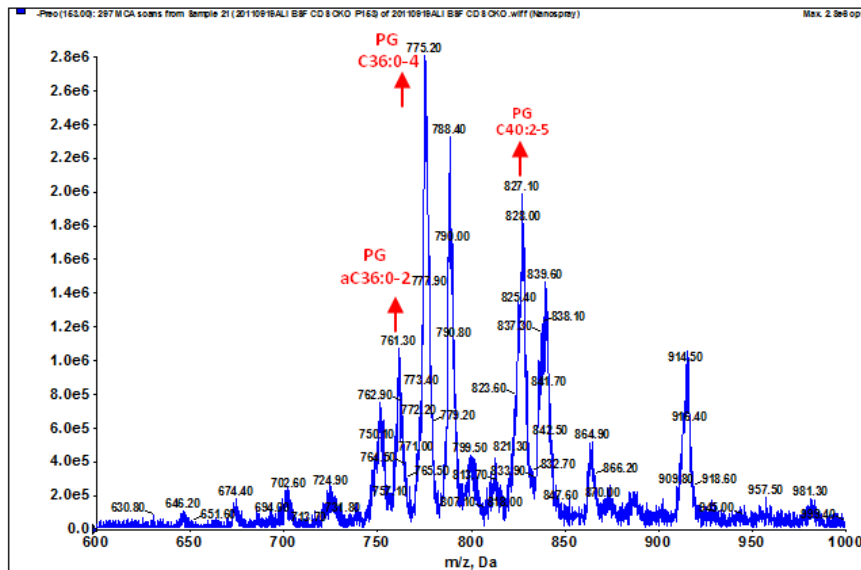


Figure 4.31. Mass spectrometric analyses of glycerophospholipids from SM and TbCDS CKO – tetracycline. Total lipids were analysed by ESI-MS in negative ion mode using precursor ion scanning for the collision induced fragment for glycerol-phosphate at 153 m/z. A. Wild type single marker cells. B. BSF TbCDS CKO cells grown in the absence of tetracycline for 42 hours. For further annotation refer to Figure 4.8.

4.6 Summary and Conclusions

Following confirmation of an open reading frame in the *T. brucei* genome which encoded CDS activity, the aim of this chapter was to show that this open reading frame expressed TbCDS activity in *T. brucei*, and to determine if it was essential in bloodstream form parasite. A secondary aim of this chapter was to examine the contribution of CDP-DAG produced by TbCDS to the synthesis of downstream phospholipids, with the hope of further elucidating the interplay between pathways of phospholipid synthesis in this organism.

Both expression of the TbCDS open reading frame, and the presence of CDS activity in *T. brucei* bloodstream form membranes has now been confirmed. The bloodstream form of the parasite is the stage which would need to be targeted by therapeutics, so showing expression and function of TbCDS in bloodstream form is essential to the parasite validates it as a drug target.

To begin investigation into the function and essentiality of TbCDS in *T. brucei*, a TbCDS RNAi knockdown cell line was created. Induction of TbCDS RNAi by the addition of tetracycline caused a growth defect which usually resulted in death by 200 hours.

This growth defect coincided with a decline in protein and total lipid synthesis, and a disproportionate decrease in the incorporation of [³H]glycerol into glycerolipid. Microscopy of these knockdown cells revealed somewhat rough, buckled cell surfaces which may be a symptom of a less flexible plasma membrane, possibly due to a disruption in the glycerophospholipid composition.

Biochemical phenotyping of the cells threw up a variety of unexpected results. Incorporation of water soluble radiolabelled precursors into phospholipids PE, PS and PI was largely unaffected by the knockdown of CDP-DAG despite a decrease in the incorporation of [³H]glycerol. These results suggest that an increase in headgroup swapping into existing lipid is masking any change in the *de novo* synthesis. This may be an adaptation to changing phospholipid composition which helps to maintain dynamic flow of stable lipids. As well as a decrease in [³H]glycerol incorporation into PI, incorporation of mannose into GPI anchors was dramatically reduced, suggesting that the cells were deficient in the pool of PI for GPI anchors, which cannot easily be labelled by exogenous inositol.

ES-MS showed the increase of certain species of neutral lipids and PG. The increase in neutral lipids could be a way in which cells deal with the accumulation of PA, but the increase in PG species was unexpected and suggested it was either extremely important to the cell or it was made by an alternative mechanism.

TbCDS RNAi knockdown caused differences in the lipid profile of PS species suggesting that CDP-DAG may contribute to its synthesis. This contradicts evidence seen in the procyclic form by Signorell and colleagues (Signorell et al., 2008) who suggested PS synthesis only occurred via headgroup exchange from PE. CDP-DAG involvement in PS synthesis has been indicated in bloodstream form by Gibellini and colleagues who saw no difference in the amount or profile of PS species when PE synthesis was disrupted. The utilisation of PC by the bloodstream form, but not the procyclic form PSS may explain all these results. Further investigation suggested that PG may be synthesised from PS via PGPS, which would explain the change in the PS pool without involving CDP-DAG as a significant source of PS, as indicated by the work of Signorell and colleagues (2008).

Due to the propensity of the TbCDS RNAi knockdown to revert, along with the knowledge that only 10% of wild type CDP-DAG levels are sufficient to maintain normal growth in yeast (Shen et al., 1996), a complete TbCDS conditional knockout was created. The TbCDS CKO had a significant growth defect and started to die after 48 hours. After 100 hours no cells were countable. However, after 120 hours revertant growth appeared in the flask. It was shown that this was due to cells breaking tetracycline control as western blot showed that the cells were again producing the HA-tagged TbCDS in the absence of tetracycline. Such revertance is characteristic of many essential genes in *T. brucei*.

This cell line showed a significant morphological phenotype, with cells stalling before abscission but after the appearance of a furrow. Unusually, these cells had two nuclei but only one kinetoplast, despite the fact they had succeeded in replicating their flagellum. This mutant is rare, but has been seen before in a knockdown of a protein kinase stimulating protein, Mob1, which was postulated to be part of a kinetoplast replication/division checkpoint in *T. brucei* (Hammarton et al., 2005). Since a link has been established between PIPs and protein kinase regulation (Franke et al., 1997) there is a possibility that the knockout of CDP-DAG is disrupting the PIP signalling pathway, which is disrupting kinetoplast replication/segregation.

The TbCDS CKO cell line had a remarkably similar biochemical phenotype to the TbCDS knockdown. *In vivo* radiolabelling showed less [³H]glycerol labelled PI but an equal amount of [³H]inositol labelled [³H]PI to the SM suggesting that whilst *de novo* synthesis was reduced, headgroup exchange of inositol into existing PI was increased. [³H]glucose incorporation into [³H]PI was also reduced, however, suggesting that in the ER, headgroup exchange of *de novo* synthesised inositol is not able to mask the decrease in PI, indicating that it may be more severely affected. Indeed, ES-MS showed the C36 PI pool which is thought to be used for GPI anchor synthesis to be further decreased relative to the C40 pool, and a cell free system assay for the synthesis of GPI anchors showed that the TbCDS CKO trypanosomes were severely hindered in their ability to make GPI anchors. This could be due to the effect of TbCDS knockout depleting PI in the correct subcellular location. This differential effect on ER localised PI for GPI anchors is likely due to the high flux that occurs through this pathway. Such high flux would mean that it utilises the declining pool of CDP-DAG quickly, and indicates that there may be two separately compartmentalised pools of CDP-DAG. As in the TbCDS RNAi but more dramatically, DAG and TAG species were increased, along with several species of PG. In both these cases the phenotype was more dramatic than that seen in the TbCDS RNAi knockdown cell line and could not only be seen by ES-MS but also by *in vivo* radiolabelling. The increase in DAG and TAG can probably be explained by a dephosphorylation of built up TbCDS substrate PA in order to make it safer for the cell. The greater increase of PG species in TbCDS CKO along with a similar disruption of the PS pool gave further evidence PS can be used as an alternative source of PG via PGPS.

Collectively, these results show that TbCDS is essential for the production of PI which is required for GPI anchors and may also be required for PIP signalling. Surprisingly, TbCDS is not essential for the production of PG, and an additional, alternative mechanism is proposed for its synthesis, e.g. from PS via PGPS. The pool of PS in *T. brucei* was altered due to depletion of TbCDS activity. However this does not give evidence that PS can be synthesised via CDP-DAG, since these results could also be explained if PS is being used as a source of PG in the absence of CDP-DAG.

Chapter 5 - Cytidine Diphosphate Diacylglycerol Synthase in Procyclic Form *Trypanosoma brucei*

5.1 Introduction

The previous chapter showed TbCDS to be essential in bloodstream form *T. brucei*, which validates it as a drug target against human and animal African Trypanosomiasis. Additionally, examination of the morphological and biochemical phenotype of the TbCDS knockdown and knockout provided information that has furthered the knowledge of lipid metabolism in the bloodstream form life cycle stage of *T. brucei*. The aim of this chapter was to assess the role of TbCDS in procyclic form *T. brucei* and in particular to see how it differs from that in the bloodstream form.

A decrease in TbCDS expression in bloodstream form *T. brucei* resulted in a cell cycle stall after the replication of the flagellum and formation of a furrow, but before the replication/segregation of the kinetoplast. This clearly indicated some problem with the kinetoplast in the cell cycle and it was proposed this was maybe due to depletion of CDP-DAG causing defects in PIPs for signalling or GPI anchor formation, thus limiting the VSG on the cell surface and causing a cell cycle stall. The cell cycle is known to differ in procyclic form *T. brucei* and therefore such CDP-DAG depletion may have a different effect. The most profound effect that depletion of CDP-DAG synthesis had on bloodstream form *T. brucei* was a decrease of PI utilised for GPI anchor biosynthesis. Procyclic form *T. brucei* do not have such a high demand for GPI anchors as they were not shown to be essential (Guther et al., 2006), so the effect of a decrease in TbCDS activity may be different. Surprisingly, PG appeared to be increased when TbCDS activity was decreased, indicating there may be an alternative pathway for PG synthesis that does not rely exclusively upon CDP-DAG. However, since the mitochondrion is far more important in the procyclic form, this likely means increased demand for the mitochondrial phospholipids PG and CL and any

alternative route of PG synthesis may not be able to compensate for this higher demand. Finally, the depletion of CDP-DAG synthesis in bloodstream form *T. brucei* did not seem to affect the amount of PS synthesised, however ES-MS analysis suggested that the abundance of various PS species had changed. This indicated that the different PS species may be made via PSS by headgroup exchange with PE rather than directly from CDP-DAG, but that an increase in base headgroup exchange from PE is able to compensate for a loss in CDP-DAG and serine. Alternatively, PS species abundance may be altered due to utilisation of specific species of PS for PG synthesis. In procyclic form, however, there is evidence of a complete dependence on headgroup exchange from PE for PS synthesis (Signorell et al., 2008). If CDP-DAG is not required for the synthesis of PS in procyclic form *T. brucei* its depletion might be expected to have no effect on the amount or distribution of different PS species, meaning any difference may be due to its utilisation for PG.

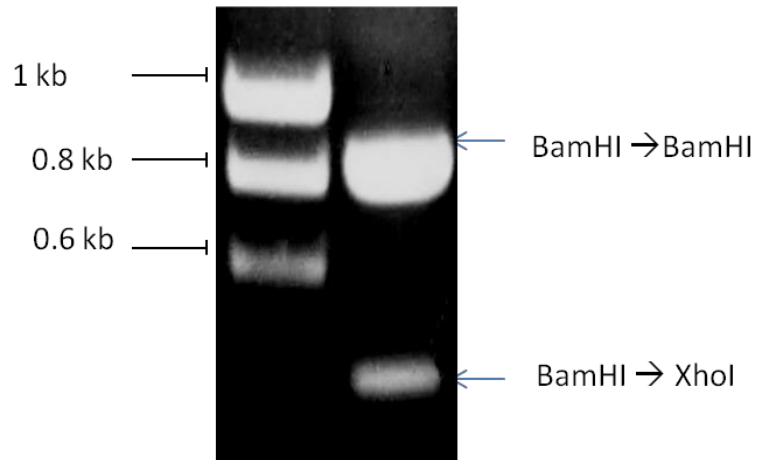
Since it seems likely that TbCDS has some significantly different roles in procyclic form *T. brucei*, depletion of its activity in this cell type may help to understand differences in lipid metabolism and lipid usages between the insect and the mammalian form of this deadly parasite.

5.2 RNAi of TbCDS in Procyclic Form *T. brucei*

Expression of TbCDS has previously been shown in procyclic form *T. brucei* (Figure 4.1), so the next step of this investigation was to see what would happen when this expression was reduced utilising an RNAi construct.

The previously obtained 400 bp TbCDS BamHI-XhoI fragment (Figure 5.1, A) was ligated into the p2T7-177 vector (Figure 5.1, B.). Like p2T7, this plasmid contains two opposing tetracycline controlled T7 polymerases which produce double stranded RNA from the DNA cloned into the multiple cloning site to induce the cell's RNAi machinery. This construct, however, is specifically targeted to the mini-chromosome DNA and is selectable with phleomycin.

A.



B.

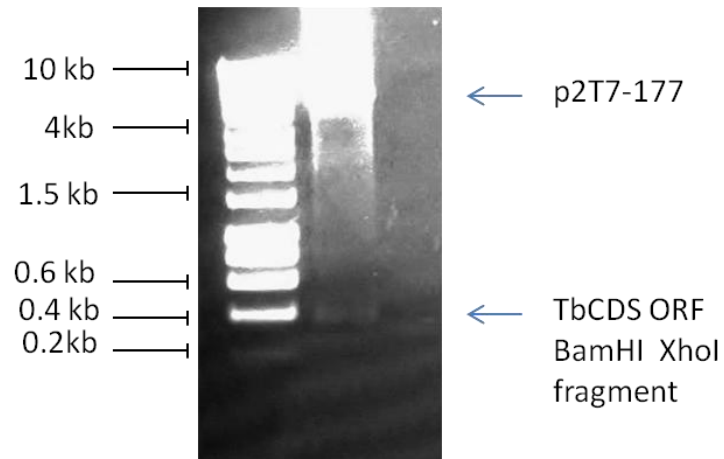


Figure 5.1. Construction of TbCDS p2T7-177 vector. (A) A TbCDS ORF PCR product amplified by the primers CDS pET32b F and R (Table 2.1) The CDS pET32b F and R primers added BamHI and XhoI restriction sites to the 5' and 3' end of the open reading frame, respectively. The TbCDS ORF also contains an internal BamHI site 800 bp downstream of the start codon so that when the PCR product was BamHI XhoI digested, two fragments were produced, one 800 bp and one 400 bp long. (B). The 400 bp BamHI XhoI fragment was then cloned into the RNAi vector p2T7-177.

The plasmid was linearised with NotI and transformed into procyclic form *T. brucei* as described in Chapter 2. Positive transformants were selected using phleomycin and TbCDS p2T7-177 clones were obtained. The TbCDS p2T7-177 containing clone with the strongest response to the addition of tetracycline was used for cell counts which were performed in the presence and absence of tetracycline.

Figure 5.2 shows growth curves for TbCDS RNAi in procyclic forms. In the first experiment, the RNAi induced cells showed a similar growth pattern to that observed in the bloodstream form, but on a slower time scale.

This is not surprising as procyclic forms have a longer doubling time. Growth appeared normal for the first 48 hours, after which there was a significant growth defect. However, cells did not die and continued at a slow or stable level of growth for more than two weeks. After about two weeks the cells started to die, and no viable cells were countable after 20 days. Repetition of the TbCDS RNAi cell counts (Figure 5.2, C-D) showed a similar growth phenotype for the first ten days, however after this time point growth seemed to revert to normal levels, possibly suggesting revertant growth.

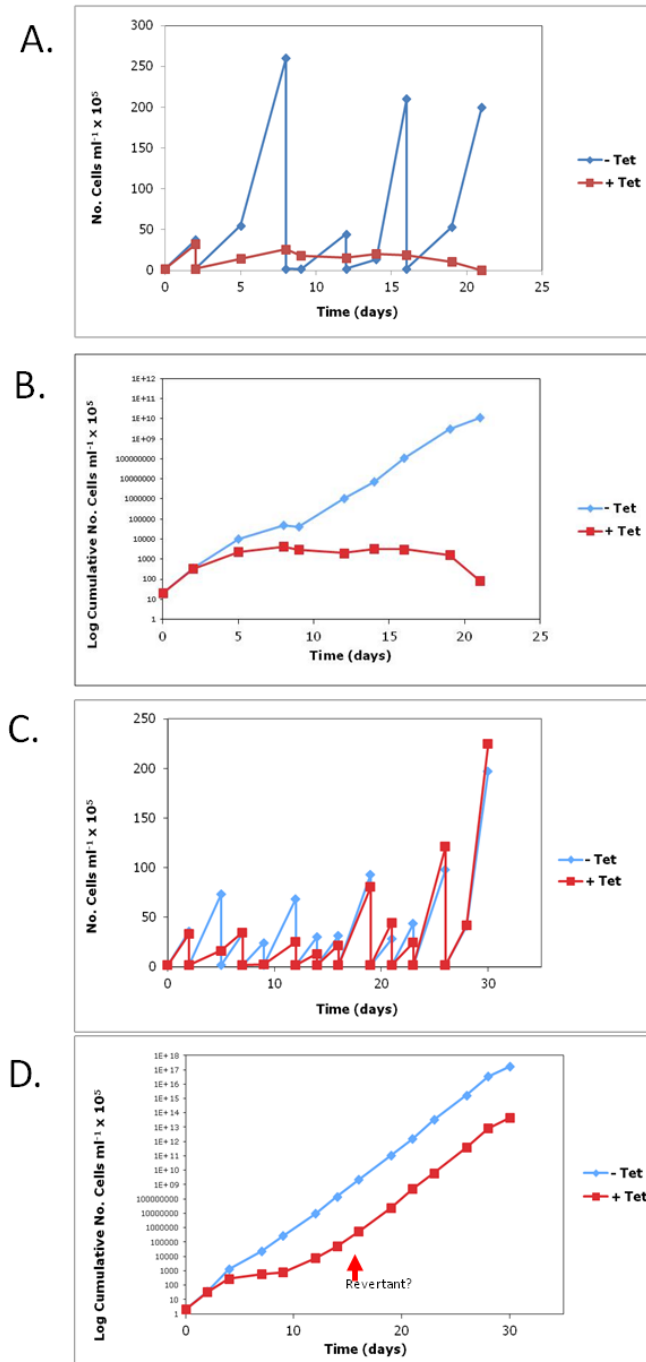


Figure 5.2. Essentiality of TbCDS in procyclic form *T. brucei*. (A) PCF TbCDS p2T7-177 RNAi cell counts 1 (A) Actual number of cells per ml of culture $\times 10^5$ after number of days cultured in the presence (+ Tet = induction of TbCDS RNAi) or absence (- Tet) of tetracycline. (B) Graph showing log cumulative number of cells over time in the presence and absence of tetracycline. (C-D) Repeat of PCF TbCDS RNAi cell counts – graph of repeat experiment showing (C) actual number of cells over time and (D) log cumulative number of cells over time.

5.2.1 Confirmation of Construct Integration

As in the bloodstream form TbCDS RNAi cell line, confirmation of the p2T7-177 copy of TbCDS integration into the genomic locus was attempted using southern blot analysis. Again, as in bloodstream form, all attempts to probe southern blots with both DIG-labelled and [³²P] labelled probes in a variety of conditions were unsuccessful, despite positive controls showing there was no problem with the protocols or reagents and PCR confirming the presence of the TbCDS and BLE ORF (Figure 5.3).

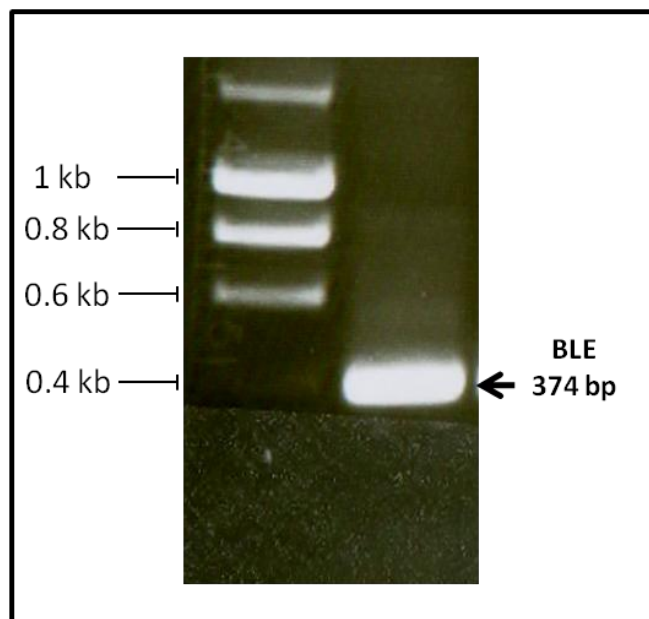


Figure 5.3. Presence of phleomycin resistance gene (BLE) from TbCDS p2T7-177 RNAi construct in procyclic form *T. brucei* genomic DNA. 1% agarose gel stained with ethidium bromide showing. Sequences for primers used are given in Table 2.1.

As before, the phleomycin resistance, along with detection of the BLE ORF by PCR were considered to be sufficient evidence of construct integration, and the morphological and biochemical phenotyping of the procyclic form TbCDS RNAi cell line was continued.

5.2.2 Morphological Phenotyping of Procytic Form TbCDS RNAi Cell line

Cells undergoing procytic form TbCDS RNAi at various points after the addition of tetracycline were carefully harvested, fixed and DAPI stained as previously described in order to closely examine the morphological phenotype. Whilst the growth phenotype of the TbCDS RNAi induced cells was not reproducible after about 14 days, something consistently seen was the presence of more than one flagellum, often with the daughter flagellum being detached (Figure 5.4). This phenotype was seen in some cells as early as 48 hours after tetracycline induction, but was present in the majority of the cells after around 14 days. In most of these mutants, the flagella appeared to be attached at either end but to loop from the membrane around the middle (Figures 5.4, B, images 1 and 2). Whilst in other cases the flagellum was only attached at one end (Figures 5.4, B, images 3 and 4). Other common mutations seen were in cell division, for example misplacement of the cleavage furrow resulting in asymmetric cell division (Figures 5.4, B, images 5-8). The number of DNA containing bodies in these cells varied, some exhibiting the normal 1N1K phenotype, but many exhibiting multinucleate phenotypes. These multinucleate cells were unusual in that they appeared to contain more nuclei than kinetoplasts, with others yet appearing to be akinetoplastic. This suggests several rounds of cell-cycle had occurred without correct kinetoplast replication/segregation, resulting in fragmentation and loss of the kinetoplast. In the bloodstream form TbCDS knockout, the cells appeared to stall after the replication of the flagellum and the formation of a cleavage furrow, but without replication of the kinetoplast (Figure 4.6). In both the bloodstream form and procytic form mutants there is clearly a problem in kinetoplast replication/segregation, but the morphological ramifications are different i.e. more striking in the procytic form due to the detached flagella. Many previous RNAi knockdowns of varying proteins have shown different cell division mutants in bloodstream form than in procytic form (Reviewed by Hammarton et al. (2007b)). For example, procytic form cells appear to lack a mitosis to cytokinesis checkpoint so inhibition of mitosis does not inhibit cytokinesis, which results in a daughter cell with one nucleus containing replicated DNA and one kinetoplast, and the other daughter cell containing only a kinetoplast and no nucleus (a zoid). In bloodstream form this does not happen and instead failure of mitosis prevents cytokinesis, but cytokinesis failure does not prevent further rounds of organelle replication, resulting in cells

with multiple nuclei and kinetoplastids (Hammarton et al., 2005, Li and Wang, 2003, Ploubidou et al., 1999). These examples show precedence for the differences in cell cycle mutants between bloodstream form and procyclic form cells. In an RNAi induced mutant of the flagellar protein FLA1, multiple nuclei were observed (sometimes more than 10) making the kinetoplasts difficult to count, however from the images it does appear possible that the number of kinetoplasts is lower than that of the nuclei (LaCount et al., 2002). In procyclic form, the segregation of the kinetoplast requires microtubule associated movement (Robinson and Gull, 1991), and the kinetoplast is tethered to the basal body of the flagellum through the tripartite attachment complex (Ogbadoyi et al., 2003). It is therefore difficult to determine how the flagella can replicate without also replicating the kinetoplast. Such a phenotype may indicate a problem with the tripartite attachment complex resulting in detachment of the kinetoplastid from the basal body. Previously, in an RNAi induced knockdown of alpha-tubulin detached flagella were shown to be a symptom of incorrect assembly of microtubules forming the flagellar attachment zone (Basal, 1998).

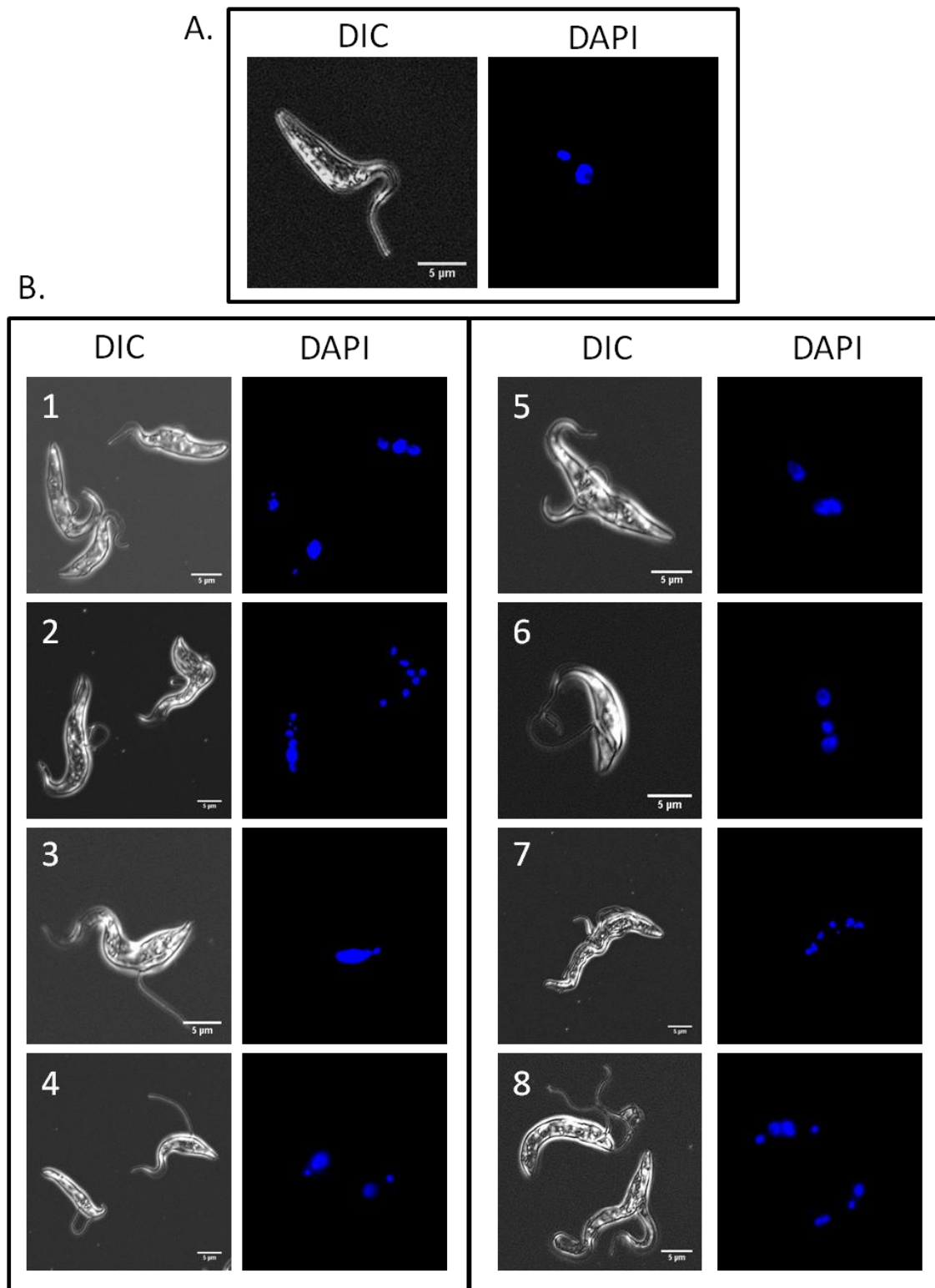


Figure 5.4. Knockdown of TbCDS in PCF cells showing detached flagella and cell-cycle stalled mutants. Cells were then fixed and stained with DAPI. (A) Morphology of DM cell. (B) morphology and DNA containing bodies of TbCDS RNAi 14 days + tetracycline cells.

It cannot be ruled out that enlarged, non-segregated kinetoplasts are being mistaken for nuclei. In procyclic form, inhibition of p166 - a protein of the tripartite attachment complex involved in kinetoplastid segregation - leads to kinetoplastids replicating but failing to segregate up to ten times, creating a kinetoplast structure far out sizing that of the nucleus (Zhao et al., 2008). In a conditional knockout of bloodstream form mitochondrial acyl carrier protein, a defect was seen where kinetoplast DNA replicated but did not segregate correctly. In the extreme case one daughter cell inherited the double sized kinetoplast whilst the other contained no kinetoplast (Clayton et al., 2011). In a procyclic form knockout of serine palmitoyl transferase, segregation of the kinetoplast was delayed but the flagella replicated. The new daughter flagellum was often detached and usually came from the same flagellar pocket as the parent flagella suggesting that the basal body and flagella pocket, like the kinetoplast, had replicated but not segregated (Fridberg et al., 2008). In this case, Fridberg and colleagues propose a role of sphingoid bases as second messengers may explain the failure of the kinetoplast to segregate, however, Clayton and colleagues suggest the perturbation in segregation seen in the acyl carrier protein knockdown was due to a physical interaction between the tripartite attachment complex and mitochondrial phospholipid (Fridberg et al., 2008, Clayton et al., 2011).

Detached flagella have been seen in *T. brucei* as a morphological phenotype of a number of mutants, particularly in knockdowns of flagellar associated proteins (Basal, 1998, LaCount et al., 2000, LaCount et al., 2002, Ralston et al., 2006, Ralston and Hill, 2006, Selvapandiyan et al., 2007). Most notably, however, is the presence of this phenotype in the knockdown of a PI-4-kinase. Knockdown of this protein showed it to be essential, and in addition to detachment of the daughter flagellum, cells had abnormal organelle positioning and a twisted morphology (Rodgers et al., 2007). A link between PIP signalling and flagellar attachment may explain the phenotype seen in these procyclic form TbCDS RNAi knockdowns due to depletion of CDP-DAG meaning the PI cycle is not functional, which would give evidence of the importance of CDP-DAG in PI signalling in both bloodstream form and especially procyclic form *T. brucei*.

5.2.3 Mitochondrial Functioning in Procyclic Form TbCDS RNAi Cell line

Since CDP-DAG is a precursor of CL, an important mitochondrial phospholipid, and IPC which is also thought to have a role in the mitochondrion, one reason for the slowed growth of the procyclics may be a loss of mitochondrial membrane potential and/or function. In order to study this, cells were stained with Mitotracker red. Mitotracker red stain is only taken up by mitochondria with an active membrane potential, so can be used to assess potential health and functionality of the mitochondrion. Exposure was maintained at 500 ms for all slides so they could be directly compared.

Mitotracker red stained the uninduced procyclic form TbCDS RNAi cells to reveal a branched, tubular structure corresponding to the mitochondrion in this life cycle stage (Figures 5.5 and 5.6 panel A). Seven days after the induction of TbCDS RNAi in the procyclic form cell line, the staining of some procyclic form TbCDS RNAi mitochondria looked similar to that of the double marker, though perhaps a slight decrease in mitochondrial staining and increase in punctuate staining. The knockdown clearly does not have an immediate dramatic effect on the mitochondrion; however there is the suggestion that the membrane potential is beginning to be affected compared with that of double markers (Figure 5.5, panel B, row 2).

By 14 days (Figure 5.6) - the stage at which the majority of cells have detached flagella - punctuate staining of the mitochondrion is far more pronounced. Similar phenotypes have been observed in *T. brucei* cells deficient in PE (Gibellini et al., 2009, Guler et al., 2008) PS, PI and CL (Serricchio and Buetikofer, 2011).

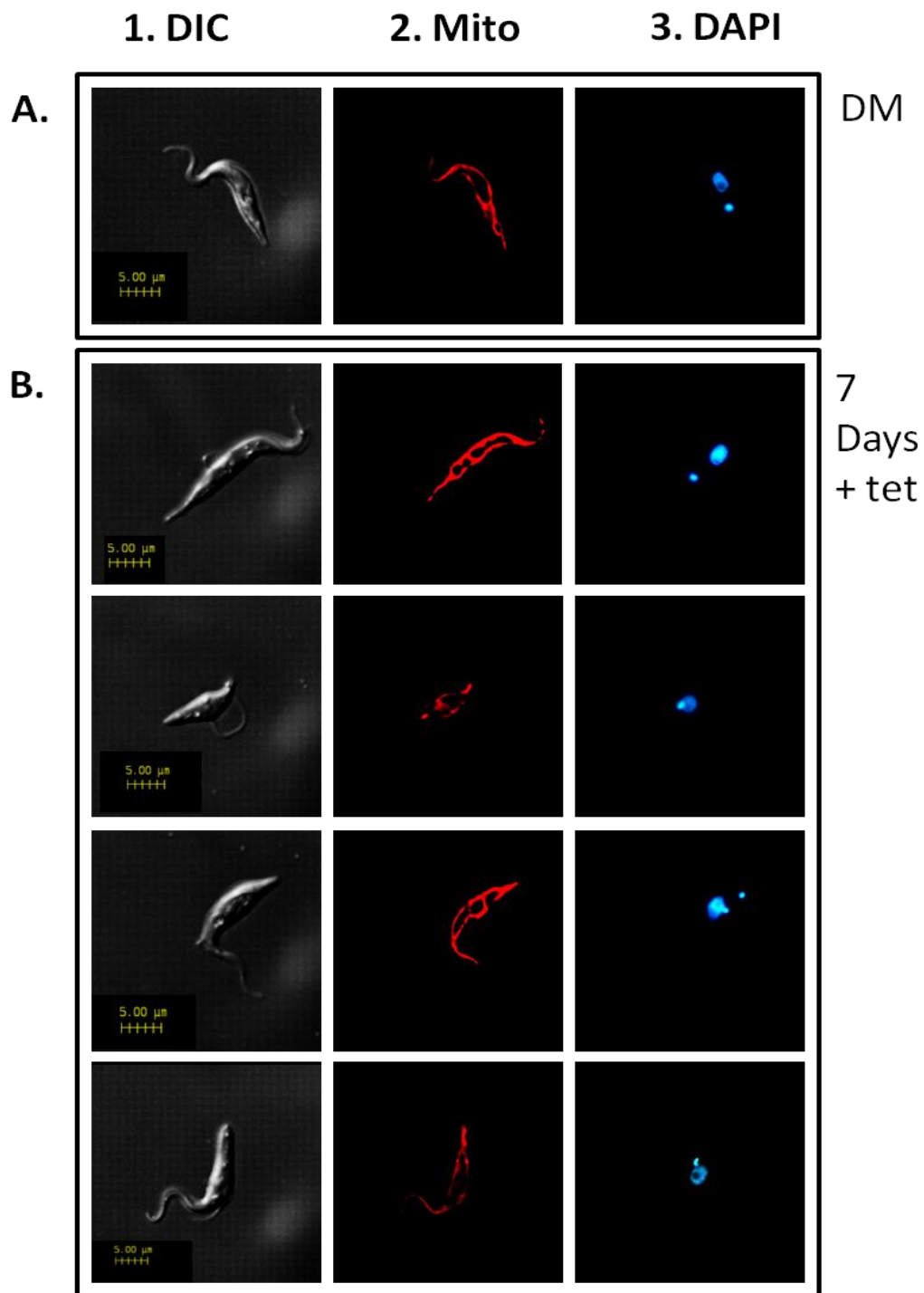


Figure 5.5. Effect of TbCDS knockdown in PCF cells on mitochondrial membrane potential 7 days + tetracycline. Mitotracker red was used to stain live cells prior to fixation. Cells were then fixed and counterstained with DAPI. (A) Morphology DM cell. (B) Morphology of TbCDS RNAi 7 days + tetracycline cells. Panel 1 – MIP rendered DIC image of fixed cells, panel 2 – mitotracker staining – Mitotracker fluorescence images were collected with the same acquisition time of 500 ms, panel 3. DAPI staining .

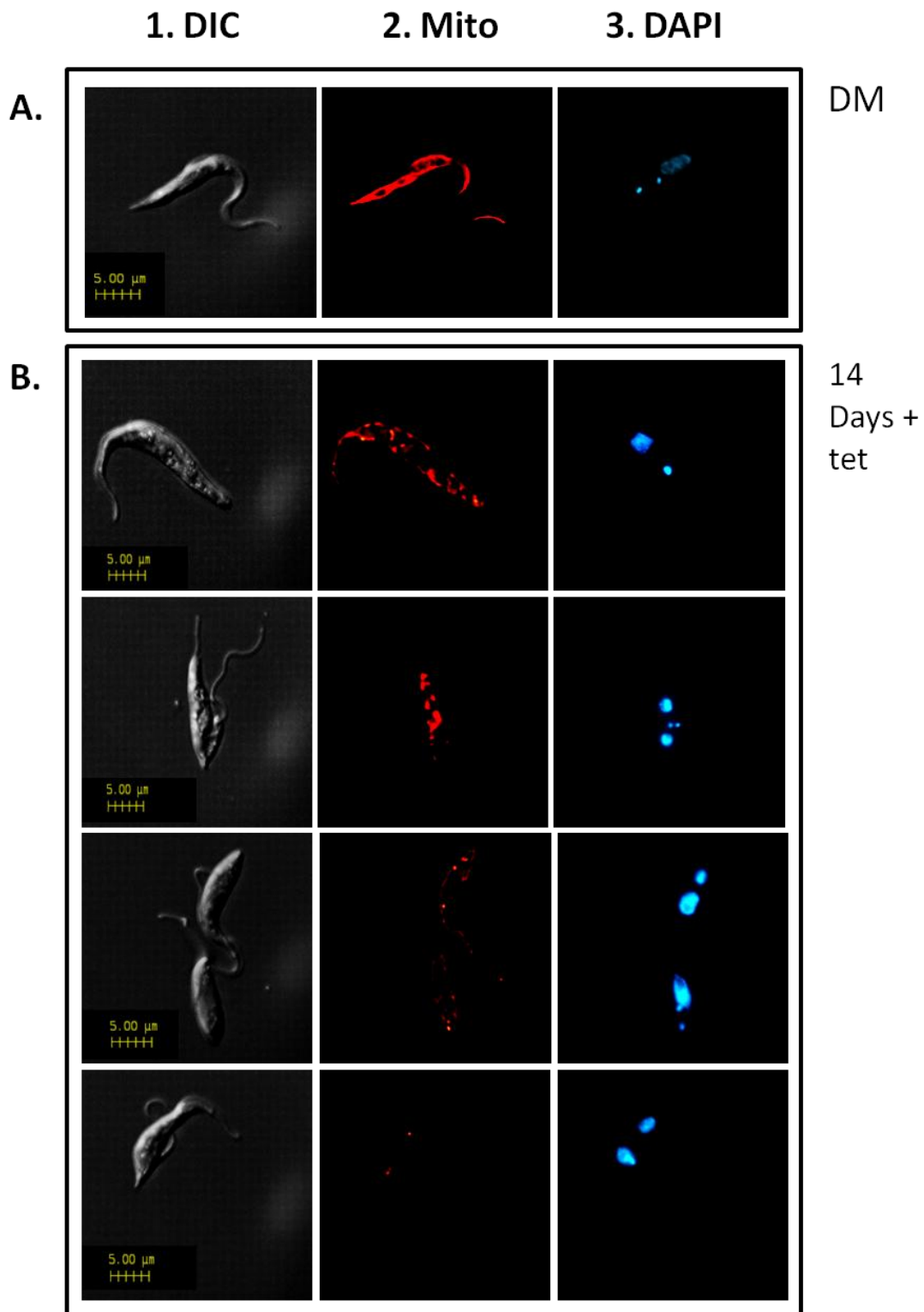


Figure 5.6. Knockdown of TbCDS in PCF cells results loss of mitochondrial membrane potential after 14 days plus tetracycline. Mitotracker red was used to stain live cells prior to fixation. Cells were then fixed and counterstained with DAPI. (A) Morphology of DM cell. (B) Morphology of TbCDS RNAi 14 days + tetracycline. Panel 1 – MIP rendered DIC image of fixed cells, panel 2 – mitotracker staining, panel 3. DAPI staining

In a knockdown of the mitochondrial acyl carrier protein, punctuate staining by Mitotracker red was observed and investigation seemed to show that these were due to localised increase in areas of membrane potential rather than mitochondrial fragmentation (Guler et al., 2008). Guler and colleagues proposed that these localised areas of increased membrane potential may correspond to areas where a key phospholipid depleted in the rest of the mitochondrion, for example PE, was sufficient to maintain membrane potential. In the case of PE in the ethanolamine-phosphate cytidyltransferase knockout (ECT) - the cells seem to fragment their mitochondrion and this leads to loss of membrane potential (Gibellini et al., 2009).

This mitochondrial fragmentation and/or loss of membrane potential is likely to be a consequence of depletion in CL and IPC as a result of their precursors PG and PI respectively, as these are both downstream products of CDP-DAG. To look more closely at these and other phospholipids in the procyclic form TbCDS RNAi knockdowns, this cell line was biochemically phenotyped.

5.2.4 Biochemical Phenotyping of Procyclic Form RNAi Cell Line

5.2.4.a In Vivo Radiolabelling

In order to more closely analyse what is occurring in the procyclic form TbCDS RNAi cells which results in slowed growth, aberrant cell division and altered mitochondria, *in vivo* radiolabelling was carried out at five days after the addition of tetracycline.

Labelling with [³⁵S]methionine (Figure 5.7, A) clearly shows that protein synthesis is occurring at normal levels at this time point, and therefore a valid point to look at biochemical phenotypes.

As in bloodstream form *T. brucei*, in procyclic form [³H]glycerol is incorporated into the backbone of DAG/PA and therefore shows all glycerolipid species. Incorporation of [³H]glycerol into the lipid fraction of TbCDS RNAi with and without the addition of tetracycline (+ and - Tet) is shown in Figure 5.7, B.1. There was a decrease in the labelling of some species in the + tetracycline cells, in particular of neutral lipids and CL (CL). A depletion in CL could certainly be responsible for the reduction in Mitotracker red staining which was seen in these mutants, since a similar phenotype was seen in a knockout of procyclic CL synthase (Serricchio and Buetikofer, 2012) although in this case the phenotype was present after just three days. However, this

difference is to be expected since here TbCDS is knocked down rather than abolished. Additionally, because TbCDS is upstream of CL it may take longer for any changes to have an effect.

Labelling of PE and PC with [³H]glycerol appeared unaffected (Figure 5.7, B.1), which is unsurprising given previous results and their synthesis via the Kennedy pathway only. However, there was not a huge reduction in labelling of PI species with [³H]glycerol, which was very surprising given that CDP-DAG is essential for PI formation. This may indicate that PI is preferentially being made because it is of the most importance to procyclic form *T. brucei*. Since PS and PI run together in this solvent system, it is possible that an increase in incorporation of [³H]glycerol into PS is masking a decrease in PI. Similarly, PG is predicted to run at a similar height as PC and therefore the incorporation of [³H]glycerol into PG cannot be determined here.

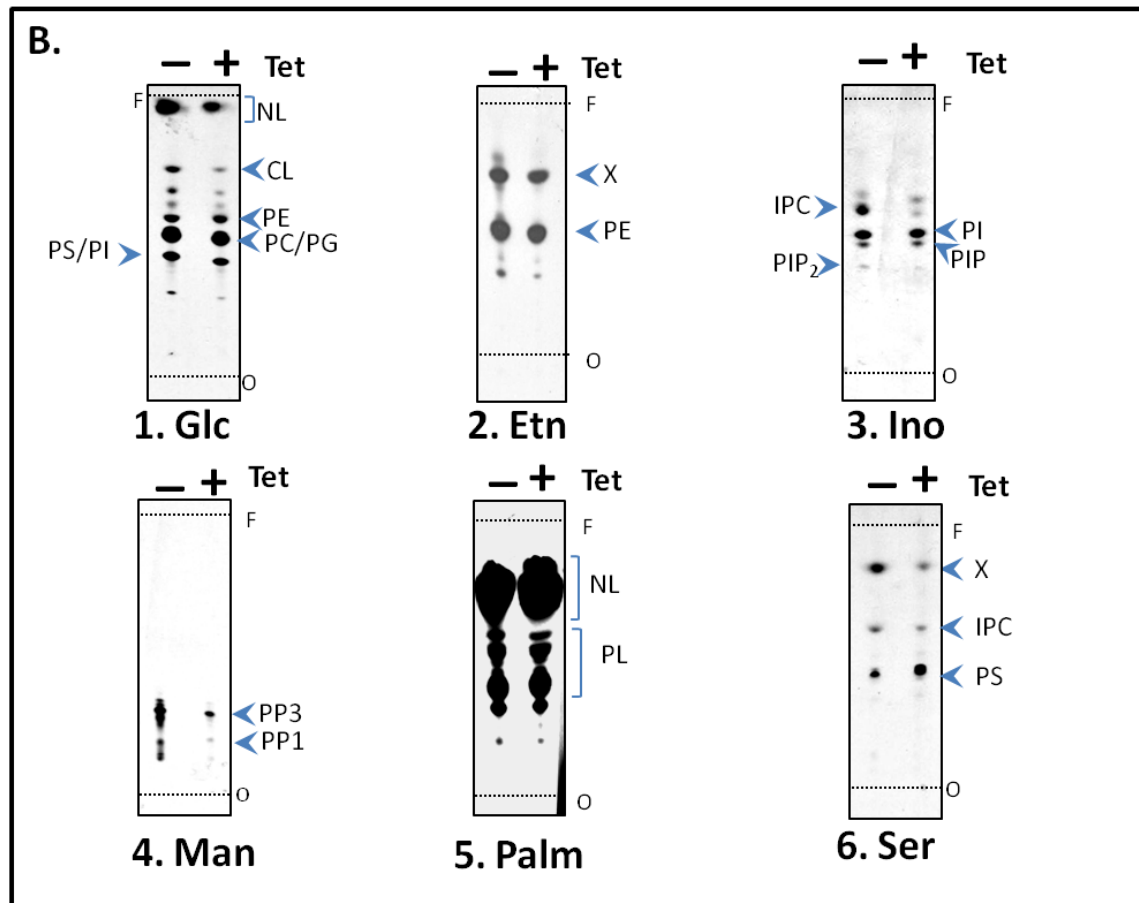
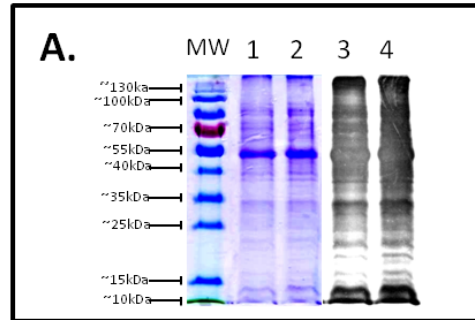


Figure 5.7. Biochemical analysis of clone 1 PCF TbCDS RNAi by *in vivo* radiolabelling 48 hours – and + tetracycline. (A) Cells were labelled with [³⁵S]methionine and protein extracts separated on a 12% SDS-PAGE gel. Proteins gels were stained with Coomassie blue (lanes 1 and 2) and put on film for radiography (lanes 3 and 4). Lanes 1 and 3 clone 1 TbCDS RNAi cells – tetracycline. Lanes 2 and 4 – clone 1 TbCDS RNAi cells 48 hours + tetracycline. (B) Autoradiographs of HPTLC plates run with the lipid fraction of cells labelled with: (1) [³H]Glycerol (2) [³H]Ethanolamine (X = unidentified band co-migrating with CL) (3) [³H]Inositol (4) [³H]Mannose (5) [³H]Palmitate (NL = neutral lipids, PL = phospholipids) (6) [³H]serine. O = origin, F = front.

To more closely examine the biosynthesis of the individual phospholipid species, radiolabelled headgroup molecules were incubated with the double marker and procyclic form TbCDS RNAi + tetracycline cells. To track the synthesis of PE [³H]ethanolamine was used. Figure 5.7, B.2 shows the TLC of [³H]ethanolamine labelled lipid and confirms what was seen in the [³H]glycerol labelling - there is no significant perturbation in the synthesis of this PE in the TbCDS RNAi cell line. As in bloodstream form, a higher band in the [³H]ethanolamine labelling is unexpected (labelled X). Again, this band co-migrates with CL and is also present in the [³H]serine labelling showing serine/ethanolamine or their metabolites are able to label CL or another hydrophobic, neutral lipid.

Also confirming what was seen in the [³H]glycerol labelling, the incorporation of [³H]inositol into PI was not decreased in the + tetracycline cells. This is not entirely surprising, since in both the TbCDS RNAi and the TbCDS knockout in bloodstream form, [³H]inositol incorporation into PI was unaltered despite incorporation of [³H]glycerol being significantly reduced. In these cases, since ES-MS showed that total PI was definitely depleted, it seemed that an increase in headgroup exchange activity of [³H]inositol into existing PI was masking this decrease in PI. If the reduction in PI is less in procyclic form TbCDS RNAi than it was in bloodstream form TbCDS RNAi it is to be expected that headgroup exchange will easily mask it, however this means no new PI is being formed, and that total PI content in the cells will decrease.

In procyclic cells, in addition to PI and PIPs, inositol is incorporated into the sphingolipid inositol phosphorylceramide (IPC). The [³H]inositol labelling showed incorporation into IPC to be dramatically decreased in the TbCDS RNAi cells compared to in the double marker. Whilst this is not an unexpected result given the role of CDP-DAG as a precursor to IPC through PI, it is perhaps surprising given that PI itself was not greatly depleted according to both the [³H]glycerol and the [³H]inositol radiolabelling results. These results may indicate that the synthesis of IPC is being sacrificed in order to maintain a pool of PI, but since IPC is essential in procyclic form *T. brucei* (Fridberg et al., 2008). This is somewhat difficult to understand, particularly given that it is not thought that PI is essential for GPI anchors though PI may well be essential for PIPs. The reduced level of IPC may indicate rapid turnover of this sphingolipid, which is essential. In fact, in cells where the production of IPC was limited by RNAi, the phenotype of the knockdowns showed many similarities to

the TbCDS knockdown, including detached flagella, delayed kinetoplast segregation and incomplete cytokinesis (Fridberg et al., 2008). However, in this case the phenotype appeared at three or six days after the addition of tetracycline, whilst in the TbCDS RNAi the phenotype is only found in the majority of cells at around two weeks after tetracycline addition. Additionally, IPC is thought to have a role in the mitochondrion, and its depletion may contribute to the decrease in mitochondrial membrane potential that is seen in the TbCDS RNAi knockdown cells. If synthesis of IPC is affected as early as 96 hours after induction of RNAi, it is surprising that the phenotype does not appear until much later, and suggests that whilst IPC normally has a high turnover rate it is able to be maintained.

To specifically look at the synthesis of GPI anchors, procyclic form TbCDS RNAi cells were labelled with [³H]mannose, which, as in bloodstream form cells is converted into GDP-[³H]mannose and dolichol-P-[³H]man allowing easy incorporation into GPI precursors in a series of three mannosylations prior to ethanolamine-phosphate capping to produce the GPI precursor PP3 (Field et al., 1992). However, unlike in bloodstream form the inositol is not deacylated, and instead a phospholipase acts to remove the acyl group in the sn-2 position on the glycerol to produce the GPI intermediate PP1 which is used to attach cell surface proteins such as procyclin (Field et al., 1991). Figure 5.7, B.4 clearly shows that the synthesis of GPI anchors in the TbCDS RNAi knockdown is greatly hindered. This is rather surprising, since levels of *de novo* PI synthesis are not greatly reduced, and GPI anchor synthesis might be expected to be less affected in the procyclic form than in the bloodstream form because there is less of a demand on PI for GPI anchors (Lillico et al., 2003, Vassella et al., 2009, Nagamune et al., 2004, Roper et al., 2005). It might be that the cells are preserving their PI pool from further metabolism, since their requirement for the PI itself is the most important, for example for membrane lipid or PIP signalling. Alternatively, since sphingolipid is essential in procyclic form *T. brucei* (Sutterwala et al., 2008) and the synthesis of mature GPI anchors is not (Guther et al., 2006, Lillico et al., 2003, Nagamune et al., 2000), it is feasible that PI made from *de novo* synthesised inositol in the ER is being shuttled away from GPI anchor synthesis and towards the synthesis of IPC which is transported to the mitochondrion (Smith, personal communication). The existence of IPC synthesis from the ER pool of PI is supported by the fact that GPI anchor synthesis is less in procyclic form compared to bloodstream form, meaning that there is extra PI (from *de novo* synthesised inositol)

available in the ER. Synthesis of IPC from the pool of excess PI in the ER in addition to its synthesis via Golgi PI would therefore make sense. However, Gonzalez-Salgado and colleagues found that knockout of the inositol transporter - which specifically depletes the Golgi pool of PI - also depleted IPC, suggesting that IPC is also made in the Golgi (Gonzalez-Salgado et al., 2012). If synthesis of IPC from the ER pool of PI was possible, it would surely have happened in this knockout. Moreover, if PI is being shuttled towards the synthesis of IPC it is clearly not enough, since IPC synthesis is clearly depleted, therefore depletion of one cannot be compensated for by the other.

In order to examine total lipid synthesis in procyclic form TbCDS RNAi cells, they were labelled with [³H]palmitate, a fatty acid which is known to be readily incorporated into procyclic form lipid. Incorporation of [³H]palmitate into the lipid fraction is shown in Figure 5.7, B.5. There is maybe a slight decrease in the labelling of all lipids in the procyclic form TbCDS RNAi cell line, but it is very subtle. Incorporation of [³H]palmitate into lipid is probably via remodelling of existing phospholipid and neutral lipids therefore little difference shows that general metabolism is unaffected.

Previous investigations have indicated there may be a difference in PS metabolism between bloodstream form and procyclic form *T. brucei*. If this is the case, the effect of TbCDS knockdown on the synthesis and metabolism of PS may be different in the two cell types. In bloodstream form TbCDS knockdown and knockout [³H]serine labelling of PS showed the synthesis of this lipid to be unaltered, suggesting its synthesis occurs via headgroup exchange from PE as is the case in higher eukaryotes, rather than from CDP-DAG as is the case in yeast and plasmodium. The TLC of the procyclic form [³H]serine labelling shown in Figure 5.7, B.6 shows the band expected to correspond to PS is certainly less in the + tetracycline lane. This result does not fit in with previous results where PE was essential for PS synthesis, suggesting synthesis via CDP-DAG was not possible, or at least did not make a significant contribution (Signorell et al., 2008). Since PE synthesis is not significantly altered, the reason for a decrease in PS is not a secondary effect of CDP-DAG on the PE pool. It is possible, however that the depletion of PS is due to another secondary effect of CDP-DAG depletion i.e. due to its use in making PG, which will be discussed later. This depletion also indicates that an increase in PE to PS headgroup swapping is unable to

compensate for the increased utilisation of PS, possibly as the depleted pool of PS is in the mitochondrion and does not have access to ER localised PE.

The TLC of [³H]serine labelling shows a large increase in its incorporation into the unidentified lipid labelled as lipid X. This phospholipid also appears in the TLC of [³H]ethanolamine labelling in bloodstream form TbCDS knockdown and knockout and in this procyclic form knockdown. This lipid co-migrates with CL, which is not currently thought to be labelled by either [³H]serine or [³H]ethanolamine. Incorporation of [³H]serine into this lipid is significantly reduced, which would support what is seen in the [³H]glycerol labelling of CL.

The middle band in the [³H]serine labelling is likely to correspond to IPC, which acquires label via the incorporation of [³H]serine into ceramide, which is then incorporated into IPC. Like the decrease of [³H]inositol into IPC, the incorporation of [³H]serine into IPC is reduced, though possibly not to the same extent. This shows that some IPC is being synthesised from PI that cannot be labelled by [³H]inositol i.e. the ER pool of PI which can only utilise inositol *de novo* synthesised in the ER. This would give further evidence for a pool of IPC in the ER.

The lowest band on the [³H]serine TLC corresponds to PS (based on co-migration with PS standard in both 180:140:9:9:23 (CHCl₃:MeOH:30% NH₃:1M NH₄Ac:H₂O) and in 10:10:3 (CHCl₃:MeOH:30% NH₃Ac:H₂O) - see appendix A. This band is increased in the procyclic form TbCDS RNAi + tetracycline, which may tie in with the earlier hypothesis that PG can be synthesised by PS via headgroup exchange catalysed by the PGPS enzyme. An increase in the PS pool may indicate that excess PA species which are being converted into DAG (as discussed earlier), and that this DAG is being shuttled into the formation of PG via PE and PS. The increase in incorporation of [³H]serine into PS may be a result the up-regulation of PSS occurring slightly before up-regulation PGPS, or the accumulation of species of PS which are not utilised by PGPS for incorporation into PG. The up-regulation of PG synthesis may be an effective way of dealing with the excess PA - which is a lipid messaging molecule of several cellular processes including apoptosis - without disturbing membrane dynamics, since PG is relatively neutral.

5.2.4.b Lipid Profile of Procyclic Form TbCDS RNAi Cell Line by ES-MS

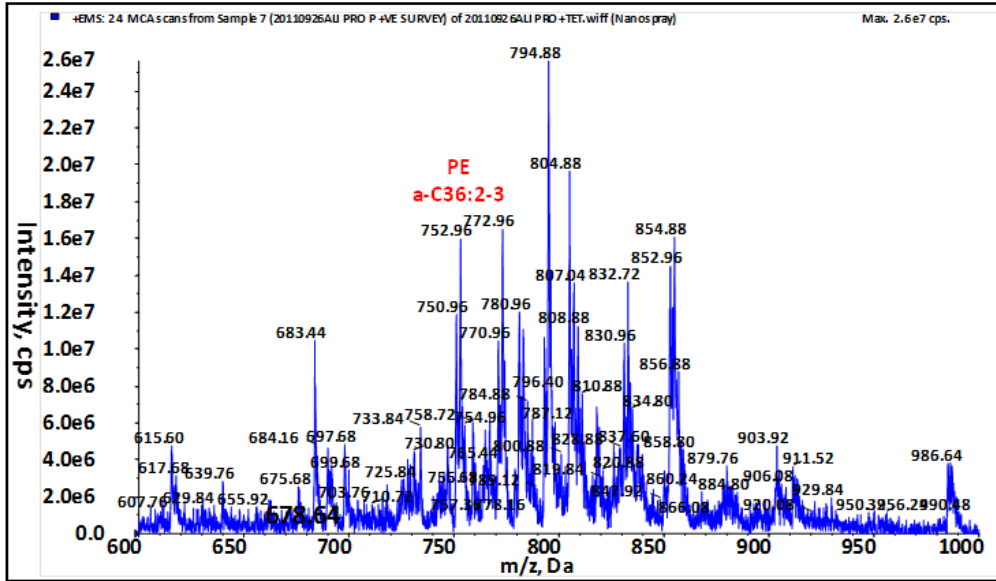
To get a closer look at how different pools of lipid were affected in the procyclic form TbCDS RNAi knockdown cell line, total cellular lipids were analysed by ES-MS.

The lipid profile of wild type *T. brucei* procyclic form shows many similarities to that of the bloodstream form, but there are also some important differences. Like the bloodstream form, the major species of phospholipids contain C18:0 in the *sn*-1 position, whilst the *sn*-2 position is occupied by unsaturated acyl groups - C18:2 in ether lipids and C18:2, C22:4 and some C20:4 in diacyl lipids. The procyclic forms contain less highly unsaturated fatty acyls than the bloodstream form (Richmond et al., 2010).

5.2.4.b.i Positive Survey Scan

Figure 5.8 shows the positive ion scan from the double marker and the TbCDS p2T7-177 + Tet. As in the bloodstream form, a scan for positive ions detects $[M+H]^+$ and $[M+Na]^+$ ions of PC and SpM species, and can also pick up positive ions of PE and PS. Since SpM species are much less common in procyclic form than bloodstream form a positive ion scan mostly represents PC species. The scans shown in Figure 5.8 are slightly confused by the presence of sodium adducts, but the four key peaks corresponding to the most common PC series are present, along with some longer and shorter chain PC species and some DAG species. There is a relative increase in two DAG at 639.6 m/z series corresponding mostly to DAG C38:7 from 0.34 to 0.55 of PC C32 and of the DAG series at 683.62 m/z, corresponding mostly to DAG C40:10 from 0.75 to 0.97 of PC C32. An increase in DAG species likely corresponds to an increase in the CDS substrate PA, which is likely dephosphorylated to DAG because this is less harmful to the cell.

A. DM



B. TbCDS p2T7-177 + tetracycline

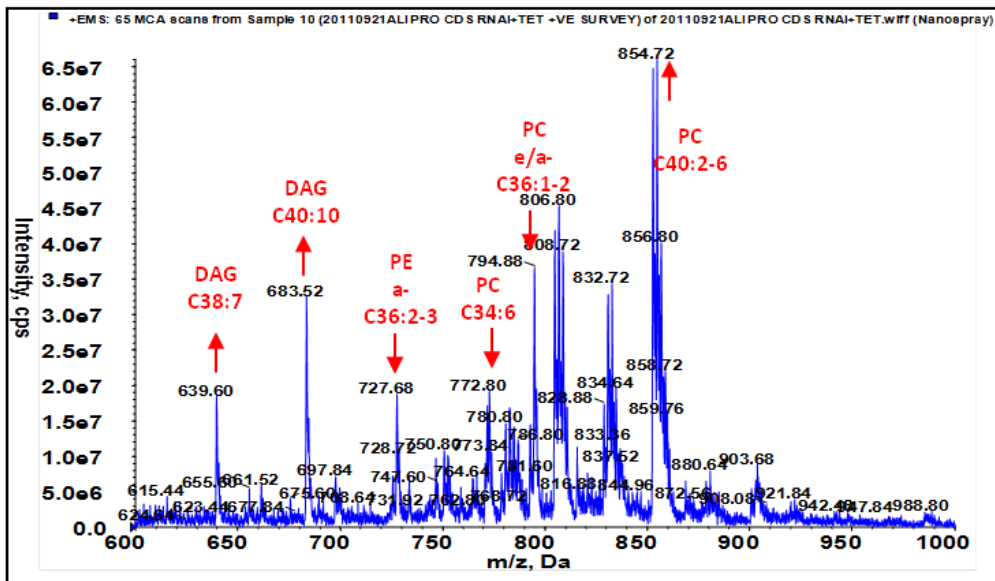


Figure 5.8. Positive ion survey scan of lipids from DM and procyclic form TbCDS RNAi + tetracycline. A. Wild type double marker (DM) cells. B. PCF TbCDS RNAi cells grown in the presence of tetracycline for 96 hours. DAG = diacylglycerol species, TAG = triacylglycerol species. Red arrows and text indicate peaks which are different in the mutant, whilst the direction of the arrow indicates whether this peak is increased or decreased in the mutant. CX:Y = X – total number of carbons, Y – total number of double bonds in fatty acid chains of lipid species. e = alkenyl-acyl- linked lipid, a = alkyl-acyl- linked lipid.

An increase in DAG species was also seen in the bloodstream form TbCDS RNAi and TbCDS knockout, but the species were different, possibly reflecting differences in lipid synthesis pathways between two cell types. As previously mentioned, this up-regulation of PA phosphatase could be signalled by the decrease in TbCDS activity, as has been shown in yeast (Shen and Dowhan, 1997) Whilst the overall abundance of PC species may be the same, there is a shift in the general abundance of PC species, which was more specifically examined in a scan for choline phosphate (Figure 5.10) and will be discussed later.

5.2.4.b.ii Negative Survey Scan

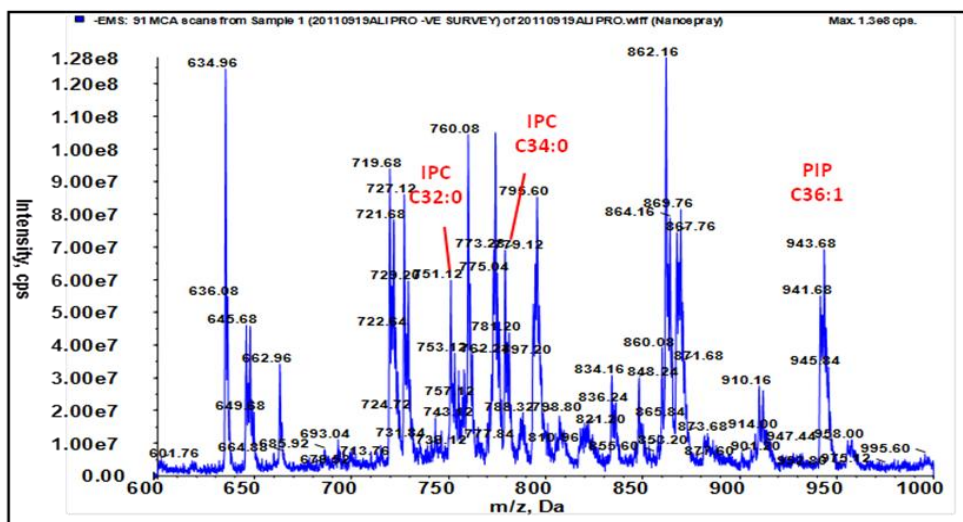
A ES-MS negative survey scan provides a good overview of the relative abundance of anionic lipid species. In procyclic form *T. brucei*, The negative survey scan detects $[M-H]^-$ of PI, PG, PS, PE, IPC and PA species. The key ion series that form peaks in procyclic form, as in bloodstream form are PE a-C36:y at 727 m/z; PS a-C36:y at 774 m/z and PI peaks at 862 m/z (C36:y) and 910 m/z (C40:y). From Figure 5.9, all these peaks are present in the double marker scan, but there are considerable differences between the double marker scan and the TbCDS RNAi mutant scans.

In the procyclic form TbCDS RNAi mutant scans (Figure 5.9, B) the main PE a-C36:y peak at 727 m/z is very much reduced in comparison to the double marker scan (Figure 5.9, A) from 0.69 of PI C36 to 0.29. This contradicts what had been seen in the *in vivo* radiolabelling and in the positive survey scan. An intense peak at 773 m/z may correspond to the PS a-C36 series, which would confirm the increase in the incorporation of $[^3H]$ serine into PS that was seen (Figure 5.7, B.6) and may correspond to a decrease in the PE series. It could also correspond to the PG C36 series, which was increased in both the bloodstream form TbCDS knockdown and knockout. Also confirming what was seen in the radiolabelling, peaks corresponding to IPC C32:0 and IPC C34:0 are decreased from 0.46 and 0.66 of PI C36 to 0.26 and 0.43 in TbCDS RNAi + tetracycline, respectively. It is difficult to say whether PI peaks are decreased relative to other peaks, since other peaks are so altered in this scan, however the ratio of PI C36:y to C40:y is decreased with respect to wild type - from 2.91 to 2.33. As in the bloodstream form mutants there is the appearance of a peak at 824.2 m/z corresponding mostly to PG C40:5 (C18:0/C22:5 - Figure 4.15, A).

In the procyclic form TbCDS RNAi + tetracycline scan, the PIP species visible on the double marker scan at 943 m/z, corresponding to PIP C36:1 is replaced by PIP C38:4.

This corresponds to a decrease which is seen in the PI C36 series relative to PI C40 species and may indicate the cells are trying to preserve this depleted pool by phosphorylating PI C38. Since PIPs are signalling molecules, such an alteration of species may have a consequence in signalling pathways, and could contribute to disruption of cell cycle events that was seen in Figure 5.4.

A. DM



B. TbCDS p2T7-177 + tetracycline

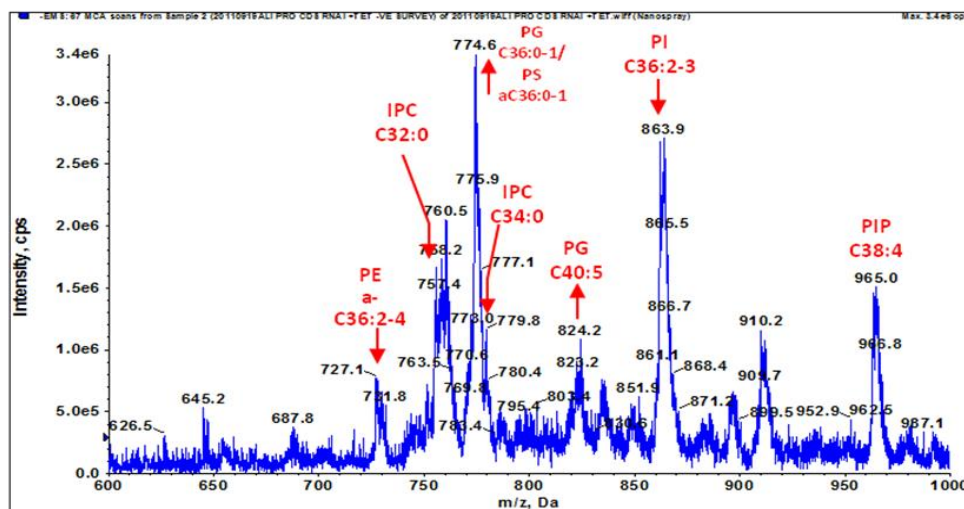


Figure 5.9. Negative survey scan of lipids from DM and procyclic form TbCDS RNAi + tetracycline. A. Wild type double marker cells (DM). B. PCF TbCDS RNAi cells grown in the presence of tetracycline for 96 hours. PI = phosphatidylinositol, IPC = inositolphosphorylceramide, TAG = triacylglycerol, PIP = phosphorylated PIs. For key to annotation, see Figure 5.8.

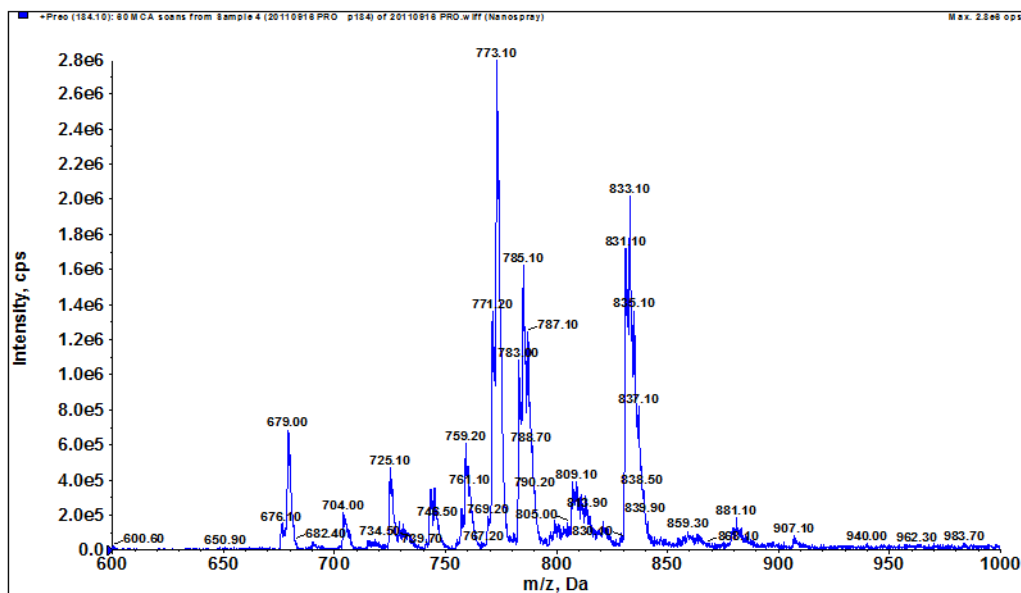
5.2.4.b.iii Choline Containing Lipid

Scanning for precursors of the unique m/z 184 ion detects all choline-phosphate containing phospholipids. As in bloodstream form the ratio of diacyl to ether PC species is about 3:1, and the four main series of PC are comprised of e/a 36:y, 36:y, 38:y and 40:y (Richmond et al., 2010). All these peaks are clear in both the double marker and the TbCDS p2T7-177 + tetracycline scans in Figure 5.10. In the TbCDS RNAi + tetracycline mutant, however, there is a shift in the relative intensities of some of these peaks, with the longer chained C40:y peak (m/z 833) showing a marked increase over e/a C36:y (m/z 774) from 0.67 in the wild type to 1.38 in TbCDS RNAi + tetracycline.

There is also a decrease in the shorter chained species like PC C28:y at m/z 679 in the induced TbCDS RNAi cell line in comparison to the double marker - from 0.42 to 0.09 of PC C36.

Such a shift in choline containing lipid was not expected due to the synthesis of these species via a separate pathway than that involving CDP-DAG and no indication in perturbation of levels by radiolabelling. An increase in the length of lipid chains may be an adaptation to perturbations in other cellular phospholipids, for example an increase in unused PA being dephosphorylated to DAG would create an increase in particular species of DAG as substrates for the Kennedy Pathway. Earlier in this work, it was suggested that synthesis of PS via PC may explain some discrepancies in PS metabolism. If PS can normally be synthesised, at least in part, from CDP-DAG, increased synthesis via PC may help to bypass any deficit in PS in the TbCDS knockdown. This may explain the alteration in relative species of PC, although does not seem particularly likely since knockdown of PE synthesis was previously shown to almost abolish PS synthesis in procyclic form *T. brucei* (Signorell et al., 2008). Additionally, the pool of PS is small compared to PC and its synthesis would be unlikely to make a particularly noticeable impact on the profile of PC species.

A. DM



B. TbCDS p2T7-177 + tetracycline

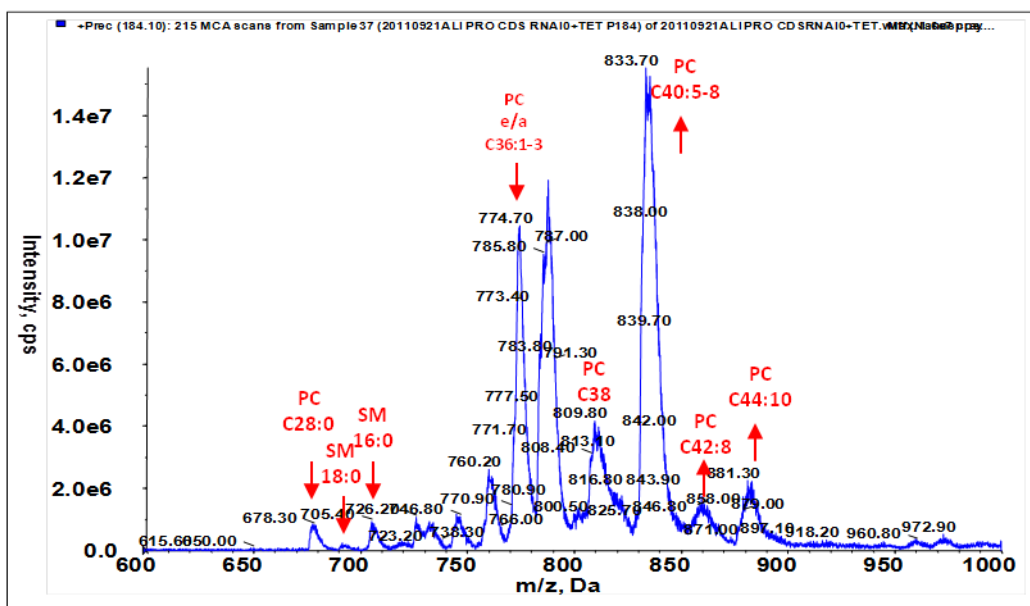
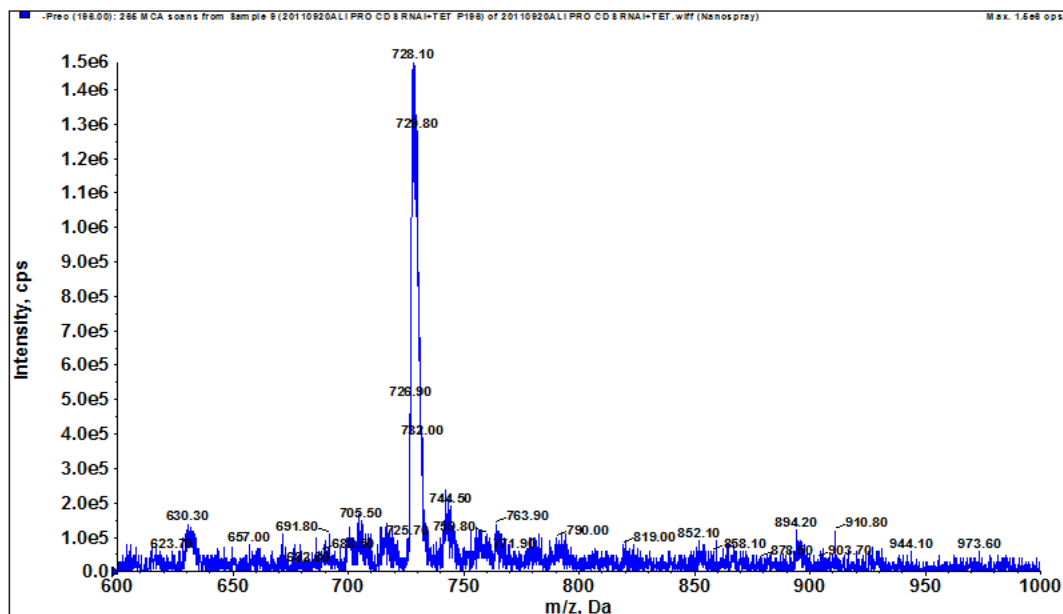


Figure 5.10. Mass spectrometric analyses of choline-phosphate containing phospholipids from DM and procyclic TbCDS RNAi + tetracycline. Total lipids were analysed by ESI-MS in positive ion mode using parent-ion scanning of the collision induced fragment for phosphorylcholine at 184 m/z. A. Wild type double marker cells (DM). B. PCF TbCDS RNAi cells grown in the presence of tetracycline for 96 hours. For further information, see Figure 5.8.

5.2.4.b.iv Ethanolamine Containing Lipid

The most abundant PE species by far in wild type procyclic form *T. brucei*, as in bloodstream form is e/a-C36:y, consisting mostly of e-C18:1/C18:2 at m/z 726 (Richmond et al., 2010). Precursor ion scanning for PE species in both the double marker and the TbCDS RNAi cell line (Figure 5.7, B.2) show this peak to be the most intense. Moreover, both scans are pretty much identical, meaning there is no change in the relative abundance of different PE species in the procyclic form TbCDS RNAi knockdown. If *in vivo* radiolabelling showed a slight decrease in the labelling of PE with [³H]ethanolamine (Figure 5.11), it must be equally effecting all species of PE and there is no unusual adaptation occurring that is resulting in an altered profile of PE species. Certainly, a lack of crosstalk between the branches of the Kennedy Pathway means adaptation would be less likely.

A. DM



B. TbCDS p2T7-177 + tetracycline

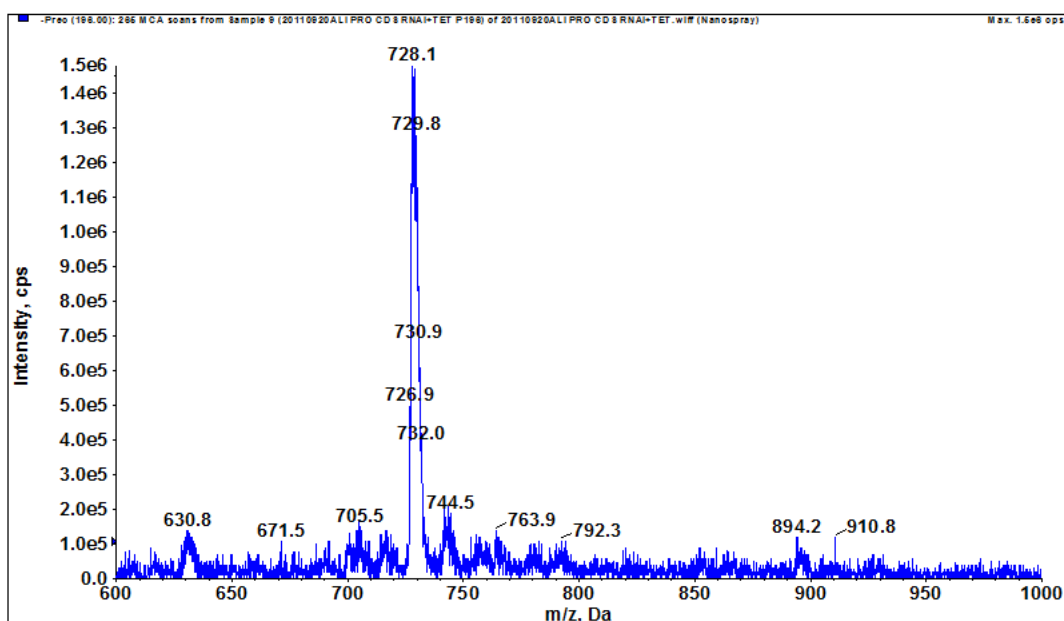


Figure 5.11. Mass spectrometric analyses of ethanolamine-containing phospholipids from DM and procyclic TbCDS RNAi + tetracycline. Total lipids were analysed by ESI-MS in negative ion mode using parent-ion scanning of the collision induced fragment for phosphorylethanolamine at 196 m/z. A. Wild type double marker cells (DM). B. PCF TbCDS RNAi cells grown in the presence of tetracycline for 96 hours. For annotation see Figure 5.8.

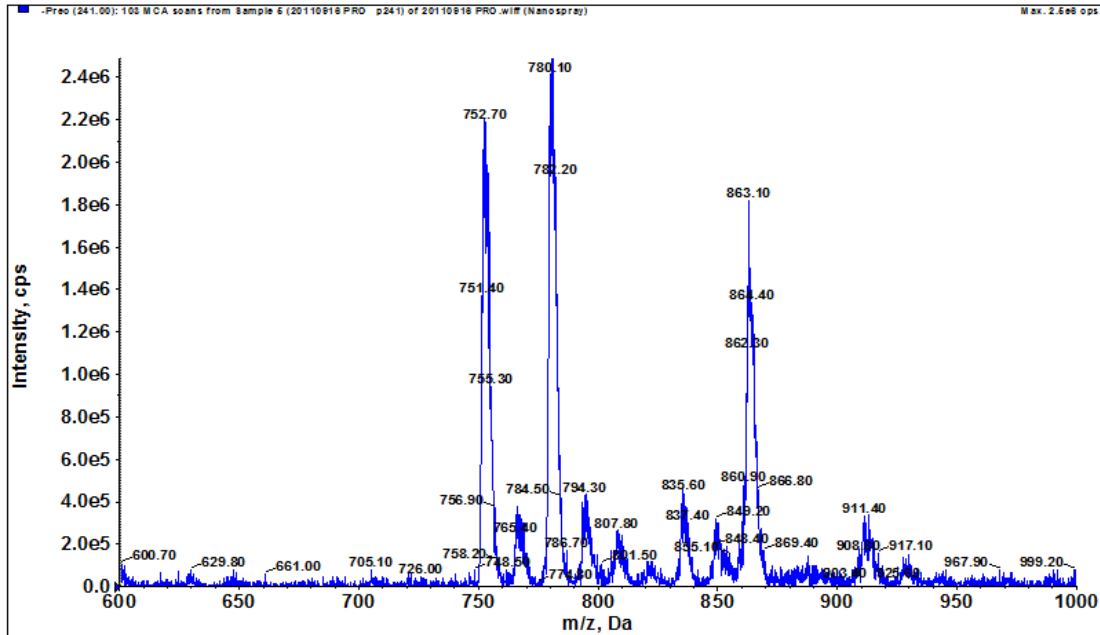
5.2.4.b.v Inositol Containing Lipid

Given the surprising lack of change in labelling of PI species in procyclic form *T. brucei* as a result of TbCDS knockdown, it was important to get a better idea of what was going on by ES-MS. Procyclic form contain the sphingolipid IPC in addition to PI, and therefore scanning for precursors of the ion fragment m/z 241 in negative ion mode also reveals IPC species. As in bloodstream form, in procyclic form the two most abundant PI species are C36:y (mostly C18:0/C18:1-2) at m/z 863 and C40:y (mostly C18:0/C22:4-22:6) at m/z 910, but the C36:y tends to be more abundant in procyclic form. Additionally, in procyclic form the presence of shorter fatty acid chain diacyl and ether species has been confirmed, which, along with IPC species at m/z 752 and m/z 780 are not usually present in bloodstream form. The p241 scan shown in Figure 5.12 gives evidence as to how the various pools of inositol-phosphate containing lipids are affected. The first obvious thing is a decrease in the abundance of C36:y PI with respect to P40:y from 0.37 in double markers to 0.19 in TbCDS p2T7-177 + tetracycline, showing that the pool of C36 PI is disproportionately affected by the decrease in CDP-DAG synthesis. Work by Guther and colleagues found that C36:0 and C36:1 PI species were preferentially incorporated into GlcNAc-PIs for GPI anchors in procyclic form - the most commonly incorporated being C36:1 composed of C18:0/C18:1 at m/z 863 (Guther et al., 2006). The relative decrease in the C36 peak ties in with the decrease that was seen in the incorporation of mannose into GPI anchors. However, there is an increase in the PI pool at m/z 849 (mostly a-C18:0/C18:1) in the TbCDS RNAi knockdown (which is also incorporated into GlcNAc-PI) relative to the pool at 835 m/z (mostly C16:0/C18:1)- from 0.17 to 0.23.

In Figure 5.12., the IPC species are represented by peaks at 752, 780 and 807 m/z which are present in both the double marker and the TbCDS RNA scans - these peaks correspond mostly to IPC C32:0, IPC C34:0 and IPC C36:0 respectively. In the *in vivo* radiolabelling, the incorporation of [^3H]inositol into IPC was dramatically decreased by the TbCDS RNAi, whilst their labelling via [^3H]serine was less affected. From the ES-MS spectra, IPC species are decreased with respect to the PI species - IPC C32 decreases from 1.39 of PI C36 to 0.95, and IPC C34 decreases from 1.23 of PI C36 to 0.55. This is the opposite of what was seen in the mitochondrial acyl carrier protein of the mitochondrion where total IPC levels remain unchanged during RNAi whilst PI levels are decreased. Interestingly, during RNAi of the mitochondrial acyl carrier protein, the 778 m/z species of IPC (C34:0) is increased relative to the 752 m/z

species (C32:0) in lipid extracts from total cells, whilst the ratio of these two species remains relatively similar in lipid extracts from mitochondria. This may suggest that a pool of IPC separate from that in the mitochondrial/ER or MAM fraction (i.e. the Golgi pool) contains a higher proportion of the C34 IPC species (Guler et al., 2008). In this procyclic form TbCDS RNAi, there is also relative increase of C34 series (780 m/z) in comparison to the C32 series (752 m/z) - from 1.13 to 1.73. This may suggest that the ER pool of IPC is more affected by the knockdown of TbCDS than the Golgi pool. However, radiolabelling results showed that total IPC (as labelled by [³H]serine) showed a less dramatic depletion than Golgi IPC (as labelled by [³H]inositol) which would contradict this. However, this could be due to the relative speed of incorporation of these two precursors into IPC species rather than due to a difference in the knockdown of these two pools.

A. DM



B. TbCDS p2T7-177 + tetracycline

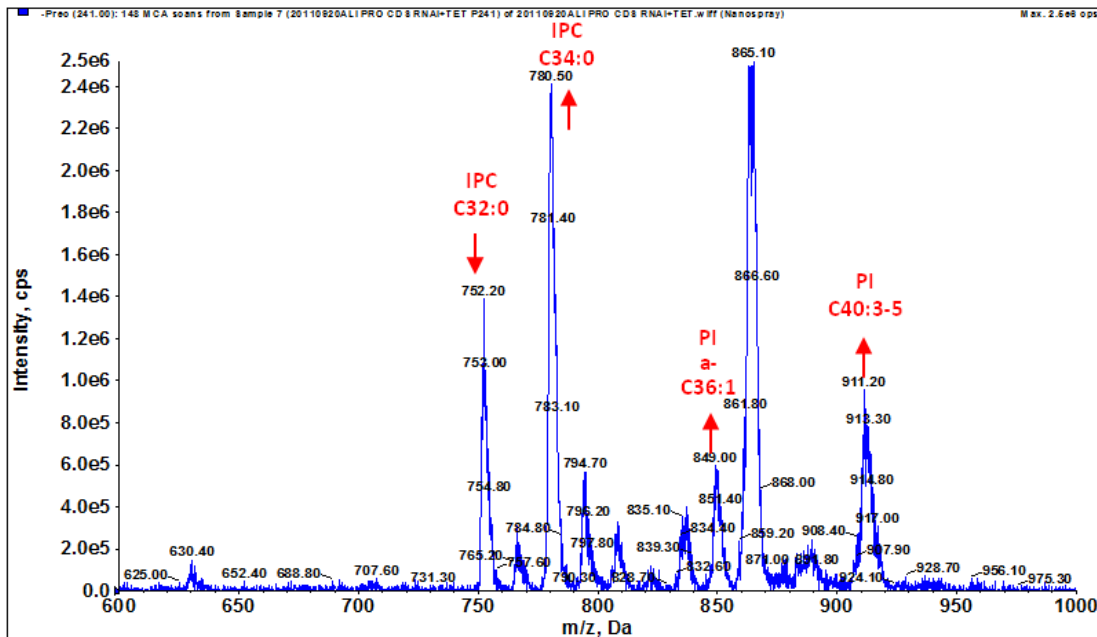
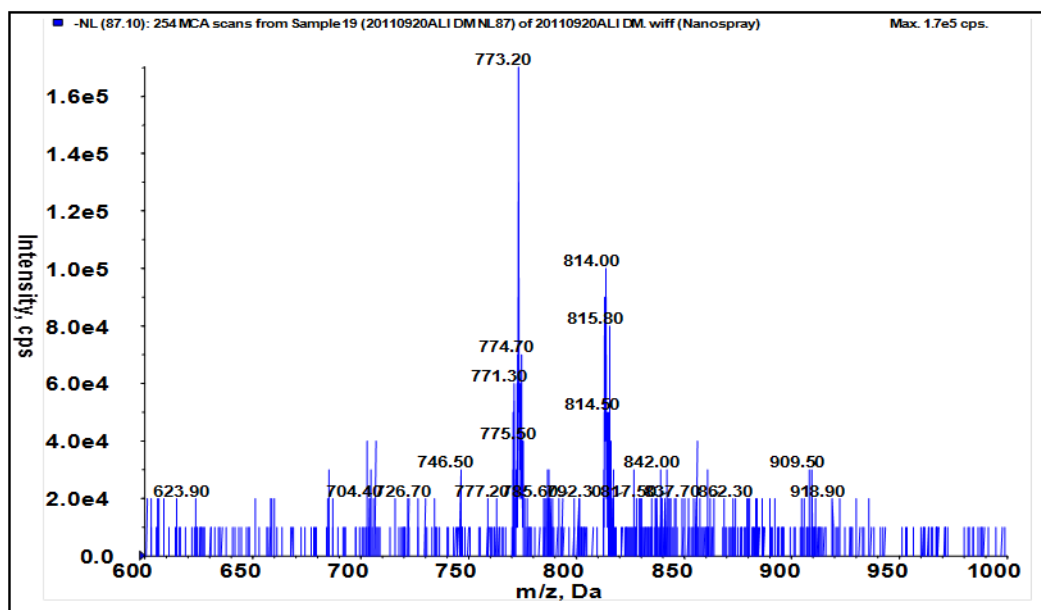


Figure 5.12. Mass spectrometric analyses of inositol-phosphate containing phospholipids from DM and procyclic TbCDS RNAi + tetracycline. Total lipids were analysed by ESI-MS in negative ion mode using parent-ion scanning of the collision induced fragment at 241 m/z. A. Wild type double marker cells (DM). B. PCF TbCDS RNAi grown in the presence of tetracycline for 96 hours. IPC = inositolphosphoryl ceramide. For further information, see Figure 5.8.

5.2.4.b.vi Serine Containing Lipid

In procyclic form total lipid samples, scanning for neutral loss of m/z 87 in negative mode identifies PS molecules. As in bloodstream form, the pool of PS species contains a variety of both diacyl and ether species. Again, in procyclic form as in bloodstream form the most intense PS signal stems from m/z 772 which corresponds to a-C18:0/C18:2. The proportion of diacyl PS species in procyclic form, however, is decreased in procyclic form with respect to bloodstream form where they make up only about 12% of total PS species as opposed to 25% in bloodstream form (Richmond et al., 2010). *In vivo* labelling of PS with [3 H]serine showed this phospholipid to be increased in procyclic form TbCDS RNAi cells. The results from the ES-MS for serine containing lipid show quite an alteration in the proportions of PS species. As in the bloodstream form, the signal of these scans is quite low so it is important not to draw too much from them, however it is notable that similar changes are seen in both bloodstream form TbCDS mutants and in the procyclic form TbCDS RNAi. In the procyclic form TbCDS RNAi scan shown in Figure 5.13, B, the most abundant species is the diacyl PS C38 (814 m/z) rather than PS a-C36 (773.2 m/z) - the ratio changes from 1.67 a-C36 to C38 to 0.63. This shift in the most intense peak was also seen in both bloodstream form mutants so is likely to be significant. It is probable that the a-C36 peak corresponds to PS produced from headgroup exchange with PE, which appears decreased on in the negative survey scan but not by radiolabelling. Since radiolabelling shows an increase in PS overall, there is likely no decrease in the PS a-C36 series, but instead an increase in the PS C38 series. This increase in the production of C38 PS could possibly come headgroup exchange with C38 PC - a species which is slightly increased in the procyclic form TbCDS RNAi, however, PS production from a lipid other than PE is not thought to be possible in procyclic form *T. brucei*, since depletion of PE has a dramatic effect on PS (Signorell et al., 2008).

A. DM



B. TbCDS p2T7-177 + tetracycline

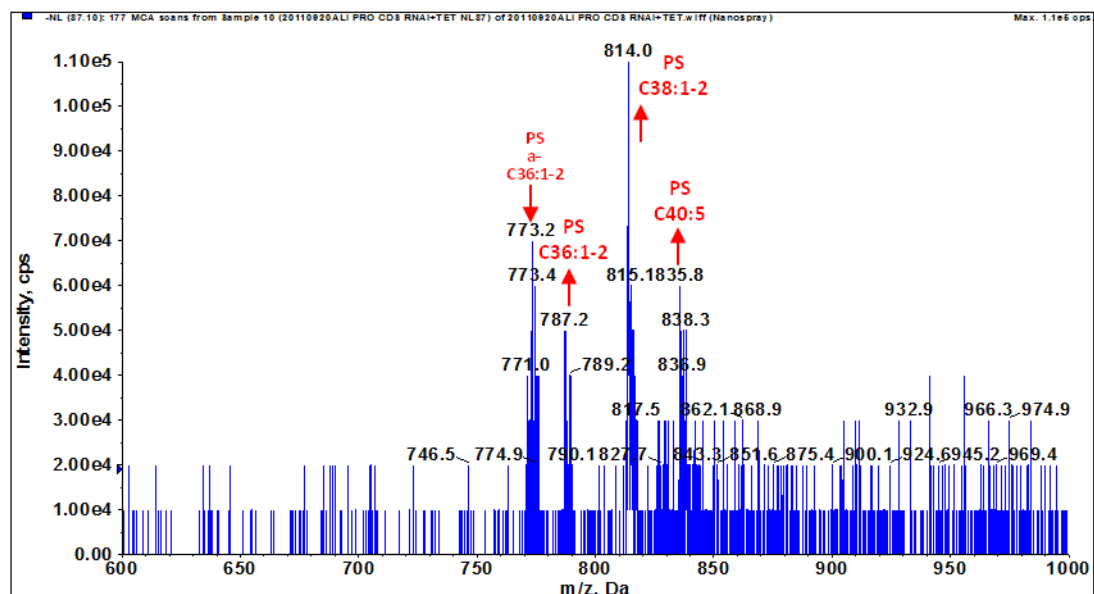


Figure 5.13. Mass spectrometric analyses of serine containing phospholipids from DM and procyclic TbCDS RNAi + tetracycline. Total lipids were analysed by ESI-MS in negative ion mode using neutral loss scanning for 87 m/z . A. wild type double marker cells (DM). B. PCF TbCDS RNAi cells grown in the presence of tetracycline for 96 hours. For further information, see Figure 5.8.

Unlike in bloodstream form TbCDS mutants, where there was a significant decrease in the intensity of the peak corresponding to PS C36 species, there is an increase in this peak in the procyclic form TbCDS RNAi scan compared to the wild type. It is worth noting that the C36 PS series is significantly decreased in procyclic form with respect to bloodstream form in normal circumstances, and if the C36 peak of PS is made from CDP-DAG rather than from headgroup exchange with PE then this would suggest that the PE exchange route is more important in the procyclic form, and therefore may explain why a knockout of part of the ethanolamine branch of the Kennedy pathway severely depleted incorporation of [³H]serine into PS in procyclic form but not in bloodstream form (Signorell et al., 2008, Gibellini et al., 2009). However, an increase in the C36 PS species in the procyclic form TbCDS knockdown is difficult to explain in this context, and may not be significant due to the low signal. There is also a similar increase in the longer chained PS C40 series at m/z 838.3 in the TbCDS RNAi knockdown, but again since this was not seen in either of the bloodstream form TbCDS mutants it may not be significant.

As in bloodstream form *T. brucei* TbCDS knockdown and knockout, it is possible that in the procyclic form this disruption in the relative distributions of PS species may be due to increase in the operation of the PG synthesis pathway via PS, as was previously discussed. Again, it is certainly worth comparing the altered PS species to altered PG species.

5.2.4.b.vii PA and PG

Scanning total lipid samples for precursors of the collision induced 153 m/z ion detects all negatively charged species containing glycerol-phosphate, but is particularly useful for detecting PA and PG species which are otherwise difficult to see. Here, we were particularly interested in PG due to its role in the mitochondrion and as a precursor to CL, also an important mitochondrial phospholipid in procyclic form *T. brucei* (Serricchio and Buetikofer, 2012).

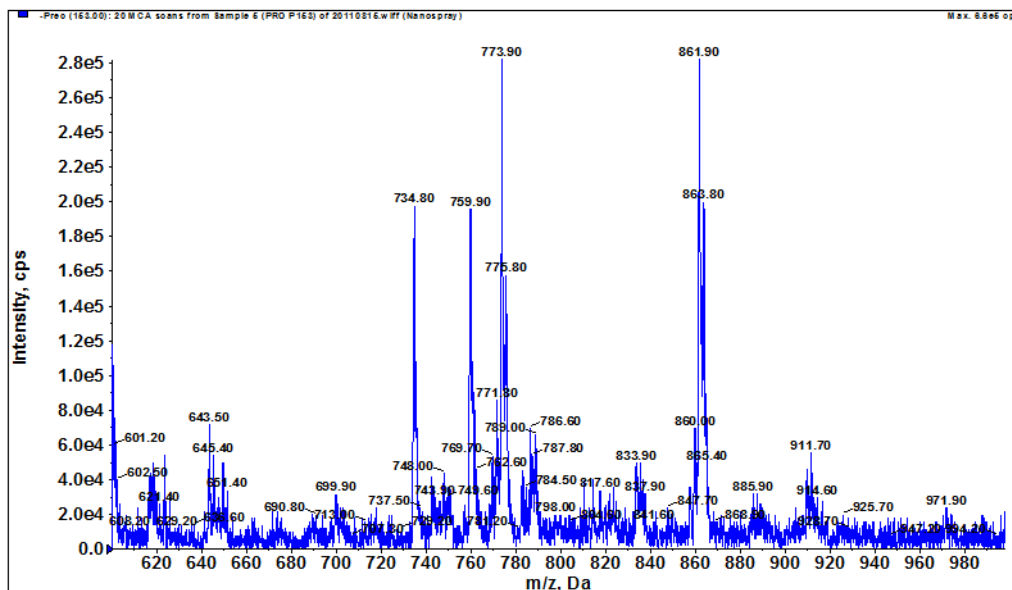
As in bloodstream form TbCDS mutants, PG species have unexpectedly increased in procyclic form TbCDS RNAi mutants (Figure 5.14). Two PG species which are increased in the procyclic form TbCDS RNAi knockdown are PG C38:3 at 800 m/z and PG C40:5 at 824 m/z - the latter of which was greatly increased in the bloodstream form TbCDS conditional knockout. Only the ether linked PG series a-C36 is decreased in the mutant - from 0.69 of PI C36 to 0.40. This a-C36 PG series is also more

saturated, with the most abundant species in the double marker scan being PG a-C36:2 and the most abundant species in the TbCDS RNAi knockdown series being PG a-C36:0. The decrease in PG a-C36 may correspond with the relative decrease that was seen in the a-C36 species of PS. Both bloodstream form and procyclic form *T. brucei* may be capable of synthesising PG via another mechanism i.e. from PS via PG as has been previously described. If PS can be used as a source for PG it may not only explain the alteration of the species profile of PS (Figure 5.13), but also the increase of PS in the procyclic form TbCDS knockdown. Both PG and PS a-C36 species are decreased, whilst C38 and C40 species of the two lipids are increased which lends support to a link between these two lipids.

Interestingly, there is also some considerable change in the PA species. A peak present at 734.8 m/z in the DM scan - possibly corresponding to PA e/a-C40:4/5 - is absent in the TbCDS RNAi knockdown whilst a peak corresponding to the diacyl series of the same C40 PA is increased in intensity - for example, from just 0.15 of PI C36 to 0.71 - and in saturation from C40:6 in the DM to C40:4 in TbCDS RNAi. A further peak in the TbCDS RNAi at 713.9 m/z which is not present in the DM may correspond to a series of e/a-C38 PA containing mostly 1 or two carbon-carbon double bonds. An increase of C40 PA species was also seen in the bloodstream form *T. brucei* ethanolamine-phosphate cytidyltransferase knockout where it was presumed to be an adaptation to a suboptimal level of PE or a build up of its precursors (Gibellini et al., 2009). Since PE levels are not disrupted here it must be a more general response to suboptimal phospholipid species.

The overall picture is one of extreme disturbance of PA and PG species in the procyclic form TbCDS RNAi knockdown, and indicates that the parasite is trying to adapt to the loss of certain lipid species by increase in synthesis of others in order to maintain membrane fluidity and integrity.

A. DM



B. TbCDS p2T7-177 + tetracycline

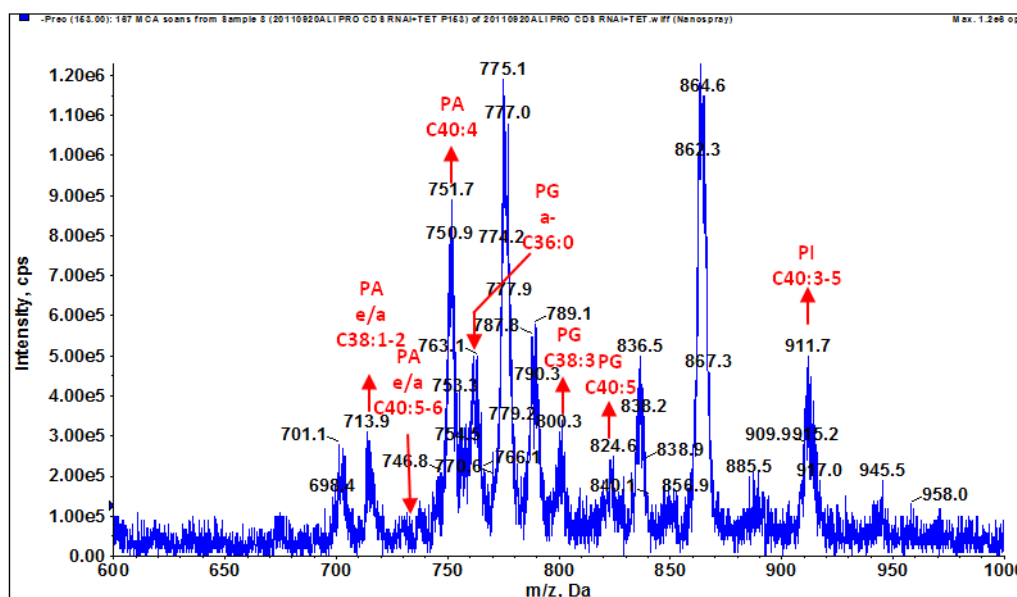
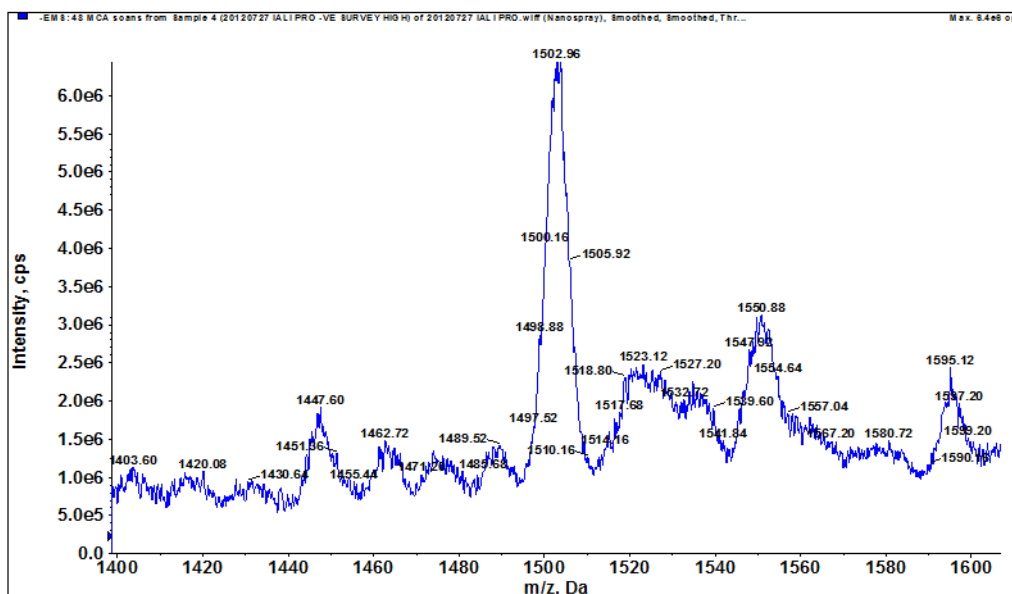


Figure 5.14 Mass spectrometric analyses of glycerol-phosphate containing phospholipids from DM and procyclic TbCDS RNAi + tetracycline. Total lipids were analysed by ESI-MS in negative ion mode using precursor ion scanning for the collision induced fragment for glycerol-phosphate at 153 m/z. A. Wild type double marker cells (DM). B. PCF TbCDS RNAi cells grown in the presence of tetracycline for 96 hours. For annotation see Figure 5.8.

5.2.4.b.viii CL

CL is clearly an important phospholipid in procyclic form *T. brucei*, since its synthesis has been proven to be essential due to its roles in the mitochondrion (Serricchio and Buetikofer, 2012). In the procyclic form TbCDS RNAi mutant, it seems likely that a reduction in CL synthesis is responsible for the observed decrease in mitochondrial membrane potential as observed by Mitotracker red staining (Figures 5.5 and 5.6), since incorporation of [³H]glycerol into CL was greatly decreased in this cell line (Figure 5.7, B.1). Previously, the presence of CL has been shown in the procyclic form mitochondrion by negative ES-MS scanning at high molecular weight. The most intense peak at around 1500 m/z has been characterised and shown to comprise mostly of C18:2/C18:0 glycerol-3-P (m/z 699) and C18:2/C22:6 glycerol-3-P (m/z 743) (Guler et al., 2008). Negative ion survey scan of total lipid between m/z 1400 and m/z 1600 revealed a peak at around 1502 m/z in the DM and the procyclic form TbCDS RNAi + tetracycline corresponding to CL. This peak was considerably larger in the DM than in the procyclic form TbCDS RNAi, confirming what was seen in the *in vivo* radiolabelling - that CL is seriously depleted in the procyclic form TbCDS RNAi mutants.

A. DM



B. TbCDS p2T7-177 + tetracycline

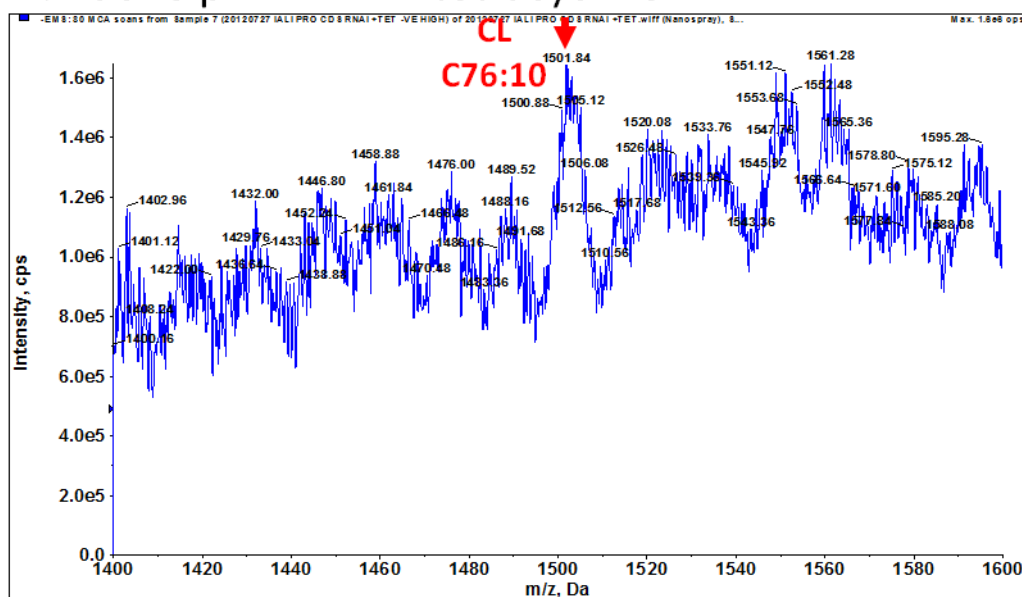


Figure 5.15. Negative survey scan of lipids from DM and procyclic TbCDS RNAi + tetracycline – high m/z.. A. Wild type double marker cells (DM). B. PCF TbCDS RNAi cells grown in the presence of tetracycline for 96 hours. CL = cardiolipin. For annotation see Figure 5.8.

It would seem that the adaptation which is able to maintain levels of PG in the mutant is either not sufficient to supply demand for CL synthesis, does not produce the PG in the correct cellular location or does not produce the correct species.

5.5 Summary and Conclusion

The open reading frame TbCDS has previously been shown to encode a functional CDS and be essential in bloodstream form *T. brucei*, thus validating it as a drug target. The next aim of this investigation was to see what role TbCDS had in the insect form procyclic *T. brucei*. Since the TbCDS had already been shown to be expressed in procyclic form, the importance of its expression was assessed by knocking down the mRNA levels via RNAi. The procyclic form TbCDS cell line exhibited a growth defect showing that TbCDS is also essential in this life cycle stage. Procyclic form cells undergoing TbCDS RNAi were aberrant in cell division, many cells being multinucleate and/or with misplaced cleavage furrows and the majority of cells containing additional, detached flagella. The number of kinetoplasts appeared to be less than the number of nuclei in these cells, however it could not be ruled out that multiple rounds of replication with failure to segregate had resulted in kinetoplasts that could be mistaken for nuclei. Together, these results suggest disruption of cell cycle that may be due to a depletion of the phosphoinositide pool for cell signalling as was seen in the bloodstream form. However, the detached daughter flagella seen in these cells indicated that there may be a problem with the tripartite attachment complex between the basal body of the flagella and the kinetoplast which was causing a failure of the kinetoplast to segregate. This could be a physical problem due to a change in its phospholipid composition and was seen in mutants of IPC synthesis (Mina et al., 2009).

Due to the role of CDP-DAG as a precursor to mitochondrial phospholipids PG and CL, and the increased size and importance of the mitochondria in procyclic form *T. brucei* in comparison to bloodstream form *T. brucei*, cells were stained with Mitotracker red at seven days and 14 days after the induction of TbCDS RNAi to assess the membrane potential of the mitochondria. At seven days there was a very slight decrease in staining and an increase in “hotspots” indicating localised areas of increased membrane potential. By 14 days the mitochondrial staining was extremely reduced and the remaining staining was punctuate, which may have been due to fragmentation or localised areas where the composition of depleted phospholipids was sufficient to maintain a membrane potential.

The lipid metabolism and profile of the procyclic form TbCDS RNAi cell line was assessed by both *in vivo* radiolabelling and ES-MS. Whilst the synthesis of total PC

species was unaffected, ES-MS showed a relative increase in longer fatty acid chained species and a concomitant decrease in shorter fatty acid chains species. This was unexpected because the CDP-DAG pathway is largely separate from the Kennedy pathway by which PC is synthesised, but may be an adaptation which gives an indication of the central role of TbCDS in phospholipid synthesis. In contrast, the profile of PE, whose synthesis is also executed by the Kennedy pathway, remained the same. Radiolabelling showed a decrease in total neutral glycerolipids and CL synthesis, and ES-MS showed the intensity of many neutral lipid species to be altered and the amount of CL to be depleted. Total inositol lipid species were decreased in the TbCDS RNAi knockdown, as shown by [³H]glycerol and [³H]inositol labelling of lipid. The synthesis of PI itself was not dramatically decreased suggesting that it is of particular importance to the procyclic form *T. brucei*. Poor incorporation of [³H]mannose into glycerolipid indicated the synthesis of GPI anchors to be greatly decreased in the procyclic form TbCDS RNAi cell line, possibly suggesting that the ER localised pool of PI was depleted, or it was being preserved for other uses e.g. PIP signalling. The synthesis of IPC from [³H]inositol was dramatically decreased in the procyclic form TbCDS RNAi knockdown, whilst [³H]serine incorporation into IPC was less affected. ES-MS showed a decrease in IPC species relative to PI species and a change in the species composition of the IPC pool, which may correspond to a decrease in the ER pool of IPC relative to the Golgi pool of IPC.

Depletion of TbCDS activity in the bloodstream form suggested that PS is made from both headgroup exchange with PE and from CDP-DAG, and that synthesis from CDP-DAG is perhaps able to completely compensate for synthesis via PE (Gibellini et al., 2009). However, previous work has indicated that in procyclic form PS synthesis is only achieved from PE (Signorell et al., 2008). Knockdown of TbCDS in procyclic form *T. brucei* resulted in an increase of [³H]serine incorporation into PS, and, similarly to what was seen in bloodstream form, the relative intensities of different PS species was dramatically altered. Since PE is not altered, this may be due to the lack of synthesis of PS occurring via CDP-DAG.

Alternatively, this affect on PS species may be due to the operation of an adaptive pathway to compensate for the reduction in CDP-DAG - for example, as previously described, the synthesis of PG via PS.

Finally, a surprising result of TbCDS RNAi in procyclic *T. brucei*, and in TbCDS knockout and knockdown in bloodstream form *T. brucei* was the increase of PG species. The lack of PG depletion following a decrease in TbCDS was completely unexpected and suggests an alternate route for its synthesis, for example via a phospholipase D like transphosphatidylation possibly by CL synthase or PGP synthase via PS and glycerol. The latter reaction would also explain the increase in PS given that CDP-DAG is not thought to be major source of its synthesis in procyclic form. However, since CL is dramatically decreased in the procyclic form TbCDS RNAi cell line this PG is clearly not sufficient for CL synthesis, either by amount, compartmentalisation or species.

Results provided here show the importance of TbCDS in procyclic form for GPI anchor synthesis, cell cycle and mitochondrial morphology, and its profound impact on the lipid profile of the cell show how central it is to phospholipid and glycolipid synthesis. Additionally, the very different effects of a reduction in TbCDS expression in the procyclic form compared to the bloodstream form emphasises just how different metabolism is between these two life cycle stages.

Chapter 6: Overexpression and Subcellular Localisation of TbCDS in *T. brucei*

6.1 Introduction

Investigation into TbCDS in both bloodstream form and procyclic form *T. brucei* showed it to be an essential gene, and mutants deficient in expression of this gene showed a diverse range of changes in phospholipid metabolism, some of which were entirely unexpected. This suggests that TbCDS has a central role in phospholipid metabolism and regulation, but that its roles are not yet properly understood. One unexpected result was a differential effect on the pool of PI for GPI anchors, indicating that there may also be more than one separately compartmentalised pool of CDP-DAG, possibly produced by a separately localised TbCDS. Additionally, disruption of cell cycle hinted at a role of TbCDS in maintaining PIPs for cell cycle related signalling. An increase in PG species indicated that their synthesis may be possible by another pathway, for example by the phospholipase D like enzyme able to transfer the glycerol headgroup to an existing phospholipid.

The aim of this chapter is to further investigate the role of TbCDS in both bloodstream form and procyclic form *T. brucei* by creation and characterisation of over-expressing cell lines and examining the subcellular location of the TbCDS protein.

Overexpression of *E. coli* CDS on a runaway replication plasmid in *E. coli* had little effect on overall phospholipid synthesis, though it did appear to increase competition for limiting CTP (Icho et al., 1985). Similarly, overexpression of human CDS1 cells had little effect COS-7 cells (Lykidis et al., 1997). Overexpression of the *E. coli* CDS improved competition for the substrate CTP (Icho et al., 1985). In yeast, an increase of CDS expression led to an increase in PIS activity, but a decrease in PSS activity and an increase in cellular PA (Shen and Dowhan, 1997).

6.2 TbCDS Overexpression in Bloodstream Form *T. brucei*

The TbCDS open reading frame was cloned into the pLEW82 overexpression vector. In pLEW82 a T7 promoter with three tetracycline operators drives the inserted gene and a constitutive 10% T7 promoter drives a phleomycin resistance gene (BLE) (Wirtz et al., 1999). This plasmid integrates into the rRNA spacer region and produces very high expression of the cloned gene producing HA-tagged protein, and is therefore excellent for subcellular localisation studies. TbCDS was PCR amplified from genomic *T. brucei* DNA using the CDS p82 F and CDS p82 R primers (Table 2.1) and cloned into pLEW82. The plasmid was linearised and transfected into bloodstream form *T. brucei* cells as described in Chapter 2, and transformants were selected for with phleomycin.

Several attempts to create a bloodstream form *T. brucei* cell line containing the pLEW82 copy of TbCDS were unsuccessful despite the success of control transformations. It was proposed that overexpression of the TbCDS may be lethal to *T. brucei*, and that the level of leaky expression of TbCDS from the T7 promoter that was occurring was sufficient to make the cells unviable. Previously, bloodstream form *T. brucei* had been transfected with a pLEW100 copy of TbCDS as a tetracycline inducible ectopic copy for the creation of a conditional knockout (Chapter 4). Tetracycline induced expression of TbCDS from the procyclin promoter (GPEET) in pLEW100 did not cause lethality in this cell line, which argued against the hypothesis that overexpression of TbCDS was lethal, although expression from GPEET is considerably lower than that from the T7 promoter and there is a chance that leaky expression from the T7 promoter may exceed expression from GPEET. In order to see the effect of TbCDS expression from the pLEW100 in TbCDS, and to address why the pLEW82 TbCDS transfected *T. brucei* were not surviving, cell counts were performed with the bloodstream form TbCDS pLEW100 cell line in the presence and absence of tetracycline.

6.2.1 Growth Phenotype of Bloodstream Form *T. brucei* over expressing TbCDS

Figure 6.1 shows growth curves from cell counts performed over 150 hours. Surprisingly, overexpression of TbCDS pLEW100 initially appeared to have a stimulatory affect on growth, however after 120 hours growth was occurring at a

normal rate. If overexpression of TbCDS is initially creating a competitive advantage, it is difficult to see why the TbCDS pLEW82 cell line was not viable. It is possible that this overexpression of TbCDS is using up more CTP than is sustainable.

To further investigate this, lipids were harvested from the bloodstream form TbCDS pLEW100 cell line 48 hours after the addition of tetracycline, analysed by ES-MS and the spectra compared with those of wild type.

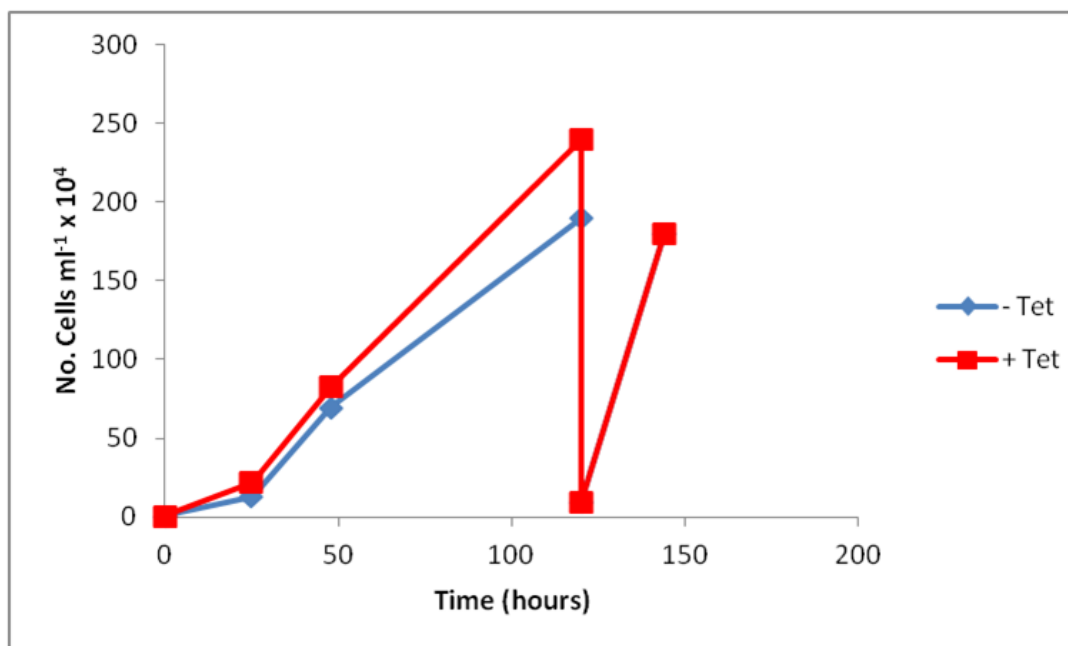


Figure 6.1. Overexpression of TbCDS in BSF *T. brucei* results in an initial increase in growth rate. Cell counts were performed in the presence and absence of tetracycline in order to switch on and off expression of the exogenous TbCDS copy inserted using pLEW 100.

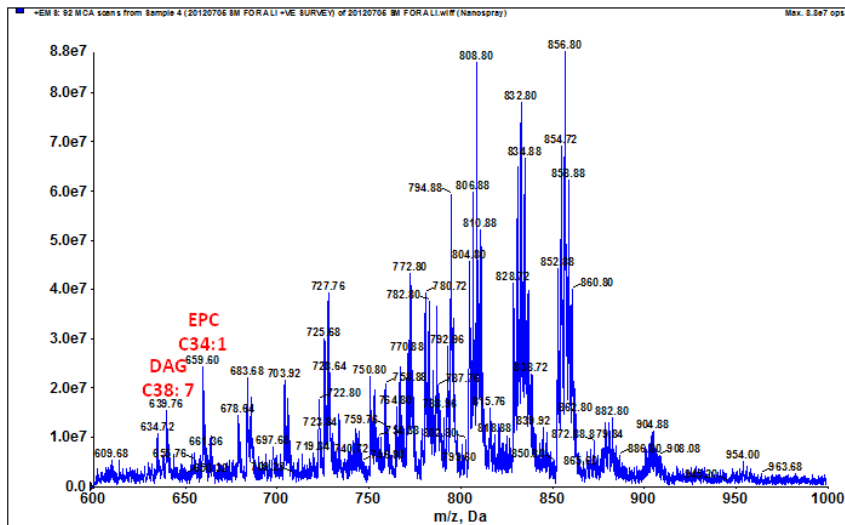
6.2.2 Lipidomics of Bloodstream Form *T. brucei* over expressing TbCDS

6.2.2.a Positive Survey Scan

A positive survey spectrum of total lipids from TbCDS pLEW100, 48 hours after the addition of tetracycline (Figure 6.2) showed a slight reduction in DAG C38:7 species at 679.76 m/z in comparison to the SM scan - from 0.16 of PC C40 in the SM to not above background in the TbCDS p100 + tetracycline. The decrease in DAG species is the converse to what was seen in the bloodstream form TbCDS p2T7 and the bloodstream form TbCDS CKO, where such species increased, probably as a result of

the phosphorylation of accumulating TbCDS substrate PA, which is not being used to synthesised downstream lipids. If the increase in TbCDS expression is increasing CDP-DAG production, PA will be getting used up at a greater rate than in wild type, and since the pool of PA species is utilised to make both CDP-DAG and DAG it is not surprising that the DAG pool is depleted. Such a depletion of DAG is likely to have a knock on affect on the Kennedy Pathways, to which it is the precursor. The positive survey scan shows an increase in PE a-C36 species, mostly a-C36:3 - from 0.44 of PC C40 to 1.04. This may be an adaptation to a decrease in other species of PE as a result of a decrease in PA for DAG. It seems unlikely that TbCDS would be using up a-C36 PA, since a-C36 species of the downstream products of TbCDS, PI or PG, are rarely found. There is a relative increase in a peak at 808.8 m/z - corresponding mostly to PC C36:4 in comparison to the peak at 856.7 m/z (PC C40:6) - from 1.23 to 2.26. A more obvious change is the decrease of the peak at 832 m/z which corresponds to the sodium adduct of the PC species C38:4 and the positive ion of PC species C40:7 from 0.87 to 0.54 of PC C40. A decrease in PC C40:7 would appear to tie in well with the knowledge that PI C40 and PG C40 species are common and likely PA C40 species are being used up by the over-expressed TbCDS, however due to the presence of sodium adducts these results are difficult to interpret on their own.

A. SM



B. TbCDS p100 + tetracycline

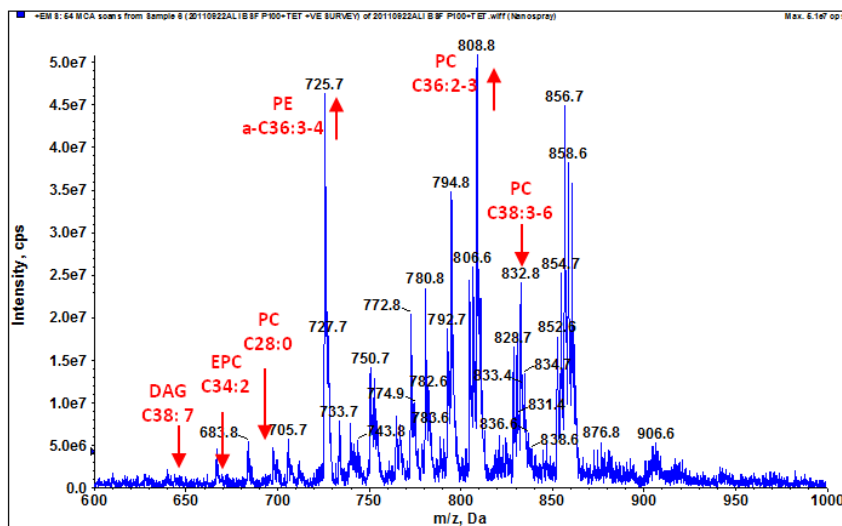


Figure 6.2. Positive ion survey scan of lipids from SM and bloodstream form and TbCDS pLEW100 + tetracycline A. Wild type single marker cells (SM). B. BSF TbCDS over-expressing cell line in the presence of tetracycline for 48 hours. DAG = diacylglycerol species, TAG = triacylglycerol species, PI = phosphatidylinositol species, PE = phosphatidylethanolamine, EPC = ethanolamine phosphorylceramide. Red arrows and text indicate peaks which are different in the mutant, whilst the direction of the arrow indicates whether this peak is increased or decreased in the mutant. CX:Y = X – total number of carbons, Y – total number of double bonds in fatty acid chains of lipid species. e = alkenyl-acyl- linked lipid, a = alkyl-acyl- linked lipid.

6.2.2.b Negative Survey Scan

Figure 6.3 shows the negative survey scan of total lipids in bloodstream form TbCDS pLEW100 compared to that of SM cells. The increase in PE a-C36 that was seen in the bloodstream form TbCDS pLEW100 compared to SM in the positive survey scan is also

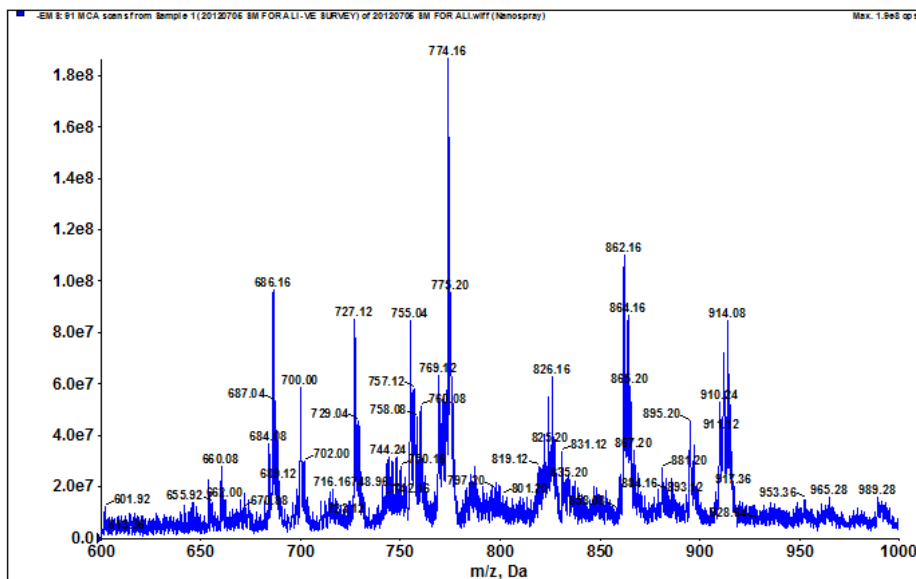
clear here (Figure 6.2) from 0.47 to 0.77 of a-C36 PS. Decreases in PA C36 (0.52 of a-C36 PS to not above background) and PA C40 (from 0.45 to 0.18 of a-C36 PS) are possibly due to increased utilisation by TbCDS for incorporation into C36 and C40 PI.

What is surprising, though, is an increase in the PG species at m/z 826 previously identified as PG C40 from 0.33 to 0.53 of PS a-C36. This species was significantly increased in both bloodstream form and procyclic form TbCDS knockdowns and the bloodstream form TbCDS CKO. That it was increased in these mutants deficient in TbCDS appeared to indicate that it was not synthesised from CDP-DAG but may, for example, be synthesised by headgroup exchange with another phospholipid, possibly PS, though PS itself is not increased. It seems strange that both depletion and increase in TbCDS should cause a similar increase in this species. It is possible that synthesis of this species of PG is easy to control for adaptive purposes, and that can be synthesised via both CDP-DAG and another alternative mechanism as described previously, and that it is synthesised as a general response to alteration in lipid content. Indeed, an increase in certain PG species have previously been observed in knockouts of ethanolamine cytidyltransferase (Gibellini et al., 2009) and choline kinase (Simon Young - manuscript in preparation) in bloodstream form *T. brucei*.

Even more surprising is that the PI species appear to be decreased relative to PS a-C3 - PI C36 decreases from 0.6 to 0.28 of PS a-C36, whilst PI C40 decreases from 0.45 to 0.37. A decrease in PI C36 at 862 m/z relative to PI C40 at m/z 914 is visible - from 1.29 PI C36:PI C40 to 0.75. This is the same that was seen in all TbCDS deficient mutants and was considered to be an indication of a decrease of the pool of PI for GPI anchors, however in the TbCDS RNAi and knockout the difference was much more pronounced. It is likely that in this case, an increase in PI C40 rather than a decrease in PI C36 is occurring, and there is an increase in PE, PG and PS. If the production of CDP-DAG is the rate limiting step, one would expect PI to increase, however If PI is not increased its production is likely to be limited by something else, possibly the production or acquisition of inositol. If PI C40 is increased relative to PI C36 it may be because the flux through the ER PI C36 pathway is accelerated so that PI pools do not build up despite the increase in PI synthesis because the excess PI is immediately utilised in GPI anchor production. The increase seen in the C40 PI pool may be a result of these PI species not being further utilised to the same extent. It could also be that too much PI in the ER is a bad thing, causing transport of this PI pool to the Golgi, or turnover by PI-PLC back to inositol-phosphate and DAG.

Interestingly, a peak appears at 963.1 m/z which could be TAG C60:5, but is more likely to be PIP C38 since it is not seen in the positive survey scan. This shows that an increase in TbCDS expression is increasing the PI C38 species which is then being dephosphorylated to PIP C38. Increase in the PIP C38:4 species was also seen in the procyclic form TbCDS RNAi where it was considered to be an indication that due to depletion of the PI C36 pool the PI C38 pool was being utilised for PIP signalling. This could also be true of the TbCDS pLEW100 overexpression mutant but in this case it would be excess of the PI C38 pool rather than depletion of the PI C36 pool which is causing the change. The PI C38 pool is a relatively minor component of total PI in *T. brucei*, and does not appear to be increased in the TbCDS pLEW100 compared to the SM. There is a possibility that this species is normally used for signalling, and its build up means the signal is not being sent.

A. SM



B. TbCDS p100 + tetracycline

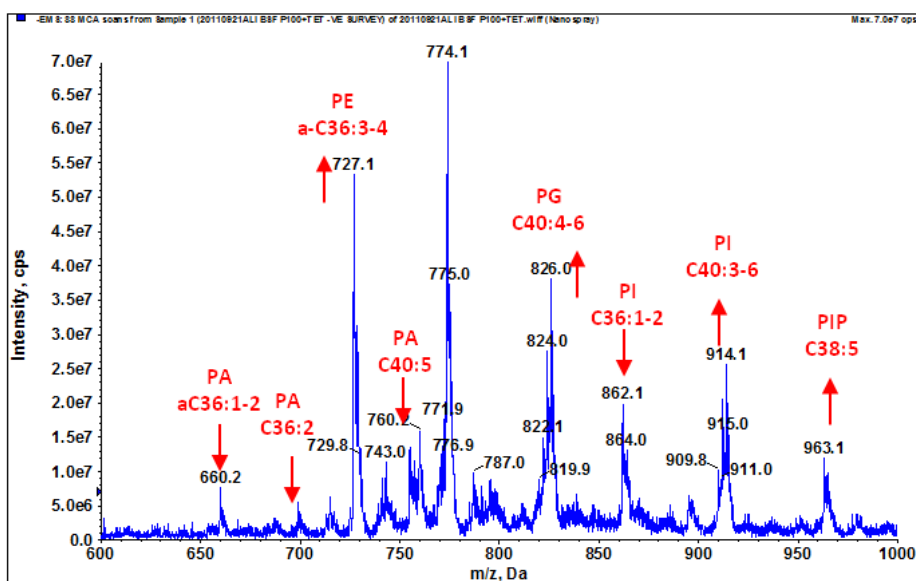
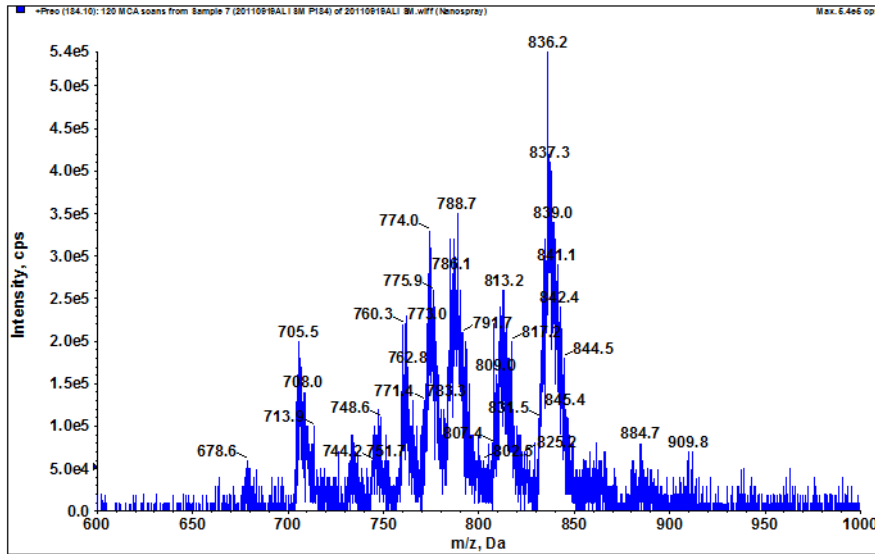


Figure 6.3 Negative survey scan of lipids from SM and bloodstream from TbCDS pLEW100 + tetracycline. A. wild type single marker cells (SM). B. BSF TbCDS RNAi cells grown in the presence of tetracycline for 42 hours. PA = phosphatidic acid species, PE = phosphatidylethanolamine species, PS = phosphatidylethanolamine species, PG = phosphatidyl glycerol, PI = phosphatidyl inositol., PIP = phosphatidylinositol-phosphate. For further annotation, see Figure 6.2.

6.2.2.c Choline-Phosphate Containing Lipids

Precursor ion scanning for choline-phosphate containing lipids (Figure 6.4) gave a clearer outline of what was happening to the pools of PC species than was obtained by a survey scan for positive ions alone, due to the presence of sodium adducts in the latter. In fact, the distribution of choline-phosphate containing lipids was not much altered. Whilst there is a slight increase in the intensity of the series containing C36 PC with respect those containing C38 (1.32 to 1.48) and C40 PC (0.63 to 0.74), there is no decrease in PC C38 compared to PC C40. Instead, there is a decrease in the series containing SpM C16:0 and C30 PC at about 706.5 m/z from 0.36 to 0.12 of PC C40, along with a slight decrease in PC C28 that was also seen in the positive survey scan. At the other end of the m/z scale the series containing C44 PC at 885 m/z is increased in comparison to in the wild type from 0.14 to 0.29 of PC C40. All these changes are identical to those seen in the bloodstream from TbCDS RNAi and TbCDS CKO, which is very surprising and may suggest some kind of adaptation mechanism to perturbation in lipids that occurs irrelevant to the lipids that are perturbed.

A. SM



B. TbCDS p100 + tetracycline

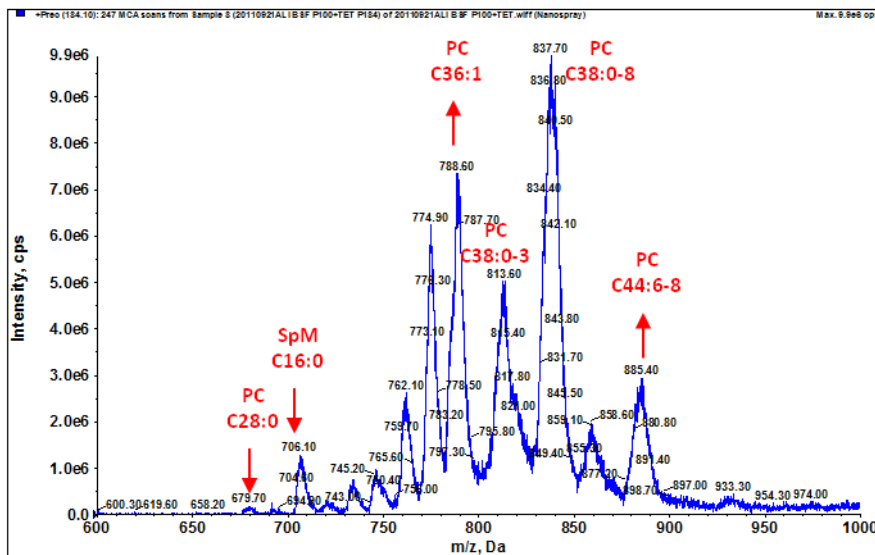
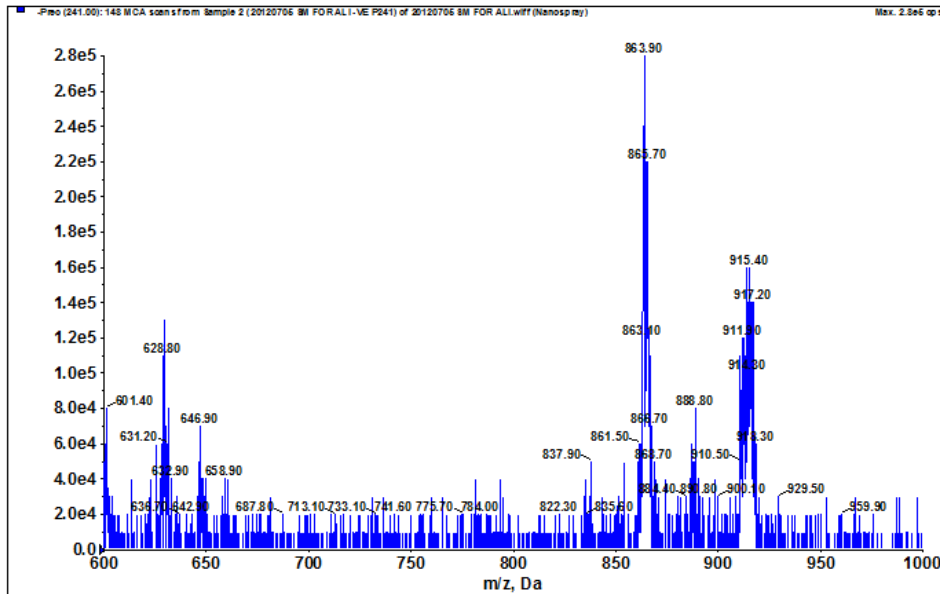


Figure 6.4. Mass spectrometric analyses of choline-phosphate containing phospholipids from SM and bloodstream form TbCDS pLEW100 + tetracycline. Total lipids were analysed by ES-MS in positive ion mode using parent-ion scanning of the collision induced fragment for phosphorylcholine at 184 m/z . A. wild type single marker cells (SM). B. BSF TbCDS p100 over-expressing cell line grown in the presence of tetracycline for 48 hours. SpM = sphingomyelin. For further annotation see Figure 6.2.

6.2.2.d Inositol-Phosphate Containing Lipids

From the scan for inositol phosphate containing lipids (Figure 6.5), the decrease in the pool containing C36 PI in comparison to the pool containing C40 PI is very obvious - from 1.24 to 0.56. Without an internal standard it is not possible to say whether this is due to an increase in PI C40 or a decrease in C36. If it is assumed that there is an increase in PI due to overexpression of TbCDS creating more CDP-DAG as precursor to TbPIS, the increase in PI C40 over PI C36 is likely because the flux through the ER PI pathway for GPI anchors is much higher and the increase in PI is immediately translated into a change in GPI, so that the absolute pool of PI does not change, however the Golgi localised pool containing C40 PI is not utilised further for GPI anchors and therefore is increased relative to the C36 series.

A. SM



B. TbCDS p100 + tetracycline

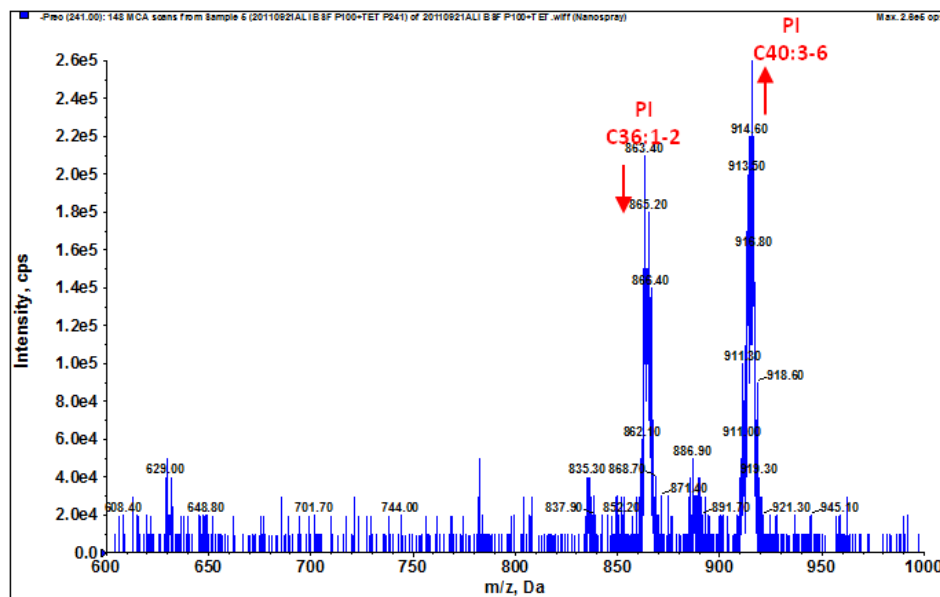


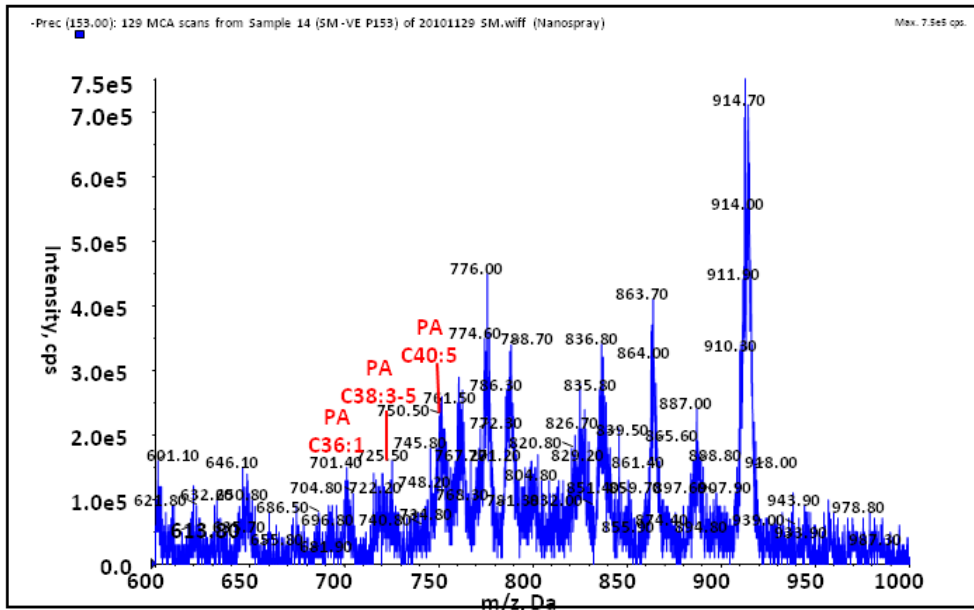
Figure 6.5. Mass spectrometric analyses of inositol-phosphate containing phospholipids from SM and bloodstream form TbCDS pLEW100 + tetracycline. Total lipids were analysed by ES-MS in negative ion mode using parent-ion scanning of the collision induced fragment at 241 m/z . A. wild type single marker cells (SM). B. BSF TbCDS p100 grown in the presence of tetracycline for 48 hours. For further annotation see Figure 6.2.

6.2.2.e Glycerol-Phosphate Containing Lipids

In the scan for glycerol-phosphate containing lipids (Figure 6.6) it is difficult to find a point for comparison between the two scans. PI species are decreased relative to PG species, which may indicate an increase in PG rather than a decrease in PI. PG C36 is increased from 1.32 to 2.42 of PG c38, whilst PG C40 increases from 0.57 to 1.46 in comparison to this peak. PI C36, however decreases from 1.2 to 0.96 and PI C40 decreases from 2.18 to 0.8 of the same, PG C38 peak. Increase in PG species was seen a response to a decrease in TbCDS in the TbCDS RNAi and TbCDS CKO, and it is therefore surprising that they are also increased as a response to an increase in TbCDS, however, as discussed earlier there is evidence that increase in PG species may be a general cellular response to glycerophospholipid synthesis disruption (Gibellini et al., 2009), Simon Young, manuscript in publication. In this case it could simply be that excess CDP-DAG is being converted to PG species because they are less charged and unlikely to perturb membrane dynamics.

The increase in PI C40 relative to PI C36 is clear here, and has been discussed earlier.

A. SM



B. TbCDS p100 + tetracycline

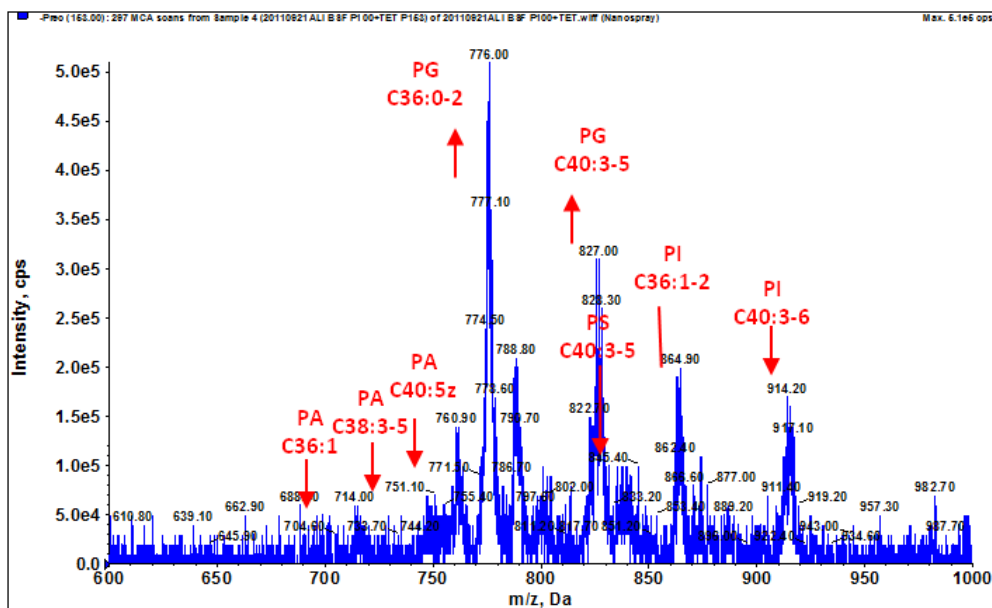


Figure 6.6. Mass spectrometric analyses of glycerol-phosphate containing phospholipids from SM and bloodstream form TbCDS pLEW100 + tetracycline. Total lipids were analysed by ES-MS in negative ion mode using precursor ion scanning for the collision induced fragment for glycerol-phosphate at 153 m/z . A. wild type single marker cells (SM). B. BSF TbCDS p100 overexpression cell line in the presence of tetracycline for 48 hours. For further annotation see Figure 6.2.

6.2.3 Subcellular Localisation of TbCDS in Bloodstream Form *T. brucei*

The differential effects that were seen of both depletion of TbCDS expression and TbCDS overexpression on the two different PI pools in bloodstream form *T. brucei* strongly suggest two separate pools of CDP-DAG that may be synthesised by separately localised TbCDS enzymes. In order to examine the subcellular localisation of TbCDS, it was necessary to create a bloodstream form *T. brucei* cell line overexpressing a tagged copy of TbCDS. pLEW100 is not the vector of choice for subcellular localisation studies due to its relatively low expression level. Clearly, TbCDS does not need to be expressed at a high level in *T. brucei* since the double knockout containing the pLEW100 copy of the TbCDS was viable in the presence of tetracycline. Moreover, expression of the TbCDS open reading frame in bloodstream form *T. brucei* has been shown to have affects on growth and biochemical phenotype. Additionally, viability of the cell line expressing only the pLEW100 TbCDS copy confirms that the protein is correctly expressed and localised. However, when total protein was extracted from bloodstream form TbCDS pLEW100 + tetracycline no HA tagged protein could be detected by Western blot. Furthermore, immunofluorescence microscopy did not detect any signal above background in fixed cells of this cell line in the presence of tetracycline. Since previous results indicate that TbCDS is being expressed from the pLEW100 construct, these results simply show that expression of the HA tagged TbCDS is below detectable levels. However, it was previously observed that in the TbCDS double knockout carrying the tetracycline induced pLEW100 copy of TbCDS, HA tagged protein was easily detectable by Western blot of total protein. This observation indicated that the expression or stability of the pLEW100 TbCDS was in some way suppressed when the cell did not need it, indicating that too much TbCDS activity is harmful for the cell - possibly, for example, due to PIP disruption or other anionic phospholipid mis-regulation. This also supports the hypothesis that the harmful effect of TbCDS overexpression was the reason for failure of transfection with pLEW82 TbCDS.

For this reason, bloodstream form TbCDS double knockouts with ectopic TbCDS pLEW100 overexpression were used for subcellular localisation studies. In order to examine the subcellular localisation of TbCDS, cells were grown in the presence of tetracycline and harvested and fixed as described in chapter 2. The cells were stained against the HA tagged protein and for the ER localised BiP protein (Bangs et al., 1993)(Figure 6.7). The strongest signal from HA-tagged TbCDS comes from the

region between the nucleus and kinetoplast, whilst punctuate staining is visible throughout the cell. Since TbCDS is a membrane protein this pattern of staining indicates that it is localised to the membrane of subcellular organelles rather than the plasma membrane. Intense staining between the nucleus and kinetoplast is indicative of a Golgi localisation, which has previously been shown in the downstream enzyme TbPIS and is consistent with a requirement of CDP-DAG for the synthesis of bulk cellular lipid, whilst perinuclear staining and staining throughout the cell could be indicative of ER localisation where TbCDS could supply CDP-DAG required for the ER localised TbPIS to make PI for GPI anchors. Some co-staining of TbCDS with the ER protein BiP does occur, particularly between the nucleus and the kinetoplast, although co-staining is not complete and some punctuate staining of TbCDS appears to occur out with the ER. Even within the ER, TbCDS is not evenly distributed and it may be present in specific areas of the ER (i.e. between the nucleus and the kinetoplast), the mitochondrial associated membranes or even, perhaps, in the mitochondrion.

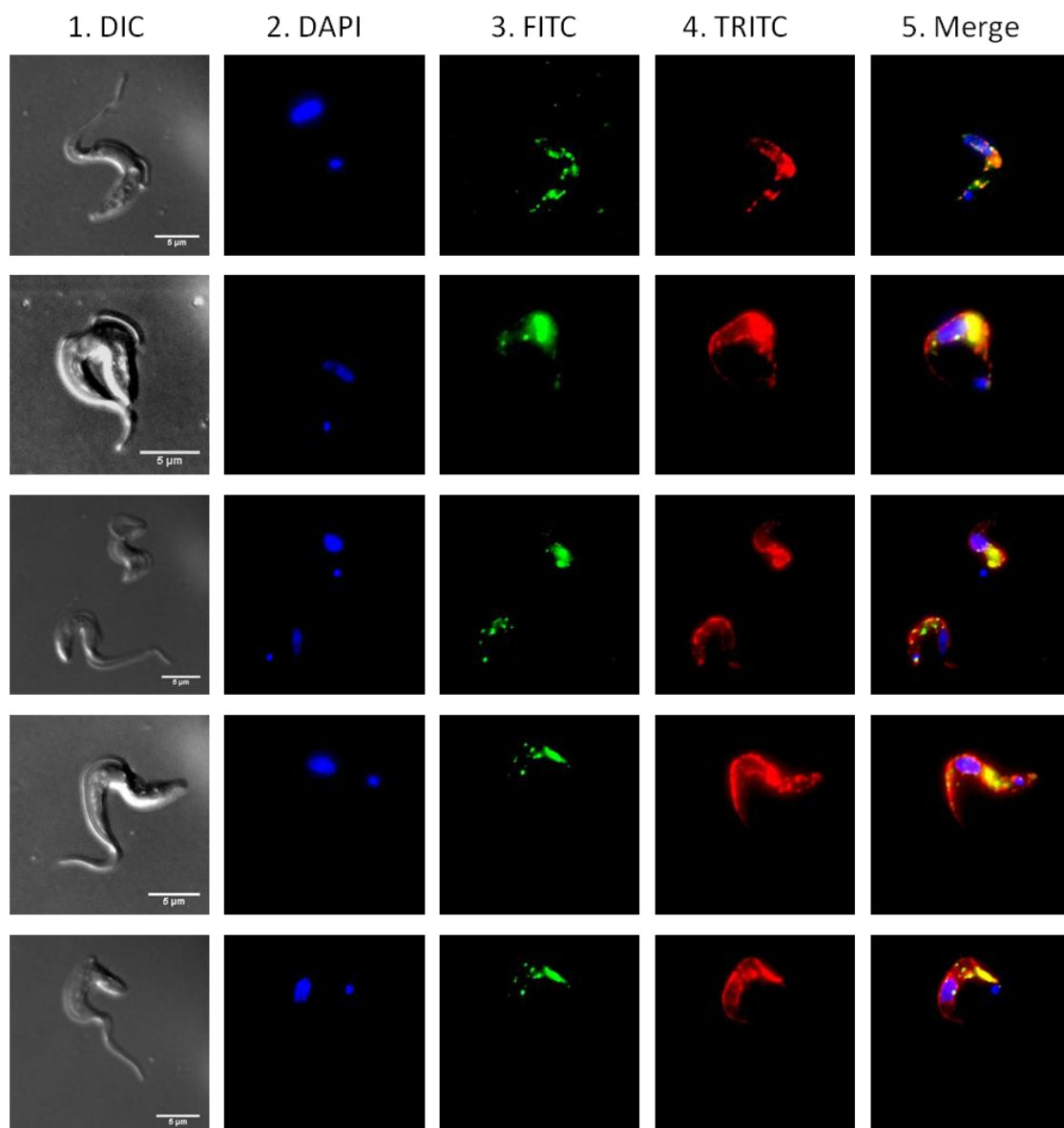


Figure 6.7. Subcellular localisation of TbCDS-HA in TbCDS conditional knockout bloodstream form *T. brucei*. Cells expressing TbCDS-HA were costained for the nuclear marker DAPI, the HA epitope and the ER marker BiP. 1. DIC image. 2. DAPI staining. 3. HA epitope staining and FITC detection. 4. BiP staining and TRITC detection. 5. Merged image.

6.3 Overexpression of TbCDS in Procyclic Form *T. brucei*

Knockdown of TbCDS in procyclic form *T. brucei* showed some phenotypic and biochemical differences compared to knockdown of TbCDS in bloodstream form *T. brucei*. The cell cycle stall - predicted to be a result of depletion in PI for PIP signalling and/or IPC - was more dramatic. The PI species themselves were less affected and instead the synthesis of IPC species, not present in the bloodstream form, was decreased. Additionally, synthesis of the mitochondrial phospholipid CL was decreased and, possibly along with IPC depletion, resulted in loss of membrane potential in the mitochondrion. These results indicate different CDP-DAG requirements between the two cell types, and therefore overexpression is likely to cause different effects in procyclic form, and subcellular localisation of TbCDS may also differ. To further investigate the difference in the function of TbCDS in the procyclic form, overexpression of this enzyme was performed in these cells.

Transformation of procyclic form *T. brucei* with the pLEW82 TbCDS construct was attempted, and several clones were obtained by selection with phleomycin. The procyclic form pLEW82 TbCDS cells were induced with tetracycline, cells were fixed and protein harvested at 48 hours after induction to look for expression of the HA-tagged TbCDS. Neither Western blot nor immunofluorescence microscopy revealed any signal from HA tagged protein in any of the clones. It seemed unlikely that expression was below detection levels, as appeared to be the case in the bloodstream form TbCDS pLEW100 cell line containing both endogenous alleles, since expression of HA-tagged protein should be clear from pLEW82 due to the strong T7 promoter in this vector. It therefore seemed that these transformants were aberrant in some way, for example losing the T7 promoter driving TbCDS but not the 10% T7 promoter driving phleomycin resistance. In any case, they were clearly not suitable for subcellular localisation experiments.

As in bloodstream form, a procyclic form TbCDS pLEW100 cell line had been created as the first stage of a conditional knockout. This TbCDS pLEW100 cell line was therefore used in order to study overexpression of TbCDS on total cellular lipids. This also allowed direct comparison with the bloodstream form pLEW100 TbCDS overexpression cell line.

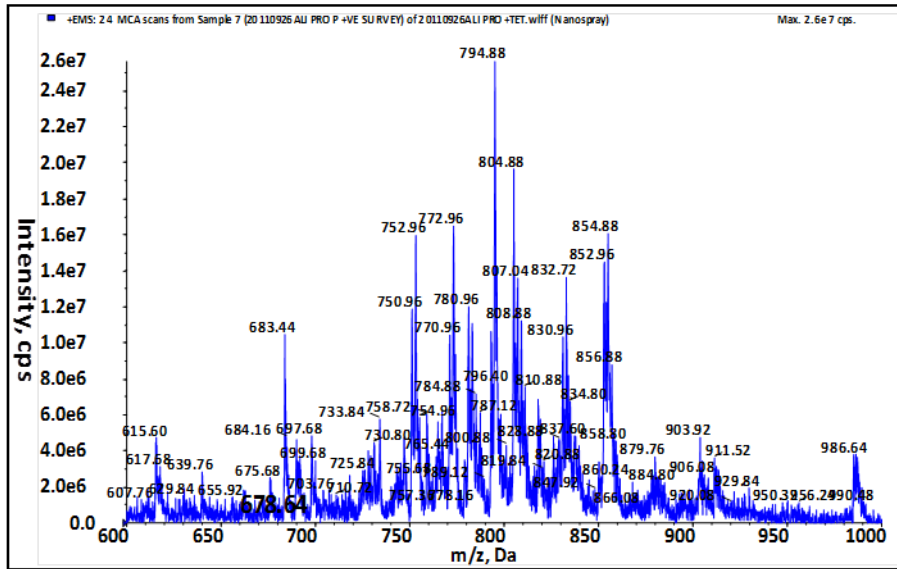
6.3.1 Lipidomics of Procyclic Form *T. brucei* overexpressing TbCDS

6.3.1.a Positive Survey Scan

The positive survey scan of total lipids from procyclic form TbCDS pLEW100 + tetracycline showed considerable differences to one from DM (Figure 6.8) but the changes were different to those in bloodstream form TbCDS pLEW100. In bloodstream form TbCDS pLEW100 the DAG series C38 was clearly decreased with respect to SM whilst the procyclic form TbCDS pLEW100 survey scan shows a significant increase in this series, mostly DAG C38:7, from 0.15 to 0.4 of PC C36. There was also a slight increase in DAG C40:10 (present as a sodium adduct at 683.6 m/z) from 0.52 to 0.71 of PC C36. An increase in DAG species was also seen in the procyclic form TbCDS RNAi knockdown where it was proposed to be due to phosphorylation of the accumulating pool of PA species as unused precursor to CDP-DAG. Here, this is clearly not the case since TbCDS is overexpressed, however excess phospholipids may be being broken down into these DAG species. Unused host fatty acids (e.g. C20:4) may also be incorporated into DAG. Since DAG is neutral it is unlikely to perturb membrane dynamics dramatically.

A change in the distribution of PC species is another surprising similarity to the procyclic form TbCDS RNAi. The intensity of shorter chained species PC a-C36 and is decreased in the procyclic form TbCDS pLEW100 relative to the peak corresponding to PC C36 - from 1.29 to 0.81 of PC C36. PC C40 is increased with respect to PC C36 from 0.79 to 1.48. The choline containing phospholipid species were studied more specifically by scanning for precursors of the unique choline-phosphate ion at 184 m/z. This is shown in Figure 6.10 and will be discussed later.

A. DM



B. TbCDS p100 + tetracycline

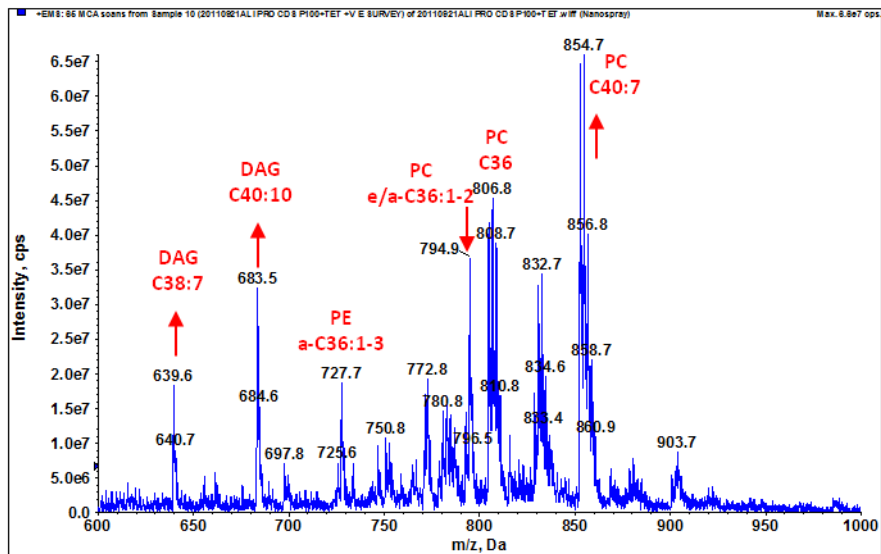


Figure 6.8. Positive ion survey scan of lipids from DM and procyclic form TbCDS pLEW100 + tetracycline. Mass spectrometric analyses of total phospholipids by positive survey scan ES-MS. A. wild type double marker (DM) cells. B. PCF TbCDS p100 overexpression cells grown in the presence of tetracycline for 48 hours. For further information see Figure 6.2.

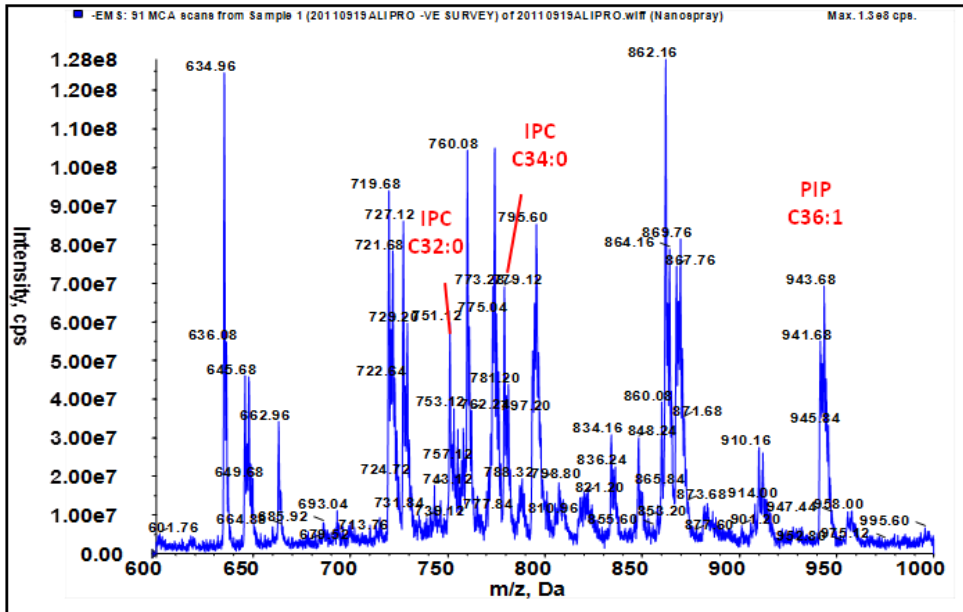
6.3.1.b Negative Survey Scan

The negative survey scan of total lipids from procyclic form TbCDS pLEW100 shows significant difference in the distribution of anionic phospholipid species compared to the DM scan (Figure 6.9). This is not surprising given the purported role of CDP-DAG in regulating ionic lipids (Sato et al., 2000). In yeast for example, overexpression of TbCDS resulted in an increase in PI synthesis and a decrease in PS synthesis (Shen and Dowhan, 1996).

Intense peaks in the DM scan at 634, 645 and 662 m/z correspond to PA species, but are probably artefacts because they are not usually present in the negative survey scan and are not visible in the glycerol-phosphate scan.

There may be a decrease in the key PE species - a-C36:2-4 - relative to other species. However, an absolute decrease in this PE species is unexpected since it was increased in the bloodstream form TbCDS pLEW100 and does not contain a lipid moiety which is common in products of the CDP-DAG pathway. Again, it is possible that there is no change in this species, and that instead the other anionic phospholipids are increased. If PE a-C36 is used as a baseline for comparison, PI species are increased - PI C36 from 1.5 to 2.6 of PE a-C36, and PI C40 from 0.33 to 0.88. and this would make sense as a result of the overexpression of TbCDS. There is also an intense peak at 774 m/z which increases from 1.2 to 2.6 of PE a-C36. This may correspond either to PS a-C36:2 or PG C36:2 and cannot be determined without further fragmentation. A large increase in PG and no change in PS would fit in best with the bloodstream form results for overexpression of TbCDS, and could easily be explained by an increase in TbCDS making more CDP-DAG for PG synthesis, whilst a modest increase in synthesis of PS a-C36 may result in a decrease in a-C36 PE, although there would not appear to be any reason for this.

A. DM



B. TbCDS p100 + tetracycline

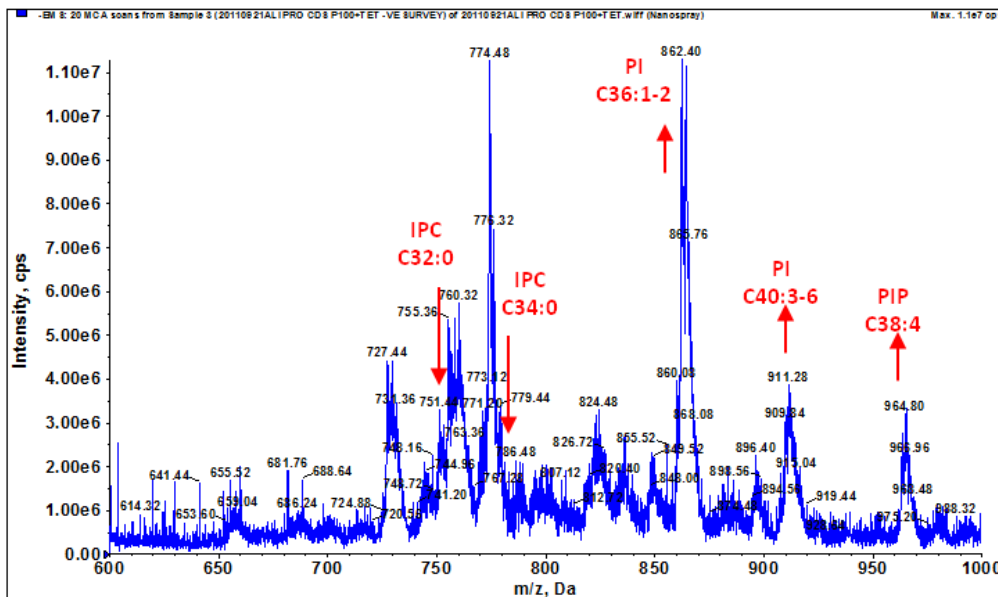


Figure 6.9. Negative survey scan of lipids. Mass spectrometric analyses of total phospholipids by negative survey scan ESI-MS. A. Wild type double marker cells (DM). B. PCF TbCDS pLEW 100 cells grown in the presence of tetracycline for 96 hours. PI = phosphatidylinositol. IPC = inositol phosphorylceramide. TAG = triacylglycerol. For key to annotation, see Figure 6.2.

Both main PI series are increased, whilst IPC species are decreased - IPC C32 from 0.66 to 0.42 and IPC C34 from 0.81 to 0.46 of PE α -C36. This would suggest that IPC synthesis is more tightly regulated and that perhaps the availability of ceramide is limiting in this life cycle stage rather than the availability of PI.

Finally, a species at 943 m/z in the DM which could be TAG C58:1 or PIP 36:1 is replaced by a peak at 964.8 m/z in the procyclic form TbCDS pLEW100 + tetracycline which could be TAG C60:4 or PIP C38:4. Since these species were not seen in the positive survey scan it seems unlikely that they are TAG species. Increase in the PIP C38:4 species seen in the procyclic form TbCDS RNAi and the bloodstream form TbCDS pLEW100 overexpression mutant, where it may be linked a decrease in the ratio of the PI C36 pool with respect to other PI species. Here there does appear to be a slight increase in the PI C38 pool.

6.2.3.c Choline-Phosphate Containing Lipids

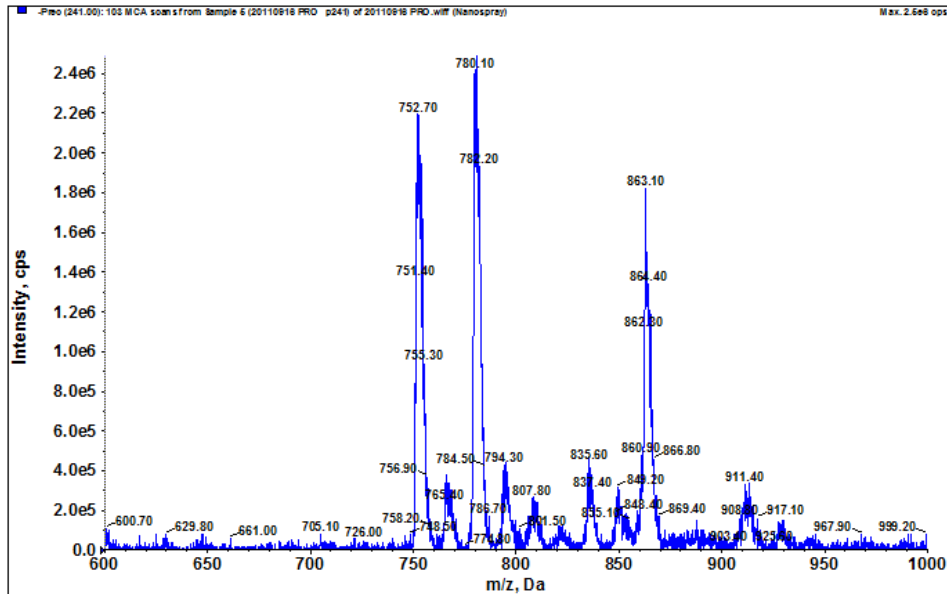
A change in the distribution of PC species was seen in the positive survey scan of TbCDS pLEW100 + tetracycline lipids in comparison to the DM positive survey scan. This was confirmed by scanning specifically for choline-phosphate containing lipids. Figure 6.10 shows precursors to choline-phosphate ion in the DM and the TbCDS pLEW100 + tetracycline and it is clear that there is a change in the ratio of PC ϵ / α -C36 to PC C40 from 1.4 to 0.66. This is a similar pattern to that which was seen in the procyclic form TbCDS RNAi knockdown and it is again extremely unexpected that overexpression of TbCDS would have similar effects to knockdown. A decrease in ϵ / α -C36:1-3 is particularly unexpected since this lipid moiety is not commonly incorporated into any of the downstream lipids of the CDP-DAG pathway.

6.2.3.d Inositol-Phosphate Containing Lipids

The scan for inositol-phosphate containing lipids shows an increase in the PI species of TbCDS pLEW100 + tetracycline with respect to the IPC species compared to the DM scan (Figure 6.11). This indicates that whilst PI species are increased by the increase in precursor CDP-DAG due to TbCDS activity, this is not translated into a corresponding increase in IPC synthesis from the increased PI, possibly due to limiting amounts of ceramide, which may be tightly regulated due to its use as a signalling molecule.

In bloodstream form *T. brucei* a significant increase in the C36 PI series was not seen, and therefore the PI C40 series appeared relatively increased. The explanation given for this was that the flux through the ER PI pathway to GPI (involving predominantly C36 PI) is very high and that any increase in PI would be utilised for incorporation into GPI anchors and therefore would not lead to an increase in the PI C36 pool. The increase the ratio of PI C36 with relative to the IPC pools of TbCDS pLEW100 that is seen in Figure 6.11 - from 0.74 to 1.2 of IPC C32 and 0.61 to 1.3 of IPC C34 - helps to confirm this, since the flux of the GPI biosynthesis pathway is not nearly as high in procyclic form due to less of a demand for GPI anchors - this is supported by the fact that there is normally less PI C36 in double marker. Therefore, the increase in the pool of PI as a result of TbCDS overexpression is not translated into an increase in GPI anchor and so PI C36 accumulates, and the increase can be seen by ES-MS. This gives further evidence that the ER and Golgi pools of PI are separately regulated in both bloodstream form and procyclic form and further indicates the need for separate pools of CDP-DAG which may be achieved by TbCDS in more than one subcellular location, as is the case with TbPIS.

A. DM



B. TbCDS p100 + tetracycline

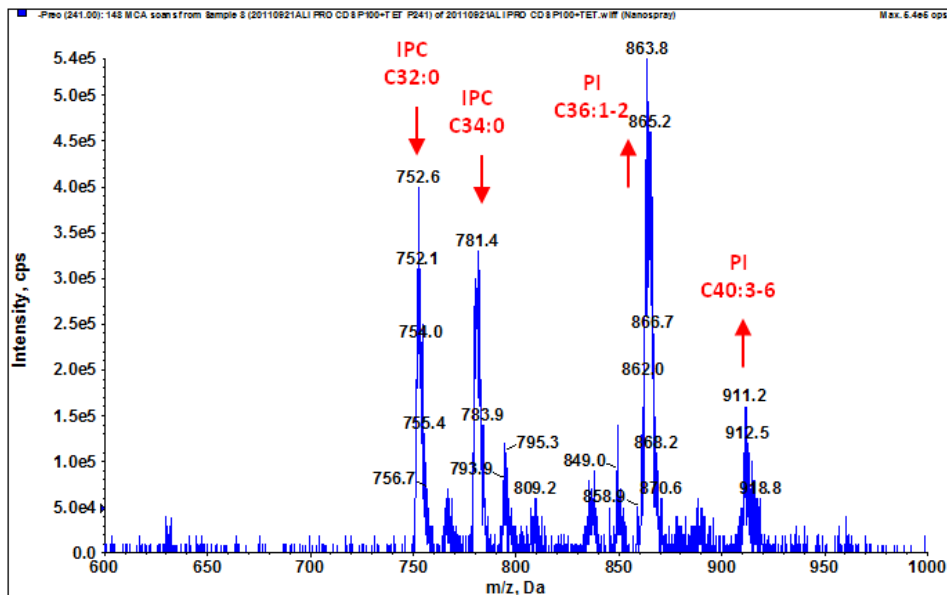
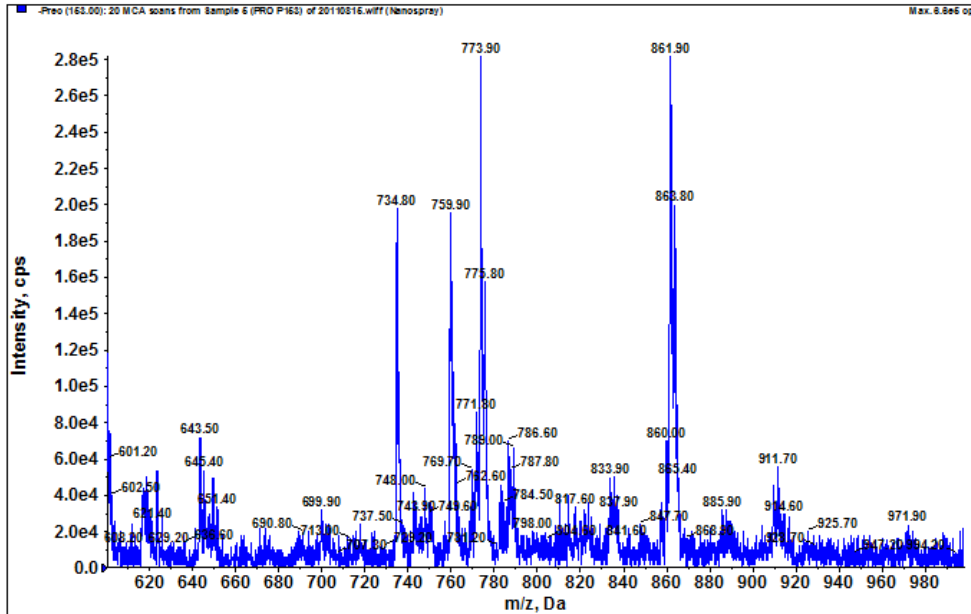


Figure 6.11. Mass spectrometric analyses of inositol-phosphate containing phospholipids. Total lipids were analysed by ESI-MS in negative ion mode using parent-ion scanning of the collision induced fragment at 241 m/z . A. wild type double marker cells (DM). B. PCF TbCDS p100 overexpression cells grown in the presence of tetracycline for 48 hours. For further information see Figure 6.2.

6.2.3.e Glycerol-Phosphate Containing Lipids

To look particularly for changes in the precursor and product phospholipids of CDP-DAG - PA and PG - which are not always easy to see in survey scans, a negative ion scan was performed for precursors of the glycerol-phosphate ion at m/z 153 (Figure 6.12). The scan is difficult to interpret because it cannot be said which phospholipids are actually increased as there is no baseline for comparison. If it is assumed that PI species are increased, as indicated from the negative survey scan, then there is a large increase in the peak at 774 m/z - from being 1:1 with the PI C36 peak to being 1.7 of it. This peak corresponds to PG C36:3 (fragmented in Chapter 7, Figure 7.9) which ties in with the increase in CDP-DAG as a precursor to PG. This increase is relative to the decrease which is seen in the corresponding alkyl-acyl-C36:2 PG species from 0.68 to 0.32 of PI C36. possibly showing that the synthesis of the PG is increased via CDP-DAG as a result of the increase in CDP-DAG synthesis, but that its synthesis from PE via PS remains the same or is decreased.

A. DM



B. TbCDS p100 + tetracycline

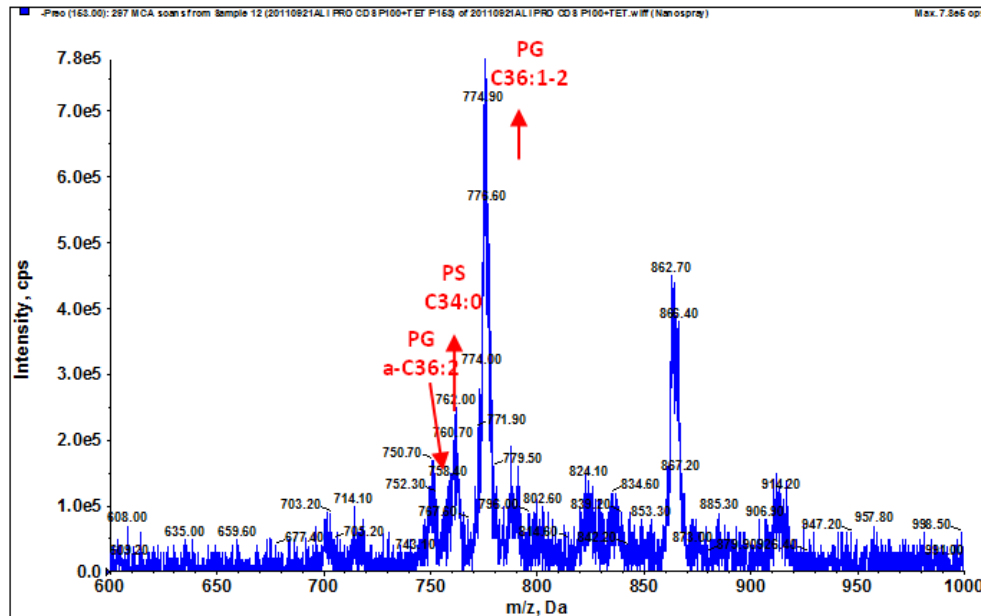
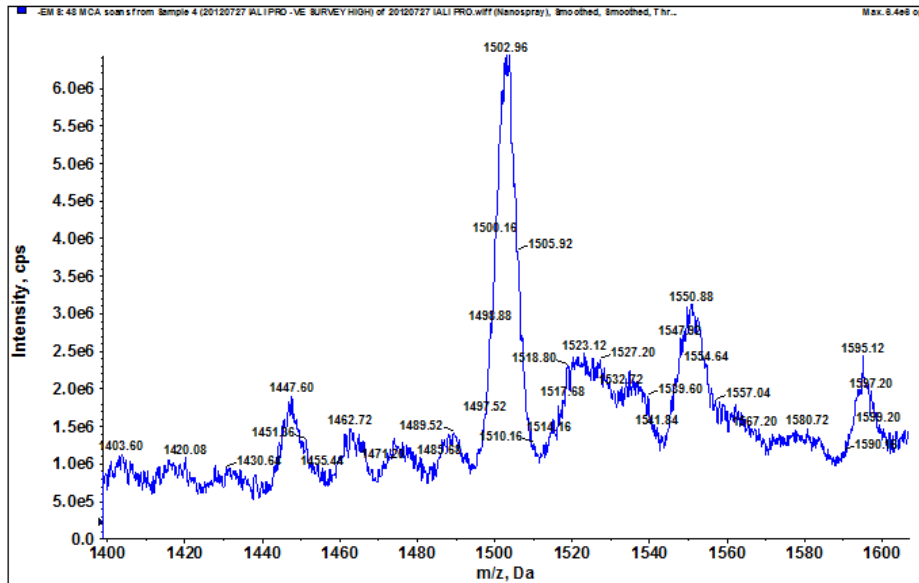


Figure 6.12. Mass spectrometric analyses of glycerol-phosphate containing phospholipids from DM and procyclic form TbCDS pLEW100 + tetracycline. Total lipids were analysed by ES-MS in negative ion mode using precursor ion scanning for the collision induced fragment for glycerol-phosphate at 153 m/z. A. Wild type double marker cells (DM). B. PCF TbCDS p100 cells grown in the presence of tetracycline for 48 hours. For further annotation see Figure 6.2.

6.2.3.f CL

Finally, in order to see if the increase in PG was being translated into an increase in the important mitochondrial phospholipid CL - which in *T. brucei* is produced from two molecules of PG - a negative survey scan was performed between 1500 and 1600 m/z (Figure 6.13). Though the resolution on the scan from TbCDS pLEW100 total lipids is not particularly clear, the peak corresponding to CL does not appear to be increased in comparison to that from double marker. This suggests that the increase in PG is not utilised further to make CL, perhaps indicating some regulatory step in the pathway, for example involving transport into the mitochondrion or between inner and outer mitochondrial membranes. The synthesis of CL may be tightly regulated due to its role in the mitochondrion in order not to disrupt membrane potential.

A. DM



B. TbCDS p100 + tetracycline

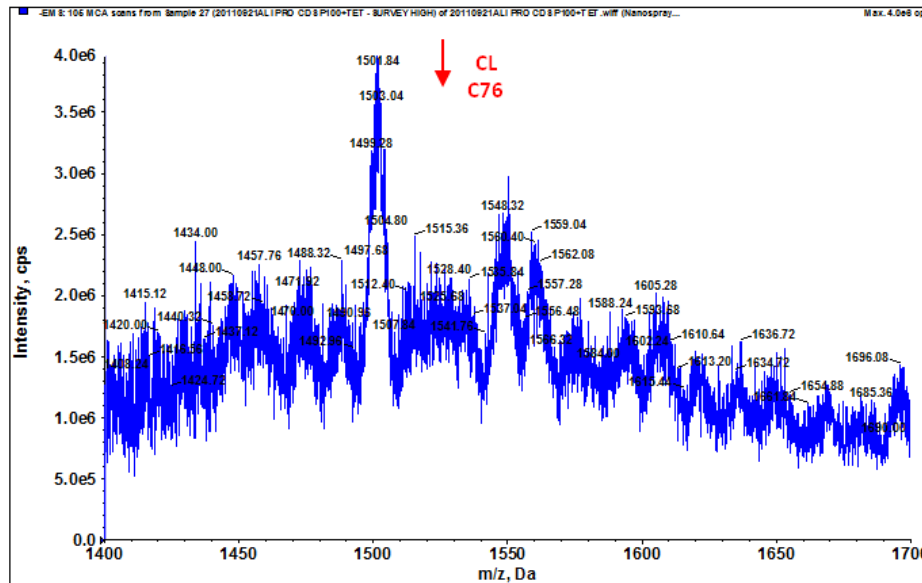


Figure 6.13. High m/z negative survey scan of lipids from DM and procyclic form TbCDS pLEW100 + tetracycline. Mass spectrometric analyses of total phospholipids by negative survey scan ES-MS. A. wild type double marker cells (DM). B. PCF TbCDS p100 overexpression cells grown in the presence of tetracycline for 48 hours. CL = cardiolipin. For annotation see Figure 6.2.

6.4 Subcellular Localisation of TbCDS in Procyclic Form *T.*

brucei

The differential effect of TbCDS knockdown and overexpression that was seen on the separate pools of PI in the procyclic form *T. brucei*, along with the presence of TbPIS in both the Golgi and the ER (Martin and Smith, 2006b) led to the suggestion that there are also separate pools of CDP-DAG. This in turn led to the hypothesis that TbCDS may itself be dually localised to both the Golgi and the ER. Furthermore, in the procyclic form an enhanced requirement for mitochondrial phospholipids PG and CL synthesised from CDP-DAG may mean a requirement for mitochondrial TbCDS, whilst the role of TbCDS in phosphoinositide signalling may indicate a separate pool of CDP-DAG specifically for this purpose, as has been proposed in mammals where it is found in a unique subcellular compartment (Kim et al., 2011). Altogether, the requirement for the essential lipid intermediate CDP-DAG may indicate that its synthesis may occur in multiple locations.

In order to look at the subcellular localisation of TbCDS in *T. brucei*, a tagged TbCDS needed to be expressed in sufficient quantities to be detectable by immunofluorescence. Despite the striking change in lipidomics that was seen in the procyclic form TbCDS pLEW100 cell line on induction with tetracycline, in procyclic form, as in bloodstream form induction of the TbCDS expression by tetracycline induction of the GPEET promoter in the pLEW100 copy did not produce sufficient HA- tagged protein to be detectable by anti-HA western or immunofluorescence. This is not particularly surprising since expression from the GPEET promoter is known to be very low, and as in the bloodstream form there was the chance that post transcriptional control was regulating the levels of TbCDS. In bloodstream form, a TbCDS null background appeared to force stronger expression of the pLEW100 TbCDS. Unfortunately a conditional double knockout of TbCDS was not available in the procyclic form, however, a procyclic form single knockout of TbCDS carrying the ectopic pLEW100 TbCDS had been created. It seemed possible that this may be sufficient to see detectable expression of the HA tagged TbCDS, since previously it had been observed that some HA tagged protein was detectable by an anti HA Western blot of the total protein from bloodstream form SKO TbCDS *T. brucei* expressing ectopic pLEW100 TbCDS. Immunofluorescence was therefore attempted

with the procyclic TbCDS SKO TbCDS p100. Cells were fixed and stained using antibodies against the HA-tag and also using anti-BiP which stains the ER.

Figure 6.14 shows the immunofluorescence images obtained from the fixed and stained procyclic form SKO TbCDS/tbcds::PURO [TbCDS-HA pLEW100] cell line. TbCDS-HA staining occurs anterior and posterior to the nucleus and also distributed in areas throughout the cell body. Since TbCDS is predicted to contain multiple hydrophobic domains it must be localised to a membrane. The staining pattern clearly indicates that the protein is not localised to the plasma membrane, and therefore must be localised to the membrane of a subcellular organelle or organelles. The pattern of TbCDS staining looks similar to that observed with the ER protein BiP and co-staining with BiP shows that in some locations the proteins co-localise, however, there are also clearly locations where TbCDS-HA is present and BiP is not. Staining between the nucleus and kinetoplastid could certainly correspond to a Golgi location in addition to the ER location as is the case in TbPIS, but further staining in non BiP staining regions anterior to the nucleus and posterior to the kinetoplast suggest the presence of TbCDS in the membrane of another subcellular organelle - possibly the mitochondrion. Certainly, the utilisation of the TbCDS product CDP-DAG as lipid precursor to essential mitochondrial phospholipids PG and CL would give good reason for such a localisation. Such extensive staining out with the area stained by BiP was not seen in the TbCDS of the bloodstream form (Figure 6.1) and would fit in with the decreased size and importance of the mitochondrion in bloodstream form.

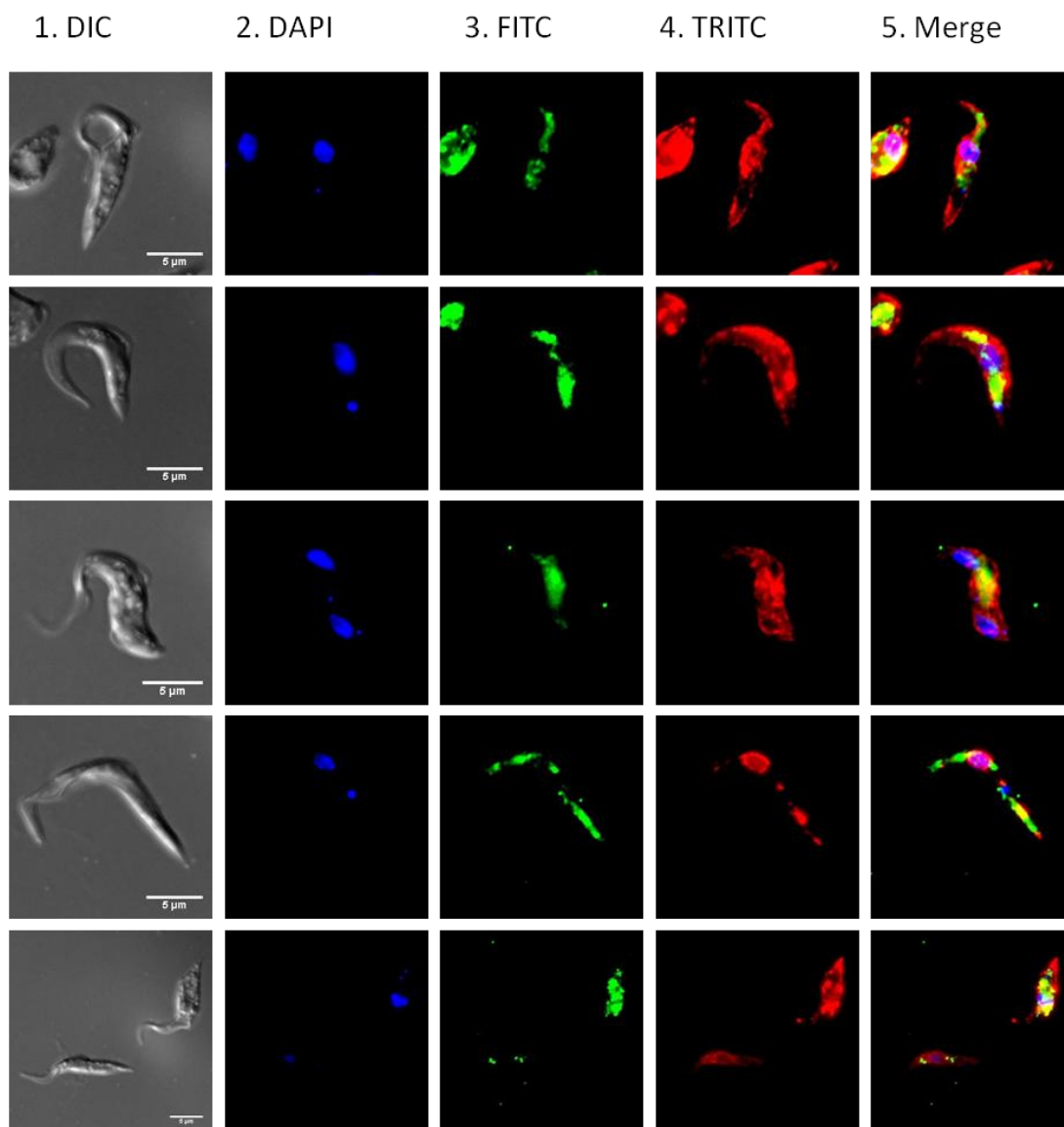


Figure 6.14. Subcellular localisation of TbCDS-HA in TbCDS single knockout, procyclic form *T. brucei*. Cells expressing TbCDS-HA were co-stained for the nuclear marker DAPI, the HA epitope and the ER marker BiP. 1. DIC image. 2. DAPI staining. 3. HA epitope staining and FITC detection. 3. BiP staining and TRITC detection. 4. Merged image.

6.5 Conclusions

RNAi knockdown and conditional knockout of TbCDS in bloodstream form *T. brucei* showed it to be essential, and a significant growth defect was also seen in procyclic form cells undergoing TbCDS RNAi. Examination of the morphological phenotypes of TbCDS activity mutants indicated a role of TbCDS in the PIP signalling in both life cycle stages, and in mitochondrial phospholipid in procyclic form. The biochemical phenotypes showed that in both cell types the separate pools of PI that have previously been described (Martin and Smith, 2006a) were differently affected by the reduction in TbCDS, indicating different flux through the two pathways and different regulation. The requirement for CDP-DAG in several different cellular locations raised the question that there may separate pools of the nucleolipid, as is seen in PI, and that this may indicate the need for more than one localisation of the TbCDS enzyme itself to serve this demand.

Another surprising result of the reduction in TbCDS seen in both life cycle stages was the increase in PG that was previously thought to be made solely from CDP-DAG. This indicated an additional, alternative route for its synthesis possibly via headgroup exchange with PS.

In order to further investigate the role of TbCDS in phospholipid synthesis, and to determine its subcellular location, both bloodstream form and procyclic form *T. brucei* were transfected with pLEW100 TbCDS copies under the control of the GPEET promoter and inducible by tetracycline.

ES-MS of lipids from bloodstream form *T. brucei* over expressing of TbCDS from the pLEW100 showed a variety of changes in the pools of cellular lipids. Decreases were seen in both PA and DAG species, which is not surprising given that PA is a substrate for TbCDS and that PA is dephosphorylated to DAG for entry into the Kennedy Pathway. There was also an increase in α -C36 PE which was considered to be an adaptation to the altered lipid levels and achievable in the absence of certain DAG species because α -C36 is not a lipid moiety which is thought to be utilised by TbCDS. An increase in PG species was also seen. This in itself is not surprising, but given that PG species were also increased in both the bloodstream form knockdown and knockout of *T. brucei* it is unusual that the effect on TbCDS could have the same effect on PG species. This may indicate that the same PG species can be made either

via TbCDS or another mechanism, and that these lipid species are produced in response to different perturbations in normal lipid composition.

PI species were not particularly increased, which could indicate either that they are tightly regulated or that flux through the pathway is such that PI does not accumulate, but something downstream (e.g. GPI anchors or PIPs) accumulates instead. There was an increase in PI C40 relative to PI C36 which would confirm that flux of PI C36 lipids is much faster due to their utilisation in the GPI biosynthetic pathway, or that accumulation of PI in the ER is disadvantageous to the cell, and excess PI is catabolised or shuttled to the Golgi. PIP C38 was also increased which may have been due to utilisation of an increased amount of PI synthesised from CDP-DAG, although an increase in this signalling molecule would be expected to be harmful to the cell and may explain why overproduction of TbCDS protein is suppressed in TbCDS pLEW100.

TbCDS overexpression for IF was achieved using the pLEW100 TbCDS in a null TbCDS background, which was found to give the best level of expression. Immunofluorescence microscopy showed TbCDS to be localised in subcellular organelles, co-localising partly with the ER protein BiP but also showing intense staining between the nucleus and kinetoplast, which indicates a Golgi location. In addition there was punctuate staining that did not co-localise with the BiP or expected position of the Golgi and may correspond to a slight mitochondrial staining. These results give some indication that TbCDS is present in multiple locations, and that as in TbPIS these may include the ER and the Golgi.

In procyclic form, overexpression of TbCDS produced some remarkably similar alterations in cellular lipid to what was seen in the procyclic form TbCDS RNAi knockdown. There was an increase in DAG species - the opposite of what was seen in the bloodstream form and there were also very similar changes in PC species and a large increase in the pools of PG species. The decrease in levels of DAG species and alterations in PC species similar to what was seen in the RNAi knockdown are difficult to explain, whilst the PG species could indicate a general response to alterations in lipid content. Unsurprisingly, there was an increase in PI species, indicating that flux through the pathway is not as much as in the bloodstream, possibly due to the decreased demand for GPI anchor synthesis in bloodstream form as compared to procyclic form. This increase in PI was not translated to an increase in IPC, indicating

that PI is not limiting for IPC synthesis and that perhaps ceramide is, or that IPC synthesis is tightly regulated due to its role as a signalling molecule. Similarly, the increases in PG did not result in an increase in CL, which may indicate that the synthesis of CL is also tightly regulated or that the PG species that are increased are not utilised by CL synthase or are not in the correct subcellular location. C36 PIP was replaced with C38 PIP in the procyclic form TbCDS pLEW100 - this was again similar to what had been seen in the TbCDS p2T7-177 CDS knockdown and in the bloodstream form TbCDS overexpression cell line and it may be due to a relative decrease in the ratio of C36 PI to other PI species.

Finally, overexpression of TbCDS in a single TbCDS knockout background was used for subcellular localisation. As in the bloodstream form, extensive staining was seen between the nucleus and the kinetoplast, indicative of a Golgi localisation, as well as some co-localisation with the ER protein BiP. However, there was also extensive staining throughout the cell which did not co stain with BiP and may indicate an additional subcellular localisation of the TbCDS protein in procyclic form - possibly the mitochondrion, which would make sense due the requirement of CDP-DAG for mitochondrial phospholipid and the importance of the mitochondrion in this life cycle stage.

Chapter 7: Overexpression and Subcellular Localisation of TbPIS in *T. brucei*

7.1 Introduction

PI synthase has previously been shown to be essential in bloodstream form *T. brucei* (Martin and Smith, 2006b). Further work by Martin and colleagues showed that in bloodstream form, the product of the TbPIS gene was localised to both the Golgi and the ER. It was hypothesised that whilst the Golgi pool of PI was used for bulk cellular phospholipid, the ER localised pool was used for the synthesis of GPI anchors. Work on the *T. brucei* inositol phosphate synthase (TbINO1) in bloodstream form confirmed that the ER localised pool of PI was almost exclusively made from *de novo* synthesised inositol which explained why GPI anchors are difficult to label with exogenous inositol (Martin and Smith, 2006a). Moreover, work on a bloodstream form TbINO1 knockout showed that Golgi PI synthesised from exogenous inositol was unable to compensate for the reduction in ER synthesised PI, and that TbINO1 was therefore essential to *T. brucei* due to its role in GPI anchor biosynthesis (Martin and Smith, 2006a).

No work has been published on the INO1 or TbPIS of procyclic form *T. brucei*, however characterisation of an inositol transporter present in the Golgi, but not the ER in procyclic form has given further evidence that there are also two pools of PI in this life cycle stage. Knockdown of this inositol transporter has shown that, similar to the situation in bloodstream form, ER PI made from *de novo* synthesised inositol cannot compensate for the reduction in Golgi PI caused by the loss of exogenous inositol transport into the cell. Furthermore, the inositol transporter knockdown had no effect on GPI anchor synthesis in procyclic form *T. brucei* (Gonzalez-Salgado et al., 2012).

Whilst these results appear to suggest that synthesis and metabolism of PI is similar in the two life cycle stages, with two pools of PI being separately compartmentalised

and utilised, manipulation of TbCDS expression levels had some contrasting consequences on the synthesis of PI and its downstream metabolites between bloodstream form and procyclic form *T. brucei*. Additionally, in both life cycle stages alteration of TbCDS expression level differentially effected the two main series of PI species, indicating that these two series of PI may not be equally distributed between the Golgi and the ER, and there is evidence that diacyl-PI with specific lipid species are preferentially utilised in the GPI anchor biosynthesis pathway in procyclic form *T. brucei* (Guther et al., 2006).

In order to further elucidate the biosynthesis and metabolism of PI in *T. brucei* and to investigate any differences between the bloodstream form and procyclic form, overexpression and subcellular localisation of TbPIS in was carried out in both life cycle stages.

7.2 TbPIS Overexpression in Bloodstream Form *T. brucei*

A cell line over-expressing TbPIS using the GPEET promoter on the pLEW100 vector had been previously created (Martin and Smith, 2006b) and was used here in order to directly compare with the TbCDS over-expressing cell line (Chapter 6). In the bloodstream form TbCDS pLEW100 cell line the addition of tetracycline caused a slight increase in growth rate for the first 48 hours. To see if the overexpression of TbPIS had a similar effect, cell counts were performed as previously described, and the results are shown in Figure 7.1, A. In fact, overexpression of TbPIS had the opposite effect on the growth of bloodstream form *T. brucei*, where a slight reduction in growth rate was seen. In the TbCDS over-expressing cells, growth rate returned to normal after 48 hours, but the growth defect seen in the TbPIS over-expressing cell line persisted across the nine days of counting. This may indicate that TbCDS protein levels are tightly regulated, which is supported by the observation that HA tagged TbCDS protein was not visible from bloodstream form or procyclic form cells over-expressing TbCDS from the GPEET promoter by Western blot or IF when both endogenous TbCDS alleles were present. Western blot of bloodstream form TbPIS pLEW100, however, showed strong signal from HA-tagged protein (Figure 7.1, B). There was a lot of aggregated, HA-tagged protein running at a high molecular weight in the SDS-PAGE gel, however this is not entirely surprising given that TbPIS, like TbCDS is a multiple trans-membrane protein. Additionally, the single band of HA-tagged protein present between 15 and 25 kDa runs rather lower than the predicted

mass of TbPIS at 25 kDa - another behaviour that could be attributed to the protein's hydrophobic nature. Nevertheless, TbPIS-HA protein was sufficient for normal growth in TbPIS double knockouts (Martin and Smith, 2006b) so must therefore be correctly expressed, localised and functional *in vivo*. To further investigate the effect of TbPIS overexpression, and in particular to examine what may be causing this slight growth defect, the biochemical phenotype of the bloodstream form TbPIS pLEW100 cells was examined by lipidomics.

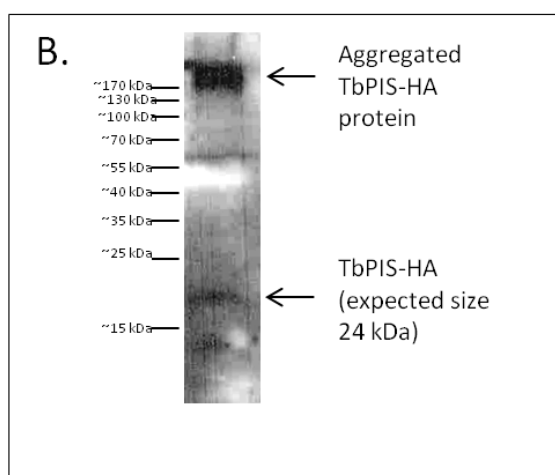
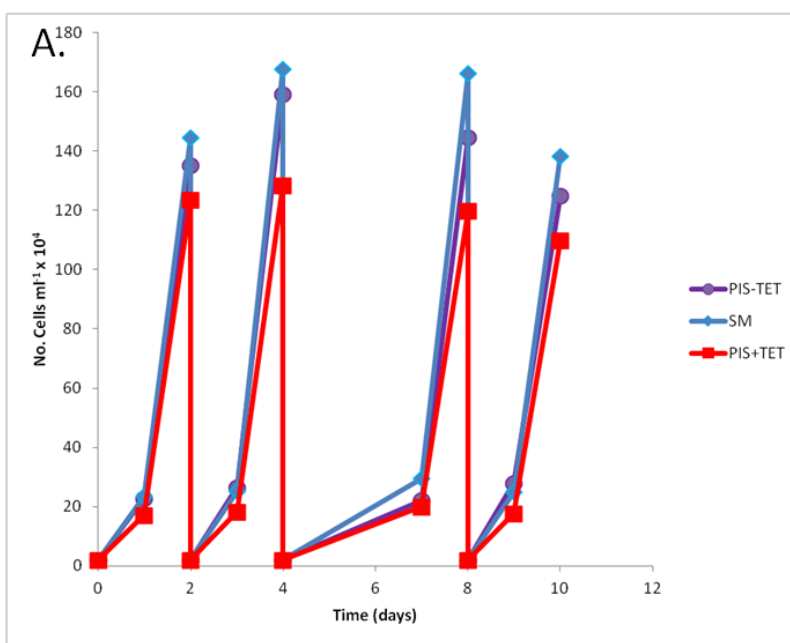


Figure 7.1. Overexpression of TbPIS in BSF *T. brucei*. A. Overexpression of TbPIS causes a decrease in growth rate. Cell counts were performed with the TbPIS pLEW 100 cell line in the presence and absence of tetracycline in order to switch the TbPIS pLEW 100 copy on and off, and with SM cells. B. HA-tagged TbPIS is detectable in total protein from BSF *T. brucei* – anti-HA Western blot showing HA-tagged TbPIS

7.2.2 Lipidomics of Bloodstream Form *T. brucei* over expressing TbPIS

7.2.2.a Positive Survey Scan

Comparison of the positive survey scan from SM cells with tetracycline induced TbPIS pLEW100 cells is shown in Figure 7.2. What is immediately obvious is a significant increase in several DAG species - DAG C36, DAG C38 and DAG C40 with respect to other peaks. For example, DAG C36 goes from below background to 0.45 of PC C42, whilst DAG C38 goes from 0.16 to 0.53 of PC C42 and DAG C40 goes from 0.25 to 0.8 of PC C42. An increase in DAG species was seen in both bloodstream form and procyclic form mutants deficient in TbCDS expression, where it was thought to be due to accumulation of the TbCDS substrate PA, which was being dephosphorylated into DAG due to the danger of PA accumulation to the cells. That it is also increased here suggests that it may instead be a response to CDP-DAG depletion, due to reduction of TbCDS expression/ activity but also due to overexpression of TbPIS, as CDP-DAG is a substrate for the TbPIS enzyme. It is highly likely that CDP-DAG has some role in controlling total lipid content in the cell, and that the reduction or altered use of CDP-DAG causes an adaptive increase in DAG that cannot be utilised by the Kennedy Pathways, which may already be operating at maximum capacity. As discussed previously, a role for CDP-DAG in controlling PA phosphatase and DAG kinase activity - as shown by in yeast (Wu and Carman, 1996, Shen and Dowhan, 1997)- is supported by these results.

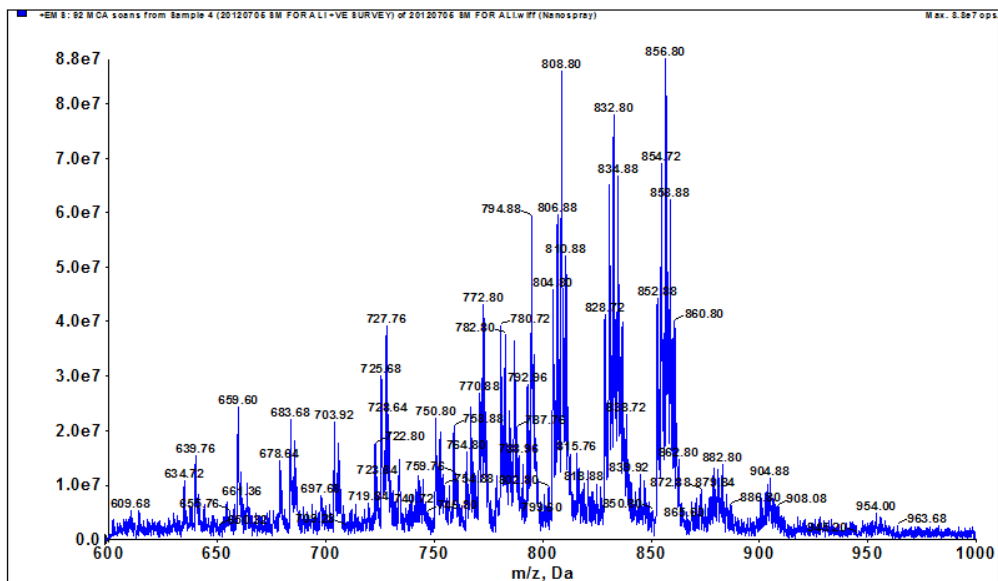
The EPC species C36:1 is also increased here - from 0.20 to 0.51 of PC C42 - which was also the case in bloodstream form TbCDS RNAi + tetracycline and bloodstream form TbCDS CKO in the absence of tet. In these cases it was coupled with a decrease in PE which was not seen here. This is clearly some adaptation to disruption of lipid pathways in the cell, but its role is not clear.

The peak corresponding to the key PS species, PS a-C36:2 is reduced with from 0.49 to 0.3 of PC C42. This could be a result of depletion in CDP-DAG, although this seems unlikely since TbCDS depletion did not have a dramatic effect on total PS synthesis in bloodstream form *T. brucei*, and PS a-C36 is thought to be derived from PE rather than from CDP-DAG. This decrease may therefore be a responsive action as well as

possible further evidence for PG formation through PS headgroup swapping (as discussed previously).

Peaks corresponding to PC species e-C38:4 and PC C40:4-7 were also decreased from 0.66 to 0.35 and 0.89 to 0.62 of PC C42, respectively. Increased utilisation of PA to make PI via CDP-DAG could be responsible for a reduction in DAG species which leads to this reduction in Kennedy Pathway products, but a visible increase in DAG species would argue that this was not happening. However, the DAG species which are accumulating do not correspond to the PC species which are accumulating. Since both e-C38:4 and C40:4-7 CDP-DAG species are incorporated into PI, it is possible that the DAG species which are accumulating are the ones which are not as readily incorporated into phospholipid, or that the enzymes which utilise these species are already at saturation. It certainly seems to indicate that overproduction of TbPIS has caused misregulation which has led to an altered phospholipid content. Peaks possibly corresponding to TAG species C56:8 (902.68 m/z) and C62:9 (986.32 m/z) are increased in the TbPIS pLEW100 scan, and the appearance and disappearance of TAG species has previously been seen in both TbCDS knockdowns and the overexpression mutants, indicating that this may be an adaptive response to phospholipid perturbation or play a role in regulating total lipid content.

A. SM



B. TbPIS p100 + tetracycline

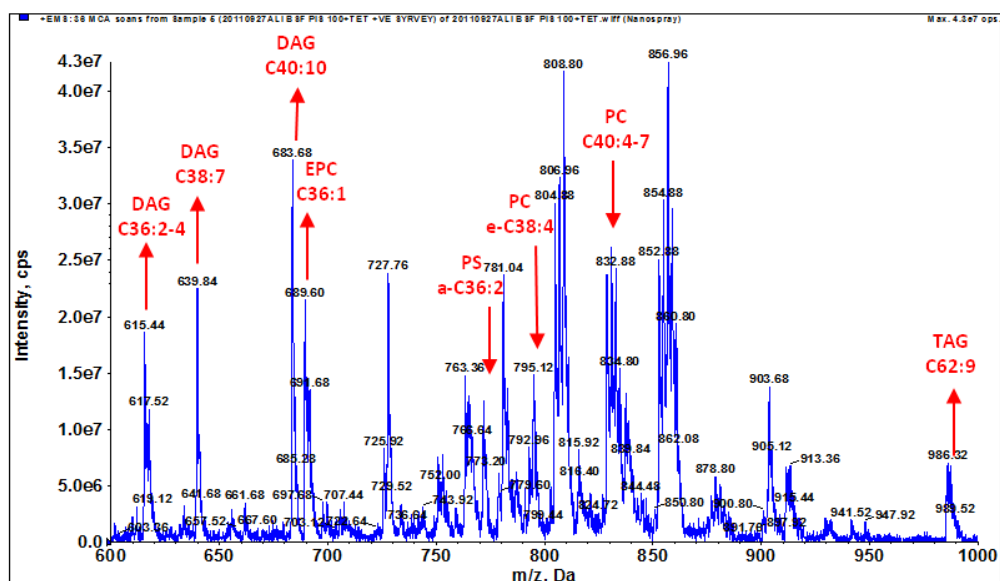


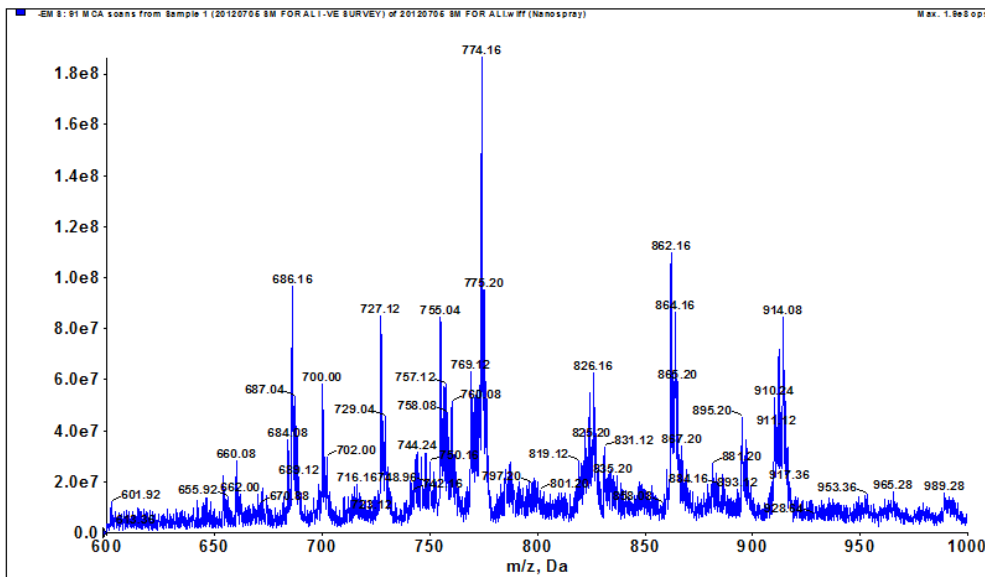
Figure 7.2. Positive ion survey scan of lipids in SM and bloodstream from TbPIS pLEW100 + tetracycline. Mass spectrometric analyses of total phospholipids by positive survey scan ES-MS. A. wild type single marker cells (SM). B. BSF TbPIS p100 overexpressing cell line in the presence of tetracycline for 48 hours. DAG = diacylglycerol species, TAG = triacylglycerol species, PS = phosphatidylserine species, PC = phosphatidylcholine species. PI = phosphatidylinositol species. Red arrows and text indicate peaks which are different in the mutant, whilst the direction of the arrow indicates whether this peak is increased or decreased in the mutant. CX:Y = X – total number of carbons, Y – total number of double bonds in fatty acid chains of lipid species. e = alkenyl-acyl- linked lipid, a = alkyl-acyl- linked lipid.

7.2.2.b Negative Survey Scan

The disappearance of PA species in the TbPIS pLEW100 + tetracycline negative survey scan (Figure 7.3) also mirrors what was seen in the TbCDS knockdown and CKO. Here, it could be a result of their utilisation by TbCDS to make CDP-DAG to meet the demand created by TbPIS pLEW100 overexpression since both species (a-C36:1-2 and C36:1-2) are incorporated into PI species.

The ratio of the PI C40 series is definitely increased relative to the PI C36 series, from 1.29 PI C36:PI 40 to 0.77 PI C36:PI C40. This is the opposite of what was seen in the TbPIS CKO (Martin and Smith, 2006b) and will be discussed later. There is also the clear appearance of a species at 963.12 m/z which is likely to correspond to PIP C38:5 and could be an indication of an increase in flux through this pathway, even if the pool of PI itself is not increased. This PIP species also appeared in bloodstream form TbCDS p100 overexpression cell line and replaced PIP C36 in procyclic form TbCDS RNAi and procyclic form TbCDS p100 overexpression cell line, where it was considered to be a response to the decrease in the ratio of PI C36 with respect to other PI species, and this could also be the case here.

A. SM



B. TbPIS p100 + tetracycline

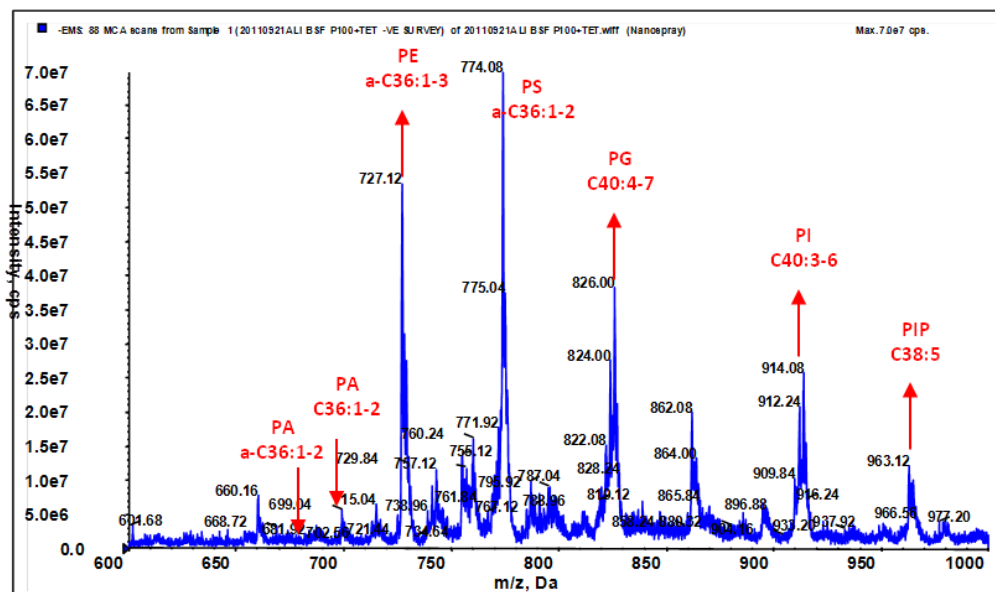
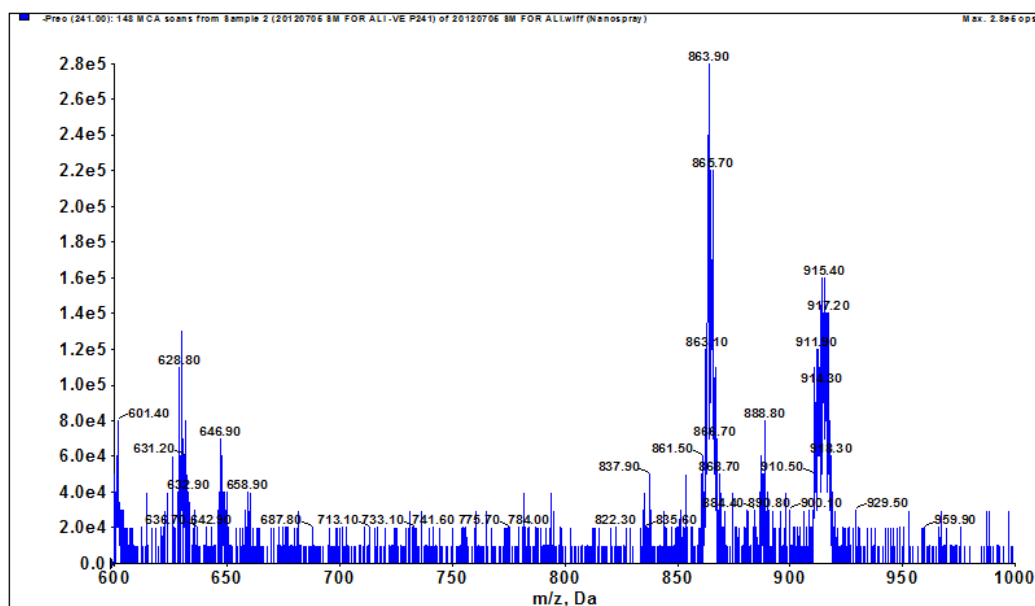


Figure 7.3 Negative survey scan of lipids in SM and bloodstream from TbPIS pLEW100 + tetracycline. Mass spectrometric analyses of total phospholipids by negative survey scan ES-MS. A. wild type single marker cells (SM). B. BSF TbPIS p100 over-expression cell line the presence of tetracycline for 48 hours. PA = phosphatidic acid species, PE = phosphatidylethanolamine species, PIP = phosphatidylinositol phosphate species, PG = phosphatidyl glycerol, PI = phosphatidyl inositol. For further annotation, see Figure 7.2.

7.2.2.c Inositol-Phosphate Containing Lipids

Figure 7.4 shows the SM and TbPIS pLEW100 + tetracycline scans specific for inositol-phosphate containing lipids. Here, the increase in the ratio of C40 PI to C36 PI is clear - from 1.15 C36 PI: C40 PI to 0.57 C36 PI:C40 PI. Previously, overexpression of TbCDS in bloodstream form *T. brucei* was also shown to increase this ratio and it was proposed that the reason for increase in the pool of C40 PI is because unlike C36 PI, which is rapidly metabolised into GPI anchors, the Golgi localised C40 PI is not under heavy demand for further metabolism into GPI anchors and therefore is allowed to accumulate. It could also be that the accumulation of PI in the ER could be detrimental to the cell, and so excess PI in this location is catabolised or shuttled into the Golgi. However, when TbPIS was knocked out in bloodstream form *T. brucei*, there was a visible increase in the ratio of C36 PI to C40 PI seen by ES-MS. If C36 PI species are more abundant in the ER and flux through the pathway is high due to their utilisation as GPI anchors, it might be expected that in a TbPIS synthase knockout, this PI series would deplete more rapidly. It is known from the INO1 knockout (Martin and Smith, 2006a) and from the inositol transporter knockout (Gonzalez-Salgado et al., 2012) that the two pathways cannot compensate for each other, but perhaps there is some mechanism by which the ER localised pathway is maintained at the expense of Golgi PI synthesis. Interestingly, in the bloodstream form TbCDS knockout and knockdown, the C36 PI peak was decreased relative to the C40 PI peak, and in the TbINO1 knockout which only affects the ER localised pool, the C36 PI peak was also very slightly decreased (Martin and Smith, 2006a). These results appear to indicate that bloodstream form *T. brucei* are able to maintain levels of C36 PI when PI synthase expression itself is lacking, but that this maintenance is not possible in the absence of either of the enzymes precursors.

A. SM



B. TbPIS p100 + tetracycline

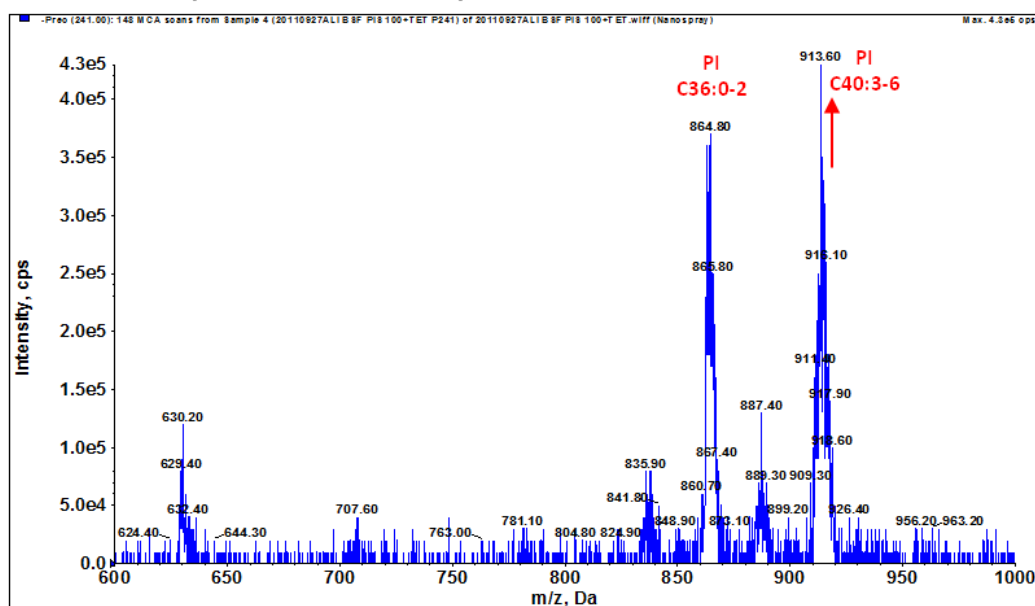


Figure 7.4. Mass spectrometric analyses of inositol-phosphate containing phospholipids in SM and bloodstream from TbPIS pLEW100 + tetracycline. Total lipids were analysed by ES-MS in negative ion mode using parent-ion scanning of the collision induced fragment at 241 m/z . A. Wild type single marker cells (SM) B. BSF TbPIS p100 grown in the presence of tetracycline for 48 hours. For further annotation see Figure 7.2.

7.2.3 Subcellular Localisation of TbPIS in Bloodstream Form *T. brucei*

Previously, TbPIS has been localised to the ER and the Golgi in bloodstream form *T. brucei* (Martin and Smith, 2006b). This work was carried out using the high overexpression level pLEW82 vector. Since subcellular localisation has already been determined in the bloodstream form, the main aim of this TbPIS localisation study was to determine if the dual localisation was also present in the procyclic form. However, a procyclic form cell line carrying TbPIS on the pLEW82 vector was not available, and therefore subcellular localisation work was carried out using the more tightly regulatable pLEW100 overexpression vector, where expression of the ectopic gene is achieved from the GPEET rather than the T7 promoter. Since the aim of this work was to directly compare the localisation of TbPIS between the two cell types, it was considered necessary to also use this lower level expression vector to carry out localisation work in bloodstream form, in case the different vectors led to any differences in expression or localisation.

The TbPIS pLEW100 bloodstream form cells were induced to express the exogenous, HA-tagged TbPIS by the addition of tetracycline. 48 hours after tetracycline induction cells were harvested, fixed and stained as described in Chapter 2. As well as staining against the HA-tag, cells were co-stained against the ER localised protein BiP. The results of the immunofluorescence are shown in Figure 7.5. As indicated from the anti-HA Western blot of total protein from the this cell line, expression of TbPIS by the GPEET promoter was strong despite the presence of both allelic copies of TbPIS, showing that this protein may not be under such tight regulation as TbCDS. The images confirm what has previously been shown by Martin and Smith, since the TbPIS protein clearly co-localises with the BiP protein, but is also present in a distinct body between the nucleus and kinetoplast, indicative of a Golgi and an ER localisation. However, as was seen with the TbCDS protein in bloodstream form, there does appear to be some staining of the TbPIS protein out-with both the Golgi and the ER, particularly in punctuate areas posterior to the nucleus and anterior to the kinetoplast.

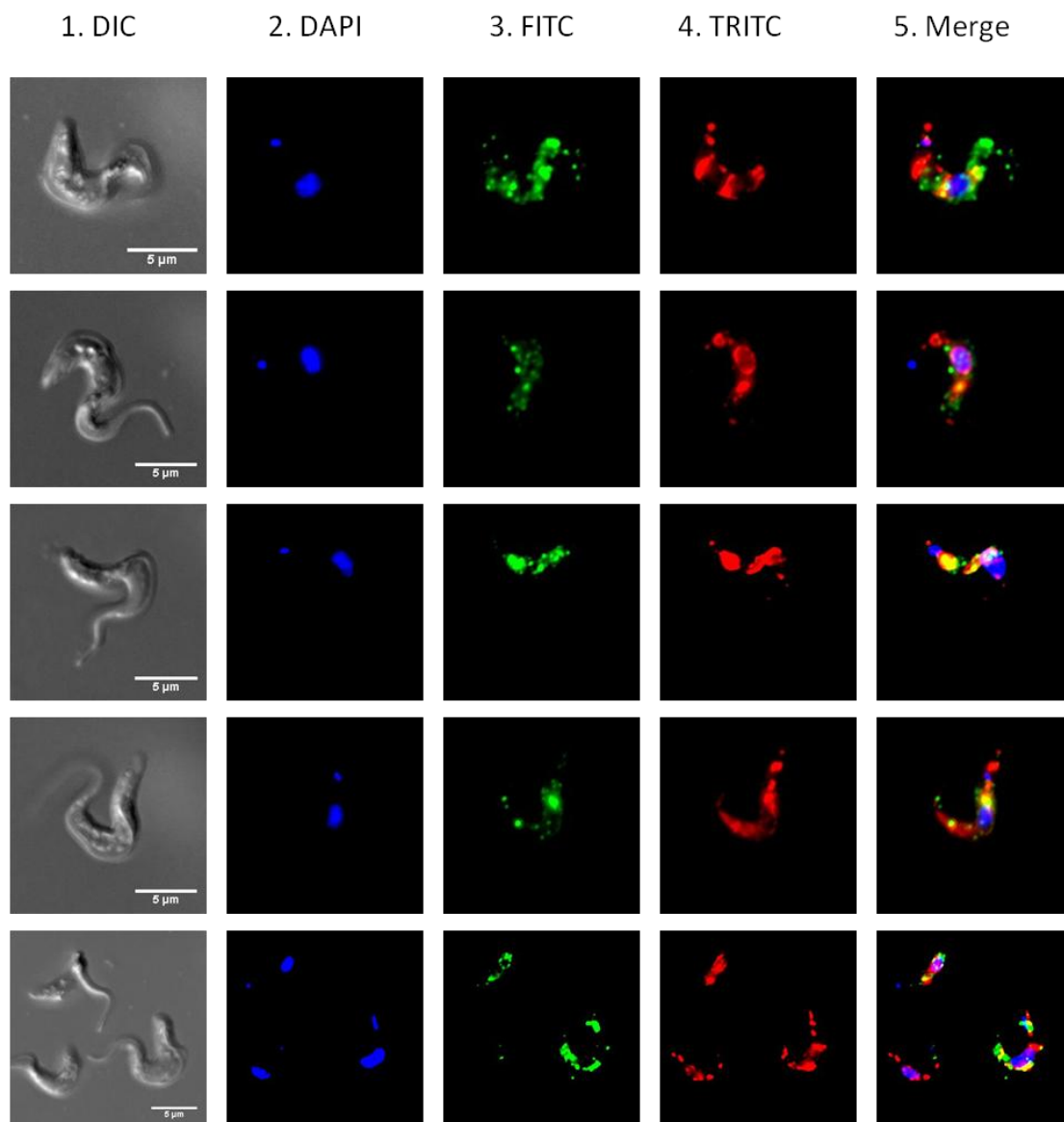


Figure 7.5. Subcellular localisation of TbPIS-HA in bloodstream form *T. brucei*. Cells expressing TbPIS-HA were costained for the nuclear marker DAPI, the HA epitope and the ER marker BiP. 1. DIC image. 2. DAPI staining. 3. HA epitope staining and FITC detection. 4. BiP staining and TRITC detection. 5. Merged image.

7.3 TbPIS Overexpression in Procyclic Form *T. brucei*

Whilst TbPIS has been well characterised and shown to be essential in bloodstream form *T. brucei*, no work has been done on this enzyme in the procyclic form. As work with TbCDS has shown, lipid metabolism between the two cell types can differ considerably, and the procyclic form reduced dependency on a huge flux through the GPI biosynthesis pathway compared to the bloodstream form is likely to mean that the requirement for TbPIS is different in the procyclic form. Work with an inositol transporter of the Golgi suggests that, as in the bloodstream form there are two separately localised pools of PI in procyclic form *T. brucei*, one in the Golgi which is used for bulk PI and at least some of the IPC synthesis, and one in the ER which utilises *de novo* synthesised inositol for PI synthesis and is responsible for supplying PI for the GPI biosynthesis pathway. This work also showed that these pools of PI cannot substitute for one another in the procyclic form (Gonzalez-Salgado et al., 2012) as is also the case in the bloodstream form (Martin and Smith, 2006a). In procyclic form the PI requirement for the synthesis of the IPC, which is not usually present in bloodstream form *T. brucei* may indicate a different dependence on the PI pools. However, in the procyclic form TbCDS RNAi knockdown it appeared that the IPC pools were reduced with respect to PI pools, and GPI anchors biosynthesis was also compromised, suggesting that the maintenance of the PI pools themselves may be a priority for the procyclic form cells. Maintaining certain levels of PI may, for example, be important in PIP signalling - alteration of which may have caused the cell cycle defects that were seen in Chapter 2 in the TbCDS RNAi knockdown cell line in the presence of tetracycline.

In order to compare the roles of TbPIS in procyclic form *T. brucei* with those in bloodstream form *T. brucei*, a cell line over-expressing TbPIS was created. Transformation of procyclic form *T. brucei* with TbPIS on the high expression level construct pLEW82 was not successful. Instead, cells were transfected with the previously created TbPIS pLEW100 construct, and selected with phleomycin. Successful transformants were grown in the presence of tetracycline in order to switch on the expression of the exogenous TbPIS from the GPEET promoter. Total protein was prepared from the TbPIS-HA over-expressing cells, separated by SDS-PAGE, Western Blotted and detected using anti-HA rat and anti-rat-HRP antibodies. Figure 7.6. shows a strong signal from HA-tagged protein in the TbCDS pLEW100

procyclic form *T. brucei* cell line. The expected size of TbCDS-HA is 25 kDa, but in bloodstream form *T. brucei*, where the TbPIS-HA has been proven to be expressed and functional much of the protein ran as aggregate, with a faint band at approximately 20 kDa. In the procyclic form, the majority of signal for the HA-tagged protein runs at around 50 kDa - double the expected size, with a further faint band running just below the 35 kDa marker. It is well known that multiple trans-membrane proteins can behave unusually on SDS-PAGE gels, and it is also possible that the procyclic form TbPIS has different post translational modifications to that of the bloodstream form TbPIS, which may cause it to run at a different size. Alternatively, the large quantity of aggregated TbPIS-HA from the bloodstream form sample may indicate suboptimal protein sample preparation, so the different running sizes could be artefacts of sample preparation.

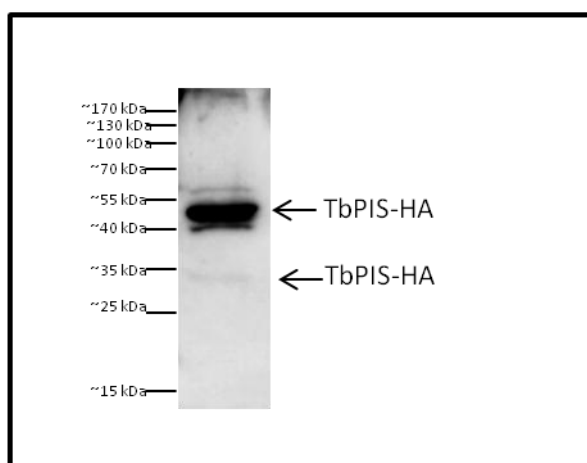


Figure 7.6. TbPIS-HA protein expressed from TbPIS pLEW100 construct in procyclic form *T. brucei*. Western blot using anti-HA to detect HA-tagged PIS from total PCF *T. brucei* TbPIS pLEW 100 protein.

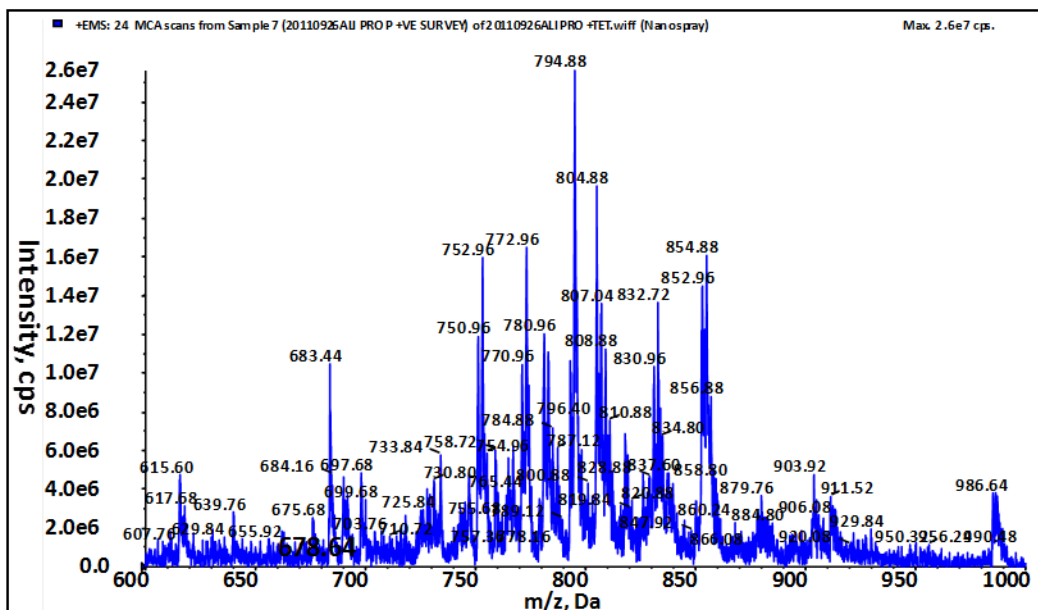
To further examine the procyclic form TbPIS pLEW100 biochemical phenotype, and in particular to ascertain whether TbPIS was functional, total lipids were harvested from these cells 48 hours after induction with tetracycline to examine the lipidomic profile by ES-MS/MS.

7.3.1 Lipidomics of Procyclic Form *T. brucei* Overexpressing TbPIS

7.3.1.a Positive Survey Scan

Figure 7.7 shows the positive survey scan of total lipids from both DM and procyclic form TbPIS pLEW100 + tetracycline. Contrary to what was seen in the bloodstream form, overexpression of TbPIS does not seem to cause any obvious differences on the profile of positive ion species. This could be taken as evidence that the exogenous TbPIS-HA is not correctly expressed or functional in the procyclic form, however further lipid scans show that this is not the case. Instead, the lack of perturbation of cationic phospholipid may indicate that pools of PC and SpM are more tightly regulated in this life cycle stage.

A. DM



B. TbPIS p100 + tetracycline

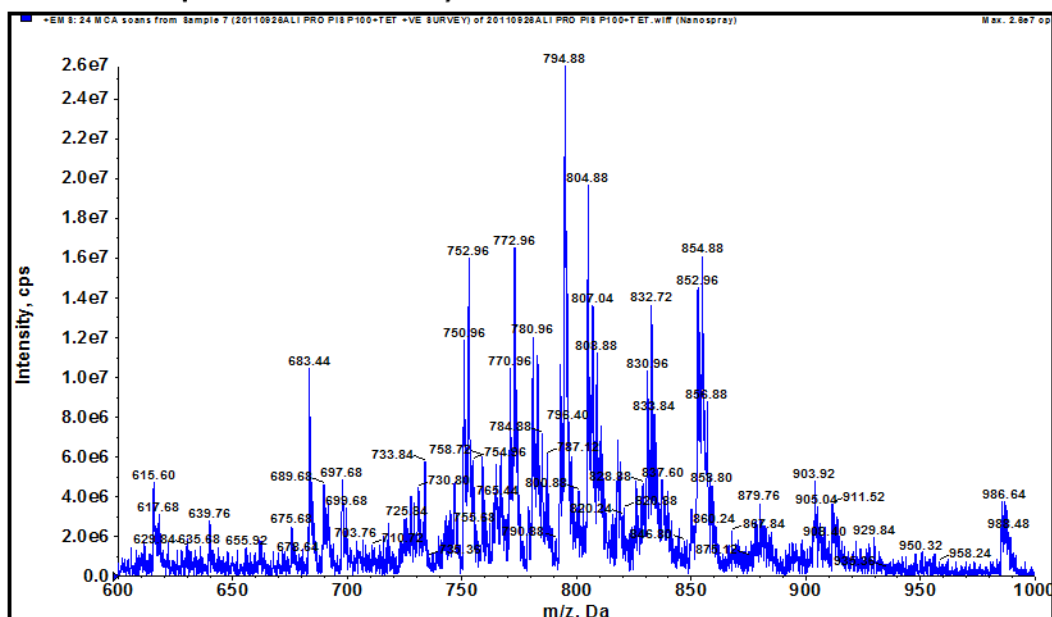


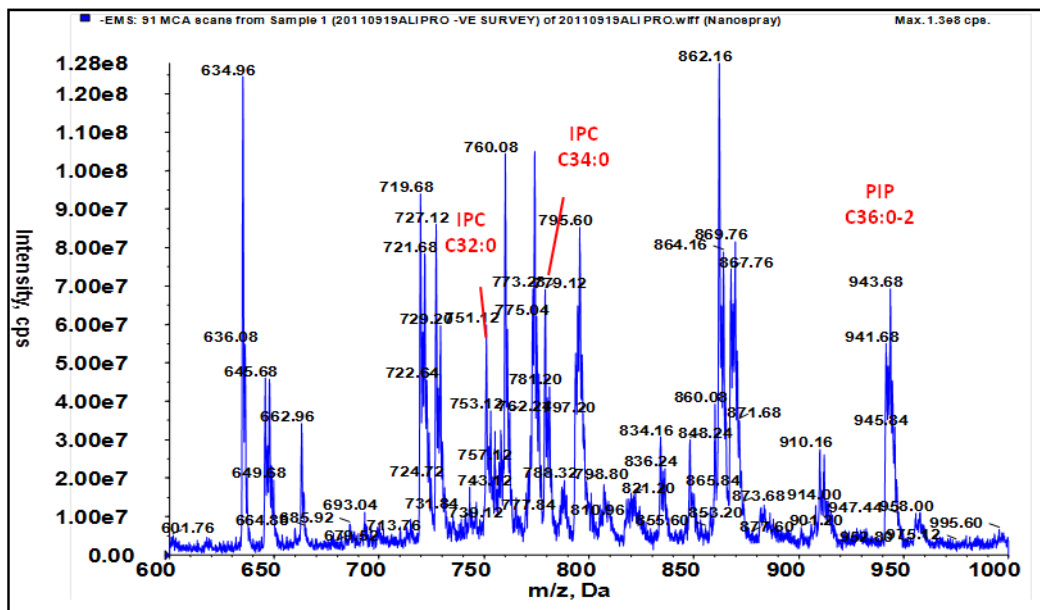
Figure 7.7. Positive ion survey scan of lipids from DM and procyclic form TbPIS pLEW100 + tetracycline. Mass spectrometric analyses of total phospholipids by positive survey scan ES-MS. A. wild type double marker (DM) cells. B. PCF TbPIS pLEW 100 overexpression cell line grown in the presence of tetracycline for 48 hours. For further information, see Figure 7.2.

7.3.1.b Negative Survey Scan

In contrast to the lack of alteration that was seen between procyclic form TbPIS pLEW100 and the DM in the positive survey scan, there are a number of interesting differences in the negative survey scan (Figure 7.8). The first obvious difference is a proportional decrease in the key PE species at m/z 727 - PE a-C36:2-3 in the TbPIS overexpression cell line compared to the other anionic lipids. An absolute decrease in this PE species is very unlikely given that the same species was unaltered in the positive survey scan (appearing as a sodium adduct in Figure 7.7 at m/z 752). A peak at 760 m/z , possibly corresponding to PE a-C38:0 is also reduced. Since no change was seen in either of these species in the positive survey scan, it is likely that neither of these species are reduced, and that instead other anionic species are increased. Using PE a-C36 as a comparison, PI C36 species are increased from 1.5 to 3.6 and PI C40 is increased from 0.31 to 0.5., IPC C32 is increased from 0.67 to 1.9 and IPC C34 is increased. There is a relative increase in the peak at around 751 m/z with respect to PE a-C36 from 0.67 to 1.9, and fragmentation of this peak confirms it to be IPC C32:0 (Figure 7.9, B). An increase in this species is not unexpected given that it is synthesised from PI. There is also an increase in the other key IPC species IPC C34:0 at 779 m/z , though to less of an extent than IPC C32 - from 0.81 to 1.23 of PE a-C36. This may suggest that the synthesis of these two different IPC series is separately regulated, possibly being differently compartmentalised although previous results have indicated that they are both synthesised in the Golgi from the same pool of PI (Gonzalez-Salgado et al., 2012).

Certainly an increase in PI and IPC species would be expected, but another of the key peaks at m/z 774 would also greatly increase. Fragmentation of this peak appears to identify it as PG C36:1 (Figure 7.9, A), an increase in which would not necessarily be expected, but was seen in both TbCDS knockdown and TbCDS over-expressing procyclic form cell lines and may indicate that production of this lipid is a response to alterations in lipid content such that membrane fluidity is maintained.

A. DM



B. TbPIS p100 + tetracycline

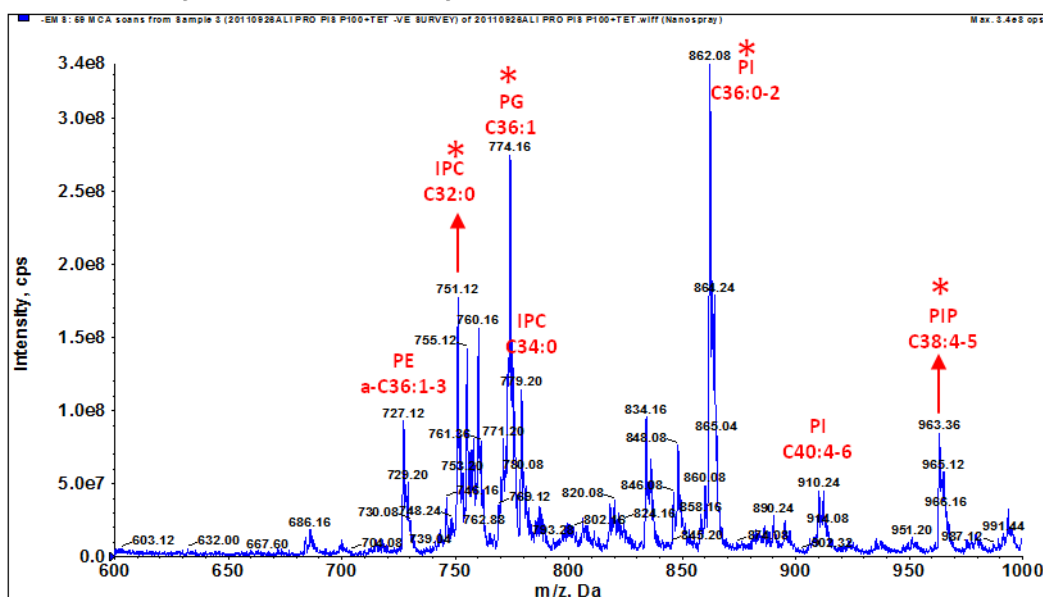
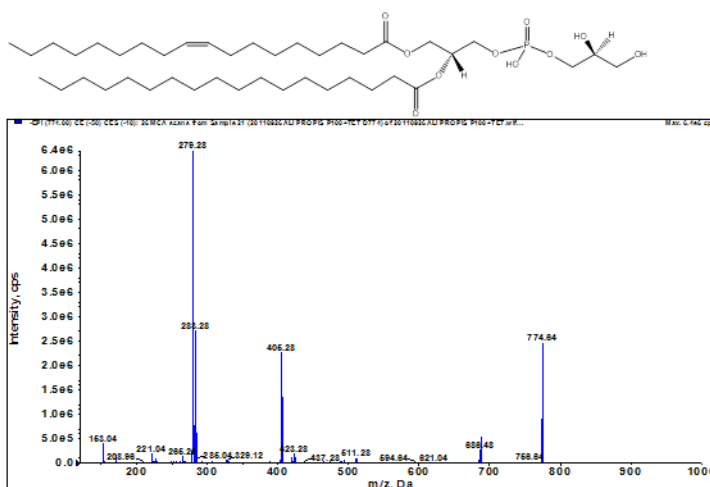
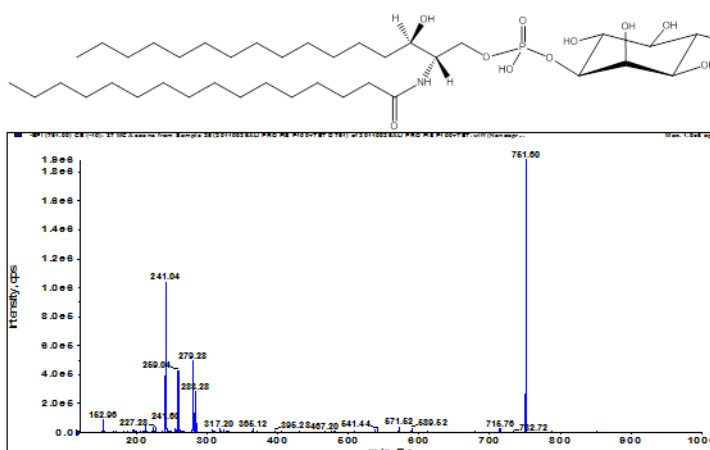


Figure 7.8. Negative survey scan of lipids from DM and procyclic form TbPIS pLEW100 + tetracycline. Mass spectrometric analyses of total phospholipids by negative survey scan ES-MS. A. Wild type double marker cells (DM). B. PCF TbPIS pLEW 100 cells grown in the presence of tetracycline for 48 hours. PI = phosphatidylinositol. IPC = inositolphosphorylceramide. PIP= phosphatidylinositol phosphate. Red asterixes indicate peaks which have been further fragmented (see Figure 7.9). For further annotation, see Figure 7.2.

A. PG C18:1/C18:0



B. IPC C32:0



C. PIP C18:2/C20:3

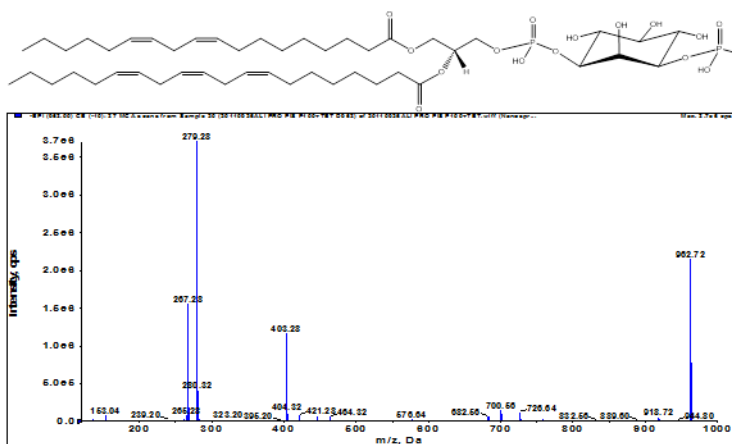


Figure 7.9. Daughter ion spectrum from A. 774 m/z $[M-H]^-$ ion, B. 751 m/z $[M-H]^-$ ion C. 963 m/z $[M-H]^-$ ion.

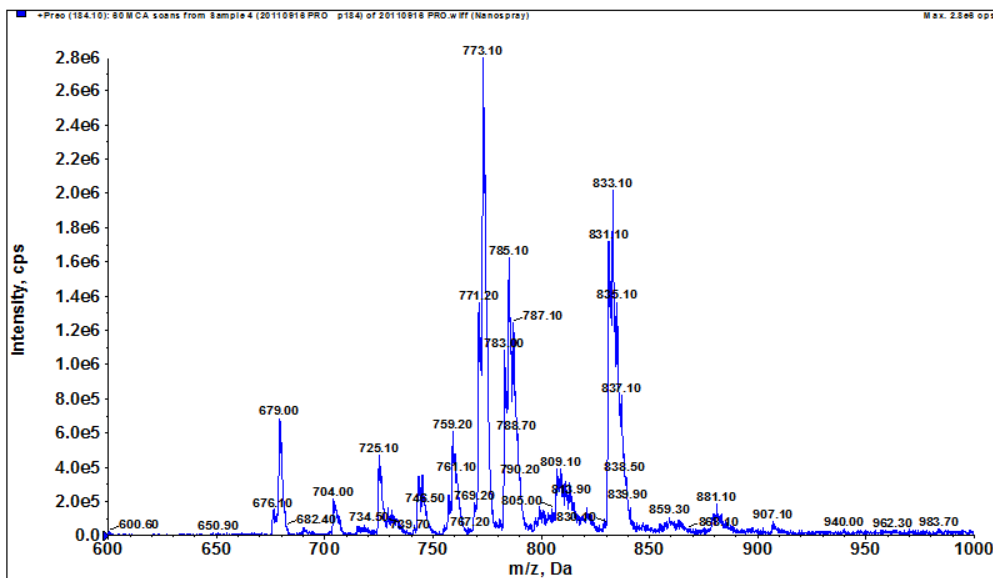
The ratio of the two key peaks of PI at 862 m/z and 910 m/z altered less than in some mutants - from 4.77 to 6.89 PI C36:PI C40. The lack of a large change in the ratio of these two series is the converse of what was seen in the bloodstream form, where flux of the two different phospholipids is very different and alterations in both TbPIS and TbCDS expression had differential effects on the two series, which may correspond to the two different subcellular localisations of the PI pools.

Finally, the PIP C36 series at 943 m/z in DM is replaced by a series at 963 m/z in the TbPIS pLEW100 negative survey scan (confirmed by further fractionation - Figure 7.9, C), indicating that PI C38 series are preferentially being phosphorylated. This was also seen in the TbCDS overexpression and knockdown mutants of both bloodstream form and procyclic form cell lines, and had been considered to be a response to a decrease in the ratio of C36 PI to other PI species. However, since the opposite is true of the PI series here, it must be some general response to lipid disruption, possibly as cessation of some signalling pathway indicating that everything is operating normally.

7.3.1.c Choline-Phosphate Containing Lipids

Confirming what was seen in the positive survey scan, the spectra showing choline-phosphate containing lipids is largely the same in procyclic form TbPIS pLEW100 + tetracycline and double marker (Figure 7.10). The only slight differences are seen at the lower end of the m/z scale, with a shift in a peak from 725 m/z to 734 m/z likely pertaining in a saturation change of the PC C32 series from the majority being PC C32:5 to the majority being PC C32:0. The significance of this increase is difficult to determine, but is presumably an adaptation to adjust to the increased inositol containing phospholipid content.

A. DM



B. TbPIS p100 + tetracycline

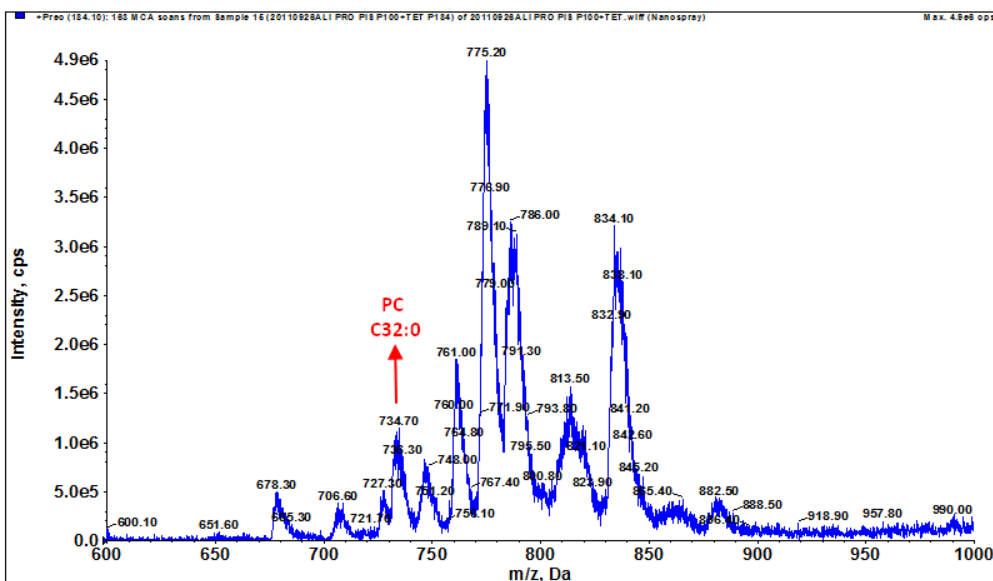
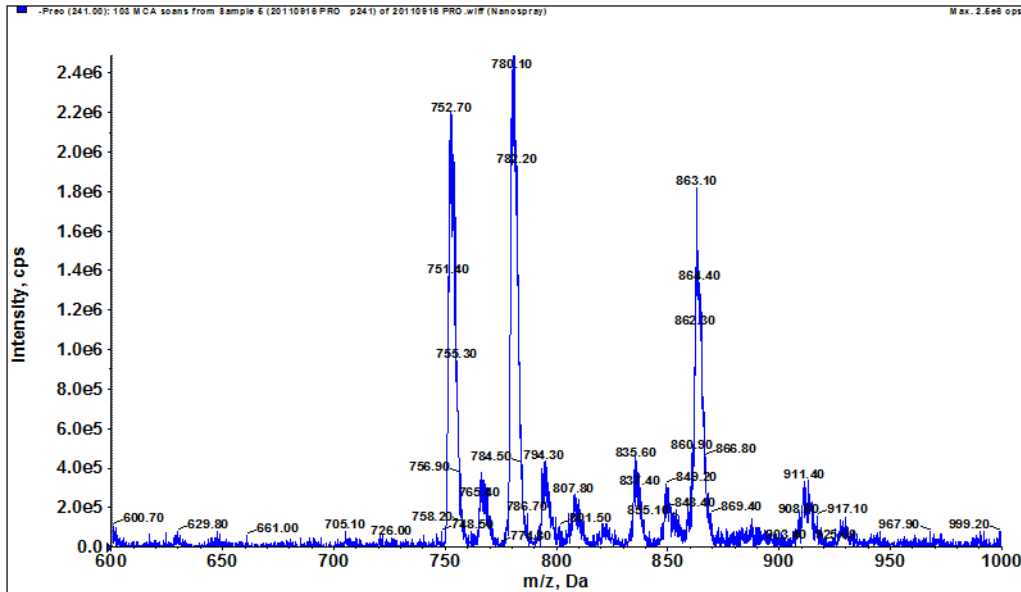


Figure 7.10. Mass spectrometric analyses of choline-phosphate containing phospholipids from DM and procyclic form TbPIS pLEW100 + tetracycline. Total lipids were analysed by ES-MS in positive ion mode using parent-ion scanning of the collision induced fragment for phosphorylcholine at 184 m/z . A. Wild type double marker cells (DM). B. PCF TbPIS p100 over-expression cells grown in the presence of tetracycline for 48 hours. For further information see Figure 7.2.

7.3.1.d Inositol-Phosphate Containing Lipids

Finally, to look at the products of the TbPIS protein more specifically, total lipids were scanned for precursors to the inositol-phosphate ion (Figure 7.11). This scan confirms what was previously seen in the negative survey scan. In the DM scan, the ratio of the two main PI series C36 and C40 at 863 m/z and 912 m/z (daughter ion scans shown in Figure 7.11) is 5:1. In the scan of PCF TbPIS pLEW 100 + tetracycline the ratio of PI C36 to PI C40 is 6:1, so not hugely increased. Therefore any increase in total PI (as suggested by the negative survey scan) is affecting both these series relatively equally. Secondly, there is a clear increase in the amount of the IPC C32 series at 750 m/z compared to the IPC C34 series at m/z 780. In the DM IPC C32 is 0.89 of IPC C34, whilst in the PCF TbPIS pLEW 100 + tetracycline IPC C32 is increased to 1.72 of IPC C34. This result is similar but more dramatic to what was seen in the procyclic form TbCDS overexpression mutant, where the ratio increased to 1.21, but is the opposite to what was seen in the PCF TbCDS knockdown where the ratio decreased to 0.58. This gives evidence that these two different series of IPC are differently regulated, possibly being synthesised or catabolised at different rates, presumably in separate compartments as may be the case for the PI used to format it. In a knockout of the mitochondrial acyl carrier protein, which depletes mitochondrial PI, an increase was seen in the C34 IPC series in lipid extracts from total cells, but not in mitochondrial extracts alone. This may suggest that the pool of PI out-with the ER/MAM - i.e. the Golgi IPC - contains a higher proportion of C34 PI than the ER/MAM fraction. If this is the case, it might be worth noting that the ER/MAM pool of PI appears to be more sensitive to PI depletion, since in the procyclic form TbCDS RNAi knockdown C32 IPC was decreased with respect to the pool of C34, and this is also seen here.

A. DM



B. TbPIS p100 + tetracycline

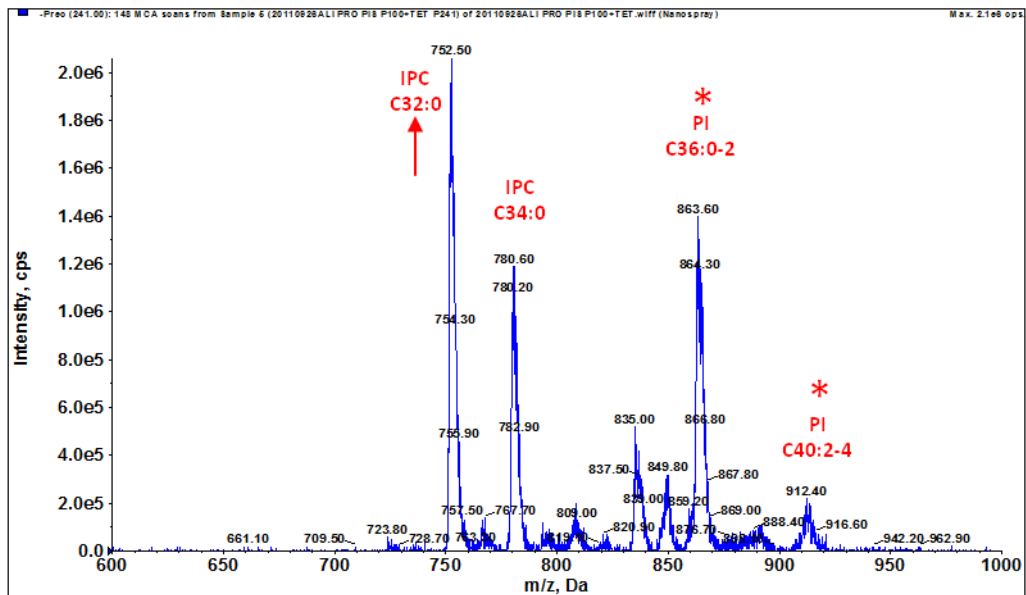
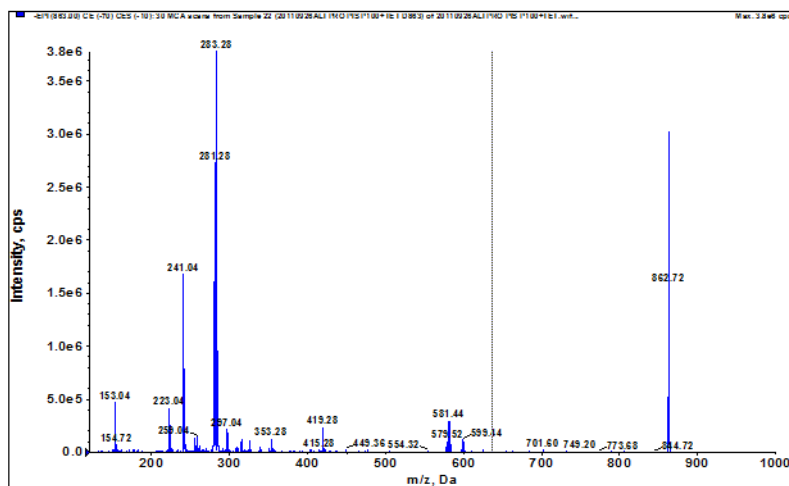
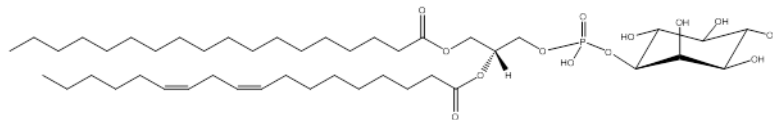


Figure 7.11. Mass spectrometric analyses of inositol-phosphate containing phospholipids from DM and procyclic form TbPIS pLEW100 + tetracycline. Total lipids were analysed by ES-MS in negative ion mode using parent-ion scanning of the collision induced fragment at 241 m/z . A. wild type double marker cells. B. PCF TbPIS p100 overexpression cells grown in the presence of tetracycline for 48 hours. Asterisks indicate species which have been further fragmented – see Figure 7.12. For further information see Figure 7.2.

A. PI 18:0/18:2



B. PI 18:0/22:6

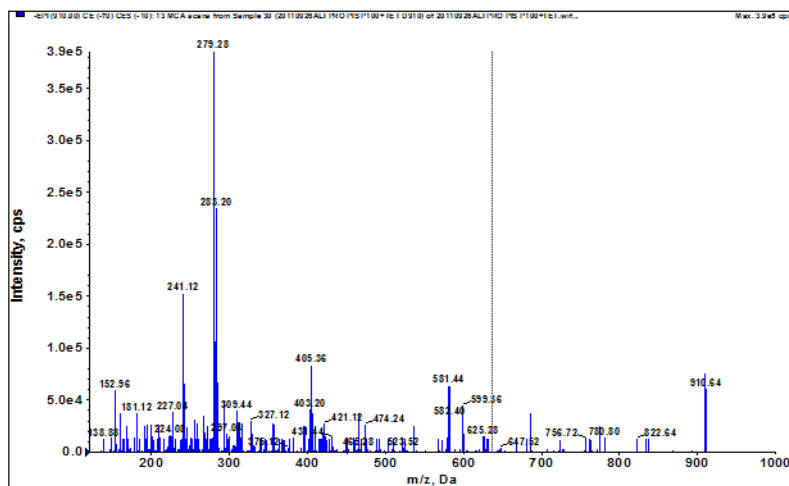
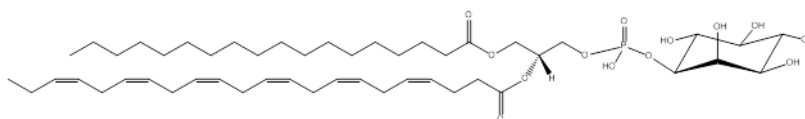


Figure 7.12. Daughter ion spectrum from A. 863 m/z [M-H]⁻ ion. B. 910 m/z [M-H]⁻ ion.

7.3.2 Subcellular Localisation of TbPIS in Procyclic Form *T. brucei*

In bloodstream form *T. brucei*, TbPIS protein has been shown to localise to both the Golgi and the ER, with Golgi TbPIS synthesising PI for bulk cellular PI from exogenous inositol and ER TbPIS synthesising PI for GPI anchors from *de novo* synthesised inositol. Whilst this has not been shown in procyclic form, the discovery of an inositol transporter that localises to the Golgi and possibly the plasma membrane, but not to the ER combined with the knowledge that knockdown of this transporter does not affect GPI anchor synthesis (Gonzalez-Salgado et al., 2012), it seems likely that TbPIS is also dually localised in procyclic form.

In order to test this hypothesis, procyclic form cells over-expressing TbPIS were induced with tetracycline. 48 hours after induction, cells were fixed and stained against both the HA tag and the ER localised protein BiP.

The results of this TbPIS-HA localisation immunofluorescence are shown in Figure 7.13. Surprisingly, very differently to what was seen in the bloodstream form TbPIS-HA cell line, HA-tagged protein was only detected in an intense spot between the nucleus and the kinetoplastid. No staining above background was seen anywhere out-with this spot, even upon exposure of the slide for several seconds. This staining is clearly not extensive enough to indicate distribution throughout the ER, although it cannot be ruled out that the protein is localised to a sub-compartment of the ER, since the BiP protein staining does cover this region. However, the size and location of the staining body is more likely to correspond to the Golgi, particularly since in some dividing cells the staining body is duplicated, as would be the case for the Golgi.

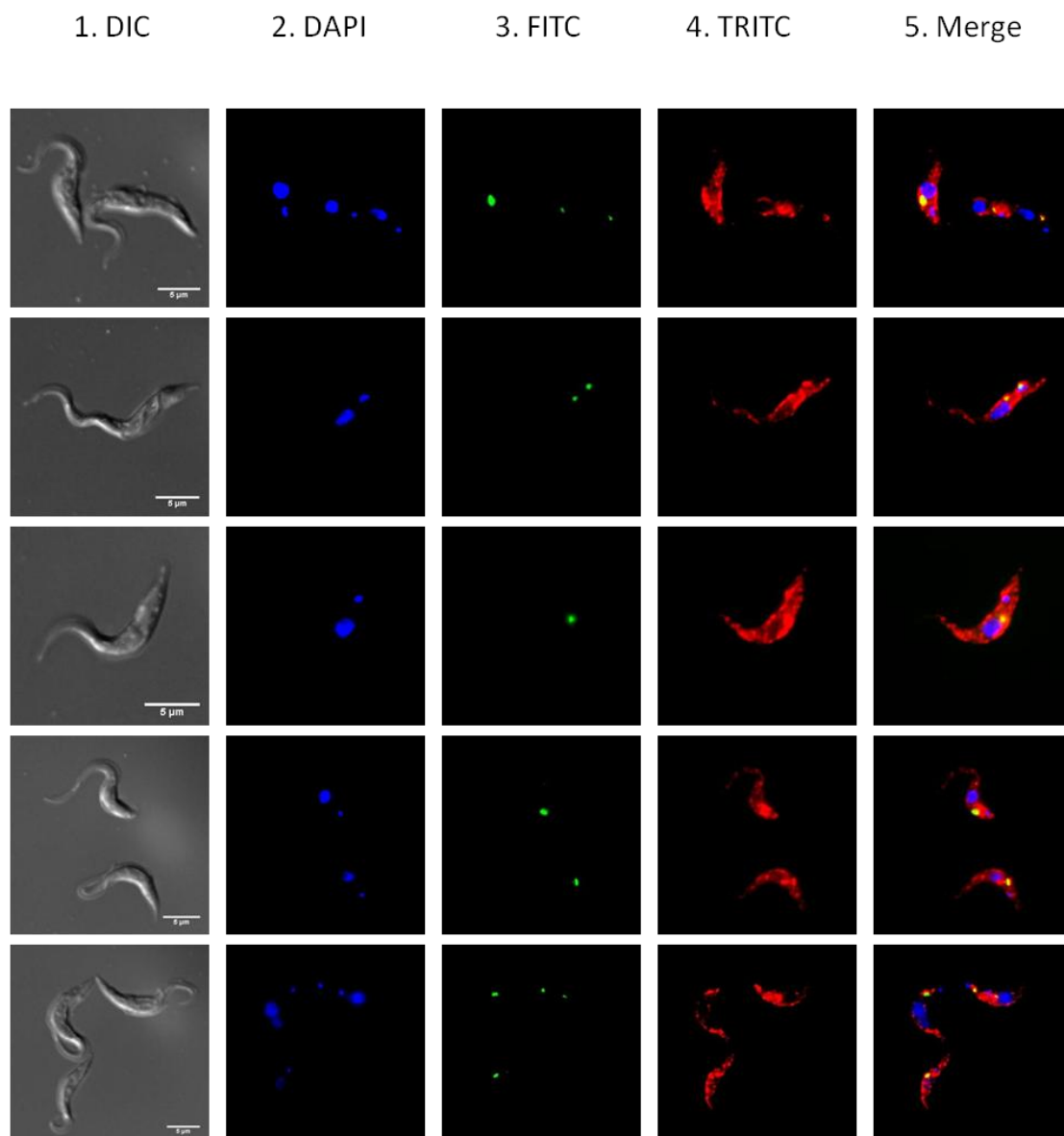


Figure 7.13. Subcellular localisation of TbPIS-HA in procyclic form *T. brucei*. Cells expressing TbPIS-HA were costained for the nuclear marker DAPI, the HA epitope and the ER marker BiP. 1. DIC image. 2. DAPI staining. 3. HA epitope staining and FITC detection. 3. BiP staining and TRITC detection. 4. Merged image.

With the results available, it can perhaps not be ruled out that the lack of ER localised TbPIS-HA protein may be due to incorrect expression of the ectopic protein meaning that it is not correctly targeted to this organelle, particularly since the HA-tagged TbPIS expressed in the procyclic form ran on SDS-PAGE in quite a different way to the same protein expressed in bloodstream form. It is, however, unclear why this would occur since the expression of TbPIS-HA in a null TbPIS background in the bloodstream form showed that it was fully functional and it seems unlikely that the

protein on the same cassette would fail to be properly processed in the procyclic form. Additionally, extra PI and IPC shows that it must be a functionally active PIS.

If TbPIS is only localised to the Golgi in the procyclic form it has dramatic ramifications for our current knowledge of phospholipid synthesis in this life cycle stage. This would mean that PI must be transported to the ER for its incorporation into GPI anchors. A less heavy dependence on GPI anchors in this life cycle stage may make this more feasible in the procyclic form than it would be in the bloodstream form as supply to the ER would not need to be quite so efficient.

However, if the Golgi pool of PI incorporating exogenous inositol supplies the GPI anchor biosynthesis pathway, it is very surprising that the knockdown of the Golgi inositol transporter had no effect on the synthesis of GPI intermediates (Gonzalez-Salgado et al., 2012). It is possible that the cells are deliberately maintaining supply of PI for GPI anchors at the expense of other phospholipids, or that the transport of PI to the ER and subsequent incorporation occurs too slowly for this pool to have been depleted in the time scale that was examined. However, exogenous radio-labelled inositol does not easily label GPI anchors in this life cycle stage (Terry Smith - personal communication).

One hypothesis which may explain this apparent contradiction may be that that in procyclic form *T. brucei* the putative inositol-phosphate transporter, which is present in the ER in the bloodstream form may be localised to the Golgi, and that somehow PI synthesis from *de novo* synthesised inositol and PI synthesis from exogenously acquired inositol are still kept separated, possibly occurring in different sub-compartments. In this scenario, the PI formed from *de novo* synthesised inositol would be transported from the Golgi to the ER for its incorporation into GPI anchors.

7.4 Conclusions

TbPIS is an essential gene in bloodstream form *T. brucei*, and the protein has been shown localise to both the Golgi and the ER (Martin and Smith, 2006b). There is evidence that in bloodstream form the ER pool of PI, which is made from *de novo* synthesised inositol, is utilised exclusively for the GPI pathway, whilst the Golgi synthesised PI, utilising exogenously acquired inositol is responsible for bulk cellular PI (Martin and Smith, 2006a). Work here suggests that the two main series of PI are not equally distributed between the two locations and alteration in the synthesis of a

PI precursor, CDP-DAG by TbCDS has different effects on the PI with these two different lipid moieties.

HA-tagged TbPIS was shown to express well in bloodstream form *T. brucei*, but its expression caused a small but consistent growth defect. This was the opposite of what occurred upon overexpression of the precursor enzyme, TbCDS, in bloodstream form *T. brucei*, which caused a slight increase in growth rate for the first 48 hours, after which growth returned to normal. This shows that the TbPIS protein is perhaps not so tightly regulated as TbCDS protein, but that the overexpression of TbPIS has detrimental effects, whilst the overexpression of TbCDS, at least in the short term, has a positive effect on cell growth, but which presumably is not sustainable, possibly due to the depletion of CTP.

bloodstream form *T. brucei* over-expressing TbPIS accumulated several species of DAG, similarly to what was seen in the TbCDS knockdown and knockout. This was previously thought to be due to the TbCDS substrate PA accumulating and being dephosphorylated into the less toxic DAG. However, these results indicate that the accumulation of DAG may in fact be a cellular response to the decrease in CDP-DAG levels, since overexpression of TbPIS would clearly also cause this reduction. In support of this, CDP-DAG levels have been shown to regulate PA phosphatase and DAG kinase in yeast (Wu and Carman, 1996, Shen and Dowhan, 1996). A decrease in PA species similar to what was seen in the bloodstream form TbCDS overexpression mutant was unexpected but may indicate that the cells are trying to adapt to the overexpression of TbPIS by upregulating TbCDS, which may utilise PA species. Generally, the lipid profile of the TbPIS overexpressing bloodstream form cell line indicated that the increase in TbPIS expression caused mis-regulation and disruption to cellular phospholipid. More specifically, an increase was seen in the ratio of the C40 PI series to the C36 PI series - the opposite to what was seen in the TbPIS CKO. This confirms what was previously seen in the bloodstream form TbCDS overexpression mutant - that there is a higher flux through the C36 pathway so that an increase in PI synthesis does not accumulate as PI but is translated into an increase in the GPI. Additionally C36 PI is more likely to be formed from *de novo* synthesised fatty acids meaning there may be more consistent traffic through this pathway. There may not be such a demand for the further utilisation of PI C40, however, so an increase in the synthesis of these species results in an accumulation of PI C40 itself.

Subcellular localisation was performed, and it was confirmed that TbPIS localises to both the ER and the Golgi, even when the HA-tagged TbPIS is expressed from a weaker promoter than what was previously attempted.

procyclic form *T. brucei* has different priorities for its PI synthesis pathways. This cell type has less dependence on a GPI anchor synthesis pathway, but PI is a precursor to the sphingolipid IPC which is not present in bloodstream form *T. brucei*. Additionally, knockdown of TbCDS expression showed that in the procyclic form, PI pools appear to be maintained at the expense of both GPI and IPC, so must in themselves be important, possibly in the maintenance of a supply of PIPs for signalling.

HA-tagged TbPIS also expressed well in procyclic form *T. brucei*. Overexpression of TbPIS did not appear to make any significant impact on the profile of positively charged lipid species, whilst there was a proportional increase in the anionic lipids PI, IPC and PG. An increase in PI and IPC are expected as products of the TbPIS protein, however the increase in PG C36:1 was unexpected and reflected what was seen in both the TbCDS knockout and knockdown, suggesting that an increase in this lipid may be some kind of cellular response to some disruption of lipid content. Replacement of PIP C36 species in DM with a peak corresponding to PIP C38 species is another alteration that was seen in both TbCDS deficient and TbCDS overexpression mutants, and could be another response to alteration of lipid content.

Contrary to what was seen in the bloodstream form, the ratio the two main PI series appeared to be unaltered. This is likely because the flux through the GPI synthesis pathway is not nearly so dramatic, combined with the utilisation of PI species to make IPC possibly evening out the demands on the two pools. Conversely, there was a large increase in the ratio of IPC C32 to IPC C34. This differential effect was seen in previous mutants and strongly suggests different regulation and possibly different localisation of IPC species with the two different lipid moieties, and may suggest that the ER/MAM pool contains more IPC C32 and that this is more sensitive to depletion of PI, which may be due to the other requirements for PI in this compartment - i.e. for GPI anchor biosynthesis.

Finally, subcellular localisation by IF showed a surprising result for procyclic form TbPIS - that unlike in bloodstream form *T. brucei* the protein does not appear to be dually localised, and signal was only seen from the Golgi. Whilst incorrect targeting

of the HA-tagged protein is possible, if these results are correct than there is the necessity of getting Golgi synthesised PI into the ER for GPI anchor biosynthesis. Certainly, less dependence upon, and less flux through the GPI biosynthesis pathway in procyclic form would make this more feasible in this cell type than it would be in the bloodstream form. One possible scenario that may explain these results is if the putative inositol-phosphate transporter was also present in the Golgi in procyclic form *T. brucei*, and somehow the two routes of PI synthesis (via de novo synthesised inositol and exogenously acquired inositol) were separated in this organelle. PI synthesised from de novo synthesised inositol would then be transported into the ER for its utilisation in GPI anchor biosynthesis. This unexpected result is an excellent example of just how different phospholipid synthesis is between the two life cycle stages.

Chapter 8: Conclusions and Future Work

T. brucei is the causative agent of Human African Trypanosomiasis, and new treatments are urgently needed. Lipid metabolism of *T. brucei* differs in many respects from that of its human host, and potentially offers a plethora of novel drug targets. In particular, *T. brucei* has a high demand for glycerophospholipids, especially those involved in the synthesis of GPI anchors and possibly for PIP signalling, as well as in sphingolipid metabolism. CDP-DAG synthase is a central enzyme in glycerophospholipid synthesis, but nothing is currently known about this enzyme in *T. brucei*. Here, TbCDS and its downstream pathways were investigated in bloodstream form and procyclic *T. brucei*.

Bloodstream Form *Trypanosoma brucei*

Results presented here give clear evidence that Tb927.7.220 encodes the only functional eukaryotic-like TbCDS which here is shown to be essential in bloodstream form *T. brucei*, genetically validating it as a drug target. Moreover, the discovery was made that related parasitic organisms *T. vivax*, *T. cruzi* and *Leishmania* species contain a second TbCDS gene of prokaryotic origin which is not present in humans, and may be worth investigating as potential drug targets in the future.

Manipulation of TbCDS expression in bloodstream form *T. brucei* has added to knowledge of glycerophospholipid synthesis, and has challenged some previous assumptions about lipid metabolism in bloodstream form *T. brucei* metabolism.

Figure 8.1 shows a revised scheme for bloodstream form glycerophospholipid synthesis pathways involving CDP-DAG, paying particular attention to their subcellular localisation. Both PI and CDP-DAG are synthesised in both the Golgi apparatus and the ER. A *myo*-inositol specific transporter pumps inositol into the Golgi, and this inositol is used along with CDP-DAG (produced by the Golgi TbCDS) to make PI via the Golgi resident PI synthase, whose active site is thought to face

towards the inside of the Golgi (Gonzalez-Salgado et al., 2012). This PI is the source of bulk cellular PI, but is not used for GPI anchor synthesis.

Inositol-3-phosphate produced from glucose-6-phosphate by INO1 in the cytoplasm is transported into the ER where it is dephosphorylated by inositol monophosphatase. This *de novo* synthesised inositol is then used for the production of PI along with CDP-DAG synthesised from the ER TbCDS via the internal facing TbPIS in the ER. This PI feeds the GPI biosynthetic pathway, which is essential for bloodstream form *T. brucei*. The high flux through the PI to GPI pathway is likely to be on a par with or higher than that of the PI synthesised in the Golgi, meaning that the dynamic pool of PI in the ER is very small as it is so rapidly used. This PI may also be used for the production of PIPs, which may occur in a mobile subcompartment of the ER as in humans (Kim et al., 2011). A cell cycle stall caused by the knockout of TbCDS could indicate that PIP signalling has a role in cell cycle regulation in bloodstream form *T. brucei*. This would give evidence of the importance of PI for PIP signalling to the parasite. Additionally, depletion of GPI anchor biosynthesis has been shown to cause a cell cycle stall due to the cells being unwilling to dilute their GPI anchored VSG on the cell surface (Smith et al., 2009).

Previous work has indicated that the synthesis of PS via CDP-DAG does not occur in *T. brucei* (Signorell et al., 2008) and in support of this, the *T. brucei* PSS enzyme shows most sequence similarity to the mammalian PSS2 headgroup exchange enzyme which utilises PE, rather than the yeast or prokaryotic PSS proteins which are CDP-alcohol phosphatidyltransferases (Nikawa et al., 1987b). However, since knockdown of PE did not affect the amount of PS in bloodstream form *T. brucei* (Gibellini et al., 2009) it is possible that the *T. brucei* PSS is also capable of utilising PC as a substrate. The production of PE through PS decarboxylation occurs in prokaryotes, yeast, and to a limited extent in mammals (reviewed in Schuiki and Daum (2009) this activity does not occur in bloodstream form *T. brucei* (Gibellini et al., 2009). Surprisingly, however, *T. brucei* does encode a functional PSD and preliminary work indicates that it is essential in bloodstream form *T. brucei* (Smith, personal communication).

For the first time, evidence is presented here that in *T. brucei* PG must be synthesised via an alternative mechanism not involving CDP-DAG as a lipid donor. The *T. brucei* gene predicted to encode PGP synthase shows sequence similarity to the *S. cerevisiae* PGPS which was previously thought to encode a PS synthase based on

sequence homology with the *E. coli* PSS (Chang et al., 1998), but has since been shown to encode a PGP synthase (Chang et al., 1998). PGPS belongs to a family of proteins with two phospholipase D domains which catalyse trans-phosphatidyl transfer reactions (Ponting and Kerr, 1996) and it is possible that they could catalyse such a reaction using PS as the lipid donor and producing PG. This reaction would not be reversible, since PGPS does not use serine as a substrate (Muller and Frentzen, 2001, Kawasaki et al., 2001). PS synthesis from PE is thought to occur in the mitochondrial associated membrane of the ER (Vance, 1990, Stone and Vance, 2000, Shiao et al., 1995) and so it would be ideally localised to feed into the mitochondrial phospholipid pathway.

It appears that the *T. brucei* cellular response to glycerophospholipid disruption that results in the feed of excess PA or DAG into the Kennedy Pathway which is converted to PG via PS, possibly this is in order to maintain a balance of cellular lipid and PG is considered a relatively harmless lipid to produce in excess. Whether PS is the major

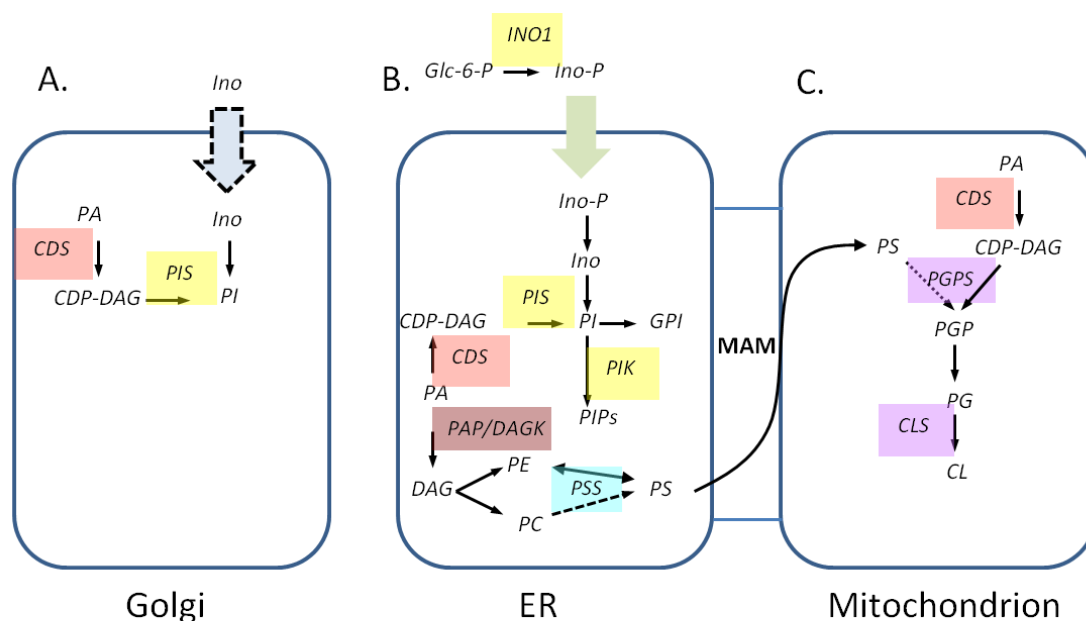


Figure 8.1. Revised pathways for glycerophospholipid synthesis in bloodstream form *T. brucei*. Enzymes for which candidate genes have been identified are indicated. Block arrows indicate transporters. MAM = mitochondrial associated membranes. **Metabolite abbreviations:** Glc-6-P = glucose-6-phosphate; PA – phosphatidic acid; CDP-DAG – cytidine diphosphate diacylglycerol; PGP – phosphatidylglycerophosphate; PG – phosphatidylglycerol, CL – cardiolipin, PS- phosphatidylserine, PE – phosphatidylethanolamine; PI – phosphatidylinositol; PIPs – phosphorylated derivatives of phosphatidyl inositol; DAG – diacylglycerol; PE – phosphatidylethanolamine; IPC – inositol phosphorylceramide. **Enzyme abbreviations:** CDS – cytidine diphosphate diacylglycerol synthase, PGPS – phosphatidylglycerolphosphate synthase, CLS – cardiolipin synthase, PIS phosphatidylinositol synthase, PIK - phosphatidylinositol kinase, PSS – phosphatidylserine synthase, PSD – phosphatidylserine decarboxylase, PAP – phosphatidic acid phosphatase, DAGK – DAG kinase. Dotted lines indicate putative pathways.

source of PG and CL under normal circumstances or whether synthesis of PGP from CDP-DAG normally produces the bulk of PG remains to be determined. In many organisms CDS is localised to the mitochondria, and there is a chance that this is also the case in bloodstream form *T. brucei*, although further co-localisation experiments and subcellular fractionation would be required to confirm this.

Procyclic Form *Trypanosoma brucei*

TbCDS reduction caused a growth defect in procyclic form *T. brucei*, suggesting that this gene is essential in the insect form of the parasite. However, in this case alteration of TbCDS expression levels also leads to a number of conclusions which both further and challenge current knowledge of glycerophospholipid metabolism in procyclic form *T. brucei*, as well as highlighting just how different glycerophospholipid biosynthesis is between the two life cycle stages. Figure 8.2 shows a revised scheme for the glycerophospholipid synthesis in procyclic form *T. brucei*, again concentrating on TbCDS and downstream pathways and their subcellular localisation.

It is known that an inositol transporter localised to the Golgi membrane is essential for viability in procyclic form *T. brucei* (Gonzalez-Salgado et al., 2012), but that this transporter is not required for the synthesis of GPI anchors. This Golgi pool of PI is further utilised for the synthesis of IPC (Gonzalez-Salgado et al., 2012). However, results here indicate that whilst TbCDS is present in both the Golgi and the ER, the TbPIS is only present in the Golgi. If this result is correct, PI synthesised in the Golgi must be transported to the ER for GPI and PIP synthesis. This seems more feasible than it would be in bloodstream form, since flux through the GPI biosynthetic pathway in procyclic form is about 10% of bloodstream form levels (Young and Smith, 2010 and references therein). However, *T. brucei*, like bloodstream form, produce the vast majority of GPI anchors from PI that is derived from *de novo* synthesised inositol, which would suggest that inositol-phosphate - the product of INO1 gene from glucose-6-phosphate - would need to be transported into the Golgi. Since it is clear that the pathway for PI produced from exogenous inositol and *de novo* synthesised inositol are separate, they must therefore be separately compartmentalised within the Golgi.

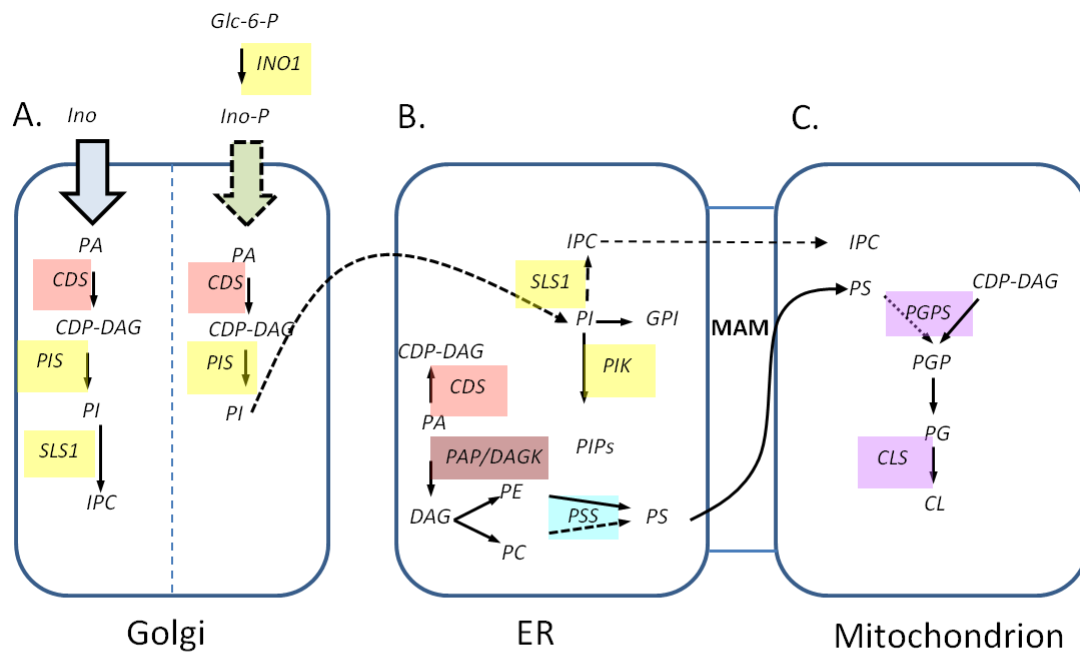


Figure 8.2. Revised pathways for glycerophospholipid synthesis in procyclic *T. brucei*. Enzymes for which candidate genes have been identified are indicated. Block arrows indicate transporters. Dashed lines indicate putative pathways, MAM = mitochondrial associated membranes. **Metabolite abbreviations:** PA – phosphatidic acid; CDP-DAG – cytidine diphosphate diacylglycerol; PGP – phosphatidylglycerophosphate; PG – phosphatidylglycerol, CL – cardiolipin, PS- phosphatidylserine, PE – phosphatidylethanolamine; PI – phosphatidylinositol; PIPs – phosphorylated derivatives of phosphatidyl inositol; DAG – diacylglycerol; PE – phosphatidylethanolamine; IPC – inositol phosphorylceramide. **Enzyme abbreviations:** CDS – cytidine diphosphate diacylglycerol synthase, *PGPS* – phosphatidylglycerolphosphate synthase, *CLS* – cardiolipin synthase, *PIS* phosphatidylinositol synthase, *PIK* - phosphatidylinositol kinase, *PSS* – phosphatidylserine synthase, *PSD* – phosphatidylserine decarboxylase, *PAP* – phosphatidic acid phosphatase, *DAGK* – DAG kinase *SLS1* – inositol phosphorylceramide synthase. Dotted lines indicate putative pathways.

Localisation of the TbPIS to the Golgi is only currently tentative for the procyclic form, and there is a chance that the HA-tagged TbCDS is not being properly expressed and/or localised. To further investigate the localisation it may be worth creating a TbCDS expression construct with a different epitope-tag, for example an N-terminal GFP fusion.

PI transported to the ER from the Golgi that is utilised for GPI anchor biosynthesis, may also be used for PIP signalling and possibly some IPC synthesis. Knockdown of CDP-DAG for the production of PI for PIPs caused a kinetoplast segregation defect and detached flagella, which may be further evidence of the importance of PIP signalling in cell cycle regulation in procyclic form *T. brucei* (Hammarton et al., 2005, Hammarton et al., 2007a, Franke et al., 1997, Rodgers et al., 2007).

PS synthesis in procyclic form *T. brucei* has already been shown to be almost completely abolished when PE is knocked down (Signorell et al., 2008) which appears

to argue against a role for PC in its production. However, the demand for synthesis of the mitochondrial phospholipids PG and CL is much higher in this life cycle stage, which may put a heavy demand on PS if this is the only route to PG (see later). If headgroup exchange activity of TbPSS with PC is less efficient than that with PE, whilst it may be sufficient for the modest requirements on the PS pool of bloodstream form *T. brucei* it is not sufficient for the procyclic form. Such a demand on the PS pool for PG and CL would argue against a significant role for CDP-DAG in its synthesis.

As in bloodstream form *T. brucei*, it seems that PG synthesis is achieved via an alternative route that does not utilise CDP-DAG, and that PG is produced as a general cellular response to alterations in glycerophospholipid, possibly to try and balance out any excesses in unwanted intermediates, such as PA. In this case, PG and CL are likely to have a larger role due to the importance of the mitochondria, as discussed earlier.

Altogether these results show that TbCDS is an essential enzyme in both procyclic form and bloodstream form *T. brucei*, and that the downstream glycerophospholipid biosynthesis pathways differ to those in mammals as well as between the *T. brucei* life cycle stages - an indication of their vastly different life styles and essential biochemical pathways i.e. GPI biosynthesis in bloodstream form and fully functional mitochondria and IPC formation in procyclic form. If TbCDS itself does not present a good drug target due to similarity to human CDSs, it is possible that this work has elucidated other genes and pathways that are different from the human host which may represent ideal novel drug targets, for example the prokaryotic type CDS in other trypanosomatids, or the TbPGPS which may display a specificity for PS which is not present in the mammalian enzyme.

References

- AGRANOFF, B. W. & FISHER, S. K. 1991. PHOSPHOINOSITIDES AND THEIR STIMULATED BREAKDOWN. *Acs Symposium Series*, 463, 20-32.
- ANDERSON, M. S. & LOPES, J. M. 1996. Carbon source regulation of PIS1 gene expression in *Saccharomyces cerevisiae* involves the MCM1 gene and the two-component regulatory gene, SLN1. *Journal of Biological Chemistry*, 271, 26596-26601.
- ANDREWS, J. & MUDD, J. B. 1985. PHOSPHATIDYLGLYCEROL SYNTHESIS IN PEA-CHLOROPLASTS - PATHWAY AND LOCALIZATION. *Plant Physiology*, 79, 259-265.
- ANTONSSON, B. 1997. Phosphatidylinositol synthase from mammalian tissues. *Biochimica Et Biophysica Acta-Lipids and Lipid Metabolism*, 1348, 179-186.
- ANTONSSON, B. E. 1994. PURIFICATION AND CHARACTERIZATION OF PHOSPHATIDYLINOSITOL SYNTHASE FROM HUMAN PLACENTA. *Biochemical Journal*, 297, 517-522.
- ANTONSSON, B. E. & KLIG, L. S. 1996. *Candida albicans* phosphatidylinositol synthase has common features with both *Saccharomyces cerevisiae* and mammalian phosphatidylinositol synthases. *Yeast*, 12, 449-456.
- ASHBURNER, B. P. & LOPES, J. M. 1995. REGULATION OF YEAST PHOSPHOLIPID BIOSYNTHETIC GENE-EXPRESSION IN RESPONSE TO INOSITOL INVOLVES 2 SUPERIMPOSED MECHANISMS. *Proceedings of the National Academy of Sciences of the United States of America*, 92, 9722-9726.
- ATKINSON, K. D., JENSEN, B., KOLAT, A. I., STORM, E. M., HENRY, S. A. & FOGEL, S. 1980. YEAST MUTANTS AUXOTROPHIC FOR CHOLINE OR ETHANOLAMINE. *Journal of Bacteriology*, 141, 558-564.
- BAELEE, M. S. & CARMAN, G. M. 1984. PHOSPHATIDYLSERINE SYNTHESIS IN SACCHAROMYCES-CEREVISIAE - PURIFICATION AND CHARACTERIZATION OF MEMBRANE-ASSOCIATED PHOSPHATIDYLSERINE SYNTHASE. *Journal of Biological Chemistry*, 259, 857-862.
- BAKER, R. R. & CHANG, H. Y. 1990. PHOSPHATIDYLINOSITOL SYNTHETASE ACTIVITIES IN NEURONAL NUCLEI AND MICROSOMAL FRACTIONS-ISOLATED FROM IMMATURE RABBIT CEREBRAL-CORTEX. *Biochimica Et Biophysica Acta*, 1042, 55-61.
- BANGS, J. D., UYETAKE, L., BRICKMAN, M. J., BALBER, A. E. & BOOTHROYD, J. C. 1993. MOLECULAR-CLONING AND CELLULAR-LOCALIZATION OF A BIP HOMOLOG IN TRYPANOSOMA-BRUCI - DIVERGENT ER RETENTION SIGNALS IN A LOWER EUKARYOTE. *Journal of Cell Science*, 105, 1101-1113.
- BARRETT, M. P., BURCHMORE, R. J. S., STICH, A., LAZZARI, J. O., FRASCH, A. C., CAZZULO, J. J. & KRISHNA, S. 2003. The trypanosomiasis. *Lancet*, 362, 1469-1480.
- BARRETT, M. P., VINCENT, I. M., BURCHMORE, R. J. S., KAZIBWE, A. J. N. & MATOVU, E. 2011. Drug resistance in human African trypanosomiasis. *Future Microbiology*, 6, 1037-1047.
- BASAL 1998. Double-stranded RNA induces mRNA degradation in *Trypanosoma brucei*. *Proceedings of the National Academy of Sciences of the United States of America*, 95, 14687-14692.
- BELENDIUK, G., MANGNALL, D., TUNG, B., WESTLEY, J. & GETZ, G. S. 1978. CTP-PHOSPHATIDIC ACID CYTIDYLTRANSFERASE FROM SACCHAROMYCES-CEREVISIAE - PARTIAL-PURIFICATION, CHARACTERIZATION, AND KINETIC-BEHAVIOR. *Journal of Biological Chemistry*, 253, 4555-4565.
- BELL, R. M., MAVIS, R. D., OSBORN, M. J. & VAGELOS, P. R. 1971. ENZYMMES OF PHOSPHOLIPID METABOLISM - LOCALIZATION IN CYTOPLASMIC AND OUTER MEMBRANE OF CELL ENVELOPE OF ESCHERICHIA-COLI AND SALMONELLA-TYPHIMURIUM. *Biochimica Et Biophysica Acta*, 249, 628-&.
- BENJAMINS, J. A. & AGRANOFF, B. W. 1969. DISTRIBUTION AND PROPERTIES OF ENZ CDP DI GLYCERIDE INOSITOL TRANSFERASE FROM BRAIN GUINEA-PIG BOVINE SERUM ALBUMIN. *Journal of Neurochemistry*, 16, 513-527.
- BERRIMAN, M., GHEDIN, E., HERTZ-FOWLER, C., BLANDIN, G., RENAULD, H., BARTHOLOMEU, D. C., LENNARD, N. J., CALER, E., HAMLIN, N. E., HAAS, B., BOHME, W., HANNICK, L., ASLETT, M. A., SHALLOM, J., MARCELLO, L., HOU, L. H., WICKSTEAD, B., ALSMARK, U.

- C. M., ARROWSMITH, C., ATKIN, R. J., BARRON, A. J., BRINGAUD, F., BROOKS, K., CARRINGTON, M., CHEREVACH, I., CHILLINGWORTH, T. J., CHURCHER, C., CLARK, L. N., CORTON, C. H., CRONIN, A., DAVIES, R. M., DOGGETT, J., DJIKENG, A., FELDBLYUM, T., FIELD, M. C., FRASER, A., GOODHEAD, I., HANCE, Z., HARPER, D., HARRIS, B. R., HAUSER, H., HOSTETTER, J., IVENS, A., JAGELS, K., JOHNSON, D., JOHNSON, J., JONES, K., KERHORNOU, A. X., KOO, H., LARKE, N., LANDFEAR, S., LARKIN, C., LEECH, V., LINE, A., LORD, A., MACLEOD, A., MOONEY, P. J., MOULE, S., MARTIN, D. M. A., MORGAN, G. W., MUNGALL, K., NORBERTCZAK, H., ORMOND, D., PAI, G., PEACOCK, C. S., PETERSON, J., QUAIL, M. A., RABBINOWITSCH, E., RAJANDREAM, M. A., REITTER, C., SALZBERG, S. L., SANDERS, M., SCHOBEL, S., SHARP, S., SIMMONDS, M., SIMPSON, A. J., TALTON, L., TURNER, C. M. R., TAIT, A., TIVEY, A. R., VAN AKEN, S., WALKER, D., WANLESS, D., WANG, S. L., WHITE, B., WHITE, O., WHITEHEAD, S., WOODWARD, J., WORTMAN, J., ADAMS, M. D., EMBLEY, T. M., GULL, K., ULLU, E., BARRY, J. D., FAIRLAMB, A. H., OPPERDOES, F., BARRET, B. G., DONELSON, J. E., HALL, N., FRASER, C. M., et al. 2005. The genome of the African trypanosome *Trypanosoma brucei*. *Science*, 309, 416-422.
- BISHOP, H. H. & STRICKLAND, K. P. 1976. STUDIES ON FORMATION BY RAT-BRAIN PREPARATIONS OF CDP-DIGLYCERIDE FROM CTP AND PHOSPHATIDIC ACIDS OF VARYING FATTY-ACID COMPOSITIONS. *Canadian Journal of Biochemistry*, 54, 249-260.
- BITTOVA, L., STAHELIN, R. V. & CHO, W. 2001. Roles of ionic residues of the C1 domain in protein kinase C- α activation and the origin of phosphatidylserine specificity. *Journal of Biological Chemistry*, 276, 4218-4226.
- BLIGH, E. G. & DYER, W. J. 1959. A RAPID METHOD OF TOTAL LIPID EXTRACTION AND PURIFICATION. *Canadian Journal of Biochemistry and Physiology*, 37, 911-917.
- BLOUIN, A., LAVEZZI, T. & MOORE, T. S. 2003. Membrane lipid biosynthesis in *Chlamydomonas reinhardtii*. Partial characterization of CDP-diacylglycerol: myo-inositol 3-phosphatidyltransferase. *Plant Physiology and Biochemistry*, 41, 11-16.
- BONNEL, S. I., LIN, Y. P., KELLEY, M. J., CARMAN, G. M. & EICHBERG, J. 1989. INTERACTIONS OF THIOPHOSPHATIDIC ACID WITH ENZYMES WHICH METABOLIZE PHOSPHATIDIC-ACID - INHIBITION OF PHOSPHATIDIC-ACID PHOSPHATASE AND UTILIZATION BY CDP-DIACYLGLYCEROL SYNTHASE. *Biochimica Et Biophysica Acta*, 1005, 289-295.
- BOWES, A. E., SAMAD, A. H., JIANG, P., WEAVER, B. & MELLORS, A. 1993. THE ACQUISITION OF LYSOPHOSPHATIDYLCHOLINE BY AFRICAN TRYPANOSOMES. *Journal of Biological Chemistry*, 268, 13885-13892.
- BREGLIA, S. A., SLAMOVITS, C. H. & LEANDER, B. S. 2007. Phylogeny of phagotrophic euglenids (Euglenozoa) as inferred from hsp90 gene sequences. *Journal of Eukaryotic Microbiology*, 54, 86-92.
- BRUN, R. & SCHONENBERGER, M. 1979. CULTIVATION AND INVITRO CLONING OF PROCYCLIC CULTURE FORMS OF TRYPANOSOMA-BRUCI IN A SEMI-DEFINED MEDIUM. *Acta Tropica*, 36, 289-292.
- CAMPBELL, D. A., THOMAS, S. & STURM, N. R. 2003. Transcription in kinetoplastid protozoa: why be normal? *Microbes and Infection*, 5, 1231-1240.
- CARMAN, G. M. & BAELEE, M. 1992. PHOSPHATIDYLSERINE SYNTHASE FROM YEAST. *Methods in Enzymology*, 209, 298-305.
- CARMAN, G. M. & FISCHL, A. S. 1992. PHOSPHATIDYLINOSITOL SYNTHASE FROM YEAST. *Methods in Enzymology*, 209, 305-312.
- CARMAN, G. M. & HAN, G.-S. 2011. Regulation of Phospholipid Synthesis in the Yeast *Saccharomyces cerevisiae*. In: KORNBERG, R. D. R. C. R. H. R. J. E. T. J. W. (ed.) *Annual Review of Biochemistry*, Vol 80.
- CARMAN, G. M. & HAN, G. S. 2007. Regulation of phospholipid synthesis in *Saccharomyces cerevisiae* by zinc depletion. *Biochimica Et Biophysica Acta-Molecular and Cell Biology of Lipids*, 1771, 322-330.
- CARMAN, G. M. & HAN, G. S. 2009. Regulation of phospholipid synthesis in yeast. *Journal of Lipid Research*, 50, S69-S73.
- CARMAN, G. M. & HENRY, S. A. 1989. PHOSPHOLIPID BIOSYNTHESIS IN YEAST. *Annual Review of Biochemistry*, 58, 635-669.

- CARMAN, G. M. & HENRY, S. A. 1999. Phospholipid biosynthesis in the yeast *Saccharomyces cerevisiae* and interrelationship with other metabolic processes. *Progress in Lipid Research*, 38, 361-399.
- CARMAN, G. M. & HENRY, S. A. 2007. Phosphatidic acid plays a central role in the transcriptional regulation of glycerophospholipid synthesis in *Saccharomyces cerevisiae*. *Journal of Biological Chemistry*, 282, 37293-37297.
- CARTER, J. R. & KENNEDY, E. P. 1966. Enzymatic synthesis of cytidine diphosphate diglyceride. *Journal of Lipid Research*, 7, 678-83.
- CHANG, S. C., HEACOCK, P. N., CLANCEY, C. J. & DOWHAN, W. 1998. The PEL1 gene (renamed PGS1) encodes the phosphatidylglycerophosphate synthase of *Saccharomyces cerevisiae*. *Journal of Biological Chemistry*, 273, 9829-9836.
- CHANG, T. H., MILNE, K. G., GUTHER, M. L. S., SMITH, T. K. & FERGUSON, M. A. J. 2002. Cloning of *Trypanosoma brucei* and *Leishmania major* genes encoding the GlcNAc-phosphatidylinositol De-N-acetylase of glycosylphosphatidylinositol biosynthesis that is essential to the African Sleeping sickness parasite. *Journal of Biological Chemistry*, 277, 50176-50182.
- CHEN, D. C., YANG, B. C. & KUO, T. T. 1992. ONE-STEP TRANSFORMATION OF YEAST IN STATIONARY PHASE. *Current Genetics*, 21, 83-84.
- CHEN, M., HANCOCK, L. C. & LOPES, J. M. 2007. Transcriptional regulation of yeast phospholipid biosynthetic genes. *Biochimica Et Biophysica Acta-Molecular and Cell Biology of Lipids*, 1771, 310-321.
- CHICHA, A., JUSTIN, A. M., JOLLIOT, A., DEMANDRE, C. & MAZLIAK, P. 1993. BIOSYNTHESIS OF THE MOLECULAR-SPECIES OF PHOSPHATIDYLINOSITOL FOUND IN MICROSOMES AND PLASMA-MEMBRANES FROM ETIOLATED MAIZE COLEOPTILES. *Plant Physiology and Biochemistry*, 31, 507-513.
- CLAROS, M. G. & VONHEIJNE, G. 1994. TOPPED-II - AN IMPROVED SOFTWARE FOR MEMBRANE-PROTEIN STRUCTURE PREDICTIONS. *Computer Applications in the Biosciences*, 10, 685-686.
- CLAYTON, A. M., GULER, J. L., POVELONES, M. L., GLUENZ, E., GULL, K., SMITH, T. K., JENSEN, R. E. & ENGLUND, P. T. 2011. Depletion of Mitochondrial Acyl Carrier Protein in Bloodstream-Form *Trypanosoma brucei* Causes a Kinetoplast Segregation Defect. *Eukaryotic Cell*, 10, 286-292.
- COBON, G. S., CROWFOOT, P. D. & LINNANE, A. W. 1974. BIOGENESIS OF MITOCHONDRIA .35. PHOSPHOLIPID SYNTHESIS INVITRO BY YEAST MITOCHONDRIAL AND MICROSOMAL FRACTIONS. *Biochemical Journal*, 144, 265-275.
- COLLIN, S., JUSTIN, A. M., CANTREL, C., ARONDEL, V. & KADER, J. C. 1999. Identification of AtPIS, a phosphatidylinositol synthase from *Arabidopsis*. *European Journal of Biochemistry*, 262, 652-658.
- COPPENS, I., BAUDHUIN, P., OPPERDOES, F. R. & COURTOY, P. J. 1988. RECEPTORS FOR THE HOST LOW-DENSITY LIPOPROTEINS ON THE HEMOFLAGELLATE TRYPANOSOMA-BRUCI - PURIFICATION AND INVOLVEMENT IN THE GROWTH OF THE PARASITE. *Proceedings of the National Academy of Sciences of the United States of America*, 85, 6753-6757.
- COPPENS, I. & COURTOY, P. J. 1995. EXOGENOUS AND ENDOGENOUS SOURCES OF STEROLS IN THE CULTURE-ADAPTED PROCYCLIC TRYPOMASTIGOTES OF TRYPANOSOMA-BRUCI. *Molecular and Biochemical Parasitology*, 73, 179-188.
- CROSS, G. A. M. 1996. Antigenic variation in trypanosomes: Secrets surface slowly. *Bioessays*, 18, 283-291.
- CUBITT, A. B. & GERSHENGORN, M. C. 1989. CHARACTERIZATION OF A SALT-EXTRACTABLE PHOSPHATIDYLINOSITOL SYNTHASE FROM RAT PITUITARY-TUMOUR MEMBRANES. *Biochemical Journal*, 257, 639-644.
- DAS, A., GALE, M., CARTER, V. & PARSONS, M. 1994. THE PROTEIN PHOSPHATASE INHIBITOR OKADAIC ACID INDUCES DEFECTS IN CYTOKINESIS AND ORGANELLAR GENOME SEGREGATION IN TRYPANOSOMA-BRUCI. *Journal of Cell Science*, 107, 3477-3483.
- DE KONING, H. P., WATSON, C. J. & JARVIS, S. M. 1998. Characterization of a nucleoside/proton symporter in procyclic *Trypanosoma brucei brucei*. *Journal of Biological Chemistry*, 273, 9486-9494.

- DE VIRVILLE, J. D., BROWN, S., COCHET, F., SOLER, M.-N., HOFFELT, M., RUELLAND, E., ZACHOWSKI, A. & COLLIN, S. 2010. Assessment of mitochondria as a compartment for phosphatidylinositol synthesis in *Solanum tuberosum*. *Plant Physiology and Biochemistry*, 48, 952-960.
- DECAMILLI, P., EMR, S. D., MCPHERSON, P. S. & NOVICK, P. 1996. Phosphoinositides as regulators in membrane traffic. *Science*, 271, 1533-1539.
- DECHAVIGNY, A., HEACOCK, P. N. & DOWHAN, W. 1991. SEQUENCE AND INACTIVATION OF THE PSS GENE OF *ESCHERICHIA-COLI* - PHOSPHATIDYLETHANOLAMINE MAY NOT BE ESSENTIAL FOR CELL VIABILITY. *Journal of Biological Chemistry*, 266, 5323-5332.
- DEFLOIRIN, J., RUDOLF, M. & SEEBECK, T. 1994. THE MAJOR COMPONENTS OF THE PARAFLAGELLAR ROD OF *TRYPANOSOMA-BRUCI* ARE 2 SIMILAR, BUT DISTINCT PROTEINS WHICH ARE ENCODED BY 2 DIFFERENT GENE LOCI. *Journal of Biological Chemistry*, 269, 28745-28751.
- DITTRICH, N. & ULBRICH-HOFMANN, R. 2001. Transphosphatidylation by immobilized phospholipase D in aqueous media. *Biotechnology and Applied Biochemistry*, 34, 189-194.
- DIXON, H., GINGER, C. D. & WILLIAMS, J. 1971. LIPID METABOLISM OF BLOOD AND CULTURE FORMS OF *TRYPANOSOMA-LEWISI* AND *TRYPANOSOMA-RHODESIENSE*. *Comparative Biochemistry and Physiology*, 39, 247-&.
- DIXON, H. & WILLIAMS, J. 1970. LIPID COMPOSITION OF BLOOD AND CULTURE FORMS OF *TRYPANOSOMA-LEWISI* AND *TRYPANOSOMA-RHODESIENSE* COMPARED WITH THAT OF THEIR ENVIRONMENT. *Comparative Biochemistry and Physiology*, 33, 111-&.
- DOERING, T. L., MASTERSON, W. J., ENGLUND, P. T. & HART, G. W. 1989. BIOSYNTHESIS OF THE GLYCOSYL PHOSPHATIDYLINOSITOL MEMBRANE ANCHOR OF THE *TRYPANOSOMA* VARIANT SURFACE GLYCOPROTEIN - ORIGIN OF THE NON-ACETYLATED GLUCOSAMINE. *Journal of Biological Chemistry*, 264, 11168-11173.
- DOWHAN, W. 1997. CDP-diacylglycerol synthase of microorganisms. *Biochimica Et Biophysica Acta-Lipids and Lipid Metabolism*, 1348, 157-165.
- ELABBADI, N., ANCELIN, M. L. & VIAL, H. J. 1994. CHARACTERIZATION OF PHOSPHATIDYLINOSITOL SYNTHASE AND EVIDENCE OF A POLYPHOSPHOINOSITIDE CYCLE IN *PLASMODIUM*-INFECTED ERYTHROCYTES. *Molecular and Biochemical Parasitology*, 63, 179-192.
- FELSENSTEIN, J. 1980a. EVOLUTIONARY TREES FROM CONTINUOUS CHARACTERS AN IMPROVED ITERATION METHOD. *The University of British Columbia. Second International Congress of Systematic and Evolutionary Biology, Vancouver, B.C., Canada, July 17-24, 1980. 1+441p. University of British Columbia: Vancouver, B.C., Canada. Paper, P195-P195.*
- FELSENSTEIN, J. 1980b. WEIGHTING OF CHARACTERS IN ESTIMATING PHYLOGENIES - AN APPROACH THROUGH LIKELIHOOD METHODS. *American Zoologist*, 20, 820-820.
- FERGUSON, M. A. J. 1997. The surface glycoconjugates of trypanosomatid parasites. *Philosophical Transactions of the Royal Society of London Series B-Biological Sciences*, 352, 1295-1302.
- FERGUSON, M. A. J. 1999. The structure, biosynthesis and functions of glycosylphosphatidylinositol anchors, and the contributions of trypanosome research. *Journal of Cell Science*, 112, 2799-2809.
- FERGUSON, M. A. J. & CROSS, G. A. M. 1984. MYRISTYLATION OF THE MEMBRANE FORM OF A *TRYPANOSOMA-BRUCI* VARIANT SURFACE GLYCOPROTEIN. *Journal of Biological Chemistry*, 259, 3011-3015.
- FIELD, M. C. & CARRINGTON, M. 2009. The trypanosome flagellar pocket. *Nature Reviews Microbiology*, 7, 775-786.
- FIELD, M. C., MENON, A. K. & CROSS, G. A. M. 1991. A GLYCOSYLPHOSPHATIDYLINOSITOL PROTEIN ANCHOR FROM PROCYCLIC STAGE *TRYPANOSOMA-BRUCI* - LIPID STRUCTURE AND BIOSYNTHESIS. *Embo Journal*, 10, 2731-2739.
- FIELD, M. C., MENON, A. K. & CROSS, G. A. M. 1992. DEVELOPMENTAL VARIATION OF GLYCOSYLPHOSPHATIDYLINOSITOL MEMBRANE ANCHORS IN *TRYPANOSOMA-BRUCI* - INVITRO BIOSYNTHESIS OF INTERMEDIATES IN THE CONSTRUCTION OF THE GPI ANCHOR

- OF THE MAJOR PROCYCLIC SURFACE GLYCOPROTEIN. *Journal of Biological Chemistry*, 267, 5324-5329.
- FISCHL, A. S. & CARMAN, G. M. 1983. PHOSPHATIDYLINOSITOL BIOSYNTHESIS IN SACCHAROMYCES-CEREVISIAE - PURIFICATION AND PROPERTIES OF MICROSOME-ASSOCIATED PHOSPHATIDYLINOSITOL SYNTHASE. *Journal of Bacteriology*, 154, 304-311.
- FISCHL, A. S., HOMANN, M. J., POOLE, M. A. & CARMAN, G. M. 1986. PHOSPHATIDYLINOSITOL SYNTHASE FROM SACCHAROMYCES-CEREVISIAE RECONSTITUTION, CHARACTERIZATION, AND REGULATION OF ACTIVITY. *Journal of Biological Chemistry*, 261, 3178-3183.
- FRANKE, T. F., KAPLAN, D. R., CANTLEY, L. C. & TOKER, A. 1997. Direct regulation of the Akt proto-oncogene product by phosphatidylinositol-3,4-bisphosphate. *Science*, 275, 665-668.
- FRIDBERG, A., OLSON, C. L., NAKAYASU, E. S., TYLER, K. M., ALMEIDA, I. C. & ENGMAN, D. M. 2008. Sphingolipid synthesis is necessary for kinetoplast segregation and cytokinesis in *Trypanosoma brucei*. *Journal of Cell Science*, 121, 522-535.
- GAILLARD, J. L., LUBOCHINSKY, B. & RIGOMIER, D. 1983. SPECIFIC-INHIBITION OF PHOSPHATIDATE CYTIDYLTRANSFERASE FROM BACILLUS-SUBTILIS MEMBRANES BY CYTIDINE MONOPHOSPHATE. *Biochimica Et Biophysica Acta*, 753, 372-380.
- GALVAO, C. & SHAYMAN, J. A. 1990. THE PHOSPHATIDYLINOSITOL SYNTHASE OF PROXIMAL TUBULE CELLS. *Biochimica Et Biophysica Acta*, 1044, 34-42.
- GANONG, B. R., LEONARD, J. M. & RAETZ, C. R. H. 1980. PHOSPHATIDIC-ACID ACCUMULATION IN THE MEMBRANES OF ESCHERICHIA-COLI MUTANTS DEFECTIVE IN CDP-DIGLYCERIDE SYNTHETASE. *Journal of Biological Chemistry*, 255, 1623-1629.
- GANONG, B. R. & RAETZ, C. R. H. 1982. MASSIVE ACCUMULATION OF PHOSPHATIDIC-ACID IN CONDITIONALLY LETHAL CDP-DIGLYCERIDE SYNTHETASE MUTANTS AND CYTIDINE AUXOTROPHS OF ESCHERICHIA-COLI. *Journal of Biological Chemistry*, 257, 389-394.
- GASCUEL, O. 1997. BIONJ: An improved version of the NJ algorithm based on a simple model of sequence data. *Molecular Biology and Evolution*, 14, 685-695.
- GEBERT, N., JOSHI, A. S., KUTIK, S., BECKER, T., MCKENZIE, M., GUAN, X. L., MOOGA, V. P., STROUD, D. A., KULKARNI, G., WENK, M. R., REHLING, P., MEISINGER, C., RYAN, M. T., WIEDEMANN, N., GREENBERG, M. L. & PFANNER, N. 2009. Mitochondrial Cardiolipin Involved in Outer-Membrane Protein Biogenesis: Implications for Barth Syndrome. *Current Biology*, 19, 2133-2139.
- GEHRIG, S. & EFFERTH, T. 2008. Development of drug resistance in *Trypanosoma brucei rhodesiense* and *Trypanosoma brucei gambiense*. Treatment of human African trypanosomiasis with natural products (Review). *International Journal of Molecular Medicine*, 22, 411-419.
- GHOSH, S., STRUM, J. C., SCIORRA, V. A., DANIEL, L. & BELL, R. M. 1996. Raf-1 kinase possesses distinct binding domains for phosphatidylserine and phosphatidic acid - Phosphatidic acid regulates the translocation of Raf-1 in 12-O-tetradecanoylphorbol-13-acetate-stimulated Madin-Darby canine kidney cells. *Journal of Biological Chemistry*, 271, 8472-8480.
- GHOSH, S., XIE, W. Q., QUEST, A. F. G., MABROUK, G. M., STRUM, J. C. & BELL, R. M. 1994. THE CYSTEINE-RICH REGION OF RAF-1 KINASE CONTAINS ZINC, TRANSLOCATES TO LIPOSOMES, AND IS ADJACENT TO A SEGMENT THAT BINDS GTP-RAS. *Faseb Journal*, 8, A1293-A1293.
- GIBELLINI, F., HUNTER, W. N. & SMITH, T. K. 2008. Biochemical characterization of the initial steps of the Kennedy pathway in *Trypanosoma brucei*: the ethanolamine and choline kinases. *Biochemical Journal*, 415, 135-144.
- GIBELLINI, F., HUNTER, W. N. & SMITH, T. K. 2009. The ethanolamine branch of the Kennedy pathway is essential in the bloodstream form of *Trypanosoma brucei*. *Molecular Microbiology*, 73, 826-843.
- GIBSON, W., PEACOCK, L., FERRIS, V., WILLIAMS, K. & BAILEY, M. 2006. Analysis of a cross between green and red fluorescent trypanosomes. *Biochemical Society Transactions*, 34, 557-559.
- GILMORE, A. P. & BURRIDGE, K. 1996. Regulation of vinculin binding to talin and actin by phosphatidyl-inositol-4-5-bisphosphate. *Nature*, 381, 531-535.

- GONZALEZ-SALGADO, A., STEINMANN, M. E., GREGANOVA, E., RAUCH, M., MAESER, P., SIGEL, E. & BUETIKOFER, P. 2012. myo-Inositol Uptake Is Essential for Bulk Inositol Phospholipid but Not Glycosylphosphatidylinositol Synthesis in *Trypanosoma brucei*. *Journal of Biological Chemistry*, 287, 13313-13323.
- GULER, J. L., KRIEGOVA, E., SMITH, T. K., LUKES, J. & ENGLUND, P. T. 2008. Mitochondrial fatty acid synthesis is required for normal mitochondrial morphology and function in *Trypanosoma brucei*. *Molecular Microbiology*, 67, 1125-1142.
- GUNZL, A., BRUDERER, T., LAUFER, G., SCHIMANSKI, B., TU, L. C., CHUNG, H. M., LEE, P. T. & LEE, M. G. S. 2003. RNA polymerase I transcribes procyclin genes and variant surface glycoprotein gene expression sites in *Trypanosoma brucei*. *Eukaryotic Cell*, 2, 542-551.
- GUTHER, M. L. S. & FERGUSON, M. A. J. 1995. THE ROLE OF INOSITOL ACYLATION AND INOSITOL DEACYLATION IN GPI BIOSYNTHESIS IN TRYPANOSOMA-BRUCI. *Embo Journal*, 14, 3080-3093.
- GUTHER, M. L. S., LEE, S., TETLEY, L., ACOSTA-SERRANO, A. & FERGUSON, M. A. J. 2006. GPI-anchored proteins and free GPI glycolipids of procyclic form *Trypanosoma brucei* are nonessential for growth, are required for colonization of the tsetse fly, and are not the only components of the surface coat. *Molecular Biology of the Cell*, 17, 5265-5274.
- HALFORD, S., DULAI, K. S., DAW, S. C., FITZGIBBON, J. & HUNT, D. M. 1998. Isolation and chromosomal localization of two human CDP-diacylglycerol synthase (CDS) genes. *Genomics*, 54, 140-144.
- HALL, B. S., GABERNET-CASTELLO, C., VOAK, A., GOULDING, D., NATESAN, S. K. & FIELD, M. C. 2006. TbVps34, the trypanosome orthologue of Vps34, is required for Golgi complex segregation. *Journal of Biological Chemistry*, 281, 27600-27612.
- HAMMARTON, T. C., KRAMER, S., TETLEY, L., BOSHART, M. & MOTTRAM, J. C. 2007a. *Trypanosoma brucei* Polo-like kinase is essential for basal body duplication, kDNA segregation and cytokinesis. *Molecular Microbiology*, 65, 1229-1248.
- HAMMARTON, T. C., LILLICO, S. G., WELBURN, S. C. & MOTTRAM, J. C. 2005. *Trypanosoma brucei* MOB1 is required for accurate and efficient cytokinesis but not for exit from mitosis. *Molecular Microbiology*, 56, 104-116.
- HAMMARTON, T. C., MONNERAT, S. & MOTTRAM, J. C. 2007b. Cytokinesis in trypanosomatids. *Current Opinion in Microbiology*, 10, 520-527.
- HAN, G. S., O'HARA, L., CARMAN, G. M. & SINIOSSOGLU, S. 2008. An unconventional diacylglycerol kinase that regulates phospholipid synthesis and nuclear membrane growth. *Journal of Biological Chemistry*, 283, 20433-20442.
- HAN, G. S., SINIOSSOGLU, S. & CARMAN, G. M. 2007. The cellular functions of the yeast lipin homolog pah1p are dependent on its phosphatidate phosphatase activity. *Journal of Biological Chemistry*, 282, 37026-37035.
- HAN, S. H., HAN, G. S., IWANYSHYN, W. M. & CARMAN, G. M. 2005. Regulation of the PIS1-encoded phosphatidylinositol synthase in *Saccharomyces cerevisiae* by zinc. *Journal of Biological Chemistry*, 280, 29017-29024.
- HARTWIG, J. H., BOKOCH, G. M., CARPENTER, C. L., JANMEY, P. A., TAYLOR, L. A., TOKER, A. & STOSSEL, T. P. 1995. THROMBIN RECEPTOR LIGATION AND ACTIVATED RAC UNCAP ACTIN FILAMENT BARBED ENDS THROUGH PHOSPHOINOSITIDE SYNTHESIS IN PERMEABILIZED HUMAN PLATELETS. *Cell*, 82, 643-653.
- HASELIER, A., AKBARI, H., WETH, A., BAUMGARTNER, W. & FRENTZEN, M. 2010. Two Closely Related Genes of Arabidopsis Encode Plastidial Cytidinediphosphate Diacylglycerol Synthases Essential for Photoautotrophic Growth. *Plant Physiology*, 153, 1372-1384.
- HATCH, G. M. 1994. CARDIOLIPIN BIOSYNTHESIS IN THE ISOLATED HEART. *Biochemical Journal*, 297, 201-208.
- HATCH, G. M. & MCCLARTY, G. 1996. Regulation of cardiolipin biosynthesis in H9c2 cardiac myoblasts by cytidine 5'-triphosphate. *Journal of Biological Chemistry*, 271, 25810-25816.
- HEACOCK, A. M. & AGRANOFF, B. W. 1997. CDP-diacylglycerol synthase from mammalian tissues. *Biochimica Et Biophysica Acta-Lipids and Lipid Metabolism*, 1348, 166-172.

- HEACOCK, A. M., UHLER, M. D. & AGRANOFF, B. W. 1996. Cloning of CDP-diacylglycerol synthase from a human neuronal cell line. *Journal of Neurochemistry*, 67, 2200-2203.
- HIRUMI, H. & HIRUMI, K. 1989. CONTINUOUS CULTIVATION OF TRYPANOSOMA-BRUCI BLOOD STREAM FORMS IN A MEDIUM CONTAINING A LOW CONCENTRATION OF SERUM-PROTEIN WITHOUT FEEDER CELL-LAYERS. *Journal of Parasitology*, 75, 985-989.
- HOLUB, B. J. & PIEKARSKI, J. 1976. BIOSYNTHESIS OF MOLECULAR-SPECIES OF CDP-DIGLYCERIDE FROM ENDOGENOUSLY-LABELED PHOSPHATIDATE IN RAT-LIVER MICROSOMES. *Lipids*, 11, 251-257.
- HOMANN, M. J., HENRY, S. A. & CARMAN, G. M. 1985. REGULATION OF CDP-DIACYLGLYCEROL SYNTHASE ACTIVITY IN SACCHAROMYCES-CEREVISIAE. *Journal of Bacteriology*, 163, 1265-1266.
- HOWE, K., BATEMAN, A. & DURBIN, R. 2002. QuickTree: building huge Neighbour-Joining trees of protein sequences. *Bioinformatics*, 18, 1546-1547.
- ICHO, T., SPARROW, C. P. & RAETZ, C. R. H. 1985. MOLECULAR-CLONING AND SEQUENCING OF THE GENE FOR CDP-DIGLYCERIDE SYNTHETASE OF ESCHERICHIA-COLI. *Journal of Biological Chemistry*, 260, 2078-2083.
- IMAI, A. & GERSHENGORN, M. C. 1987. INDEPENDENT PHOSPHATIDYLINOSITOL SYNTHESIS IN PITUITARY PLASMA-MEMBRANE AND ENDOPLASMIC-RETICULUM. *Nature*, 325, 726-728.
- INGLIS-BROADGATE, S. L., OCAKA, L., BANERJEE, R., GAASENBEEK, M., CHAPPLE, J. P., CHEETHAM, M. E., CLARK, B. J., HUNT, D. M. & HALFORD, S. 2005. Isolation and characterization of murine Cds (CDP-diacylglycerol synthase) 1 and 2. *Gene*, 356, 19-31.
- IWANYSZYN, W. M., HAN, G. S. & CARMAN, G. M. 2004. Regulation of phospholipid synthesis in *Saccharomyces cerevisiae* by zinc. *Journal of Biological Chemistry*, 279, 21976-21983.
- JACKSON, M., CRICK, D. C. & BRENNAN, P. J. 2000. Phosphatidylinositol is an essential phospholipid of mycobacteria. *Journal of Biological Chemistry*, 275, 30092-30099.
- JANMEY, P. A. 1994. PHOSPHOINOSITIDES AND CALCIUM AS REGULATORS OF CELLULAR ACTIN ASSEMBLY AND DISASSEMBLY. *Annual Review of Physiology*, 56, 169-191.
- JANSSENS, P. G. & DEMUYNCK, A. 1977. CLINICAL-TRIALS WITH NIFURTIMOX IN AFRICAN TRYPANOSOMIASIS. *Annales De La Societe Belge De Medecine Tropicale*, 57, 475-480.
- JELSEMA, C. L. & MORRE, D. J. 1978. DISTRIBUTION OF PHOSPHOLIPID BIOSYNTHETIC-ENZYMES AMONG CELL COMPONENTS OF RAT-LIVER. *Journal of Biological Chemistry*, 253, 7960-7971.
- JETTON, N., ROTHBERG, K. G., HUBBARD, J. G., WISE, J., LI, Y., BALL, H. L. & RUBEN, L. 2009. The cell cycle as a therapeutic target against *Trypanosoma brucei*: Hesperadin inhibits Aurora kinase-1 and blocks mitotic progression in bloodstream forms. *Molecular Microbiology*, 72, 442-458.
- JIANG, F., RYAN, M. T., SCHLAME, M., ZHAO, M., GU, Z. M., KLINGENBERG, M., PFANNER, N. & GREENBERG, M. L. 2000. Absence of cardiolipin in the *crd1* null mutant results in decreased mitochondrial membrane potential and reduced mitochondrial function. *Journal of Biological Chemistry*, 275, 22387-22394.
- JOHNSON, S. C., DAHL, J., SHIH, T. L., SCHEDLER, D. J. A., ANDERSON, L., BENJAMIN, T. L. & BAKER, D. C. 1993. SYNTHESIS AND EVALUATION OF 3-MODIFIED 1D-MYO-INOSITOLS AS INHIBITORS AND SUBSTRATES OF PHOSPHATIDYLINOSITOL SYNTHASE AND INHIBITORS OF MYOINOSITOL UPTAKE BY CELLS. *Journal of Medicinal Chemistry*, 36, 3628-3635.
- JUSTIN, A. M., KADER, J. C. & COLLIN, S. 2002. Phosphatidylinositol synthesis and exchange of the inositol head are catalysed by the single phosphatidylinositol synthase 1 from *Arabidopsis*. *European Journal of Biochemistry*, 269, 2347-2352.
- JUSTIN, A. M. & MAZLIAK, P. 1992. COMPARISON OF THE MOLECULAR-SPECIES PATTERNS OF PHOSPHATIDIC-ACID, CDP-DIACYLGLYCEROLS AND PHOSPHATIDYLINOSITOL IN POTATO-TUBER, PEA LEAF AND SOYBEAN MICROSOMES - CONSEQUENCES FOR THE SELECTIVITY OF THE ENZYMES CATALYZING PHOSPHATIDYLINOSITOL BIOSYNTHESIS. *Biochimica Et Biophysica Acta*, 1165, 141-146.
- KATOH, K., KUMA, K., TOH, H. & MIYATA, T. 2005. MAFFT version 5: improvement in accuracy of multiple sequence alignment. *Nucleic Acids Research*, 33, 511-518.

- KATOH, K., MISAWA, K., KUMA, K. & MIYATA, T. 2002. MAFFT: a novel method for rapid multiple sequence alignment based on fast Fourier transform. *Nucleic Acids Research*, 30, 3059-3066.
- KATOH, K. & TOH, H. 2008. Recent developments in the MAFFT multiple sequence alignment program. *Briefings in Bioinformatics*, 9, 286-298.
- KAWASAKI, K., KUGE, O., YAMAKAWA, Y. & NISHIJIMA, M. 2001. Purification of phosphatidylglycerophosphate synthase from Chinese hamster ovary cells. *Biochemical Journal*, 354, 9-15.
- KELLEY, M. J., BAILIS, A. M., HENRY, S. A. & CARMAN, G. M. 1988. REGULATION OF PHOSPHOLIPID BIOSYNTHESIS IN SACCHAROMYCES-CEREVISIAE BY INOSITOL - INOSITOL IS AN INHIBITOR OF PHOSPHATIDYLSERINE SYNTHASE ACTIVITY. *Journal of Biological Chemistry*, 263, 18078-18085.
- KELLEY, M. J. & CARMAN, G. M. 1987. PURIFICATION AND CHARACTERIZATION OF CDP-DIACYLGLYCEROL SYNTHASE FROM SACCHAROMYCES-CEREVISIAE. *Journal of Biological Chemistry*, 262, 14563-14570.
- KENNEDY, P. G. E. 2004. Human African trypanosomiasis of the CNS: current issues and challenges. *Journal of Clinical Investigation*, 113, 496-504.
- KENT, C. 1995. EUKARYOTIC PHOSPHOLIPID BIOSYNTHESIS. *Annual Review of Biochemistry*, 64, 315-343.
- KIM, Y. J., GUZMAN-HERNANDEZ, M. L. & BALLA, T. 2011. A Highly Dynamic ER-Derived Phosphatidylinositol-Synthesizing Organelle Supplies Phosphoinositides to Cellular Membranes. *Developmental Cell*, 21, 813-824.
- KINNEY, A. J. & CARMAN, G. M. 1990. ENZYMES OF PHOSPHOINOSITIDE SYNTHESIS IN SECRETORY VESICLES DESTINED FOR THE PLASMA-MEMBRANE IN SACCHAROMYCES-CEREVISIAE. *Journal of Bacteriology*, 172, 4115-4117.
- KLEZOVITCH, O., BRANDENBURGER, Y., GEINDRE, M. & DESHUSSES, J. 1993. CHARACTERIZATION OF REACTIONS CATALYZED BY YEAST PHOSPHATIDYLINOSITOL SYNTHASE. *Febs Letters*, 320, 256-260.
- KOPKA, J., LUDEWIG, M. & MULLERROBER, B. 1997. Complementary DNAs encoding eukaryotic-type cytidine-5'-diphosphate-diacylglycerol synthases of two plant species. *Plant Physiology*, 113, 997-1002.
- KOREH, K. & MONACO, M. E. 1986. THE RELATIONSHIP OF HORMONE-SENSITIVE AND HORMONE-INSENSITIVE PHOSPHATIDYLINOSITOL TO PHOSPHATIDYLINOSITOL 4,5-BISPHOSPHATE IN THE WRK-1 CELL. *Journal of Biological Chemistry*, 261, 88-91.
- KUCHLER, K., DAUM, G. & PALTAUF, F. 1986. SUBCELLULAR AND SUBMITOCHONDRIAL LOCALIZATION OF PHOSPHOLIPID-SYNTHESIZING ENZYMES IN SACCHAROMYCES-CEREVISIAE. *Journal of Bacteriology*, 165, 901-910.
- KUGE, O. & NISHIJIMA, M. 1997. Phosphatidylserine synthase I and II of mammalian cells. *Biochimica Et Biophysica Acta-Lipids and Lipid Metabolism*, 1348, 151-156.
- KYTE, J. & DOOLITTLE, R. F. 1982. A SIMPLE METHOD FOR DISPLAYING THE HYDROPATHIC CHARACTER OF A PROTEIN. *Journal of Molecular Biology*, 157, 105-132.
- LACOUNT, D. J., BARRETT, B. & DONELSON, J. E. 2002. Trypanosoma brucei FLA1 is required for flagellum attachment and cytokinesis. *Journal of Biological Chemistry*, 277, 17580-17588.
- LACOUNT, D. J., BRUSE, S., HILL, K. L. & DONELSON, J. E. 2000. Double-stranded RNA interference in Trypanosoma brucei using head-to-head promoters. *Molecular and Biochemical Parasitology*, 111, 67-76.
- LANGLEY, K. E. & KENNEDY, E. P. 1978. PARTIAL-PURIFICATION AND PROPERTIES OF CTP - PHOSPHATIDIC-ACID CYTIDYLYLTRANSFERASE FROM MEMBRANES OF ESCHERICHIA-COLI. *Journal of Bacteriology*, 136, 85-95.
- LAVIE, Y. & AGRANOFF, B. W. 1996. Inhibition of neuroblastoma cell phosphatidylinositol 3-kinase by CDP-diacylglycerol and phosphatidate. *Journal of Neurochemistry*, 66, 811-816.
- LEE, S. H., STEPHENS, J. L. & ENGLUND, P. T. 2007. A fatty-acid synthesis mechanism specialized for parasitism. *Nature Reviews Microbiology*, 5, 287-297.
- LEE, S. H., STEPHENS, J. L., PAUL, K. S. & ENGLUND, P. T. 2006. Fatty acid synthesis by elongases in trypanosomes. *Cell*, 126, 691-699.

- LI, P. P., WARSH, J. J. & STANACEV, N. Z. 1988. INVITRO AND EXVIVO EFFECTS OF ANTIDEPRESSANTS ON RAT-BRAIN MEMBRANE-BOUND PHOSPHATIDYLINOSITOL SYNTHETASE-ACTIVITY. *Neurochemical Research*, 13, 789-795.
- LI, Z. Y. & WANG, C. C. 2003. A PHO80-like cyclin and a B-type cyclin control the cell cycle of the procyclic form of *Trypanosoma brucei*. *Journal of Biological Chemistry*, 278, 20652-20658.
- LILLICO, S., FIELD, M. C., BLUNDELL, P., COOMBS, G. H. & MOTTRAM, J. C. 2003. Essential roles for GPI-anchored proteins in African trypanosomes revealed using mutants deficient in GP18. *Molecular Biology of the Cell*, 14, 1182-1194.
- LITEPLO, R. G. & SRIBNEY, M. 1980. THE STIMULATION OF RAT-LIVER MICROSOMAL CDP-DIACYLGLYCEROL FORMATION BY GUANOSINE TRIPHOSPHATE. *Canadian Journal of Biochemistry*, 58, 871-877.
- LIU, Y., BOUKHELIFA, M., TRIBBLE, E., MORIN-KENSICKI, E., UETRECHT, A., BEAR, J. E. & BANKAITIS, V. A. 2008. The Sac1 phosphoinositide phosphatase regulates golgi membrane morphology and mitotic spindle organization in mammals. *Molecular Biology of the Cell*, 19, 3080-3096.
- LOEWEN, C. J. R., GASPAR, M. L., JESCH, S. A., DELON, C., KTISTAKIS, N. T., HENRY, S. A. & LEVINE, T. P. 2004. Phospholipid metabolism regulated by a transcription factor sensing phosphatidic acid. *Science*, 304, 1644-1647.
- LUCK, D. J. L. 1984. GENETIC AND BIOCHEMICAL DISSECTION OF THE EUKARYOTIC FLAGELLUM. *Journal of Cell Biology*, 98, 789-794.
- LYKIDIS, A. 2007. Comparative genomics and evolution of eukaryotic phospholipid biosynthesis. *Progress in Lipid Research*, 46, 171-199.
- LYKIDIS, A., JACKSON, P. D., ROCK, C. O. & JACKOWSKI, S. 1997. The role of CDP-diacylglycerol synthetase and phosphatidylinositol synthase activity levels in the regulation of cellular phosphatidylinositol content. *Journal of Biological Chemistry*, 272, 33402-33409.
- MALAQUIAS, A. T. & OLIVEIRA, M. M. 1999. Phospholipid signalling pathways in *Trypanosoma cruzi* growth control. *Acta Tropica*, 73, 93-108.
- MARCELLO, L. & BARRY, J. D. 2007. Analysis of the VSG gene silent archive in *Trypanosoma brucei* reveals that mosaic gene expression is prominent in antigenic variation and is favored by archive substructure. *Genome Research*, 17, 1344-1352.
- MARTIN, D., GANNOUN-ZAKI, L., BONNEFOY, S., ELDIN, P., WENGELNIK, K. & VIAL, H. 2000. Characterization of *Plasmodium falciparum* CDP-diacylglycerol synthase, a proteolytically cleaved enzyme. *Molecular and Biochemical Parasitology*, 110, 93-105.
- MARTIN, K. L. & SMITH, T. K. 2006a. The glycosylphosphatidylinositol (GPI) biosynthetic pathway of bloodstream-form *Trypanosoma brucei* is dependent on the de novo synthesis of inositol. *Molecular Microbiology*, 61, 89-105.
- MARTIN, K. L. & SMITH, T. K. 2006b. Phosphatidylinositol synthesis is essential in bloodstream form *Trypanosoma brucei*. *Biochemical Journal*, 396, 287-295.
- MASLOV, D. A., YASUHIRA, S. & SIMPSON, L. 1999. Phylogenetic affinities of Diplonema within the euglenozoa as inferred from the SSU rRNA gene and partial COI protein sequences. *Protist*, 150, 33-42.
- MASTERSON, W. J. 1990. BIOSYNTHESIS OF THE GLYCOSYL PHOSPHATIDYLINOSITOL ANCHOR OF TRYPANOSOMA-BRUCI VARIANT SURFACE GLYCOPROTEIN. *Biochemical Society Transactions*, 18, 722-724.
- MASTERSON, W. J., DOERING, T. L., HART, G. W. & ENGLUND, P. T. 1989. A NOVEL PATHWAY FOR GLYCAN ASSEMBLY - BIOSYNTHESIS OF THE GLYCOSYL-PHOSPHATIDYLINOSITOL ANCHOR OF THE TRYPANOSOME VARIANT SURFACE GLYCOPROTEIN. *Cell*, 56, 793-800.
- MASTERSON, W. J., RAPER, J., DOERING, T. L., HART, G. W. & ENGLUND, P. T. 1990. FATTY-ACID REMODELING - A NOVEL REACTION SEQUENCE IN THE BIOSYNTHESIS OF TRYPANOSOME GLYCOSYL PHOSPHATIDYLINOSITOL MEMBRANE ANCHORS. *Cell*, 62, 73-80.
- MATTHEWS, K. R. 2005. The developmental cell biology of *Trypanosoma brucei*. *Journal of Cell Science*, 118, 283-290.

- MCPHEE, F., LOWE, G., VAZIRI, C. & DOWNES, C. P. 1991. PHOSPHATIDYLINOSITOL SYNTHASE AND PHOSPHATIDYLINOSITOL INOSITOL EXCHANGE-REACTIONS IN TURKEY ERYTHROCYTE-MEMBRANES. *Biochemical Journal*, 275, 187-192.
- MENON, A. K., EPPINGER, M., MAYOR, S. & SCHWARZ, R. T. 1993. PHOSPHATIDYLETHANOLAMINE IS THE DONOR OF THE TERMINAL PHOSPHOETHANOLAMINE GROUP IN TRYPANOSOME GLYCOSYLPHOSPHATIDYLINOSITOLS. *Embo Journal*, 12, 1907-1914.
- MENON, A. K., MAYOR, S. & SCHWARZ, R. T. 1990a. BIOSYNTHESIS OF GLYCOSYL-PHOSPHATIDYLINOSITOL LIPIDS IN TRYPANOSOMA-BRUCI - INVOLVEMENT OF MANNOSYLPHOSPHORYLDOLICHOL AS THE MANNOSE DONOR. *Embo Journal*, 9, 4249-4258.
- MENON, A. K., SCHWARZ, R. T., MAYOR, S. & CROSS, G. A. M. 1990b. CELL-FREE SYNTHESIS OF GLYCOSYL-PHOSPHATIDYLINOSITOL PRECURSORS FOR THE GLYCOLIPID MEMBRANE ANCHOR OF TRYPANOSOMA-BRUCI VARIANT SURFACE GLYCOPROTEINS - STRUCTURAL CHARACTERIZATION OF PUTATIVE BIOSYNTHETIC INTERMEDIATES. *Journal of Biological Chemistry*, 265, 9033-9042.
- MILNE, K. G., FIELD, R. A., MASTERTON, W. J., COTTAZ, S., BRIMACOMBE, J. S. & FERGUSON, M. A. J. 1994. PARTIAL-PURIFICATION AND CHARACTERIZATION OF THE N-ACETYLGALACTOSAMINYL-PHOSPHATIDYLINOSITOL DE-N-ACETYLASE OF GLYCOSYLPHOSPHATIDYLINOSITOL ANCHOR BIOSYNTHESIS IN AFRICAN TRYPANOSOMES. *Journal of Biological Chemistry*, 269, 16403-16408.
- MILNE, K. G., GUTHER, M. L. S. & FERGUSON, M. A. J. 2001. Acyl-CoA binding protein is essential in bloodstream form *Trypanosoma brucei*. *Molecular and Biochemical Parasitology*, 112, 301-304.
- MINA, J. G., PAN, S. Y., WANSADHIPATHI, N. K., BRUCE, C. R., SHAMS-ELDIN, H., SCHWARZ, R. T., STEEL, P. G. & DENNY, P. W. 2009. The *Trypanosoma brucei* sphingolipid synthase, an essential enzyme and drug target. *Molecular and Biochemical Parasitology*, 168, 16-23.
- MOENS, F., DEWILDE, M. & NGATO, K. 1984. CLINICAL-TRIAL OF NIFURTIMOX IN HUMAN AFRICAN TRYPANOSOMIASIS. *Annales De La Societe Belge De Medecine Tropicale*, 64, 37-43.
- MOK, A. Y. P., MCDUGALL, G. E. & MCMURRAY, W. C. 1992. CDP-DIACYLGLYCEROL SYNTHESIS IN RAT-LIVER MITOCHONDRIA. *Febs Letters*, 312, 236-240.
- MONACO, M. E. & ADELSON, J. R. 1991. EVIDENCE FOR COUPLING OF RESYNTHESIS TO HYDROLYSIS IN THE PHOSPHOINOSITIDE CYCLE. *Biochemical Journal*, 279, 337-341.
- MONACO, M. E. & FELDMAN, M. 1997. Extraction and stabilization of mammalian CDP-diacylglycerol synthase activity. *Biochemical and Biophysical Research Communications*, 239, 166-170.
- MONACO, M. E., FELDMAN, M. & KLEINBERG, D. L. 1994. IDENTIFICATION OF RAT-LIVER PHOSPHATIDYLINOSITOL SYNTHASE AS A 21 KDA PROTEIN. *Biochemical Journal*, 304, 301-305.
- MOORE, T. S. 1982. PHOSPHOLIPID BIOSYNTHESIS. *Annual Review of Plant Physiology and Plant Molecular Biology*, 33, 235-259.
- MOREIRA, D., LOPEZ-GARCIA, P. & VICKERMAN, K. 2004. An updated view of kinetoplastid phylogeny using environmental sequences and a closer outgroup: proposal for a new classification of the class Kinetoplastea. *International Journal of Systematic and Evolutionary Microbiology*, 54, 1861-1875.
- MORITA, Y. S., PAUL, K. S. & ENGLUND, P. T. 2000. Specialized fatty acid synthesis in African trypanosomes: Myristate for CPI anchors. *Science*, 288, 140-143.
- MULLER, F. & FRENTZEN, M. 2001. Phosphatidylglycerophosphate synthases from *Arabidopsis thaliana*. *Febs Letters*, 509, 298-302.
- NAGAI, Y., AOKI, J., SATO, T., AMANO, R., MATSUDA, Y., ARAI, H. & INOUE, K. 1999. An alternative splicing form of phosphatidylserine-specific phospholipase A(1) that exhibits lysophosphatidylserine-specific lysophospholipase activity in humans. *Journal of Biological Chemistry*, 274, 11053-11059.
- NAGAMUNE, K., ACOSTA-SERRANO, A., UEMURA, H., BRUN, R., KUNZ-RENGGLI, C., MAEDA, Y., FERGUSON, M. A. J. & KINOSHITA, T. 2004. Surface sialic acids taken from the host

- allow trypanosome survival in Tsetse fly vectors. *Journal of Experimental Medicine*, 199, 1445-1450.
- NAGAMUNE, K., NOZAKI, T., MAEDA, Y., OHISHI, K., FUKUMA, T., HARA, T., SCHWARZ, R. T., SUTTERLIN, C., BRUN, R., RIEZMAN, H. & KINOSHITA, T. 2000. Critical roles of glycosylphosphatidylinositol for *Trypanosoma brucei*. *Proceedings of the National Academy of Sciences of the United States of America*, 97, 10336-10341.
- NAGAMUNE, K., OHISHI, K., ASHIDA, H., HONG, Y. C., HINO, J., KANGAWA, K., INOUE, N., MAEDA, Y. & KINOSHITA, T. 2003. GPI transamidase of *Trypanosoma brucei* has two previously uncharacterized (trypanosomatid transamidase 1 and 2) and three common subunits. *Proceedings of the National Academy of Sciences of the United States of America*, 100, 10682-10687.
- NICKELS, J. T., BUXEDA, R. J. & CARMAN, G. M. 1994. REGULATION OF PHOSPHATIDYLINOSITOL 4-KINASE FROM THE YEAST *SACCHAROMYCES-CEREVISIAE* BY CDP-DIACYLGLYCEROL. *Journal of Biological Chemistry*, 269, 11018-11024.
- NIGOU, J. & BESRA, G. S. 2002. Cytidine diphosphate-diacylglycerol synthesis in *Mycobacterium smegmatis*. *Biochemical Journal*, 367, 157-162.
- NIKAWA, J., KODAKI, T. & YAMASHITA, S. 1987a. PRIMARY STRUCTURE AND DISRUPTION OF THE PHOSPHATIDYLINOSITOL SYNTHASE GENE OF *SACCHAROMYCES-CEREVISIAE*. *Journal of Biological Chemistry*, 262, 4876-4881.
- NIKAWA, J., TSUKAGOSHI, Y., KODAKI, T. & YAMASHITA, S. 1987b. NUCLEOTIDE-SEQUENCE AND CHARACTERIZATION OF THE YEAST PSS GENE ENCODING PHOSPHATIDYLSERINE SYNTHASE. *European Journal of Biochemistry*, 167, 7-12.
- NIKAWA, J. & YAMASHITA, S. 1981. CHARACTERIZATION OF PHOSPHATIDYLSERINE SYNTHASE FROM *SACCHAROMYCES-CEREVISIAE* AND A MUTANT DEFECTIVE IN THE ENZYME. *Biochimica Et Biophysica Acta*, 665, 420-426.
- NIKAWA, J. I., KODAKI, T. & YAMASHITA, S. 1988. EXPRESSION OF THE *SACCHAROMYCES-CEREVISIAE* PIS-GENE AND SYNTHESIS OF PHOSPHATIDYLINOSITOL IN *ESCHERICHIA-COLI*. *Journal of Bacteriology*, 170, 4727-4731.
- NUCCIO, M. L., ZIEMAK, M. J., HENRY, S. A., WERETILNYK, E. A. & HANSON, A. D. 2000. cDNA cloning of phosphoethanolamine N-methyltransferase from spinach by complementation in *Schizosaccharomyces pombe* and characterization of the recombinant enzyme. *Journal of Biological Chemistry*, 275, 14095-14101.
- OGBADOYI, E. O., ROBINSON, D. R. & GULL, K. 2003. A high-order trans-membrane structural linkage is responsible for mitochondrial genome positioning and segregation by flagellar basal bodies in trypanosomes. *Molecular Biology of the Cell*, 14, 1769-1779.
- OHTSUKA, T., NISHIJIMA, M. & AKAMATSU, Y. 1993a. A SOMATIC-CELL MUTANT DEFECTIVE IN PHOSPHATIDYLGLYCEROPHOSPHATE SYNTHASE, WITH IMPAIRED PHOSPHATIDYLGLYCEROL AND CARDIOLIPIN BIOSYNTHESIS. *Journal of Biological Chemistry*, 268, 22908-22913.
- OHTSUKA, T., NISHIJIMA, M., SUZUKI, K. & AKAMATSU, Y. 1993b. MITOCHONDRIAL DYSFUNCTION OF A CULTURED CHINESE-HAMSTER OVARY CELL MUTANT DEFICIENT IN CARDIOLIPIN. *Journal of Biological Chemistry*, 268, 22914-22919.
- OSMAN, C., VOELKER, D. R. & LANGER, T. 2011. Making heads or tails of phospholipids in mitochondria. *Journal of Cell Biology*, 192, 7-16.
- OVERATH, P. & ENGSTLER, M. 2004. Endocytosis, membrane recycling and sorting of GPI-anchored proteins: *Trypanosoma brucei* as a model system. *Molecular Microbiology*, 53, 735-744.
- PALAVALLI, L. H., BRENDZA, K. M., HAAKENSON, W., CAHOON, R. E., MCLAIRD, M., HICKS, L. M., MCCARTER, J. P., WILLIAMS, D. J., HRESKO, M. C. & JEZ, J. M. 2006. Defining the role of phosphomethylethanolamine N-methyltransferase from *Caenorhabditis elegans* in phosphocholine biosynthesis by biochemical and kinetic analysis. *Biochemistry*, 45, 6056-6065.
- PARRIES, G. S. & HOKINNEAVERSON, M. 1984. PHOSPHATIDYLINOSITOL SYNTHASE FROM CANINE PANCREAS - SOLUBILIZATION BY NORMAL-OCTYL GLUCOPYRANOSIDE AND STABILIZATION BY MANGANESE. *Biochemistry*, 23, 4785-4791.

- PARRIES, G. S. & HOKINNEAVERSON, M. 1985. INHIBITION OF PHOSPHATIDYLINOSITOL SYNTHASE AND OTHER MEMBRANE-ASSOCIATED ENZYMES BY STEREOISOMERS OF HEXACHLOROCYCLOHEXANE. *Journal of Biological Chemistry*, 260, 2687-2693.
- PARSONS, M. 2004. Glycosomes: parasites and the divergence of peroxisomal purpose. *Molecular Microbiology*, 53, 717-724.
- PATNAIK, P. K., FIELD, M. C., MENON, A. K., CROSS, G. A. M., YEE, M. C. & BUTIKOFER, P. 1993. MOLECULAR-SPECIES ANALYSIS OF PHOSPHOLIPIDS FROM TRYPANOSOMA-BRUCI BLOOD-STREAM AND PROCYCLIC FORMS. *Molecular and Biochemical Parasitology*, 58, 97-105.
- PAUL, K. S., JIANG, D., MORITA, Y. S. & ENGLUND, P. T. 2001. Fatty acid synthesis in African trypanosomes: a solution to the myristate mystery. *Trends in Parasitology*, 17, 381-387.
- PAULUS, H. & KENNEDY, E. P. 1960. The enzymatic synthesis of inositol monophosphatide. *The Journal of biological chemistry*, 235, 1303-11.
- PAYS, E., COQUELET, H., TEBABI, P., PAYS, A., JEFFERIES, D., STEINERT, M., KOENIG, E., WILLIAMS, R. O. & RODITI, I. 1990. TRYPANOSOMA-BRUCI - CONSTITUTIVE ACTIVITY OF THE VSG AND PROCYCLIN GENE PROMOTERS. *Embo Journal*, 9, 3145-3151.
- PEPIN, J., MILFORD, F., MEURICE, F., ETHIER, L., LOKO, L. & MPIA, B. 1992. HIGH-DOSE NIFURTIMOX FOR ARSENO-RESISTANT TRYPANOSOMA-BRUCI-GAMBIENSE SLEEPING SICKNESS - AN OPEN TRIAL IN CENTRAL ZAIRE. *Transactions of the Royal Society of Tropical Medicine and Hygiene*, 86, 254-256.
- PESSI, G., KOCIUBINSKI, G. & BEN MAMOUN, C. 2004. A pathway for phosphatidylcholine biosynthesis in Plasmodium falciparum involving phosphoethanolamine methylation. *Proceedings of the National Academy of Sciences of the United States of America*, 101, 6206-6211.
- PIAZZA, G. J. & MARMER, W. N. 2007. Conversion of phosphatidylcholine to phosphatidylglycerol with phospholipase D and glycerol. *Journal of the American Oil Chemists Society*, 84, 645-651.
- PLOUBIDOU, A., ROBINSON, D. R., DOCHERTY, R. C., OGBADOYI, E. O. & GULL, K. 1999. Evidence for novel cell cycle checkpoints in trypanosomes: kinetoplast segregation and cytokinesis in the absence of mitosis. *Journal of Cell Science*, 112, 4641-4650.
- PONTING, C. P. & KERR, I. D. 1996. A novel family of phospholipase D homologues that includes phospholipid synthases and putative endonucleases: Identification of duplicated repeats and potential active site residues. *Protein Science*, 5, 914-922.
- PULIDO, J. A., DELHOYO, N. & PEREZALBARSANZ, M. A. 1992. THE EFFECTS OF DIFFERENT HEXACHLOROCYCLOHEXANES AND CYCLODIENES ON GLUCOSE-UPTAKE AND INOSITOL PHOSPHOLIPID-SYNTHESIS IN RAT-BRAIN CORTEX. *Life Sciences*, 50, 1585-1596.
- RAETZ, C. R. H. 1976. PHOSPHATIDYLSERINE SYNTHETASE MUTANTS OF ESCHERICHIA-COLI - GENETIC-MAPPING AND MEMBRANE PHOSPHOLIPID COMPOSITION. *Journal of Biological Chemistry*, 251, 3242-3249.
- RAETZ, C. R. H. & KENNEDY, E. P. 1973. FUNCTION OF CYTIDINE DIPHOSPHATE-DIGLYCERIDE AND DEOXYCYTIDINE DIPHOSPHATE-DIGLYCERIDE IN BIOGENESIS OF MEMBRANE LIPIDS IN ESCHERICHIA-COLI. *Journal of Biological Chemistry*, 248, 1098-1105.
- RAETZ, C. R. H., WICKNER, W. T., KENNEDY, E. P., HIRSCHBE.CB & DOWHAN, W. 1972. MEMBRANE-BOUND PYROPHOSPHATASE IN ESCHERICHIA-COLI CATALYZING HYDROLYSIS OF CYTIDINE DIPHOSPHATE-DIGLYCERIDE. *Journal of Biological Chemistry*, 247, 2245-&.
- RALSTON, K. S. & HILL, K. L. 2006. Trypanin, a component of the flagellar dynein regulatory complex, is essential in bloodstream form African trypanosomes. *Plos Pathogens*, 2, 873-882.
- RALSTON, K. S., LERNER, A. G., DIENER, D. R. & HILL, K. L. 2006. Flagellar motility contributes to cytokinesis in Trypanosoma brucei and is modulated by an evolutionarily conserved dynein regulatory system. *Eukaryotic Cell*, 5, 696-711.
- RASBAND, W. S. 1997-2012 ImageJ. U.S. National Institutes of Health, Bethesda, Maryland.
- RICHMOND, G. S., GIBELLINI, F., YOUNG, S. A., MAJOR, L., DENTON, H., LILLEY, A. & SMITH, T. K. 2010. Lipidomic analysis of bloodstream and procyclic form Trypanosoma brucei. *Parasitology*, 137, 1357-1392.

- RIFKIN, M. R., STROBOS, C. A. M. & FAIRLAMB, A. H. 1995. SPECIFICITY OF ETHANOLAMINE TRANSPORT AND ITS FURTHER METABOLISM IN TRYPANOSOMA-BRUCI. *Journal of Biological Chemistry*, 270, 16160-16166.
- ROBINSON, D. R. & GULL, K. 1991. BASAL BODY MOVEMENTS AS A MECHANISM FOR MITOCHONDRIAL GENOME SEGREGATION IN THE TRYPANOSOME CELL-CYCLE. *Nature*, 352, 731-733.
- ROBINSON, D. R., SHERWIN, T., PLOUBIDOU, A., BYARD, E. H. & GULL, K. 1995. MICROTUBULE POLARITY AND DYNAMICS IN THE CONTROL OF ORGANELLE POSITIONING, SEGREGATION, AND CYTOKINESIS IN THE TRYPANOSOME CELL-CYCLE. *Journal of Cell Biology*, 128, 1163-1172.
- RODGERS, M. J., ALBANESI, J. P. & PHILLIPS, M. A. 2007. Phosphatidylinositol 4-kinase III-beta is required for golgi maintenance and cytokinesis in *Trypanosoma brucei*. *Eukaryotic Cell*, 6, 1108-1118.
- ROPER, J. R., GUTHER, M. L. S., MACRAE, J. I., PRESCOTT, A. R., HALLYBURTON, I., ACOSTA-SERRANO, A. & FERGUSON, M. A. J. 2005. The suppression of galactose metabolism in procyclic form *Trypanosoma brucei* causes cessation of cell growth and alters procyclin glycoprotein structure and copy number. *Journal of Biological Chemistry*, 280, 19728-19736.
- ROPER, J. R., GUTHER, M. L. S., MILNE, K. G. & FERGUSON, M. A. J. 2002. Galactose metabolism is essential for the African sleeping sickness parasite *Trypanosoma brucei*. *Proceedings of the National Academy of Sciences of the United States of America*, 99, 5884-5889.
- SAITO, S., GOTO, K., TONOSAKI, A. & KONDO, H. 1997. Gene cloning and characterization of CDP-diacylglycerol synthase from rat brain. *Journal of Biological Chemistry*, 272, 9503-9509.
- SAKAGAMI, H., AOKI, J., NATORI, Y., NISHIKAWA, K., KAKEHI, Y., NATORI, Y. & ARAI, H. 2005. Biochemical and molecular characterization of a novel choline-specific glycerophosphodiester phosphodiesterase belonging to the nucleotide pyrophosphatase/phosphodiesterase family. *Journal of Biological Chemistry*, 280, 23084-23093.
- SAMAD, A., LICHT, B., STALMACH, M. E. & MELLORS, A. 1988. METABOLISM OF PHOSPHOLIPIDS AND LYSOPHOSPHOLIPIDS BY TRYPANOSOMA-BRUCI. *Molecular and Biochemical Parasitology*, 29, 159-169.
- SATO, N., HAGIO, M., WADA, H. & TSUZUKI, M. 2000. Requirement of phosphatidylglycerol for photosynthetic function in thylakoid membranes. *Proceedings of the National Academy of Sciences of the United States of America*, 97, 10655-10660.
- SCHUIKI, I. & DAUM, G. 2009. Phosphatidylserine Decarboxylases, Key Enzymes of Lipid Metabolism. *Iubmb Life*, 61, 151-162.
- SELVAPANDIYAN, A., KUMAR, P., MORRIS, J. C., SALISBURY, J. L., WANG, C. C. & NAKHASI, H. L. 2007. Centrin1 is required for organelle segregation and cytokinesis in *Trypanosoma brucei*. *Molecular Biology of the Cell*, 18, 3290-3301.
- SERON, K., DZIERSZINSKI, F. & TOMAVO, S. 2000. Molecular cloning, functional complementation in *Saccharomyces cerevisiae* and enzymatic properties of phosphatidylinositol synthase from the protozoan parasite *Toxoplasma gondii*. *European Journal of Biochemistry*, 267, 6571-6579.
- SERRICCHIO, M. & BUETIKOFER, P. 2011. *Trypanosoma brucei*: a model micro-organism to study eukaryotic phospholipid biosynthesis. *Febs Journal*, 278, 1035-1046.
- SERRICCHIO, M. & BUETIKOFER, P. 2012. An essential bacterial-type cardiolipin synthase mediates cardiolipin formation in a eukaryote. *Proceedings of the National Academy of Sciences of the United States of America*, 109, E954-E961.
- SHEADER, K., VAUGHAN, S., MINCHIN, J., HUGHES, K., GULL, K. & RUDENKO, G. 2005. Variant surface glycoprotein RNA interference triggers a pre-cytokinesis cell cycle arrest in African trypanosomes. *Proceedings of the National Academy of Sciences of the United States of America*, 102, 8716-8721.
- SHEN, H. & DOWHAN, W. 1996. Reduction of CDP-diacylglycerol synthase activity results in the excretion of inositol by *Saccharomyces cerevisiae*. *Journal of Biological Chemistry*, 271, 29043-29048.

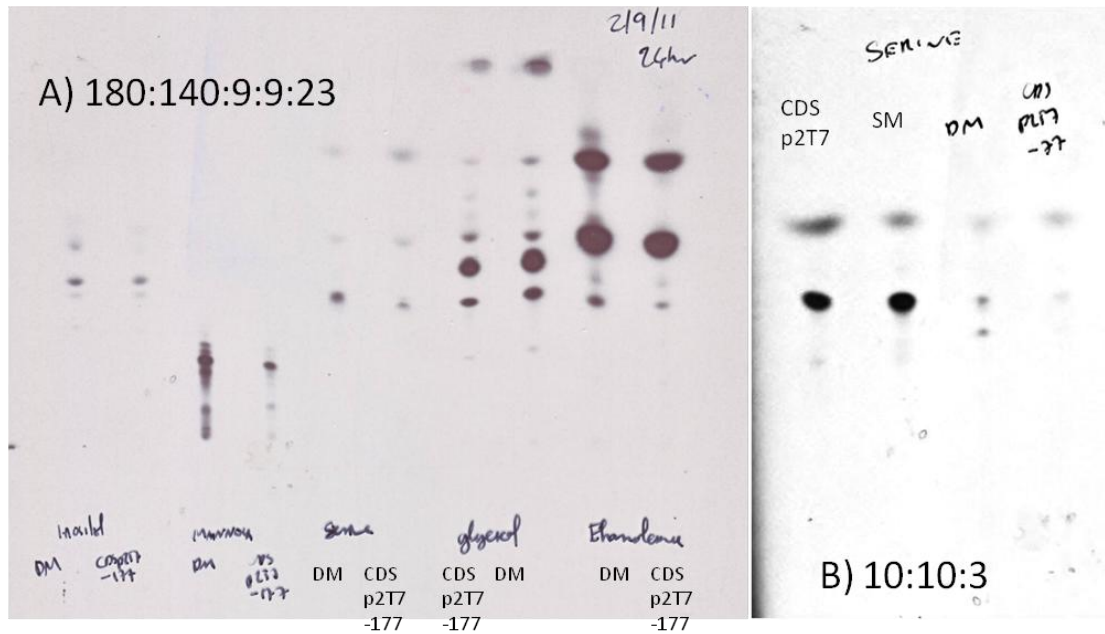
- SHEN, H. F. & DOWHAN, W. 1997. Regulation of phospholipid biosynthetic enzymes by the level of CDP-diacylglycerol synthase activity. *Journal of Biological Chemistry*, 272, 11215-11220.
- SHEN, H. F., HEACOCK, P. N., CLANCEY, C. J. & DOWHAN, W. 1996. The CDS1 gene encoding CDP-diacylglycerol synthase in *Saccharomyces cerevisiae* is essential for cell growth. *Journal of Biological Chemistry*, 271, 789-795.
- SHERWIN, T. & GULL, K. 1989. THE CELL-DIVISION CYCLE OF TRYPANOSOMA-BRUCI-BRUCI - TIMING OF EVENT MARKERS AND CYTOSKELETAL MODULATIONS. *Philosophical Transactions of the Royal Society of London Series B-Biological Sciences*, 323, 573-&.
- SHIAO, Y. J., LUPO, G. & VANCE, J. E. 1995. EVIDENCE THAT PHOSPHATIDYLSERINE IS IMPORTED INTO MITOCHONDRIA VIA A MITOCHONDRIA-ASSOCIATED MEMBRANE AND THAT THE MAJORITY OF MITOCHONDRIAL PHOSPHATIDYLETHANOLAMINE IS DERIVED FROM DECARBOXYLATION OF PHOSPHATIDYLSERINE. *Journal of Biological Chemistry*, 270, 11190-11198.
- SIEVERS, F., WILM, A., DINEEN, D., GIBSON, T. J., KARPLUS, K., LI, W., LOPEZ, R., MCWILLIAM, H., REMMERT, M., SOEDING, J., THOMPSON, J. D. & HIGGINS, D. G. 2011. Fast, scalable generation of high-quality protein multiple sequence alignments using Clustal Omega. *Molecular Systems Biology*, 7.
- SIGNORELL, A., RAUCH, M., JELK, J., FERGUSON, M. A. J. & BUETIKOFER, P. 2008. Phosphatidylethanolamine in *Trypanosoma brucei* is organized in two separate pools and is synthesized exclusively by the Kennedy pathway. *Journal of Biological Chemistry*, 283, 23636-23644.
- SIMARRO, P. P., DIARRA, A., POSTIGO, J. A. R., FRANCO, J. R. & JANNIN, J. G. 2011. The Human African Trypanosomiasis Control and Surveillance Programme of the World Health Organization 2000-2009: The Way Forward. *Plos Neglected Tropical Diseases*, 5.
- SIMPSON, A. G. B., INAGAKI, Y. & ROGER, A. J. 2006. Comprehensive multigene phylogenies of excavate protists reveal the evolutionary positions of "primitive" eukaryotes. *Molecular Biology and Evolution*, 23, 615-625.
- SIMPSON, A. G. B., LUKES, J. & ROGER, A. J. 2002. The evolutionary history of kinetoplasts and their kinetoplasts. *Molecular Biology and Evolution*, 19, 2071-2083.
- SIMPSON, A. G. B. & ROGER, A. J. 2004. Protein phylogenies robustly resolve the deep-level relationships within Euglenozoa. *Molecular Phylogenetics and Evolution*, 30, 201-212.
- SMITH, T. K. & BUETIKOFER, P. 2010. Lipid metabolism in *Trypanosoma brucei*. *Molecular and Biochemical Parasitology*, 172, 66-79.
- SMITH, T. K., CROSSMAN, A., BRIMACOMBE, J. S. & FERGUSON, M. A. J. 2004. Chemical validation of GPI biosynthesis as a drug target against African sleeping sickness. *Embo Journal*, 23, 4701-4708.
- SMITH, T. K., VASILEVA, N., GLUENZ, E., TERRY, S., PORTMAN, N., KRAMER, S., CARRINGTON, M., MICHAELI, S., GULL, K. & RUDENKO, G. 2009. Blocking Variant Surface Glycoprotein Synthesis in *Trypanosoma brucei* Triggers a General Arrest in Translation Initiation. *Plos One*, 4.
- SPARROW, C. P. & RAETZ, C. R. H. 1985. PURIFICATION AND PROPERTIES OF THE MEMBRANE-BOUND CDP-DIGLYCERIDE SYNTHETASE FROM *ESCHERICHIA-COLI*. *Journal of Biological Chemistry*, 260, 2084-2091.
- SRIBNEY, M., DOVE, J. L. & LYMAN, E. M. 1977. STUDIES ON SYNTHESIS OF CDP-DIACYLGLYCEROL - STIMULATION BY GTP AND INHIBITION BY ATP AND FLUORIDE. *Biochemical and Biophysical Research Communications*, 79, 749-755.
- STEPHENS, J. L., LEE, S. H., PAUL, K. S. & ENGLUND, P. T. 2007. Mitochondrial fatty acid synthesis in *Trypanosoma brucei*. *Journal of Biological Chemistry*, 282, 4427-4436.
- STONE, S. J. & VANCE, J. E. 2000. Phosphatidylserine synthase-1 and -2 are localized to mitochondria-associated membranes. *Journal of Biological Chemistry*, 275, 34534-34540.
- SUMIDA, S. & MUDD, J. B. 1970. STRUCTURE AND BIOSYNTHESIS OF PHOSPHATIDYL INOSITOL IN CAULIFLOWER INFLORESCENCE. *Plant Physiology*, 45, 712-&.

- SUTTERWALA, S. S., HSU, F.-F., SEVOVA, E. S., SCHWARTZ, K. J., ZHANG, K., KEY, P., TURK, J., BEVERLEY, S. M. & BANGS, J. D. 2008. Developmentally regulated sphingolipid synthesis in African trypanosomes. *Molecular Microbiology*, 70, 281-296.
- TAKAI, Y., KISHIMOTO, A., IWASA, Y., KAWAHARA, Y., MORI, T. & NISHIZUKA, Y. 1979. CALCIUM-DEPENDENT ACTIVATION OF A MULTIFUNCTIONAL PROTEIN-KINASE BY MEMBRANE PHOSPHOLIPIDS. *Journal of Biological Chemistry*, 254, 3692-3695.
- TANAKA, S., NIKAWA, J., IMAI, H., YAMASHITA, S. & HOSAKA, K. 1996. Molecular cloning of rat phosphatidylinositol synthase cDNA by functional complementation of the yeast *Saccharomyces cerevisiae* *pis* mutation. *Febs Letters*, 393, 89-92.
- TETLEY, L., TURNER, C. M. R., BARRY, J. D., CROWE, J. S. & VICKERMAN, K. 1987. ONSET OF EXPRESSION OF THE VARIANT SURFACE GLYCOPROTEINS OF TRYPANOSOMA-BRUCI IN THE TSETSE-FLY STUDIED USING IMMUNOELECTRON MICROSCOPY. *Journal of Cell Science*, 87, 363-372.
- THOMPSON, R. J. 1977. BIOSYNTHESIS OF CYTIDINE DIPHOSPHATE DIACYLGLYCEROL IN MAMMALIAN CEREBRAL-CORTEX. *Biochemical Society Transactions*, 5, 49-51.
- THOMPSON, W. & MACDONALD, G. 1975. ISOLATION AND CHARACTERIZATION OF CYTIDINE DIPHOSPHATE DIGLYCERIDE FROM BEEF LIVER. *Journal of Biological Chemistry*, 250, 6779-6785.
- TRIPODI, K. E. J., BUTTIGLIERO, L. V., ALTABE, S. G. & UTTARO, A. D. 2006. Functional characterization of front-end desaturases from trypanosomatids depicts the first polyunsaturated fatty acid biosynthetic pathway from a parasitic protozoan. *Febs Journal*, 273, 271-280.
- TYERYAR, K. R., VONGTAU, H. O. U. & UNDIH, A. S. 2008. Diverse antidepressants increase CDP-diacylglycerol production and phosphatidylinositide resynthesis in depression-relevant regions of the rat brain. *Bmc Neuroscience*, 9.
- VAN DEN ABEELE, J., CLAES, Y., VAN BOCKSTAELE, D., LE RAY, D. & COOSEMANS, M. 1999. *Trypanosoma brucei* spp. development in the tsetse fly: characterization of the post-mesocyclic stages in the foregut and proboscis. *Parasitology*, 118, 469-478.
- VAN DEN BOSSCHE, P. & DELESPAUX, V. 2011. Options for the control of tsetse-transmitted livestock trypanosomosis. An epidemiological perspective. *Veterinary Parasitology*, 181, 37-42.
- VAN HELLEMOND, J. J. & TIELENS, A. G. M. 2006. Adaptations in the lipid metabolism of the protozoan parasite *Trypanosoma brucei*. *Febs Letters*, 580, 5552-5558.
- VANCE, J. E. 1990. PHOSPHOLIPID-SYNTHESIS IN A MEMBRANE-FRACTION ASSOCIATED WITH MITOCHONDRIA. *Journal of Biological Chemistry*, 265, 7248-7256.
- VANCE, J. E. 2008. Thematic review series: Glycerolipids. Phosphatidylserine and phosphatidylethanolamine in mammalian cells: two metabolically related aminophospholipids. *Journal of Lipid Research*, 49, 1377-1387.
- VANCE, J. E. & STEENBERGEN, R. 2005. Metabolism and functions of phosphatidylserine. *Progress in Lipid Research*, 44, 207-234.
- VANDERPLOEG, L. H. T., VALERIO, D., DELANGE, T., BERNARDS, A., BORST, P. & GROSVELD, F. G. 1982. AN ANALYSIS OF COSMID CLONES OF NUCLEAR-DNA FROM TRYPANOSOMA-BRUCI SHOWS THAT THE GENES FOR VARIANT SURFACE GLYCOPROTEINS ARE CLUSTERED IN THE GENOME. *Nucleic Acids Research*, 10, 5905-5923.
- VARGAS, L. A., MIAO, L. X. & ROSENTHAL, A. F. 1984. INHIBITION OF PLATELET PHOSPHATIDYLINOSITOL SYNTHETASE BY AN ANALOG OF CDP-DIACYLGLYCEROL. *Biochimica Et Biophysica Acta*, 796, 123-128.
- VASSELLA, E., OBERLE, M., URWYLER, S., RENGGLI, C. K., STUDER, E., HEMPHILL, A., FRAGOSO, C., BUTIKOFER, P., BRUN, R. & RODITI, I. 2009. Major Surface Glycoproteins of Insect Forms of *Trypanosoma brucei* Are Not Essential for Cyclical Transmission by Tsetse. *Plos One*, 4.
- VAZIRI, C., DOWNES, C. P. & MACFARLANE, S. C. 1993. DIRECT LABELING OF HORMONE-SENSITIVE PHOSPHOINOSITIDES BY A PLASMA-MEMBRANE-ASSOCIATED PTDINS SYNTHASE IN TURKEY ERYTHROCYTES. *Biochemical Journal*, 294, 793-799.
- VICKERMAN, K. 1974. *THE ULTRASTRUCTURE OF PATHOGENIC FLAGELLATES*.
- VICKERMAN, K. 1985. DEVELOPMENTAL CYCLES AND BIOLOGY OF PATHOGENIC TRYPANOSOMES. *British Medical Bulletin*, 41, 105-114.

- VICKERMAN, K. & PRESTON, T. M. 1976. Comparative Cell Biology of the Kinetoplastid flagellates. In: LUMSDEN, W. H. R. & EVANS, D. A. (eds.) *Biology of the Kinetoplastida*. London: Academic Press.
- VOELKER, D. R. & FRAZIER, J. L. 1986. ISOLATION AND CHARACTERIZATION OF A CHINESE-HAMSTER OVARY CELL-LINE REQUIRING ETHANOLAMINE OR PHOSPHATIDYLSERINE FOR GROWTH AND EXHIBITING DEFECTIVE PHOSPHATIDYLSERINE SYNTHASE ACTIVITY. *Journal of Biological Chemistry*, 261, 1002-1008.
- VOLTA, M., BULFONE, A., GATTUSO, C., ROSSI, E., MARIANI, M., CONSALEZ, G. G., ZUFFARDI, O., BALLABIO, A., BANFI, S. & FRANCO, B. 1999. Identification and characterization of CDS2, a mammalian homolog of the *Drosophila* CDP-diacylglycerol synthase gene. *Genomics*, 55, 68-77.
- VOLTA, M., BULFONE, A., ROSSI, E., MARIANI, M., CONSALES, G., ZUFFARDI, O., BALLABIO, A., BANFI, S. & FRANCO, B. 1998. Identification and expression studies of mammalian homologs of the *Drosophila* CDP-diacylglycerol synthase (CDS) gene: implications for the evolution of phototransduction mechanisms. *European Journal of Human Genetics*, 6, P6032.
- VONHEIJNE, G. 1992. MEMBRANE-PROTEIN STRUCTURE PREDICTION - HYDROPHOBICITY ANALYSIS AND THE POSITIVE-INSIDE RULE. *Journal of Molecular Biology*, 225, 487-494.
- WANG, Z. F., MORRIS, J. C., DREW, M. E. & ENGLUND, P. T. 2000. Inhibition of *Trypanosoma brucei* gene expression by RNA interference using an integratable vector with opposing T7 promoters. *Journal of Biological Chemistry*, 275, 40174-40179.
- WATANABE, R., MURAKAMI, Y., MARMOR, M. D., INOUE, N., MAEDA, Y., HINO, J., KANGAWA, K., JULIUS, M. & KINOSHITA, T. 2000. Initial enzyme for glycosylphosphatidylinositol biosynthesis requires PIG-P and is regulated by DPM2. *Embo Journal*, 19, 4402-4411.
- WAUGH, M. G., MINOGUE, S., CLAYTON, E. L. & HSUAN, J. J. 2011. CDP-diacylglycerol phospholipid synthesis in detergent-soluble, non-raft, membrane microdomains of the endoplasmic reticulum. *Journal of Lipid Research*, 52, 2148-2158.
- WEEKS, R., DOWHAN, W., SHEN, H. F., BALANTAC, N., MEENGs, B., NUDELMAN, E. & LEUNG, D. W. 1997. Isolation and expression of an isoform of human CDP-diacylglycerol synthase cDNA. *DNA and Cell Biology*, 16, 281-289.
- WHITE, D. A., ALBRIGHT, F. R., LENNARZ, W. J. & SCHNAITM.CA 1971. DISTRIBUTION OF PHOSPHOLIPID-SYNTHESIZING ENZYMES IN WALL AND MEMBRANE SUBFRACTIONS OF ENVELOPE OF *ESCHERICHIA-COLI*. *Biochimica Et Biophysica Acta*, 249, 636-&.
- WICKSTEAD, B., ERSFELD, K. & GULL, K. 2002. Targeting of a tetracycline-inducible expression system to the transcriptionally silent minichromosomes of *Trypanosoma brucei*. *Molecular and Biochemical Parasitology*, 125, 211-216.
- WILLIAMSON, F. A. & MORRE, D. J. 1976. DISTRIBUTION OF PHOSPHATIDYLINOSITOL BIOSYNTHETIC ACTIVITIES AMONG CELL FRACTIONS FROM RAT-LIVER. *Biochemical and Biophysical Research Communications*, 68, 1201-1205.
- WINZELER, E. A., SHOEMAKER, D. D., ASTROMOFF, A., LIANG, H., ANDERSON, K., ANDRE, B., BANGHAM, R., BENITO, R., BOEKE, J. D., BUSSEY, H., CHU, A. M., CONNELLY, C., DAVIS, K., DIETRICH, F., DOW, S. W., EL BAKKOURY, M., FOURY, F., FRIEND, S. H., GENTALEN, E., GIAEVER, G., HEGEMANN, J. H., JONES, T., LAUB, M., LIAO, H., LIEBUNDGUTH, N., LOCKHART, D. J., LUCAU-DANILA, A., LUSSIER, M., M'RABET, N., MENARD, P., MITTMANN, M., PAI, C., REBISCHUNG, C., REVUELTA, J. L., RILES, L., ROBERTS, C. J., ROSS-MACDONALD, P., SCHERENS, B., SNYDER, M., SOOKHAI-MAHADEO, S., STORMS, R. K., VERONNEAU, S., VOET, M., VOLCKAERT, G., WARD, T. R., WYSOCKI, R., YEN, G. S., YU, K. X., ZIMMERMANN, K., PHILIPPSSEN, P., JOHNSTON, M. & DAVIS, R. W. 1999. Functional characterization of the *S-cerevisiae* genome by gene deletion and parallel analysis. *Science*, 285, 901-906.
- WIRTZ, E., LEAL, S., OCHATT, C. & CROSS, G. A. M. 1999. A tightly regulated inducible expression system for conditional gene knock-outs and dominant-negative genetics in *Trypanosoma brucei*. *Molecular and Biochemical Parasitology*, 99, 89-101.
- WIRTZ, K. W. A. 2006. Phospholipid transfer proteins in perspective. *Febs Letters*, 580, 5436-5441.
- WONG, K., VALDEZ, P. A., TAN, C., YEH, S., HONGO, J.-A. & OUYANG, W. 2010. Phosphatidylserine receptor Tim-4 is essential for the maintenance of the

- homeostatic state of resident peritoneal macrophages. *Proceedings of the National Academy of Sciences of the United States of America*, 107, 8712-8717.
- WU, L., NIEMEYER, B., COLLEY, N., SOCOLICH, M. & ZUKER, C. S. 1995. REGULATION OF PLC-MEDIATED SIGNALING IN-VIVO BY CDP-DIACYLGLYCEROL SYNTHASE. *Nature*, 373, 216-222.
- WU, W. I. & CARMAN, G. M. 1996. Regulation of phosphatidate phosphatase activity from the yeast *Saccharomyces cerevisiae* by phospholipids. *Biochemistry*, 35, 3790-3796.
- YANG, Y. Z., CAO, J. S. & SHI, Y. G. 2004. Identification and characterization of a gene encoding human LPGAT1, an endoplasmic reticulum-associated lysophosphatidylglycerol acyltransferase. *Journal of Biological Chemistry*, 279, 55866-55874.
- YOUNG, S. A. & SMITH, T. K. 2010. The essential neutral sphingomyelinase is involved in the trafficking of the variant surface glycoprotein in the bloodstream form of *Trypanosoma brucei*. *Molecular Microbiology*, 76, 1461-1482.
- YUN, O., PRIOTTO, G., TONG, J., FLEVAUD, L. & CHAPPUIS, F. 2010. NECT Is Next: Implementing the New Drug Combination Therapy for *Trypanosoma brucei gambiense* Sleeping Sickness. *Plos Neglected Tropical Diseases*, 4.
- ZHAO, Z., LINDSAY, M. E., CHOWDHURY, A. R., ROBINSON, D. R. & ENGLUND, P. T. 2008. p166, a link between the trypanosome mitochondrial DNA and flagellum, mediates genome segregation. *Embo Journal*, 27, 143-154.

Appendix A



Appendix A. Radiolabelling from A) [^3H]inositol, [^3H]mannose, [^3H]serine, [^3H]glycerol and [^3H]ethanolamine labellings run in 180:140:9:9:23 CHCl_3 :MeOH:30% NH_3 : 1 M NH_4Ac :H , B. [^3H]serine labelling run in 10:10:3 CHCl_3 :MeOH:H $_2$ O wild type single marker (SM), wild type double marker (DM), BSF CDS p2T7 RNAi + tetracycline (CDS p2T7) and PCF CDS p2T7 RNAi + tetracycline (CDS p2T7-177).